The Synthesis-Enabled Stereochemical Elucidation of the Marine Natural Products Hemicalide and Phormidolide A

A thesis submitted for the degree of Doctor of Philosophy
at the University of Cambridge

Nelson Y. S. Lam

Trinity College

Department of Chemistry

August 2019

Declaration

This thesis is the result of my own work and includes nothing which is the outcome of work done in collaboration except as declared in the Preface and specified in the text. It is not substantially the same as any that I have submitted, or, is being concurrently submitted for a degree or diploma or other qualification at the University of Cambridge or any other University or similar institution except as declared in the Preface and specified in the text. I further state that no substantial part of my thesis has already been submitted, or, is being concurrently submitted for any such degree, diploma or other qualification at the University of Cambridge or any other University or similar institution except as declared in the Preface and specified in the text. It does not exceed the prescribed word limit of 60,000 words, excluding experimental data.

_____

Nelson Yuen Sum Lam

August 2019

Part of the work described in this thesis has been published in the following peer-reviewed articles:

Han, B. Y.; Lam, N. Y. S.; MacGregor, C. I.; Goodman, J. M.; Paterson, I. *Chem. Commun*. **2018**, *54*, 3247–3250.

Lam, N. Y. S.; Muir, G.; Rao Challa, V.; Britton, R.; Paterson, I. *Chem. Commun.* **2019**, *55*, 9717–9720.

Acknowledgements

If I have seen further than others it is by standing upon the shoulders of giants

The work described in this thesis would not have been possible without the abundant support and camaraderie of my mentors, collaborators and friends.

I am indebted to Prof. Ian Paterson for the opportunity to be part of a team with decades of world-leading expertise in organic synthesis. His principled perspectives and incredible breadth of knowledge have made for many fantastic discussions that I hope will continue for years to come. I am also grateful for my academic mentors, Profs. Jonathan Goodman, David Spring, Rob Britton (SFU) and Christian Hartinger (Auckland), who have given me their advice over the years.

I am fortunate to have worked with a fantastic team of scientists during my PhD. Above all, I am very grateful to Dr. Bing Yuan Han for his guidance and solidarity, and Garrett Muir for his ceaseless enthusiasm in our ongoing project towards phormidolide A. Both were instrumental for the advances we have made towards our projects and their names deserve to be in equal standing alongside mine on the front cover of this thesis. I am particularly grateful for Drs. Bing Yuan Han and Andrew Phillips for taking the time to proofread my thesis. Additionally, none of this research would have been possible without Nic Davies, Naomi Hobbs and Carlos Davies for their excellent technical support, and Dr. Peter Grice, Duncan Howe and Andrew Mason for their fountain of NMR expertise.

Moving halfway around the world has been made easier by the wonderful lab environment created by everyone in the Paterson group past and present, as well as the Spring and Phipps groups who share our lab space. These people have all contributed to the dynamic atmosphere that is Lab 122. The four years have been fruitful not just in the pursuit of knowledge, but also in forging lifelong friendships. Through the ups and many downs of PhD life, I am indebted to the support from my fellow lab mates, and my friends near and far: Ruth, Dråkšo, Sarah, Brieuc, Paula, Sofia, Jesse, Mark, Catherine, Micah, Ryan and Anthony to name a few. I have to especially thank Rachel, my fellow PhD companion, with whom over our four years celebrated the joys with food and weathered the storms with more food.

Finally, I would like to express my gratitude to the people and organisations who have supported my time in Cambridge through their generous funding: Dr. Nigel Evans, Sir Noel Robinson and the Woolf Fisher Trust, and Eashwar Krishnan, Tzo-Tze Ang and Trinity College.

Abstract

The structural complexity and biological activity of marine natural products have made them attractive targets for synthetic chemists. In cases where their relative and/or absolute configuration is unknown, total synthesis becomes a powerful method to enable their structural elucidation, as highlighted in Part I. This thesis discusses synthetic efforts towards two marine natural products, hemicalide (**1**) and phormidolide A (**2**), with the end goal of establishing and/or confirming the compound's full stereochemistry.

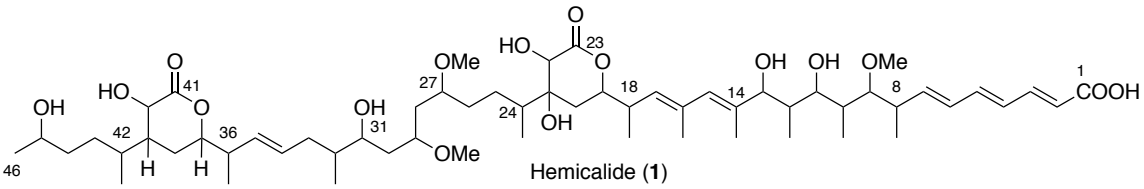

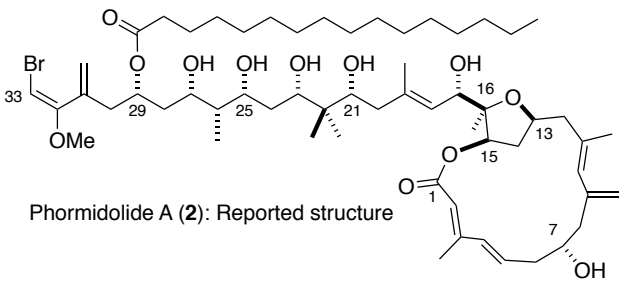

Hemicalide's low isolation yield from its marine sponge source meant that none of the 21 stereocenters were assigned in the original patent literature. Previous computational and synthetic work by Ardisson and Cossy, as well as the Paterson and Goodman groups, have narrowed down the possibilities for the C1-C15, C16-C25 and C35-C46 fragments to a single diastereomer with reasonable confidence. However, the relative configuration between fragments and the absolute stereochemistry remains unknown. Part II describes the synthesis of the C16-C28 dihydroxylactone fragment, which was used to successfully assemble a diastereomer of the C1-C28 truncate. Comparisons with the alternative configuration synthesised by Han enabled the definitive assignment of the relative configuration between the C1-C15 and the C16-C25 region of hemicalide. These studies also illuminated the nature of the C1 carboxyl group in the natural product.

Phormidolide A possesses several fascinating structural motifs. Its terminal bromomethoxydiene (BMD) motif in particular, is unprecedented among natural products. Furthermore, inconclusive stereochemical evidence presented in the literature meant that a synthesis-guided stereochemical evaluation is required. Part III discusses synthetic efforts to the natural product, involving the expedient synthesis of the C18-C23 vinyl iodide and the C25-C33 side chain bearing the unique BMD motif. Towards the end goal of a total synthesis, this chapter also illustrates the evolution of the fragment coupling strategy, which led to the reassignment of seven of the 11 stereocentres present in phormidolide A.

Table of Contents

Abbreviations

Å	Ångstrom
Ac	Acetyl
aq.	Aqueous
BBN	Borabicyclo[3.3.1]nonane
BINOL	1,1'-Bi-2-naphthol
Bn	Benzyl
brsm	Based on recovered starting material
Bu or *n*Bu	*n*-Butyl
Bz	Benzoyl
cat.	Catalytic
CBS	Corey-Bakshi-Shibata
CoA	Coenzyme A
COSY	^{1}H-^{1}H correlation spectroscopy
conv.	Conversion
Cp	Cyclopentadienyl
CSA	Camphorsulfonic acid
Cy	Cyclohexyl
dr	Diastereomeric ratio
d, dd, ddd	Doublet, doublet of doublets, doublet of doublets of doublets
dt	Doublet of triplets
dba	Dibenzylideneacetone
DBU	1,8-Diazabicyclo[5.4.0]undec-7-ene
DCC	*N,N'*-Dicyclohexylcarbodiimide
DDQ	2,3-Dichloro-5,6-dicyano-1,4-benzoquinone
DEAD, DIAD	Diethyl/Diisopropyl azodicarboxylate
DFT	Density Functional Theory
DIBAL	Diisobutylaluminium hydride
DIPCl	Diisopinocampheylborane chloride
DIPEA	Diisopropylethylamine
DMAP	4-Dimethylaminopyridine
DMF	*N,N*-Dimethylformamide
DMP	Dess-Martin Periodinane
DMSO	Dimethyl sulfoxide
ee	Enantiomeric excess

EDC	1-Ethyl-3-(3-dimethylaminopropyl)carbodiimide
eq.	Equivalents
ESI	Electrospray ionisation
Et	Ethyl
g, mg	Gram(s), milligram(s)
h	Hour(s)
HMBC	Heteronuclear Multiple Bond Correlation Spectroscopy
HMDS	Hexamethyldisilazide
HMPA	Hexamethylphosphoramide
HPLC	High Performance Liquid Chromatography
HWE	Horner-Wadsworth-Emmons
Hz, MHz	Hertz, Megahertz
IC_{50}	Half maximal inhibitory concentration
Imid.	Imidazole
Ipc	Isopinocampheyl
*i*Pr	Isopropyl
IR	Infrared Spectroscopy
J	^{1}H-^{1}H coupling constant
KR	Ketoreductase
L	Unspecified ligand
LD_{50}	Median lethal dose
LDA	Lithium diisopropylamide
LLS	Longest linear sequence
lut.	2,6-Lutidine
M	Unspecified metal; Molar
Me	Methyl
min.	Minute(s)
mL, μL	Milli/microlitre(s)
mmol, μmol	Milli/micromole(s)
MNBA	2-Methyl-6-nitrobenzoic anhydride
MS	Molecular sieves or mass spectrometry
Ms	Mesyl (methanesulfonyl)
MTPA	α-Methoxy-α-(trifluoromethyl)phenylacetate
nM	Nanomolar
NHC	*N*-Heterocyclic carbene
NMP	*N*-Methylpyrrolidinone

NMO	*N*-Methylmorpholine *N*-oxide
NMR	Nuclear Magnetic Resonance Spectroscopy
NOE	Nuclear Overhauser Effect
NOESY	Nuclear Overhauser Effect Spectroscopy
NCS, NBS, NIS	*N*-Chloro/bromo/iodosuccinimide
PE 30-40/40-60	Petroleum Ether, boiling point 30-40 °C or boiling point 40-60 °C
Ph	Phenyl
Pin	Pinacol
PMB	*para*-Methoxybenzyl
ppm	Parts per million
PMBTCA	*para*-Methoxybenzyl trichloroacetimidate
PPTS	Pyridinium *para*-toluenesulfonate
py	Pyridine
q	Quartet
Quant.	Quantitative
R	Unspecified substituent
r.t.	Room Temperature
R_f	Retention factor
sp.	Species
t	Triplet
TASF	Tris(dimethylamino)sulfonium difluorotrimethylsilicate
TBAF/I	Tetrabutylammonium fluoride/iodide
TBAT	Tetrabutylammonium diflurotriphenylsilicate
TBS	*tert*-Butyldimethylsilyl
*t*Bu	*tert*-Butyl
TC	Thiophene-2-carboxylate
TCBC	2,4,6-Trichlorobenzoyl chloride
TEMPO	(2,2,6,6-Tetramethylpiperidin-1-yl)oxy
TES	Triethylsilyl
Tf	Trifluoromethanesulfonyl
THF	Tetrahydrofuran
TIPS	Triisopropylsilyl
TLC	Thin layer chromatography
TMDS	Tetramethyldisiloxane
TMS	Tetramethylsilane *or* trimethylsilyl
Ts	Tosyl (*para*-toluenesulfonyl)

Nomenclature

Compound numbering

The numbering system used for hemicalide and its associated fragments follows that of Carletti et *al.*.[1] Substituents are defined by the skeletal carbon to which they are attached. The complete numbering scheme for hemicalide is shown in **Figure 1**.

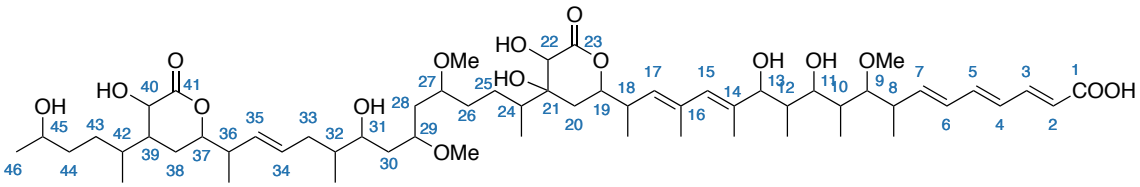

Figure 1. *Numbering scheme for hemicalide*

The numbering system used for the carbon skeleton of phormidolide A follows that of Williamson et *al.*[2], with the exception of skeletal substitutions (e.g. hydroxyl, methyl, methoxy and methylene groups), which are denoted by the skeletal carbon to which they are attached. The complete numbering scheme for phormidolide A is shown in **Figure 2**.

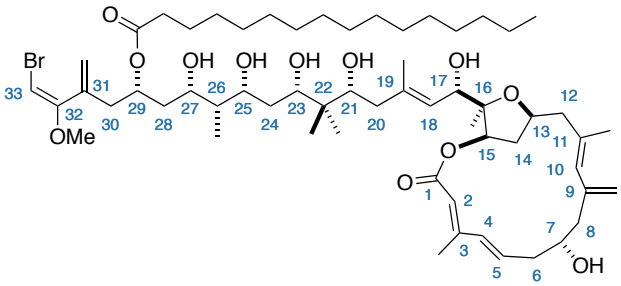

Figure 2. *Numbering scheme for phormidolide A*

Metal enolate and olefin geometry

The geometry of olefins and metal enolates are assigned based on the accepted IUPAC convention. *E* olefins are defined by having the highest priority groups located on opposite sides of the double bond. *Z* olefins are defined by having the highest priority groups located on the same side. Metal enolates follow an analogous assignment, however, by convention, the metal-oxygen is always defined as the highest priority group (**Figure 3**).

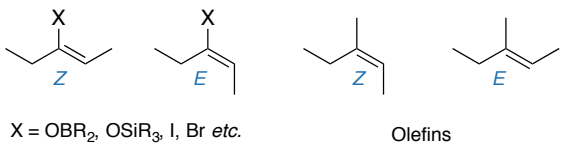

Figure 3. *General examples of enolate and olefin geometries*

Stereochemical relationships

The relative stereochemical relationship between two substituents are defined by the convention set out by Masamune.[3] A *syn* relationship has the two substituents pointing in the same direction relative to the plane of the carbon skeleton when drawn in a linear fashion, whereas an *anti* relationship has the two substituents pointing in opposite direction (**Figure 4**).

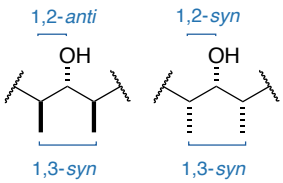

Figure 4. *Examples of stereochemical relationships*

Part I – Introduction

1.1. Marine Natural Products and their Characterisation

The marine environment accounts for over 70% of the Earth's total area, and in it harbours a plethora of biodiversity.[4] This breadth of marine flora and fauna flows down into the breadth of secondary metabolites many of these organisms produce. In facing the inherent problem of efficacy in high dilution, many of these secondary metabolites produced by marine organisms have evolved over time to be highly potent binders of specific biological targets, or incredibly toxic towards other living organisms.[5]

Throughout history, humankind's interdependence with nature has led to the extensive use of terrestrial natural products in treating ailments.[6] Largely owing to their inaccessibility, marine natural products have only recently started to enter the medicinal repertoire.[7] Though marine natural products have comparatively occupied a minute period of history as compared to terrestrial compounds, over 20,000 marine natural products have been discovered in the last fifty years.[8] Indeed, their diverse range of bioactivities have resulted in the clinical validation of many promising compounds.[9] Underpinning any further discovery however is the successful structural elucidation of these compounds of interest. In order for these compounds to be realised as clinical candidates, or for any further activity-guided optimisation to occur, their 2D and 3D structures must be unambiguously determined. This is by no means a simple task given the often-complex architectures underscored by a non-trivial isolation procedure that often only generates meagre amounts of the novel compound from a huge amount of biomass.[10]

As such, isolation chemists are often faced with the daunting task of determining the structure of a complex compound and ascertaining its biological activity, all from tiny amounts of material. In the past, with limited experimental data, the unambiguous structural elucidation was often only achieved through X-ray diffraction studies of single crystals. Nowadays, complex structures can be routinely solved by chemists employing an array of spectroscopic (especially NMR) techniques, elucidating complex structures that previously would have in the past, taken a team of eminent scientists many years to achieve.[11] It is to no surprise that the overall advancement in natural product research has evolved symbiotically with advances in characterisation techniques, such that it is now possible to fully solve a structure with ever smaller amounts of material. In particular, advances in long-range NMR techniques,[12] along with detailed conformational analyses from coupling constant data of these molecules[13] can often be used synergistically to unambiguously reveal the relative configuration of a novel compound.

However, these inferential experimental techniques are often insufficient to allow for the full structural determination. To alleviate these problems, many state-of-the-art computational techniques, such as the DP4 algorithm,[14] have been developed to allow the application of statistical methods in assigning likely candidate structures for a natural product. Beyond this, recent advances in cryo-electron microscopy (EM)[15] has meant that these techniques are becoming more relevant for small molecules, rather than large biomolecules for which they have found a niche. In the realm of natural products research, the increased ease of genome mining has allowed for the use of DNA sequence information to help identify enzymes that catalyse similar reactions in related compounds which can often aid in the structural elucidation of natural products.[16,17]

These aforementioned contemporary structural elucidation tools do not provide all the solutions and *ab initio* methods, including DP4, become prohibitively costly to run on large and especially flexible molecules;[14,18,19] the nascent cryo-EM technology for small molecules rely on the sample being a solid and abundant in reasonable quantities often not feasible after an isolation campaign,[15] and the use of bioinformatics as a prospective tool can seldom fully rationalise the stereochemistry of a natural product. For these reasons, synthesis still remains the undisputed arbiter of structural proof. Beyond chemical derivisation and degradation, a total synthesis of a natural product followed by its spectroscopic comparison gives an unambiguous proof of a compound's overall constitution and 3D structure.

1.2. The Role of Synthesis in Correcting Stereochemical Misassignments

As characterisation techniques become more advanced and the analytical toolkit becomes more diverse, it should logically follow that assignment errors should accordingly decrease. Interestingly, however, taking what arguably is the most powerful tool for characterisation – the NMR spectrometer, the continual improvement of an NMR magnet's field strength over the last few decades correlates positively to the number of misassignments reported in the literature.[20] This seemingly contradictory observation reflects that the improvement in sensitivity does not fundamentally alter how analyses are conducted. Rather than increasing the accuracy of spectroscopic assignments, the correlation is attributed to better spectrometers enabling the elucidation of increasingly limited amounts from extracts, leading to a greater number of new natural products isolated.[20] Additionally, these structural misassignments often reflect on the inherent weaknesses of each technique, some of which cannot be resolved even if a combination of techniques are used.[11] By way of example, even the seemingly infallible X-ray crystallographic technique has its drawbacks; the fact that crystallographic techniques struggle to discern between atoms that do not contain hydrogen atoms led to the structural misassignment of the antibiotic kinamycin C (**3**, **Figure 5a**).[21]

In these cases, the nature of inferential structural elucidation methods, such as NMR spectroscopy, are limited in its ability to definitively resolve stereochemical ambiguities, as a diverse set of structural outcomes

could plausibly be accounted for by the same set of spectra.[22] Because of this, comparative methods enabled by synthesis remain as the crowning method for stereochemical determination. The power of synthesis shines through when discerning between diastereomers, especially ones containing distal stereoclusters. In cases where the molecule is particularly flexible, *ab initio* NMR methods often cannot generate meaningful predictions for which structures are likely to be correct, as the plurality of low energy conformers often precludes accurate NMR predictions.[14] In these cases, the unambiguous stereochemical assignment of a natural product is achieved through its total synthesis. Prominent examples in which the total synthesis of a compound has resulted in their structural reassignment include the marine natural products callipeltoside A (**4, Figure 5b**) by Trost[23] and azaspiracid-1 (**5, Figure 5c**) by Nicolaou.[24]

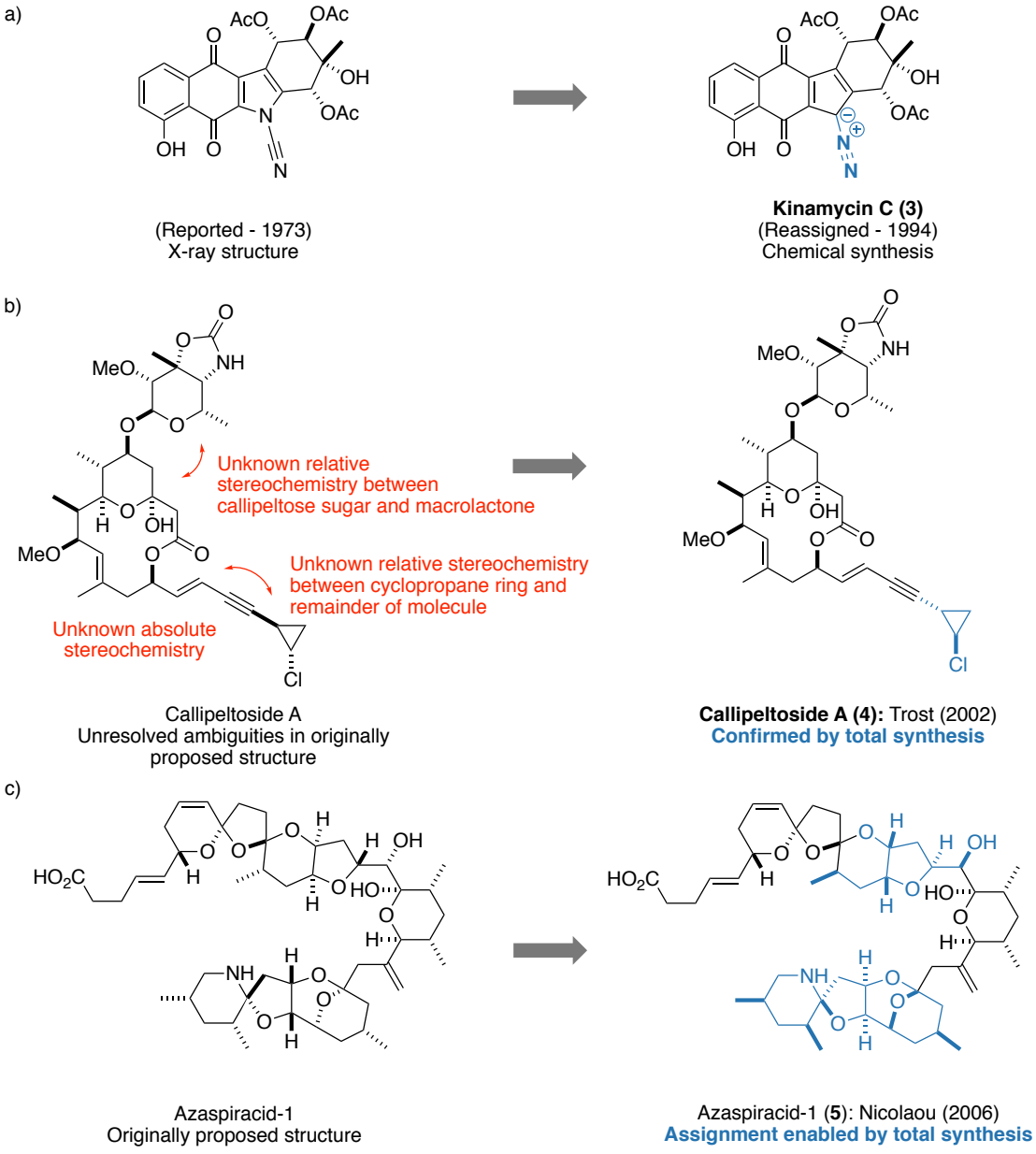

Figure 5. *Stereochemical revisions of a) kinamycin C (**3**), b) callipeltoside A (**4**) and c) azaspiracid-1 (**5**)*

These synthesis-enabled assignments and reassignments have continued to the present day; a cursory search on a literature database containing the terms "synthesis" and "stereochemical revision/reassignment" generated over 30 results from January 2016 until present (August 2019) across a wide range of terrestrial and marine natural products. To demonstrate the crucial role of synthesis in enabling such reassignments, three recent examples from the marine natural product literature are highlighted below.

One prominent class of compound that has garnered a lot of research attention is the mandelalide family of natural products, with four research groups reporting its successful total synthesis since 2013.[25–28] In particular, the most potent congener, mandelalide A, registered mid-nM activity across a range of cancer cell lines, and consequentially has been the focal point of synthetic effort across research groups. In 2014, Fürstner *et al.* reported a first total synthesis of the originally reported structure for mandelalide A (**6**, **Figure 6**), which revealed spectroscopic inconsistencies that signified the misassignment of several stereocentres.[29] Later that year, the Ye group also achieved a total synthesis of the proposed structure, which corroborated Fürstner's claims.[25] At this point, Ye noted that mandelalide A was structurally homologous to a related natural product, madeirolide A (**7**),[30] which contains a different THF configuration compared to mandelalide A. Speculating that both natural products have a common biosynthetic origin, Ye revised the configuration of the THF fragment and generated further diastereomers of mandelalide A for spectroscopic comparisons. In doing so, Ye found structure **6a** to closely match the natural product, which formed the basis of the reassignment. The ambiguities with mandelalide A did not stop here however, as the different groups that have achieved successful total syntheses have recorded disparate biological activities for the compound. While the general consensus in the community affirms the cytotoxicity of the mandelalides, it goes to show biological studies even in the same cell lines may not be an absolute indication of a compound's activity.[31]

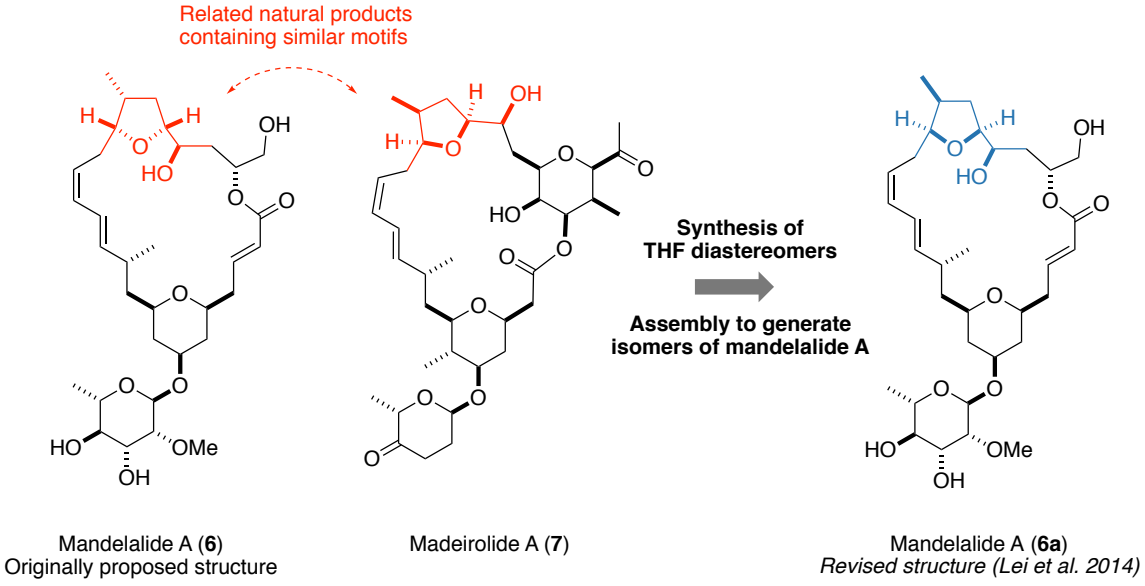

Figure 6. *Proposed and revised structure for mandelalide A (**6** and **6a**), as compared with madeirolide A (7)*

First reported in 2015, iriomoteolide-2a was isolated from a dinoflagellate found off the coast of Japan, and was determined to exhibit nanomolar activity across a range of cancer cell lines.[32] In the quest for its total synthesis, Fuwa *et al.* found spectroscopic anomalies after the successful synthesis of its originally reported structure **8** (**Figure 7**).[33] To probe the source of this incongruity, Fuwa *et al.* were able to systematically generate model substructures to verify the configuration within each of the regions of the natural product. This led to identifying the tetrahydrofuran (THF) motif, as well as a single carbinol stereocentre being misassigned, to which the incorporation of revised fragments led to a structure (**8a**) that was spectroscopically identical to the natural product.[34] Notably, this feat of a wholly synthesis-enabled stereochemical reassignment of iriomoteolide-2a was enabled by the highly modular synthesis of the natural product, allowing for the facile incorporation of fragments to rapidly verify the veracity of its configuration. Owing to the isolated stereoclusters, it is unsurprising that traditional elucidation techniques failed to pinpoint the correct diastereomer, and it ultimately required a synthetic proof to confidently determine its overall 3D structure. In fact, Fuwa *et al.* harnessed the power of synthesis to prove the absolute configuration of iriomoteolide-2a (**8b**) through synthesising both enantiomers and comparing their chiral-HPLC retention times with the natural product.

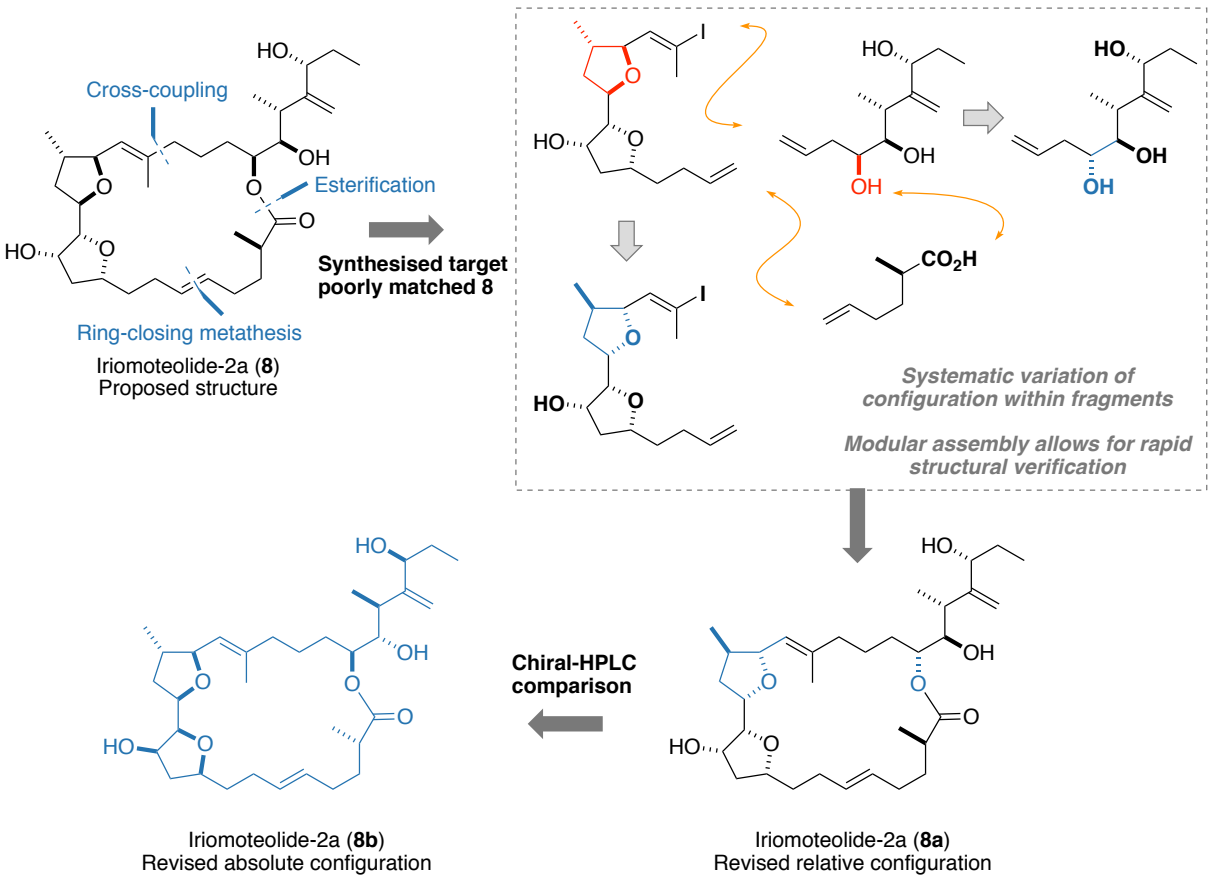

Figure 7. *Reported structure for iriomoteolide-2a (**8**) and the process leading to the revision of relative configuration to **8a**, and finally its absolute configuration to **8b***

The final example pertains to the baulamycin family of natural products, which perhaps best represents the synergistic role synthesis plays, among other contemporary techniques, in the unambiguous stereochemical elucidation of a natural product. Towards their ongoing campaign for the discovery of novel antibiotic agents, Sherman *et al.* reported the baulamycin family of siderophore antibiotics from a library of marine microbes in 2014.[35] Owing to the scarcity of material, no attempt was made at ascertaining its absolute configuration, though the relative configuration was initially determined by *J*-based coupling constant analysis. Its promising bioactivity has drawn interest from at least two research groups, with Goswami *et al.* achieving a total synthesis of the reported structure for baulamycin A (**9**) in early 2017.[36] However, the clear deviations from the reported NMR values for the natural product suggested that the structure was misassigned.

Later in 2017, Aggarwal *et al.* disclosed a comprehensive stereochemical reassignment of the baulamycins, correcting five out of seven stereocentres and definitively assigning the absolute configuration of the natural product (**Figure 8**).[37] This was initially achieved through a combination of *ab initio* NMR predictions and statistical analyses, which allowed for the reassignment of C10-C1'. The elucidation of the remaining methyl configured stereocentres nominally would be challenging using spectroscopy, but in this case, an elegant synthesis enabled by Aggarwal's lithation-borylation methodology allowed for its facile determination. By using a pre-encoded mixture of enantiomers, a statistically defined mixture of four diastereomers was generated, which could be compared with the natural product to readily determine its relative configuration. A final optical rotation comparison further allowed the unambiguous absolute stereochemical assignment of the baulamycins, that was unable to be achieved by the isolation chemists. Overall, this resulted in the reassignment of baulamycin A and B from **9** and **10**, to **9a** and **10a** respectively.

These examples are among many in the chemical literature on the decisive role synthesis has played in the unambiguous stereochemical assignment of natural products. In cases where related natural products have been isolated, homology from biosynthetic proposals can guide a synthesis-enabled reassignment, as evidenced by the reassignment of mandelalide A. Developing modular syntheses where major groups of stereocentres are isolated in single fragments also contributes to the expeditious identification of stereochemical anomalies, which was exemplified in iriomoteolide-2a. Finally, the reassignment of the baulamycins represents the power in incorporating elegant syntheses with computational techniques in tackling what otherwise would be an intractable number of candidates. Each of these examples highlight the multifaceted problems stereochemical inconsistencies bring, which demand multifaceted solutions in order to solve them.

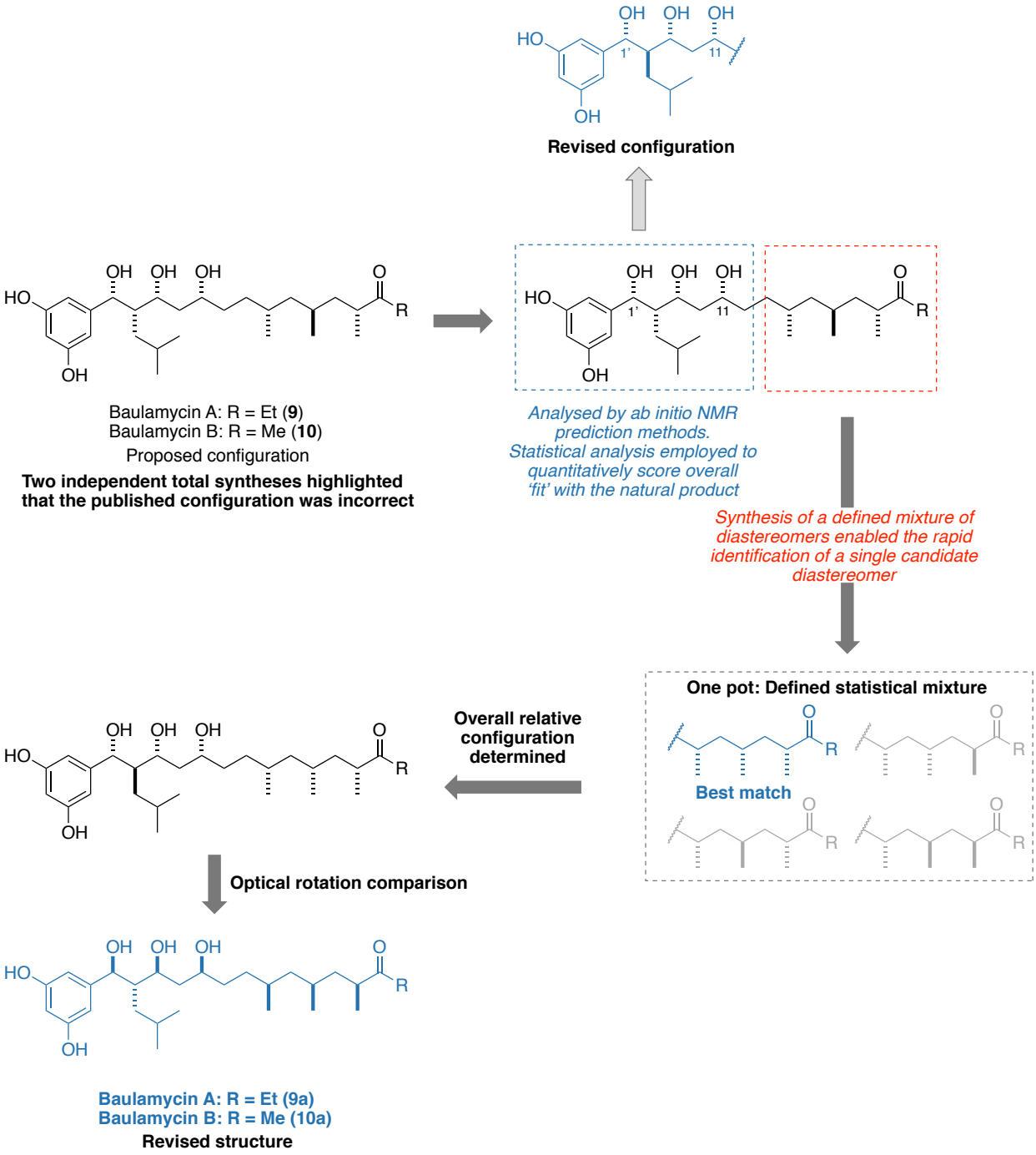

Figure 8. *The proposed configuration of the baulamycins, and the workflow employed to result in its relative and absolute stereochemical reassignment*

1.3. Summary

The continual advances in characterisation techniques have facilitated a much greater structural diversity of compounds to be isolated and elucidated from nature. This in turn, has inspired the development of state-of-the-art analytical methods for their elucidation, as well as novel synthetic methods for their synthesis. However, these methods are not perfect, and mistakes still happen. In many cases, advanced techniques are unable to resolve ambiguities, and a judicious synthetic chemistry campaign can still be used as the final tool to definitively pin down a compound's true identity, as exemplified by the three recent case studies illustrated in this section.

This thesis will highlight the prominent role synthesis has played in the stereochemical elucidation of two marine polyketides, hemicalide and phormidolide A. Chapter two discusses work towards the natural product hemicalide, a potent cytotoxin that possesses a seemingly intractable stereochemical problem. Chapter three furthers this with results presented for phormidolide A, a compound that has evolved into a continually moving target. Both sections ultimately will highlight the decisive role synthesis has played in the structural elucidation of natural products that otherwise cannot be easily accomplished through other means.

Part II – Hemicalide

2. Introduction

2.1. Isolation, 2D structural elucidation and biological activity of hemicalide

First appearing in the patent literature in 2011, hemicalide (**1**) was isolated from the marine sponge *Hemimycale* sp. around the Torres Islands of Vanuatu by CNRS-Pierre Fabre Laboratories and the Institut de Recherche pour le Développement. A bioassay-guided fractionation from 5 kg of *Hemimycale* sp. afforded 0.5 mg of the active component hemicalide.[1] ESI-MS identified a $[M–H]^-$ pseudomolecular ion signal at m/z = 1061.6780, which corresponded to a molecular formula of $C_{59}H_{97}O_{16}$. The planar structure of hemicalide was assigned from extensive 1D- and 2D-NMR studies, which revealed a 46-carbon skeleton bearing 21 stereocentres. Major features observed include a conjugated trienic acid (C1-C7), a contiguous polyproprionate stereohexad (C8-C13), a conjugated diene (C14-C17), an α,β-dihydroxylactone (C19-C23) and an α-hydroxylactone (C37-C41) (**Figure 9**).[1] Unfortunately, further derivatisation or degradation studies to ascertain both the relative and absolute stereochemistry of the molecule were not conducted owing to the scarce supply of the material, leaving all 21 stereocentres unassigned.

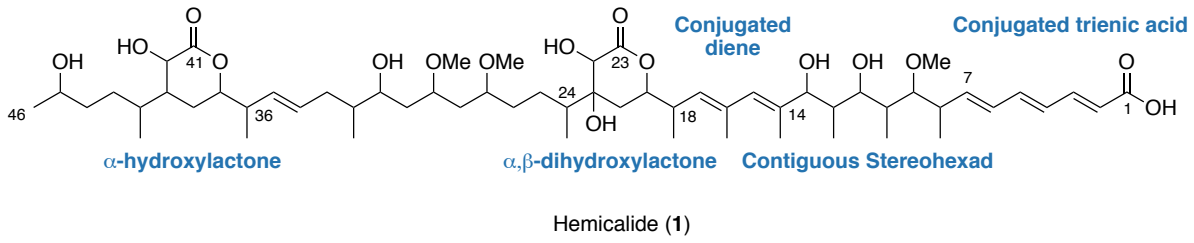

Figure 9. *Planar structure of hemicalide, with major structural features highlighted*

Hemicalide was found to be highly cytotoxic across a number of cell lines (**Table 1**). Preliminary attempts at elucidating hemicalide's mechanism of action pointed towards microtubule destabilisation.[1] At a dose of 5-50 nM, immunohistochemical labeling of α-tubulin in HeLa cells found no microtubule skeleton for cells in interphase. Mitotic cells additionally were found arrested in prometaphase without microtubules.[1] Other well-known antimitotic natural products, such as paclitaxel, epothilone B and discodermolide inhibit microtubule polymerisation during the metaphase/anaphase boundary.[38] These observations suggest that hemicalide inhibits the formation of the microtubule network in a novel manner; a valuable property as a potential anticancer agent in light of rising drug resistance towards existing cancer chemotherapeutics.[39]

Hemicalide presents itself as an attractive natural product for synthetic chemists and biologists due to its structural complexity, stereochemical uncertainty, and more importantly, the need for further biological studies into its novel mechanism of action. Additionally, with the advent of targeted anticancer therapies such as antibody-drug conjugates (ADC), hemicalide's picomolar potency and novel mode of action make it a prime candidate as a potential payload in an ADC context.[40]

***Table 1**. Antiproliferative activity of hemicalide across six different cancer cell lines*

Cell line	Disease	IC_{50} (nM)
A549	Non small cell lung cancer	0.82
BxPC3	Pancreatic cancer	0.47
LoVo	Colon cancer	0.081
MCF7	Breast cancer	0.011
Namalwa	Burkitt's lymphoma	1.1
SK-OV-3	Ovarian cancer	0.33

2.2. Current progress towards the stereochemical assignment of hemicalide

Despite the promising biological effects exhibited by hemicalide from nascent investigations, further elucidation of its mode of action and subsequent development cannot occur if its 3D architecture is left undetermined. In this case, the 21 unassigned stereocentres of hemicalide produce 2^{21} possible stereoisomers. To simplify the task of ascertaining the relative configuration of the molecule, the Ardisson group began by examining isolated stereoclusters, notably the C1-C15 polypropionate (**11**), the C18-C24 dihydroxylactone (**12**) and the C36-C46 hydroxylactone (**13**) regions (**Figure 10**). An overview of the current progress towards the complete stereochemical assignment of hemicalide is presented below.

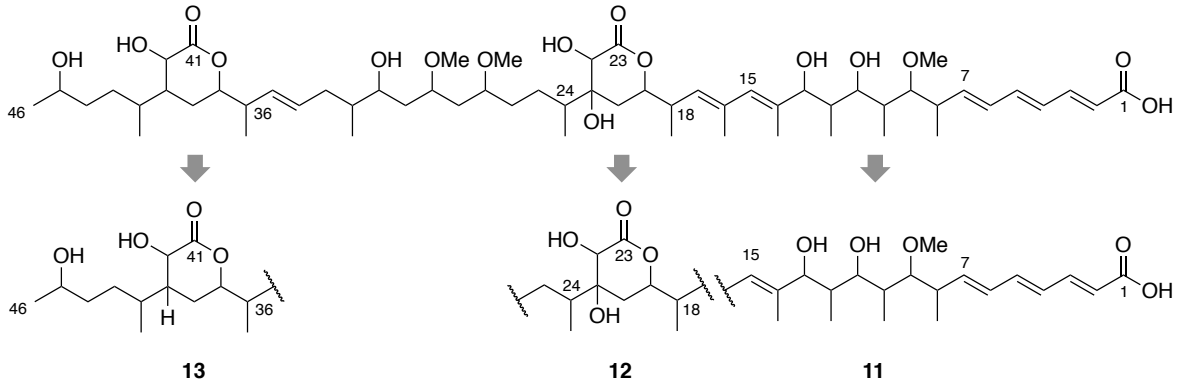

***Figure 10.** Major regions in hemicalide for focusing the initial stereochemical elucidation by Ardisson et al.*

2.2.1. *Assignment of the C1-C15 polypropionate stereohexad*

On initial examination of the ^{13}C NMR spectrum for hemicalide, Ardisson noticed that the chemical shift for the signal attributed to Me12 was unusually low (7.6 ppm). Comparisons with typical polyketide motifs pointed to Me12 as being part of a C10-C13 *syn-syn* stereotriad.[41] The same phenomenon was not observed for Me10, ruling out a *syn-syn* relationship for the substituents across C9-C11 and indicating that the stereotriad must likely to contain a *syn-anti*, *anti-syn* or an *anti-anti* configuration (**Figure 11a**). These two observations allowed Ardisson to reduce the number of diastereomers to consider from 32 down to six. Following the synthesis of all six candidate diastereomers and detailed spectroscopic comparisons with the natural product, Ardisson concluded diastereomer **11a** was the best match to hemicalide. During the course of this study, Ardisson noticed significant deviations in chemical shifts in the C1-C7 trienoic acid region of their fragments from hemicalide, though notably, the perturbations did not extend into the aliphatic region (C8 onwards). By deprotonating a model acid **14** to form **15,** Ardisson speculated that these deviations may be attributed to hemicalide being isolated as the carboxylate salt rather than the free acid (**Figure 11b**).

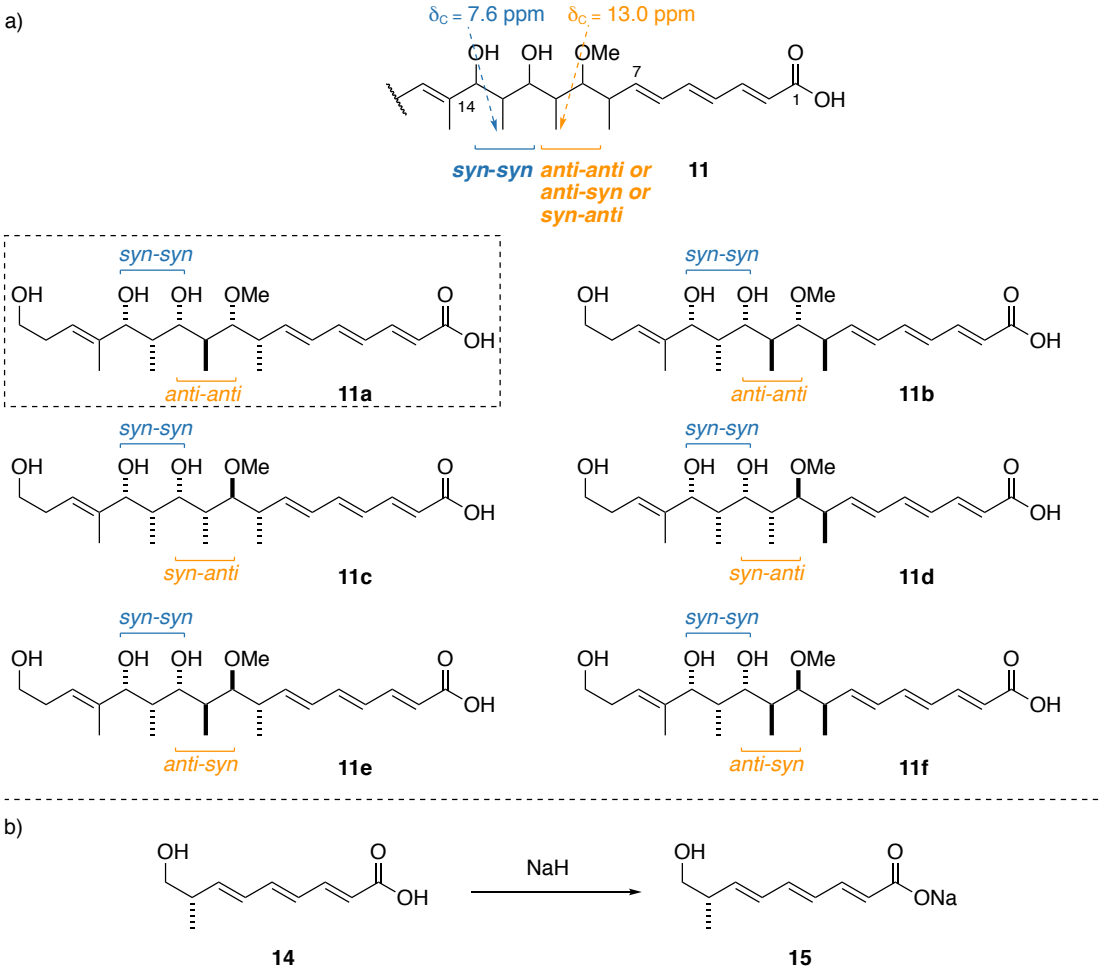

Figure 11. *a) Diagnostic spectroscopic data for the C1-C15 polypropionate region, leading to diastereomers **11a-f** analysed by Ardisson to determine **11a** as the most likely candidate structure. b) Synthesis of model carboxylate salt **15** by Ardisson to conclude that the C1 carboxyl group was likely to be deprotonated in hemicalide*

Using the DP4 Gauge-including atomic orbital (GIAO)-NMR shift prediction methodology, Smith and Goodman independently arrived at the same conclusion regarding relative stereochemistry of the stereohexad in the C1-C15 fragment.[14] The DP4 method allows the prediction of a compound's relative stereochemistry from a given set of diastereomers. This is achieved through *ab initio* calculations of ^{1}H and ^{13}C NMR chemical shifts for each candidate diastereomer. Comparing the differences between the theoretical shifts with the experimental data *via* the DP4 algorithm gives rise to an overall probability for the candidate diastereomer fitting the experimental NMR data. As enantiomers show identical chemical properties and thus, display identical NMR spectra, the DP4 method cannot be used to assign the absolute stereochemistry of a compound.[14]

2.2.2. Assignment of the C18-C24 dihydroxylactone

For the C18-C24 region, Ardisson narrowed down the set of possible diastereomers to four based on NOE and coupling constant analyses (**Figure 12a**).[42] Synthesis of all four diastereomers (**16a-d**) and comparing their NMR data to hemicalide led to the conclusion that the diastereomer **16c**, containing the 18,19-*anti* relationship, was the most likely candidate (**Figure 12b**). Interestingly, DP4 calculations performed in the Paterson group by MacGregor for the C18-C25 region identified diastereomer **17** (**Figure 12c**) as the most likely candidate (99%),[43] which contradicted Ardisson's assignment with its key 18,19-*syn* relationship. Ardisson's 18,19-*anti* assignment hinged upon a qualitative comparison of the H19 proton signal, reasoning that the 18,19-*anti* diastereomer, which exhibited a ddd multiplicity, was a closer match for the experimental hemicalide data compared to the 18,19-*syn* relationship. This was not considered to be conclusive by MacGregor given that the analogous H37 oxymethine proton appeared as a ddd in the C36-C42 fragment **18** (**Figure 12d**),[44] which exhibited a 36,37-*syn* relationship. Furthermore, Ardisson's synthesis of the C1-C25 fragment involved an intermediate **19**, which, despite the 18,19-*anti* relationship, exhibited a dt multiplicity for the H19 proton.[45]

A recent synthesis by the Paterson group of a model C16-C28 fragment **20**, with structural features more similar to the natural product than that synthesised by Ardisson, reinforced MacGregor's findings. The chemical shift, multiplicity and *J* values for the model C16-C28 fragment **20** proved to be a better match to the natural product, thus providing a more confident assignment of the relative stereochemistry in the C18-C25 dihydroxylactone fragment.[43]

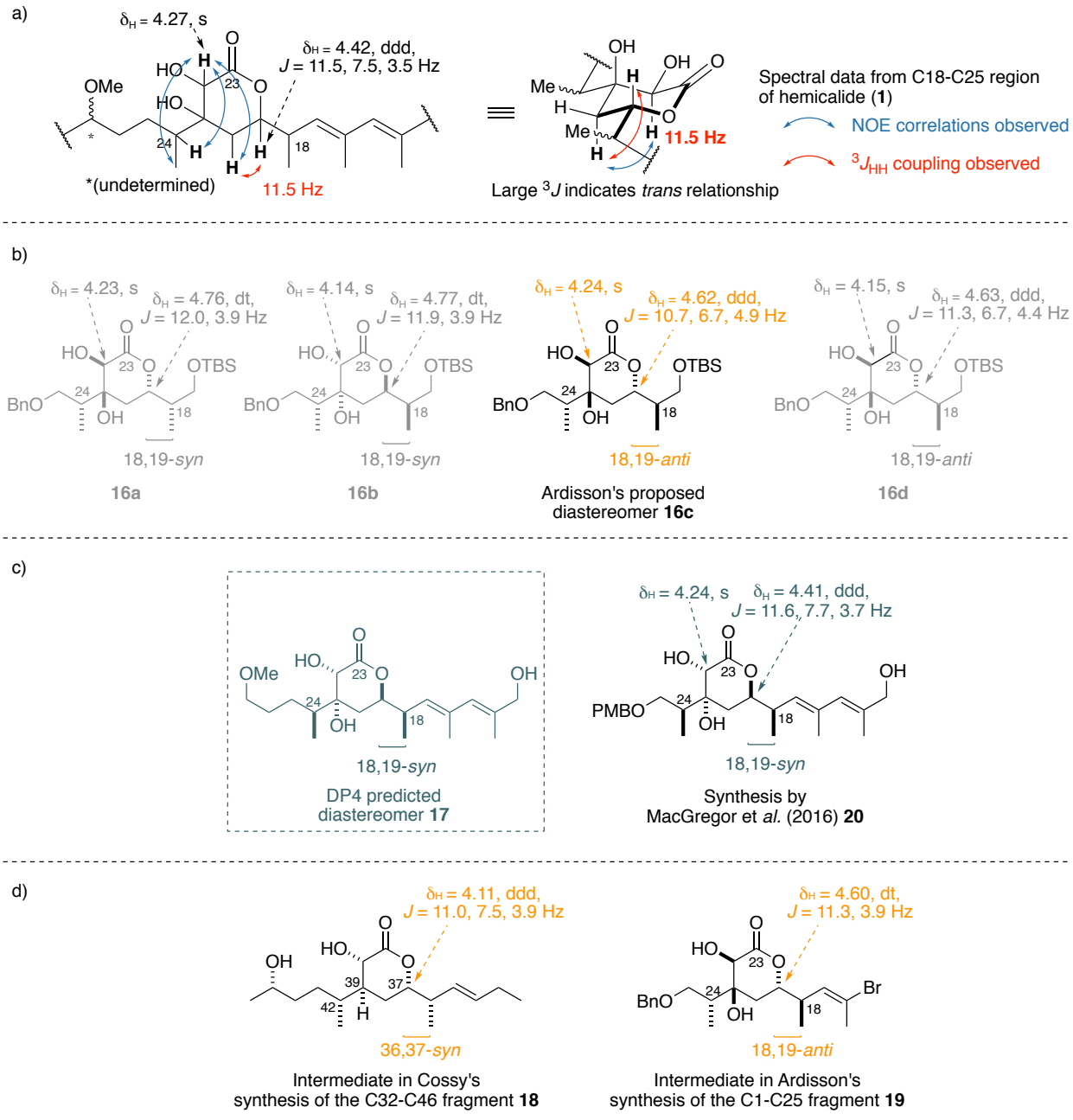

Figure 12. *a) Original spectroscopic data for the C18-C25 region, highlighting the relative chemical assignment of the δ-lactone b) Diastereomers analysed by Ardisson to determine* ***16c*** *as the most likely candidate structure c) DP4 predicted diastereomer* ***17*** *and model fragment* ***20*** *as synthesised by MacGregor et al. d) Late stage intermediates* ***18*** *and* ***19*** *that appeared to contradict Ardisson's original assignment*

2.2.3. *Assignment of the remainder of hemicalide: the C25-C46 region*

The C36-C46 hydroxylactone contains the final stereochemically dense fragment present in hemicalide. Analogous to the assignment of the C18-C25 dihydroxylactone, observation of key NOE correlations and coupling constants allowed Ardisson/Cossy to reduce the number of diastereomers to consider from 32 to eight (**Figure 13a**).[44] During the course of their study, it became apparent that the distal nature of the C45 carbinol stereocentre relative to the C36-C42 hydroxylactone meant that the two candidate C45 epimers could not be differentiated spectroscopically. By arbitrarily defining the C45 stereocentre, Ardisson/Cossy further reduced the number of candidate diastereomers to four, whereby spectroscopic comparisons with the natural product revealed **21a** to be the best match with hemicalide (**Figure 13b**). In parallel, DP4 calculations performed by MacGregor on a model C36-C46 fragment (**22**, **Figure 13c**) corroborated the relative configuration proposed by Ardisson/Cossy.[46]

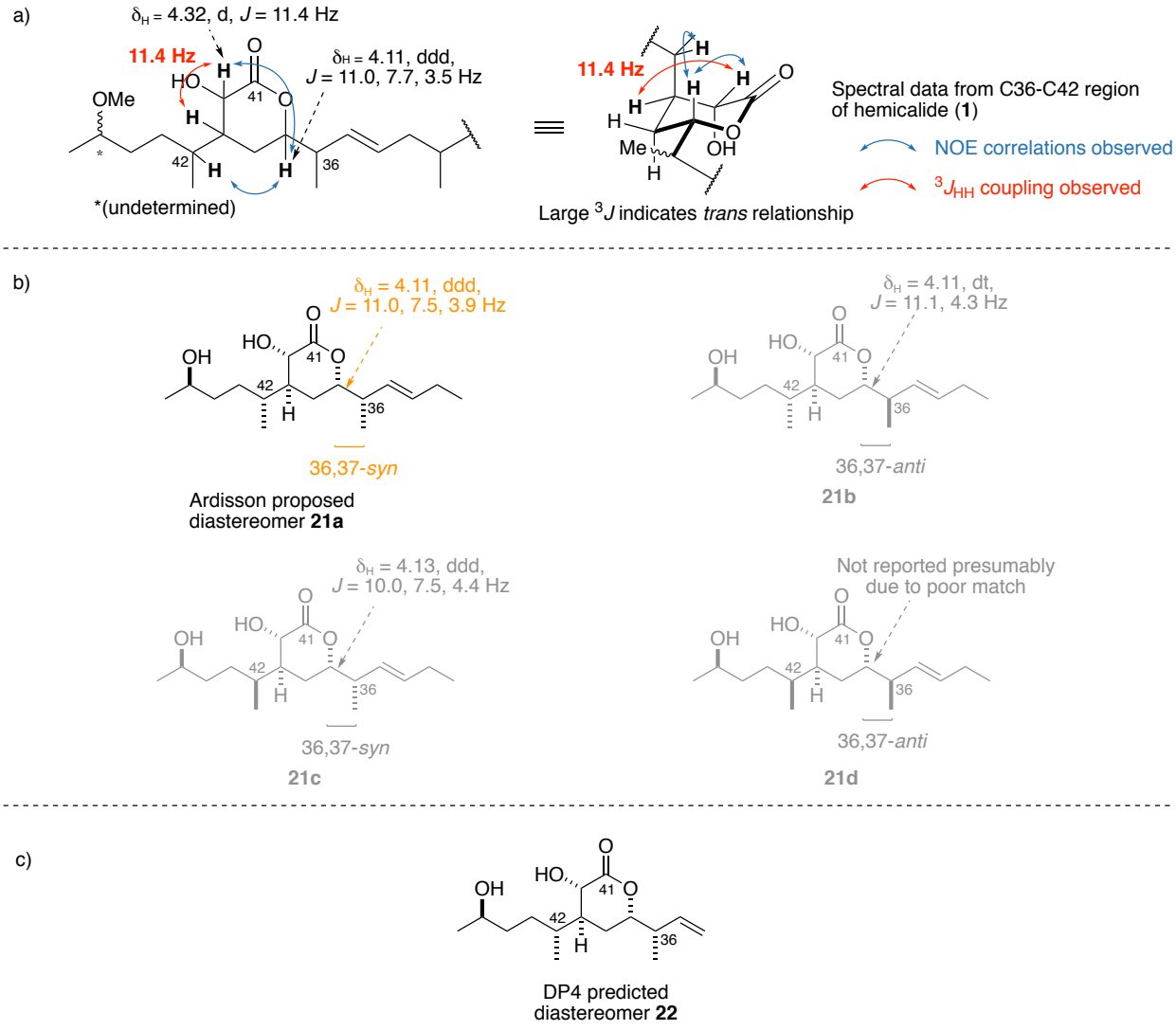

Figure 13. *a) Original spectroscopic data for the C36-C42 region, highlighting the relative chemical assignment of the δ-lactone b) Diastereomers analysed by Ardisson/Cossy to determine* ***21a*** *as the most likely candidate structure. c) DP4 predicted diastereomer* ***22*** *as conducted by MacGregor et al.*

At this stage, the relative configuration of 16 of the 21 stereocentres in hemicalide have been assigned, corroborated both by synthesis and computational studies. Aside from C45, which remains configurationally elusive despite attempts at synthetic verification, the four remaining unassigned stereocentres are contained within the C25-C34 polyacetate region. MacGregor attempted DP4 calculations to determine the most likely diastereomer for the C25-C34 region. However, the region's inherent flexibility led to multiple low energy conformations, which could not be further refined as the chemical shifts for the methylene protons in this region were obscured in a 22H multiplet in the ^{1}H NMR spectrum for hemicalide. These limitations meant that overall, no candidate C25-C34 diastereomers could be assigned with high confidence.[46]

Recently, Ardisson and Cossy reported the synthesis of a structure **23** corresponding to the full carbon skeleton of hemicalide, bearing the revised 18,19-*syn* configuration in the C18-C24 dihydroxylactone (**Figure 14**).[47] While the Ardisson and Cossy were unable to achieve a full deprotection in **23**, the large chemical shift deviations between **23** and hemicalide, in particular in the C28-C32 polyacetate region provided compelling evidence that the natural product is likely to not contain the published configuration. In particular, the large ^{13}C chemical shift deviations (>1.0 ppm) recorded for C26, C28, Me32 and C33 is a diagnostic indication that hemicalide probably possesses the opposite relative configuration, namely 27,29-*anti* and 31,32-*syn*, to the structure published by Ardisson and Cossy.

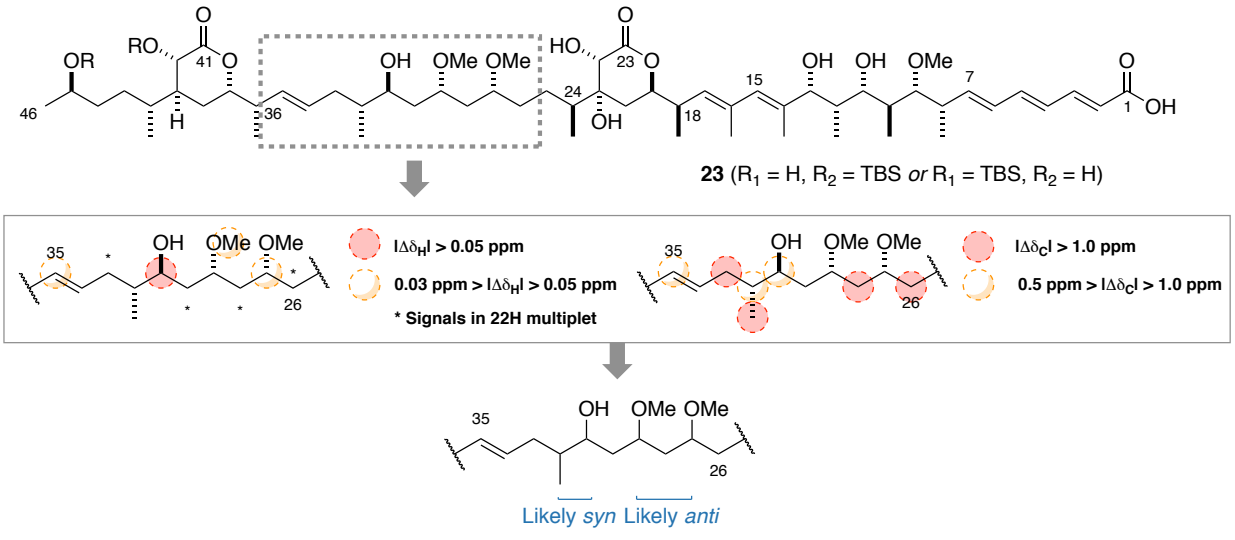

Figure 14. *Structure of* ***23*** *as synthesised by Ardisson and Cossy, highlighting the C26-C36 polyacetate region and the large chemical shift deviations compared with hemicalide*

2.2.4. Relative configuration between the C1-C15 and C16-C25 region

With the relative configuration established within the three regions, the next unanswered question was the diastereomeric relationship between each stereocluster. Initial forays into this were undertaken by the Ardisson and Cossy groups, who first reported a synthesis of the C1-C27 truncate **24** featuring the incorrect 18,19-*anti* configuration in the dihydroxylactone fragment.[45] After MacGregor's reassignment, the Ardisson and Cossy groups revised their synthesis of their C1-C27 fragment to contain the updated 18,19-*syn* configuration in **25**,[48] and incorporated this updated configuration in their synthesis of the full carbon skeleton **23.**[47] Analysis of the NMR deviations between truncates **24, 25** (containing the revised 18,19-*syn* configuration) and **23** pleasingly affirmed our reassignment, with compounds **23** and **25** bearing the revised stereochemistry resulting a far closer fit to the spectroscopic data for hemicalide (**23**: ($\Sigma|\Delta\delta_H|$ = 0.20 ppm; $\Sigma|\Delta\delta_C|$ = 4.3 ppm**; 25**: $\Sigma|\Delta\delta_H|$ = 0.26 ppm; $\Sigma|\Delta\delta_C|$ = 3.8 ppm)* compared with truncate **24** ($\Sigma|\Delta\delta_H|$ = 0.76 ppm; $\Sigma|\Delta\delta_C|$ = 10.9 ppm) (**Figure 15**).

In the three aforementioned cases (**23, 24** and **25**), the Ardisson and Cossy groups targeted the synthesis of the C1-C27 truncate containing a 13,18-*anti* relationship between the two fragments; one of the two possible permutations present in hemicalide. Considering that both fragments represent over half of the carbon skeleton of the natural product, the comparatively large total ^{1}H and ^{13}C deviations seen in **23** ($|\Sigma\Delta\delta_H|$ = 0.20 ppm; $\Sigma|\Delta\delta_C|$ = 4.3 ppm) and **25 (**$\Sigma|\Delta\delta_H|$ = 0.26 ppm; $\Sigma|\Delta\delta_C|$ = 3.8 ppm) and and the absence of the alternative 13,18-*syn* diastereomer for comparison led us to suspect that the reported 13,18-*anti* configuration may have been erroneously assigned for hemicalide (**Figure 16**).

* Comparisons were made between H/C8 to H/C24 owing to the variability in the C1-C7 trienoic region due to the protonation state of C1, and the lack of structural homology beyond H/C24

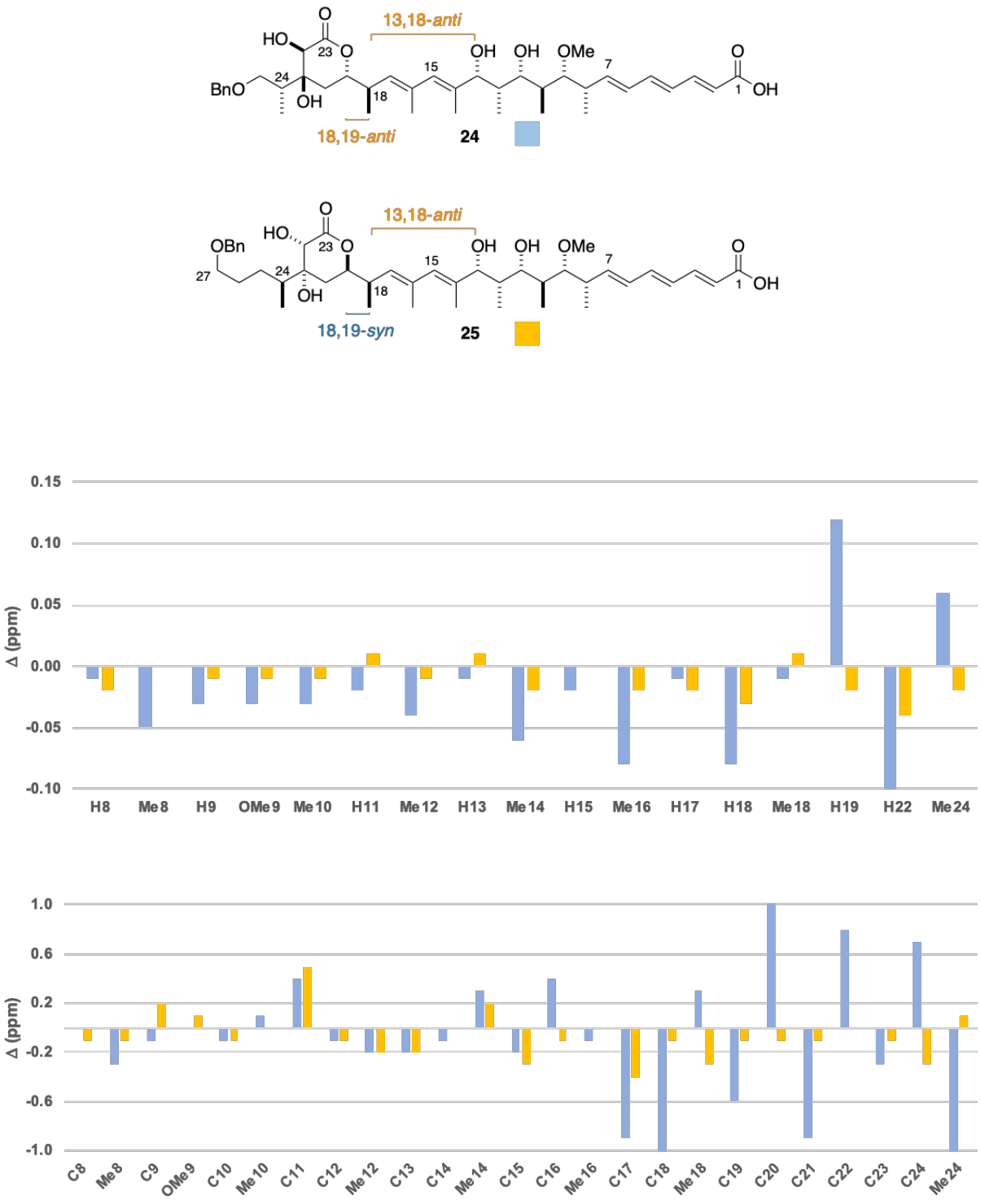

Figure 15. *Bar graphs showing the ^{1}H (top) and ^{13}C (bottom) chemical shift difference between truncate* ***24*** *(blue), truncate* ***25*** *(orange) and hemicalide, highlighting the improved correlations after reassigning to the 18,19-syn configuration*

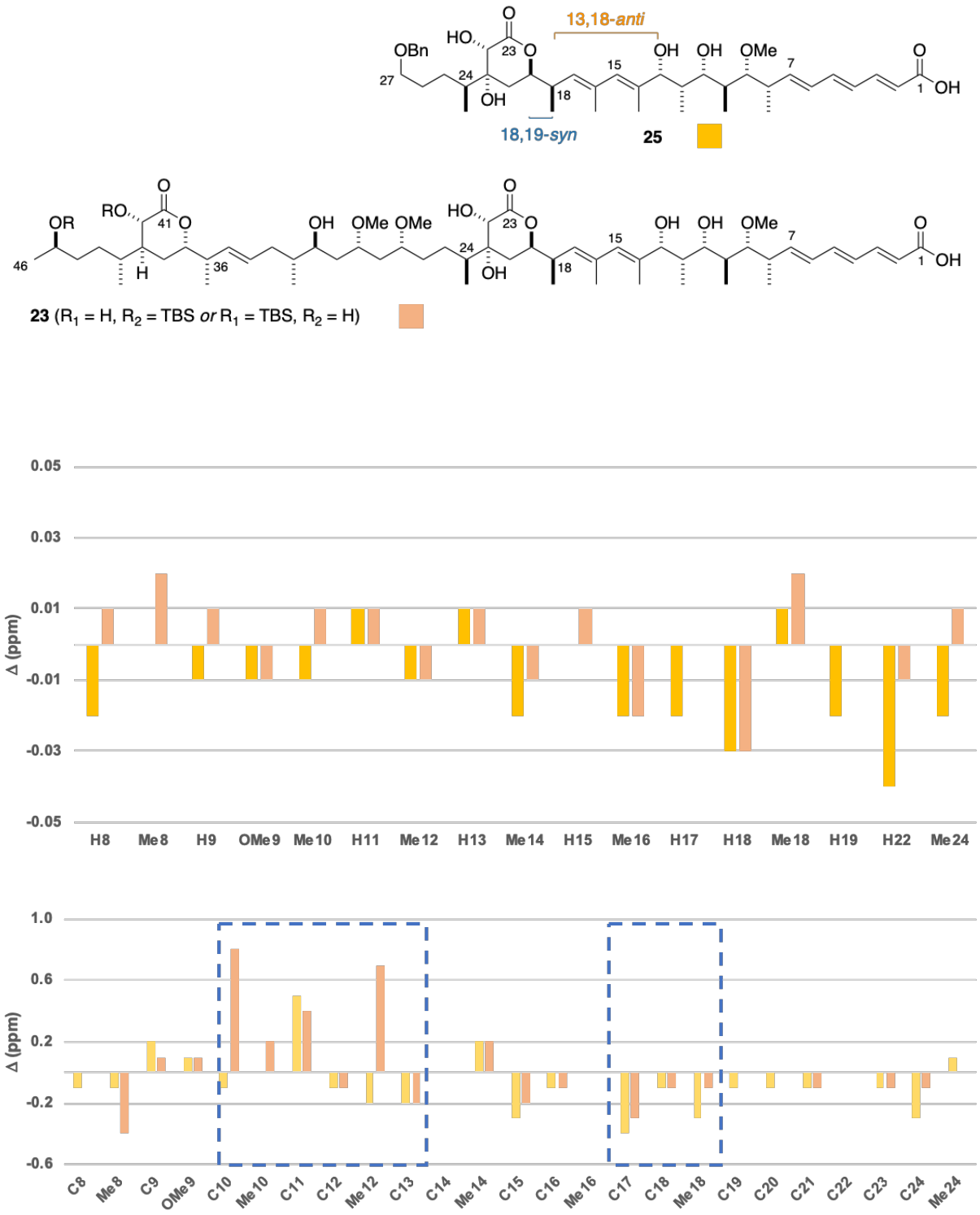

Figure 16. *Bar graphs showing the ^{1}H (top) and ^{13}C (bottom) chemical shift difference between truncate **25**, **23** and hemicalide, highlighting the large deviations (in **blue**) that are especially noticeable in the ^{13}C NMR shift comparisons*

2.3. Previous synthetic work towards hemicalide

As highlighted in section **2.2**, to date, two research groups have reported ongoing synthetic efforts towards the total synthesis of hemicalide, namely the Ardisson/Cossy groups working in collaboration, and the Paterson group. This section will outline the major synthetic routes each group has achieved towards the synthesis of key fragments.

2.3.1. Synthesis of the C1-C15 region

The C1-C15 region can be further divided into two subregions, the C1-C7 trienoic acid fragment and the C8-C15 polypropionate stereohexad. Both the Ardisson and Paterson groups approached this fragment by disconnecting across C6-C7 *via* an HWE olefination to deliver the 6*E* olefin geometry (**Scheme 1a**). This reveals a C1-C6 phosphonate and the C7-C15 aldehyde. The dense oxygenation as typified in polyketides within the C7-C15 fragment can be readily constructed *via* a series of highly diastereoselective aldol/reduction sequences, which retrosynthetically reveals Roche ester **26** and oxazolidinone **27** as the chiral building blocks for this fragment.

Ardisson's synthesis of the C1-C15 polypropionate region commenced from (*S*)-Roche ester (*S*)-**26,** which was derivatised into aldehyde **27** following a three-step sequence involving TBS protection, DIBAL reduction and Swern oxidation (**Scheme 1b**). At this point, a diastereoselective Paterson boron-mediated aldol reaction[49] with lactate-derived ketone **28** and aldehyde **27** gave **29**, where the newly formed hydroxyl centre was methylated. Reduction of the ketone and the benzoyl ester with $LiBH_4$, followed by an oxidative cleavage of the intermediate diol reveals aldehyde **30**, which engaged in an Evans' aldol reaction[50] with oxazolidinone **27** to afford the 1,2-*syn* adduct diastereoselectively. The oxazolidinone auxiliary was transformed to Weinreb amide **31**, and the free hydroxyl group transiently protected as the TMS ether in **32** to allow for the addition of the lithiated species derived from **33** into Weinreb amide **32** to give ketone **34**. The final stereocentre in this fragment was set by a 1,3-*syn* reduction mediated by $Zn(BH_4)_2$, following the deprotection of the TMS ether in **34** on treatment with Amberlyst-15 resin. The resulting diol was protected as the cyclic siloxane, the vinyl silane treated with NIS to effect a Si/I exchange and the terminal TBS ether cleaved to reveal the C7 alcohol **35.** Dess-Martin oxidation of alcohol **35** afforded aldehyde **36**, which could undergo an HWE olefination with phosphonate **37** to furnish the full C1-C15 fragment **38**. The Ardisson synthesis of the C1-C15 fragment proceeds in 19 steps in the longest linear sequence from (*S*)-**26**, with 17.5% overall yield.

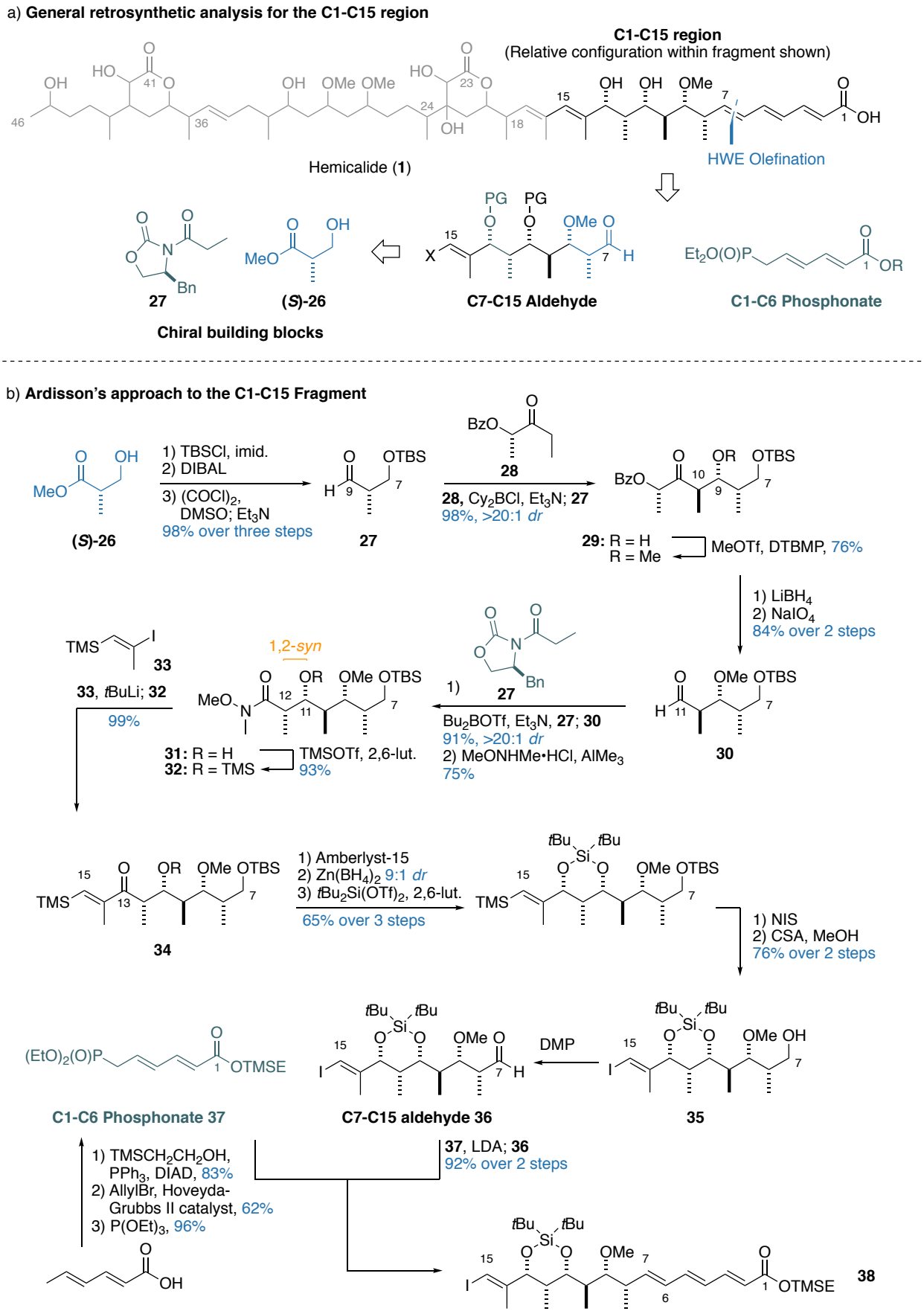

Scheme 1. *a) General retrosynthesis of the C1-C15 fragment. b) Ardisson's synthesis of the C1-C15 fragment* ***38****.*

DTBMP = di-tert-butyl-4-methylpyridine

Analogously, the Paterson approach to the C1-C15 fragment **39** commenced with an Evans' aldol reaction between oxazolidinone ***ent*-27** and aldehyde **40**, itself obtained in four steps from diethyl methylmalonate *via* ester **41** (**Scheme 2**).[51] Subsequent TES protection of aldol adduct **42** and reductive auxiliary cleavage revealed aldehyde **43**, which engaged with (*S*)-Roche ester derived ketone **44** in a boron-mediated aldol reaction with excellent diastereoselectivity (>20:1 *dr*). The aldol adduct was protected as the TES ether and followed by a diastereoselective reduction with DIBAL to afford the 1,3-*syn* product **45**. Methylation to give **46** followed by PMB deprotection, subsequent oxidation and HWE olefination with phosphonate **47** gave the full C1-C15 carbon skeleton **39**. Overall, the Paterson synthesis of the C1-C15 fragment proceeded in 11 steps in the longest linear sequence from aldehyde **40**, in 11% overall yield. Notably, all of the key stereoinducing processes in the Paterson synthesis were highly selective; generating a single diastereomer in all instances. As the synthesis is diastereoselective from ***ent*-27** and **(*S*)-44** as its chiral sources, the enantiomer can be readily accessed, and the synthesis is scalable to generate gram-scale quantities of intermediate **46**.

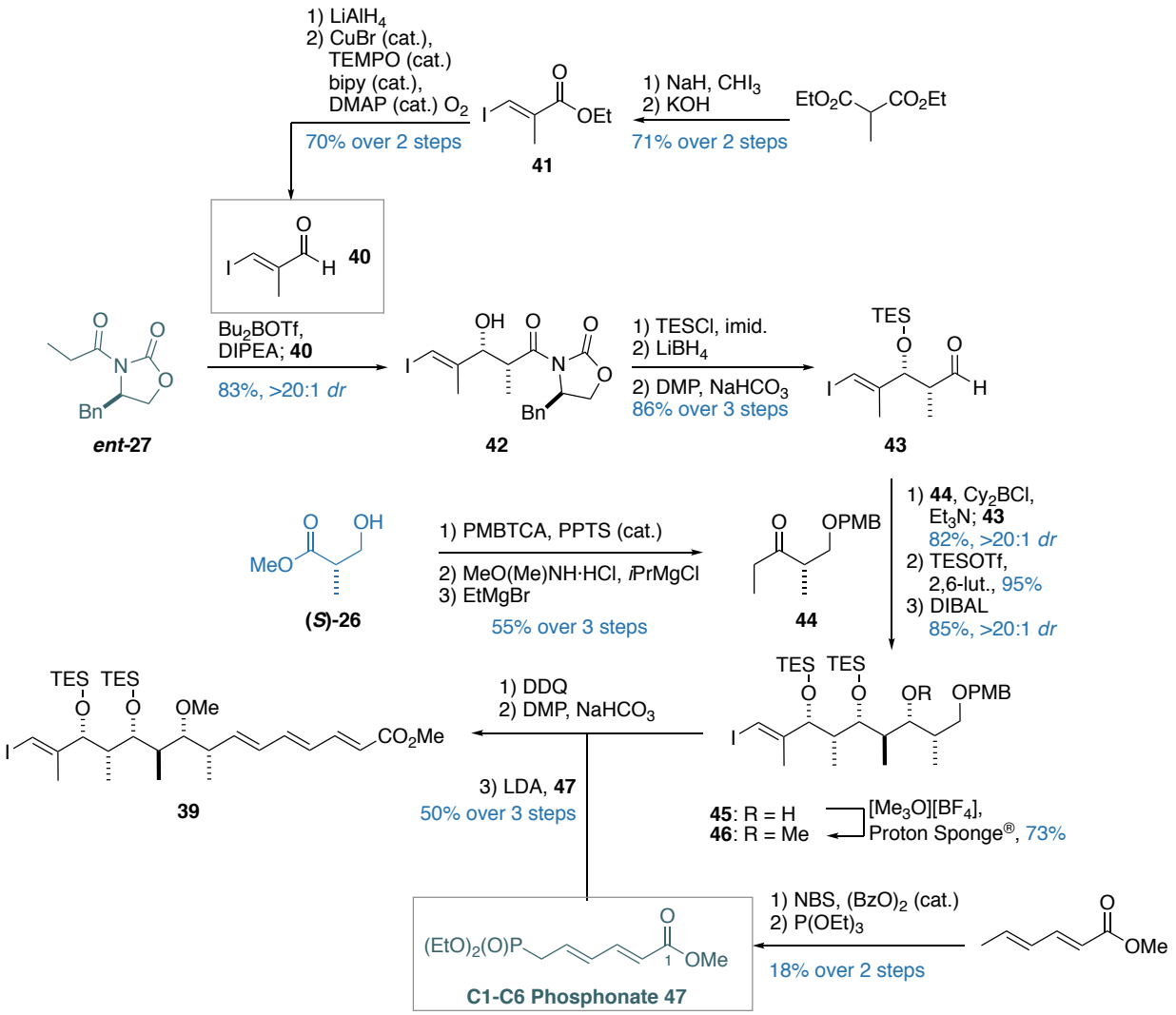

Scheme 2. *The Paterson synthesis of the C1-C15 fragment* ***39****. Bipy = 2,2'-bipyridine*

2.3.2. Synthesis of the revised C16-C25 region

Alongside the C1-C15 fragment, both the Ardisson/Cossy groups, as well as the Paterson group have reported on the synthesis of the C16-C25 region. A key feature in the C16-C25 dihydroxylactone fragment is the 21,22-*syn* diol motif, which can be generated from a substrate-controlled dihydroxylation of a cyclic enoate intermediate. At this point, the 1,4-*syn* relationship between Me24 and OH19 allows for a substrate-controlled addition of a suitable carbon nucleophile into a chiral aldehyde. These features are highlighted in the general retrosynthesis shown in **Scheme 3a**.

To experimentally validate the DP4 predicted structure bearing the 18,19-*syn* relationship, the Paterson group disclosed a synthesis of the C16-C25 region commencing with a diastereoselective Ipc-boron-mediated aldol reaction between ketone **48** and aldehyde **49** (**Scheme 3b**), both of which derived from the same enantiomer of Roche ester (*S*)-**26**. From the aldol adduct **50**, a four-step sequence involving TBS protection, enolate addition, silyl deprotection and dehydration gave the key cyclic enoate intermediate **51**. MacGregor *et al.* found that the pivotal dihydroxylation step to yield diol **52** could not be allowed to proceed to completion owing to competing oxidation at the C16 vinyl iodide. Following a *bis*-TES protection, PMB deprotection and Dess-Martin oxidation, the fragment could then be elaborated *via* an HWE olefination and conjugate reduction to afford the C16-C28 fragment **53**. For NMR comparisons, MacGregor intercepted intermediate **52** and subjected that to a Stille coupling with stannane **54** to give triol **20**. This was used to confirm that the revised C16-C25 dihydroxylactone with the 18,19-*syn* relationship was indeed a closer match to the natural product by detailed NMR comparison than that reported by the Ardisson/Cossy groups.

During the dihydroxylation step, MacGregor attributed the competing oxidation of the C16 vinyl iodide to the electronic similarity between the enoate olefin and the vinyl iodide. This was identified as a potential bottleneck, and as such, a second approach by intercepting the electronically deactivated vinyl dibromide **55** as an intermediate was investigated by Thompson (**Scheme 3c**).[52] While the planned dihydroxylation step was able to proceed to completion without observing any unwanted oxidation at the vinyl dibromide, this synthesis suffered from the intractability of aldehyde derived from PMB ether **55**, with Thompson noting that it was highly prone to degradation, as well as the poor efficiency of the *trans*-selective Stille cross coupling, proceeding in an unoptimised 16% yield from intermediate **56**. The shortcomings Thompson observed in this revised route did not appear to outweigh the singular weakness of the original route, and thus the earlier route to the C16-C25 dihydroxylactone was preserved.

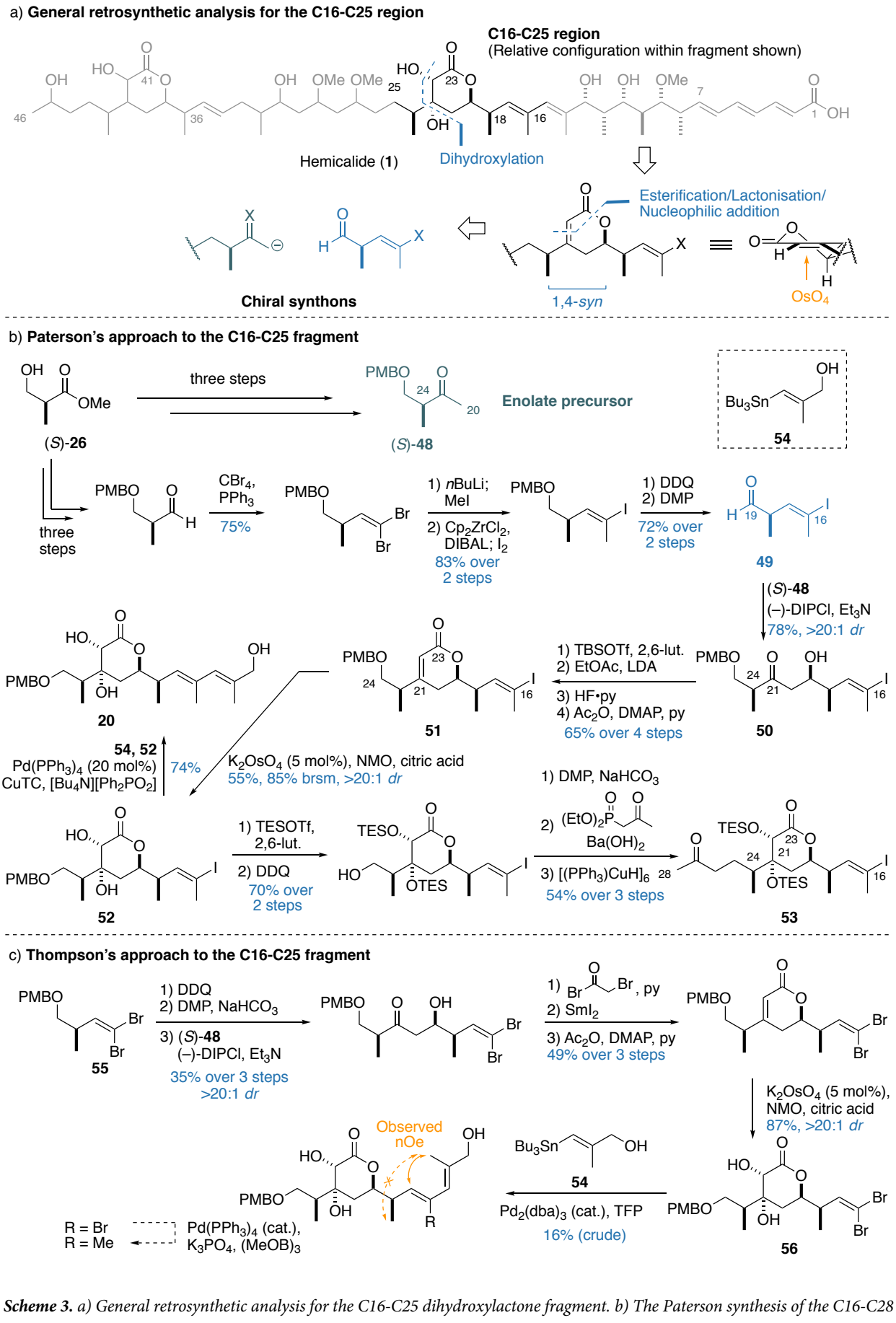

Scheme 3. *a) General retrosynthetic analysis for the C16-C25 dihydroxylactone fragment. b) The Paterson synthesis of the C16-C28 fragment* ***53****. c) Thompson's approach to the C16-C25 fragment via vinyl dibromide* ***55****. TFP = tri(2-furyl)phosphine*

Following the disclosure of our group's reassignment and synthesis, the Ardisson/Cossy group reported two routes to the reassigned C16-C25 region. The first iteration commenced with a Dias allylation[53] of allylsilane **57** and the analogous bromoaldehyde **58** (both derived from (*S*)-Roche ester (*S*)-**26**) to give alcohol **59** (9:1 *dr*) (**Scheme 4**). Subsequent ozonolysis of the C21 olefin followed by acetylation gave ester **60**, which underwent an intramolecular Reformatsky reaction (SmI_2), elimination and dihydroxylation sequence to configure all the stereocentres present in the C16-C25 lactone (**61**).

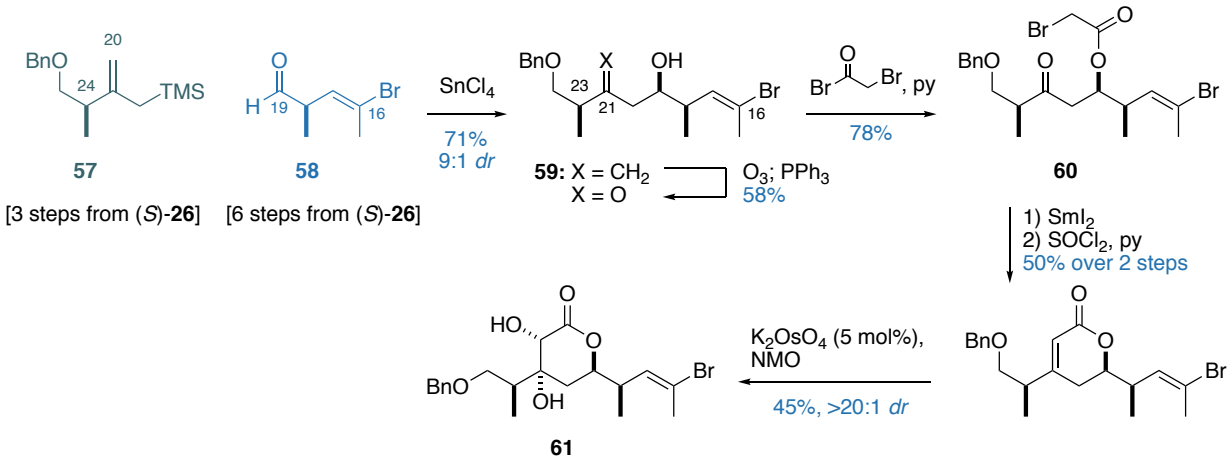

Scheme 4. *Ardisson/Cossy's synthesis of the C16-C25 fragment* ***61***

Subsequent to this initial sequence, Cossy disclosed an alternative ring-closing metathesis (RCM) route towards the synthesis of the dihydroxylactone fragment that obviates the need for the ozonolysis of the C21 olefin as well as the subsequent elimination step to reform the cyclic enoate system. Synthesis of the allylation precursor proceeded in eight steps from (*S*)-citronellol **62**. The sequence began with a silyl protection, ozonolysis followed by a reduction to afford alcohol **63**. The C27 alcohol was benzyl protected, and the primary TES ether subjected to Swern conditions, resulting in the concomitant desilylation and oxidation of the TES ether to the aldehyde. This intermediate was then α-methylenated under Mannich conditions to afford intermediate **64** (**Scheme 5**). To transform this to the allylation precursor, a reduction followed by esterification installed the allylic ester **65**, whereby a Tsuji-Trost-like displacement of the allylic ester *via* an *in situ* generated $Bu_3SnAlEt_2$ reagent under Pd catalysis installed the stannane handle in **66**. Subsequent allylation was effected under Williams' conditions to give the adduct **67** in 7.3:1 *dr*. Subsequently, the acrylate ester was installed on C19 to give **68**, where the use of Nolan's metathesis catalyst facilitated the required ring closure to form enoate **69**. Employing the improved dihydroxylation conditions reported in the Paterson synthesis allowed the facile conversion to the dihydroxylactone fragment, which was *bis*-TES protected to afford the C16-C27 fragment of hemicalide **70**.

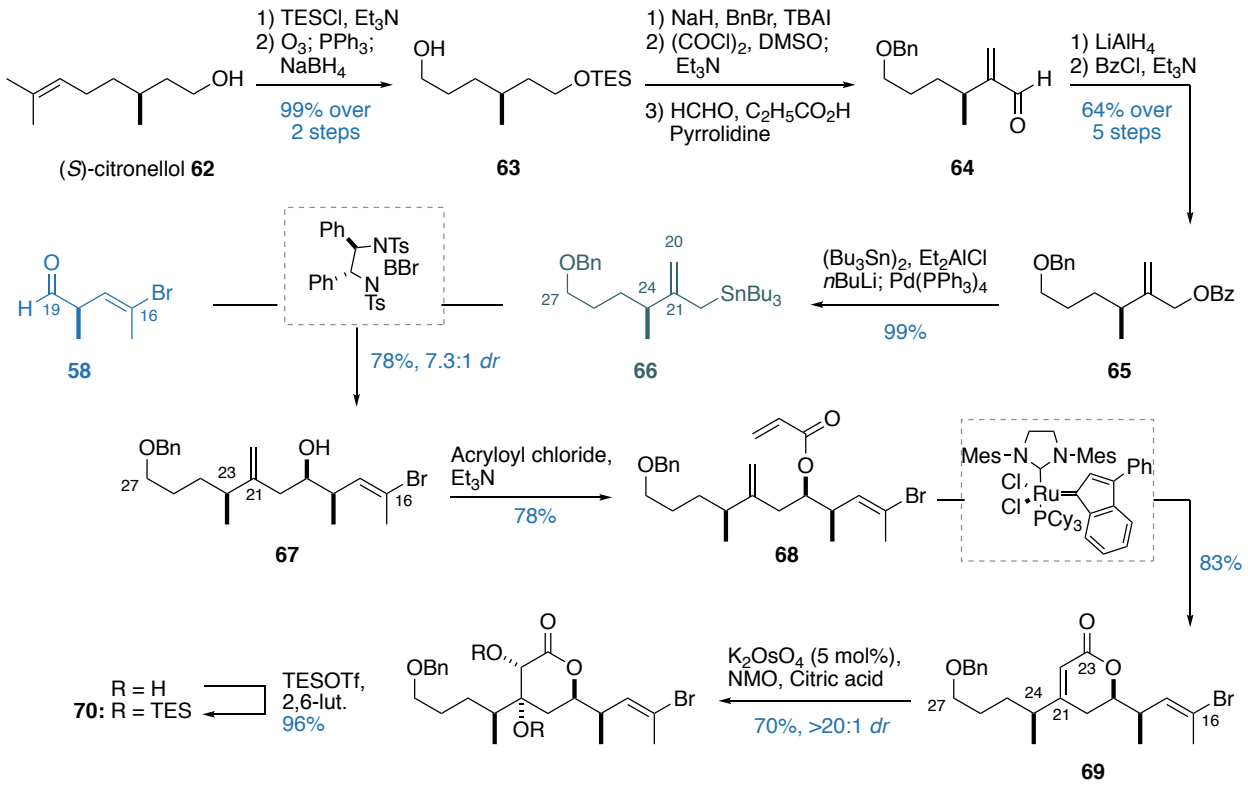

Scheme 5. *Ardisson/Cossy's second synthesis of the C16-C27 fragment* ***70*** *via an RCM approach*

2.3.3. Synthesis of the C35-C46 region

The C34-C46 hydroxylactone fragment is structurally homologous to the C16-C25 dihydroxylactone except for three aspects, namely the absence of an olefinic methyl substitution at C34, the lack of oxygenation at C39, as well as the all *syn*-configuration across the C36-C42 stereocentres.

Alongside the report on the stereochemical assignment of the C34-C46 region, the Cossy group disclosed an 11-step synthesis of the C35-C46 region, where the major disconnection involves a diastereoselective Rh-catalysed conjugate addition of the 'ate'-complex derived from boronate **71** into cyclic enoate **72** (**Scheme 6**). The synthesis of cyclic enoate **72** commenced with (*S*)-Roche ester (*S*)-**26**. A four-step sequence involving PMB protection, transformation to the corresponding Weinreb amide, reduction and allylation using the Duthaler allyltitanium reagent provided alcohol **73**, which after esterification and an RCM afforded the cyclic enoate **72**. Synthesis of the boronate partner **71** commenced with the TBS ether **74**, where cross metathesis with alkene **75** gave vinyl boronate **71** in a 5.7:1 ratio of *Z*/*E* isomers favouring the desired geometry. The required Rh-catalysed conjugate addition was achieved with moderate diastereoselection (4.9:1 *dr*) to give the full C35-C46 skeleton **76**. Next, an α-oxidation mediated by Davis oxaziridine installed the C40 stereocentre in **77** with excellent diastereoselectivity (>20:1 *dr*). The final C42 stereocentre was set by a hydroxyl-directed hydrogenation catalysed by Crabtree's catalyst of the trisubstituted olefin with modest selectivity (1:1.7 *dr*), delivering the desired configuration **78** as the minor diastereomer.

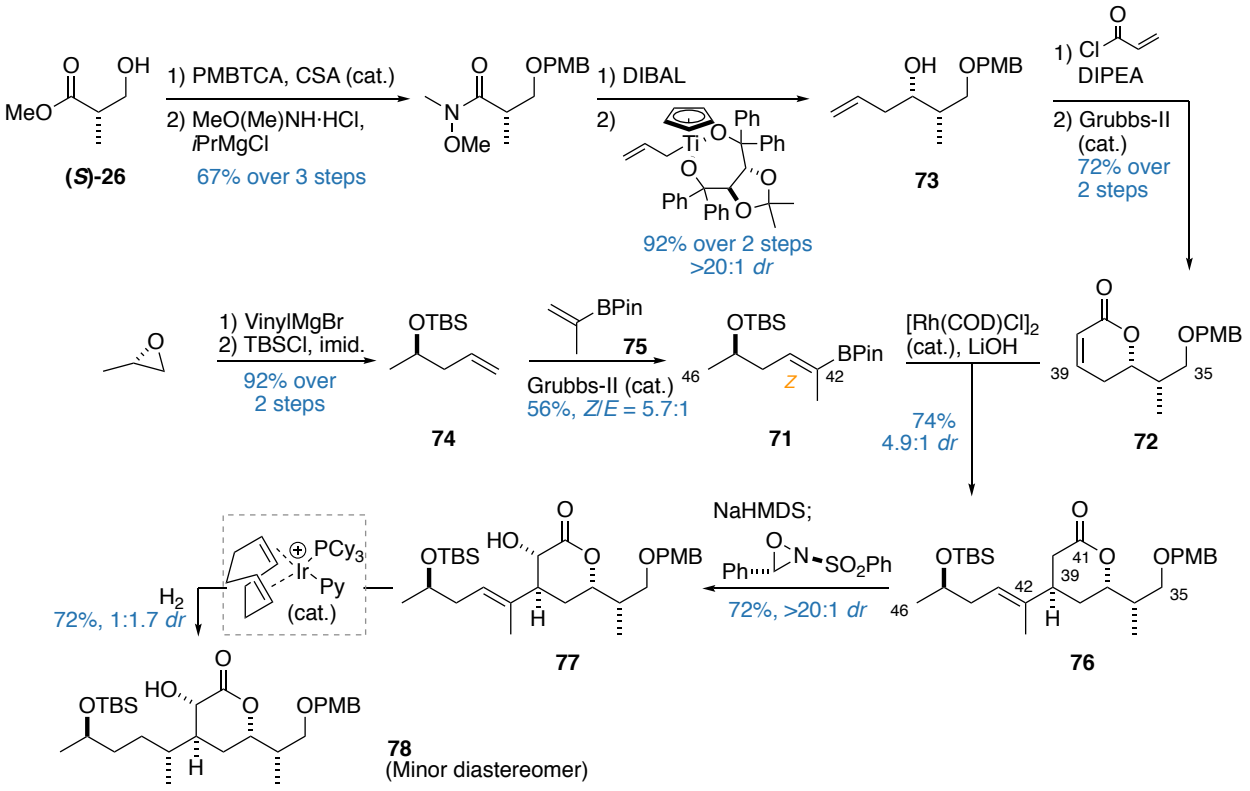

Scheme 6. *Cossy's synthesis of the C35-C46 fragment* ***78****. COD = cyclooctadiene*

While the poor selectivity of the olefin reduction was useful for the flexible generation of diastereomeric candidates in a 'diversity-oriented' manner, the confident assignment of this region now necessitates a focused 'target-oriented' approach. Recognising the structural homology between the C16-C25 dihydroxylactone with the C35-C46 fragment, the as-yet unreported Paterson synthesis conducted by Stockdale utilises methodology from the previously reported synthesis of the C16-C25 dihydroxylactone to allow the use of common starting materials (**Scheme 7**). An analogous Ipc-boron-mediated aldol reaction between aldehyde **79** and ketone (*R*)-**48**, both synthesised in three-steps from (*S*)-**26** and (*R*)-**26** respectively, gave adduct **80** diastereoselectively (>20:1 *dr*). Protection as the TBS ether followed by the addition of the lithium enolate derived from ester **81** enabled an *in situ* Peterson olefination that afforded enoate **82** primarily as a single geometric isomer. At this point, TBS deprotection enabled a hydroxyl-directed hydrogenation of the enoate olefin, catalysed by Crabtree's catalyst, to install the C39 stereocentre with useful selectivity (*ca.* 4:1 *dr*), which can be lactonised under acidic conditions to give lactone **83**. An α-oxidation mediated by Davis oxaziridine followed by silyl protection and PMB deprotection reveals the free alcohol **84**, which after oxidation could be homologated *via* an HWE olefination. At this point, a CBS reduction can selectively install the C45 stereocentre, and the olefin and benzyl groups could be reduced through hydrogenation to afford the C35-C46 fragment **85**.

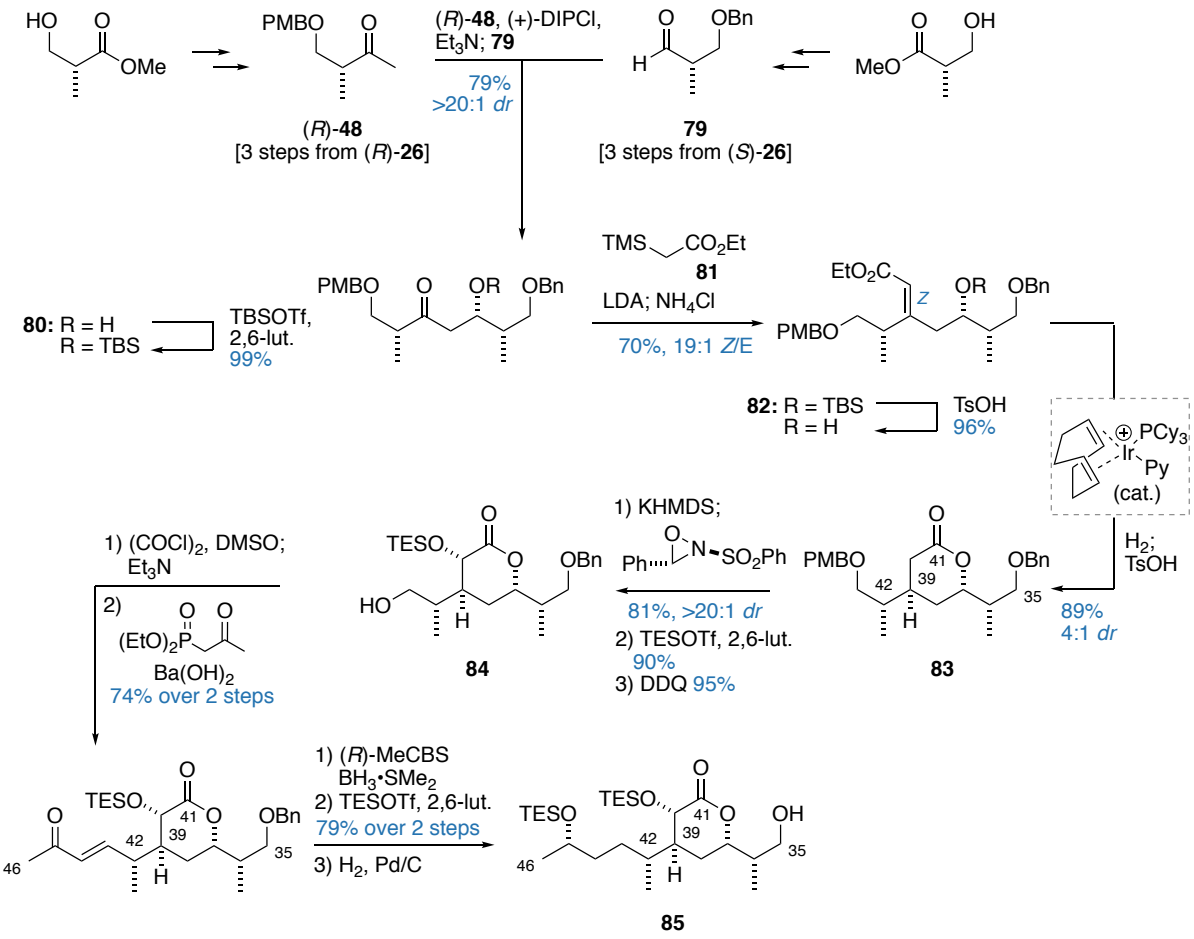

Scheme 7. *The Paterson synthesis of the C35-C46 fragment* ***85****, as currently conducted by Stockdale*

2.3.4. *Fragment union studies: Ardisson/Cossy's synthesis of the full carbon skeleton of hemicalide*

With the major fragments synthesised and reported by the Ardisson and Cossy groups, the next synthetic goal is to realise a suitable fragment coupling strategy to construct the complete carbon backbone of hemicalide. Concurrent with the Paterson group's ongoing campaign, the Ardisson/Cossy groups have recently reported a synthesis of the carbon backbone of hemicalide,[47] details of which are outlined below.

Ardisson/Cossy proposed to disconnect hemicalide across C15-C16 *via* a Suzuki coupling, C27-C28 *via* an aldol reaction and the C34 olefin *via* a Julia-Kocienski olefination (**Scheme 8**). Retrosynthetically, this reveals the C1-C15 fragment **38**, the C16-C27 fragment **86** and the C35-C46 fragment **87**, where details of the synthetic route have been previously discussed. Additionally, the retrosynthetic analysis reveals the previously undisclosed C28-C34 ketosulfone unit **88** bearing the two of the five undefined stereocentres proposed to bridge the C16-C27 and the C35-C46 fragments together.

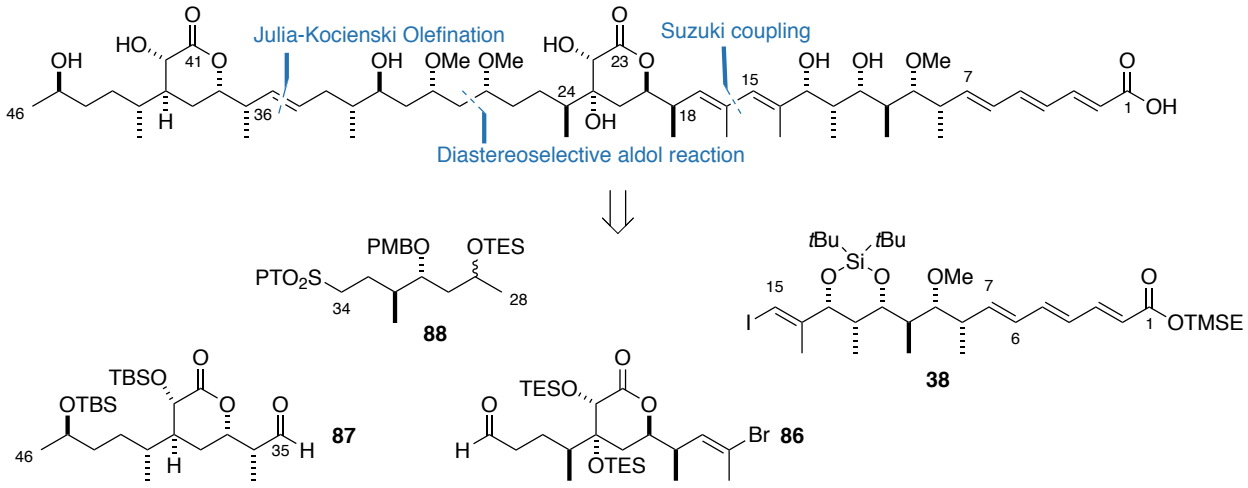

Scheme 8. *The Ardisson/Cossy approach to hemicalide, revealing four major fragments*

Synthesis of the C28-C34 ketosulfone commenced with a Duthaler-type crotylation of aldehyde **89** to give alcohol **90** diastereoselectively (**Scheme 9**). Subsequent protection of C31 as the PMB ether followed by a 9-BBN-mediated hydroboration/oxidation sequence installs the C34 alcohol in **91**, which can be displaced in a Mitsunobu manner to afford sulfide **92**. At this point, Ardisson/Cossy curiously reports a silyl protecting group switch, deprotecting the C29 TBS ether under fluorous conditions and reinstalling a TES ether. Following this sequence, an *m*CPBA-mediated oxidation of the intermediate sulfide generates the sulfone coupling partner **93** in anticipation of the planned olefination reaction.

The required aldehyde functionality on the C35-C46 fragment was attained by a three-step sequence from intermediate **78** (synthesis described in **2.3.3**). Subjecting aldehyde **94** and sulfone **93** under Julia-Kocienski olefination conditions delivered the C28-C46 fragment **95** in a moderate yield but with excellent geometric control. At this point, a selective C29 desilylation under fluorous conditions, followed by oxidation delivers

the C29 ketone **96**. This was subjected to a boron-mediated aldol reaction with the C16-C27 aldehyde **97** (synthesised in two steps from the reported intermediate **70**). While in this instance the diasteroselection of the aldol addition was not reported, in a previous communication, it was indicated that the 1,5-*anti* adduct proceeded in moderate stereocontrol (*ca.* 4:1 *dr*).[48] In this account, the intermediate boron aldolate intermediate was not isolated and immediately subjected to a $LiBH_4$-mediated reduction to deliver the 29,31-*syn* diol diastereoselectively. After a *bis*-methylation to give **98**, Ardisson/Cossy reported a two-step protecting group switch at C31 from a PMB to a TES ether. While the electron-rich PMB ether is better able to promote the remote 1,5-stereocontrol during the aldol step,[54] presumably this switch was conducted to streamline the eventual global deprotection. At this point, intermediate **99** bearing the C16-C46 fragment was transformed to the requisite boronate in **100**, in anticipation of the planned Suzuki coupling with the full C1-C15 truncate **38**.

While Ardisson/Cossy have previously employed a Suzuki coupling for the synthesis of their C1-C27 truncate, *via* the boronate derivative of the C16-C27 fragment **61**,[45,48] this two-step sequence (C16 borylation followed by cross-coupling) was poor yielding (13% over two steps), which the authors attributed to the inefficiency of the borylation step. Attempts at conducting a global deprotection was carried out using a two-step procedure (TASF; HF·py), but the authors were unable to remove the TBS protecting group at either C40 or C45. As discussed in section **2.2.4**, the large NMR shift deviations, alongside with the lack of a suitable alternative model for comparison led us to suspect that this published structure, in particular between the C1-C15 and the C16-C25 regions, as well as the C27-C32 polyacetate region, did not reflect the true stereochemical nature of hemicalide.

At this point, it is worth noting that the lack of further experimental and spectroscopic data from the isolation group means that a synthesis-based stereochemical elucidation of hemicalide is the only method to conclusively ascertain its overall configuration. Towards this end goal, the key weakness in the strategy presented is the reliance of the pre-installed C31 stereocentre to singularly configure the C27 stereocentre (*via* a 1,5-*anti* aldol). The diastereoselective nature of this transformation means that it is far more challenging to install the alternative, but equally probable 27,31-*syn* configuration. Therefore, our approach needed to pay particular attention in developing a flexible strategy in configuring all as-yet unknown stereocentres in an efficient and predictable manner.

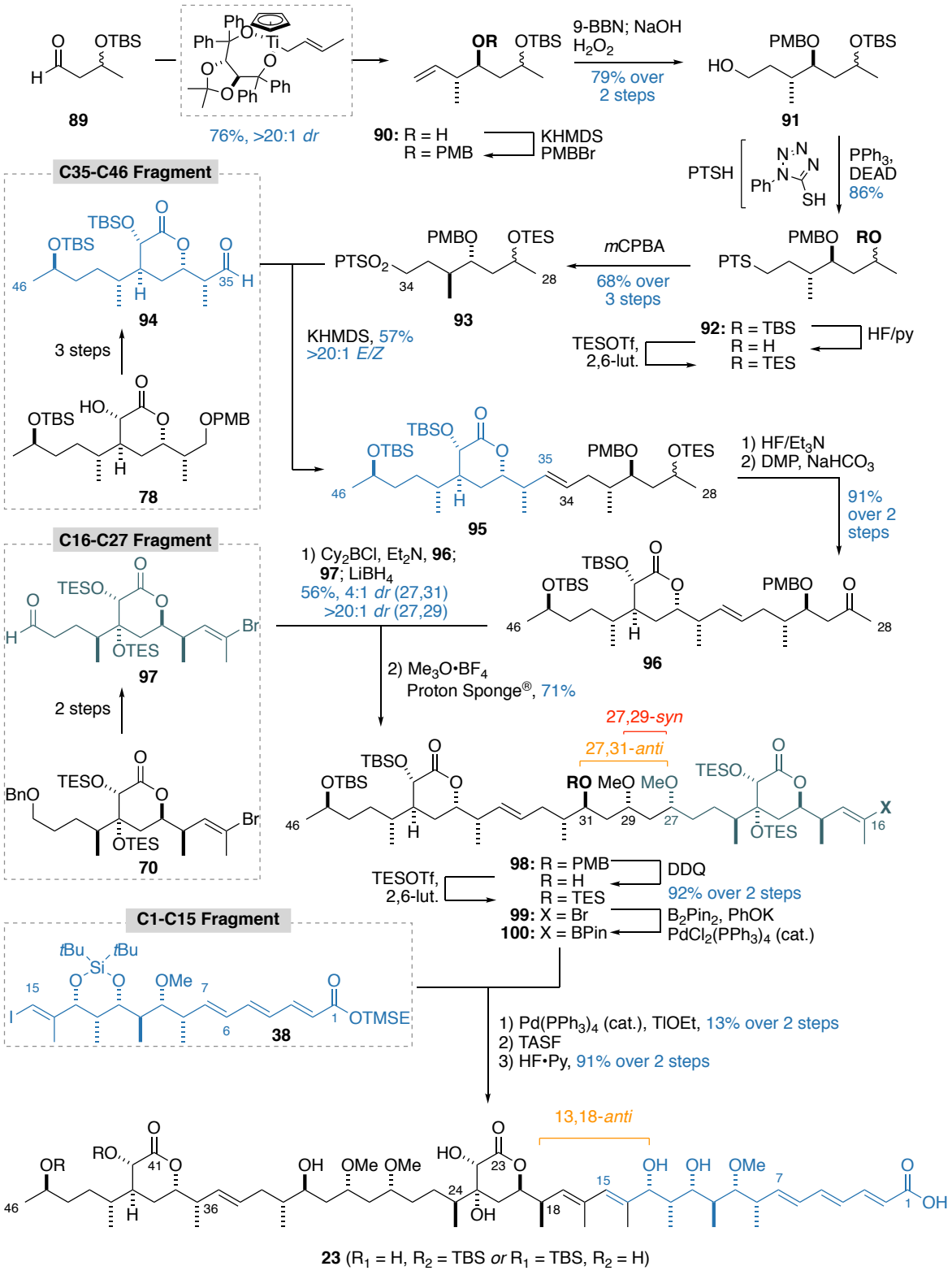

Scheme 9. *Ardisson/Cossy's synthesis of the carbon backbone of hemicalide* ***23***. *Note that the final global desilylation could not proceed to completion, leaving a TBS ether remaining at either the C40 or the C45 hydroxyl centre.*

2.4. Summary

As a highly potent and a mechanistically unique cytotoxic polyketide natural product, hemicalide has garnered the interest of chemists and biologists alike for its potential as a novel anticancer agent. Owing to its scarce supply, the isolation team were unable to determine the relative and absolute configuration of all 21 stereocentres, leaving NMR data as the only available evidence for researchers to piece together its stereochemical identity.

Through focusing their analyses to selected stereochemically rich regions, the Ardisson and Cossy groups have established the stereochemistry of the C1-C15 polypropionate and the C36-C42 hydroxylactone region, as well as proposing the 18,19-*anti* relationship for the C18-C24 dihydroxylactone (**Figure 17**). Independently, the Paterson group corroborated two of the three assignments through the DP4 algorithm but reassigned the dihydroxylactone region from an 18,19-*anti* to an 18,19-*syn* relationship. These results were experimentally confirmed with an improved correlation shown for truncate **20** to the natural product relative to truncate **16c** as synthesised by Ardisson and Cossy.

Furthermore, the Ardisson/Cossy and the Paterson groups have reported on synthetic studies towards various fragments. This included a synthesis of the C1-C15 region as well as the revised C16-C25 region. On top of this, Ardisson/Cossy have reported a synthesis of the C36-C42 hydroxylactone as part of the stereochemical assignment of the aforementioned region. Towards achieving a total synthesis, Ardisson/Cossy have also shown an iteration of their fragment union strategy between the three major fragments to afford the full carbon skeleton of hemicalide. However, the large NMR shift deviations between several major fragments, and the absence of alternative configurations for comparison hints towards the conclusion that fragment **23** is unlikely to bear the correct configuration between C1-C15 and C16-C25 regions, as well as within the C27-C32 polyacetate region.

Overall, this section outlined how 16 of the 21 stereocentres present within the three stereoclusters in hemicalide were assigned and the routes taken to achieve fragment synthesis; these are summarised in **Figure 17**. The knowledge obtained from preliminary stereochemical elucidation, as well as the strength and deficiencies of previous studies forms the basis for the next section in the ongoing study towards a synthesis-enabled stereochemical elucidation of hemicalide.

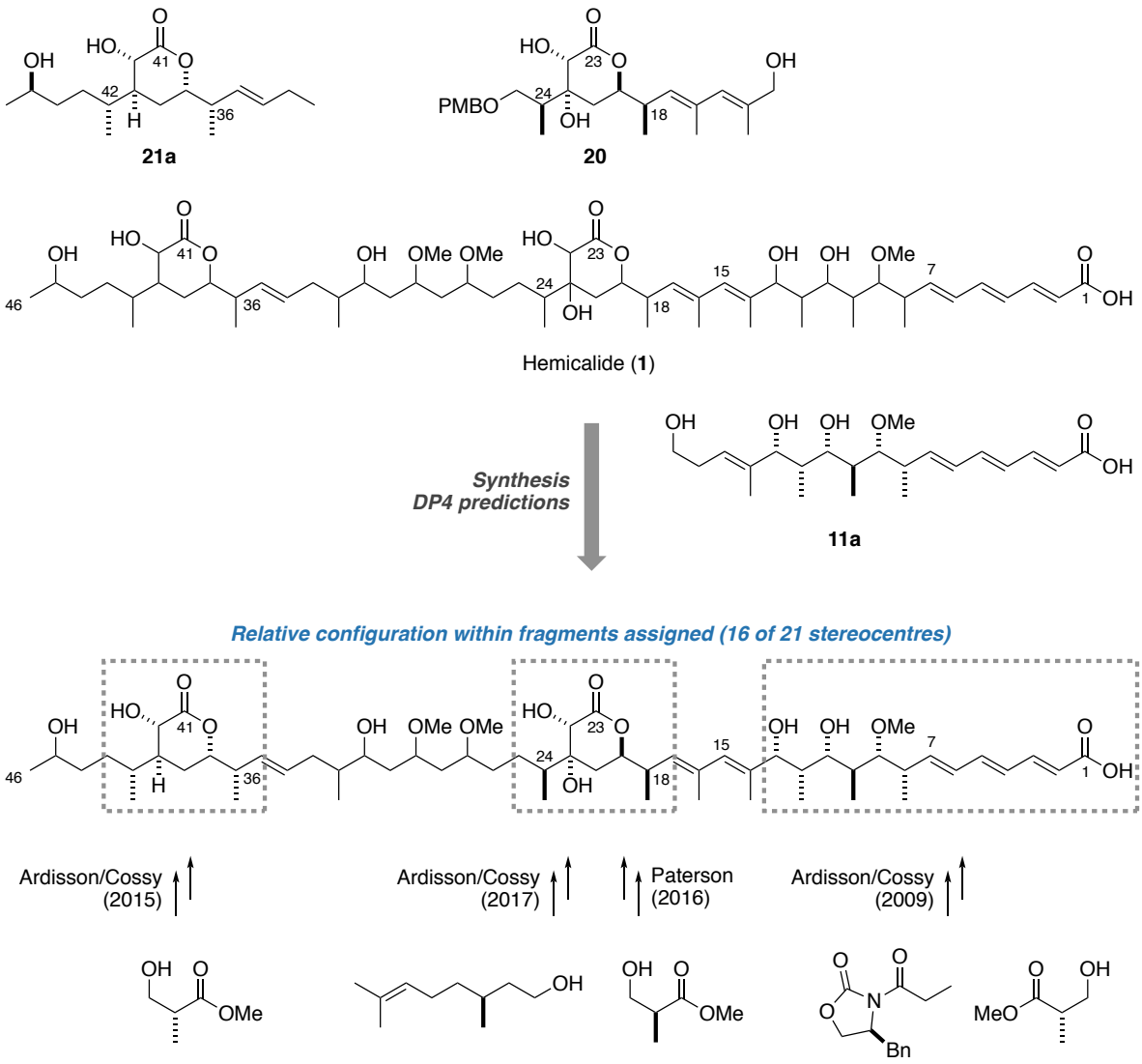

Figure 17. *Summary of the current work on the stereochemical assignment, as well as the synthesis of hemicalide*

3. Results and Discussion

The work described in this section was carried out in collaboration with Bing Yuan Han. His results were crucial to the project and are presented alongside the author's results. Unless otherwise stated, all reactions described were performed by the author and all stated yields are those obtained by the author.

3.1. The Paterson approach to hemicalide

In order to facilitate investigations towards determining the relative configuration between each known cluster, a convergent and stereoflexible approach is required, especially towards accessing the unassigned C27-C34 polyacetate region. The Paterson approach towards hemicalide proposes an enantioselective boron-mediated aldol reaction/diastereoselective reduction/*bis*-methylation sequence to configure the four possible diastereomers arising from C27 and C29 stereocentres at a late stage. Retrosynthetically, this reveals a C1-C28 fragment **101**, and a C29-C46 fragment **102.** The success of this end-game strategy depends on the *complete* reagent-control enforced by the chiral ligands on the boron Lewis acid; therefore, it is important to employ a silyl protecting group at C31, known to be a poorer contributor to 1,3-stereoelectronic effects as a measure to minimise any stereoinduction by the substrate in the closed aldol transition state.[55] The C29-C46 fragment **102** can be further disconnected at C33-C34 *via* cross-metathesis to give the C34-C46 alkene **103** and C29-C33 alkene **104** containing the remainder of the unknown stereocentres (**Scheme 10**).

The poor efficacy in installing the requisite Bpin handle for the C15-C16 cross coupling, alongside with the harsher conditions employed for the Suzuki reaction served as a cautionary tale for our synthetic design of the C1-C28 fragment **101**. Disconnecting at the same C15-C16 bond, our fragment union needed to be mild and highly efficient, and flexible enough to enable the facile access of either permutation of coupling handles. With promising results obtained from a model Stille coupling to afford model truncate **20,** the Stille coupling was adopted, which retrosynthetically reveals the C1-C15 polypropionate **39** and the C16-C28 dihydroxylactone **53**. Notably, the required stannyl handle could be flexibly installed at either C15 or C16 vinyl iodide through a Wulff-Stille reaction. The Stille coupling has proven to be a highly robust C_{sp^2}-C_{sp^2} bond forming strategy in the context of natural product synthesis in the Paterson group,[56] and was anticipated to provide efficient entry to the C1-C28 truncate of hemicalide.

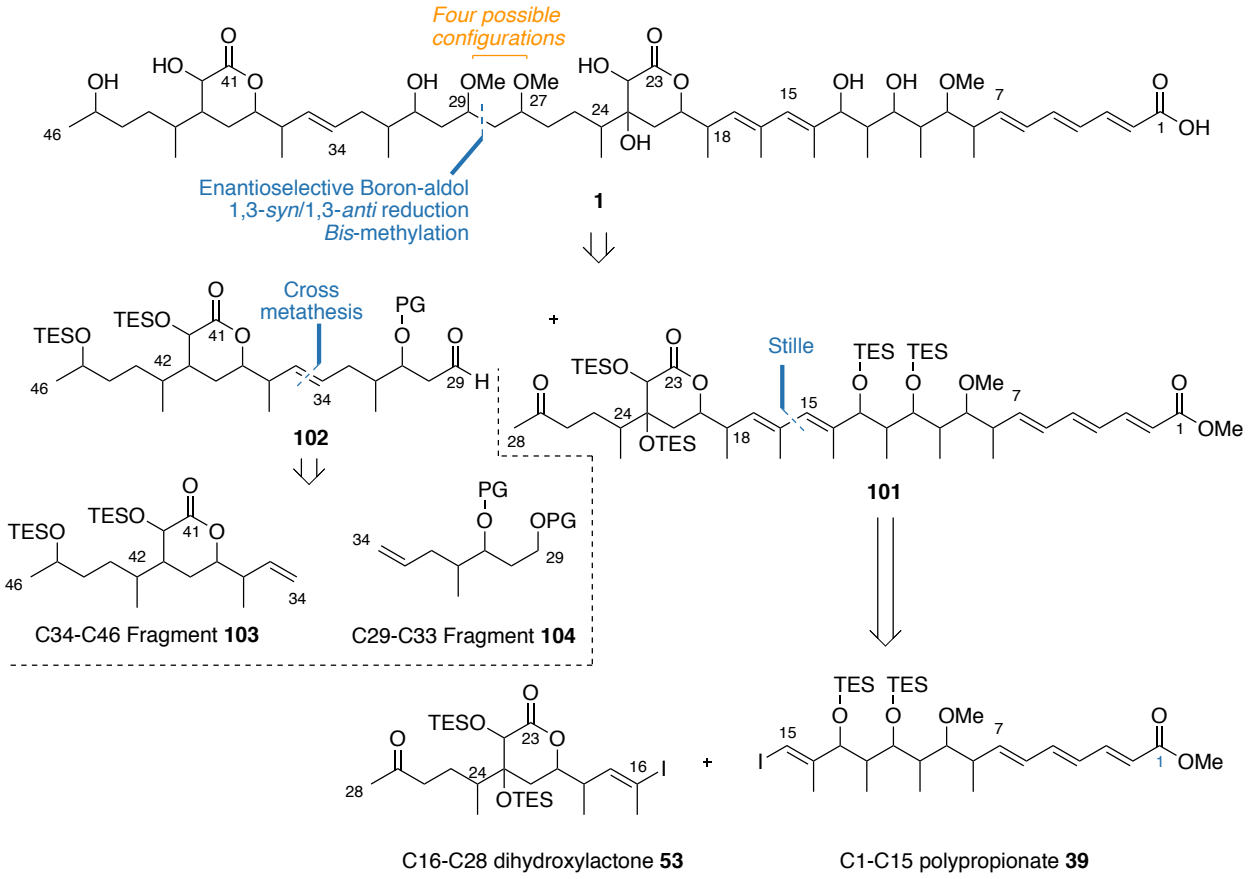

Scheme 10. *Overall disconnection strategy for hemicalide. PG denotes an unspecified protecting group.*

As highlighted in the previous section, previous work directed towards determining the relative configuration between the C1-C15 and the C16-C25 fragments have singularly targeted the 13,18-*anti* configuration, of which in the absence of the alternative 13,18-*syn* configuration, did not provide a compelling argument for the definitive assignment of the C1-C28 fragment of hemicalide. Thus, the short-term goal involves synthesising both possible diastereomers (**102** and **103**) of the reassigned C1-28 fragment as shown in **Figure 18** to ascertain the relative configuration between each fragment. Additionally, since the C1-C28 truncate constitutes over 60% of the natural product, it was hypothesised that this truncate may also exhibit bioactivity. Without any further characterisation that points towards the absolute stereochemistry of hemicalide, being able to biologically screen both enantiomers of the correct C1-C28 diastereomer could hint towards the absolute configuration of hemicalide, with the enantiomer corresponding to the one present in hemicalide putatively being more active than the other. Therefore, in light of this end goal of a synthesis-enabled elucidation of the C1-C28 region, as well as an activity-guided determination of the putative absolute configuration, both enantiomers of the C1-C15 and C16-C28 fragments are required. Concurrently with this work, Han developed a scalable approach to both enantiomers of the C1-C15 fragment, leaving the synthesis of the enantiomeric C16-C28 fragment ***ent*-53** based on the synthesis by MacGregor and Han as the next step in the hemicalide project.

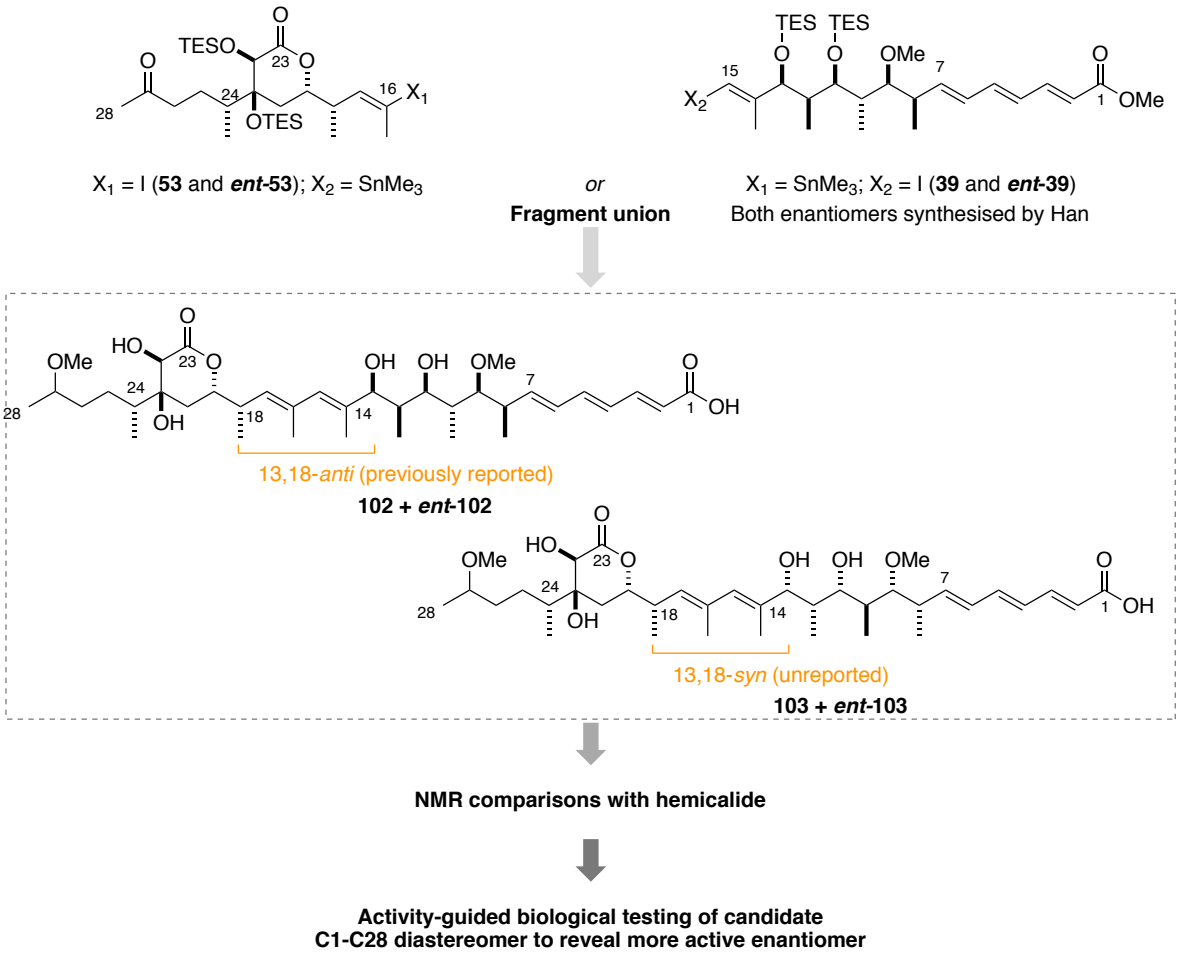

Figure 18. *Proposed workflow towards assigning the relative and absolute configuration of C1-C28 of hemicalide, highlighting the two possible diastereomers (13,18-anti, and 13,18-syn) that could exist in this region*

3.2. Synthesis of the opposite enantiomeric series for the C16-28 fragment

*3.2.1. Synthesis of the aldol adduct **ent-50***

Synthesis of the enantiomeric C16-C28 fragment ***ent*-53** commenced with PMB protection of (*R*)-Roche ester (*R*)-**26** to afford PMB ether **104** in excellent yield (99%). This was followed by reduction with $LiAlH_4$ to yield the primary alcohol **105** (93%). A subsequent Swern oxidation afforded the aldehyde **106**, which was directly submitted to the Corey-Fuchs reaction[57] to avoid racemisation of the aldehyde (80% over two steps). Vinyl dibromide ***ent*-55** was then treated with *n*BuLi and MeI to afford the alkyne **107** (98%) (**Scheme 11a**).

Transformation of alkyne **107** to vinyl iodide **108** was achieved by hydrozirconation with the Schwartz reagent ($Cp_2Zr(H)Cl$)[58] (**109**) generated *in situ* from Cp_2ZrCl_2 and DIBAL, followed by trapping of the organozirconium species with iodine. The regio- and stereoselectivity of this reaction arises from a *syn*-stereospecific addition of the hydrozirconium species across the alkyne (**TS-I** and **II**), with the large [Cp_2ZrCl] species adding on the least hindered end.[59] In theory, employing an excess of the Schwartz reagent improves the regioselectivity by a reversible second addition of the hydrozirconium species across the vinylzirconium intermediates (**TX-III** and **IV**). σ-bond rotation followed by a β-hydride elimination of the more hindered organozirconium species favours the formation of the major regioisomer as the thermodynamic product (**Scheme 11b**).[58] In the author's hands, this transformation was capricious and particularly dependent on reagent quality, where older supplies of Cp_2ZrCl_2 additionally afforded appreciable amounts of the regioisomeric vinyl iodide.

Subsequent PMB deprotection with DDQ afforded alcohol **110** (93%), which was oxidised with DMP to afford the required aldehyde ***ent*-49**. Due to its volatility and risk of racemisation at the C18 centre, aldehyde ***ent*-49** was always prepared fresh and directly submitted into the subsequent aldol reaction with minimal purification.

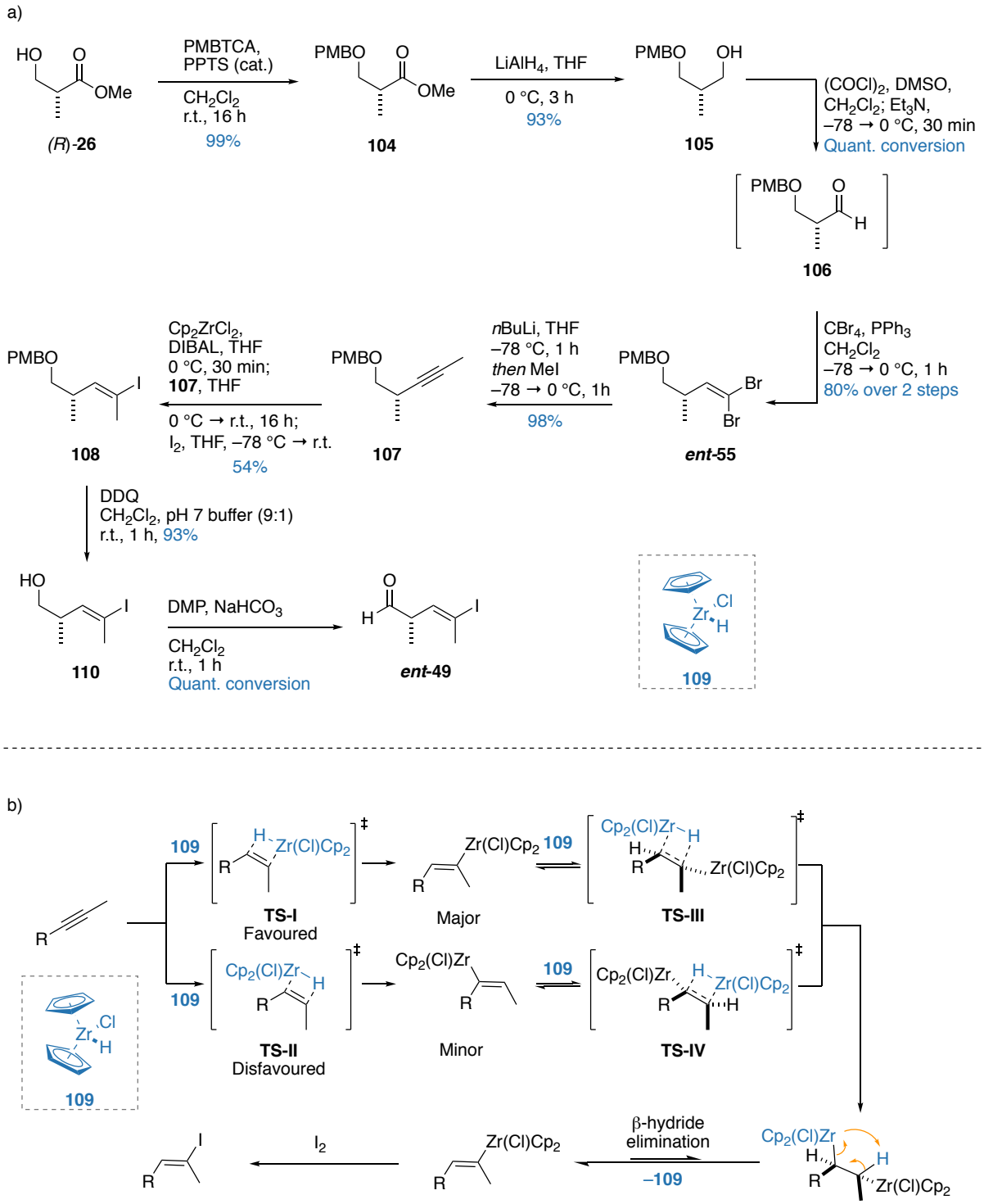

Scheme 11. *a) Synthesis of aldehyde* ***ent-49*** *from (R)-Roche ester (R)-**26**.*

b) Mechanism of the hydrozirconation with Schwartz reagent ***109***

The required methyl ketone ***ent*-48** was synthesised from a methylation of Weinreb amide **111** with MeMgBr. Grignard additions into Weinreb amides circumvent the issue of over-addition through the formation of a stable tetrahedral chelate **112** that does not decompose until aqueous workup, thereby avoiding the formation of the more electrophilic ketone under the reaction conditions. With ***ent*-48** and ***ent*-49** in hand, the required 1,4-*syn* boron aldol reaction was conducted employing the chiral boron reagent (+)-DIPCl (**Scheme 12a**). The reaction proceeds *via* a six-membered transition state (**Scheme 12b**),[60] where aldehyde ***ent*-49** and the boron enolate derived from ***ent*-48** are thought to sit in a boat conformation to facilitate the formation of the stabilising formyl-H bond between the electron-rich oxygen and the activated aldehyde.[60] Two diastereomeric transition states **TS-V** and **TS-VI** can then be drawn. **TS-V** is favoured as the allylic strain between C20 and Me24 on the enolate is minimised.[61] Additionally, **TS-V** also has the enolate approaching the aldehyde in a Felkin-Anh manner. The Ipc ligands enhances the selectivity by destabilising **TS-VI** with the unfavoured steric interaction between the Ipc Me group and the boron enolate, leading to the 1,4-*syn* diastereomer ***ent*-50** as the anticipated major product.[61]

The absolute configuration of the C19 stereocentre was confirmed by Mosher ester analysis. Compounds **113** and **114** were formed by reaction of ***ent*-50** with (*S*)- and (*R*)-MTPA respectively under Steglich esterification conditions (DCC, DMAP) (**Scheme 13**).[62] MTPA derivatives of secondary alcohols preferentially adopt a conformation in which the carbinol proton, ester carbonyl and CF_3 groups on the MTPA ester lie in the same plane (**Figure 19a**).[63] This results in the protons lying on the same side as the MTPA Ph group to be diamagnetically shielded (shifted upfield) relative to the protons lying on the same side as the OMe group. Thus, the protons lying adjacent to the (*S*)-MTPA Ph group will be shielded compared to the analogous protons in the (*R*)-MTPA derivative.[64] Thus, proton signals with $\Delta\delta < 0$ ($\Delta\delta = \Delta\delta_S - \Delta\delta_R$) would lie on the left-hand side of the (*R*)-MTPA plane from the perspective of the CF_3 group, and *vice versa* for $\Delta\delta > 0$ (**Figure 19b**).[65] Calculating $\Delta\delta$ (**Table 2**) and applying the model described in **Figure 19** showed that the C21 center had the desired *S* configuration, which corroborated the assignments based on mechanistic predictions and analogous literature reactions.

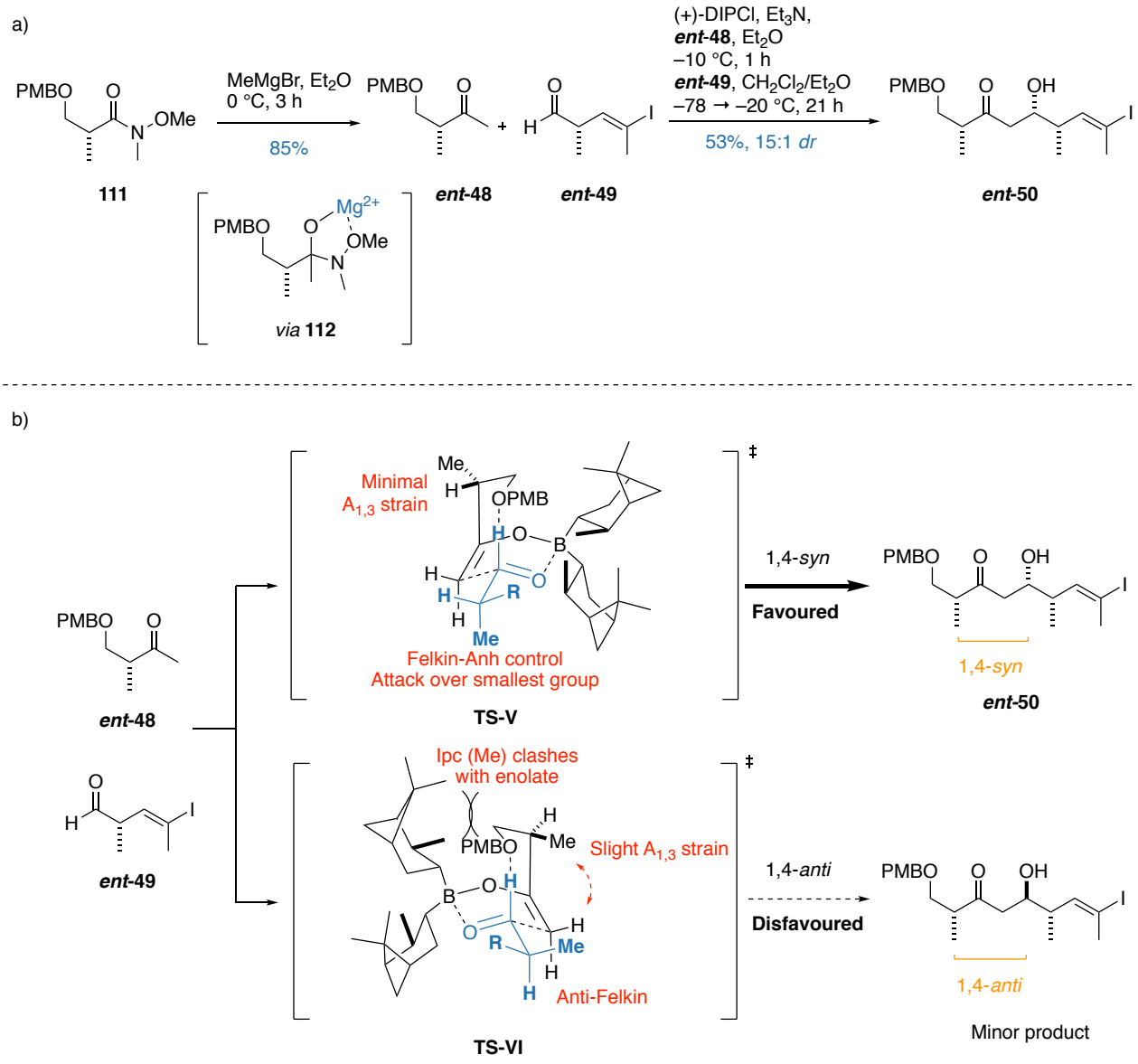

Scheme 12**. a) Synthesis of **ent-50** from **ent-48** and **ent-49

*b) Transition states for the aldol reaction of **ent-48** and **ent-49***

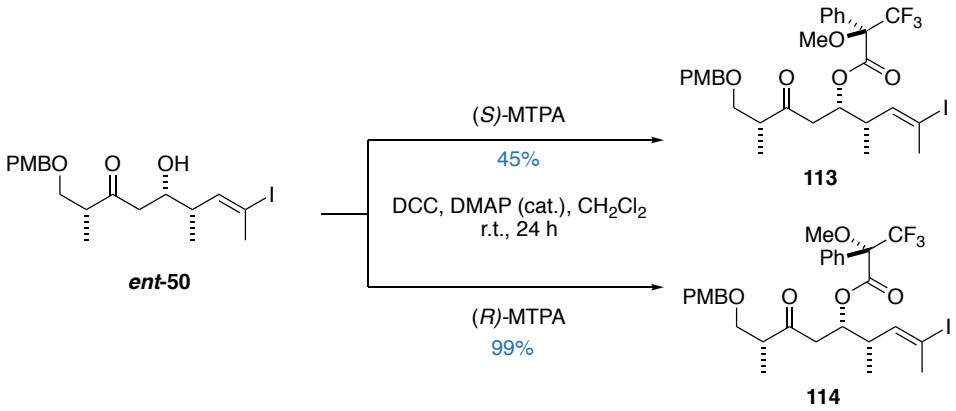

Scheme 13. *Synthesis of (R)- and (S)-MTPA derivatives of* ***ent-50***

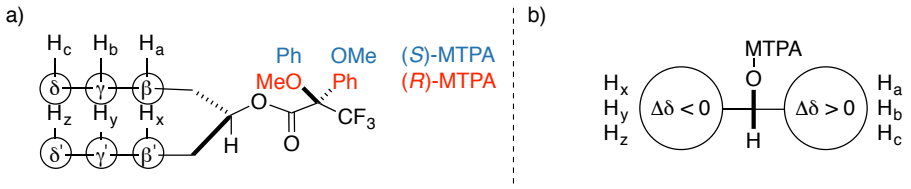

Figure 19. *a) Diagram highlighting the preferred conformation of the MTPA derivative b) Model to assist the absolute configuration of a carbinol centre*

Table 2. *List of chemical shifts for MTPA derivatives* ***113*** *and* ***114***

Proton	**δH (*S*)-MTPA** (ppm)	**δH (*R*)-MTPA** (ppm)	$\Delta\delta_{S\text{-}R}$ (ppm)
H25a	3.49	3.52	−0.03
H25b	3.41	3.44	−0.03
H24	(2.75)	(2.84)	−0.09
Me24	0.93	0.99	−0.06
H20a	2.84	(2.84)	0.00
H20b	2.75	(2.84)	−0.09
H19	5.42	5.42	0.00
H18	(2.87)	(2.81)	+0.06
Me18	0.91	0.86	+0.05
H17	5.98	5.86	+0.12
Me16	2.39	2.32	+0.07

() denotes signals obscured in multiplets, where chemical shifts were determined from COSY spectrum

3.2.2. *Synthesis of the dihydroxylactone* ***ent*-52**

Subsequent TBS protection of ***ent*-50** afforded TBS ether **115**, which was subjected to a lithium aldol reaction with the enolate generated from EtOAc and LDA to furnish ester **116** in excellent yields (99% and 98% respectively) as an inconsequential 3.5:1 mixture of diastereomers, as the formed hydroxyl group would eventually be dehydrated (**Scheme 14**). On a multigram scale, the material can be telescoped from ***ent*-50** to ester **116** without chromatographic purification, as all byproducts generated from these two steps are either volatile or chemically inert.

At this point, the TBS ether needed to be removed to facilitate the formation of lactone **117**. While the transformation of ***ent*-50** to **117** could, in theory, be performed without intermediary silyl protection, MacGregor found that any attempts at effecting the lithium aldol reaction with the free C19 OH resulted in elimination or retro-aldol processes occurring. In the original route, MacGregor and Han employed fluorous conditions (HF·py) to cleave the TBS ether and effect an *in situ* lactonisation, but this procedure was difficult to execute on scale. The required deprotection/lactonisation sequence was found to best proceed under acidic conditions (TsOH, MeOH), although careful monitoring was required as the unselective E1 dehydration of C21 was found to be the side product if the reaction was left for too long. Under optimised conditions developed by Han, lactone **117** could then be selectively dehydrated *via* an intermediate tertiary acetate into the cyclic enoate ***ent*-51**, where the combination of a weak base and a poorer leaving group promoted the E1cb-like pathway over other unselective pathways. Pleasingly, all transformations up until this point can be carried out on a multigram scale to ensure a sustainable supply of the enoate intermediate ***ent*-51**; the largest of which afforded 3.0 g of the cyclic enoate in a single operation.

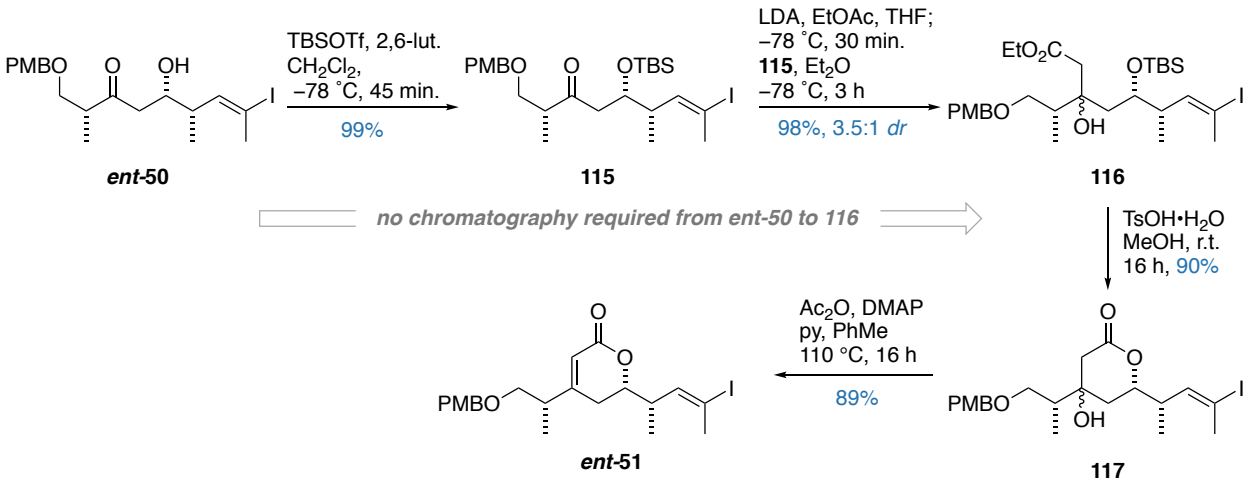

Scheme 14**. Synthesis of **ent-51** from **ent-50

The final two stereocentres in this fragment were installed by a modified Upjohn dihydroxylation from the *in situ* generation of OsO_4 (**Scheme 15a**). After optimisation, Han found that the addition of citric acid, employed by Sharpless to improve the yield of dihydroxylations of electron deficient alkenes, led to the more efficient conversion to the desired diol ***ent*-52**.[66] Notably, a sub-stoichiometric amount of the terminal oxidant NMO (0.5 eq. relative to enoate ***ent*-51**) was required to prevent the overoxidation to the undesired hydroxyketone **118**, attributed to electronic similarities between the enoate and vinyl iodide olefins. This was not observed in Ardisson/Cossy's case, as their vinyl bromide resulted in a more electron deficient olefin, which allowed for the complete selectivity for the enoate olefin. However, both diol ***ent*-52** and the unreacted starting material could be reliably isolated and resubmitted (79% brsm), and the reaction could be carried out on a one-gram scale without significant loss in material throughput.

Under the reaction conditions, $K_2OsO_4{\cdot}2H_2O$ is oxidised by NMO from Os^{VI} to the active Os^{VIII} species, which engages in a [3+2] cycloaddition with the olefin to deliver the osmate ester *syn*-stereospecifically. Under heterogeneous conditions, water is able to slowly displace the osmate complex to liberate the *syn*-diol product, which upon catalyst reoxidation by NMO closes the catalytic cycle (**Scheme 15b**). A catalyst deactivation pathway involves a second [3+2] cycloaddition with another equivalent of olefin to afford the diester **119**, which could be hydrolysed to form complex **120** and subsequently deprotonated to afford the kinetically inert dianion **121**. As this is resistant to diester hydrolysis, dianion **121** functionally cannot reenter the catalytic cycle and is a deleterious pathway for this reaction. In particular, electron withdrawing groups on the olefin reduce the pKa for complex **120**, allowing for weak bases, such as *N*-methylmorpholine (NMM) generated from NMO reduction, to deprotonate **120** to result in the unwanted dianion **121**.[66]

The addition of citric acid promotes catalyst turnover in two ways: Firstly, citric acid serves as a ligand for the Os complex; its enhanced hydrophilicity accelerates the rate limiting hydrolysis step and reduces the rate of the second [3+2] cycloaddition, suppressing the catalyst from entering the deactivation pathway. Secondly, the acidic conditions suppresses the unwanted deprotonation of complex **120** to form the inert dianion **121**; both of which help promote the catalytic efficiency of the Os catalyst in the dihydroxylation of electron poor olefins.[66]

This transformation uniformly delivers a single diastereomer of the desired product. The excellent diastereoselectivity of this transformation can be rationalised by drawing the lactone as the half-chair conformer, where the lowest energy conformer places the C16-C18 side chain pseudoequatorial. In this conformer, the active OsO_4 species is disfavoured from a bottom face by the pendant side chain to result in the *syn*-dihydroxylation installing the OHs on the top face (**Scheme 15c**). As the enoate bears the *E* geometry and therefore possesses two low energy conformers, the Houk model[67] predicts that the C24 allylic stereocentre would minimally impact the stereochemical outcome of this reaction.[68]

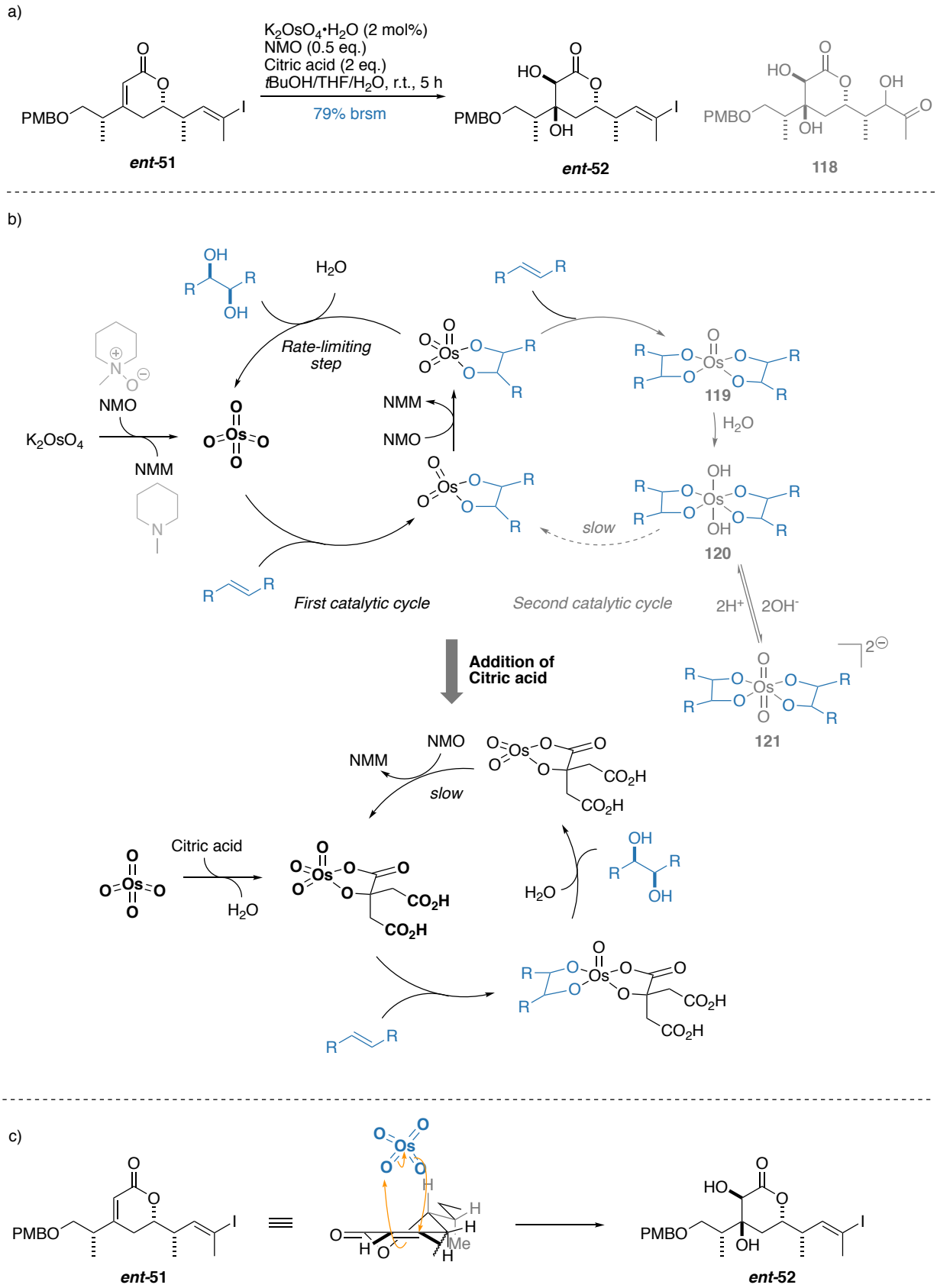

Scheme 15. *a) Dihydroxylation of* ***ent-51*** *to form* ***ent-52****. b) Mechanism of the OsO_4-catalysed dihydroxylation, and the mechanism with citric acid as the additive. c) Stereochemical rationalisation of the dihydroxylation reaction*

*3.2.3. Completion of the enantiomeric C16-C28 fragment **ent-53***

With diol ***ent*-52** in hand, *bis*-TES protection followed by oxidative PMB removal in **122** gave alcohol **123**, which underwent Dess-Martin oxidation to afford aldehyde **124 (Scheme 16a)**. To avoid the risk of epimerisation at C24, aldehyde **124** was immediately used in the $Ba(OH)_2$-mediated HWE olefination with ketophosphonate **125**. Upon treatment of **125** with $Ba(OH)_2$, the Ba^{2+} is able to coordinate between the carbonyl and phosphoryl oxygens, which reduces the pK_a of the methylene protons. This allows for facile deprotonation to generate the corresponding carbanion, which rapidly and reversibly adds into aldehyde **124** to generate a mixture of *syn* and *anti* diastereomers (**Scheme 16b**). The subsequent cyclisation to form the oxaphosphatane intermediate is a much slower process, but is reversible and is faster for the *anti* diastereomer. At this point, the oxaphosphatane collapses irreversibly to give the *E* olefin. Owing to the slow oxaphosphatane formation that favours the *anti* configuration coupled with the fast collapse to form the olefin, the equilibrium mixture of *syn* and *anti*-**126** favours the formation of *anti*-**126**, which leads to the preferential formation of the *E* over the *Z* olefin configuration. With aldehyde **124** and ketophosphonate **125**, the HWE olefination proceeded smoothly (77% over two steps) to deliver the enone **127** as a single geometric isomer.

The completion of the enantiomeric C16-C28 fragment ***ent*-53** was achieved by a conjugate reduction of the enone using Stryker's reagent (70%). Han found that optimal results were achieved by using a freshly prepared solution of the reagent, where the active copper hydride species was generated *in situ*. Although only a catalytic amount of Cu was required, Han found better results employing a stoichiometric amount of Cu in this reaction. Mechanistically, the copper hydride species undergoes a conjugate addition into the enone. The resulting copper enolate can then be reduced by TMDS present in solution to regenerate the active catalyst, as well as liberating the silyl enol ether **128**, which upon protonation forms the product (**Scheme 16c**).

Overall, the enantiomeric fragment ***ent*-53** was synthesised in 18 steps in 5.5% overall yield from (*R*)-Roche ester (*R*)-**26**, which was comparable to Han's synthesis of **53** (4.4%). Notably, multigram quantities of the key cyclic enoate intermediate have been prepared, enabling the goal of achieving fragment union to give the two possible diastereomers between the C1-15 and the C16-C25 region.

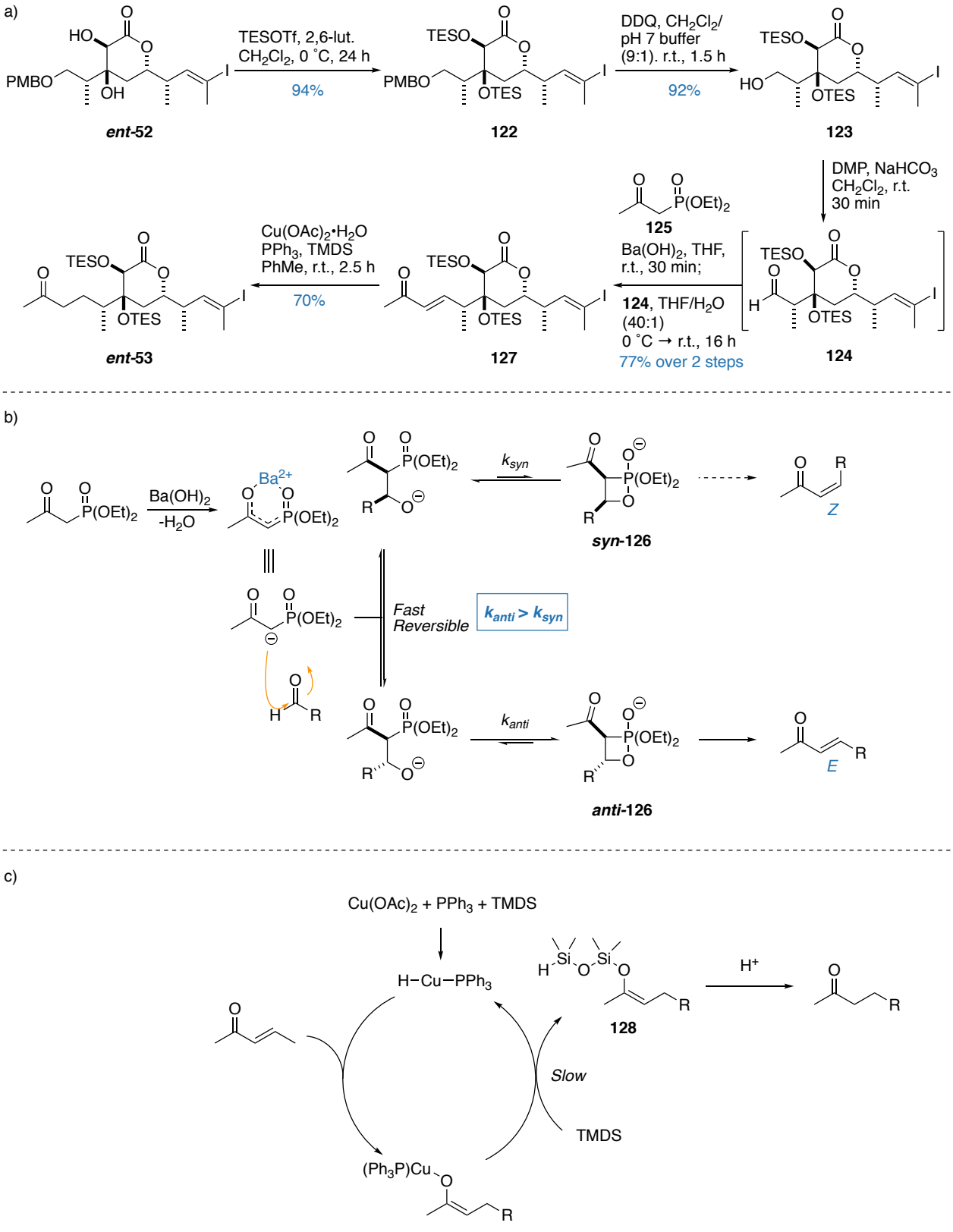

Scheme 16. *a) Synthesis of the enantiomeric C16-C28 fragment* ***ent-53*** *from diol* ***ent-52.*** *b) Mechanism of the Ba(OH)₂-mediated HWE olefination reaction to selectively generate the E-enone. c) Mechanism of the copper-catalysed conjugate reduction*

3.3. Fragment union, derivatisation of the C1-C28 truncate and NMR comparisons

With adequate supplies of the C16-C28 vinyl iodide ***ent*-53** in hand, and access to both enantiomers of the C1-C15 fragment **39**, the synthesis of both diastereomers of the C1-C15 and C16-C25 fragment was within reach. During exploratory studies, Han found that the corresponding stannane derived from the C16-C28 vinyl iodide was highly unstable, being prone to protodestannylation processes. Alongside this, Han was able to transform the C1-C15 vinyl iodide **39** to the corresponding stannane **129** *via* a Wulff-Stille reaction (**Scheme 17a**).[69] These two results pointed towards employing the C1-C15 vinyl stannane and the C16-C28 vinyl iodide as the two coupling handles for the Stille cross coupling to synthesise the full C1-C28 truncate.

Employing Fürstner's modified Stille conditions ($Pd(PPh_3)_4$, CuTC), vinyl iodide ***ent*-53** and stannane **129** were smoothly reacted to form the full C1-C28 truncate **101a** bearing the 13,18-*syn* configuration. The Fürstner modification of the Stille coupling has been a general and reliable method of executing cross-couplings of complex substrates in the context of natural product synthesis, successfully used in the context of leiodermatolide,[70] iejimalide B[71] and rubriflordilactone A.[72] The proposed catalytic cycle for the copper-mediated palladium-catalysed Stille cross coupling begins by the oxidative addition of palladium into a carbon-halogen bond, followed by a transmetallation event and an irreversible reductive elimination to release the cross-coupled product and regenerate the catalyst (**Scheme 17b**). The exact role of copper is not fully elucidated, but it is known that the addition of Cu^{I} accelerates the rate of reaction by equilibrating the poorly nucleophilic organostannane into the more nucleophilic organocuprate. The transient organocuprate allows for a more facile transmetallation event onto the Pd^{II} centre, accelerating what otherwise is the rate-determining step of the catalytic cycle. However, as this exchange is in dynamic equilibrium, the accumulation of tin disfavours the formation of the organocuprate as the reaction proceeds and overtime, reduces the beneficial effect promoted by Cu. To circumvent this, Fürstner reported a solution by employing a thiocarboxylate ligand on the copper to sequester the tin species formed.[73] Additionally, Fürstner reported that the thiocarboxylate ligand alone was insufficient for the complete removal of tin, and further added the phosphinate salt $[n\text{Bu}_4\text{N}][\text{Ph}_2\text{PO}_2]$ to help drive the equilibrium towards the right hand side. This was a notable improvement to employing fluoride sources[74] as the terminal sequestering agent for its improved functional group tolerance, especially towards silyl groups. In the author's hands, the omission of the phosphinate salt did not impair the efficacy of this reaction, and was able to deliver the coupled product **101a** (72%) from near equimolar amounts of both reaction partners.

The remainder of this section will detail with the synthesis of the 13,18-*syn* diastereomeric series. Towards the end goal of achieving a detailed NMR comparison between the two diastereomers, the alternative 13,18-*anti* diastereomeric series starting from ketone **101b** was pursued concurrently by Han.

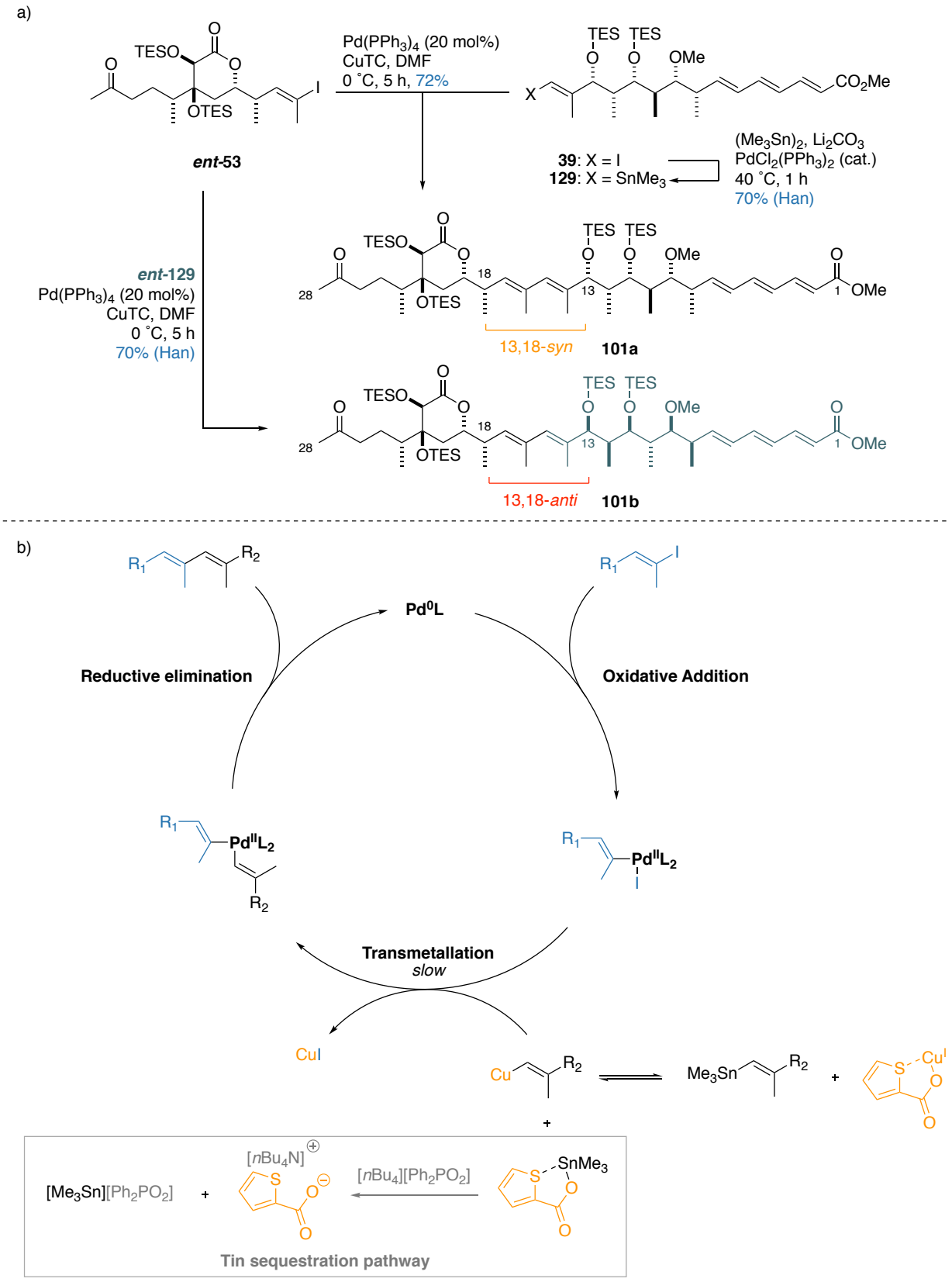

Scheme 17. *a) The Stille coupling of* ***ent-53*** *and* ***129*** *to form the C1-C28 truncate* ***101a****. The corresponding 13,18-anti diastereomer* ***101b*** *was analogously synthesised by Han. b) Mechanism for the palladium catalysed-CuTC-mediated Stille coupling*

3.3.1. Derivatisation of the C1-C28 fragment for NMR comparison

The C1-C28 ketone fragment **101a** represents a major branching point for the total synthesis of hemicalide, as the methyl ketone handle can be used for the planned aldol/reduction/methylation endgame sequence. For purposes of NMR comparisons however, the silyl protecting groups needed to be removed. While it may seem like a tempting solution to globally desilylate truncate **101a**, earlier studies by MacGregor and Han on the C16-C28 ketone **53** showed that desilylation resulted in the concomitant hemiacetal engagement to give **130**, an unrelated structure that would complicate spectroscopic analyses (**Scheme 18a**). Furthermore, noting that the natural product contains a methyl ether at C27, it was therefore sensible to transform the C27 ketone to the corresponding methyl ether to aid NMR comparisons.

Initial efforts were directed towards asymmetrically reducing C27 to obtain the configurationally pure alcohol. However, attempts at reducing ketone **101a** mediated by the CBS reagent were met with poor selectivity (**Scheme 18b**), presumably arising from the poor discrimination of two similarly sized substituents around the ketone. Arising from this was the observation that both C27 epimers exhibited *quasi* identical ^{1}H and ^{13}C NMR spectra in the C1-C24 region; an observation echoed by Cossy during their investigation of C45 relative to the C35-C42 region.[44] While minute differences were seen near C27, the distal stereocentre appeared to minimally affect the spectra arising from the remainder of the truncate.

As such, for ease of material throughput, an unselective reduction mediated by $NaBH_4$ was conducted. Initial attempts at effecting this transformation were met with what appeared to be the concomitant conjugate reduction of the trienoate system. This was found to be attributed to residual amounts of $Pd(PPh_3)_4$ that coeluted with the ketone product, which upon treatment with $NaBH_4$, could catalytically reduce the trienoate *via* an intermediary palladium-hydride species. Rechromatographing ketone **101a** appeared to solve this problem, and alcohol **131** was cleanly delivered in 95% yield as a mixture of epimers at C27. Alcohol **131** could then be methylated using Meerwein's salt to deliver methyl ether **132**. Gratifyingly, despite the epimeric mixture at C27, intermediates **131** and **132** exhibited clear NMR signals in the C1-C24 region that allowed for their facile characterisation. Using an analogous sequence, Han synthesised the corresponding 13,18-*anti* methyl ether **133** in comparable yields.

3.3.2. Global silyl deprotection of the C1-C28 truncate

At this point, all that remained was the global desilylation of four TES ethers, and the hydrolysis of the C1 methyl ester to give the model C1-C28 truncates. Unexpectedly, the global desilylation of **132** to afford tetraol **134** proved to be a much bigger challenge than anticipated. While MacGregor and Han reported the facile deprotection of **53**[43] **(Scheme 18a)** and C1-C15 truncate ***ent*-39** to give **130** and **135** respectively[75] using HF·py, the same conditions led to only partial deprotection for the full truncate, with increasing concentration of HF·py and time of exposure leading to degradation of the fragment.

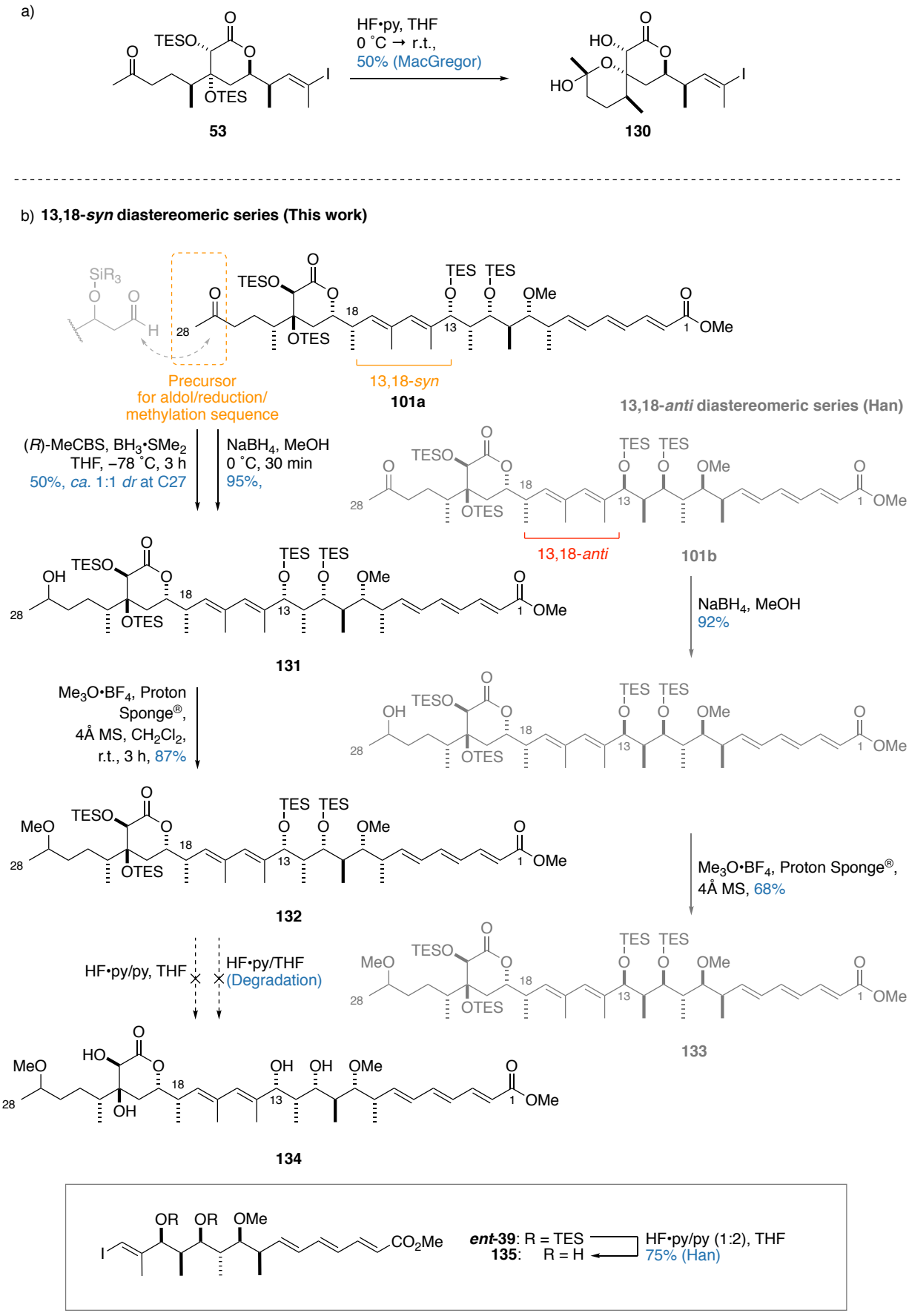

Scheme 18. *a) Desilylation of* ***53*** *results in the formation of hemiacetal* ***130*** *as observed by MacGregor. b) Synthesis of the 13,18-syn-methyl ether* ***132*** *from ketone* ***101a.*** *The synthesis of the 13,18-anti methyl ether* ***133*** *conducted by Han is presented alongside*

Using model fragments **122** and ***ent*-39** as a surrogate for the C1-C15 and the C16-C28 region respectively, three curious observations were found: Firstly, there were *no* common reagents (acidic, acidic fluorous or basic fluorous) that could deprotect all four silyl protecting groups simultaneously (**Table 3**). Secondly, acidic conditions (TsOH) or acidic fluorous conditions (i.e. HF·py and HF/MeCN) appeared to chemoselectively deprotect the C11 and C13 bearing OTES groups, leaving the C21 and C22 OTES groups intact that degraded upon prolonged exposure at high concentration. Thirdly, basic fluoride-mediated deprotection conditions (unbuffered TBAF and TASF) appeared to chemoselectively deprotect the C21 and C22 OTES groups, with degradation observed in the C1-C15 fragment upon prolonged exposure.

Working with what appeared to be a razor-thin margin of reactivity, a cross-over experiment was conducted to establish the stability of the respective diols to the various deprotection conditions (**Table 4**). Knowing that a suitable buffered solution of HF·py could cleanly deprotect the C1-C15 region, attention turned towards establishing a set of conditions that could cleanly deprotect the C16-C28 region without degrading the free C1-C15 diols. From this, it appeared that TASF was the reagent of choice to effect this deprotection whilst preserving the integrity of the remainder of the molecule, and as such, a two-step procedure involving a short exposure of the full truncate to HF·py to cleave the C11,C13 TES ethers, followed by treatment with TASF to remove the C21 and C22 TES ethers was implemented. Notably, this set of condition is the exact reverse sequence to what Ardisson/Cossy employed.[45,48] While TASF is a common reagent required for the deprotection of trimethylsilylethyl esters (the ester present in Ardisson/Cossy's truncate),[76–78] no rationale was given in their report on why this exact sequence was necessary.

Frustratingly, using what appeared to be the optimised conditions on the fully protected C1-C28 fragment **132** gave irreproducible results. While the HF·py deprotection was facile, delivering the C11,C13 diol quantitatively, the subsequent treatment with TASF was capricious; at best, the deprotection proceeded to give tetraol **134** with 50% yield, but in worst cases, the deprotection degraded the entire fragment (**Scheme 19**). With no apparent reason for this observation and a need for a reliable deprotection strategy, a better solution was clearly required to deliver not just the C1-C28 truncate, but for the eventual global deprotection of the fully protected hemicalide in the total synthesis campaign.

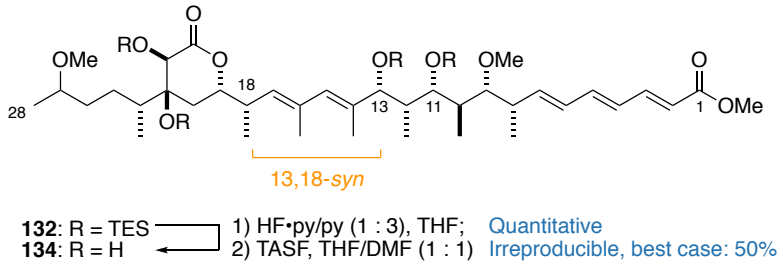

Scheme 19. *Attempts at global desilylation of* ***132*** *using HF·py and TASF*

Table 3. *Summary of conditions for model deprotection studies of the protected C1-C15 truncate* ***ent-39*** *and the protected C16-C25 truncate* ***122***

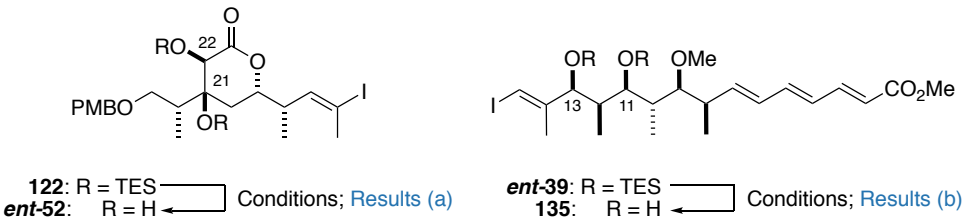

Conditions	122 → *ent*-52: Results (a)	*ent*-39 → 135: Result (b)
HF·py/py (1 : 2), 3 – 24 h	No reaction (24 h)	Complete conv. to diol (3 h)
HF·py/py (1 : 1), 3 – 24 h	No reaction (24 h)	Complete conv. to diol (3 h)
HF·py (neat), 3 - 6 h	No reaction (3 h) Degradation (6 h)	Complete conv. to diol (3 h) Degradation (6 h)
TsOH, MeCN, H_2O, 3 h	No reaction (3 h)	Complete conv. to diol (3 h)
HF (aq.), MeCN, 5 – 30 min	No reaction (30 min)	Complete conv. to diol (5 min) Degradation observed (30 min)
PPTS, MeOH, 24 h	No reaction (24 h)	No reaction (24 h)
TBAF, 3 h	Variable results	Degradation (3 h)
TASF, 1 – 3 h	Complete conv. to diol (1 h)	Degradation (3 h)

Table 4. *Summary of conditions for model deprotection studies of C1-C15 diol* ***134*** *and the protected C16-C25 truncate* ***122***

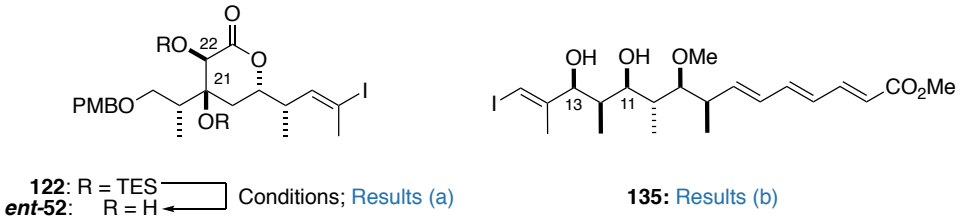

Conditions	122 → *ent*-52: Results (a)	135: Result (b)
TBAF, 1 – 3 h	No reaction. Degradation upon prolonged exposure	No reaction
TASF, 3 h	Complete conversion to diol	No reaction

Faced with this obstacle, reversing the sequence of steps was attempted, as reported by Ardisson/Cossy, to observe if this gives a better result. Interestingly, treatment with TASF (2 eq.) on the full truncate gave a mixture of *mono*/*bis*/*tris* and *tetrakis* deprotected silyl groups, but attempts at pushing this reaction with additional equivalents of TASF only served to degrade the fragment. As expected from exploratory studies, the first two silyl groups to come off were reliably from C21 and C22, and it was reasoned that if this *bis*-desilylation was allowed to proceed to completion, then treatment with HF·py should cleanly remove the remaining silyl groups. Pleasingly, by using 5 eq. of TASF (1.25 eq. per TES group) followed by treatment with buffered HF·py, this sequence not only provided a reliable means for global desilylation, but was able to reproducibly give the tetraol in very good yields over two steps (95% over two steps) (**Scheme 20**). It is worth noting that on model systems, treatment of the protected C1-C15 truncate with TASF resulted in apparent degradation, serving a reminder that results from model studies may not translate into the real system. To date, the reason why these two sets of silyl group are apparently chemically orthogonal to each other remain unclear.

With the tetraol **134** in hand, the final ester hydrolysis could be conducted. Initial attempts at using KOTMS gave complex mixtures, but employing $Ba(OH)_2 \cdot 8H_2O$ in MeOH reliably gave the 13,18-*syn* free acid **103** (50%) (**Scheme 20**). The modest yield was attributed to the high hydrophilicity of the free acid making purification difficult. In an analogous sequence from **133**, Han was able to effect the global deprotection using the aforementioned conditions to give tetraol **136** (67% over two steps) followed by methyl ester hydrolysis (50%) to afford the 13,18-*anti* truncate **102**. This represents the first time both diastereomers of the C1-C28 region of hemicalide has been made to enable NMR comparisons with the natural product.

3.4. NMR comparisons of the C1-C28 truncates with hemicalide

During the course of synthesising free acid **103**, it was encouraging to observe noticeable chemical shift differences between the 13,18-*syn* and the 13,18-*anti* diastereomers of all intermediates in $CDCl_3$. These served as promising indicators that a synthesis-enabled elucidation of the relationship between the C1-C15 and the C16-C25 fragment of hemicalide was indeed possible, despite the distal 1,6-relationship between the two stereoclusters.

3.4.1. *NMR comparisons between the 13,18-syn and 13,18-anti acids*

Due to the lack of structural homology beyond H25, as well as the fluctuating chemical shifts of the C1-C7 trienoic acid region which was attributed to the 'salt effect' claimed by Ardisson,[41] NMR comparisons were restricted to the C8-Me24 region of the truncate. Initially, a comparison with the 13,18-*anti* truncate with previously published structures by Ardisson/Cossy was made to corroborate the synthesised structure. Pleasingly, truncate **102** displayed good homology to previously published structures bearing the 13,18-*anti* relationship (**23** and **25**), giving further credence to the configuration that was synthesised (**Figure 20** and **Figure 21**).

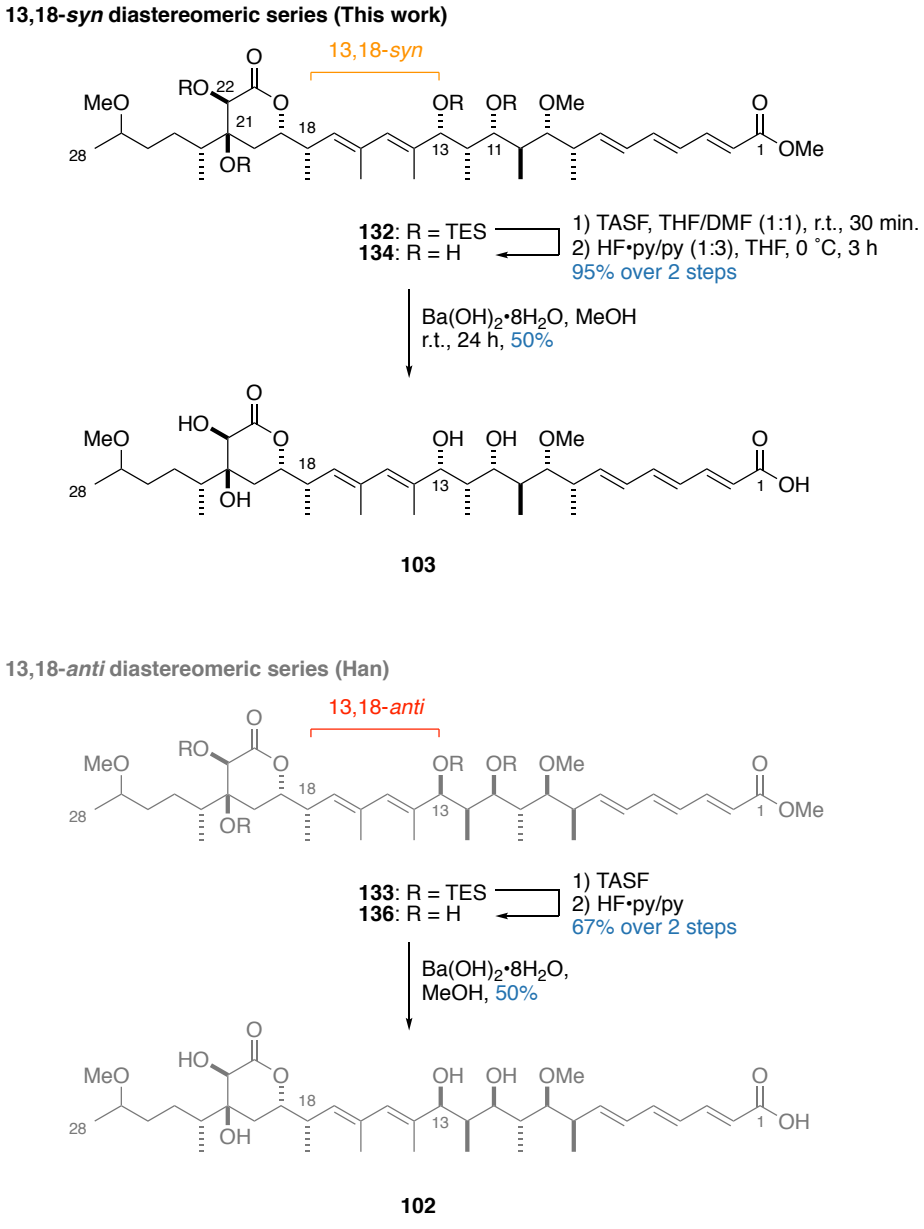

Scheme 20. *Synthesis of 13,18-syn acid* ***103*** *and the 13,18-anti acid* ***102*** *(Han)*

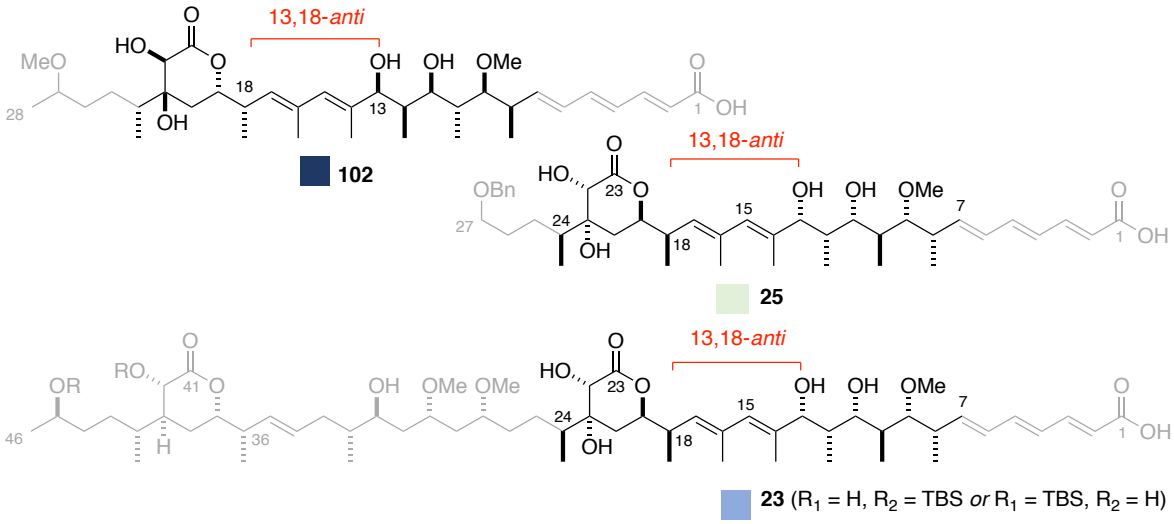

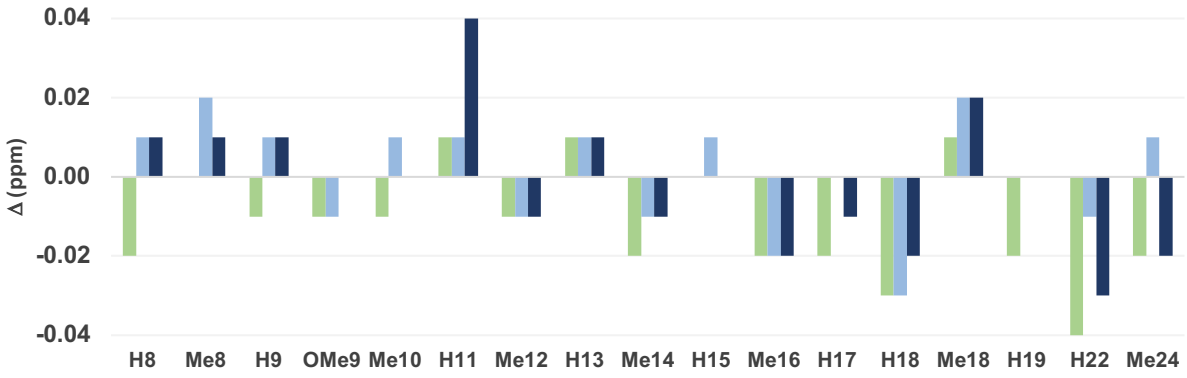

Figure 20. *Bar graph comparing [1]H NMR shift difference between* ***23****,* ***25****(Ardisson/Cossy)* ***102*** *(Han) and hemicalide*

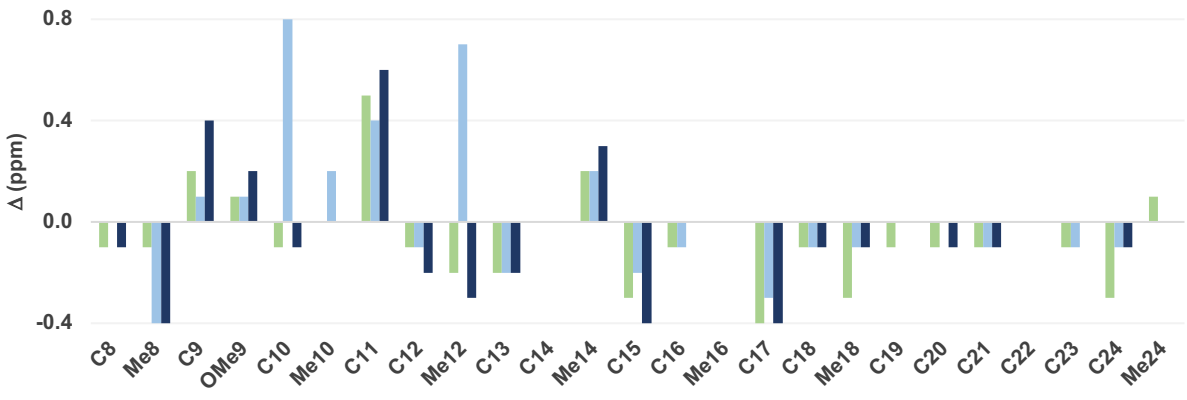

Figure 21. *Bar graph comparing [13]C NMR shift difference between* ***23****,* ***25****(Ardisson/Cossy),* ***102*** *(Han) and hemicalide*

While comparison of the 13,18-*syn* and 13,18-*anti* methyl ester truncates **134** and **136** seemed to suggest that the 13,18-*anti* diastereomer was a better fit for the natural product, upon ester hydrolysis, the 13,18-*syn* diastereomer **103** possessed remarkable homology to hemicalide ($\Sigma|\Delta\delta_H|$: 0.05 ppm, $\Sigma|\Delta\delta_C|$: 0.8 ppm; **Table 5**, entry 1), compared to the 13,18-*anti* diastereomer **102** ($\Sigma|\Delta\delta_H|$: 0.22 ppm, $\Sigma|\Delta\delta_C|$: 4.1 ppm; **Table 5**, entry 3). For **103**, the maximum chemical shift deviation did not exceed 0.01 and 0.1 ppm for ^{1}H and ^{13}C respectively, with many signals aligning exactly with the chemical shifts reported for hemicalide (i.e. $\Delta\delta$ = 0 ppm). This is in contrast with the 13,18-*anti* truncate **102**, where the maximum ^{1}H and ^{13}C deviations recorded were 0.04 and 0.6 ppm. In particular, several large deviations that were unaccounted for in the 13,18-*anti* truncate **102** exhibited a perfect match in the 13,18-*syn* truncate **103**. These included C11 ($\Delta\delta_C$ = 0.6 ppm for **102**, $\Delta\delta_C$ = 0.0 ppm for **103**), C15 ($\Delta\delta_C$ = –0.4 ppm for **102**, $\Delta\delta_C$ = 0.0 ppm for **103**) and C17 ($\Delta\delta_C$ = –0.4 ppm for **102**, $\Delta\delta_C$ = 0.0 ppm for **103**). These results are graphically represented in **Figure 22** for ^{1}H, and **Figure 23** for ^{13}C chemical shift differences.

3.4.2. NMR comparisons between the 13,18-syn and 13,18-anti salts

From preliminary studies published by Ardisson, the natural product was reported to be isolated as the carboxylate salt. Because of this, it was thought that improved correlations could be achieved between both diastereomers with the natural product across the whole molecule by deprotonating the C1 acid. This was achieved by treating truncates **103** and **102** in d_4-MeOD with Na_2CO_3 to give **137** and **138** respectively (**Scheme 21**). Interestingly, both truncates exhibited poorer correlations in C8-Me24 regions (13,18-*syn* **137**: $\Sigma|\Delta\delta_H|$: 0.09 ppm, $\Sigma|\Delta\delta_C|$: 1.7 ppm - **Table 5** entry 2; 13,18-*anti* **138**: $\Sigma|\Delta\delta_H|$: 0.22 ppm, $\Sigma|\Delta\delta_C|$: 4.3 ppm - **Table 5** entry 4) to the natural product, with no improved correlations observed in the C1-C7 trienoic acid region for both ^{1}H (**Figure 24**) and ^{13}C chemical shifts (**Figure 25**).

***Table 5**. Summary of ^{1}H and ^{13}C shift differences, represented as total sum of errors and maximum errors, between truncates **103, 137, 102, 138, 25, 23** and hemicalide (**1**)*

	$\Sigma|\Delta\delta_H|$ (ppm)[†]	**Max $|\Delta\delta_H|$ (ppm)**	**$\Sigma|\Delta\delta_C|$ (ppm)**	**Max $|\Delta\delta_C|$ (ppm)**
1. 13,18-*syn* acid 103	**0.05**	**0.01**	**0.8**	**0.1**
2. 13,18-*syn* salt **137**	0.08	0.02	1.7	0.2
3. 13,18-*anti* acid **102**	0.22	0.04	4.1	0.6
4. 13,18-*anti* salt **138**	0.22	0.04	4.3	0.7
5. Cossy 13,18-*anti* acid **25**	0.26	0.04	3.8	0.5
6. Full skeleton (13,18-*anti*) **23**	0.20	0.03	4.3	0.8

[†] Absolute errors taken from H/C8 to Me24. $|\Delta|$ = δ(experimental) – δ(reported)

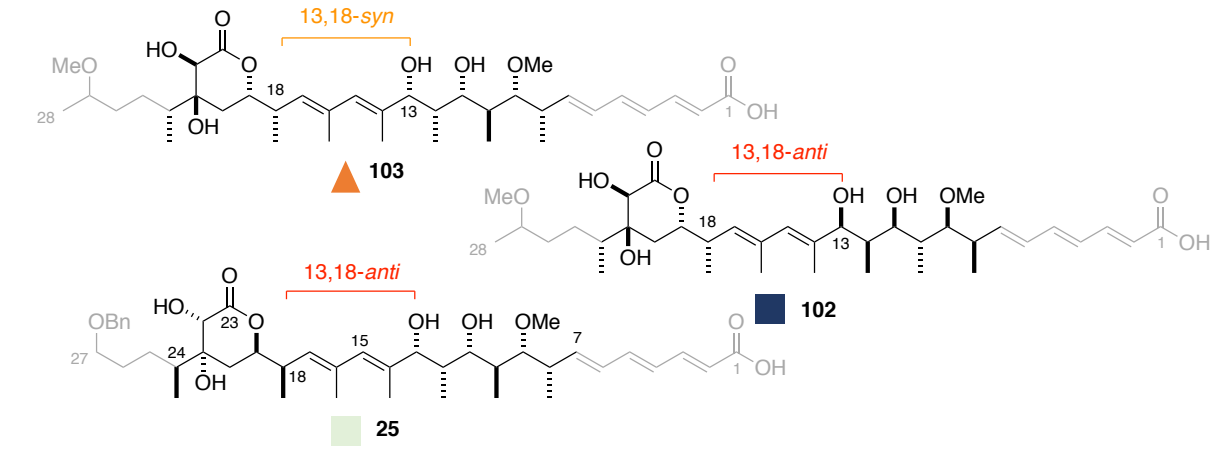

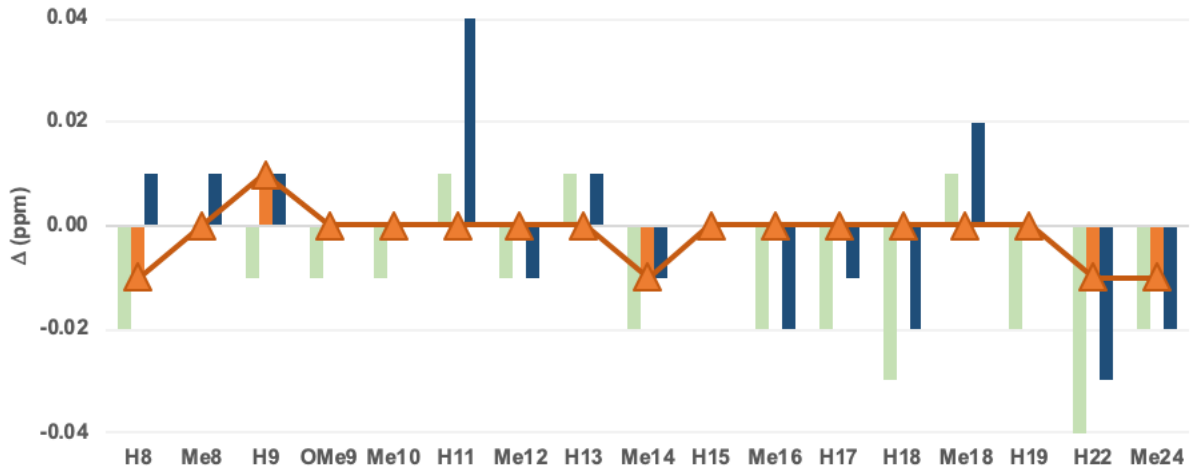

Figure 22. *Bar graph comparing [1]H NMR shift difference between* ***103****,* ***102*** *(Han),* ***25*** *(Ardisson/Cossy) and hemicalide (****1****)*

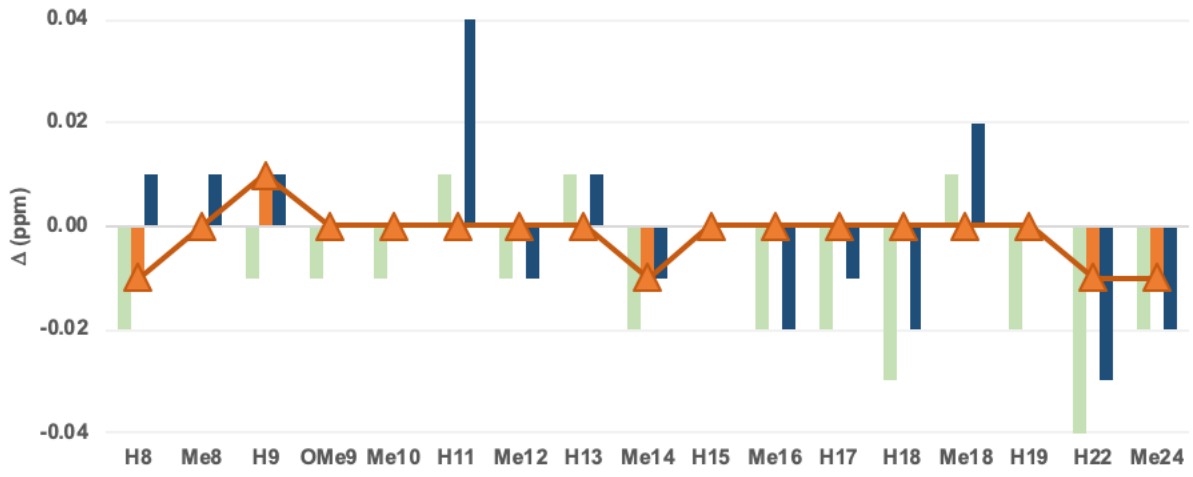

Figure 23. *Bar graph comparing [13]C NMR shift difference between* ***103****,* ***102*** *(Han),* ***25*** *(Ardisson/Cossy) and hemicalide (****1****)*

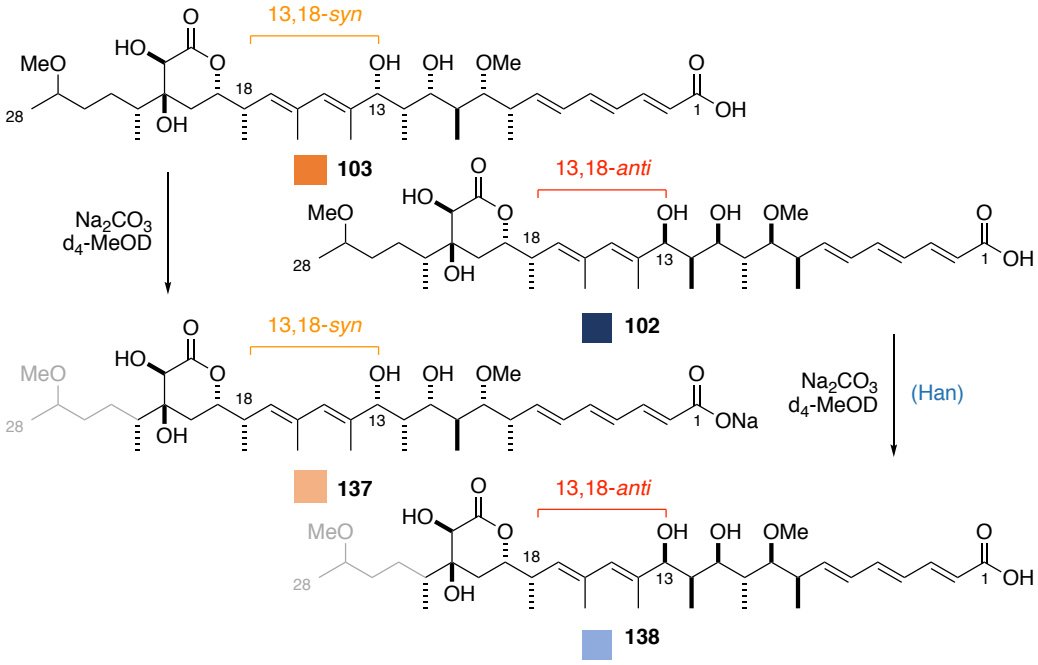

Scheme 21. *Transforming 13,18-syn acid* ***103*** *and 13,18-anti acid* ***102*** *to their corresponding carboxylate salts* ***137*** *and* ***138***

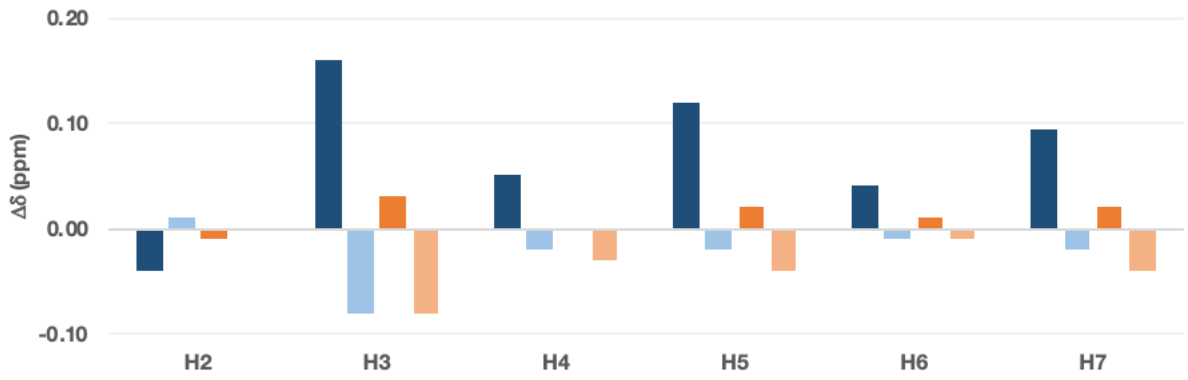

Figure 24. *Bar graph comparing* ^{1}*H NMR shift difference between* ***103, 102*** *(Han),* ***137, 138*** *(Han) and hemicalide (****1****) for H2-H7*

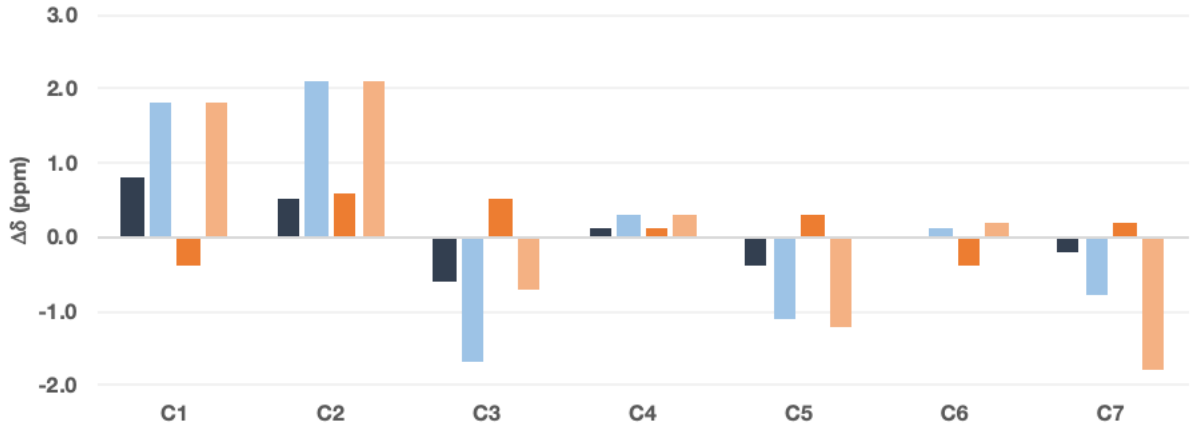

Figure 25. *Bar graph comparing* ^{13}*C NMR shift difference between* ***103, 102*** *(Han),* ***137, 138*** *(Han) and hemicalide (****1****) for C1-C7*

Initially, the poorer correlations were attributed to the unknown nature of the C1 counterion, but this was quickly dismissed as a plausible explanation for two reasons: Firstly, the choice of a polar 'protic' NMR solvent (d_4-MeOD), suggests that any counterion would not remain strongly bound to the C1 carboxylate. Secondly, the presence of a counterion would have minimal effects on the overall electronics of the C1-C7 system, which was what was indirectly observed by inspecting the NMR shifts. At this point, it was noted that the trienoic acid ^{1}H NMR resonances acquired during the purification of the free acid appeared to linearly move following HCl workup, chromatographic purification (with MeOH/AcOH), during drying and finally in its fully deprotonated state (**Figure 26**). This highlighted a chemical shift dependence of the C1-C7 trienoic acid region on the protonation state of C1. The implications of this points towards the fact that hemicalide was likely isolated as the free acid, which upon several rounds of chromatographic purification, was spectroscopically analysed in its partially deprotonated state *rather* than isolating the parent natural product as its carboxylate salt. Importantly, as this effect did not extend beyond the C1-C7 trienoic acid region, all the conclusions obtained from the NMR studies for the C8-C24 region of the 13,18-*syn* and 13,18-*anti* free acids **103** and **102** can be taken with confidence.

Overall, the excellent homology of 13,18-*syn* truncate **103** points towards the 13,18-*syn* configuration between the C1-C15 and the C16-C25 region in hemicalide, contrary to what was reported. Additionally, these findings refuted Ardisson's original claim that hemicalide was isolated as the carboxylate salt, suggesting instead that the natural product was isolated as the free acid and spectroscopically analysed in its partially deprotonated state. However, a full confirmation of its stereochemistry must wait until the natural product has been synthesised and its biological activity compared.

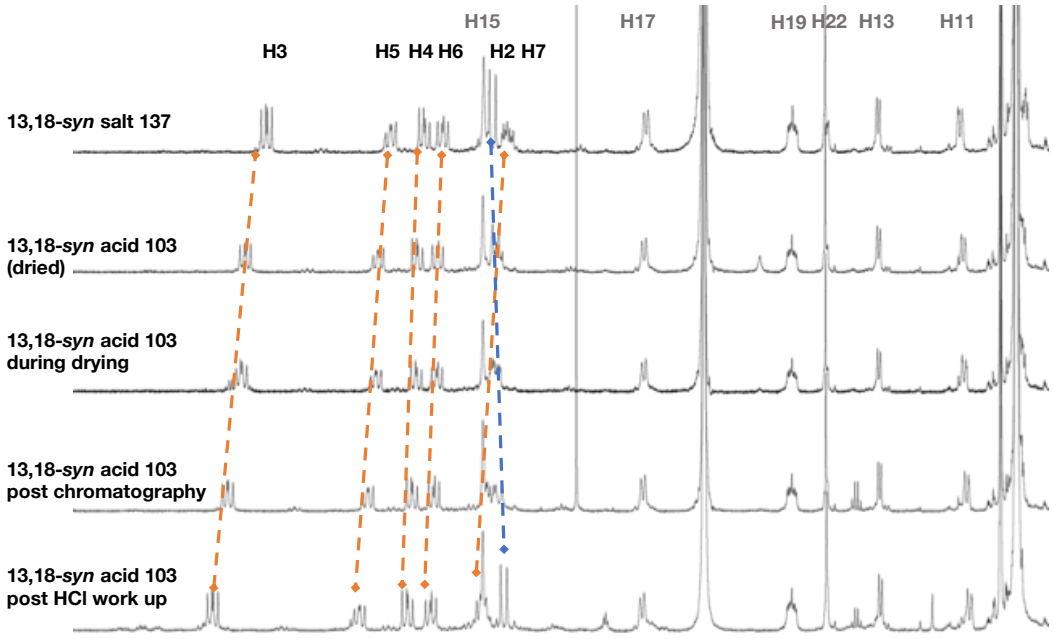

Figure 26. *Series of ^{1}H NMR spectra highlighting the chemical shift dependence of the C1-C7 trienoic acid region on the protonation state of C1. Note that signals beyond C8 do not exhibit this effect on various C1 protonation states*

4. Hemicalide: Conclusions and Future Work

4.1. Conclusions

The results described in this chapter detail the successful synthesis of a model 13,18-*syn* C1-C28 truncate of hemicalide for spectroscopic comparisons with the natural product, as summarised in **Scheme 22**. This was enabled by a scalable synthesis of the enantiomeric C16-C28 fragment ***ent*-53** in 5.5% overall yield over 18 steps in the LLS from (*R*)-Roche ester (*R*)-**26**. Alongside with the corresponding 13,18-*anti* diastereomer as synthesised by Han, this resulted, for the first time, in a detailed NMR comparison between the two possible configurations for the C1-C15 and the C16-C25 regions of the molecule. In doing so, this revealed that the 13,18-*syn* diastereomer was a far closer fit to hemicalide as opposed to the 13,18-*anti* configuration reported by Ardisson/Cossy.[51] This conclusion was made more robust with the good homology of Han's 13,18-*anti* truncate **102** with both the C1-C27 truncate **25** and the full carbon skeleton **23** by Cossy, giving confidence that the 13,18-*anti* configuration is clearly an incorrect diastereomer for hemicalide. In light of the previous work conducted by the Ardisson/Cossy and Paterson groups described at the beginning of this chapter, this result further reduces the number of candidate diastereomers of hemicalide from over 2 million down to 128. This fortunate result arising from the assignment of the distal 1,6-related stereoclusters augurs well for the synthesis-enabled stereochemical elucidation of hemicalide.

Secondly, the synthesis of the diastereomeric acids has allowed the interrogation of the claim that hemicalide was isolated as the carboxylate salt. The observed chemical shift dependence of the C1-C7 region of the molecule to the C1 protonation state along with poorer correlations for the salts of both truncates led to the conclusion that hemicalide was isolated as the free acid instead.

Moreover, this synthesis validated several key steps in the endgame that are useful for the ongoing synthetic campaign towards hemicalide. Notably, the highly effective Stille coupling as a fragment union strategy between the C1-C15 and the C16-C28 regions of the molecule, as well as providing useful intelligence into the endgame of the synthesis, including the seemingly inexplicable silyl deprotection step. Finally, the scalable synthesis of the enantiomeric C16-C28 fragment has ensured a ready supply of advanced productive intermediates that will be useful for the ongoing total synthesis campaign by Stockdale.

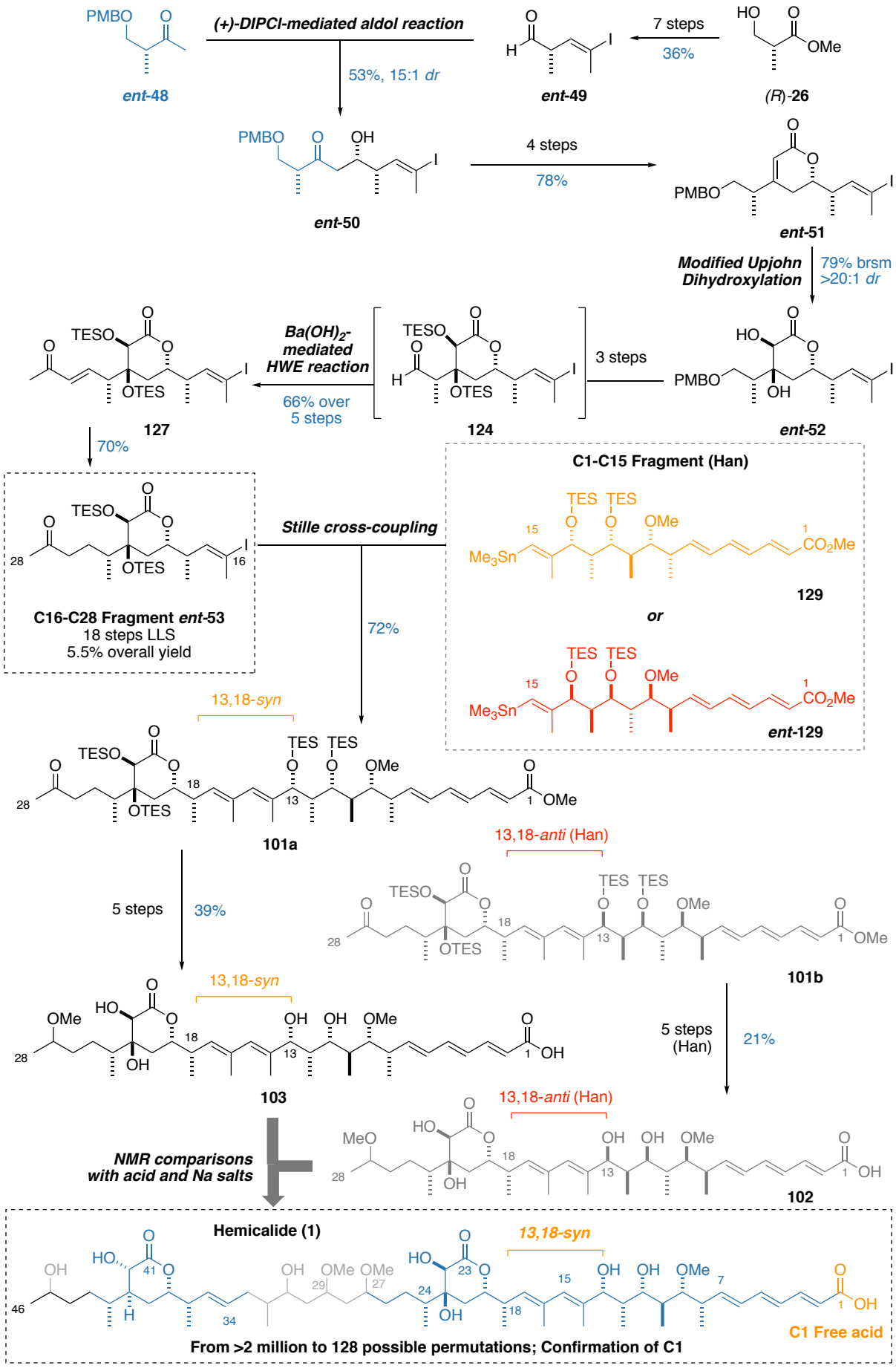

Scheme 22. *Summary of current progress towards hemicalide (**1**) as outlined in this chapter*

4.2. Future work

The successful synthesis of the C1-C28 truncate, while validating and confirming several key steps important in the planned total synthesis of the natural product, marks a significant milestone towards the end goal of a synthesis-enabled stereochemical elucidation of hemicalide. As such, this section will detail the immediate future work pertaining to the C1-C28 truncate, as well as how key lessons in this synthesis can inform how best to tackle the remaining regions of the molecule.

4.2.1. Future work in the C1-C28 fragment

The inability to remove all silyl protecting groups in one operation merits further attention in the continued strategy evolution. The peculiar reactivity may be partly attributable to the hindered nature of the TES groups in the dihydroxylactone compared to ones on the C1-C15 region. While a degree of chemical orthogonality could be useful for the site-selective incorporation of covalent modification, such as linkers in an ADC context, the lack of a common set of deprotection conditions across all silyl groups, especially right at the end of a synthetic campaign, only serves to hinder efforts in total synthesis. To this end, an immediate improvement that may benefit the desilylation efficiency could be the incorporation of more labile TMS groups (as exemplified in **139**) rather than TES groups in this region (**Scheme 23a**). The strategic use of TMS groups has proven instrumental in the context of several total syntheses, such as leiodermatolide[70] and rhizopodin,[79] and perhaps would allow the facile deprotection at the end of the synthesis. Here, the judicious choice of protecting groups is a particularly important consideration in light of Ardisson/Cossy's recent failures at the global deprotection of the full skeleton of hemicalide.[47]

The stereochemical elucidation of the C1-C28 truncate marks an important proof-of-concept study for the ability to assign the relative configuration of hemicalide from only the listed ^{1}H and ^{13}C NMR chemical shifts. However, for a full elucidation of its stereochemistry as well as looking ahead towards analogue design, the absolute configuration of hemicalide needs to be determined. Given that direct NMR techniques are unable to ascertain a molecule's absolute configuration, the only piece of information that could aid determining the absolute configuration of hemicalide is its biological activity. As the C1-C28 fragment constitutes over 60% of the natural product, it is hypothesised that this truncate may exhibit activity in cancer cell lines. Here, the synthesis of the enantiomeric 13,18-*syn* C1-C28 truncate ***ent*-103** would allow a comparison with **103**. By identifying the more active truncate from enantiomers of the C1-C28 region, this can give an indication towards which enantiomeric series to pursue for a total synthesis (**Scheme 23b**). If these truncates prove to be active, **103** and ***ent*-103** can also serve as probes towards ascertaining the as-yet unknown biological mode of action and begin to develop a comprehensive SAR study for this otherwise elusive natural product. Altogether, beginning to examine the biological properties of the C1-C28 truncate can be a revealing exercise in the context of developing hemicalide as a novel anticancer agent.

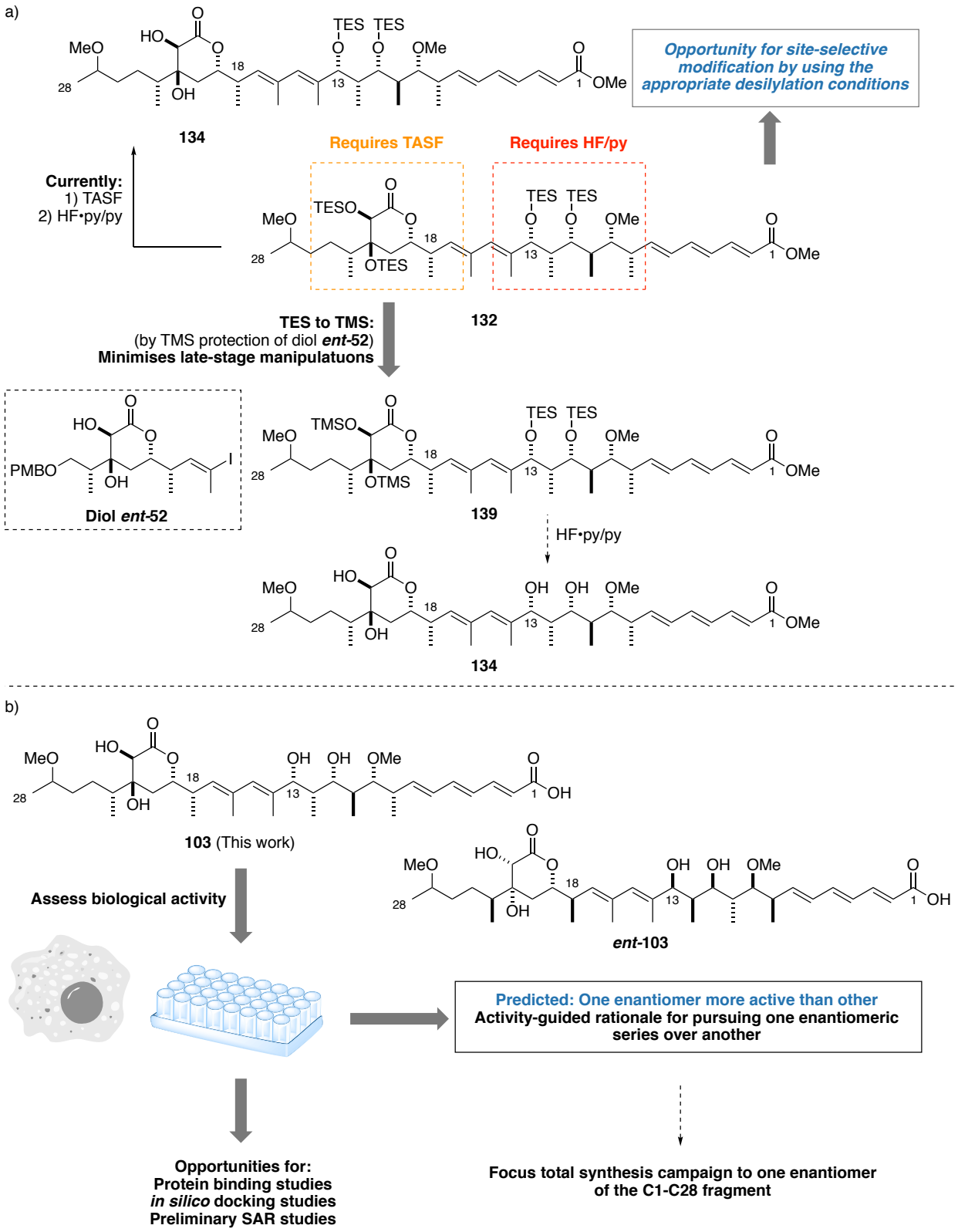

Scheme 23. *a) Replacing the inert C21 and C22 TES ethers for more labile TMS ethers in* ***139*** *should allow for a more facile global deprotection. b) Assessing the biological activity of truncates* ***103*** *and its enantiomer* ***ent-103*** *can help illuminate the likely correct enantiomer for hemicalide, as well as revealing needed data on how hemicalide may exert its mechanism of action*

4.2.2. Beyond the C1-C28 region: towards the stereochemical elucidation of hemicalide

The C32-C46 region of hemicalide contains a hydroxylactone motif that is structurally analogous to the synthesised C16-C25 fragment. Therefore, intelligence gathered from exploratory studies during the synthesis of the C16-C25 dihydroxylactone was anticipated to be broadly useful towards developing a robust synthesis of the terminal C35-C46 hydroxylactone.

During the synthesis of model truncate **102** and **103**, exploratory studies were conducted to see what the best method was to configure C27 relative to the dihydroxylactone. Unsurprisingly, enantioselective methods (e.g. MeCBS-catalysed borane reductions) proved ineffective owing to the poor steric differentiation around the prochiral carbonyl. This outcome was deemed unimportant as the resulting C27 stereocentre was planned to be set *via* an enantioselective aldol reaction, but the same process cannot be applied to the analogous C45 stereocentre. The steric hypothesis led to a test scale CBS reduction on enone **127**, posited to be a better substrate owing to the 'larger' alkene unit compared to the methyl group, which delivered the allylic alcohol **140** in useful selectivities (5:1 *dr*) (**Scheme 24a**). This outcome resulted in the overall retrosynthetic analysis for the C35-C46 region (**141**), where the distal C45 alcohol can be set in either configuration *via* a CBS reduction using the appropriate catalyst (**Scheme 24b**). While it was originally thought that a directed hydrogenation mediated by a suitable homogenous catalyst may allow the selective removal of the allylic olefin to give **142**, test scale studies on model substrates failed to deliver any activity. This led to the incorporation of a benzyl protecting group at C35, anticipated to be concomitantly cleaved alongside with the reduction of the C43 double bond over Pd/C under hydrogenative conditions. To this end, Stockdale has obtained promising results validating this route towards the C32-C46 hydroxylactone (see **Scheme 7** in section **2.3.3)** and has highlighted how the observations made during the synthesis of the C16-C25 fragment have assisted us in the strategy development for the C35-C46 hydroxylactone.

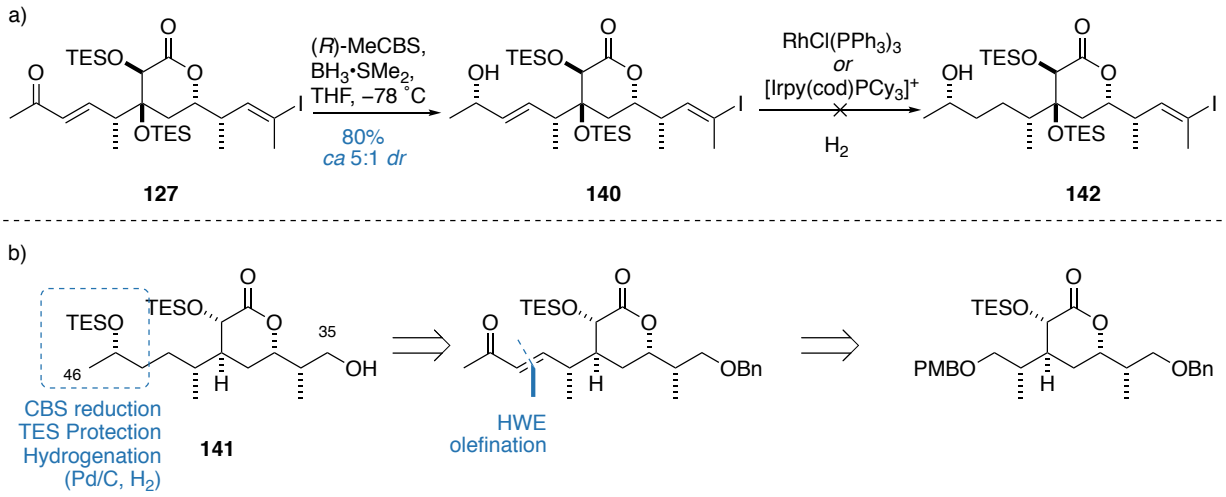

***Scheme 24**. a) Attempt at the enantioselective reduction of C27. b) Results from preliminary studies guiding the Paterson group approach to the C35-C42 hydroxylactone as currently conducted by Stockdale*

The configurationally elusive C27-C32 polyacetate region, containing four stereocentres, ideally needs to be elucidated before coupling with either the C1-C25 region, or the C35-C46 hydroxylactone. To this end, Han has completed preliminary efforts towards building a library of model compounds for spectroscopic comparisons with the natural product (**Figure 27**), which, in comparison with the data presented by Cossy (see **Figure 14** in section **2.2.3**), should allow for the clear elimination of unlikely diastereomers in this region. Here, even eliminating a few possibilities drastically reduces the number of diastereomeric possibilities to consider.

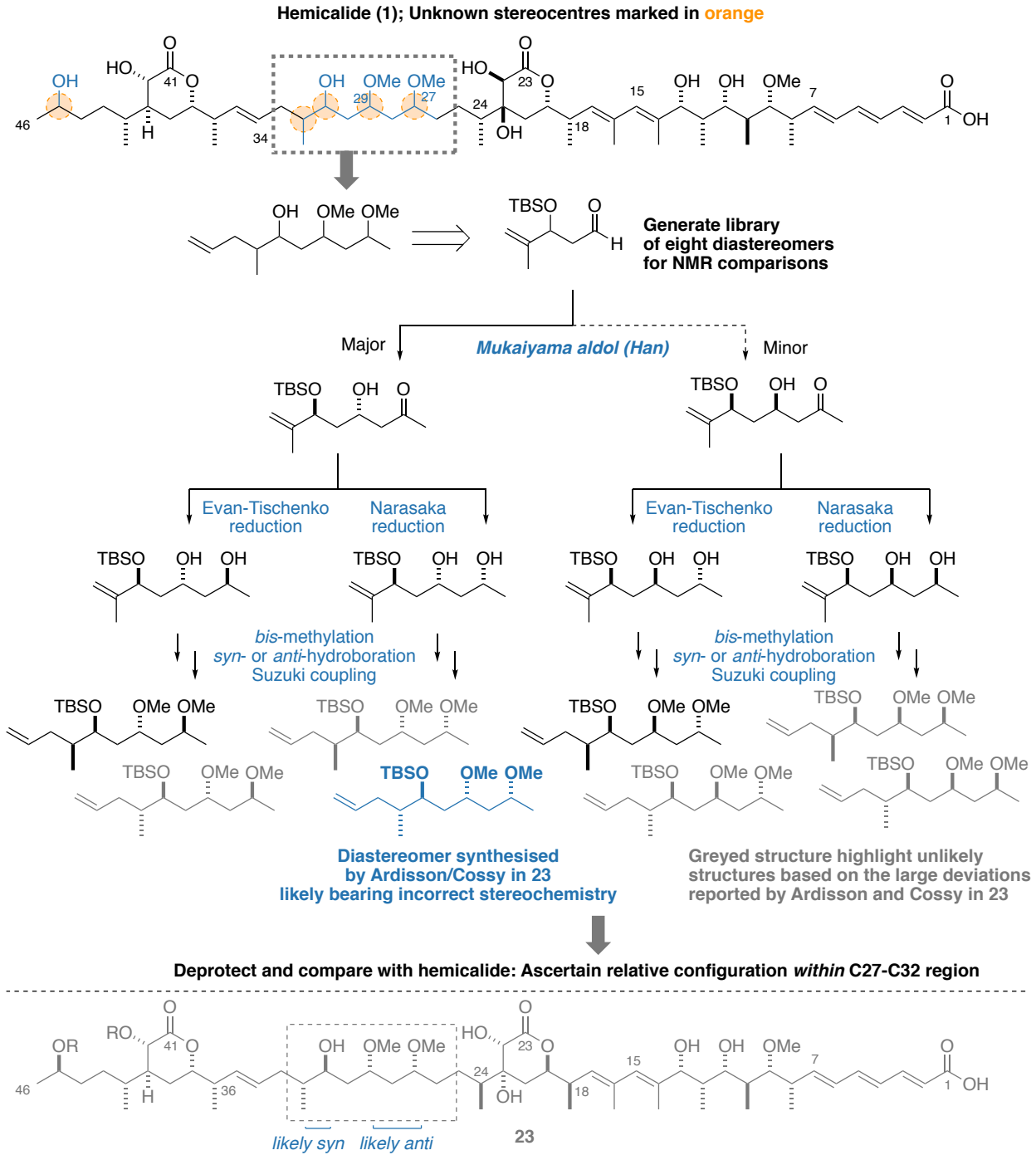

Figure 27. *Preliminary efforts by Han in generating a library of diastereomers for the C27-C32 region, compared with Ardisson/Cossy truncate* ***23*** *which likely bears the wrong configuration in the C29-C32 region*

To probe the diastereomeric relationship between the C27-C32 and the C35-C46 regions, a modular approach can be developed by employing a cross-metathesis disconnection across C34-C35, which thermodynamically favours the formation of *E*-olefins (**Scheme 25**).[80] In doing so, this allows the facile appendage of alkene **103a** with candidate C27-C32 truncates, deemed to contain the most probable configuration in hemicalide. This can help rapidly narrow down the possibilities for the remaining segment of hemicalide down to a more tractable number. Once the likely diastereomers for the C27-C46 region are identified, a focused synthesis of the C29-C46 aldehyde can take place. In this case, the cross-metathesis partner – alkene **143** – contains two stereocentres, that can be set up by an enantioselective crotylation of a suitably protected aldehyde **144**, followed by a hydroboration/oxidation/Wittig olefination sequence. Alkene **143** can then engage in a cross-metathesis reaction with the C35-C46 alkene **103a**, of which the resulting truncate can be treated under Swern conditions, anticipated to result in the concomitant primary TES group cleavage and oxidation[81] to give the required C29-C46 aldehyde **145** in anticipation for the planned endgame sequence.

The C1-C28 ketone **146** and the C29-C46 aldehyde **145** can then be subjected to the enantioselective DIPCl-mediated aldol reaction to configure C29, followed by either a 1,3-*syn* or 1,3-*anti* reduction to configure C27 – marking the assembly of all 21 stereocentres in hemicalide. *Bis*-methylation of the resulting diol gives the fully protected skeleton of hemicalide **147**. A global deprotection mediated by HF·py/py would then remove all silyl protecting groups, including the now more labile C21 and C22 TMS ethers, followed by methyl ester hydrolysis to give diastereomeric candidates of hemicalide.

At this point, detailed NMR comparisons with hemicalide can then be undertaken to further refine the number of diastereomeric candidates. Any particularly close matches with the natural product can be tested in cancer cell lines, which alongside with the biological data obtained for enantiomers of the C1-C28 fragment, can help point towards the likely absolute stereochemistry of hemicalide.

The present chapter detailing the synthesis-enabled stereochemical elucidation of the C1-C28 truncate of hemicalide, while representing a milestone towards the overall narrative, exemplifies the power of synthesis and spectroscopic analysis in discerning a molecule's relative configuration. These preliminary results give confidence that a full stereochemical assignment of a molecule as complex as hemicalide, from sparse initial NMR data, is indeed possible.

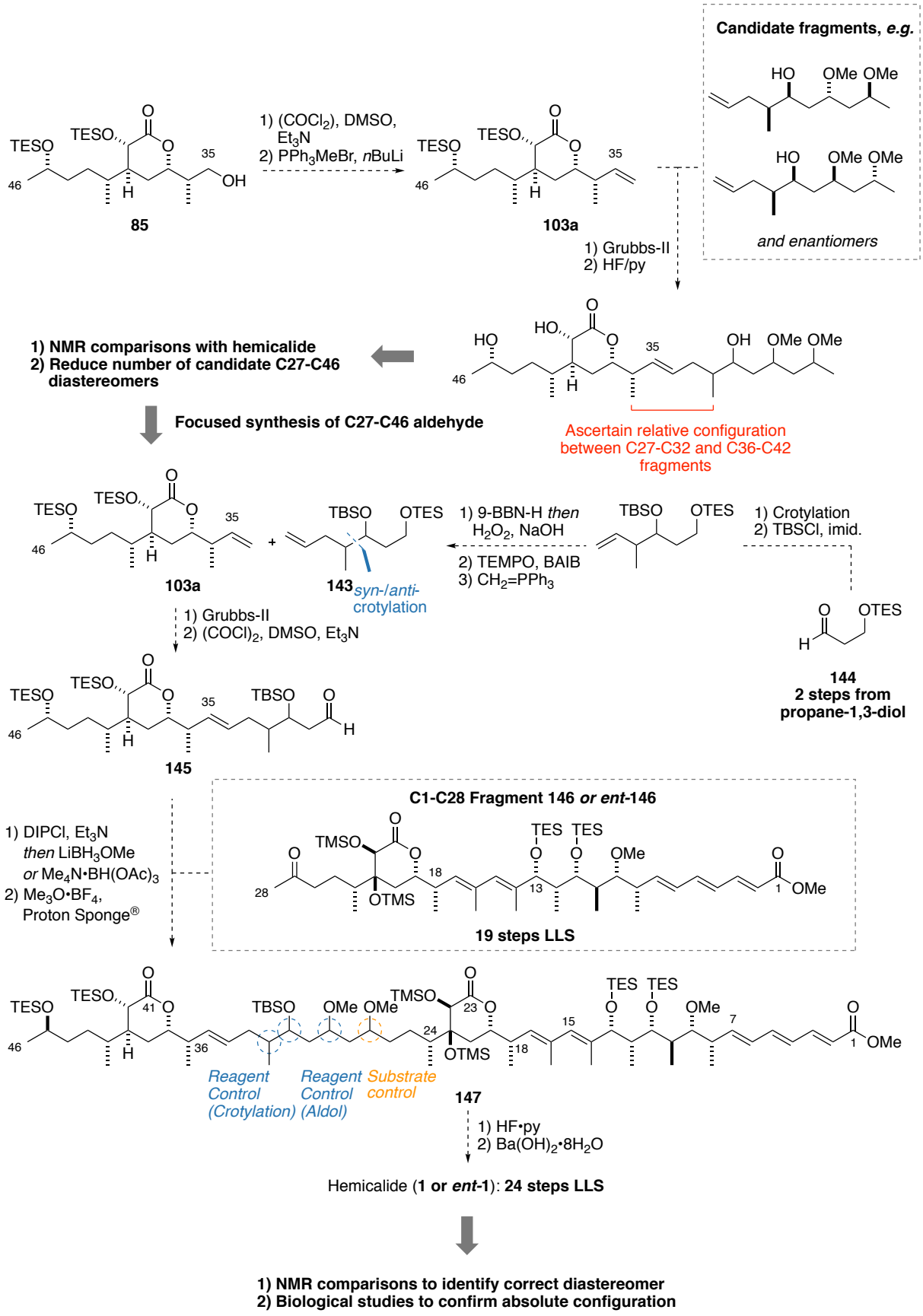

Scheme 25. *Illustration of the proposed workflow for the stereochemical elucidation of hemicalide (**1**), and a proposal for the endgame of the total synthesis. BAIB = bisacetoxyiodobenzene*

Part III - Phormidolide A

5. Introduction

5.1. Isolation and biological activity of phormidolide A

Phormidolide A (**2**) was reported by Williamson *et al.* in 2001, as part of a campaign to discover novel natural product anticancer leads.[2] The compound was isolated from the marine cyanobacteria *Leptolyngbya* sp.[82‡] collected off the coast of Sulawesi, Indonesia.[2] Culture of the bacteria, extraction and chromatography yielded 10–20 mg of phormidolide A from 7–10 g of wet biomass.

During its isolation, Williamson *et al.* found that the crude cyanobacteria extract showed potent and specific inhibitory activity towards the Ras-Raf protein-protein interaction.[2] Such interaction is an important component within the mitogen-activated signal transduction cascade mediating cell division, which is often upregulated in various cancers, making the active compound attractive as a drug target.[83] While separation of the mixture gave phormidolide A as the major component, interestingly, it was found to be inactive in the National Cancer Institute (NCI) *in vitro* 60-cell line assay, though it did exhibit potent brine shrimp toxicity (LD_{50} = 1.5 μM).[2,84] Instead, activity-guided isolation revealed a novel, but as-yet unreported, chlorophyll-type pigment completely unrelated to phormidolide A.[2]

For a compound of this architectural complexity, present in relatively abundant quantities in the organism, to exhibit no significant *in vitro* activity is an intriguing observation. As the cyanobacteria must expend a significant proportion of its metabolic resource in its biosynthesis, Williamson *et al.* surmised that phormidolide A must have an adaptive significance for the organism,[2] perhaps playing a role in deterring predators. The exact biological mechanism of action of phormidolide A remains unknown.

---

‡ The original isolation paper stated that the cyanobacteria *Phormidium* sp. produced phormidolide A; hence the etymology of the compound's name. A later analysis published by Bertin et *al.* showed that the producing cyanobacteria was misclassified, and was in fact derived from the *Leptolyngbya* sp.[82]

5.2. Structural and stereochemical determination of phormidolide A

The planar structure of phormidolide A was determined using a combination of HRMS, 1D- and 2D-NMR experiments. Recognising that type I polyketides are synthesised endogenously from acetate and propionate building blocks,[85] a ^{13}C-enriched sample of phormidolide A was obtained by supplementing the cyanobacteria culture with ^{13}C-enriched acetate. This allowed the elucidation of its skeletal connectivity by observing ^{13}C-^{13}C couplings through Incredible Natural Abundance Double Quantum Transfer Experiment (INADEQUATE) NMR experiments. At this point, the authors noted the homology in NMR data compared to a related natural product oscillariolide (**148**), discovered a decade prior by Murakami et *al.*, both containing the unique bromomethoxydiene motif not found in any other natural products (**Figure 28a**).[2,86] For the internal olefins of phormidolide A, the double-bond geometry was determined to be all *E* through the combination of coupling constant analysis (large $^{3}J_{HH}$ value for C4-C5) and diagnostic NOE correlations (for all remaining olefins) (**Figure 28b**). NOE correlations within the C13-C16 THF ring allowed the assignment of the relative stereochemistry of this region, which agrees with that assigned in oscillariolide (**148**).

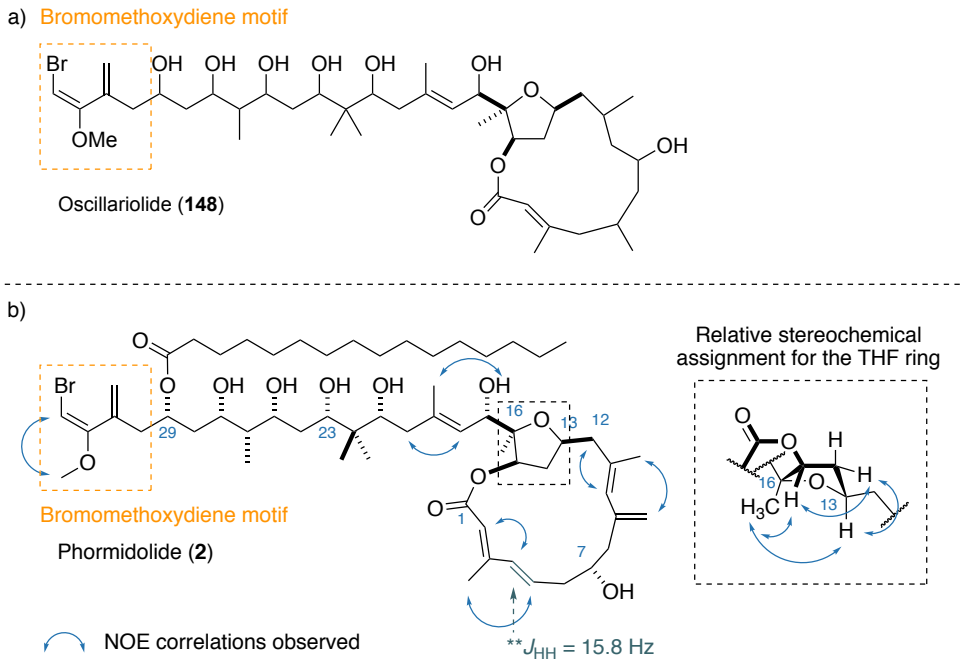

Figure 28. *a) The planar structure of oscillariolide (**148**). Note that the original isolation report did not assign the relative and absolute configuration of the macrolactone and side chain.[86] b) NOE correlations observed in phormidolide A used to determine olefin geometries and the relative configuration of the THF*

5.2.1. Relative configuration of C18-C33 region of phormidolide A

The relative stereochemistry for the remainder of the molecule was determined by a combination of *J*-based configurational analysis and chemical derivatisation. The 1,3-*syn* relative stereochemistry of the OH groups on C21, C23, C25 and C27, was determined through forming the diacetonide derivative **149** of phormidolide A with 2,3-dimethoxypropane and PPTS (**Figure 29a**). Rychnovsky's ^{13}C NMR analysis[87] of the diacetonide and the observed NOE enhancements led to the *syn* assignment within the C21-C23, and C25-C27 stereoclusters in accordance with the characteristic ^{13}C NMR signals observed for *syn* 1,3-diols. Here, the *syn*-acetonide occupies a chair conformation, where the axial and equatorial methyl groups on the acetonide resonate at *ca.* 19.5 and 30.0 ppm respectively, as shown in **Figure 29a**. Notably, the alternative 1,3-*anti* diol forces the acetonide into a twist-boat geometry, where both methyl groups are in a pseudoequatorial environment and resonate at *ca.* 25.0 ppm.[87]

The relative configuration of the polyol side chain was then determined and corroborated by detailed coupling constant analysis. This was conducted with the assumption that acyclic systems exist in a series of staggered rotamers. Murata's *J*-based configurational analysis was then applied to determine the favoured conformer by taking into account NOE correlations, $^{2,3}J_{CH}$ and $^{3}J_{HH}$ coupling constants.[13,88] $^{3}J_{HH}$ and $^{3}J_{CH}$ coupling constants follow the Karplus relationship, such that substituents with small torsion angles (i.e. a *gauche* relationship) give smaller *J* values, whereas large torsion angles (i.e. an *anti* relationship) give larger *J* values.[13,89,90] $^{2}J_{CH}$ shows the relationship between a proton and an oxygen on the adjacent carbon, where small and large $^{2}J_{CH}$ values indicate *anti* and *gauche* respectively.[13] The combination of *J* values and NOE correlations then allow the unambiguous determination of the favoured rotamer and hence the relative configuration at a specific carbon.

By way of example, the assignment of C29 relative to C27 can be obtained by observing a large $^{3}J_{HH}$ coupling constant between H28b and H29, placing the two protons *anti* to each other. An additional NOE enhancement between H28b with Me26 supports a *syn* relationship between Me26 and H28b, which is substantiated by NOE enhancement of H28a to H29, H28 and H26 *but not to Me26*. Finally, the smaller $^{3}J_{HH}$ values for H28a supports a *gauche* arrangement between H27, H28a and H29, giving the *syn* configuration of C29 relative to C27; these diagnostic spectroscopic observations for the assignment of H29 are highlighted in **Figure 29b**. In combination with the acetonide analysis described above, the *J*-based analysis conclusively ascertained the all-*syn* relative configuration between C21, 23, 25, 26, 27 and C29 stereocentres.

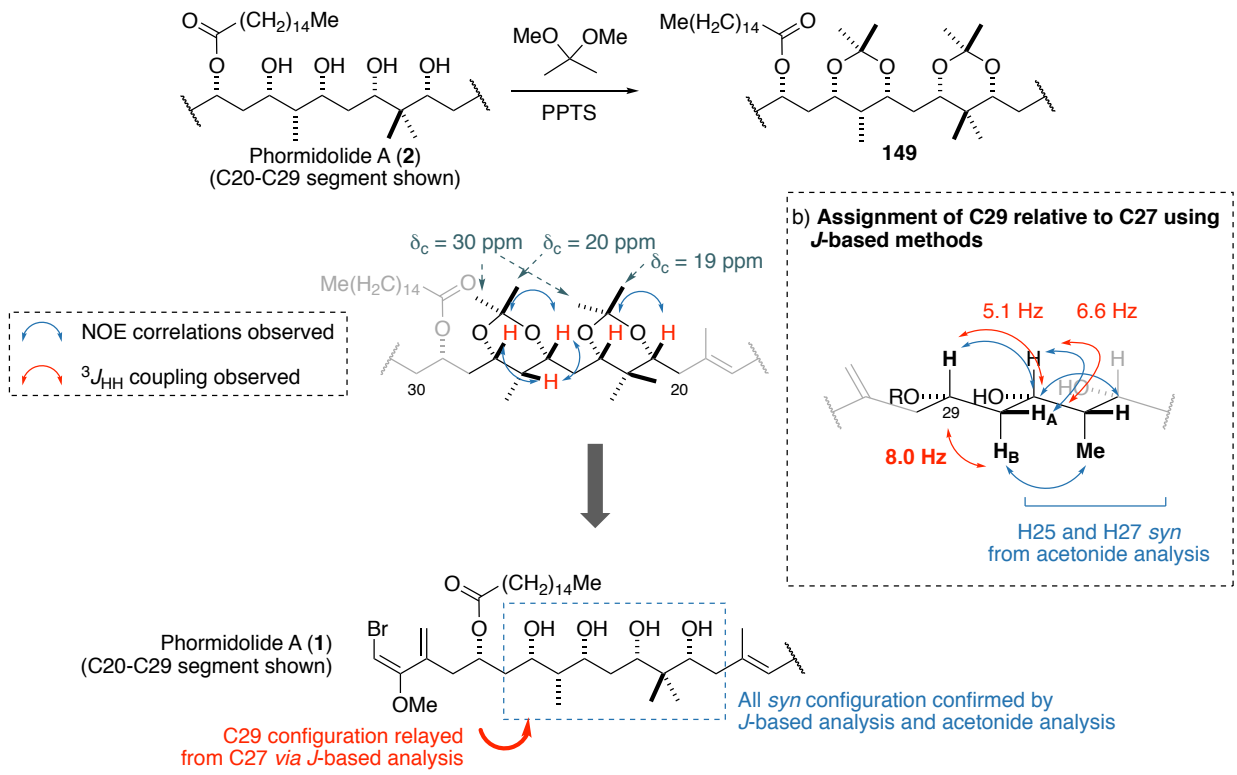

Figure 29. *a) Diacetonide derivative* ***149****, showing the diagnostic chemical shifts and NOE correlations, as well as the relative configuration between the C19-C21, and C23-C25 acetonides. b) Murata's J-based configurational analysis applied to the assignment of C29 relative to C27*

5.2.2. Relative and absolute configuration of C1-C18 region of phormidolide A

At this point, Williamson *et al.* extended the *J*-based methodology for the assignment of the remainder of the molecule, namely relaying the stereochemical information from C7 to the C13-C16 THF region, and onto the pendant side chain of phormidolide A. While there is strong evidence for the relative configuration of the C18-C33 side chain, the relative configuration between the macrolactone and the side chain is ambiguous based on the analysis presented. Williamson *et al.* assumed that stereochemical information can be relayed across planar sp^2 regions of the molecule, an assumption that is inconclusive unless there are direct long-range correlations between adjacent sp^3 centers on either side of the double bond. In the case of C7, the analysis tentatively predicted the reported relative configuration of C7 to the THF ring owing to the conformational requirement imposed by the macrolactone, eliminating the alternative configuration as a possibility (**Figure 30a**). While it appeared that there was conclusive evidence presented for the relative stereochemistry of C17 to the THF ring, the absence of a crucial long range interaction between the immediately adjacent sp^3 centers of the C18-19 olefin precluded a conclusive relative assignment of the macrolactone and the side chain (**Figure 30b**).

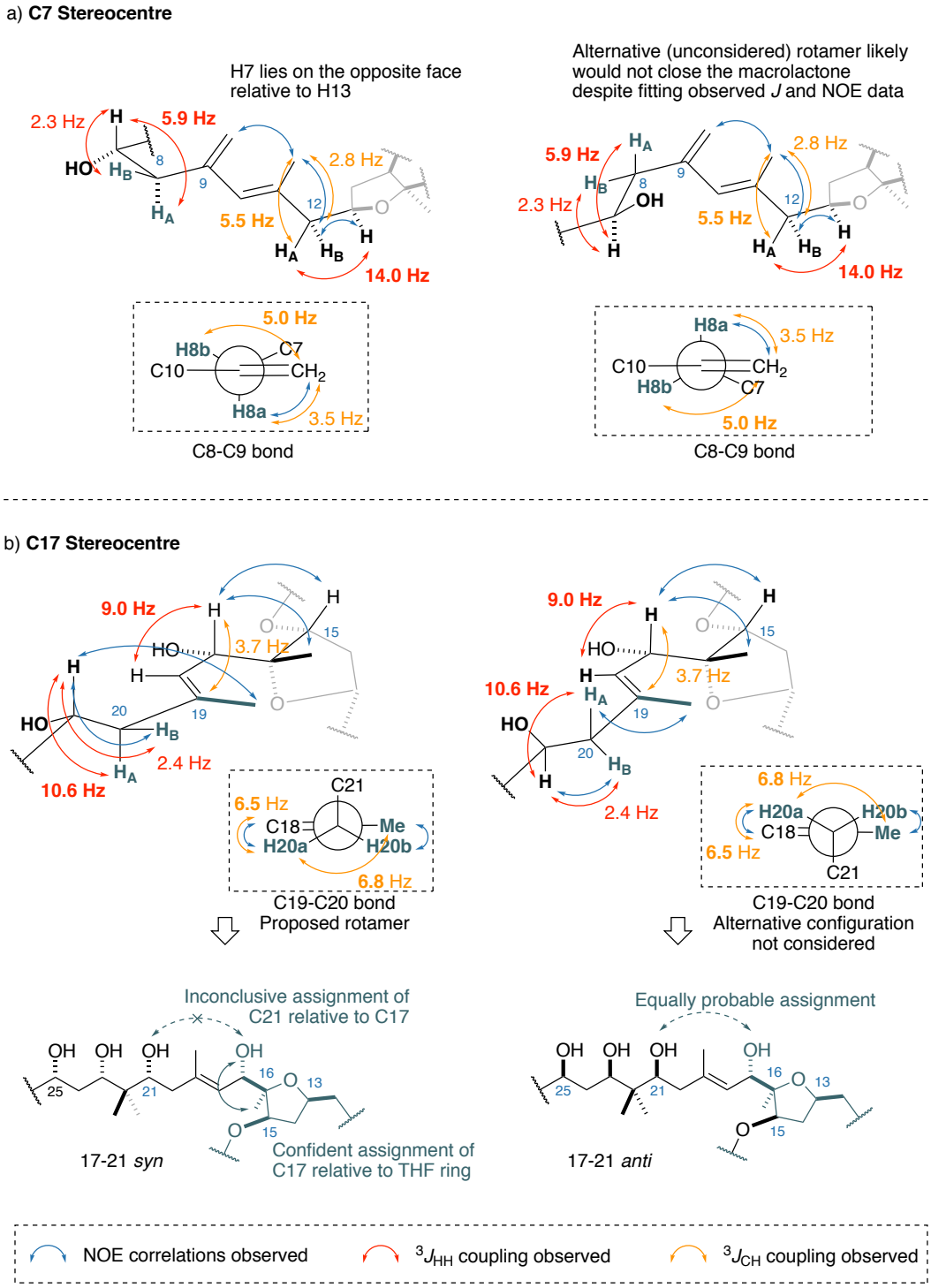

***Figure 30**. a) Determination of the stereochemistry at C7 relative to C13 b) Determination of the stereochemistry at C17 relative to C15 and C16. Key ^{1}H-^{1}H and ^{13}C-^{1}H coupling constants used to determine the relative configuration are highlighted, with large coupling constants displayed in **bold**.*

In the initial isolation report, the absolute stereochemistry of phormidolide A was determined by variable temperature NMR experiments on the di-(*R*)-methoxyphenylacetate (MPA) ester derivative **150** of the previously formed diacetonide, without requiring the synthesis of the diastereomeric ester (**Figure 31**).[91] As the stereochemistry of C7 was determined relative to the macrolactone, the absolute stereochemistry for the C1-C17 portion was assigned to be 7*R*, 13*S*, 15*R*, 16*R* and 17*R*. Williamson et *al.* extended the absolute configurational assignment to the remainder of the polyol side chain as 21*R*, 23*S*, 25*R*, 26*R*, 27*S*, 29*S*. However, the inconclusive evidence from the published *J*-based analysis (*vide supra*) precludes what we believe to be the definitive absolute stereochemical assignment of the C18-C33 region of phormidolide A relative to the macrolactone.

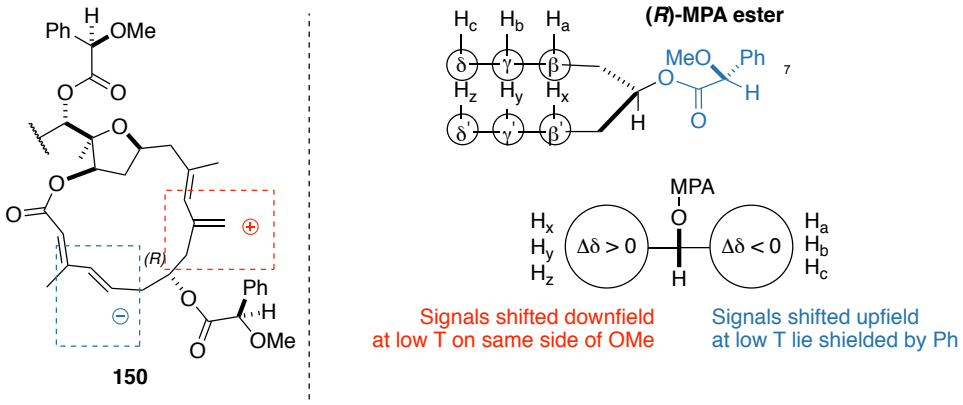

***Figure 31**. Fragment of the di-MPA ester derivative **150** of phormidolide A diacetonide shown, highlighting the assignment of the C7 stereocentre without requiring the diastereomeric ester as described by Latypov et al.*[91]

5.2.3. The biosynthesis of phormidolide A and its stereochemical implications

A subsequent publication from the Gerwick group elucidated the biosynthetic mechanism for the synthesis of phormidolide A through a combination of feeding experiments and bioinformatics.[82] As described previously, the carbon skeleton for phormidolide A is primarily derived from acetate metabolism, with ^{13}C NMR enhancements observed for C1-C30 when the cyanobacteria was supplemented with ^{13}C-carboxyl labelled acetate (**Figure 32**). The alternative ^{13}C-methyl labelled acetate on the other hand, showed enhancements at Me3, $=CH_2$9, Me11 and Me19, indicating that these centres were installed *via* the action of 3-hydroxy-3-methyl-glutaryl (HMG)-CoA synthase/dehydration sequence.[92] Furthermore, additional supplementation of ^{13}C-^{18}O-acetate indicated ^{18}O incorporation for all oxygens in the natural product except for the oxygen bridging C13 and C15 in the THF ring, indicating that the THF oxygen is not acetate derived. Finally, a feeding experiment conducted with *S*-(^{13}C-methyl)-methionine indicated that Me16, Me20a/b, Me26 and OMe32 arose from methyltransferase action with *S*-adenosoylmethionine as the methyl transfer reagent.

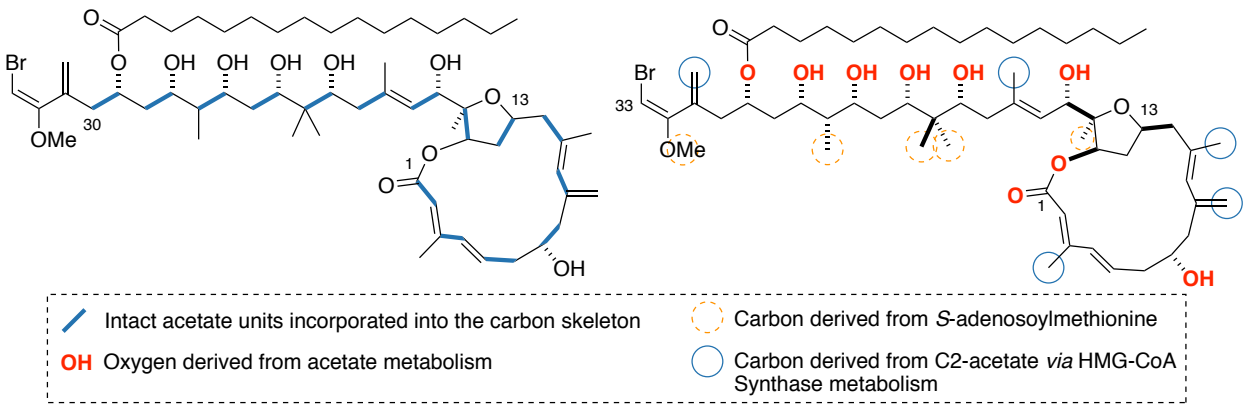

Figure 32. *Overview of atom sources of phormidolide A as determined by feeding studies (excluding the palmitoyl group)*

At this stage, only the THF ether oxygen and the atoms as part of the C31-C33 region of phormidolide A were left unaccounted for. To probe the source for C31-C33, the authors conducted additional feeding experiments with various carbon sources. While no incorporation was observed with labelled alanine, glycine and propionate, ^{13}C enrichment was observed with uniformly ^{13}C glucose. Surmising that the three-carbon fragment in this region was derived from metabolites from glycolysis,[93] the authors conducted additional feeding experiments with ^{13}C-labelled glycerate and pyruvate, though no further enrichment was observed in both cases. This putatively suggested that an upstream glycolytic intermediate from glycerate[94] was responsible for the C31-C33 region of phormidolide A (**Figure 33a**).

The observations obtained from the feeding experiments were used to guide the full characterisation of the gene cluster responsible for the biosynthesis of phormidolide A. Through sequence homology analysis, the authors found, among other enzymes, ten ketoreductases – responsible for setting the configuration of all carbinol stereocentres, four methyltransferases – responsible for Me16, Me20a/b, Me26 and OMe32 and an additional region containing HMG-CoA synthase and related tailoring enzymes, responsible for the installation of Me3, $=CH_2$9, Me11 and Me19. Finally, four enoyl-CoA hydratases were predicted to configure the C2, C4, C10 and C18 olefins. On top of this, the authors found a region encoding for a monooxygenase, explaining the origin of the THF ether oxygen, and a domain that specifically shuttles 1,3-bisphosphoglycerate into polyketide synthase pathways, pointing towards the biogenesis of the C31-C33 region. This allowed for the biosynthesis of phormidolide A to be proposed: following the dephosphorylation of 1,3-bisphosphoglycerate, the intermediate is transferred to the acyl carrier protein (ACP), where the substrate is dehydrated and *O*-methylated. An HMG-CoA synthase/decarboxylase sequence installs the C31 methylene before the chain is elaborated towards C1 from the action of ketosynthases and other modifying enzymes. The THF motif is postulated to be formed from a C-H hydroxylation at H16, followed by a cyclisation to close the five-membered ring. Finally, the full carbon skeleton of phormidolide A is released from the ACP *via* macrolactonisation onto C1, where further tailoring enzymes, including a halogenase and a fatty acid ligase, installs the terminal vinyl bromide and the C29 palmitoyl chain to complete the biosynthesis of phormidolide A (**Figure 33b**).

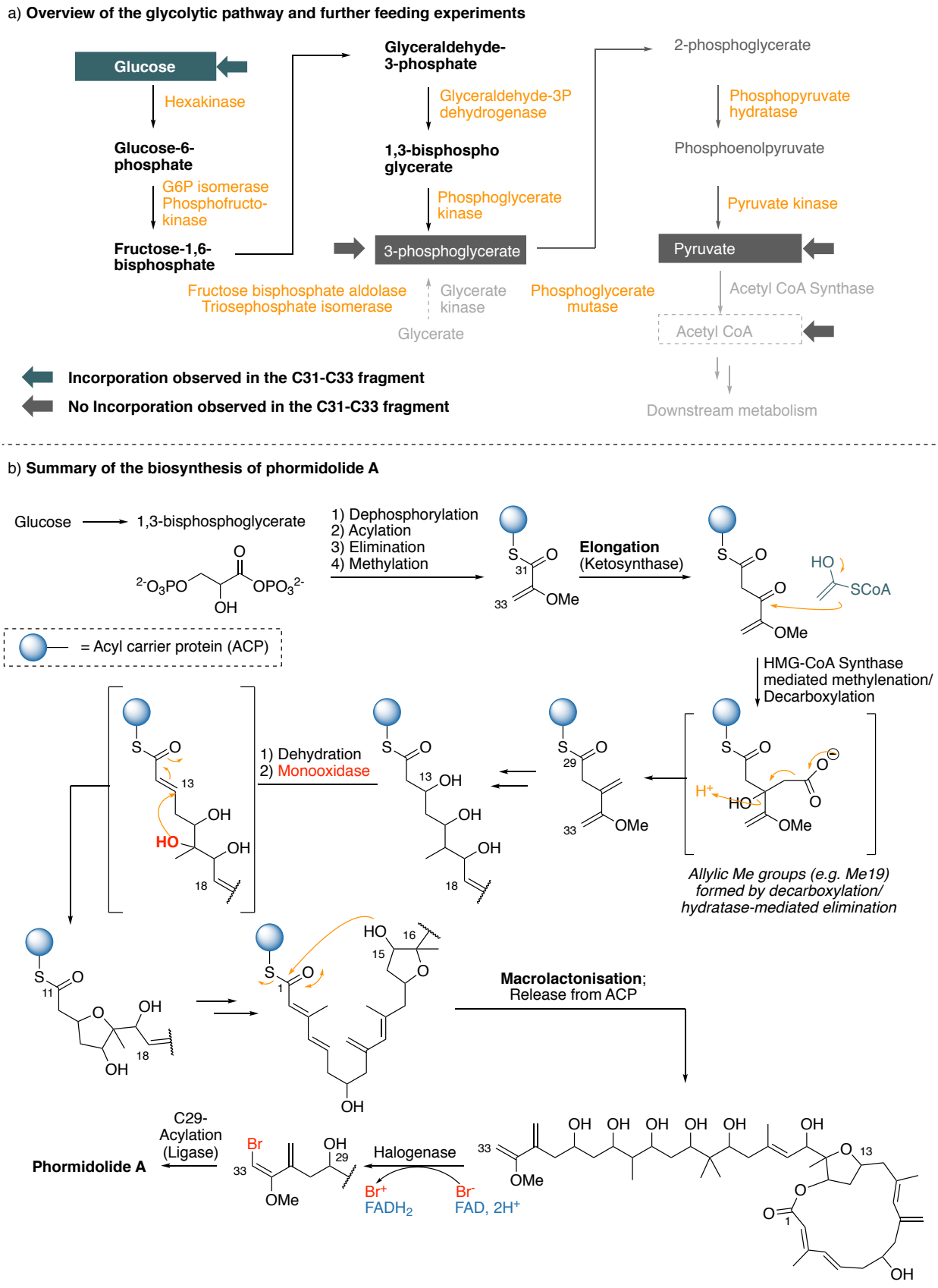

Figure 33. *a) The glycolysis pathway (enzymes coloured in orange) and the conclusions obtained from feeding studies to determine the source of the C31-C33 unit. Note that glycerate enters the glycolytic pathway via glycerate kinase.*[94] *b) Overview of the biosynthesis of phormidolide A, including the likely mechanisms for THF formation and vinyl bromide formation*

The full elucidation of the biosynthesis of phormidolide A was seen to be noteworthy for the resolving the stereochemical ambiguities previously identified. In polyketide natural products, the configuration at carbinol centres are set by the action of ketoreductases, of which specific amino acid residues in the enzymes' active site are considered to be particularly diagnostic for setting the absolute configuration of the carbinol centre.[95] Generally, Type A ketoreductases containing a conserved tryptophan (W) motif at the active site predictably generate L-configured hydroxyacyl motifs. Type B ketoreductases on the other hand, contain a conserved leucine-aspartate-aspartate (LDD) motif at the active site, of which the second aspartate located at residue 1758 (D1758) is considered to be particularly diagnostic for the generation of D-configured hydroxyacyl motifs (**Figure 34a**).[96] Analysis of the ketoreductase sequences showed that nine out of ten ketoreductases present contained the D1758 residue as typified in Type B ketoreductases, although none contained the signature LDD motif. The remaining ketoreductase – responsible for configuring C15 – did not contain signature amino acid residues that allowed for a straightforward classification. This data would have predicted that at least 90% of the carbinol stereocentres present in phormidolide A would be D-configured, directly challenging the proposed stereochemical assignment of the natural product (**Figure 34b**).

To investigate this incongruity, the authors synthesised the triacetonide derivative of phormidolide A (**151**) and generated the diastereomeric Mosher esters at C7, which were reported to confirm the 7*R* (7L) configuration originally reported by Williamson *et al.*. The authors resolved this contradiction by noting that several ketoreductases, despite containing the predictive D1758 residue, can anomalously give L-configured carbinol centres.[95] This logic was extended to the remainder of the natural product, citing that the D1758 residue was not considered to be predictive for generating the L-carbinol configuration in the biosynthesis of phormidolide A. This chain of reasoning however, in the author's opinion, fails to deliver a convincing argument for the stereochemistry of phormidolide A, especially when underscored by the ambiguous *J*-based analyses presented by in the original isolation paper.

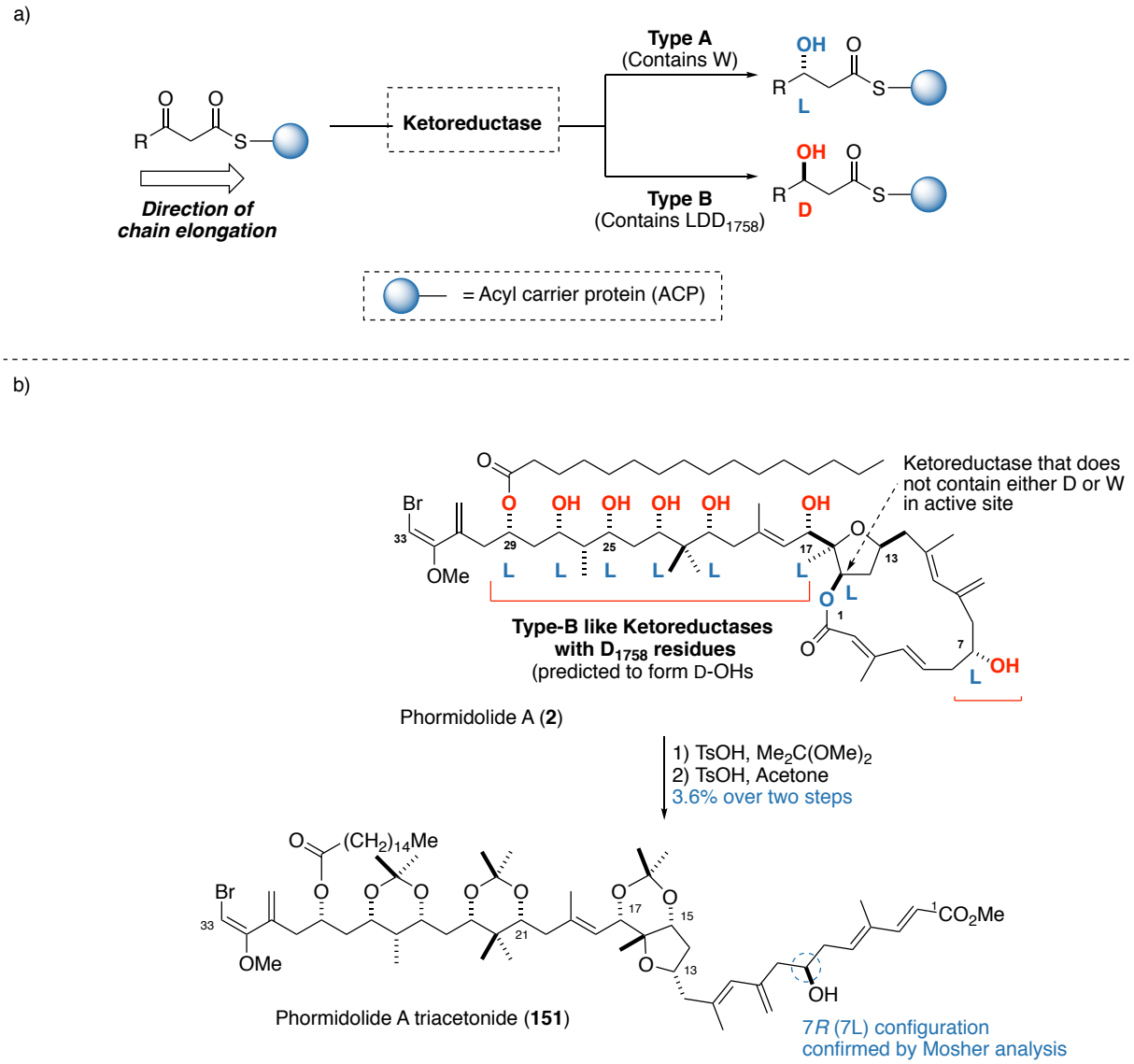

Figure 34. *a) General scheme highlighting the differential stereochemical outcome from Type A and Type B ketoreductases on a growing polyketide chain. b) Excerpt from the ketoreductase sequence responsible for the biosynthesis of phormidolide A*[82]*, highlighting the presence of the diagnostic D1758 residue predictive for D-OH. This is presented alongside an annotated diagram of phormidolide A, showing that despite the presence of D1758, all carbinols present in phormidolide A are L-configured.*

5.3. Related congeners to phormidolide A: oscillariolide and phormidolides B-D

As previously noted, phormidolide A shares a close structural homology with oscillariolide (*vide supra*), consisting of a near identical polyol side chain (minus the pendant C29 fatty acid) linked to a macrolactone containing an embedded tetrasubstituted THF ring.[86] Here, the main structural differences lie in the macrolactone ring; oscillariolide possesses a 14-membered macrolactone with a different substitution and unsaturation pattern compared to the 16-membered macrolactone of phormidolide A. The relative and absolute stereochemistry for the macrolactone ring of oscillariolide has, to date, not been determined.

In 2015, Lorente *et al.* reported the isolation of phormidolide B and C from sponges of the *Petrosiidae* family collected off the coast of Tanzania.[84] Phormidolide B (**152**) and C (**153**) differ only by the fatty acid appended on the side chain (**Figure 35a**). Their homology to phormidolide A and oscillariolide, both produced by cyanobacteria, suggest that both compounds were produced by symbiotic bacteria in the sponge.[82] Analogous to phormidolide A and oscillariolide, both phormidolide B and C contain the conserved polyol side chain, complete with the bromomethoxydiene motif at its terminus. Similar to oscillariolide, phormidolide B and C contain a 14-membered macrolactone with an embedded THF ring, differing in its oxygenation, substitution and unsaturation patterns. Notably, the THF ring for phormidolide B and C possesses a different relative configuration of its substituents and lacks the quaternary centre seen in both oscillariolide and phormidolide A.

In the original isolation report, the configuration of C3 in the macrolactone, alongside the C19-C27 side chain of phormidolide B and C were undefined. However, a later publication (and all subsequent publications thereafter) by the Álvarez group arbitrarily defined C3 in an *anti* relationship to C7 (**Figure 35b**) with no explicit justification given for their assignment.[97] Perhaps noting the structural homology to phormidolide A, the remainder of the side chain was defined in the same publication, with an analogous 15,19-*syn* relative configuration across the C16 double bond. While the authors claimed that the NMR data for macrocycle **154** were *"in accordance with* the (NMR shifts from the macrocycle) *described* (in) *phormidolide B and C"*, with any "*small difference*" attributed to the absence of the side chain, a cursory inspection of their published data showed large ^{13}C NMR shift deviations from the natural product that likely points towards a different macrocyclic configuration for phormidolides B and C (**Figure 36**).[§] To date, there have been no reports attempting to elucidate the absolute configuration for phormidolides B and C.

[§] The analysis conducted was limited by the fact that neither the ^{1}H or ^{13}C data published was assigned to any proton or carbon signals of the natural product.[97] Hence, a rudimentary ^{13}C NMR comparison was the only way to assess whether or not the published configuration was correct

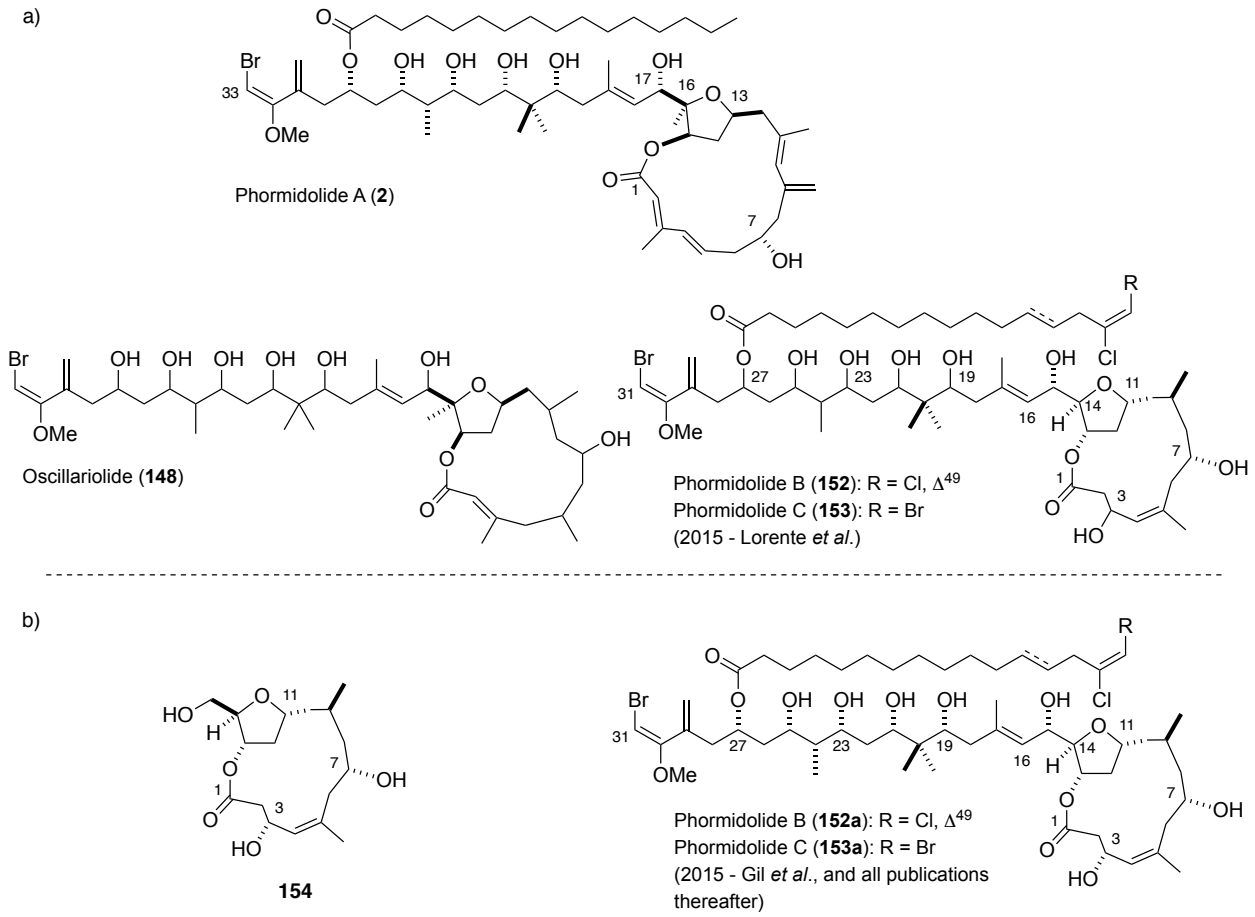

Figure 35. *a) Structures of phormidolide A, as compared with oscillariolide and the initially reported structures for phormidolides B and C. b) Subsequent reports by the Álvarez group gave an arbitrary assignment of C3 (relative to C7), as well as C19 relative to C15.*

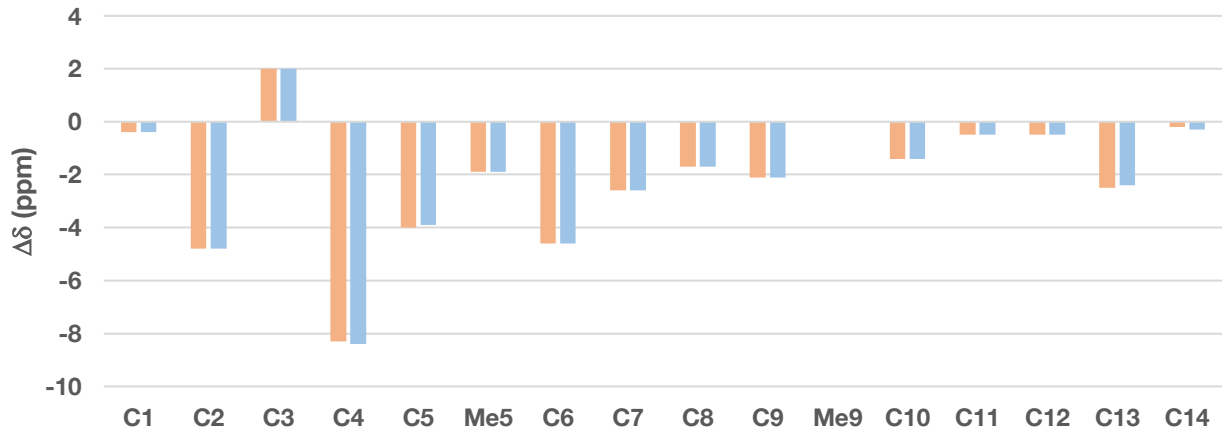

Figure 36. *Bar chart showing the ^{13}C NMR difference between macrocycle **154** with phormidolide B (**152**) (orange) and C (**153**) (blue). Note the particularly poor NMR correlation between the C1-C5 region, where very large deviations are observed*

While untested on cancer cell lines, oscillariolide was found to inhibit the division of fertilised starfish eggs at a concentration of 0.5 μg/mL, and higher concentrations resulted in uneven cell division.[86] Compared with phormidolide A's lack of observed cytotoxicity in the NCI 60 cell line assay, phormidolide B and C demonstrated low micromolar activity against lung (A-549), colon (HT-29) and breast (MDA-MB-231) cancer cell lines (**Table 6**), making them to date, the only compounds from the family to kill cancer cells. However, like phormidolide A and oscillariolide, the mechanism of action with which these molecules exert their cytotoxicity remains unelucidated.[97]

Table 6. *IC_{50} values (in μM) for phormidolide B and C in cancer cell lines*

	A-529 (lung)	**HT-29 (colon)**	**MDA-MB-231 (breast)**
Phormidolide B	1.4	1.3	1.0
Phormidolide C	1.3	0.8	0.5

Finally, the latest publication from the Álvarez group disclosed the identity of phormidolide D (**155**) as a synthetic target (**Figure 37**), despite no prior reference to its isolation or characterisation.[98] Phormidolide D is structurally identical to phormidolide C, differing only on the acyl chain, with phormidolide D containing a vinyl dichloride rather than a vinyl chlorobromide. Additionally, phormidolide D is structurally identical to phormidolide B except for an extra degree of saturation on the pendant acyl chain. While no explicit reference was made to its isolation, phormidolide D is a plausible congener given its very high degree of structural homology to related compounds, implying that all the synthetic machinery required for its biosynthesis is present. There was no biological data associated with phormidolide D, although one might assume that it would exhibit similar bioactivities to phormidolides B and C.

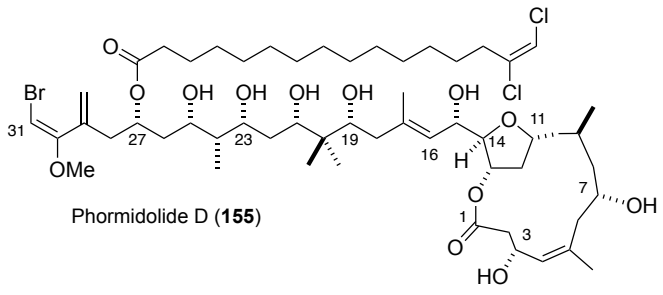

Phormidolide D (**155**)

Figure 37. *Structure of phormidolide D (**155**)*

5.4. Previous synthetic efforts towards congeners of phormidolide A

To the best of our knowledge, phormidolide A and oscillariolide have not been the target of a synthetic campaign since their isolation over a decade ago. The first members of the family to be synthetically targeted were phormidolides B-D, with initial studies reported by the Álvarez group in 2015.[84] This section will outline the synthetic efforts as reported by the Álvarez group towards phormidolides B-D.

5.4.1. Álvarez's synthesis of the macrolactone region in phormidolides B-D

As part of the initial isolation report, the Álvarez group disclosed a synthetic approach towards the 14-membered macrolactone present in phormidolides B, C (and D) to probe the configuration of the THF motif (**Scheme 26**). From 2-deoxy-D-ribose (**156**), a sequence involving a Wittig olefination/cyclisation as the main steps gave the substituted THF motif as a 1:1.5 mixture of C11 epimers, with the desired product **157** as the minor component**.** The required C9 stereocentre was installed *via* a diastereoselective conjugate addition of MeMgBr (>20:1 *dr*) into **158** to afford adduct **159**, with the facial selectivity of the addition dictated by the phenylalanine-derived oxazolidinone. Next, the C7 stereocentre was configured *via* a Paterson (–)-DIPCl-mediated aldol reaction between aldehyde **160** and the enolate derived from acetone, giving the aldol adduct **161** in 7:1 *dr*. The required Julia-Kocienski olefination was conducted with sulfone **162** and aldehyde **163** to give the trisubstituted olefin **164** in modest geometric control (2.3:1 *Z/E*). Subsequent manipulations revealed the *seco* acid, which was subjected to Yamaguchi macrolactonisation conditions to give the protected macrocycle **165** in modest yields (39%). Following the same sequence of reactions, the C14 epimer of the macrocycle could be obtained starting from 2-deoxy-L-ribose **166**, although curiously, the same macrolactonisation step generated a 5:1 mixture of C13 macrolactone epimers **167** and **168**.

The first-generation approach to the phormidolide B-D macrolactone was achieved in a modest 0.2% overall yield over 21 steps LLS from deoxyribose. In a later communication, the Álvarez group disclosed a second-generation synthesis of the same macrolactone,[97] employing a diastereoselective allylstannane addition as its key step (**Scheme 27**). Addressing the poorly selective cyclisation step in the synthesis of the THF core, the revised route employed a diastereoselective Sakurai allylation of **169** (itself derived in five steps from deoxyribofuranose **170**) to give alkene **171**. After ozonolysis of alkene **171**, an analogous route was employed to give aldehyde **172**. The synthesis of the allylstannane coupling partner started from the previously reported aldehyde **163**. A three-step procedure afforded xanthane **173**, whereby a [3.3]-sigmatropic rearrangement followed by stannylation under radical conditions gave allylstannane **174** as a mixture of isomers. Employing $SnCl_4$ as the Lewis acid allowed for a remarkably selective 1,5-*anti* allylation onto aldehyde **172** (>20:1 *dr*), configuring the trisubstituted olefin in **175** as a single geometry. This step was rationalised by the geometrically convergent trans-stannylation step with $SnCl_4$, affording a chelated structure **176**. Upon aldehyde addition, the Sn moiety could then chelate and activate aldehyde **172**,

enforcing a closed transition state where the aldehyde R group lies equatorial, and the bulky OTIPS group is projected away from the ring. Though undiscussed, it is also conceivable that additional selectivity in this reaction can be conferred through further chelation of the C1 acyloxy group onto the Sn Lewis acid, rigidifying the overall transition state geometry. Finally, improvements to the overall macrolactonisation process were achieved by using Shiina's protocol (67%) to give the protected macrocycle **177** in 3.7% overall yield over 16 steps LLS from D-deoxyribose. Across both routes, the Álvarez group did not report any evidence for the definitive assignment of C3, which appears to be inconclusive based from the data presented (see discussion in section **5.3**; *vide supra*).

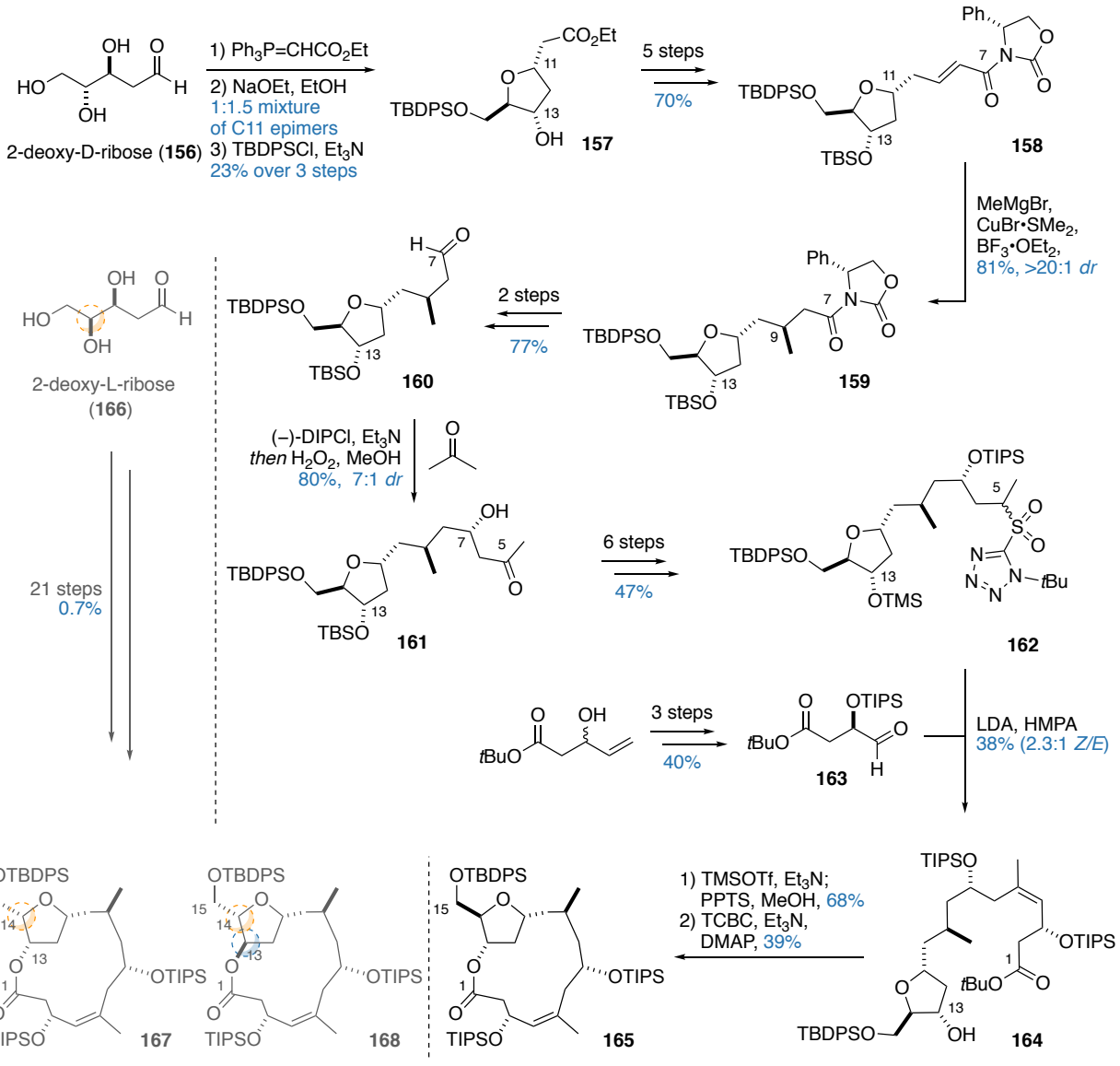

***Scheme 26**. First generation route towards macrocycle **165, 166** and **167** as reported by the Álvarez group.*

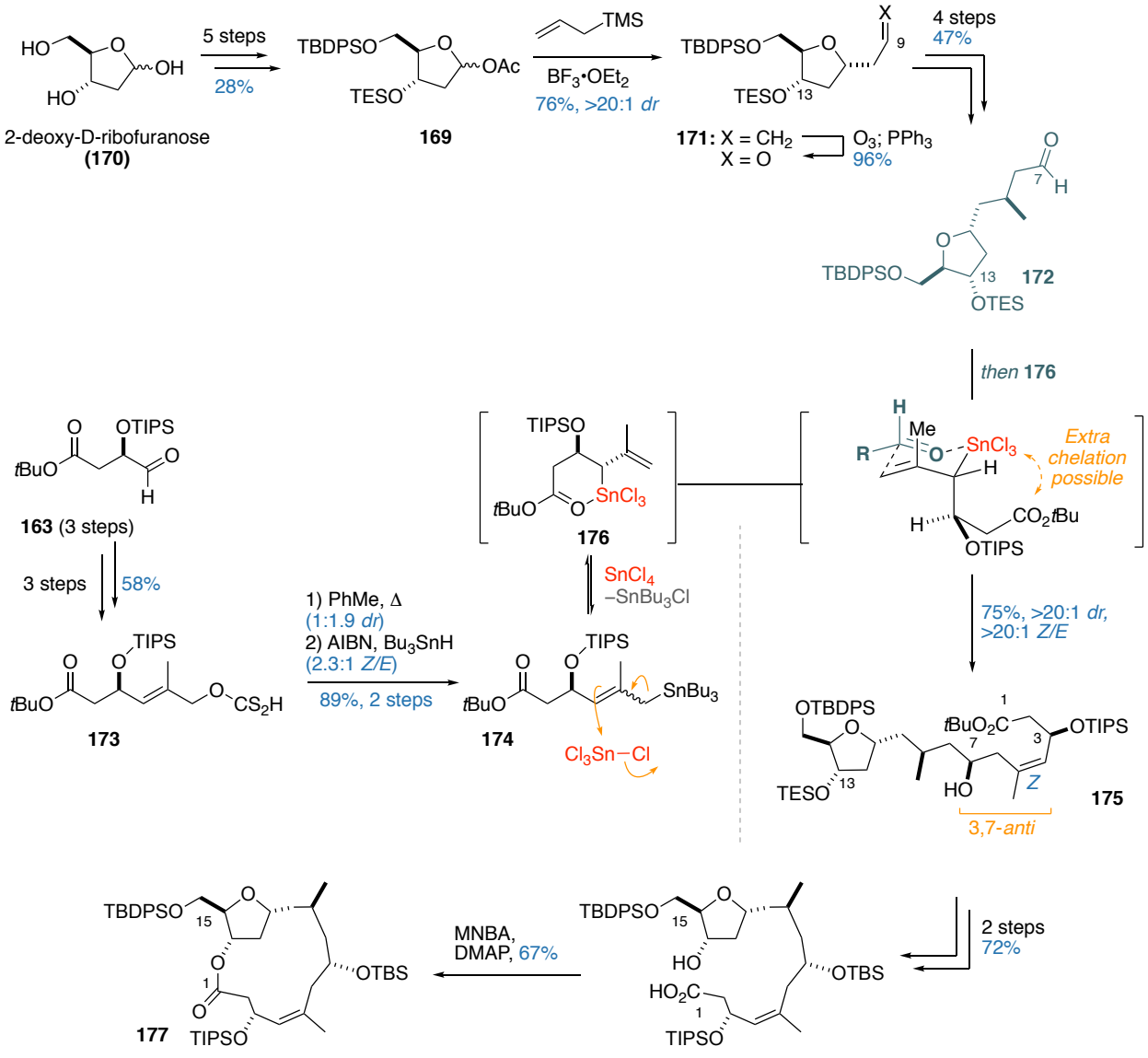

Scheme 27. *Second-generation route by the Álvarez group employing a diastereoselective allylstannane addition to generate macrocycle* ***177****. AIBN = Azobisisobutyronitrile*

5.4.2. Álvarez's approach towards the side chain of the phormidolides

More pertinent to the planned total synthesis of phormidolide A was a recent publication from the Álvarez group, which highlighted their efforts towards synthesising the conserved polyol side chain common to oscillariolide, and phormidolide A, B and C.

Focusing on what arguably appears to be the most delicate portion of the polyol side chain, the Álvarez group achieved the synthesis of the conserved bromoenol ether moiety based on chemistry developed by Edvardsen et *al.*,[99] and demonstrated its coupling to a model side chain fragment (**Scheme 28a**).[100] Beginning with 1,3-dibromo-2,2-dimethoxypropane (**178**), treatment with acetyl bromide followed by dehydrobromination yielded the bromoenol ether as a 1:1 *E*/*Z* mixture.[99] UV irradiation successfully isomerised the double bond to the required *E* geometry in a 49:1 *E*/*Z* ratio. The methyl ketone *E*-**179** was installed through acetoxylation followed by a series of redox adjustments and functional group manipulations to give ketone *E*-**179**. Despite what effectively is an eight-step 'functional group interconversion' sequence from acetone, the overall process requires only three chromatographic purifications, and is claimed to be workable on gram scale. The same report also disclosed more direct routes that failed to give the desired *E* geometry; the direct acid-mediated dehydromethoxylation of **180** gave the *Z* enol ether *Z*-**179** exclusively. Similarly, the base-mediated dehydrobromination of intermediate **181** singly gave the *Z*-**179** and attempts to isomerise *Z*-**179** either failed to give any reactivity or resulted in its degradation.

Using this chemistry, the Álvarez group published a follow-up account on employing fragment *E*-**179** as a productive precursor for their approach towards the common polyol sidechain across all phormidolide congeners (**Scheme 28b**).[101] Starting with oxazolidinone ***ent*-27**, an Evans' *syn*-aldol followed by *mono*-PMB protection gave **182**, which after a two-step cleavage of the auxiliary gave aldehyde **183**, that underwent a Mukaiyama aldol reaction to give the major product **184** as dictated by Felkin-Anh control (6:1 *dr*). A four-step sequence then revealed aldehyde **185**, which engaged with the silyl enol ether **186** derived from ketone *E*-**179** to give the undesired C27[**] configuration **187** with excellent diastereoselectivity (>20:1 *dr*). At this point, two transformations were required to generate the protected side chain; a C29 ketone methylenation and configurational inversion at C27. To achieve this, Álvarez resorted to a three-step sequence (silyl protection, methylenation, silyl deprotection) to install the olefin in **188**, followed by a further three steps to invert C29 and acylate to give the protected C18-C31 fragment of phormidolide **189**. Overall, a synthesis of a representative side chain of the phormidolide congeners took 18 steps LLS and 19% yield from propan-

[**] Compound numbering for phormidolide B-D. This would correspond to C29 in phormidolide A

1,3-diol, with the installation of the methylene olefin and inversion and derivation of C29 accounting for six of those steps.

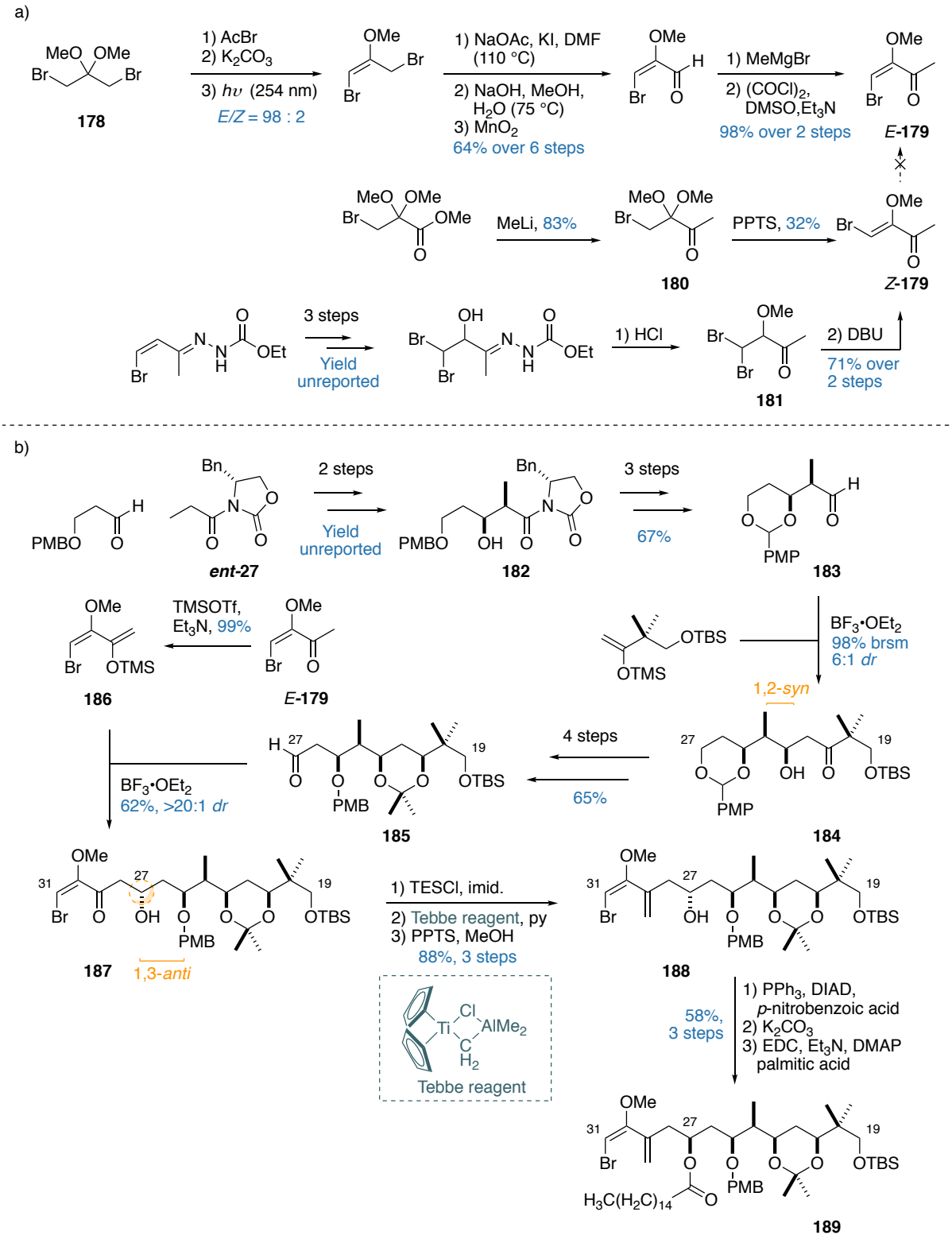

Scheme 28. *a) Synthesis of E-**179** as reported by the Álvarez group, presented alongside shorter routes that failed to deliver the same product. b) The Álvarez synthesis of the protected sidechain of the phormidolides **189***

Importantly, Álvarez's synthesis of the bromoenol ether fragment highlighted the reaction conditions this potentially delicate moiety can withstand. These included prolonged heating under basic conditions towards the synthesis of *E*-**179** (**Scheme 28a**), and as demonstrated in the synthesis of **189**, a surprising tolerance to both Lewis acidic and Brønsted acidic conditions. These results echoed the results from the Gerwick group where during the synthesis of the triacetonide derivative of phormidolide A, Bertin *et al.* showed that the parent natural product remained stable during prolonged acidic treatment with TsOH.[82]

5.4.3. Attempted endgame for phormidolide C and D as reported by Álvarez

With the synthesis of the two major fragments of phormidolides B-D reported, the Álvarez group disclosed two further reports on their attempts at effecting a fragment union between the side chain of the phormidolides with the macrocycle. A preliminary publication presented a study on the addition of vinylmetallic reagents into chiral formyltetrahydrofuran motifs present in phormidolides B and C[††] highlighted that a Nozaki-Hiyama-Kishi (NHK) reaction between model aldehyde **190** with vinyl iodide **191** was the most effective (**Scheme 29a**). This gave the adduct **192** in moderate yields (but modest isolated yields) with moderate diastereocontrol favouring the reported C15 geometry, which was deemed acceptable for a fragment coupling strategy.[102]

A more recent paper published concurrently with our group's ongoing campaign reported an attempted synthesis of phormidolides C and D.[98] In this report, the Álvarez group disclosed their overall retrosynthesis for the natural products, where an NHK reaction between aldehyde **193** and vinyl iodide **194** was proposed to elaborate the macrocycle and configure C15 (**Scheme 29b**). A Mukaiyama aldol reaction dictated by Felkin-Anh control was proposed to append on the C23-C31 side chain (**195**) and form the full carbon skeleton of phormidolide C-D, as previously demonstrated in the synthesis of **184**. The synthesis of vinyl iodide **194** required six steps from aldehyde **196**, involving a resolution of racemate **197** by the chromatographic separation of the diastereomeric (*R*)-methoxyphenylacetate esters of **197 (Scheme 29c)**. Despite its prior efficacy, the NHK reaction between aldehyde **193** and vinyl iodide **194** to afford **198** proved to be low yielding and delivered the undesired configuration. Finally, an attempt was made to realise the Mukaiyama aldol reaction between the silyl enol ether derivative of **198** and **199**, although no reaction was observed despite the analogous synthesis of **184** proceeding in high yield (see **Scheme 28b**). No concrete explanation was given for this disparate observation, although the authors did tentatively attribute the lack of reactivity to steric factors prohibiting silyl enol ether from being an effective nucleophile.

[††] This publication predated the disclosure of phormidolide D, but these results were employed in their studies towards the synthesis of phormidolides B and D

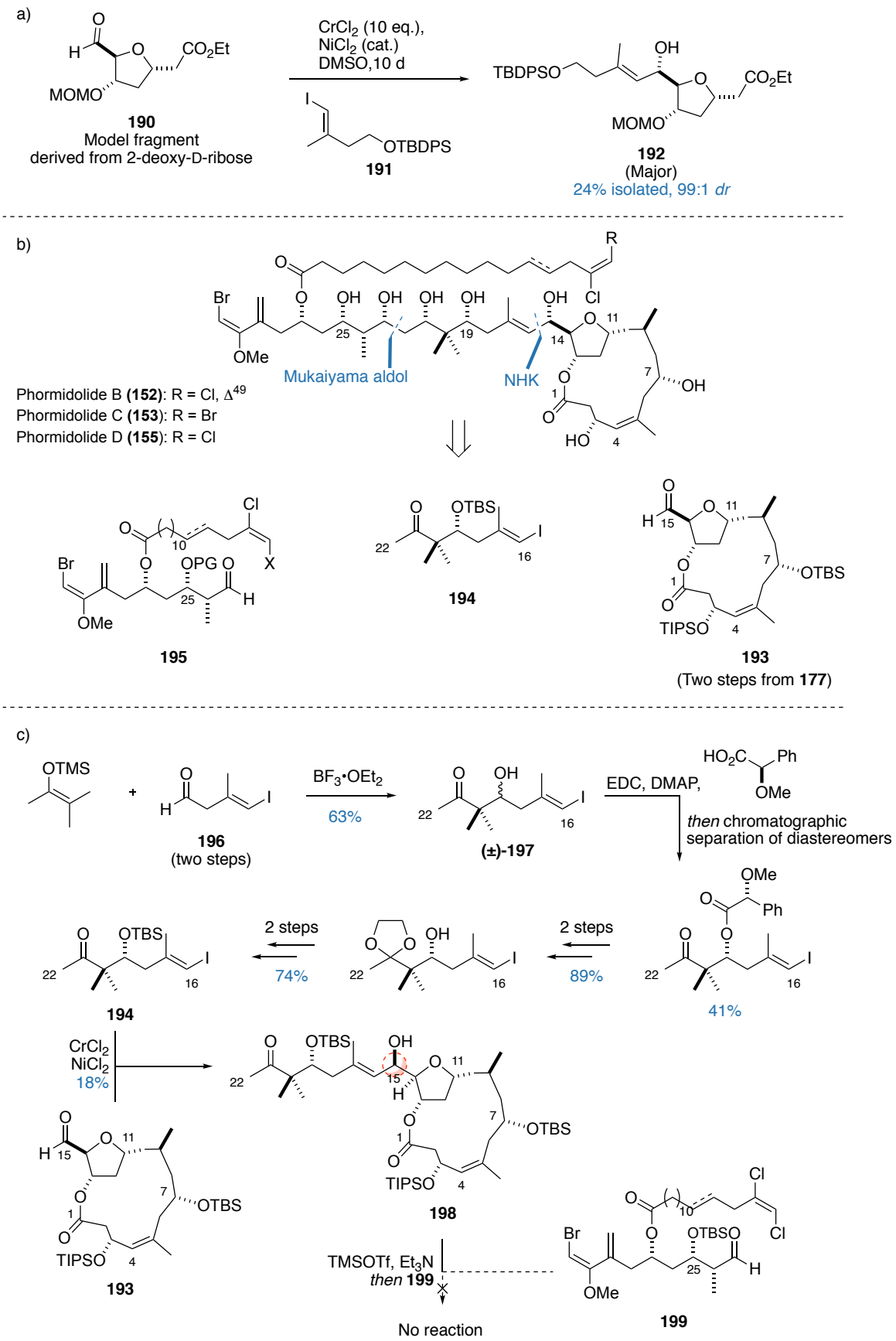

Scheme 29. *a) Model vinylmetal addition into aldehyde* ***190*** *identified that the NHK reaction was the most effective for fragment union. b) The Álvarez approach to the phormidolides C and D. c) Attempted total synthesis as disclosed by Álvarez highlighting their synthesis of the C16-C22 region*

5.5. Phormidolide A: a summary

Phormidolide A is a complex marine natural product that contains a breadth of intriguing structural features, including a unique THF-embedded macrolactone core and an all-*syn* polyol backbone terminating in the signature bromomethoxydiene motif (**Figure 38**). Perhaps owing to the apparent lack of bioactivity, phormidolide A has received little interest from the synthetic community since its isolation, though it is clear from its potent brine shrimp toxicity that the natural product has a distinct, but unknown eukaryotic target, with its production conferring some evolutionary advantage for its producer. Additionally, a reexamination of the original *J*-based analysis has raised questions on the stereochemical veracity of the structural assignment, that remained unresolved despite achieving a full elucidation of its biosynthesis.

All of these contrary observations have generated more questions than answers for this intriguing natural product. This has resulted in phormidolide A becoming an increasingly attractive target, particularly in order to resolve the stereochemical contradictions that were presented by the Gerwick group. Furthermore, a reliable synthetic route towards phormidolide A would enable us to interrogate the conundrum of its apparent lack of biological activity, especially in the presence of moderately active congeners isolated from discrete locations worldwide. These unanswered questions posed by phormidolide A could therefore all be addressed by its successful total synthesis.

This section highlighted the only other research group to date that has published work on synthetic studies towards the phormidolides. The Álvarez group has demonstrated that the bromomethoxydiene is indeed synthetically tractable, although the installation of this motif is marred with significant amounts of seemingly redundant protecting group and redox manipulations. Additionally, the deficiencies discussed in the previous studies have demonstrated the need for high yielding and highly stereoselective fragment union strategies in appending the polyol side chain onto the macrolactone. Encouragingly however, the initial work Álvarez laid out towards the synthesis of the conserved polyol side chain points to the unexpected robustness of the bromoenol ether moiety, which augurs well that such a motif could be installed early on and withstand the demands imposed by a total synthesis campaign.

In light of these aforementioned challenges and opportunities, the following sections will detail the author's eventful journey towards the total synthesis of phormidolide A, highlighting the unexpected obstacles and discoveries we encountered, and the implications this has on the continual strategy evolution towards this intriguing class of natural product.

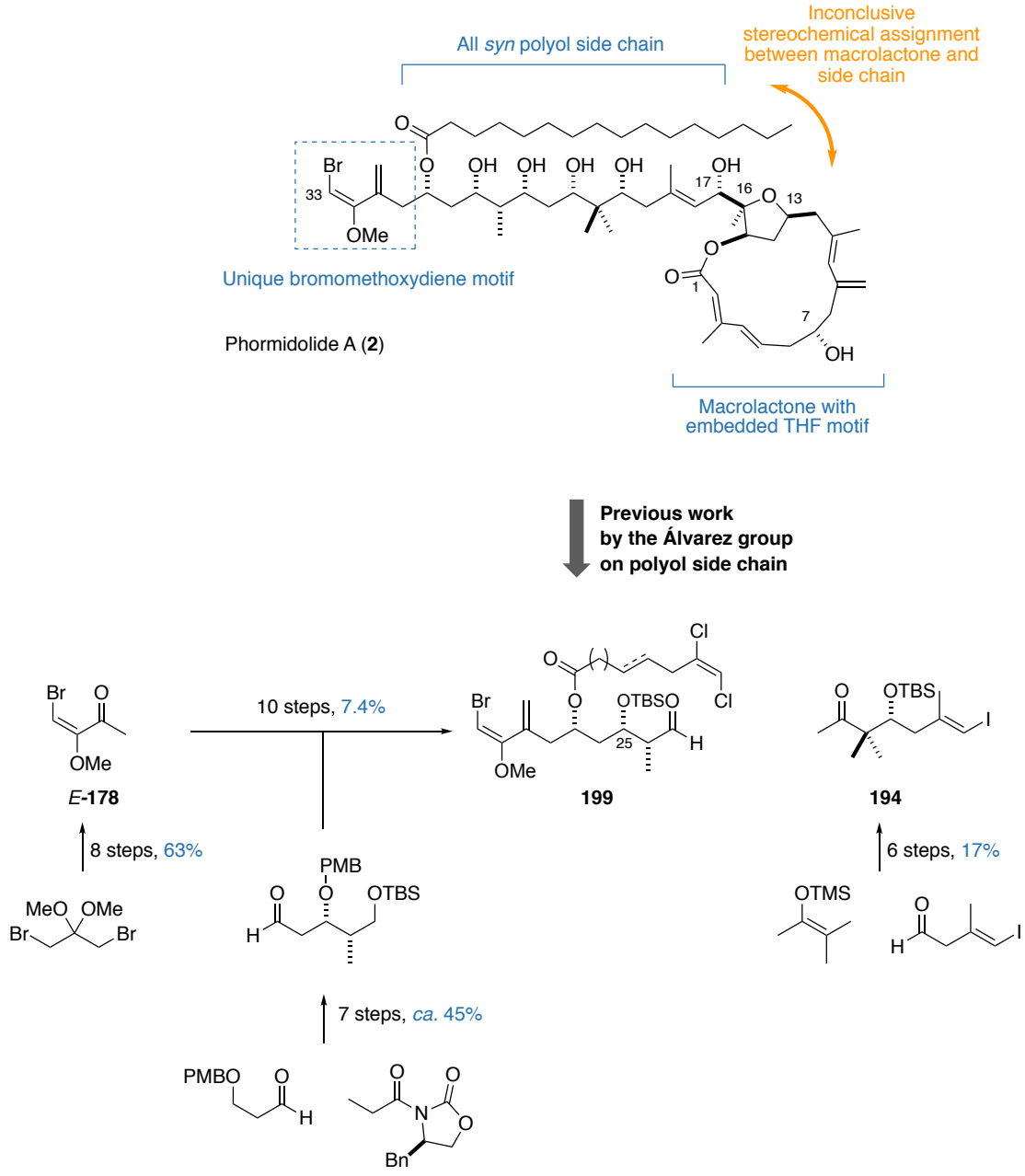

***Figure 38**. Summary of phormidolide A, including previous work conducted by the Álvarez group towards the all-syn polyol side chain*

6. Results and Discussion

6.1. Overview of initial synthetic plan

The synthetic campaign towards phormidolide A is a collaboration between the Paterson group and the Britton group at Simon Fraser University. Recognising that phormidolide A contains two structural domains of similar complexity, the initial synthetic effort was evenly divided, with the Britton group tackling the C1-C17 macrolactone, and the Paterson group approaching the C18-C33 polyol side chain (**Scheme 30a**).

The initially planned endgame strategy for phormidolide A was anticipated to be a chelation-controlled vinylmetal addition to forge the C17-C18 bond, and a Mukaiyama aldol reaction to form the C24-C25 bond. These two reactions were expected to configure C17 and C25 selectively (**Scheme 30b**); the vinylmetal addition was expected to proceed with the nucleophile approaching from the small Me group, to give the reported C17 configuration selectively.[103] Based on extensive literature precedent, a similar Mukaiyama aldol reaction to one reported by the Álvarez group[98,101] was envisioned to deliver the Felkin-Anh product, with the bulky nucleophile overriding the competing 1,3-Evans' polar product.[104] Taking into account the inconsistent result reported by the Álvarez group for the Mukaiyama aldol addition, employing a smaller silyl protecting group was hoped to improve the outcome of this reaction. Retrosynthetically, this reveals the macrocycle **200**, the C18-C24 vinyl iodide **201** and the C23-C33 aldehyde **202**. The chelation-controlled vinylmetal addition will have to arise from a lithiated intermediate, and transmetallated to a suitable metallic reagent to generate the active nucleophile. Noting that the relative configuration between the C1-C17 macrolactone and the C18-C33 polyol side chain requires verification, a stereoflexible synthesis of the C18-C33 fragment is needed to readily access both enantiomeric series of the fragments constituting the polyol side chain. This is not a necessary requirement for the macrolactone as the absolute configuration has been determined in previous studies.

For completeness, the planned Britton group's synthetic approach towards the C1-C17 macrolactone is included and shown in **Scheme 30c**. The C1-C17 macrolactone **200** can be disconnected into three key fragments by various C-C coupling reactions and a Mitsunobu macrolactonisation. Of the three fragments, the C13-C17 THF moiety **203** can be constructed from dioxanone **204** and aldehyde **205** by employing tandem α-chlorination L-proline-catalysed aldol chemistry that the Britton group has developed.[105,106]

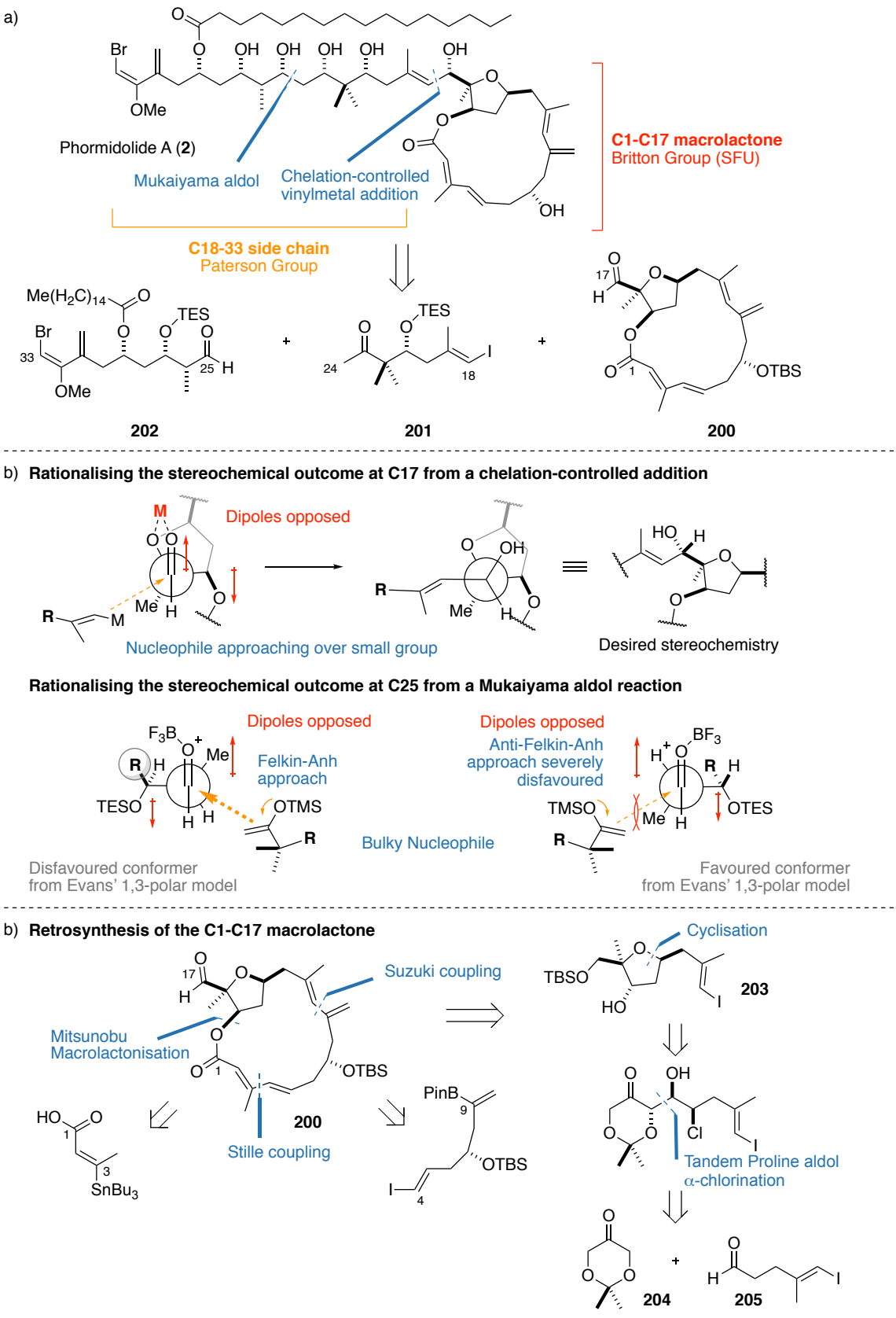

Scheme 30. *a) Proposed endgame strategy for the synthesis of phormidolide A b) Stereochemical rationalisation for the chelation-controlled vinylmetal addition, and for the Mukaiyama aldol reaction. c) Proposed retrosynthesis of the C1-C17 macrolactone by the Britton group*

6.2. Synthesis of the C18-C24 fragment

Noting that the planned total synthesis hinges on the successful bidirectional fragment union of the C18-C24 fragment to both the macrocycle and the remainder of the side chain, it was prudent therefore to commence our synthetic campaign with the linchpin that joins the two fragments together. Here, a synthesis of the C18-C24 fragment would allow an early verification on the feasibility of the proposed endgame strategy. The C18-C24 fragment **201** can be disconnected across the C21-C22 bond *via* either an Ipc boron-mediated aldol reaction or an enantioselective Mukaiyama aldol reaction. Retrosynthetically, this reveals aldehyde **196** and an enolate equivalent **207** or **208** as the required building block (**Scheme 31**)

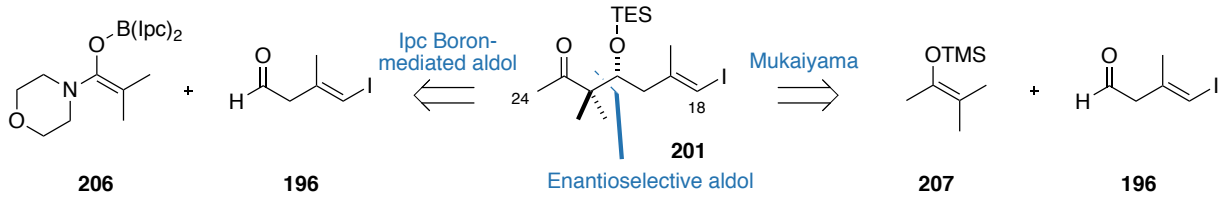

Scheme 31. *Retrosynthesis of the C18-C24 fragment*

Following a modified protocol by Wipf,[107] the synthesis of aldehyde **196** commenced with a *syn*-stereospecific Negishi carboalumination[108] of 3-butyn-1-ol (**208**) catalysed by zirconocene dichloride (**Scheme 32**). The regioselectivity of the reaction can be rationalised by **TS-VII**, where the bulky zirconocene dichloride is thought to act as a Lewis base to both activate the Me_3Al species and enforce the terminal regioselectivity of the addition. The addition of stoichiometric amounts of water is known to dramatically accelerate the rate of carboalumination although the exact mechanism in which this occurs is unknown.[107] Wipf noted this phenomenon and putatively attributed the increased reactivity to **TS-VIII**, where hydrolysis of **TS-VII** replaces the bridging Cl with an O; a better Lewis base for Me_3Al, which results in the rate enhancement for the formation of intermediate **209**. The intermediate can then be trapped *in situ* by the addition of iodine to afford the vinyl iodide **210** in 87% yield.[108,109] Screening a series of oxidation conditions found DMP oxidation to afford the desired aldehyde **196** cleanly, with other reagents resulting in either isomerisation to the conjugated enal or decomposition of the olefinic system. As aldehyde **196** is volatile and highly prone to degradation, it was always freshly prepared and stored in dry CH_2Cl_2 over 4 Å MS prior to its use in subsequent transformations.

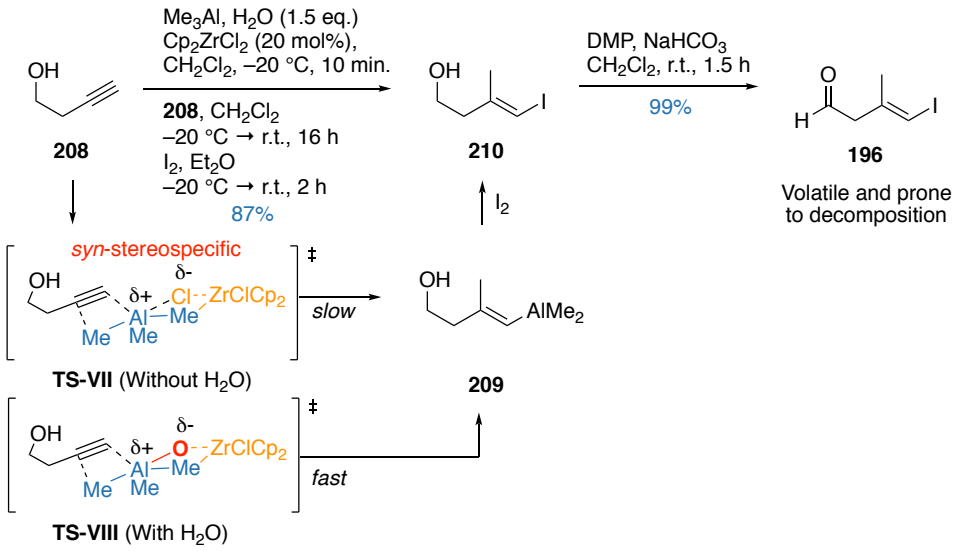

Scheme 32. *Synthesis of aldehyde* ***196*** *from 3-butyn-1-ol (****208****) via a Negishi carboalumination*

To configure the C21 stereocentre, initial investigations focused on employing Roush's reductive boron aldol conditions.[110] The rationale behind this methodology involves an *in situ* generation of an Ipc boron enolate from a 1,4-reduction of an acrolyl morpholinamide derivative, cited as a Weinreb amide substitute.[110,111] Addition of an aldehyde facilitates an Ipc boron-mediated aldol reaction, with the facial selectivity dictated by the steric interaction between the methyl group on the Ipc ligand and the axial morpholinamide moiety on the boron enolate (**Scheme 33**). For the enolate derived from treating carboxamide **211** with (+)-$(Ipc)_2BH$, the aldol reaction proceeds *via* **TS-IX** to afford the aldol adduct **212** as the major product. **TS-X** is disfavoured due to destabilising steric interactions as previously described (see **Scheme 12**), resulting in ***ent*-212** as the minor product. However, this strategy was quickly found to be intractable given problems encountered with reproducing the Roush group's results on a published substrate (**Scheme 34**). Specifically, employing hydrocinnamaldehyde under reoptimised conditions gave at best a 10% yield of the expected product **213**, compared with the 61% yield reported for the same reaction.

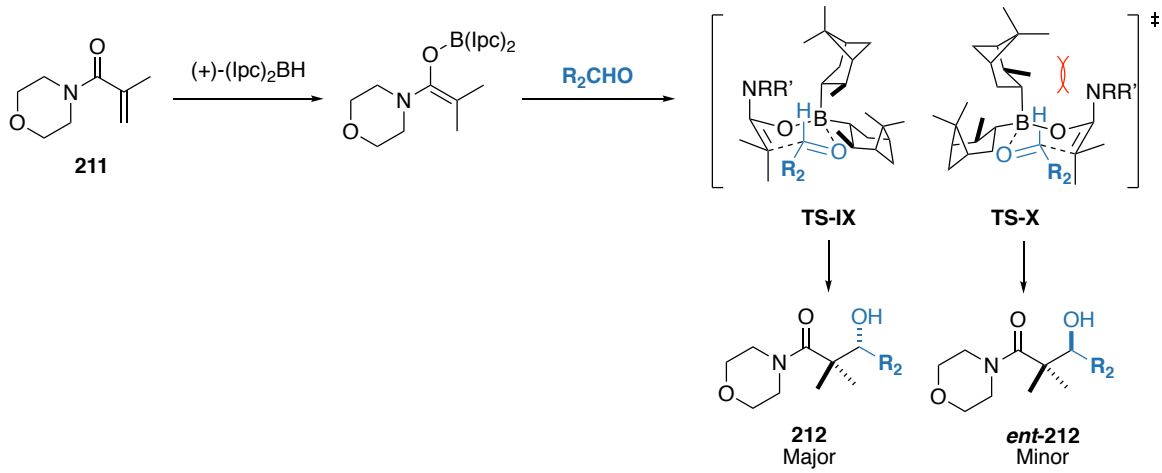

Scheme 33. *Proposed mechanism and transition states for Roush's reductive boron aldol procedure*

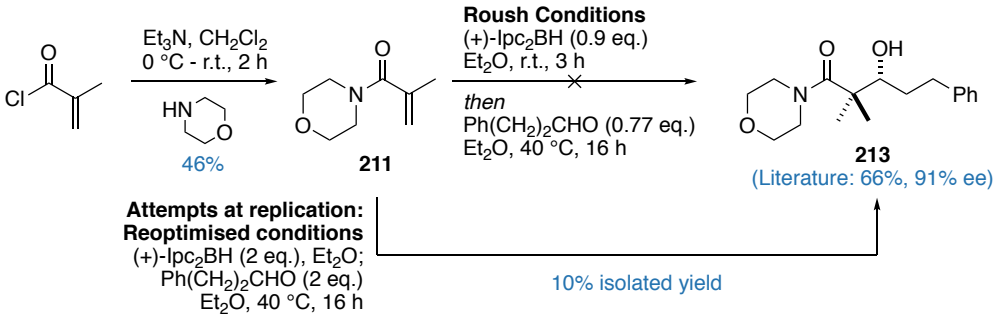

Scheme 34. *Attempted replication of Roush's reductive boron-mediated aldol methodology on a published substrate*

Deciding that this approach was not viable, attention then turned towards utilising a Mukaiyama aldol reaction between silyl enol ether **207** and aldehyde **196** to furnish the C18-24 fragment. Silyl enol ether **207** was synthesised under published conditions from methyl isopropyl ketone,[112] yielding a 9:1 mixture of silyl enol ethers **207** and **214**. Employing achiral Lewis acids such as $BF_3{\cdot}OEt_2$ or $TiCl_4$ afforded racemic aldol adduct **197** in good yields (64–68%) (**Scheme 35**). As both boron- and titanium-based Lewis acids gave good results in the racemic reaction, initial attempts at effecting an enantioselective Mukaiyama aldol reaction were focused on employing chiral boron and titanium Lewis acids. Two examples that have been employed in total syntheses are Kiyooka's valine-derived oxazaborolidinones[113,114] and the catalytic use of Ti(BINOL) complexes derived from a 1:1 mixture of either $TiCl_4$ or $Ti(O\textit{i}Pr)_4$ with (*R*)- or (*S*)-BINOL.[115,116]

Mechanistically, Kiyooka's oxazaborolidinone-mediated Mukaiyama aldol reaction proceeds *via* a bidentate coordination of the carbonyl oxygen and formyl hydrogen to the oxazaborolidinone boron and oxygen respectively.[117] The isopropyl group of the valine skeleton sets up a concave and a convex face for the complex. Additionally, the phenyl ring on the tosyl group faces away from the isopropyl group to further block the concave face. As a result, incoming nucleophiles preferentially attack from the more accessible convex face *syn* to the isopropyl group (**Scheme 36a**).[113,117] The Ti-BINOL catalytic process is, on the other hand, less defined. Studies have failed to pinpoint a specific catalyst structure for the $TiCl_4$ or $Ti(O\textit{i}Pr)_4$ derived BINOL complexes,[116] though contrary to the prevailing paradigm for the Mukaiyama aldol reaction,[118] proposals have been put forth suggesting that the complex participates in a closed transition state highlighted in **Scheme 36b** to rationalise the concerted migration of the silyl group.

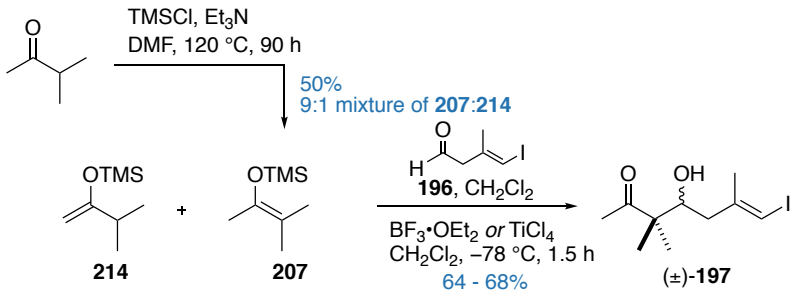

Scheme 35. *Synthesis of racemic aldol adduct* ***197*** *from aldehyde* ***196*** *and silyl enol ether* ***207***

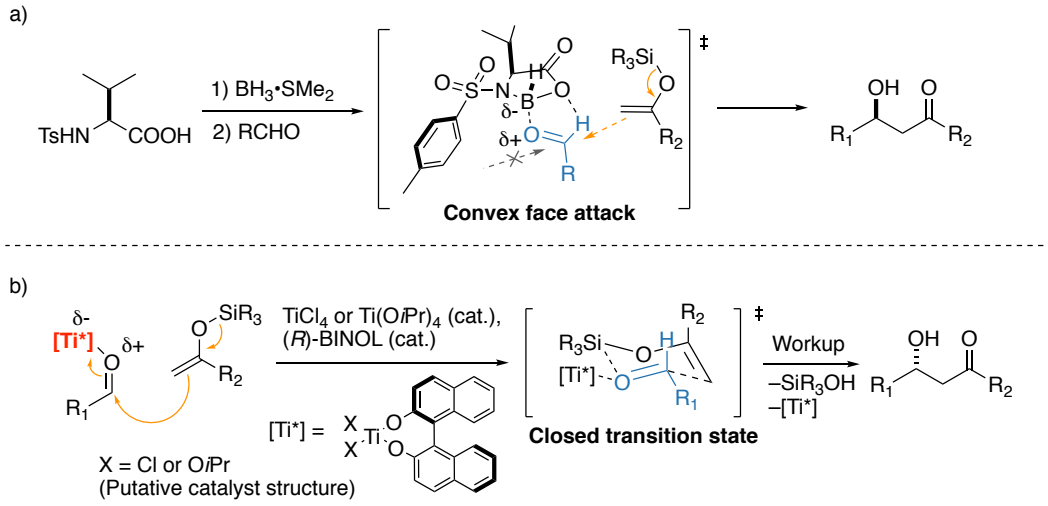

Scheme 36. *a) Stereochemical rationalisation for Mukaiyama aldols with Kiyooka's oxazaborolidinone complex*
b) Speculative mechanism for a Ti-BINOL-mediated Mukaiyama aldol reaction

Attempts to replicate these conditions on silyl enol ether **207** and aldehyde **196** employing Kiyooka's complex derived from L-tosylvaline (**215**) only resulted in reducing aldehyde **196** to the alcohol **210** (**Scheme 37a**). Exchanging the boron reagent to BCl_3 on the other hand returned a mixture of starting material and isomerised aldehyde *E*- and *Z*-**216**. Similar results were observed upon employing Ti-BINOL systems, where the 1:1 combination of $TiCl_4$ and (*S*)-BINOL at various catalytic loadings either did not result in any conversion or returned the isomerised aldehyde (**Scheme 37b**). The same reaction carried out with 1:1 Ti(O*i*Pr)$_4$ and (*S*)-BINOL did not result in any conversion. Observing the isomerisation of aldehyde **196** into enals *E*- and *Z*-**216** suggested that these Lewis acids activated the carbonyl enough to result in double bond migration, but were not strong enough to facilitate the nucleophilic attack of the silyl enol ether onto the carbonyl centre.

At this point, it was thought that the silyl enol ether **207** was not electron-rich enough, and therefore nucleophilic enough to facilitate an asymmetric Mukaiyama aldol reaction. This was reinforced by Mayr et

al., who claimed that silyl enol ether **207** was of the order of 10^3 to 10^4 fold less nucleophilic than the silyl ketene acetal derived from methyl isobutyrate.[119] Coupled with the fact that literature applications of these asymmetric methodologies used the more nucleophilic silyl ketene acetal suggested employing the silyl ketene acetal **217** to effect the asymmetric Mukaiyama aldol reaction, followed by the conversion of ester **218** to ketone **201** *via* Weinreb amide **219** would be a more productive approach (**Scheme 37c**).

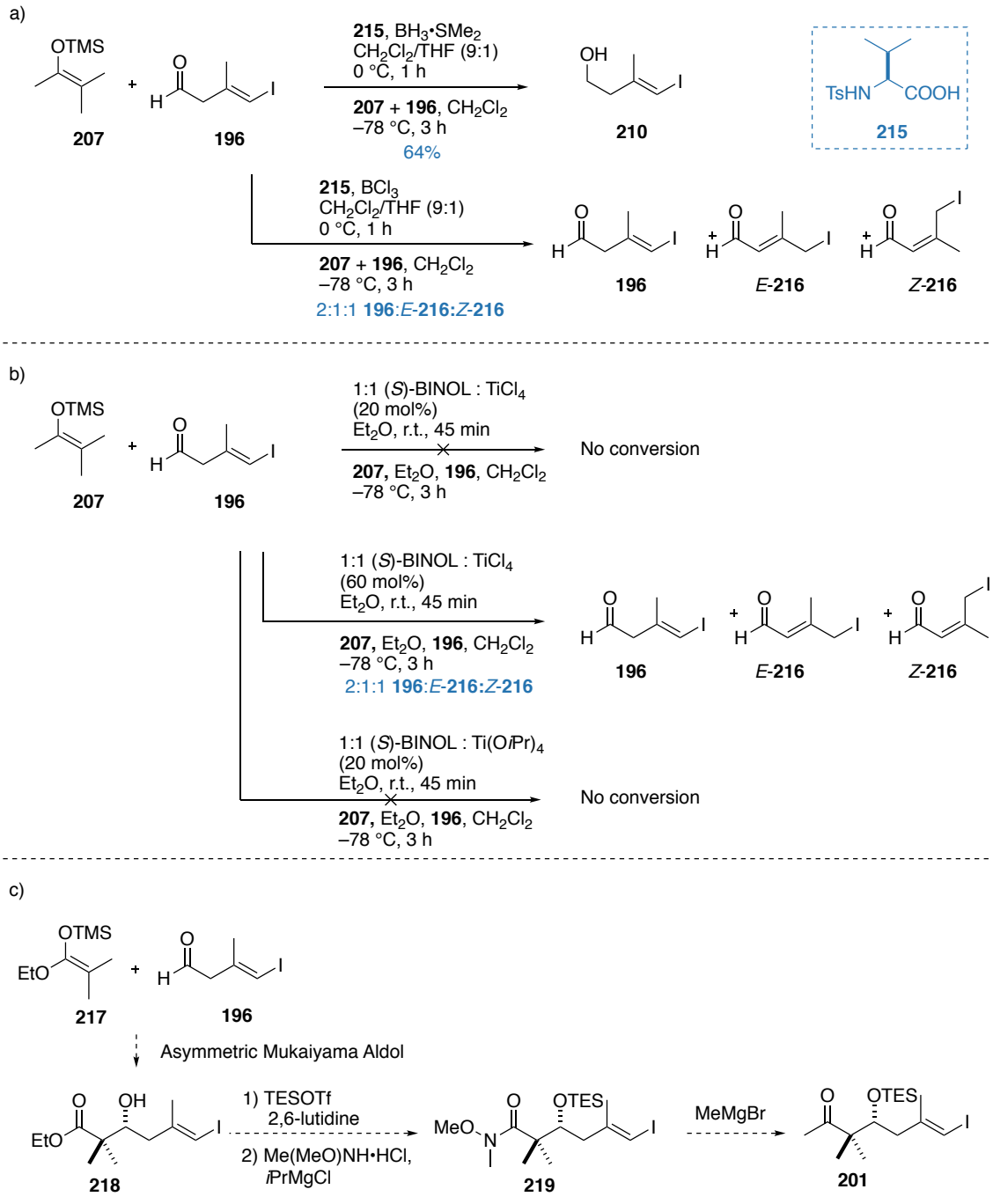

Scheme 37. *Attempted synthesis of* ***197*** *using a) Kiyooka's oxazaborolidinone complex b) Ti-BINOL complex. c) Revised synthesis of ketone* ***201*** *from silyl ketene acetal* ***217*** *and aldehyde* ***196***

Silyl ketene acetal **217** can be readily derived from ethyl isobutyrate in good yield (88%).[120] Gratifyingly, submitting silyl ketene acetal **217** and aldehyde **196** with Kiyooka's complex derived from L-tosylvaline (**215**) afforded the aldol adduct **218** in 67% yield and in 91% *ee via* **TS-XI** (**Scheme 38a**). Attempts to employ a Ti-BINOL catalyst for this reaction afforded no conversion for the catalyst derived from $Ti(OiPr)_4$, and poor yields and selectivity (29%, 2% *ee*) for the catalyst derived from $TiCl_4$. The elucidation of the absolute stereochemistry at C21 was attempted by forming diastereomeric Mosher esters, however the subsequent analysis proved to be inconclusive due to inconsistent signs around the carbinol H21 proton. At this stage, the anticipated stereochemical outcome was assumed by comparison with analogous reactions in the literature, which suggested the (*R*) configuration was obtained at the C21 centre from using L-tosylvaline **215**.[114,121] With a view to probing the diastereomeric relationship between the macrolactone and the side chain, the enantiomeric ester ***ent*-218** can be readily synthesised by using the enantiomeric D-tosylvaline ***ent*-215** as the chiral promoter.

TES protection of the aldol adduct **218** afforded the TES ether **220** in excellent yield, though the subsequent conversion to the Weinreb amide proved to be stubborn for both the protected and the unprotected substrate, resulting in no conversion or degradation under a variety of basic (*i*PrMgCl or *n*BuLi) or Lewis acidic (Me_3Al) conditions. Instead, an alternative approach to convert ester **220** directly into ketone **201** as described by Kikkawa and Yorifuji was employed.[122,123] Subjecting ester **220** directly with MeMgBr in excess Et_3N at 80 °C cleanly afforded the required methyl ketone **201** in excellent yield (92%), with no sign of Mg/I exchange or double addition occurring (**Scheme 38b**). As with typical Grignard addition to esters, the first equivalent of MeMgBr adds to form the ketone. For esters with no α-protons, conducting the reaction in excess Et_3N enolises the newly formed methyl ketone. This prevents the second equivalent of Grignard adding to the more electrophilic ketone carbonyl, thus enabling the selective transformation of esters into ketones without over-addition to form the undesired tertiary alcohol (**Scheme 38c**).[122]

Overall, the C18-C24 fragment **201** was synthesised enantioselectively in five steps from 3-butyn-1-ol alcohol in 53% overall yield, or in 60% yield over three steps from aldehyde **196.** This is in contrast with the 17% reported yield over six steps from aldehyde **196** by the Álvarez group (**Scheme 38d**). Notably, this result represents over a 3.5-fold improvement in yield compared with the analogous route, is executed in half the number of steps and does not contain a resolution step where half the material is discarded in the process.

At this point, the tentatively assigned absolute configuration at C21 could be confirmed by Mosher ester analysis. TBAF deprotection of TES ether **201** afforded alcohol (*R*)-**197** in good yield (79%). The crude alcohol (*R*)-**197** was then esterified with (*S*) or (*R*)-MTPA under Steglich conditions (DCC, DMAP)[62] to afford the diastereomeric Mosher esters **221** and **222** respectively (**Scheme 39**).

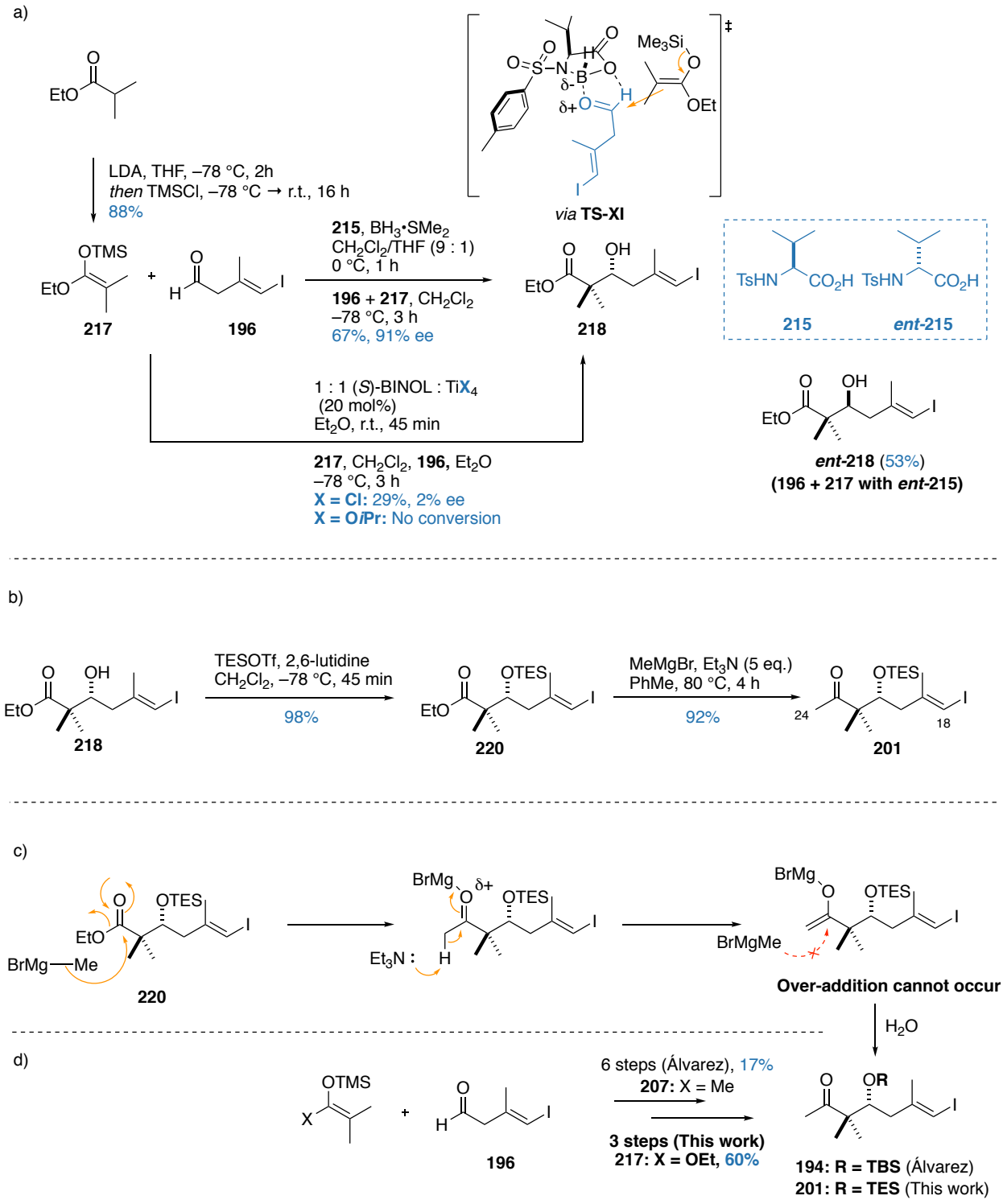

Scheme 38. *a) Synthesis of* ***218*** *using a) Kiyooka's oxazaborolidinone complex. Results from employing the Ti-BINOL complex for an enantioselective Mukaiyama aldol reaction are also shown. b) Completing the synthesis of the C18-C24 fragment* ***201****. c) Mechanism for the direct conversion of ester* ***220*** *to ketone* ***201****. d) Comparison with the Álvarez route towards ketone* ***194,*** *noting the 3.5-fold improvement in yield*

MTPA derivatives of secondary alcohols preferentially adopt a conformation in which the carbinol proton, ester carbonyl and CF_3 groups on the MTPA ester lie in the same plane (**Figure 19a**).[63] This results in the protons lying on the same side as the MTPA Ph group to be diamagnetically shielded (shifted upfield)

relative to the protons lying on the same side as the OMe group. This means that the protons lying adjacent to the (*S*)-MTPA Ph group will be shielded compared to the analogous protons in the (*R*)-MTPA derivative.[64] Thus, proton signals with $\Delta\delta < 0$ ($\Delta\delta = \Delta\delta_S - \Delta\delta_R$) would lie on the left-hand side of the (*R*)-MTPA plane from the perspective of the CF_3 group, and *vice versa* for $\Delta\delta > 0$ (**Figure 19b**).[65] Calculating $\Delta\delta$ (**Table 7**) and applying the model described in **Figure 19** showed that the C21 centre had the desired *R* configuration, which corroborated the assignments based on mechanistic predictions and analogous literature reactions.

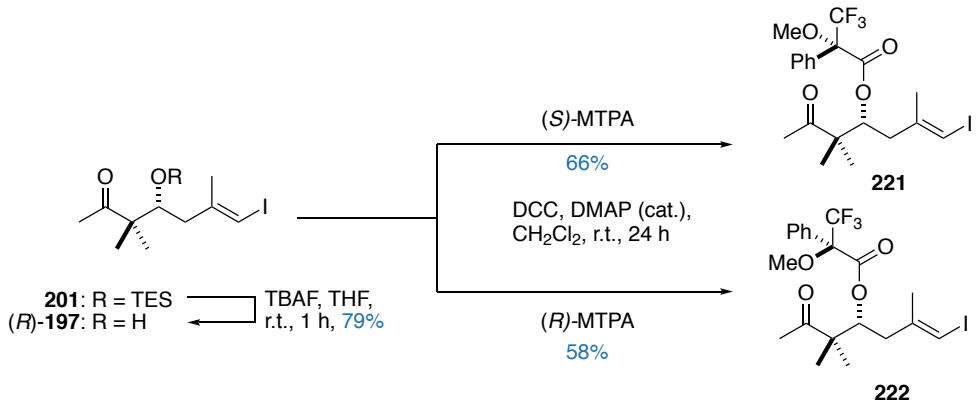

Scheme 39. *Synthesis of Mosher esters **221** and **222***

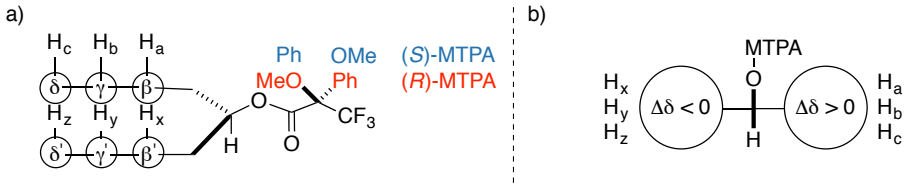

Figure 39. *a) Diagram highlighting the preferred conformation of the MTPA derivative b) Model to assist the absolute configuration of a carbinol center*

Table 7. *List of chemical shifts for MTPA derivatives **221** and **222**. The carbinol proton H21 is excluded from the analysis*

Proton	**δH (*S*)-MTPA** (ppm)	**δH (*R*)-MTPA** (ppm)	$\Delta\delta_{S-R}$ (ppm)
H24	2.11	2.13	−0.02
Me22a	1.13	1.17	−0.04
Me22b	1.12	1.15	−0.03
H21	5.69	5.66	+0.03
H20a	2.45	2.43	+0.02
H20b	2.32	2.31	+0.01
Me19	1.94	1.93	+0.01
H18	5.95	5.94	+0.01

6.2.1. *Fragment union investigations with a model side chain*

With the C18-C24 fragment **201** in hand, an investigation into the proposed Mukaiyama aldol addition with a suitable model aldehyde was conducted. While ketone **201** was inert to standard silyl enol ether formation conditions (LDA, TMSCl), employing TMSOTf and Et_3N allowed the quantitative formation of the corresponding silyl enol ether **223**. Interestingly, the planned Mukaiyama aldol reaction between **223** and model aldehyde **224** was unsuccessful in generating adduct **225**, consistently returning ketone **201** and its deprotected variant (*R*)-**197** across a variety of reaction conditions. Similarly, attempts at varying the enolate metal substituent by employing a Cy_2BCl-mediated aldol reaction also produced no product (**Scheme 40**).

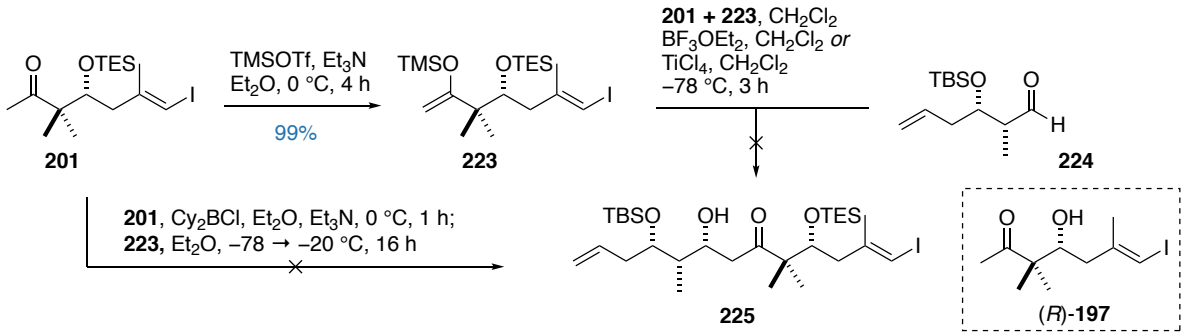

Scheme 40. *Investigations into the planned Mukaiyama aldol reaction between silyl enol ether* ***223*** *and model aldehyde* ***224***

These results echoed Álvarez's observations, where no reactivity was observed for an analogous Mukaiyama aldol reaction between the silyl enol ether derived from ketone **198** and aldehyde **199** (see **Scheme 29** in section **5.4.3**). Noting that perhaps the problem lay with the steric encumbrance of any enolate derivatives of ketone **201**, an alternative C23-C24 disconnection was envisaged, with the nucleophilic component being the enolate derivative of ketone **226** attacking into a C18-C23 aldehyde **227** (**Scheme 41a**). This transformation has been employed in Menche's studies towards the total synthesis of rhizopodin,[124] where a 1,4-*syn* diastereocontrol was enhanced by the use of the DIPCl reagent to configure the carbinol oxygen next to a gem-dimethyl group (**Scheme 41b**). Notably, this route also presents the opportunity of effecting an *in situ* 1,3-*syn* reduction of the boron aldolate intermediate, to configure two stereocentres selectively. This strategy has been employed in the Paterson group towards the synthesis of patellazole B (**Scheme 41c**).[18]

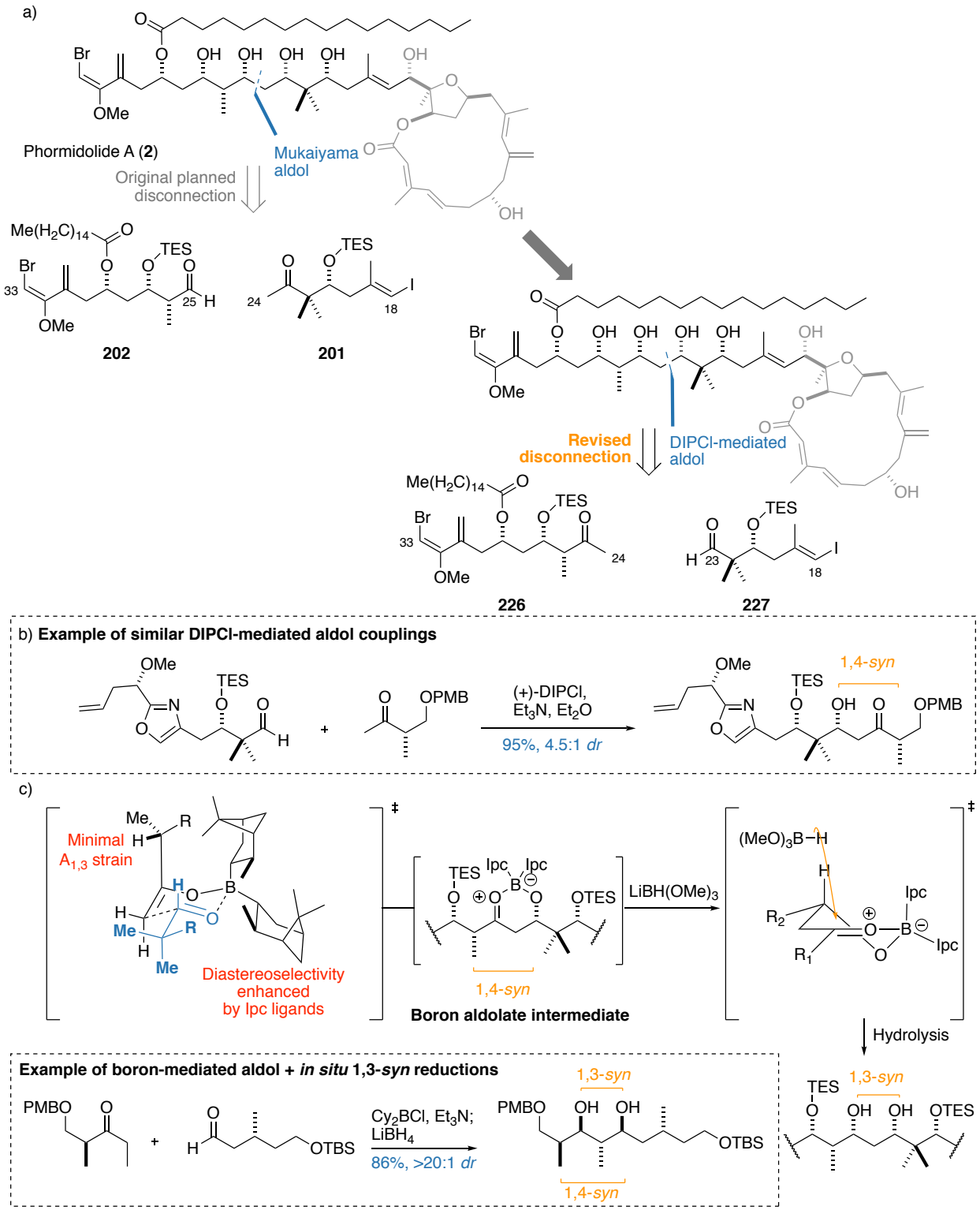

Scheme 41. *a) The original and revised retrosynthesis for phormidolide A. b) DIPCl-mediated aldol as performed by Mench in rhizopodin. c) Rationale for employing DIPCl-mediated aldol/1,3-syn reduction sequence, with an example by Paterson in patellazole B*

To test this proposal, ester **220** was selectively reduced to the corresponding aldehyde **227** by treatment with DIBAL at –78 ˚C (**Scheme 42**). After the initial hydride attack, the formed tetrahedral intermediate **228** is stable at low temperatures, preventing the over addition of the reducing agent into what would be aldehyde carbonyl centre. This tetrahedral intermediate is then hydrolysed upon workup to selectively give aldehyde **227**. The DIPCl-mediated aldol reaction was trialed with model ketone **229** and aldehyde **227**. Promisingly, the reaction forged the C-C bond to give adduct **230** in modest yields and demonstrates a viable proof-of-concept that such a fragment union strategy is possible. Due to the small scale of the test reaction, an attempt at corroborating the stereochemistry at C23 was not conducted.

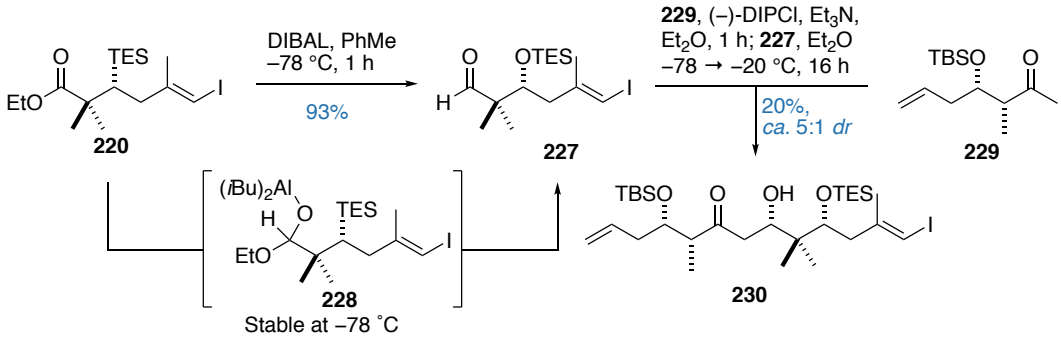

Scheme 42. *Model DIPCl-mediated aldol reaction between aldehyde* ***227*** *and model ketone* ***229***

The expeditious synthesis of the C18-C24 fragment **201** has demonstrated that the planned Mukaiyama aldol reaction was not a viable method for the synthesis of phormidolide A. Aided by the functional group flexibility of ester intermediate **220**, the alternative C18-C23 aldehyde **227** was also readily synthesised. As the planned chelation-controlled vinylmetal addition would now have to discriminate between two aldehyde carbonyl groups, it was deemed inappropriate to maintain the aldehyde functionality for the C18-C23 fragment. Thus, the revised retrosynthesis for phormidolide A reveals alcohol **231** (or a protected variant thereof) in the C18-C23 fragment and macrolactone **200 (Scheme 43a)**. These compounds were readily accessed again from ester **220**; conducting the aforementioned DIBAL reduction with warming to –40 ˚C reliably gave alcohol **232**, which could be TMS protected in high yields to give **233** (**Scheme 43b**). Similarly, the same sequence of reactions can be conducted for the enantiomeric series. After silyl protection of alcohol ***ent*-218**, an analogous reduction of ***ent*-220** and silyl protection of ***ent*-232** gave silyl ether ***ent*-233**. The stereochemical integrity of ***ent*-233** was verified relative to **233** by their optical rotation data, which were similar in magnitude but opposite in sign.

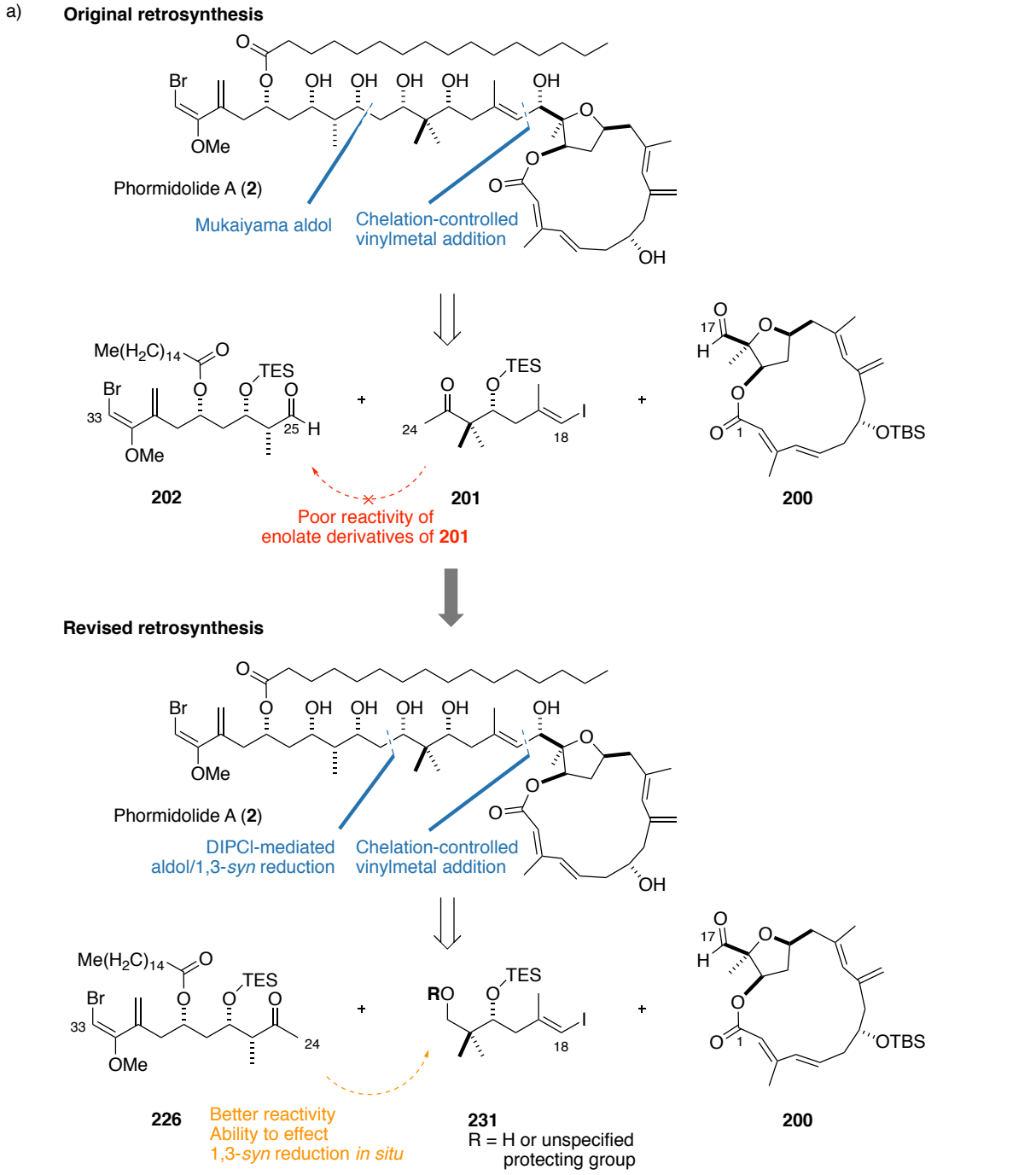

Scheme 43. *a) Original and revised retrosynthesis for phormidolide A, taking into account the key lessons learnt from preliminary fragment union studies. b) Synthesis of alcohol* ***232*** *and silyl ether* ***233*** *from ester* ***220.*** *The synthesis of the enantiomeric fragment* ***ent-233*** *from* ***ent-218*** *is also described*

6.3. Fragment union studies with the C10-C17 THF fragment

The work described in this section was carried out in collaboration with Garrett Muir and Venugopal Rao Challa at Simon Fraser University. Their results were crucial to the project and are presented alongside the author's results. Unless otherwise stated, all reactions described were performed by the author and all stated yields are those obtained by the author.

With some understanding gained for a suitable fragment union strategy between a C18-C23 fragment and the remainder of the side chain, attention now turned towards investigating the planned chelation-controlled vinylmetal addition. To facilitate this, a synthesis of a suitable model THF aldehyde was required. To this end, Muir and Rao Challa developed a scalable route towards constructing the substituted THF core present in phormidolide A; an overview of which is described below:

The synthesis commenced with a Negishi carboalumination of alkyne **234** to give vinyl iodide **235**. Subsequent Dess-Martin oxidation afforded aldehyde **205**, which was engaged in a tandem α-chlorination L-proline-mediated desymmetrising aldol reaction with dioxanone **204 (Scheme 44)**. The initial α-chlorination, mediated by NCS, generates an epimeric mixture of α-chloroaldehyde **236**. In the presence of L-proline and dioxanone **204**, an enantiodefined enamine forms, which selectively reacts with one enantiomer of α-chloroaldehyde at a faster rate as shown in **TS-XII**. This preferentially generate one enantiomer of the product, with the diastereoselectivity of the reaction defined by the preferred geometry of the substituents following the Houk-List model.[106,125] As α-chloroaldehyde is readily epimerisable under the reaction conditions, a dynamic kinetic resolution occurs to result in the convergent formation of a single enantiomer **237** from a racemic mixture of **236**. In Muir's hands, this afforded chlorohydrin **237** in moderate yields and diastereoselectivity, but with excellent enantiocontrol.

Subsequent methyl Grignard addition into **237** followed by a microwave-assisted intramolecular S_N2 cyclisation/acetal deprotection gave triol **238** comprising the full skeleton of the THF motif, though containing an extra degree of oxygenation at C14. This was removed through a three-step sequence, where triol **238** was selectively protected as the siloxane alcohol. The C14 hydroxyl group could then be removed *via* triflation followed by hydride displacement to give siloxane **239**. Removal of the cyclic silyl protecting group followed by *mono*-TBS protection at C17 then gave alcohol **203**.

In alcohol **203** however, the C15 configuration is epimeric to the natural product. Recognising that a suitable model for the vinylmetal addition would require a functionality reminiscent of the macrolactone,

it was decided that appending a dimethylacrylate ester would allow for an adequate representation. In particular, this would mean that the chosen organometallic reagent would have to tolerate the presence of the C15 ester, an important variable to control in terms of chemoselectivity. Muir attempted to correct the C15 geometry *via* a Mitsunobu inversion, using either dimethylacrylic acid or *p*-nitrobenzoic acid as the nucleophile. However, both attempts failed to give any reaction, which was presumed to be attributed to the steric constraints imposed by the proximate C16 quaternary centre. With the intermolecular variant failing to deliver any reactivity, this result has also meant that the planned Mitsunobu macrolactonisation strategy was unlikely to be a feasible reaction for the synthesis of the phormidolide A macrocycle.

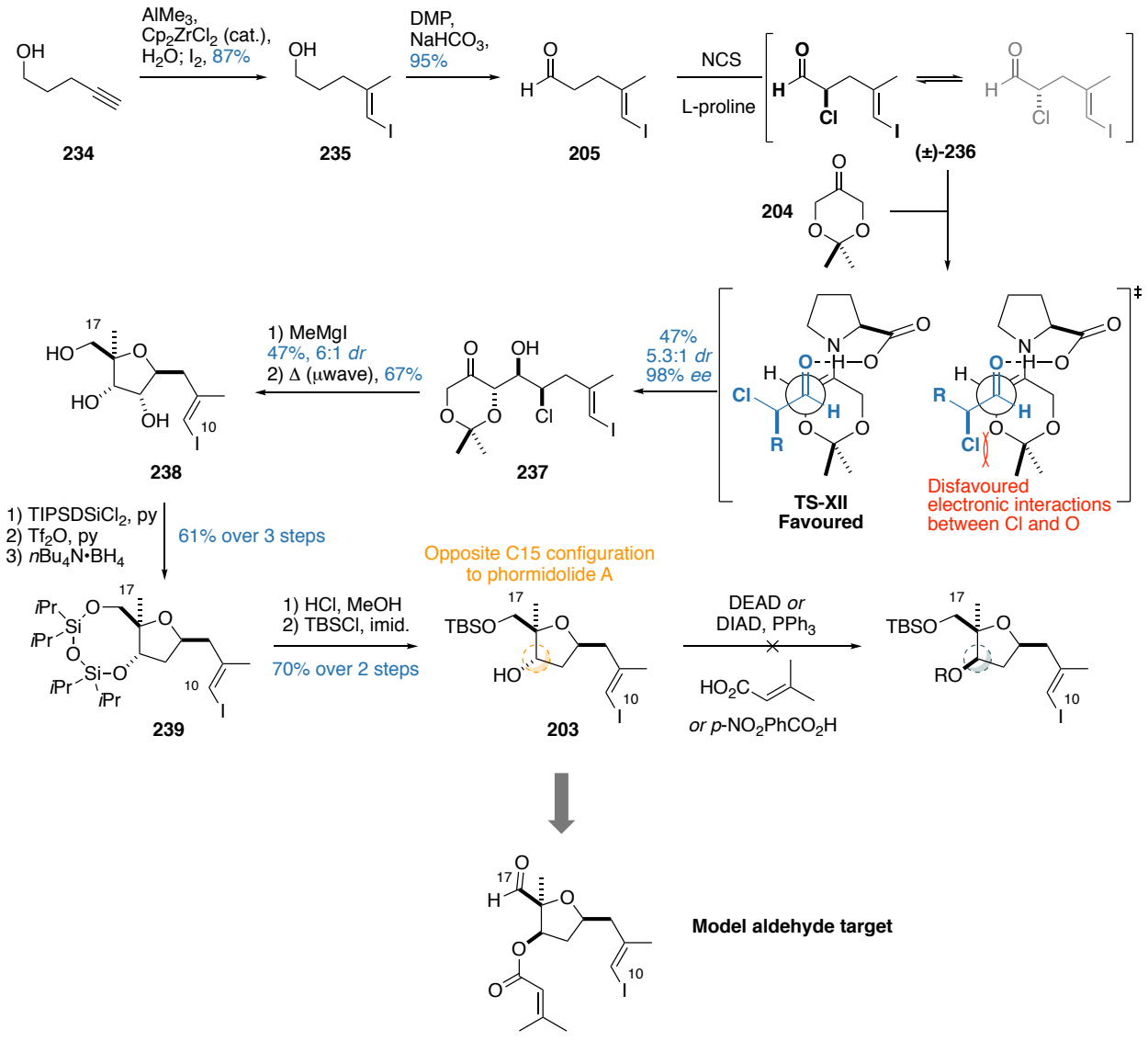

Scheme 44. *Synthesis of fragment* ***203*** *as conducted by Muir and Rao Challa*

6.3.1. *Derivatisation of the C10-C17 THF fragment*

The inability to concomitantly invert and esterify to form the desired dimethylacrylate ester meant that the configuration at C15 in **203** would have to be corrected in a more circuitous manner, involving an oxidation/reduction sequence *via* ketone **240**. Fortunately, oxidation to ketone **240** was readily accomplished under Dess-Martin conditions (**Scheme 45**). Here, it was surmised that a hydride reduction would preferentially occur on the convex face of ketone **240** as defined by the pseudoequatorial C13 and C16 substituents shown in **TS-XIII**. A screen of reducing agents (results summarised in **Table 8**) found that DIBAL (entry 6) was able to cleanly invert the configuration of C15 in an efficient manner, proceeding to give **241** in near quantitative yields over two steps.

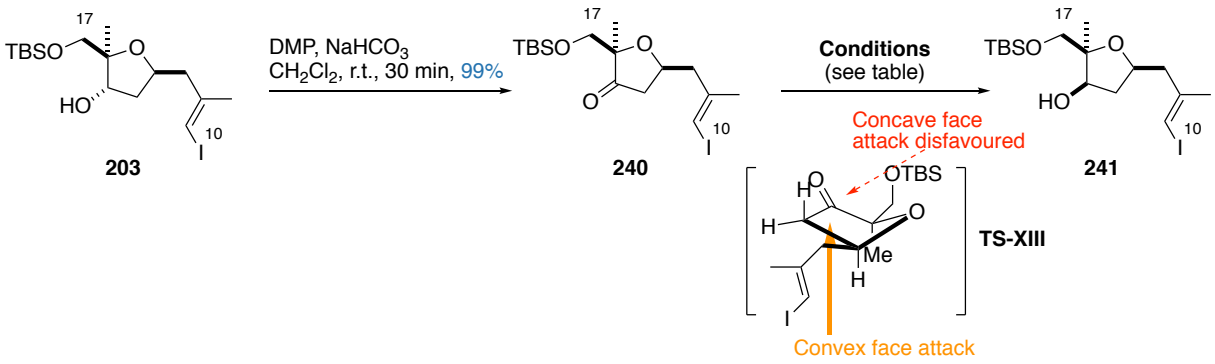

Scheme 45. *Inversion of alcohol* ***203*** *via ketone* ***240***

Table 8. *Summary of reducing agents trialled for the reduction of ketone* ***240***

Entry	Hydride source	Conditions	Yield and ratio of 241:203
1.	$NaBH_4$[‡‡]	EtOH, r.t., 3 h	Yield unreported, 3:1 *dr*
2.	$NaBH_4$	*i*PrOH/CH_2Cl_2 (1:1), –60 °C,	98%, 5:1 *dr*
3.	$NaBH_4$, $CeCl_3{\cdot}7H_2O$	EtOH, –78 → –10 °C, 2.5 h	62%, 5:1 *dr*
4.	L-Selectride	THF, –78 °C, 1 h	No reaction
5.	K-Selectride	THF, –78 °C, 1 h	No reaction
6.	**DIBAL**	**CH_2Cl_2, –78 °C, 1 h**	**99%, >20:1 *dr***

[‡‡] Result obtained by Muir

Presumably due to the steric congestion surrounding the C15 hydroxyl group, the subsequent esterification of **241** with acid **242** did not proceed under standard Steglich conditions (DCC, cat. DMAP). Gratifyingly, trialling both Keck[126] and Yamaguchi[127] esterification protocols efficiently delivered the desired ester **243** (**Scheme 46a**). While notionally a straightforward transformation, the esterification reaction can be challenging especially in the context of macrolactone formation. The demands of requiring mild conditions, high reactivity yet low substrate concentration has resulted in the development of wide-ranging esterification conditions, though the majority of these proceed *via* an activated acyl-DMAP intermediate.[128]

Developed in response to the poor efficacy sometimes observed for the Steglich conditions, Keck extended the Steglich protocol through the addition of stoichiometric amounts of DMAP·HCl, noting that the proton-transfer step towards the formation of the active acyl-DMAP intermediate can become prohibitively rate-limiting, especially under high dilution conditions (**Scheme 46b**).[126] The Yamaguchi esterification involves the initial formation of a mixed anhydride with the reacting acid and TCBC. The subsequent addition of DMAP to this mixture selectively acylates the less hindered non-aromatic carboxyl group, liberating trichlorobenzoic acid as the stoichiometric byproduct (**Scheme 46c**).[127] The formation of the highly electrophilic acyl-DMAP intermediate enables the alcohol to attack as the nucleophile to generate the required ester linkage. As the Keck protocol was operationally more straightforward than the Yamaguchi esterification, this was selected for the synthesis of ester **243**.

Subsequent C17 silyl deprotection to form alcohol **244** using TsOH/MeOH proceeded in moderate yields that were unable to be improved by using alternative desilylation conditions. The final Dess-Martin oxidation of **244** into aldehyde **245** proved stubborn and could not be pushed to completion, and in the author's hands, caused a degree of protodeiodination of the C10 vinyl iodide that was not ameliorated by added base or conducting the reaction in the dark. However, a screen of alternative oxidation conditions conducted by Muir highlighted the instability of the C10 vinyl iodide motif towards other oxidising agents. In particular, oxidations proceeding *via* a sulfonium-based mechanism such as those developed by Swern[129] and Parikh-Doering[130] caused extensive degradation. This meant that while suboptimal, the Dess-Martin oxidation provided an adequate solution to generate the required aldehyde **245** for investigations into the planned chelation-controlled vinylmetal addition.

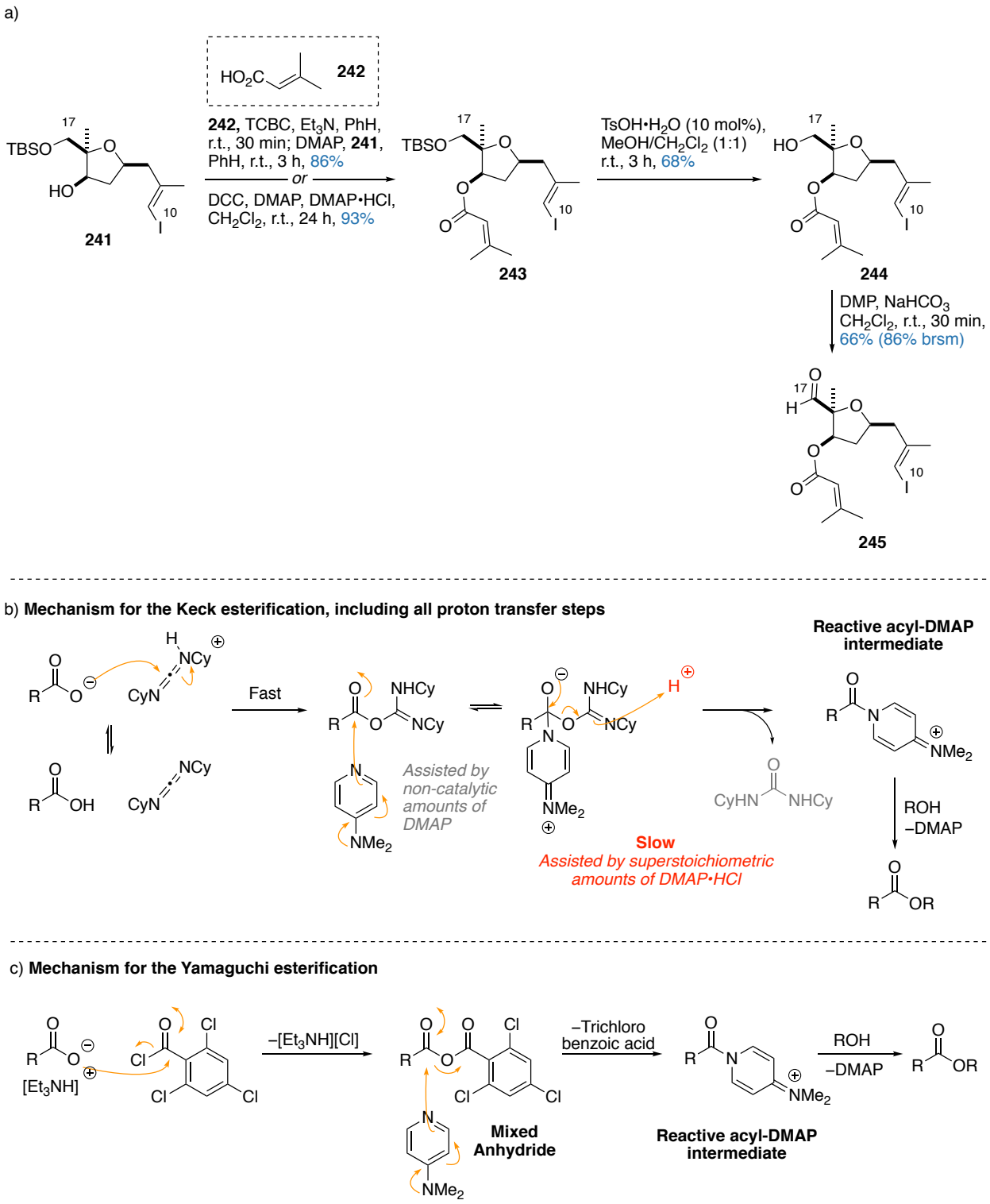

Scheme 46. *a) Synthesis of aldehyde* ***245****. b) Mechanism for the Keck esterification. C) Mechanism for the Yamaguchi esterification*

6.3.2. Investigation into the vinylmetal addition to the C10-C17 aldehyde

With both the model C10-C17 aldehyde **245** and the C18-C23 vinyl iodide **233** in hand, the pivotal vinylmetal addition could now be evaluated. Taking inspiration from Evans' total synthesis of phorboxazole B, which included a chelation-controlled Grignard addition of **246** into **247** to generate adduct **248** as one of the critical fragment union step (**Scheme 47a**),[103] an analogous procedure was adopted. This procedure involves the generation of a vinyl lithium species arising from Li/I exchange, to which this can be transmetallated onto a suitable metallic reagent – in this case $MgBr_2 \cdot OEt_2$ to generate a vinyl Grignard species. To improve the efficacy of this reaction, the highly reactive vinyl lithium reagent could ostensibly be transmetallated onto a variety of alternative metals, such as titanium and zinc, to generate a diverse range of organometallic reagents. In Evans' study, alternative organometallic reagents were inferior in terms of chelation control and reactivity as compared to the generated Grignard reagent, and as such, the *in situ* generation of the vinyl Grignard was considered to be the most promising strategy towards forming the C17 stereocentre and the C17-C18 bond.

The study commenced by treating vinyl iodide **233** with two eq. of *t*BuLi, followed by the addition of a freshly prepared solution of $MgBr_2 \cdot OEt_2$ and aldehyde **245**. As the initial Li/I exchange generates an alkyl halide species, which itself is prone to base-mediated elimination reactions, two equivalents of *t*BuLi are necessary to ensure that the formed vinyl lithium species does not get quenched through competing protodelithiation resulting from the elimination reaction of *t*BuI (**Scheme 47b**). The use of one equivalent of **233** and two equivalents of *t*BuLi failed to give complete Li/I exchange and only minimal amounts of the addition product was formed. Reasoning that this was due to adventitious moisture quenching either the *t*BuLi reagent, or the vinyl lithium intermediate, it was necessary to therefore increase the number of equivalents of vinyl iodide **233**. Gratifyingly, employing 6.5 eq. of vinyl iodide **233** relative to aldehyde **245**, 13 eq. of *t*BuLi and 19 eq. of $MgBr_2 \cdot OEt_2$ (or 2 eq. of *t*BuLi and *ca.* 2.9 eq. of $MgBr_2 \cdot OEt_2$ relative to vinyl iodide **233**) effected a clean addition to afford adduct **249** (77%), in 5:1 *dr*, with no competing addition into the C15 ester. Operationally, the excess alkene **250** formed as the byproduct of the reaction can be easily separated by chromatographic elution with neat PE 40-60, allowing for the facile isolation of the desired product **249**.

At this point, an opportunity to streamline the procedure by saving two steps was recognised by using vinyl iodide with the C23-bearing alcohol **232** as the vinylmetal addition precursor (**Scheme 47c**). Here, treating vinyl iodide **232** with excess NaH, followed by the above sequence of events failed to generate any of the required adduct **251**, surmised as due to incomplete alcohol deprotonation followed by the self-quenching of the lithiated species. As there was already a functional solution, this higher-risk/higher-reward strategy was not pursued further.

a) **Example of a chelation-controlled vinyl Grignard addition in Evans' synthesis of phorboxazole B**

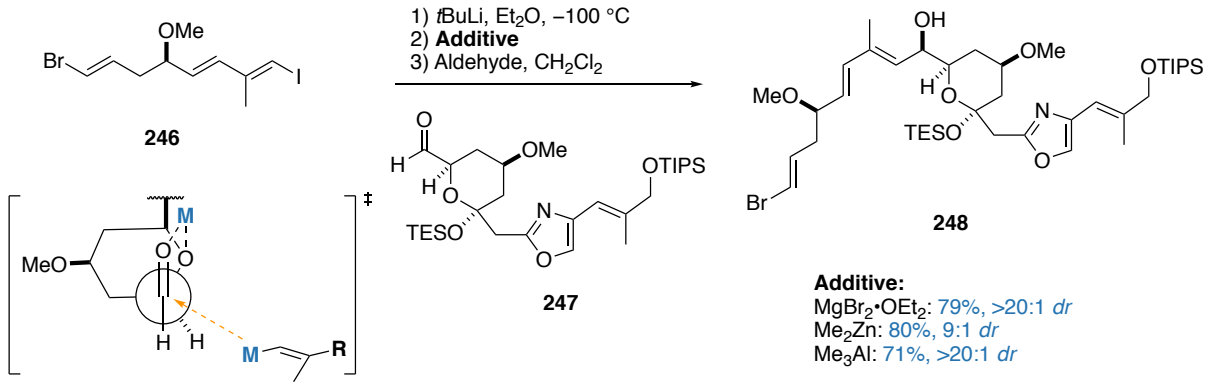

b) **Schematic for the chelation-controlled vinylmetal addition of 233 into 245**

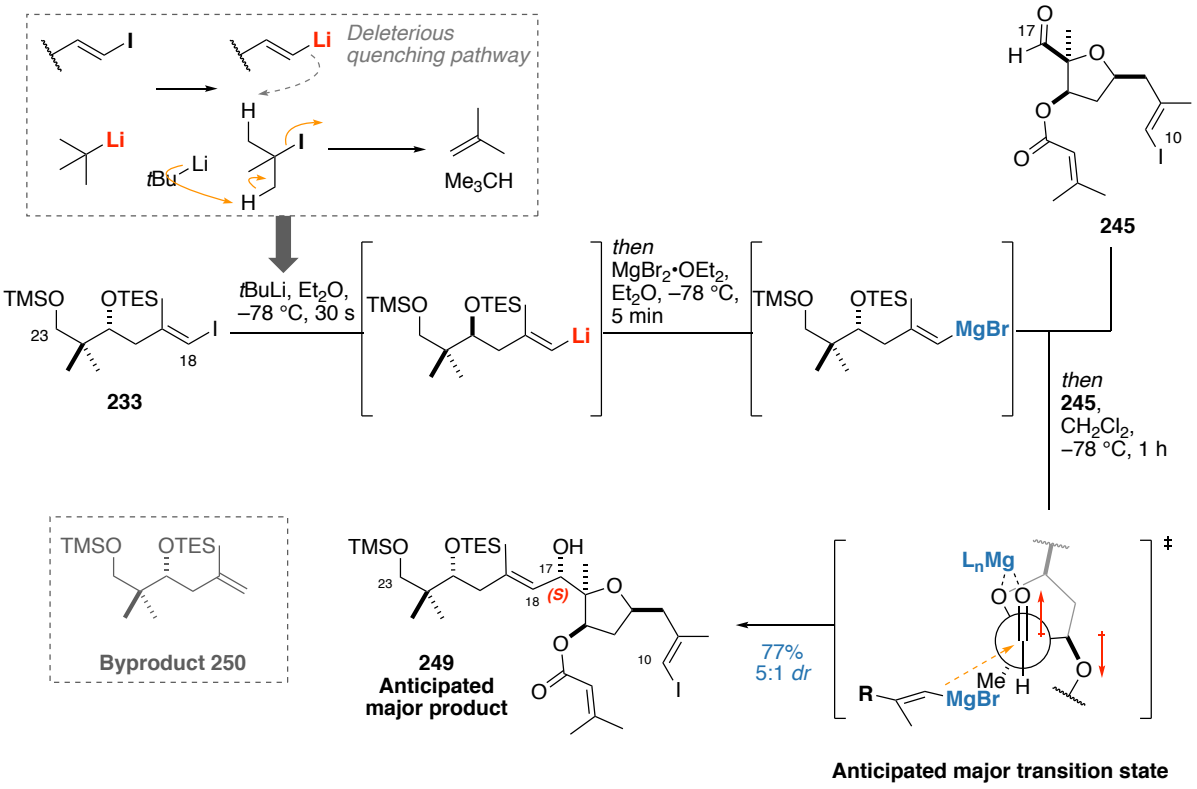

c) **Schematic for the chelation-controlled vinylmetal addition of 232 into 245**

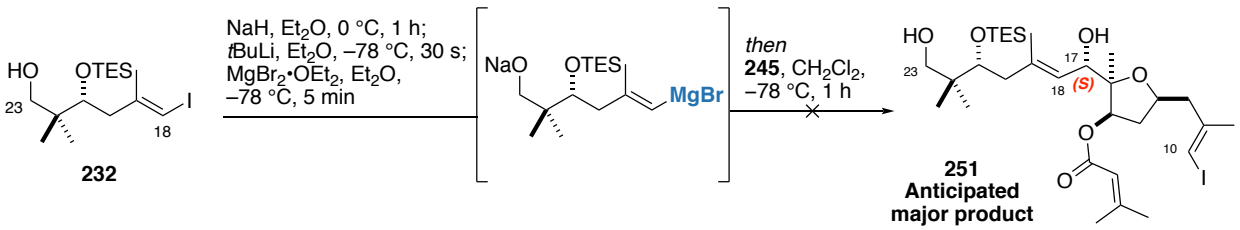

Scheme 47. *a) Excerpt from Evans' synthesis of phorboxazole B, employing a chelation-controlled vinyl Grignard addition. b) Synthesis of the anticipated major product* ***249*** *from* ***233*** *and* ***245****. c) Attempted synthesis of* ***251*** *from* ***232*** *and aldehyde* ***245***

With the requisite bond formed, the next immediate goal was ascertaining the stereochemical outcome of the addition. Noting that the configuration at C15 was conclusively proved by Muir through Mosher analysis and NOE studies of previous intermediates, a proof of the configuration at C17 can be obtained through Rychnovsky's analysis of the corresponding C15,C17-acetonide. Additionally, the Gerwick group has reported the detailed the spectroscopic data for the phormidolide A triacetonide derivative (**151**), which fortuitously allows for further corroboration of the stereochemical outcome at C17, as well as giving supporting evidence for the configuration in this region of the natural product. To do this, adduct **249** was deprotected under acidic conditions and the crude triol subjected to basic hydrolysis conditions to cleave the C15 ester. The corresponding diacetonide **252** can then be readily generated from the crude tetraol on treatment with $(MeO)_2CMe_2$ and PPTS (**Scheme 48**).

As discussed in section **5.2.1**, Rychnovsky's acetonide analysis provides a reliable method for the stereochemical assignment of 1,3-related diols. Unexpectedly, applying the aforementioned analysis to diacetonide **252** gave diagnostic ^{13}C chemical shifts for the 1,3-*anti* acetonide, corresponding to the undesired C17 epimer (*i.e.* **253**) as the major product arising from the Grignard addition (**Scheme 48**). This result was corroborated by NOE analysis of the acetonide, with the NOE enhancements conforming to the expected twist-boat geometry for the 1,3-*anti* acetonide (**Figure 40**). These incongruous observations led to the initial consideration that perhaps the rigid THF ring conformationally locks the acetonide in an atypical conformation, though a literature search of similar 1,3-*anti* systems on THF rings showed very similar NMR shifts to diacetonide **252**,[131] giving further support for the relative configuration of diacetonide **252**.

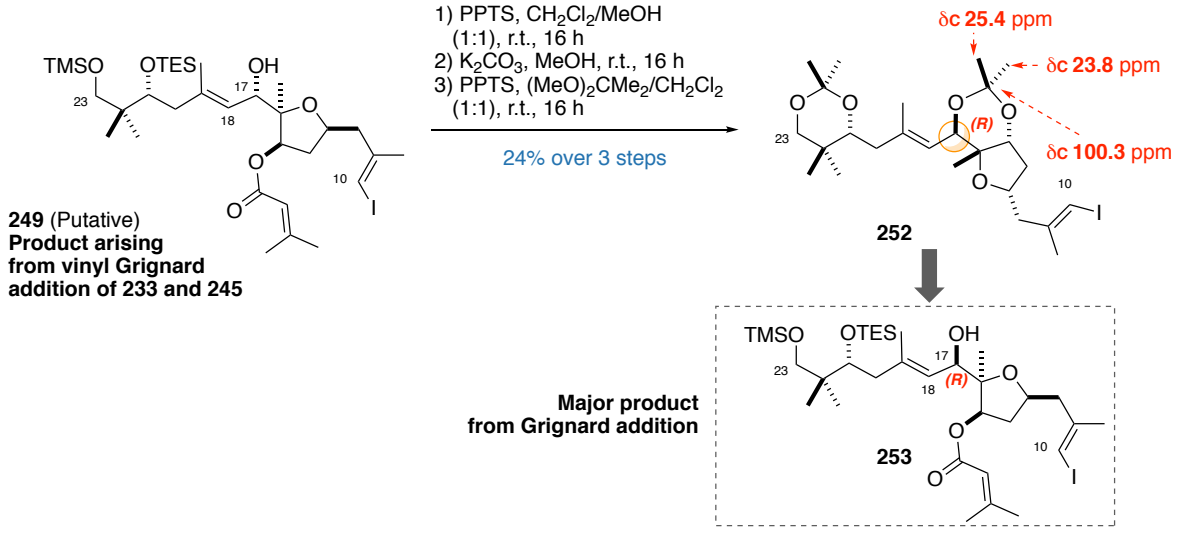

Scheme 48. *Synthesis of diacetonide* ***252****, with* ^{13}C *NMR shifts shown that are diagnostic for the 1,3-anti acetonide*

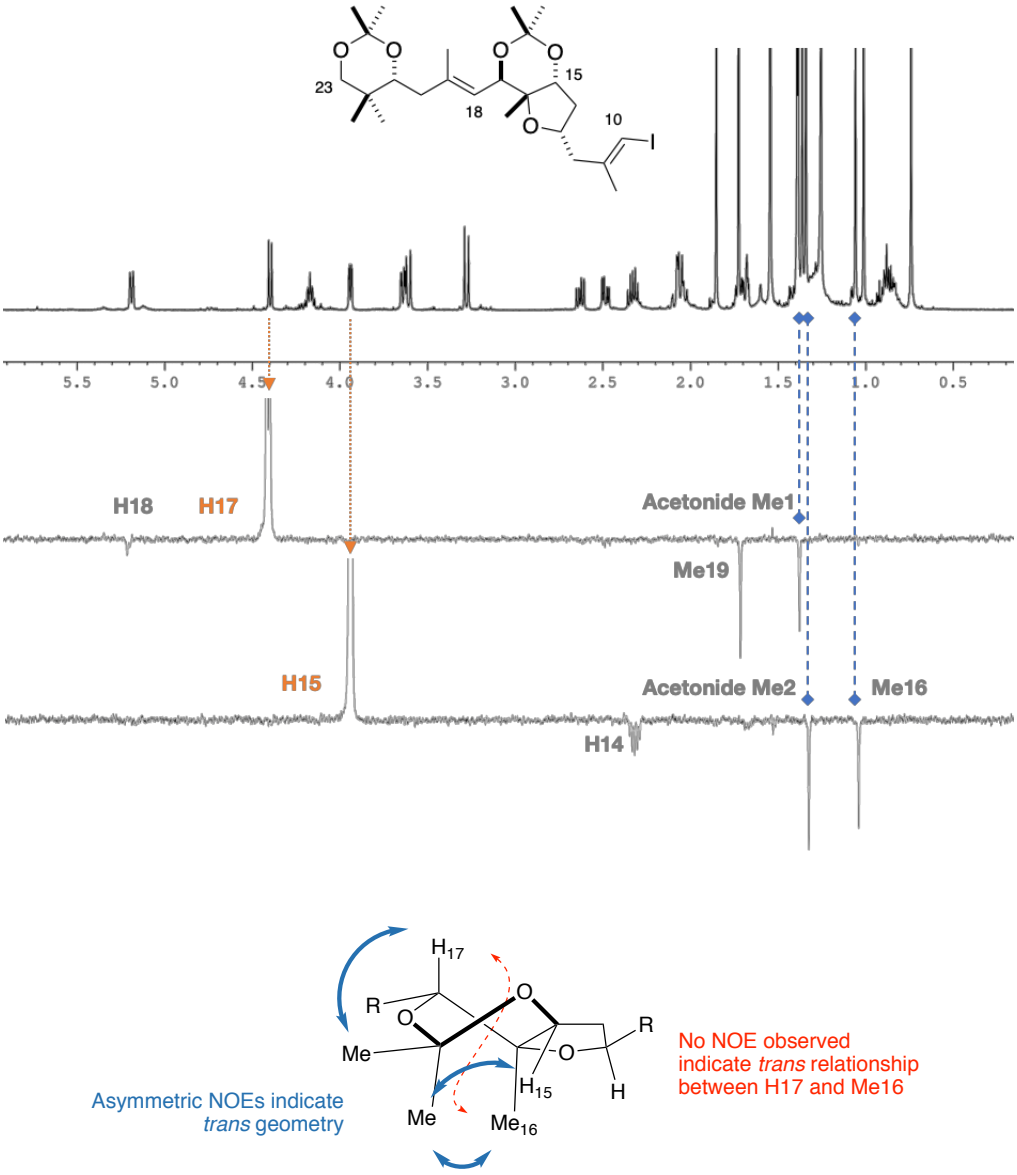

Figure 40. *Observed NOE correlations for* ***252****. Irradiated signals are denoted in orange, while observed NOE correlations from the irradiated signals are denoted in grey. The expected twist boat geometry imposed by the 1,3-anti diol is supported by observing a strong correlation between H15 and Me16 to one of the acetonide Me, and H17 showing a correlation to the other acetonide Me. This indicates that H15 and Me16 sit on one side of the acetonide, while H17 sits on the other, placing H15 and H17 anti to each other in this ring.*

Postulating that perhaps chelation-control was inoperative in this reaction, a control experiment for the vinylmetal addition was conducted where $MgBr_2{\cdot}OEt_2$ was omitted. It was hypothesised that if the omission of $MgBr_2{\cdot}OEt_2$ (i.e. a direct vinyl lithium addition into aldehyde **245**) gave a similar result to the inclusion of $MgBr_2{\cdot}OEt_2$, then it was suggestive that in practice the reaction was proceeding under polar Felkin-Anh control. The exclusion of $MgBr_2{\cdot}OEt_2$ gave the epimeric C17 adduct as the major product in 4:1 *dr* (**Scheme 49**), though a degree of competing protodeiodination was observed at C10 due to competing Li/I exchange

with the vinyl lithium species in the reaction. Again, the stereochemical outcome of this addition was corroborated by synthesising the corresponding acetonide **254**, which was determined to be in a 1,3-*syn* relationship according to diagnostic ^{13}C NMR shifts and reinforced by NOE enhancements (**Figure 41**). This outcome was supported by synthesising the diastereomeric Mosher esters of **249** and analysed following desilylation. Calculating the Δδ values obtained from esters (*R*)- and (*S*)-**255** established the 17*S* configuration of **249** as anticipated from the polar Felkin-Anh controlled addition of the vinyl lithium to aldehyde **245** (see **Scheme 49** and **Table 9**).

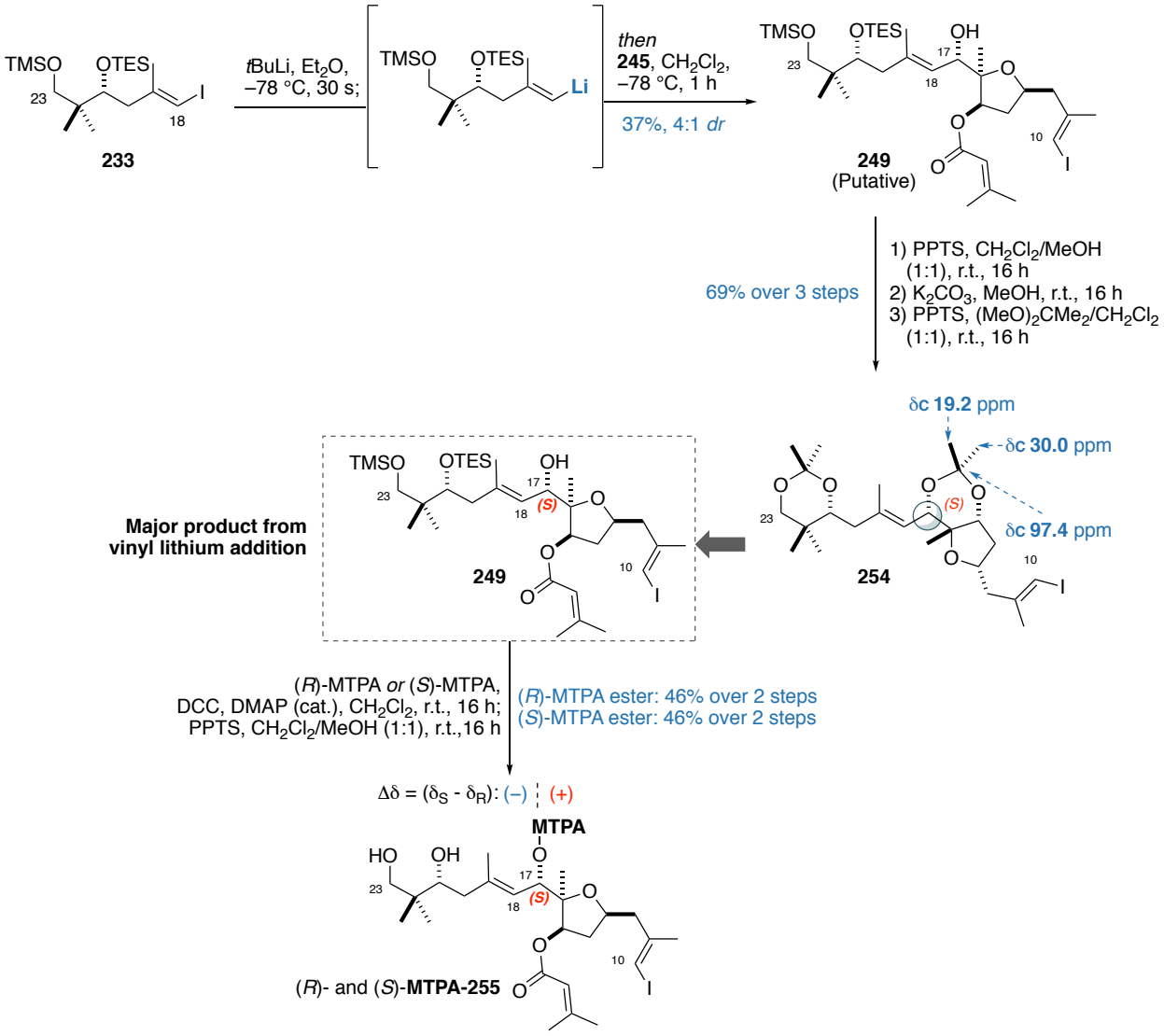

Scheme 49. *The vinyl lithium addition of* ***233*** *into aldehyde* ***245****, and the synthesis of the corresponding diacetonide* ***254****. The absolute stereochemistry at C17 was further corroborated by the synthesis of the diastereomeric Mosher esters (R)- and (S)-MTPA-* ***255***

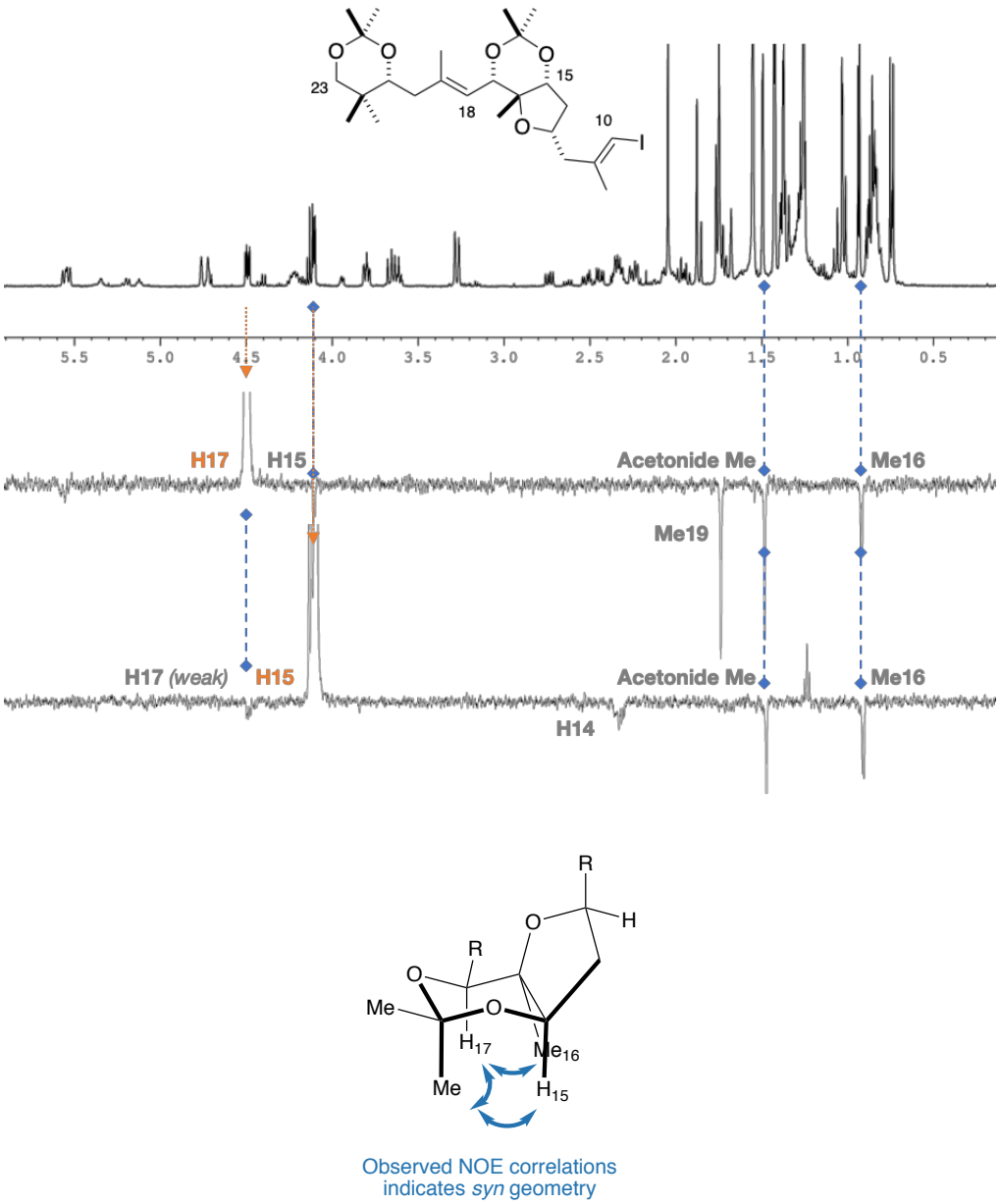

Figure 41. *Observed NOE correlations for* ***254****. Irradiated signals are denoted in orange, while observed NOE correlations from the irradiated signals are denoted in grey. The expected chair geometry imposed by the 1,3-syn diol is supported by a strong enhancement of one of the acetonide Me with all of H15, Me16 and H17. This signifies that all three substituents are sitting on the same side of the ring. Additionally, the other acetonide Me does not show any NOE enhancements to H15, Me16 and H17. This observation places H15 and H17 syn to each other in the ring, and therefore a 15,17-syn relationship exists between them*

***Table 9**. Diagnostic ^{1}H NMR signals for the configurational assignment of 17S*

Proton	**δH (*S*)-MTPA** (ppm)	**δH (*R*)-MTPA** (ppm)	$\Delta\delta_{S-R}$ (ppm)
H13	4.18	4.09	+0.09
H14A	2.43	2.13	+0.30
H14B	1.65	1.10	+0.55
H15	5.04	4.95	+0.09
Me16	1.17	1.14	+0.03
H17	5.81	5.73	+0.08
H18	5.14	5.33	-0.19
Me19	1.75	1.76	-0.01
H20A	2.11	2.17	-0.06
H20B	1.94	1.97	-0.03
H21	3.48	3.53	-0.05

These results revealed that chelation-control was indeed operative in the vinyl Grignard addition, although unexpectedly, the result suggested that the 'small' group where the nucleophile traverses over was not the methyl group, but in fact over the THF ester as shown in **TS-XIV** (**Scheme 50a**). Additionally, it highlights that the proximate Me16 was exerting a disproportionately large influence against the incoming nucleophile. Conversely, it affirms the polar Felkin-Anh approach for the vinyl lithium addition in the synthesis of **249** *via* **TS-XV**. Related examples in the literature, as reported by Myers *et al.* do indeed have nucleophiles traversing over a methyl substituent as the small group under chelation control (**Scheme 50b**).[132] In a structurally more similar example by Wolfrom and Hanessian,[133] the expected chelation-control product for a THF-containing aldehyde (omitting the analogous Me group) gave the major product as expected, highlighting that the outcome for the Grignard addition into aldehyde **245** to give **253** is indeed anomalous.

To rationalise this counterintuitive outcome, a DFT optimisation of a model chelated structure **256** was conducted. Interestingly, the lowest energy conformers all position the carbonyl C=O bond and the ether oxygen coplanar to each other, leading to a lowest-energy conformation where Me16 was projected perpendicularly away from the plane (**Figure 42**). A cursory analysis of this structure revealed that there was in fact a clear pocket where the nucleophile could readily traverse, which was located towards C15 and the THF. A similar approach on the opposite side is blocked by the protruding Me16 group, leading to the observed product as the major diastereomer under chelation-control. This model however, must be considered preliminary as solvated organomagnesium reagents rarely exist as a single species in their monomeric forms,[134] and proximal Lewis basic groups such as the C15 acyloxy group could further participate in chelation.[135] All these factors mean that the true transition state structure is likely to be more complex than that proposed in **TS-XIV**.

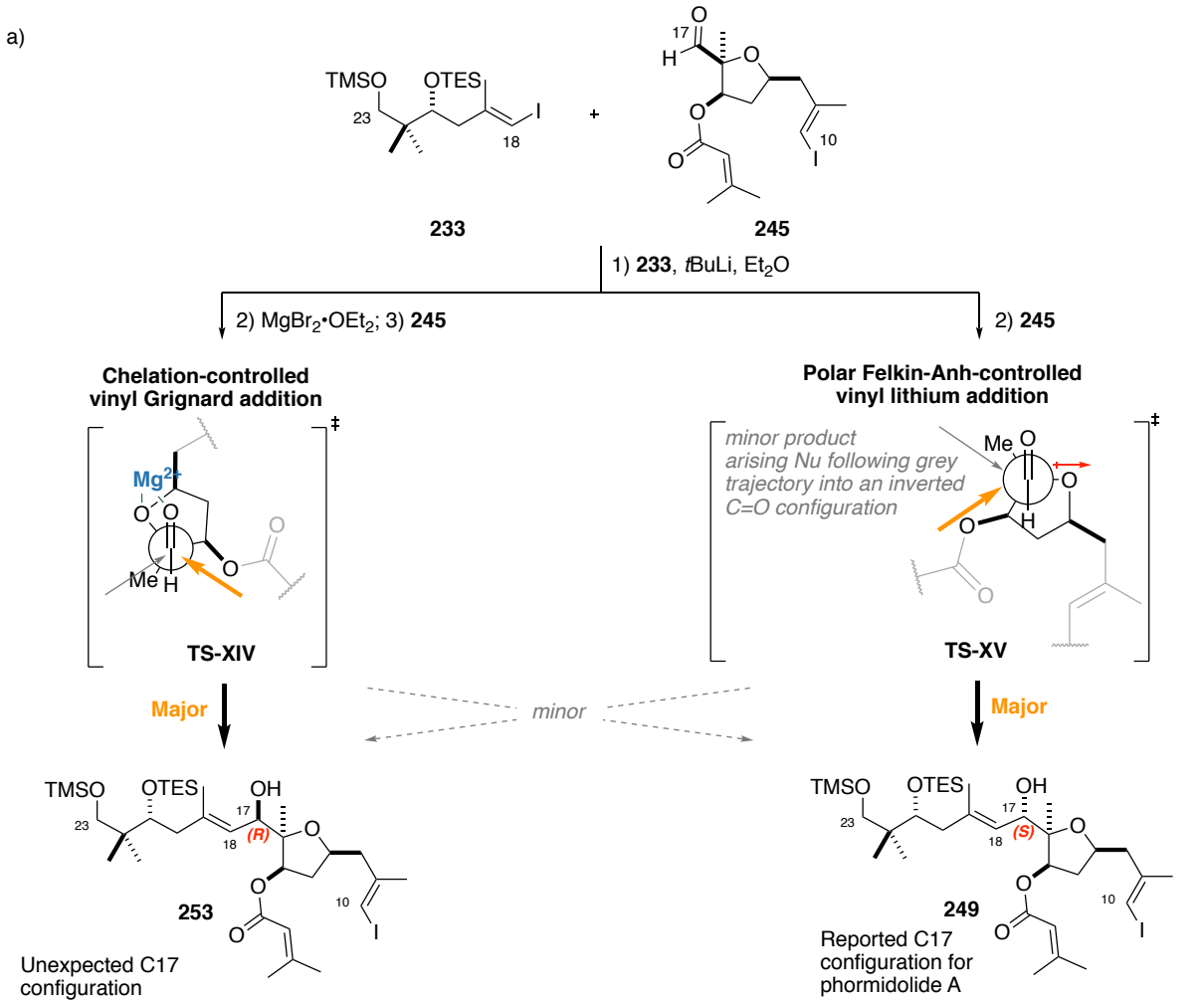

b) **Other literature examples of Grignard additions giving the expected product**

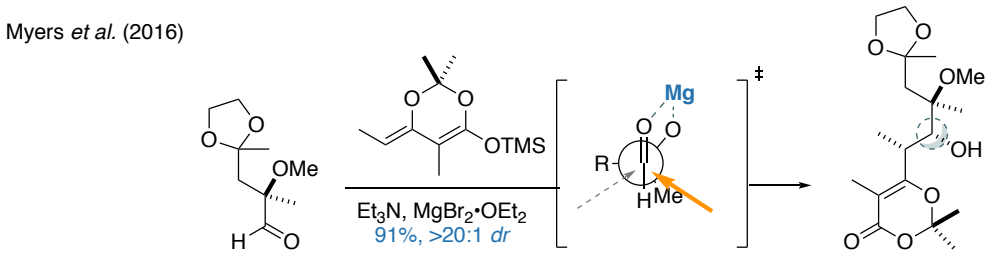

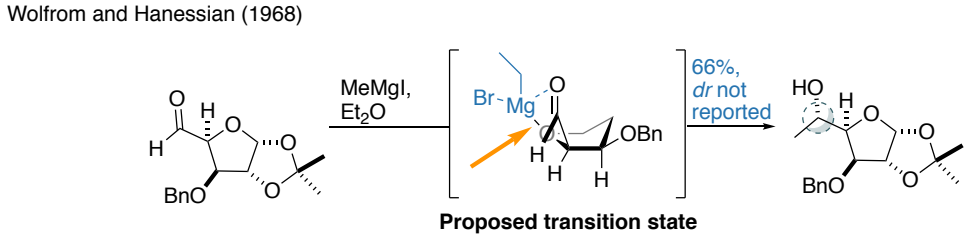

Scheme 50. *a) Transition state schematics rationalising the major products observed in the chelation-controlled vinyl Grignard addition, and the polar Felkin-Anh dictated vinyl lithium addition leading to adduct* ***253*** *and* ***249*** *respectively, b) Relevant literature examples of chelation-controlled additions into aldehydes that give the expected product*

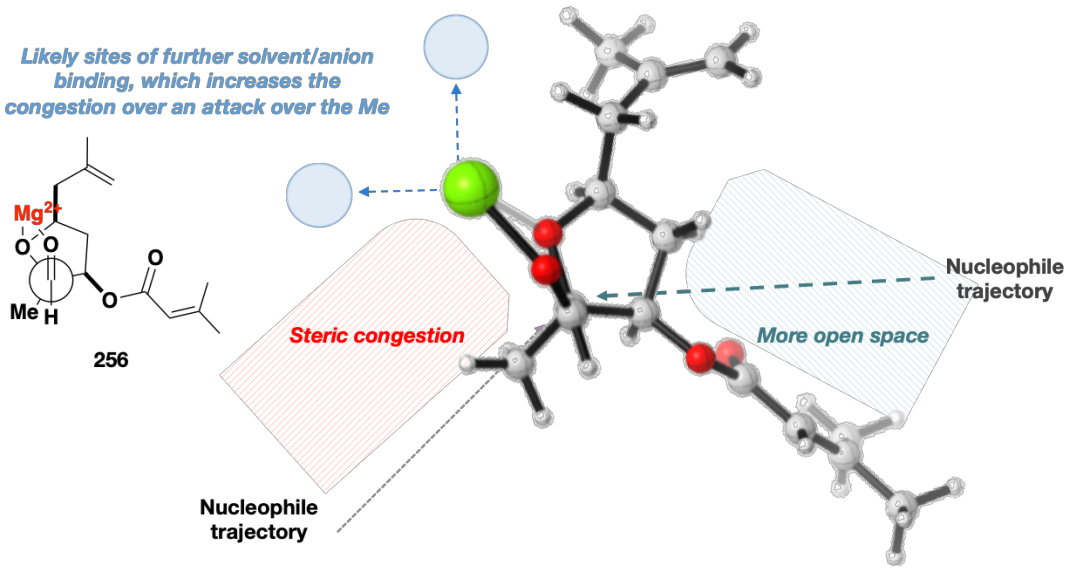

Figure 42. *B3LYP 6-31G(d,p) optimised structure of a model Mg-chelated structure* ***256****, rationalising the observed diastereoselectivity for the chelation-controlled vinyl Grignard addition*

6.3.3. The stereochemical reassignment of phormidolide A and the implication for its biosynthesis

With the two diastereomeric acetonides **252** and **254** and the NMR data for phormidolide A triacetonide **151** in hand, a further stereochemical corroboration was sought for the C10-C23 region of phormidolide A. Interestingly however, diacetonide **252** (arising from the counterintuitive chelation-controlled addition), rather than diacetonide **254** (which has the reported configuration for C15 and C17) proved to be the better match to the triacetonide derivative of phormidolide A! In particular, the phormidolide A triacetonide derivative **151** appeared to display excellent homology to the ^{1}H and ^{13}C shifts for the acetonide regions, *with the ^{13}C signals for the acetonide methyl groups diagonistic for what appeared to the anti acetonide, rather than the reported syn acetonide* (**Figure 43**).

Because the clear spectroscopic observations that were presented unambiguously determined the configuration of diacetonide **252** and **254**, this perplexing observation *vis-à-vis* phormidolide A triacetonide **151** led to the conclusion that either C15 or the C17 centre was missassigned. A thorough review of NOE data of the natural product and comparison with known synthetic intermediates towards aldehyde **245** ruled out C15 as the suspect stereocentre. Specifically, all intermediates bearing the reported 15*R* geometry contain ^{1}H signals at *ca.* 2.30-2.40 ppm, and 1.60-1.70 ppm for the diastereotopic protons of H14 (N.B.: in phormidolide A, these resonate at 2.33 and 1.57 ppm, and in phormidolide A triacetonide **151** at 2.32 and 1.75 ppm). The alternative 15*S* configuration on the other hand, shows ^{1}H signals for H14 at *ca.* 1.95 and 1.90 ppm, which do not agree with the natural product (**Figure 44**). Alongside this, key NOE correlations observed by Muir in these intermediates were also in strong support for the reported C15 configuration, leaving C17 as the likely culprit centre.

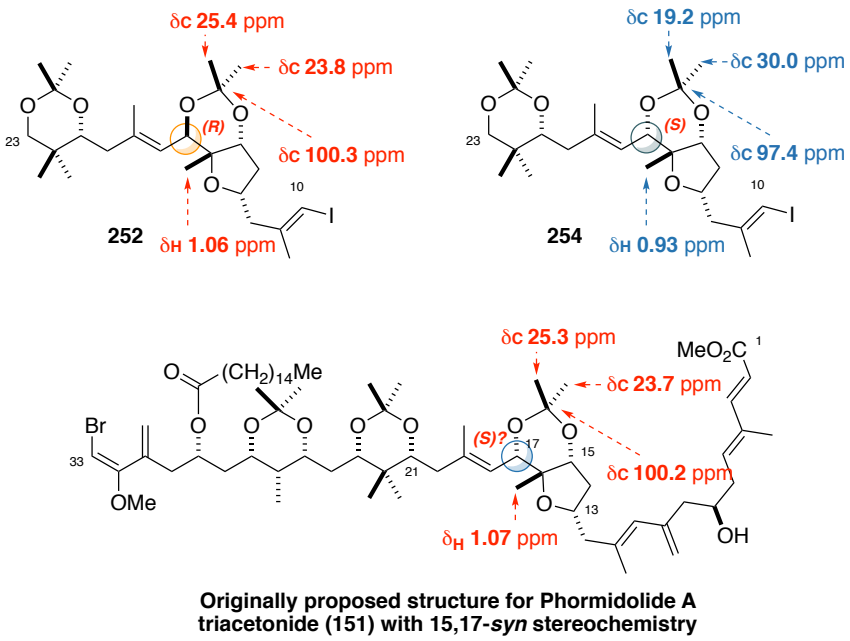

Figure 43. *Diagnostic NMR signals for diacetonides* ***252*** *and* ***254*** *as compared with the phormidolide A triacetonide derivative* ***151****, highlighting the large chemical shift deviations recorded between the reported 17S configuration*

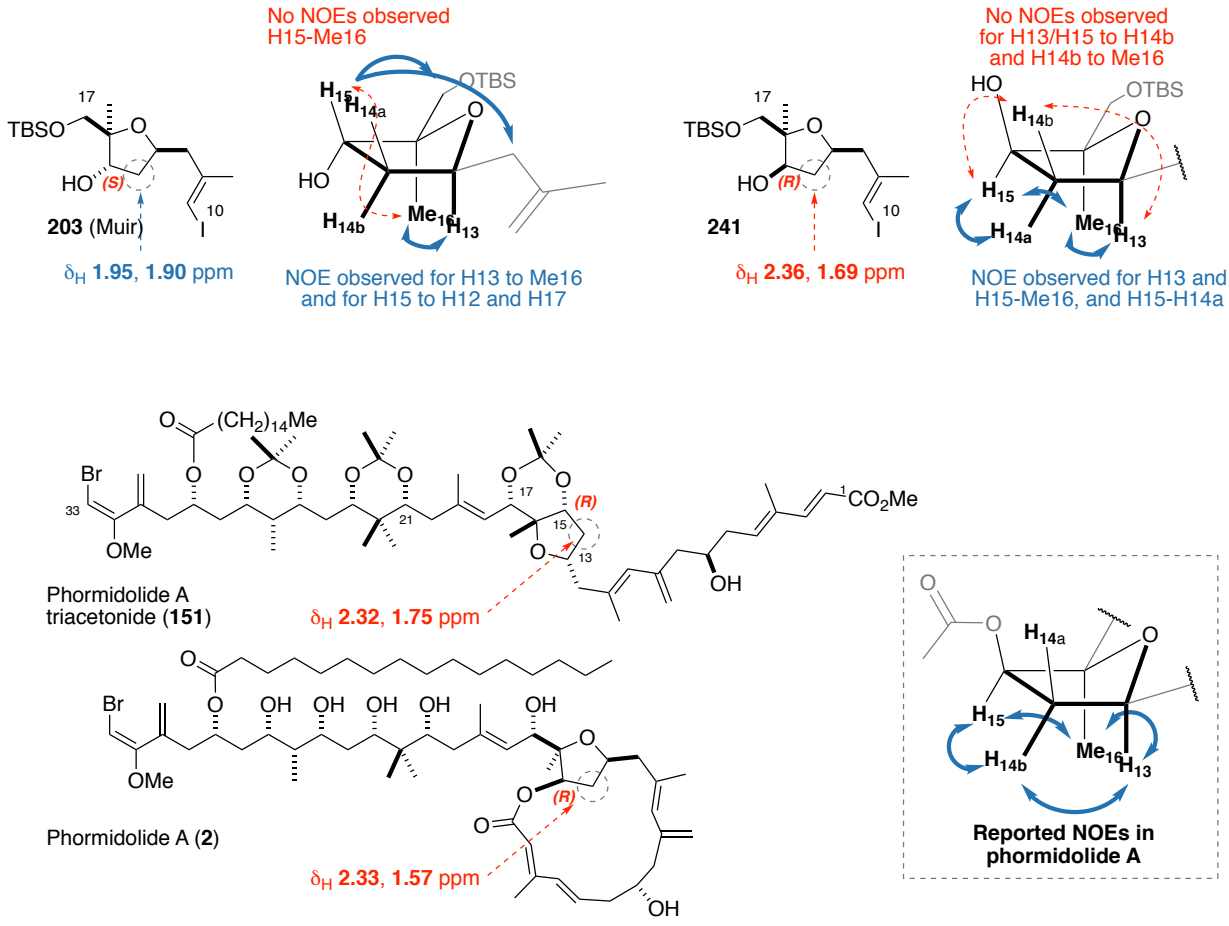

Figure 44. *The* ^{1}*H NMR and NOE comparisons of alcohols* ***203*** *and* ***243*** *with phormidolide A and phormidolide A triacetonide* ***151*** *reveals that the 15R configuration is correctly assigned*

At this point, a thorough re-examination of the $^{2/3}J$ and NOE data as reported in the isolation paper was conducted. A reanalysis of the reported NOE enhancements, taking into account all *J* values gave two possible conformers for the C16-C18 region. In the isolation paper, Williamson *et al.* presented one of two possible conformations surrounding C17 (**Table 10** and **Figure 45**).[2] While taking into account all *J* values, the reported conformation places H18 and Me16 too far away to observe the reported NOE enhancement. Instead, the alternative C17 epimer that takes into account all reported *J* values positions H18 in a proximal geometry to Me16, which accounts for the strong observed NOE correlation. This reanalysis, alongside with the interpretation of the data obtained by comparing **252**, **254** to phormidolide A triacetonide **151**, reinforces the proposed reassignment from 17*S* to 17*R*.

Table 10. *Excerpt of the NOE and ^{3}J data used for the assignment of C17 from the original isolation paper. The key strong NOE enhancement between Me16 (C37 in the original isolation paper) and H18 is highlighted in orange. St = strong; Wk = weak*

Atom #	^{13}C (ppm)	^{1}H (ppm)	NOESY	COSY (Hz)	HMBC (Hz)
13	76.7	4.48	12b, 14b, Me11, Me16	14a (0.0), 14b (ovlp), 12a (14.0), 12b (5.0)	11 (<0.5), 16 (10.6)
14	34.8	1.57	15	15 (0.0), 13 (0.0)	13 (<0.5), 12 (4.1)
		2.33	13, 15, 2	15 (4.8), 13 (ovlp)	13 (<0.5), 12 (4.5)
15	79.6	5.15	12a, 14a, 17 (st), Me16 (wk), 18 (wk)	14a (0.0), 14b (4.8)	17 (<0.5), Me16 (5.5)
16	86.9	-			
17	69.7	4.70	Me19, 15 (st), Me16 (wk)	18 (9.0)	19 (3.7), 16 (5.6), 15 (5.5), Me16 (5.0)
18	127.0	5.40	Me16 (st), 20a, 15 (wk)	17 (9.0)	20 (6.0), 16 (0.8), Me19 (10.0)
19	137.4				
Me16	21.0	1.19	13, 17 (wk), 15, 18 (st)		

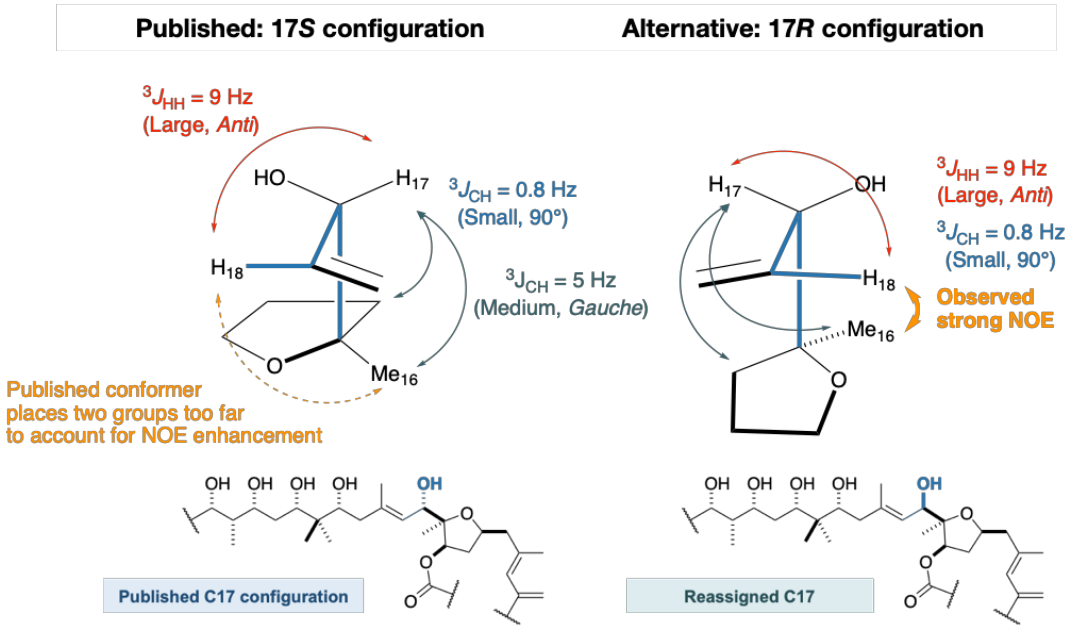

Figure 45. *Conformers taking into account all published J values for phormidolide A, highlighting an unconsidered conformer for 17R that better explains the observed strong NOE between H18 and Me16*

As previously discussed in section **5.2.2**, the inconclusive evidence presented for the *J*-based configurational analysis between C17 and C21 meant that the relative configuration for the C1-C18 region to the side chain was considered to be uncertain. In light of this reassignment, it was prudent to check whether or not C21 was configured correctly by synthesising the alternative C21 epimer of adduct **253** and its corresponding diacetonide. Taking note of the lessons learnt from hemicalide (see section **3.4**), it was hoped that the distal 1,5-related stereocentres would exhibit clear NMR differences for the diacetonide to allow for the unambiguous assignment of the configuration between these two regions. Starting with ***ent*-233** and aldehyde **245**, an analogous chelation-controlled vinyl Grignard addition delivered adduct **256**, which could then be transformed to the corresponding diacetonide **257** containing the epimeric C21 stereocentre. The Grignard addition gave the now expected 17*R* configuration, as confirmed by Rychnovsky's acetonide analysis of **257 (Scheme 51)**.

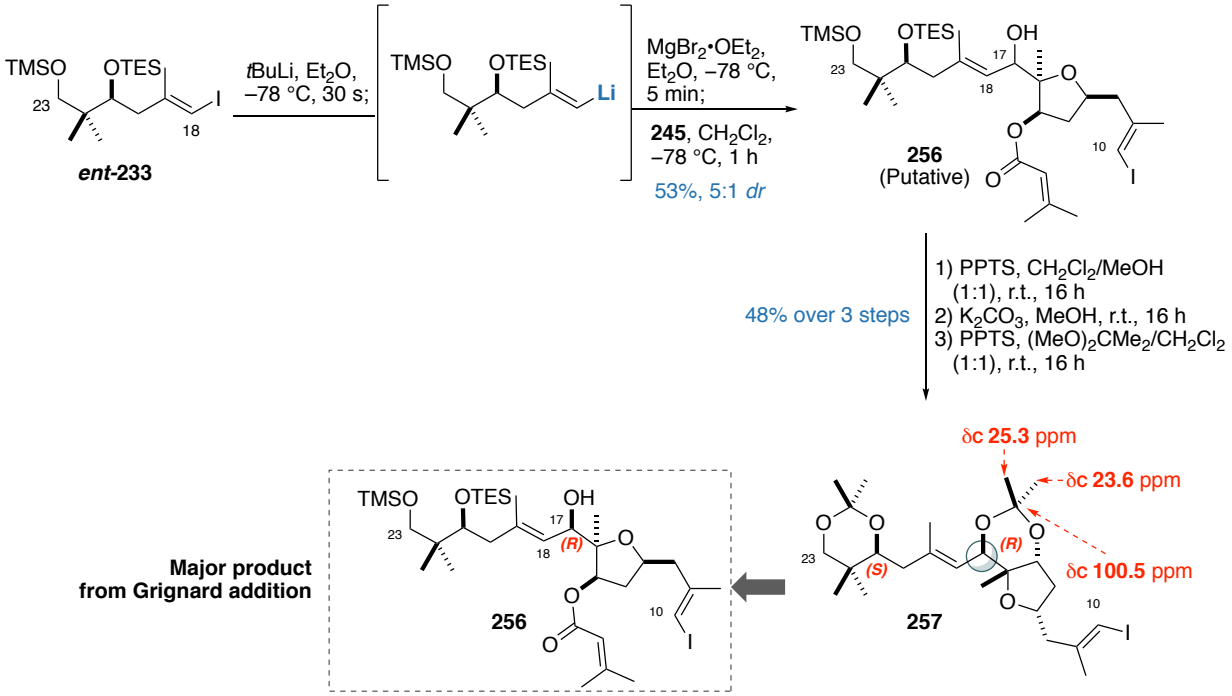

Scheme 51. *Synthesis of adduct* ***256****, and the corresponding diacetonide* ***257****, confirming the 17R configuration arising from the chelation-controlled Grignard addition*

With the three diastereomeric acetonide **252**, **254** and **257** in hand, a detailed spectroscopic comparison with phormidolide A triacetonide **151** was conducted. On initial inspection, diacetonide **254** containing the reported 17*S* and 21*S* configuration was immediately eliminated as a plausible diastereomer for phormidolide A on the basis of the large chemical shift deviations (data summarised in **Table 11** and **Figure 46**, graphical comparisons in **Figure 47** and **Figure 48**). For the remaining diacetonides containing the revised 17*R* configuration but differing in the configuration of C21, the ^{13}C NMR shift differences were particularly diagnostic, revealing that diacetonide **252** was a poorer fit for the natural product compared to diacetonide **257** (**Figure 49** and **Figure 50**). These results allowed for the conclusive reassignment of both

C17 and C21 from the reported 17*S* and 21*S* configuration, to their corresponding epimers: 17*R* and 21*R*. As the configuration of the remainder of the side chain was conclusively relayed back to C21 *via J*-based analysis and corroborated by the diacetonide derivative, these results mean that the reported 17*S*, 21*S*, 23*R*, 25*S*, 26*R*, 27*R*, 29*R* configuration present in the natural product needs to be revised to their corresponding epimers (**Figure 46**), *i.e. a reassignment of seven of the 11 stereocentres present in phormidolide A*. Noteworthily, this revelation was enabled through the unexpected and serendipitous stereochemical outcome from the chelation-controlled vinyl Grignard addition of vinyl iodide **233** and aldehyde **245**.

Table 11. *Summary of ^{1}H and ^{13}C shift differences, represented as total sum of errors and maximum errors between* ***252***, ***254***, ***257*** *and phormidolide A triacetonide* ***151****. Absolute errors taken from H/C10-H/C21, inclusive of acetonide proton and carbon signals.*

	Σ $\|\Delta\delta_H\|$ (ppm)*	Max $\|\Delta\delta_H\|$ (ppm)	Σ $\|\Delta\delta_C\|$ (ppm)*	Max $\|\Delta\delta_C\|$ (ppm)
257 (21-*epi*-15,17-*anti*)	**0.24**	**0.08**	**3.2**	**1.5**
252 (15,17-*anti*)	0.32	0.11	8.2	2.7
254 (15,17-*syn*)	1.34	0.37	30.0	8.2

*$|\Delta| = \delta$(Experimental) – δ(Reported)

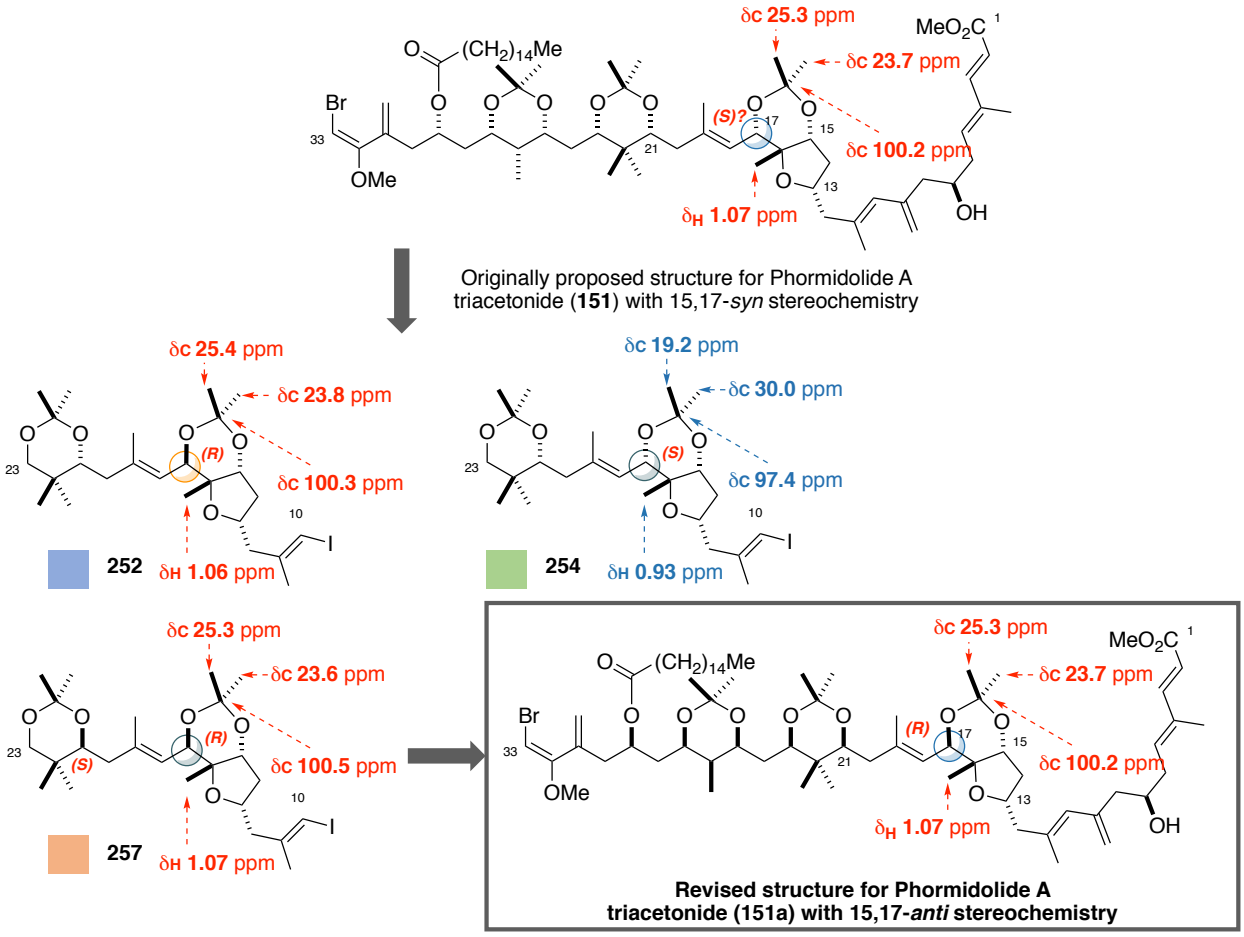

Figure 46. *Comparison between diacetonides* ***252***, ***254*** *and* ***257*** *with phormidolide A triacetonide* ***151****, leading to the reassignment of phormidolide A as shown in* ***151a***

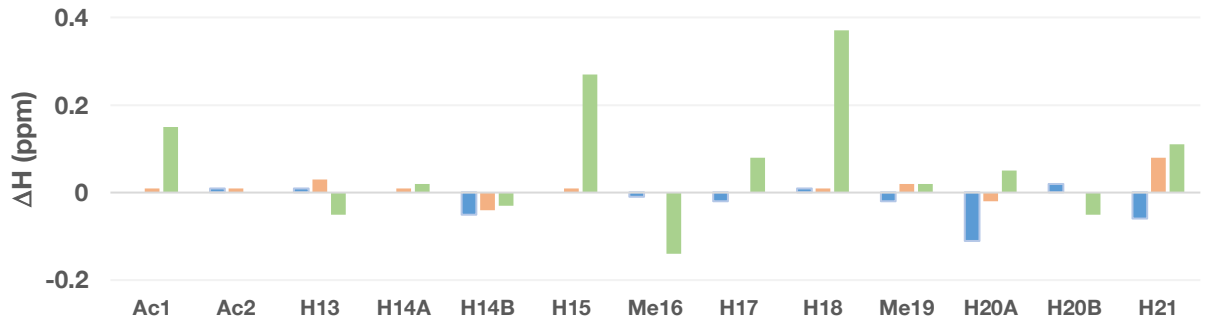

Figure 47. *Bar chart showing [1]H NMR shift differences of diacetonides* ***252, 254*** *and* ***257*** *between H13-H21.(Legend in* ***Figure 46****)*

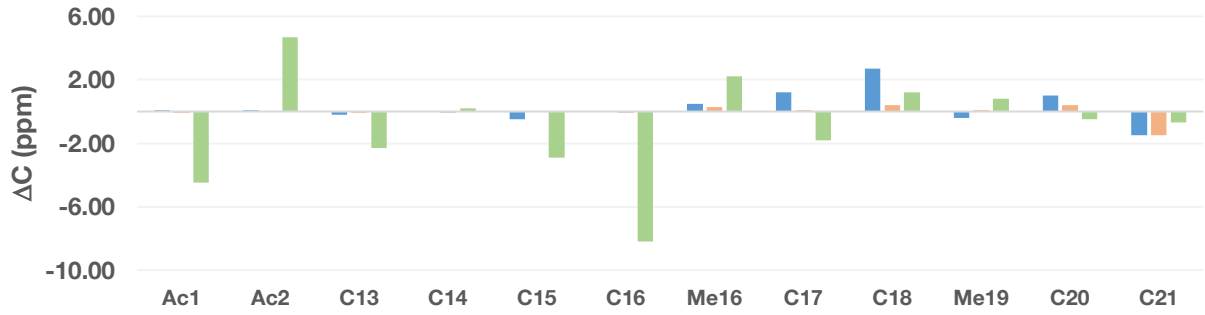

Figure 48. *Bar chart showing [13]C NMR shift differences of diacetonides* ***252, 254*** *and* ***257*** *between C13-C21 (Legend in* ***Figure 46****)*

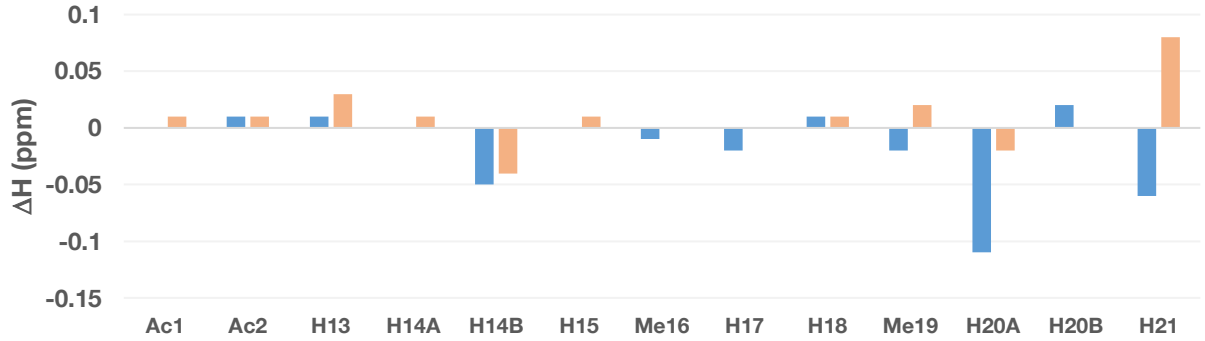

Figure 49. *Bar chart showing [1]H NMR shift differences of* ***252*** *and* ***257*** *between H13-H21 (Legend in* ***Figure 46****)*

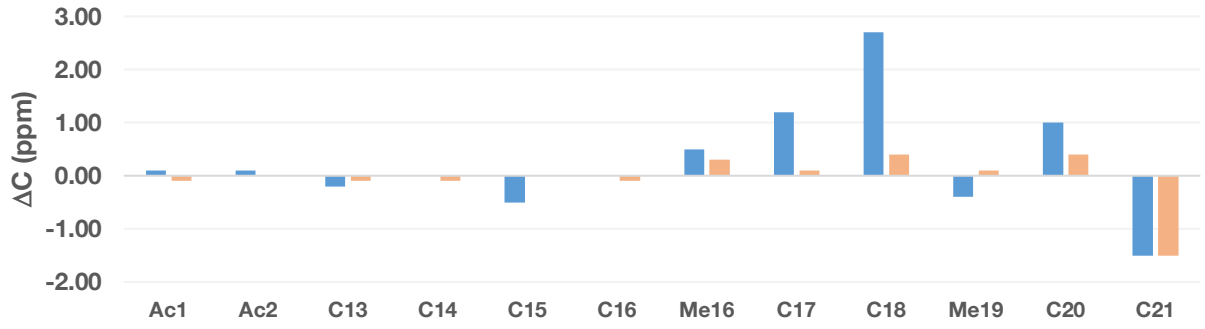

Figure 50. *Bar chart showing [13]C NMR shift differences of* ***252*** *and* ***257*** *between C13-C21 (Legend in* ***Figure 46****)*

The revised configuration of phormidolide A from **2** to **2a** may now be accounted for by the proposed biosynthetic hypothesis put forth by Bertin *et al.* (**Figure 51**).[82] In this paper, Bertin *et al.* highlighted that all ketoreductase-configured stereocentre present in phormidolide A were L-configured, despite the fact that the ketoreductases responsible for its configuration appeared to predict the formation of D-configured hydroxyl groups (for a detailed discussion, see section **5.2.3**). The reassignment of the carbinol stereocentres at C17, C21, C23, C25 and C29 leads to the corresponding D epimer. This revelation is now concordant with the observation that the type B-like ketoreductases present in the biosynthesis of phormidolide A catalyse the formation of D-OHs, leaving OH7 as the single anomalous L-OH formed by a D1758-containing ketoreductase, rather than *all* the ketoreductases being anomalous.

Importantly, this present section leads to the resolution of the stereochemical conundrum for phormidolide A at the outset of this work. Thus, through the synthesis of three diastereomeric acetonides, conclusive evidence was provided for the reassignment of both C17 and C21, and therefore the remainder of the side chain relative to the macrolactone. Gratifyingly, this stereochemical reassignment was justified by the reported biosynthesis of the natural product, giving further support for the conclusions from this study.

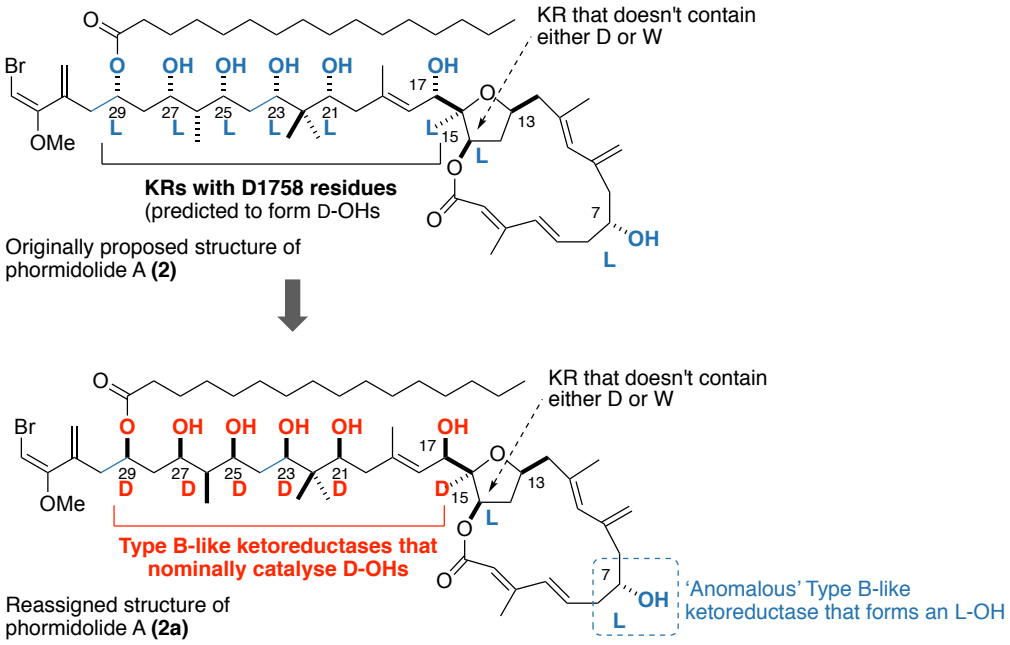

Figure 51. *Annotation of the configuration and the ketoreductases (KRs) responsible for setting the carbinol stereocentres in phormidolide A, highlighting that this proposed reassignment better rationalises the configuration for the natural product.*

6.4. Revised retrosynthetic analysis of phormidolide A

The previous section detailed the expeditious synthesis of the C18-C23 vinyl iodides **233** and ***ent*-233**, which has enabled the verification of a key fragment coupling strategy as well as the crucial stereochemical reassignment of the natural product. At this point, the cumulative lessons learnt from the journey so far merit a further discussion of the proposed retrosynthetic analysis for phormidolide A.

The revised endgame for phormidolide A involves a (+)-DIPCl-mediated aldol reaction with the C25-C33 ketone ***ent*-226** and a suitable aldehyde intermediate, followed by an *in situ* 1,3-*syn* reduction (**Scheme 52**). As the configuration of phormidolide A was now deemed to be secure, pursuing both enantiomers of the side chain was no longer necessary. The planned chelation-controlled Grignard addition has proven to be effective at installing the now desired configuration at C17 with model aldehyde **245**. However, this unexpected and serendipitous result, ostensibly resulting from the nucleophile attacking into the carbonyl from the same face as the C15 ester (**TS-XIV**), meant that the stereocontrol in of this addition was likely to diminish with the full macrocycle in place. This was anticipated to be case as the full macrocycle would result in greater steric hindrance for the desired nucleophile trajectory (**TS-XVI**), whereas fortuitously in our model studies, the C15 dimethylacrylate ester appeared to minimally contribute to the steric bulk. The outcome of this would diminish, if not completely overturn the facial selectivity for the addition. Balancing the opportunities that had arisen from the model chelation-controlled vinyl Grignard addition and the risk of poor selectivity with the macrocycle in place, it was clear that the installation of the C18-C23 region should precede macrocyclisation, ideally with a C15 ester moiety in place.

Additionally, the lack of reactivity arising from the intermolecular Mitsunobu inversion at C15 means that a Mitsunobu macrolactonisation process was unlikely to succeed. With the success of both the Keck and Yamaguchi conditions, the ring-closing step for the C1-C17 macrolactone was revised to a Yamaguchi macrolactonisation, a reaction successfully employed in the synthesis of many complex macrolide natural products within the Paterson group. The synthesis of this *seco* acid would arise from a basic hydrolysis of a methyl ester precursor. Considering that the dimethylacrylate ester was proven to undergo facile basic hydrolysis (K_2CO_3), the appendage of the dimethylacrylate ester at C15 served both as a protecting group and as a functionality to help maintain the diastereoselectivity in the Grignard addition. Retrosynthetically, this reveals the linear C1-C17 aldehyde **258** and the C18-C23 vinyl iodide ***ent*-233** as the chosen precursors for the planned chelation-controlled Grignard addition.

Revised retrosynthesis of reported phormidolide A

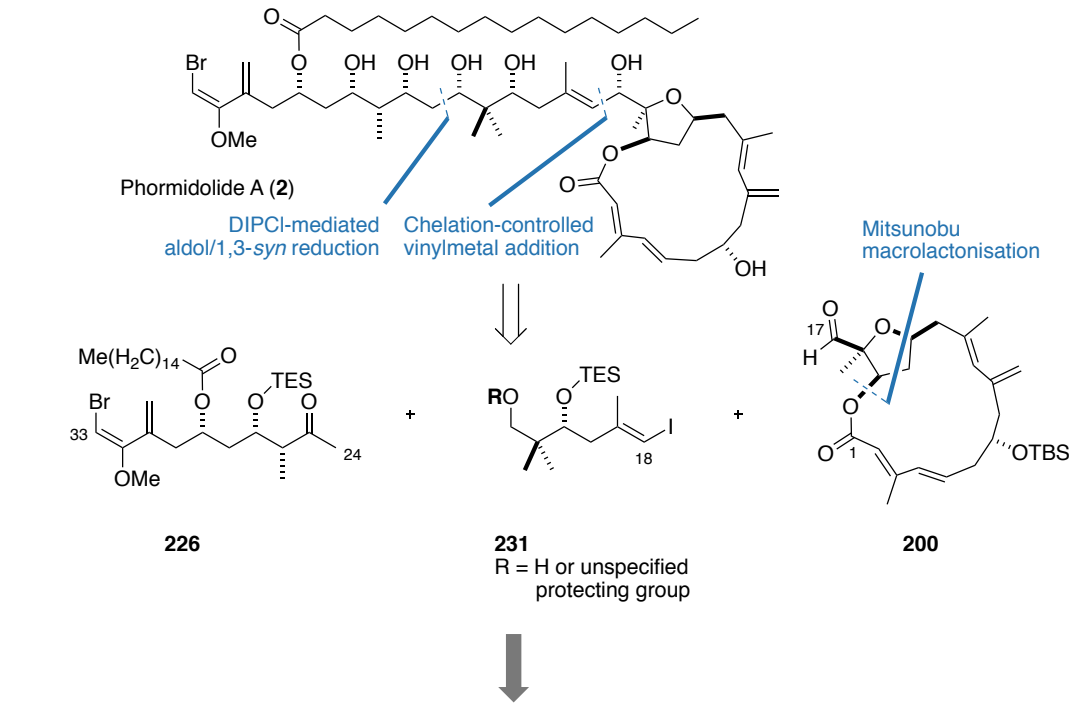

Retrosynthesis of reassigned phormidolide A

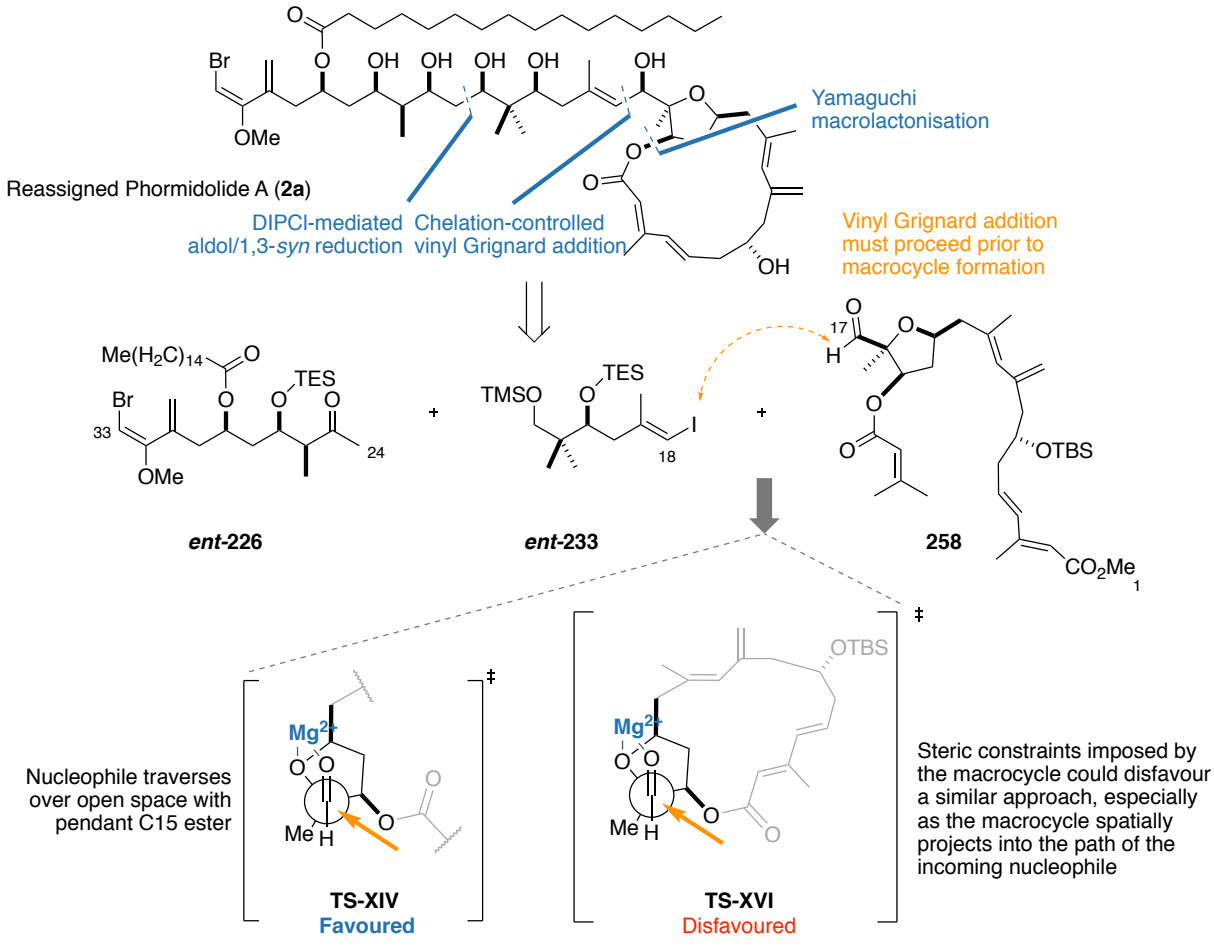

Scheme 52. *Revised retrosynthesis for reassigned phormidolide A*

6.5. Synthesis of the C24-C33 side chain

The C24-C33 fragment ***ent*-226** contains three stereocentres and terminates in the signature bromomethoxydiene motif characteristic of the phormidolide family of natural products. Leveraging the 1,4-*syn* relationship between Me26 and the oxygen bearing stereocentre at C29 in **259**, the fragment can be disconnected across C28-C29 *via* a diastereoselective boron-mediated aldol reaction followed by a 1,3-*syn* reduction to configure both C27 and C29, to reveal known ketone (*S*)-**48** and aldehyde **260** as the requisite starting material (**Scheme 53**).

With many examples, including those from the Paterson group of similar types of 1,4-*syn* aldol reactions, the challenge here is to develop a concise synthesis of aldehyde **260** containing the bromomethoxydiene motif. At the upper limit, one could intercept Álvarez's synthesis of ketone *E*-**179**, itself requiring eight steps, and homologate to generate aldehyde **260**. However, this solution was deemed circuitous and attempts at developing a more concise method towards installing this motif were investigated.

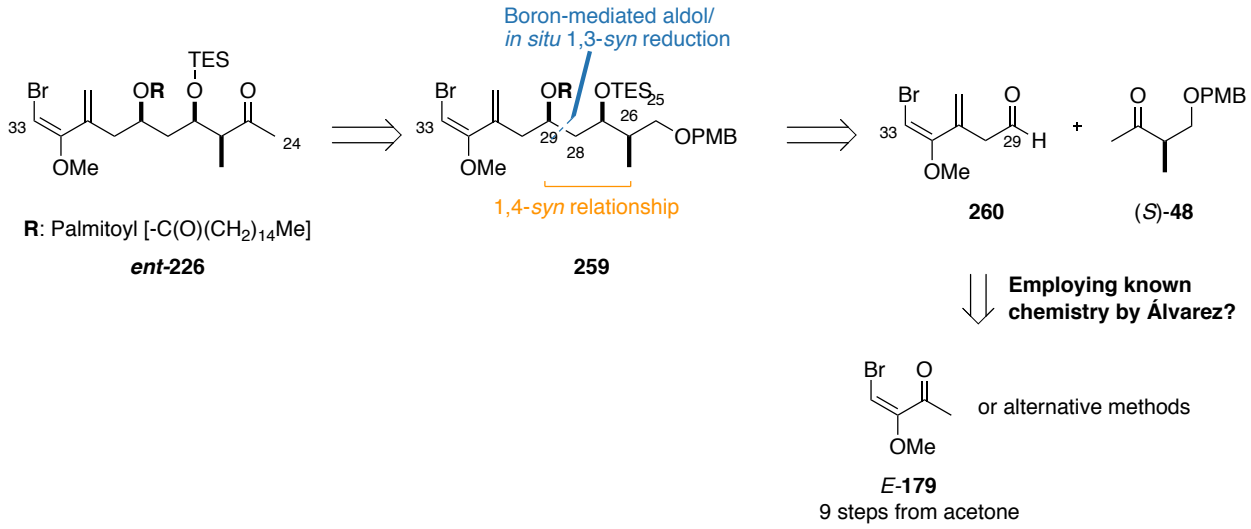

Scheme 53. *Retrosynthesis of the C24-C33 fragment* ***ent*-226** *to reveal aldehyde* ***260*** *and ketone (S)-****48***

6.5.1. Initial approach: towards a more efficient manner of installing the bromomethoxydiene motif

Beyond the sequence developed by Álvarez, the bromomethoxydiene motif could conceptually arise from two further means: a transition-metal catalysed *trans*-functionalisation of an alkyne, or through a direct electrophilic bromination/elimination sequence from a suitable methoxyenol ether precursor (**Scheme 54a**). Drawn by the possibility of installing this elusive functionality in a single operation, initial studies were focused on identifying a suitable protocol to carry out a formal methoxymetalation-bromodemetalation sequence on a model alkyne **261** to generate **262** (**Scheme 54b**). This was hypothesised to proceed *via* an *anti*-stereospecific methoxymetalation process following alkyne activation by a suitable

π-Lewis acid. The subsequent intermediate could then be trapped out by a source of electrophilic bromine to generate the required functionality. However, a range of gold-catalysed[136–138], silver-catalysed and mercurative[139,140] protocols failed to give any product or gave **263** as the major product (results summarised in **Table 12**). Notably, no olefinic protons were observed in the crude product mixture, which suggested that any processes that were operative reacted further with the electron rich enol ether intermediate, to result in the undesired dimethoxyacetal as a putative product.[141]

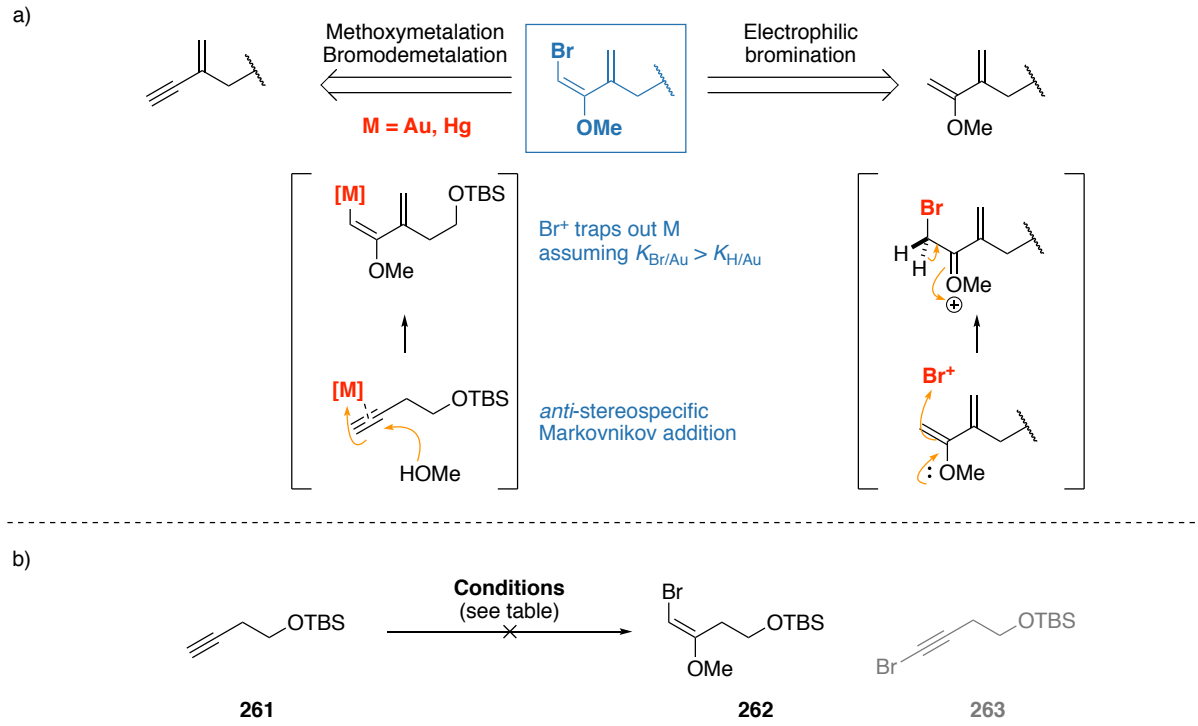

Scheme 54. *a) Alternative methods to synthesise the bromomethoxydiene motif. b) Attempts at effecting a metal-catalysed synthesis of the bromomethoxyenol ether*

Table 12. *Summary of conditions trialled for the transformation of **261** to **262***

Conditions	Solvent	Result
NBS (1 eq.), r.t., 3 – 24 h	DCE/MeOH (1:1)	**263** observed
$AuClPPh_3$ (5 mol%), r.t., 3 – 24 h	DCE/MeOH (1:1)	No reaction
$AuClPPh_3$ (5 mol%), NBS (1 eq.), r.t., 3 – 24 h	DCE/MeOH (1:1)	No reaction
$AgSbF_6$ (5 mol%), r.t., 3 – 24 h	DCE/MeOH (1:1)	No reaction
$AgSbF_6$ (5 mol%), NBS (1 eq.), r.t., 3 – 24 h	DCE/MeOH (1:1)	**263** observed
$AuClPPh_3$ (5 mol%), $AgSbF_6$ (10 mol%), r.t., 3 – 24 h	DCE/MeOH (1:1)	No reaction
$AuClPPh_3$ (5 mol%), $AgSbF_6$ (5 mol%), NBS (1 eq.) r.t., 3 – 24 h	DCE/MeOH (1:1)	Degradation
$HgCl_2$ (75 mol%), Et_3N (1.5 eq.), 60 °C, 2 h	MeOH	Degradation

With no promising results attained, this method was deemed unviable and attention turned towards investigating the second proposal for constructing the bromomethoxydiene – the direct electrophilic bromination of a suitable enol ether. This mirrors the proposed biosynthesis of phormidolide A, where it was conjectured that a halogenase enzyme, responsible for oxidising Br^- to Br^+, was responsible for the late-stage bromination of the enol ether precursor, with the configuration of this system set by the α-deprotonation of a favoured conformer (**Scheme 54a**, *vide supra*).

To pursue this biomimetic proposal, a model alkoxyenol ether compound was needed, of which the ethoxy analogue was initially targeted owing to availability of starting materials. The synthesis commenced with the tin-mediated Barbier allylation of dibromide **263** with formaldehyde to give alcohol **264**,[142] which was then protected as the TBS ether **265** to avoid potential interference from the pendant hydroxyl group (**Scheme 55**). A Stille cross-coupling with stannane **266**[§§] was then conducted to give the highly unstable ethoxyenol diene **267**, that needed to be used crude in subsequent transformations as it was prone to hydrolysing into the corresponding ketone **268**. Interestingly, the Stille cross-coupling did not proceed at all under the otherwise reliable Fürstner-type conditions ($Pd(PPh_3)_4$, CuTC). Instead, a screen of conditions revealed that reacting vinyl bromide **265** and stannane **266** under $Pd(PPh_3)_4$ conditions, with CuI and LiCl as required additives reliably gave the desired product.

Frustratingly, subjecting ethoxyenol diene **267** to a variety of electrophilic bromine sources either gave the unwanted bromoketone **269** or caused the degradation of the starting material. In all cases, it appeared that the base-mediated α-deprotonation required to generate bromomethoxydiene **270** is disfavoured relative to other lower energy pathways. These include an E2-like mechanism with the liberated base from the reaction, or less likely, an S_N2 mechanism to remove the ethyl group from the charged oxonium species.

Even though the presence of the ethyl group opens up the possibility for an extra E2 pathway that otherwise would not be present with the native methyl analogue, this study shows that the preferred intermolecular reactivity is the bimolecular interaction at the alkyl ether rather than the required α-deprotonation. In the case of the methoxyenol ether, one could plausibly extend this observation to conducting an S_N2 mechanism to decompose the exposed methyl oxonium intermediate, rather than approaching and deprotecting the more hindered α-position to generate the required product. Altogether, this study is revealing in that the biosynthetic machinery required for this transformation is likely to contain a proximal basic residue in the halogenase active site to facilitate the α-deprotonation instead of a dealkylative pathway in order to generate the bromomethoxydiene motif.

[§§] Stannane **266** was synthesised by Dr. Simon Williams

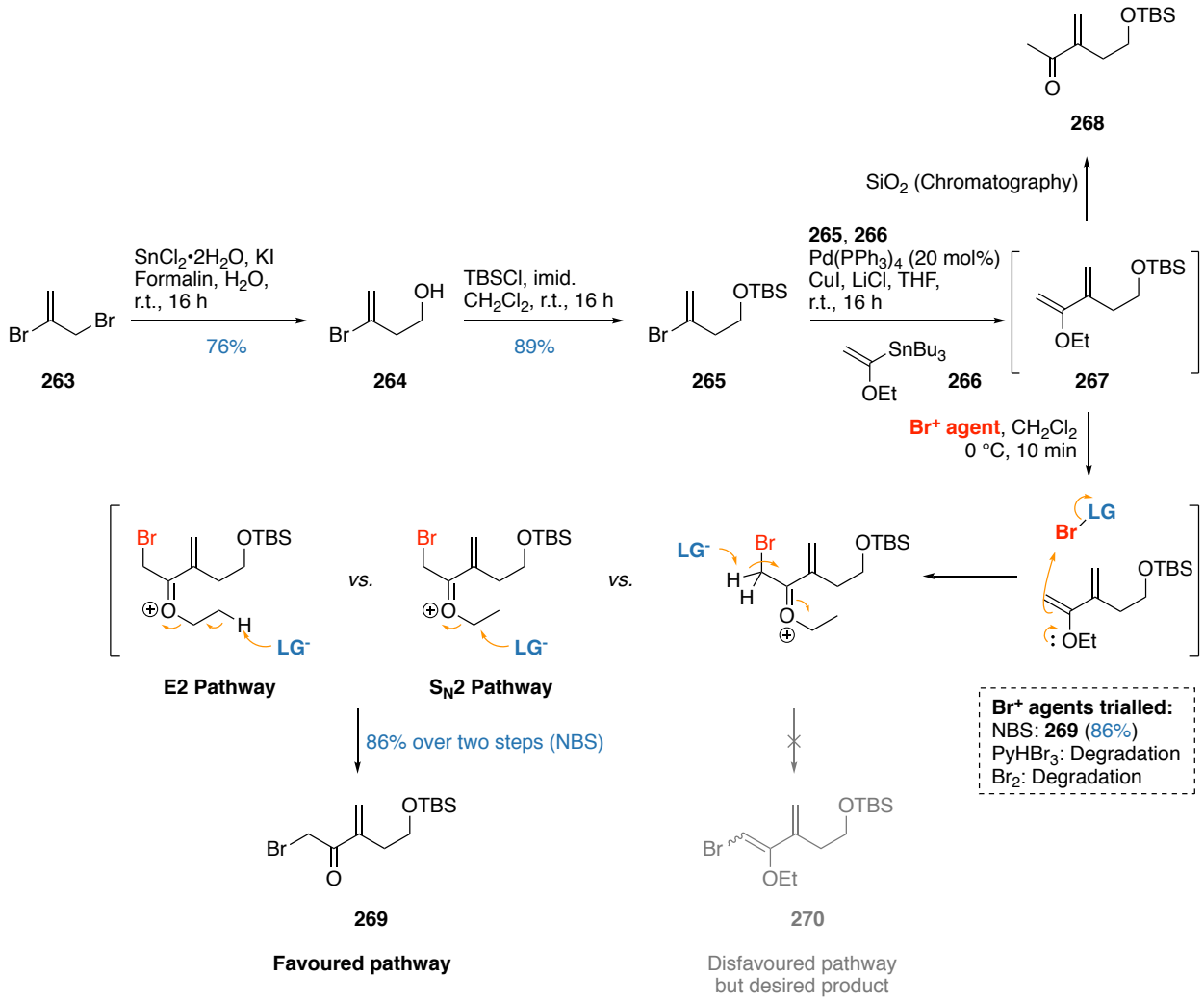

Scheme 55. *Attempted biomimetic synthesis of* ***270*** *resulted in the formation of bromoketone* ***269***

With some quantities of the bromoketone **269** present, a final attempt to transform this into bromomethoxydiene **270**, *via* the intermediate enolate was sought. In this case, it was hypothesised that treatment with a suitable base in the presence of a cation scavenger could generate the 'naked' enolate, which could then be alkylated using an electrophilic methyl source to generate the requisite functionality.[143] Unfortunately, the treatment of bromoketone with NaHMDS in the presence of 15-crown-5, followed by treatment with methyl triflate did not give any meaningful results (**Scheme 56**).

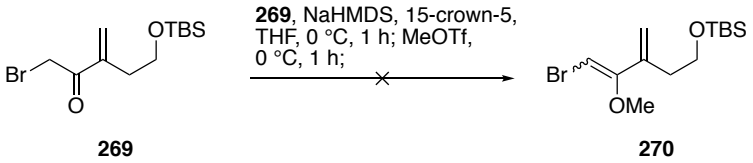

269 **270**

Scheme 56. *Attempted synthesis of* ***270*** *from* ***269***

To better understand the intrinsic reactivity of the bromomethoxydiene system, a series of preliminary DFT studies were conducted in conjunction with Reid. Specifically, these studies aimed to rationalise why Álvarez was unable to isomerise ketone *Z*-**179** but could readily isomerise dibromide **271**, as well as predicting whether or not biasing towards either kinetic or thermodynamic control could favour the geometry of the bromomethoxydiene motif. DFT optimisations of *Z*- and *E*-**179** revealed that the *E* isomer was higher in energy owing to the proximal interaction with the carbonyl group. This was not the case with dibromide **271**, where the *E* isomer was lower in energy as it allayed the interaction between Br and OMe in the *Z* isomer (**Figure 52**). By this observation also, the presence of the methylene group in *Z*-**272** would also thermodynamically disfavour isomerisation to the *E* isomer (*E*-**272**) present in the natural product; an observation that was reinforced by DFT (**Figure 53**). As product selectivity in isomerisation processes are dependent on relative product energies, this study shows that generating the disfavoured *E* geometry with any substitution at C31 *via* double bond isomerisation would be a futile method.

These results meant that a thermodynamic-controlled approach, unless employing Álvarez's published route, was an infeasible venture. To probe whether or not one could kinetically bias the reaction to favour the transition state leading to the *E* product over the *Z*, further computationally-guided investigation was conducted. Here, two routes were surveyed for their geometric selectivity: one involving the kinetic α-deprotonation of bromoketone **273** to generate **274** (**Figure 54**), and the second involving a base-mediated E2 elimination of dibromide **275** as reported by Álvarez. In both instances, the transition state possessing the conformer leading to the *Z* geometry was lower in energy than the alternative conformer, highlighting that the *Z*-bromomethoxydiene is both the kinetically and thermodynamically favoured product.

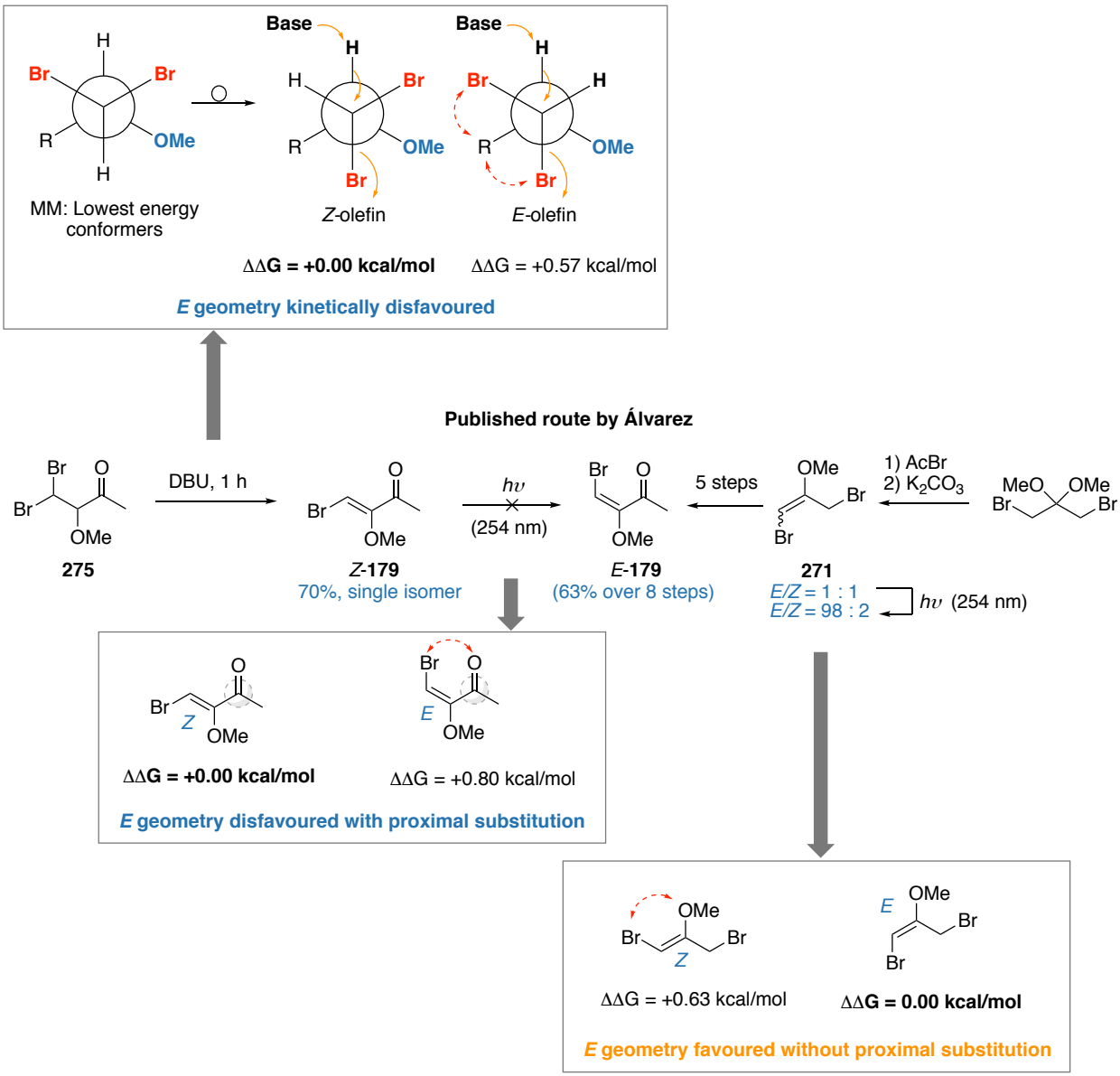

Figure 52. *Summary of DFT studies on various pathways as described by Álvarez conducted in collaboration with Reid, with red lines highlighting the interactions that presumably disfavour a particular geometry. All energies were calculated at the MO6-2X/LACVP** level of theory*

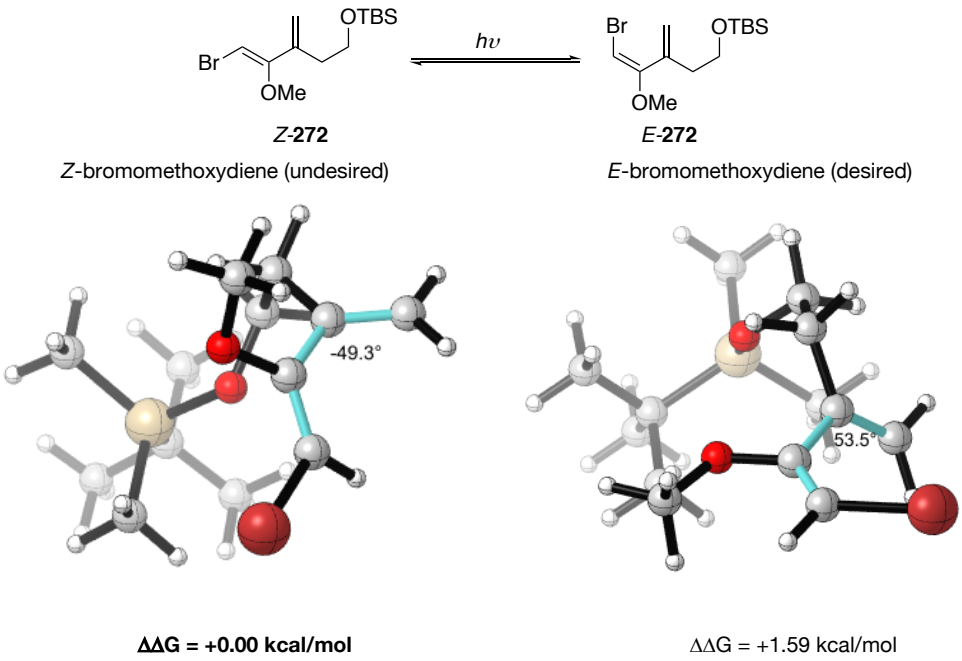

Figure 53. *DFT optimised structures as calculated (in collaboration with Reid) for E and Z-**272**, highlighting that the undesired Z-**272** isomer is the thermodynamically favoured isomer. All energies were calculated at the MO6-2X/LACVP** level of theory*

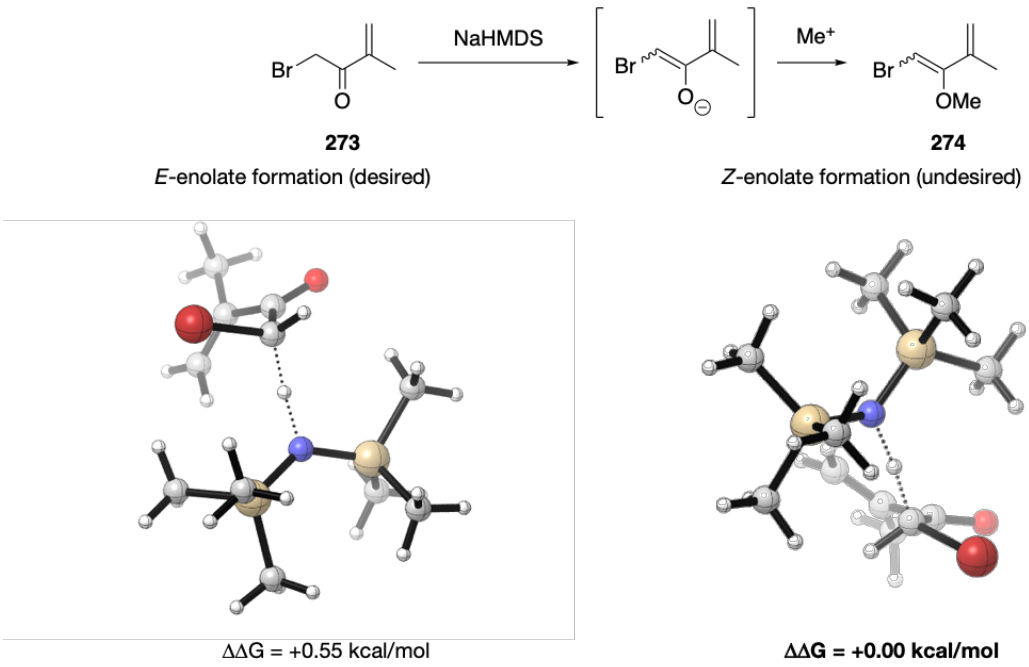

Figure 54. *DFT optimised transition states as calculated (in collaboration with Reid) for the enolisation of **273** mediated by NaHMDS, highlighting that the Z-enolate is the kinetically favoured enolate. All energies were calculated at the MO6-2X/LACVP** level of theory, using THF as an implicit solvent model*

6.5.2. *Intercepting Álvarez's bromomethoxydiene synthesis towards aldehyde* ***260***

At this juncture, there were two ways to resolve the synthetic impasse imposed by this motif: either conceive of a new and untested approach, or intercept the known optimised route as developed by Álvarez. After due consideration, adapting Álvarez's chemistry to align with our planned retrosynthesis was viewed as the more pragmatic strategy.

Moving forward, the synthesis of alcohol **276** commenced with a bromomethoxylation of acetone to generate dibromide **178** (**Scheme 57**). Despite the poor yield of this reaction, this reaction could readily be conducted on a 40 g scale and was operationally facile. The subsequent bromination of **178** with AcBr proceeded smoothly to generate tribromide **277**. While Álvarez reported the use of K_2CO_3 for the required elimination, in the author's hands the reaction proved to be poor yielding. Fortunately, direct treatment of **277** with *i*Pr_2NH cleanly generated *Z*-**271** as a single isomer, which can be isomerised to form predominantly *E*-**271** as a 10:1 mixture of geometric isomers. At this point, an acetate displacement of the allylic bromide was conducted, followed by basic hydrolysis to afford allylic alcohol **276** in good yields. This sequence was found to be highly scalable, operationally straightforward and did not require chromatography, verifying Álvarez's claim in their original report.

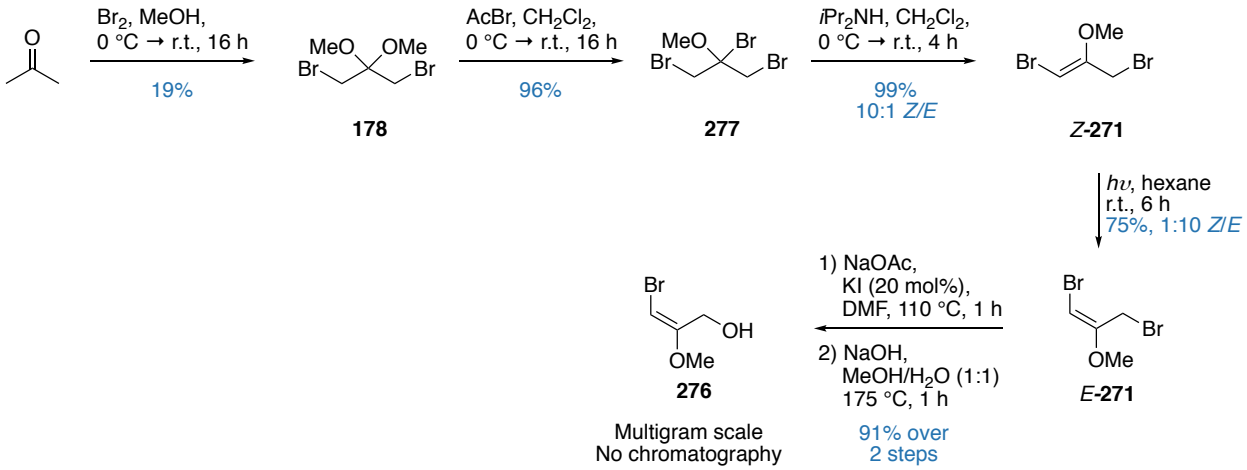

Scheme 57. *Synthesis of alcohol* ***276*** *from acetone*

Allylic oxidation of alcohol **276** mediated by MnO_2 smoothly gave the volatile aldehyde **278**. At this point, two routes were considered to generate the required aldehyde **260**: the first route involves a nucleophilic homologation of aldehyde **278** *via* an aldol reaction with the lithium enolate derived from ethyl acetate (**Scheme 58**). The second route involves a one-carbon electrophilic homologation from the silyl enol ether derived from ketone **179**. Both intermediates could then be derivatised to generate aldehyde **260** required for the total synthesis.

With the ready availability of intermediates, the first route was trialled. The aldol reaction of **278** to generate the β-hydroxyester **279** with the lithium enolate from ethyl acetate was only modestly yielding. At this point, attempts at installing the C31 methylene unit in **280** through further oxidation to ketoester **281** followed by Wittig olefination resulted in enol **282** as the only product. Attempts at reducing ester **279** to the diol followed by selective *mono*-silylation to give **283** also proved ineffective. Alongside the poor efficacy of the aforementioned steps, came the realisation that such convoluted solutions were unattractive for the synthesis of aldehyde **260**.

The pursuit of the second route required the synthesis of known silyl enol ether **186**. From aldehyde **278**, this involved a methyl Grignard addition to generate alcohol **284**. A subsequent oxidation to ketone **179** followed by enolisation mediated by TMSOTf smoothly gave silyl enol ether **186**. From here, a one-carbon homologation was necessary between the nucleophilic silyl enol ether **186** and a suitable one-carbon electrophile. This outwardly simple operation however, was non-trivial, with scant literature examples detailing methods for such a transformation. One such method detailed by Kobayashi involved an aqueous Mukaiyama aldol reaction with formaldehyde catalysed by $Yb(OTf)_3$.[144] While generating β-hydroxyketone **285** in moderate yields, this reaction generated a myriad of inseparable byproducts that remained inseparable even after further derivation.

While evidently the more promising solution, this aforementioned second route is marred by poor step-economy. To access aldehyde **260** after following Kobayashi's protocol, the primary alcohol would have to be transiently protected. At this point, the ketone functionality may then be methylenated, and the protected C29 group then be deprotected and oxidised to generate aldehyde **260**. Overall, this represents a 15-step synthesis (from acetone) for a five-carbon fragment, which leads to a 21-step synthesis for the C24-C33 fragment! Clearly, a much better solution was needed to ensure a sustainable supply of material that is concise enough in execution to afford the C24-C33 fragment ***ent*-226**.

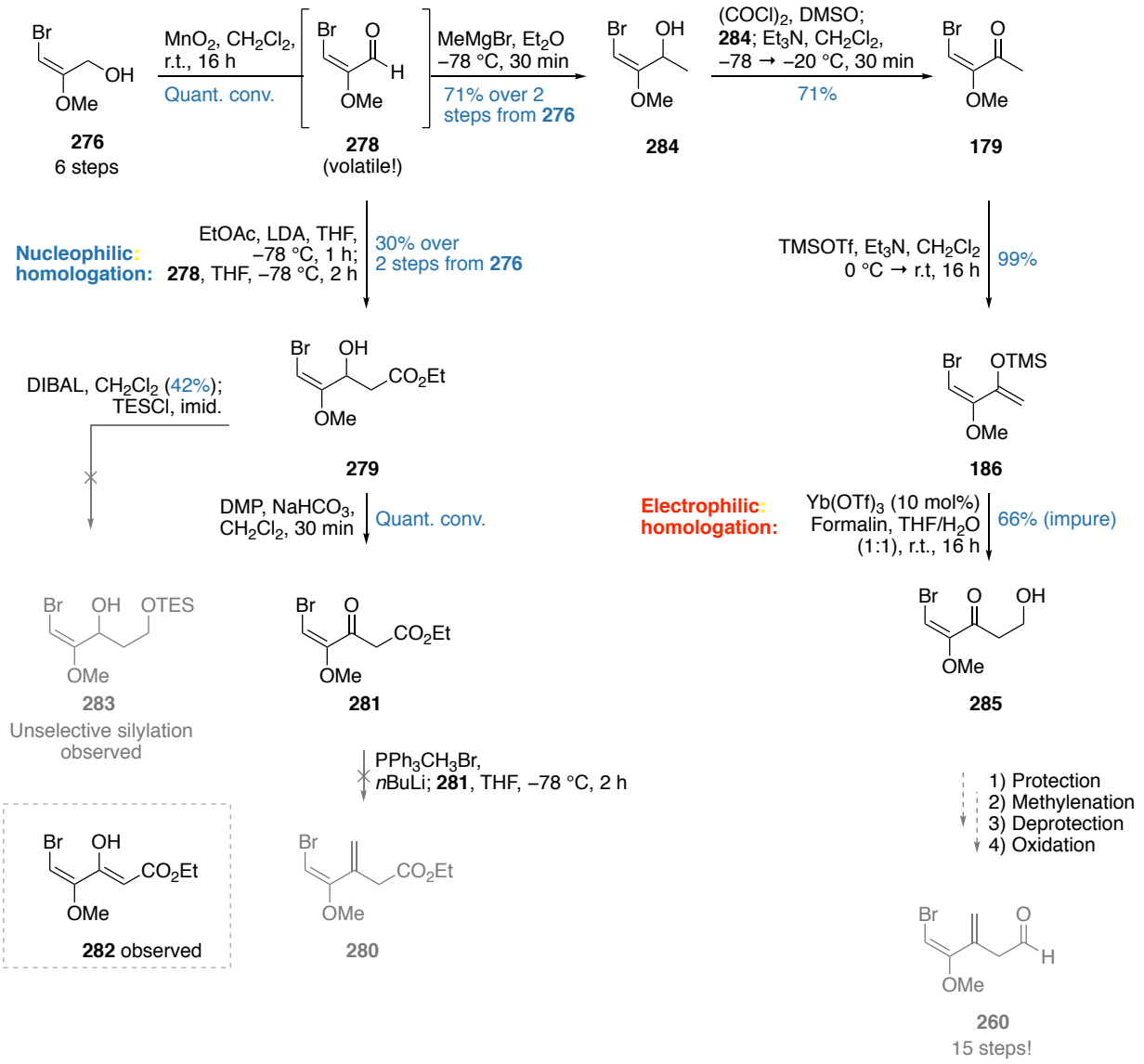

Scheme 58. *Attempted synthesis of aldehyde* ***260*** *through intercepting aldehyde* ***278*** *or silyl enol ether* ***186***

6.5.3. The Sakurai allylation approach towards the synthesis of the C24-C33 fragment

Faced with a need to develop a more concise route, a fundamental overhaul of the planned retrosynthesis was necessary. An analysis of both the author's proposed route in the previous section, as well as the synthesis undertaken by the Álvarez group highlighted the main source of inefficiency lay in the manipulations required to facilitate the C31 olefination. In light of this, two major avenues for improvement were identified: firstly, the synthesis would be more streamlined if the C31 olefin could be installed at an early stage. Secondly, the C31 olefin should ideally be utilised as part of a coupling handle to ensure a facile reaction with a suitable C25-C29 fragment.

Bearing these considerations in mind, an alternative strategy was developed involving disconnecting across the C29-C30 bond *via* a Sakurai allylation (**Scheme 59**). This would reveal allylsilane **286** and aldehyde **287**,

which could be readily accessed through an allylation/oxidation sequence from a Roche ester derived aldehyde **106** *via* alkene **288**. Allylsilane **286**, containing the wholly intact bromomethoxydiene motif, could potentially be generated from a double Grignard addition/Peterson olefination sequence from a suitable ester precursor **289**. This planned route would circumvent the unnecessary protecting group and redox manipulations to hopefully deliver a more concise synthesis of the C24-C33 fragment.

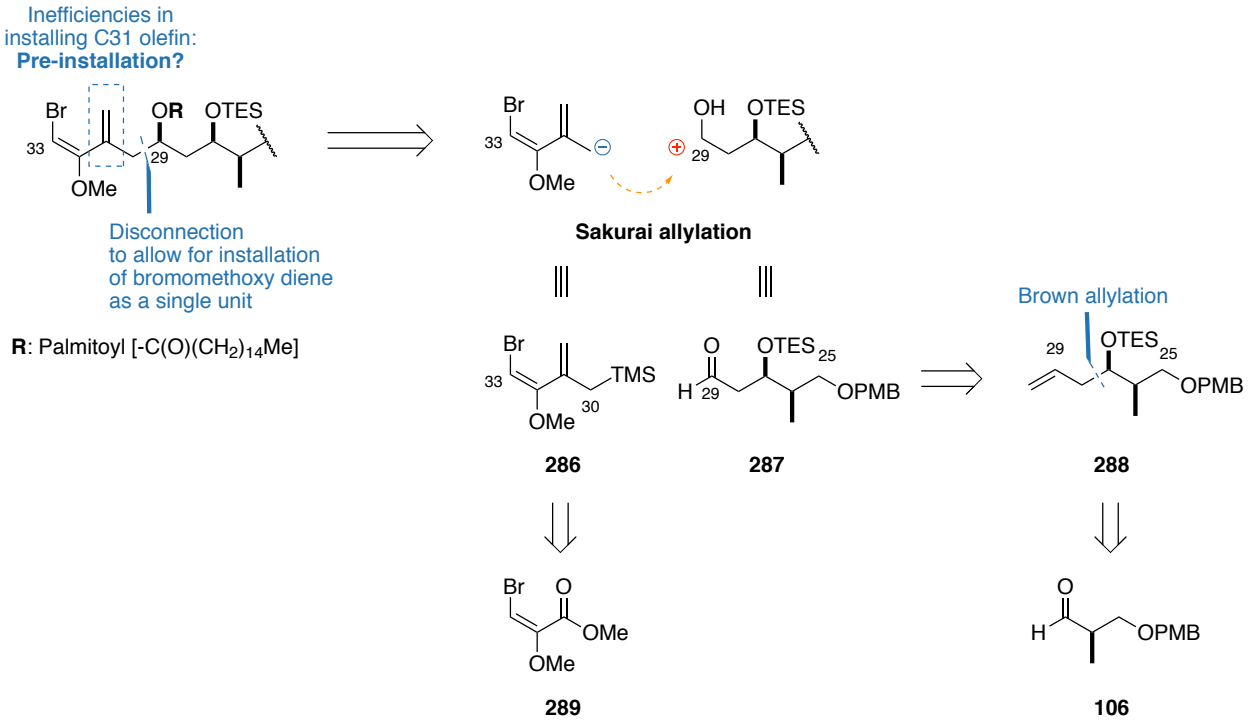

Scheme 59. *Revised retrosynthetic analysis for the C24-C33 region featuring a Sakurai allylation to forge the C29-C30 bond*

As the precursor for allylsilane **286**, access to the ester **289** was necessary. Ester **289** required redox manipulation of the already synthesised aldehyde **278**. Typically, this might involve a Pinnick oxidation followed by methylation to generate ester **289**. However, an opportunity was identified in economising this process which avoids the manipulation of volatile intermediates. Following Scheidt's example, allylic alcohols can be oxidised directly to the corresponding esters through treatment with MnO_2 and a source of alcohol in the presence of an *N*-heterocyclic carbene (NHC) catalyst.[145] The mechanism proceeds firstly with the MnO_2-mediated oxidation of allylic alcohol to the corresponding aldehyde, which then is attacked by the NHC catalyst to generate a doubly-activated carbinol centre (**Scheme 60a**). Further oxidation of the secondary alcohol by MnO_2 results in an acyl-azolium species, which can be readily attacked by the latent alcohol nucleophile to liberate the desired ester while regenerating the NHC catalyst. In this reaction, Scheidt identified that the catalyst derived from dimethyltriazolium iodide (**290**) was the most efficacious, and this catalyst was employed for this study towards the synthesis of ester **289**.

Drawn by the potential to effect a one-step oxidation from alcohol **276** to ester **289**, Scheidt's protocol was initially trialled; however, this procedure proved to be only modestly yielding. Utilising aldehyde **278** as the

precursor for the oxidation on the other hand, gave methyl ester **289** in reproducibly good yields (**Scheme 60b**). Ester **289** was then subjected to a double Grignard addition with $TMSCH_2MgCl$ mediated by $CeCl_3$.[146] The resulting alcohol **291** could then be subjected to acid-mediated Peterson olefination. Nominally, this reaction is easily facilitated by stirring over SiO_2.[146,147] However, for alcohol **291**, no conversion to the desired allylsilane was observed under these conditions. Recognising that perhaps the synthesis of the thermodynamically disfavoured *E*-bromomethoxydiene required a stronger source of acid than SiO_2, the olefination was further trialled with PPTS in MeOH, which gratifyingly gave the desired allylsilane **286** in good yields. Overall, the synthesis of allylsilane proceeded in nine steps from acetone, which favourably compares with Álvarez's synthesis of silyl enol ether **186**, itself also proceeding in nine steps from acetone.

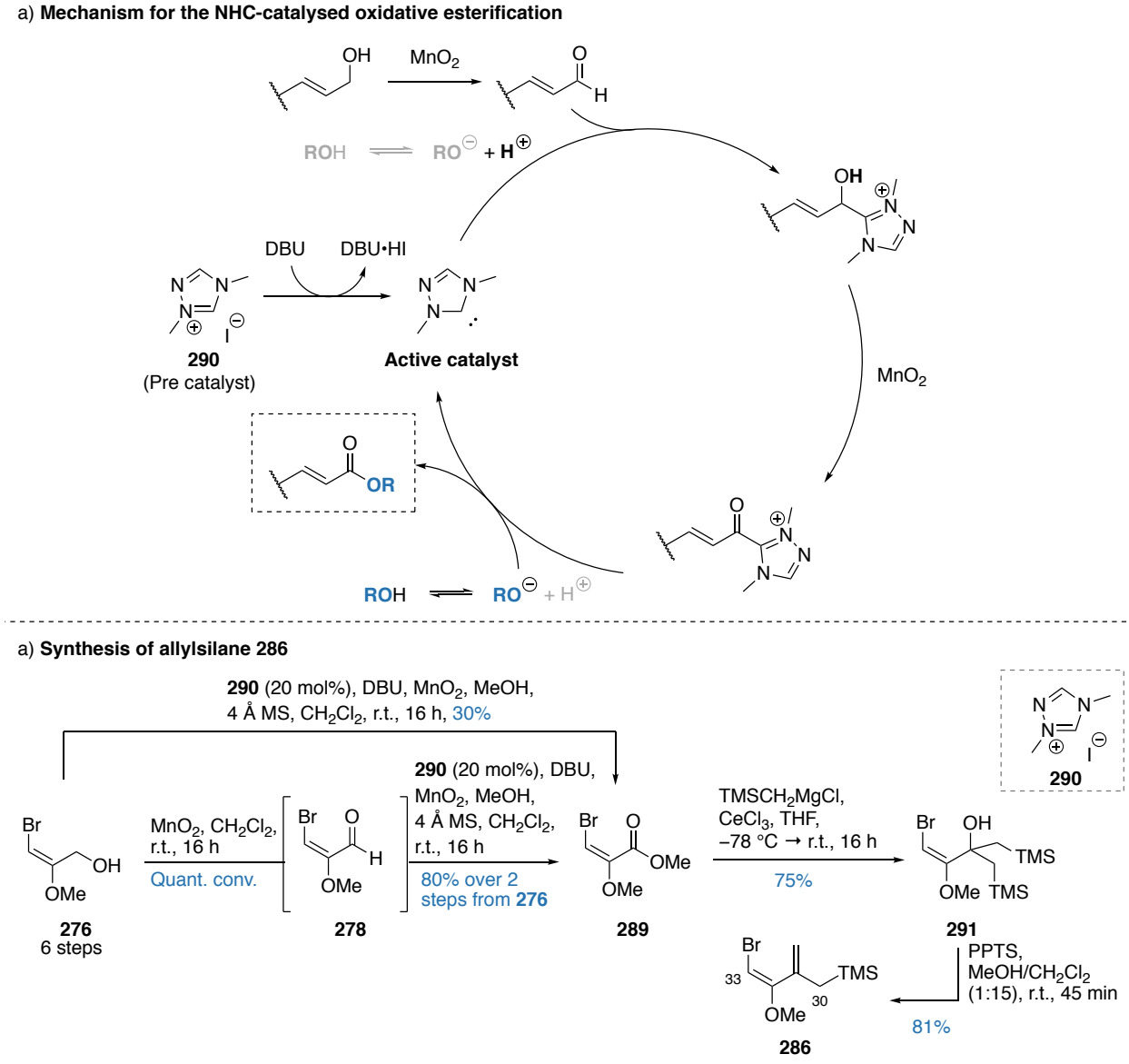

Scheme 60. *a) Mechanism of Scheidt's NHC-catalysed oxidative esterification. b) Synthesis of allylsilane* ***280*** *from* ***276***

The synthesis of the required aldehyde coupling partner **287** commenced with a Brown allylation of aldehyde **106 (Scheme 61a)**.[148] The reaction proceeds *via* a highly ordered six-membered transition state, where aldehyde **106** is activated by the Lewis acidic boron centre bearing Ipc ligands. The carbonyl

coordination causes a transient formation of an anionic complex, which renders the γ-carbon of the allyl group nucleophilic.[149] The stereoselectivity of this reaction is controlled by the chiral Ipc ligands (**TS-XVII**) and reinforced by the Felkin-Anh preference of the aldehyde **106**, and so disfavouring the formation of the minor diastereomer (**TS-XVIII**).[150] In the author's hand, the Brown allylation reaction proceeded reliably with excellent diastereocontrol (>20:1 *dr*) and generated alcohol **292** in good yields. From a previous study in the opposite enantiomeric series, the absolute configuration at C27 was confirmed by the synthesis of diastereomeric Mosher esters (*R*)- and (*S*)-MTPA-**293**, which confirmed the *R* configuration in ***ent*-292** (and therefore the *S* configuration for alcohol **292**) (**Scheme 61b** and **Table 13**).

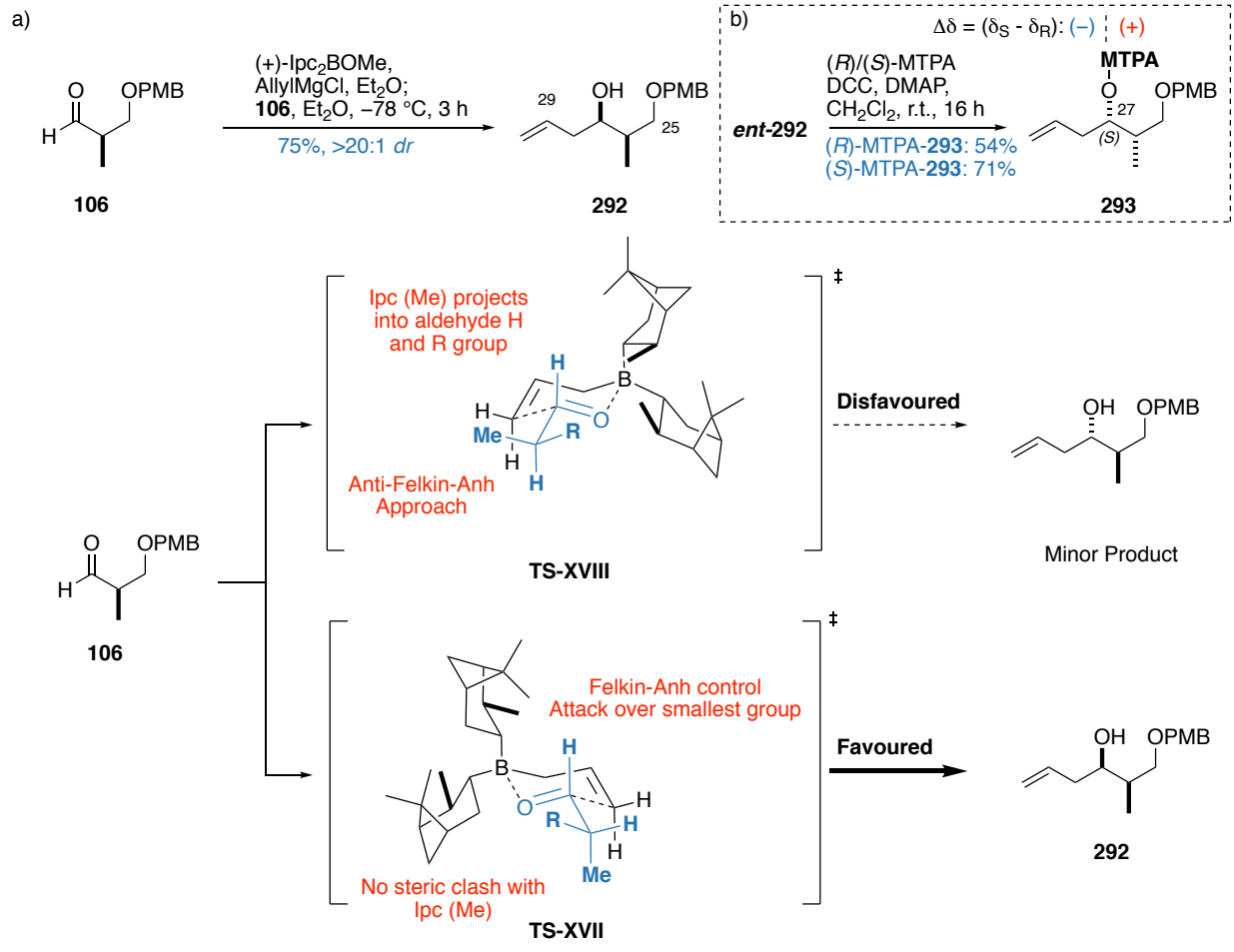

Scheme 61. *a) Synthesis of alcohol* ***292*** *via TS-****XVII****. b) Synthesis of Mosher esters (R)- and (S)-MTPA-****293*** *to confirm the 27S configuration in* ***ent*-292**

***Table 13**. Diagnostic ^{1}H NMR signals for the configurational assignment of 27S (in **ent-292**)*

Proton	**δH (*S*)-MTPA** (ppm)	**δH (*R*)-MTPA** (ppm)	$\Delta\delta_{S\text{-}R}$ (ppm)
H25	3.26	3.16	+0.10
H26	2.07	2.05	+0.02
Me26	0.92	0.87	+0.05
H27	5.34	5.40	−0.06
H28a	2.44	2.50	−0.06
H28b	2.33	2.40	−0.07
H29	5.67	5.75	−0.08

Following allylation, alcohol **292** was subsequently protected as the TES ether **288** before subjecting to ozonolysis conditions to unmask the C29 aldehyde in **287** (**Scheme 62a**). As the PMB group in **288** was also susceptible to oxidation to the corresponding ester under these conditions, the ozonolysis was carefully monitored by the use of Sudan Red as the indicator,[151] which undergoes a colour change to signify the completion of alkene ozonolysis. A reductive workup of the intermediate ozonide mediated by PPh_3 then reveals aldehyde **287** and formaldehyde as the volatile byproduct. In the authors hands, the ozonolysis proved to be variable in yield that was not aided by changing the reductive workup procedure (e.g. to Me_2S) or reaction temperature.

With allylsilane **286** and aldehyde **287** in hand, the pivotal Sakurai allylation can now be investigated. The majority of Sakurai allylations in the literature involve the Lewis acidic activation of the carbonyl (e.g. $BF_3{\cdot}OEt_2$[152] and $TiCl_4$[153]) (**Scheme 62b**), which enables the nucleophilic allylic olefin to attack into the electrophilic carbonyl centre to leave behind a carbocation stabilised by hyperconjugative effects from silicon.[154] A latent nucleophile could then attack into the TMS group to reform the double bond. A survey of these conditions with allylsilane **286** and aldehyde **287** only resulted in extensive degradation, which was shown to arise from the instability of aldehyde **287** under Lewis acidic conditions rather than the allylsilane **286** (results summarised in **Table 14**). Interestingly, a trial reaction between allylsilane **286** and isobutyraldehyde showed *no reaction* in the presence of $BF_3{\cdot}OEt_2$, highlighting that the allylsilane unit was not nucleophilic enough to attack into the C29 carbonyl despite activation with a strong Lewis acid.

With this in mind, attention was turned towards improving the nucleophilicity of the allylsilane system through Lewis base activation. A suitable Lewis base (most commonly fluoride) would coordinate to the Si and generate a transient 'ate' complex.[155] This renders the terminal γ-carbon more nucleophilic, which could in theory allow for the more facile allylation onto the C29 carbonyl (**Scheme 62b**). However, a screen of acidic and basic fluoride sources was met with failure, which highlighted the poor reactivity of allylsilane **286** under these conditions and also the incompatibility of the aldehyde substrate **287** to fluorous conditions. Postulating that the lability of the TES group in **287** played a role, the TBS analogue **294** was

also synthesised (**Scheme 62a**). Following the poor reproducibility of the ozonolysis step, an alternative method for transforming alkene **295** to aldehyde **294** was sought, involving a dihydroxylation of **295** followed by the periodate-mediated oxidative cleavage of the crude material. Gratifyingly, this sequence was highly reproducible, scalable to a gram scale and generated aldehyde **294** quantitively from alkene **295**.

Frustratingly, subjecting aldehyde **294** bearing the TBS ether to the Sakurai reaction with allylsilane **286** saw no improvement under the same range of conditions. Notably, the extensive degradation seen in both **287** and **294** was typified by the appearance of olefinic protons, signifying an eliminative process as a potential degradation pathway in both cases (**Table 14**). On a positive note, the stability of the bromomethoxydiene motif under neat HF·py conditions was a promising indication that a global desilylation step could proceed under mildy acidic fluorous conditions.

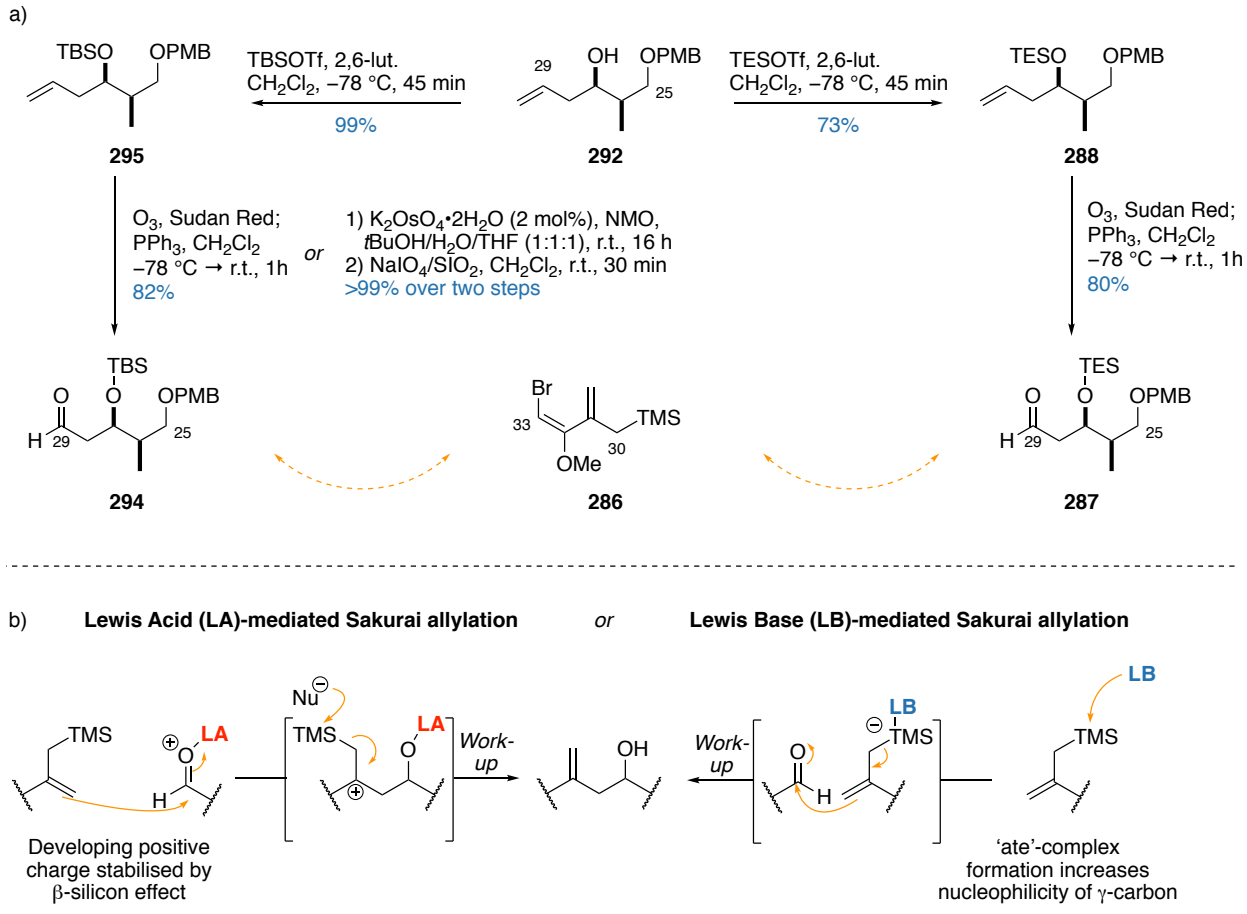

***Scheme 62**. a) Synthesis of aldehydes **287** and **294**. b) General mechanism for the Lewis acid and Lewis base mediated Sakurai allylation reaction*

Table 14. *Overview of all conditions trialled for the Sakurai allylation of* ***286*** *and aldehydes* ***287*** *or* ***294***

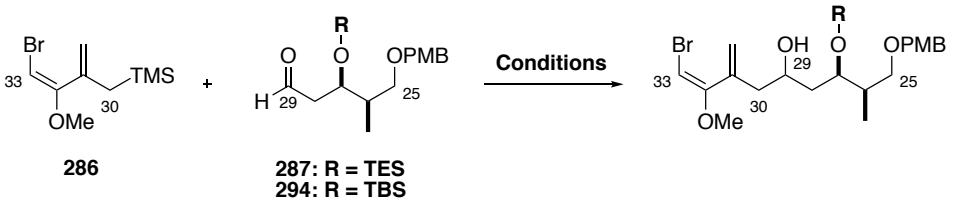

Aldehyde	Conditions	Result
287	**286**, $TiCl_4$, CH_2Cl_2, –78 °C, 1 h	Degradation of **286** and **287**
287	**286**, $BF_3.OEt_2$, CH_2Cl_2, –78 °C, 1 h	Degradation of **287** only
287	**286**, $MgBr_2{\cdot}OEt_2$, Et_2O, –78 °C, 1 h	Degradation of **286** and **287**
287	$BF_3.OEt_2$, CH_2Cl_2, –78 °C, 5 min	Degradation of **287**
Isobutyraldehyde	**286**, $BF_3.OEt_2$, CH_2Cl_2, –78 °C, 1 h	No reaction
287	**286**, TBAF; **287**, THF, 0 °C, 1 h	Degradation of **287** only
294	**286**, TBAF; **294**, THF, 0 °C, 1 h	Degradation of **294** only
287	**286**, TBAT; **287**, THF, 0 °C, 1 h	No reaction
294	**286**, TBAT; **294**, THF, 0 °C, 1 h	No reaction
287	**286**, TASF; **287**, THF, 0 °C, 1 h	Degradation of **286** and **287**
294	**286**, TASF; **294**, THF, 0 °C, 1 h	Degradation of **286** and **294**
287	**286**, HF·py; **287**, THF, 0 °C, 1 h	No reaction

N.B.: All Lewis acids were used in equimolar amount to the aldehyde in the reaction mixture.
All fluoride sources were used in equimolar amount to allylsilane in the reaction mixture

So far, the planned allylation did not proceed with either the Lewis acid activation of aldehydes **287** and **294**, or the Lewis base activation of allylsilane **286**. In both cases, the instability of the aldehydes to both sets of reaction conditions outweighed any potential reactivity, if any, of allylsilane **286**. These failures made it evident that the allylsilane system was not nucleophilic enough, and the Si present in **286** would have to be replaced with a more electropositive metal to facilitate the required nucleophilic attack.

In 2004, Dias and Steil published a report detailing the use of $SnCl_4$ as a Lewis acid for a diastereoselective allylsilane addition onto aldehydes.[53] In this report, rather than proposing a standard Lewis acid activation of the aldehyde, previous NMR studies had highlighted that a rapid Si/Sn transmetallative process was involved to generate the allyltrichlorostannane as the active allylation reagent.[156] In particular, the trichlorostannyl motif has the further ability to act as a Lewis acid to activate the aldehyde partner, leading to a highly diastereoselective closed transition state for the allylation (**Scheme 63a**).

Attracted to the idea of simultaneously improving the nucleophilicity of the allyl unit and the presence of a Lewis acid to activate the carbonyl group, the Dias protocol was pursued. Gratifyingly, the low temperature treatment of allylsilane **286** with a solution of $SnCl_4$ followed by the addition of aldehyde **294** gave the allylated product **296** as a 1:1.3 mixture of C29 epimers (**296a**:**296b**) in 72% yield (**Scheme 63b**). The alternative TES ether analogue **287** proved less efficacious, with numerous presumed degradation products observed in the course of the reaction. Importantly, both C29 epimers were separable by chromatography, which allowed for the unambiguous stereochemical elucidation through synthesis of the corresponding acetonides **297** and **298**.

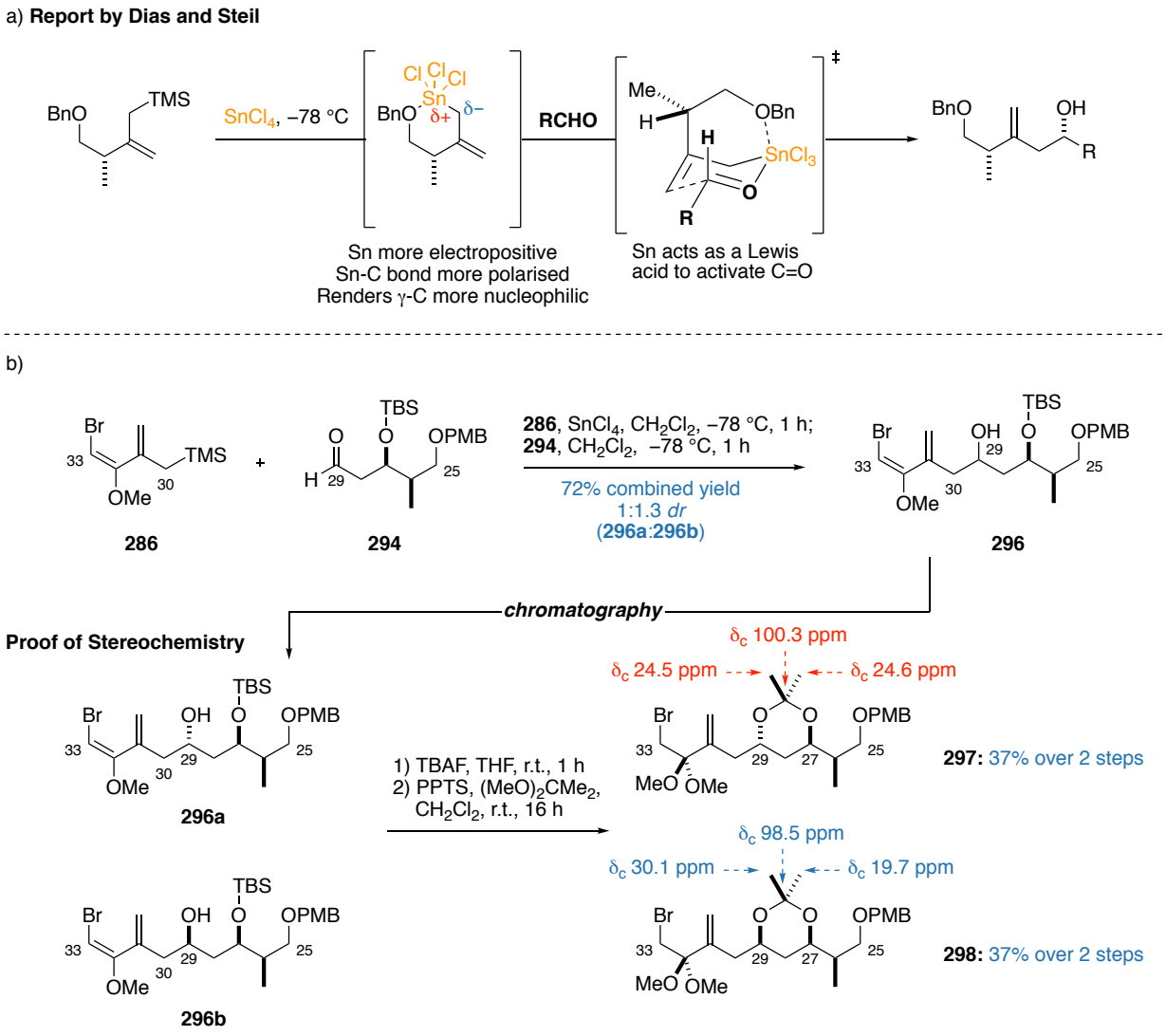

Scheme 63. *a) Sakurai allylation mediated by Sn/Si transmetallation as described by Dias and Steil. b) Synthesis of* ***296a*** *and* ***296b****, and their respective acetonides* ***297*** *and* ***298*** *confirming the stereochemical outcome of the allylation*

Finally, it is worthy to remark on the minimal diastereoselectivity observed for this reaction. The selectivity arising from a non-chelation controlled nucleophilic addition into β-alkoxyaldehydes is typically controlled by the Evans' polar model, which preferentially generates 1,3-*anti* related adducts.[55,157] The poor selectivity in this reaction echoes results observed by Evans *et al.* for additions into β-siloxyaldehydes, with poorer

selectivity observed compared to additions proceeding *via* closed transition states.[104,158] In this case, the near equimolar ratio of products suggests transition states leading to the desired 27,29-*syn* and undesired 27,29-*anti* products are similar in energy. While not investigated in this thesis, one could potentially bias the stereochemical outcome at C29 by introduce chiral chelating ligands (such as BINOL-type scaffolds) to occupy the remaining coordination sphere around Sn. This could increase the energy difference between the diastereomeric transition states in such a way that it would begin to favour the formation of the desired 29*S* product.

6.5.4. Completion of the C24-C33 fragment

The poor selectivity of the allylation step was not considered to be an issue given the fact that both diastereomers are readily separable. This means that a direct esterification of the 27,29-*syn* product **296b** would afford ester **299** containing the required C29 palmitoyl functionality. Building on promising reactivity shown by Álvarez, a Mitsunobu esterification on the 27,29-*anti* product **296a** could separately be conducted to converge onto ester **299** with the desired C29 configuration. While the esterification of **296b** with palmitic acid under Steglich conditions readily gave ester **299**, subjecting the alternative 27,29-*anti* adduct **296a** to Mitsunobu conditions with palmitic acid as the nucleophile resulted in no reaction (**Scheme 64**). As it was known that Mitsunobu esterifications proceed more efficiently when the pro-nucleophile is more acidic,[159] it was surmised that palmitic acid was not acidic enough to enable the transformation. As such, in an analogous manner to Álvarez's route,[101] a Mitsunobu inversion with *p*-nitrobenzoic acid followed by ester hydrolysis was conducted to correct the configuration at C29 for **296a**. This sequence generated **296b** bearing the correct geometry in moderate yields and was in all respects identical to the 27,29-*syn* product generated from the allylation reaction.

With a single diastereomer of ester **299** in hand, all that is required for the completion of this fragment is the transformation of the C25 terminus into the corresponding methyl ketone. This was accomplished with an oxidative cleavage of the C25 PMB ether to afford alcohol **300**. A subsequent Swern oxidation to the aldehyde, followed by a chemoselective Grignard addition conducted at low temperatures gave an epimeric mixture of alcohol **301**, which was subjected to a final Swern oxidation to give the completed C24-C33 methyl ketone **302**.

Following the nine-step synthesis of allylsilane **286** and the seven-step synthesis of aldehyde **294**, five more steps were required to give the completed C24-C33 fragment **302** in 14 steps LLS from acetone. The work presented in this section is a marked procedural improvement over Álvarez's 17-step synthesis from acetone (see section **5.4.2** and **5.4.3**), and has enabled a ready supply of an advanced intermediate for the ongoing synthetic campaign.

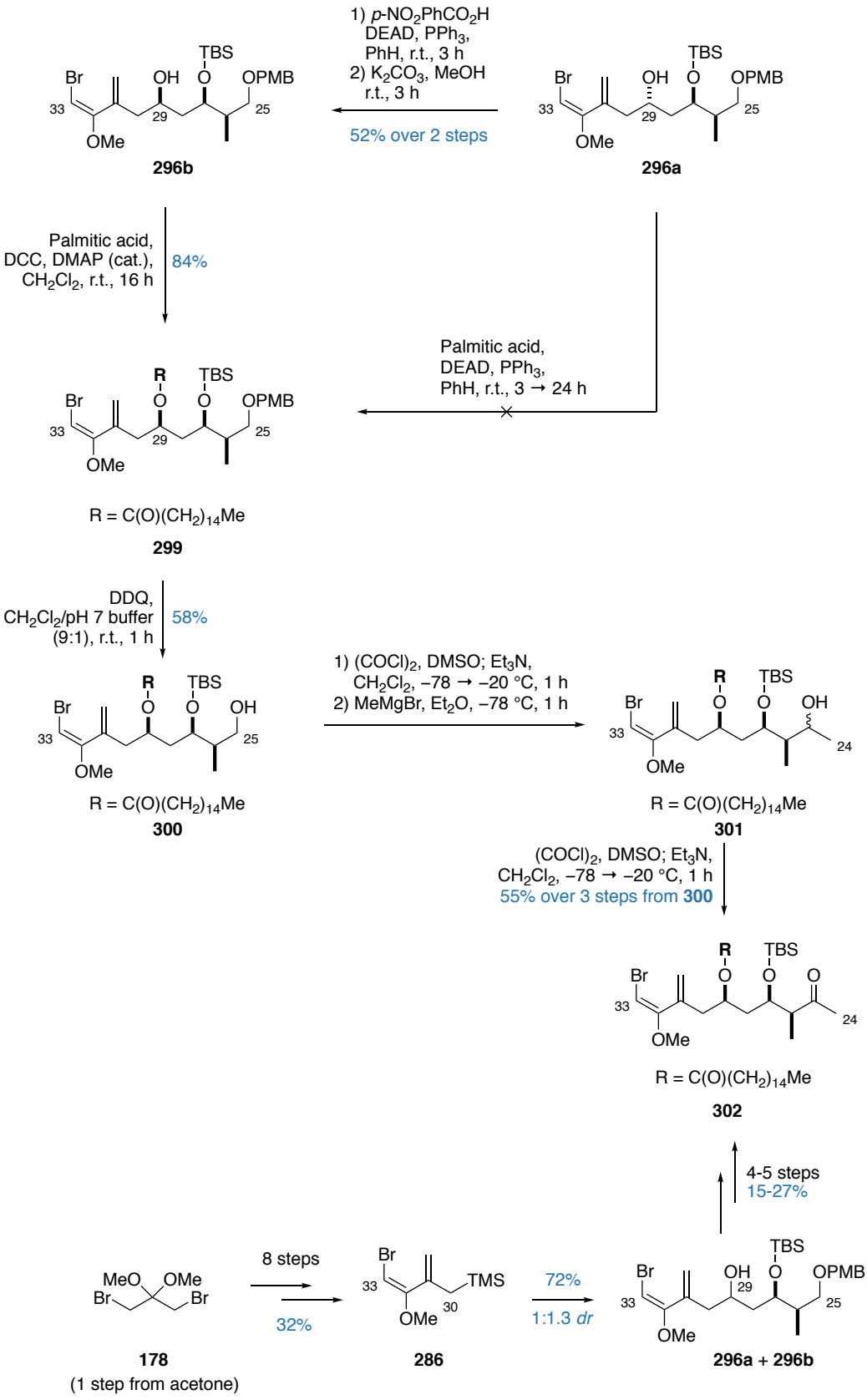

Scheme 64. *Completion of the C25-C33 fragment* ***302***

6.6. Towards the synthesis of the C1-C17 macrolactone

The work described in this section was carried out in collaboration with Garrett Muir at Simon Fraser University. His results were crucial to the project and are presented alongside the author's results. Unless otherwise stated, all reactions described were performed by the author and all stated yields are those obtained by the author.

The three major disconnections planned for the phormidolide macrocycle represent three potential locations to execute the required macrocyclisation. These are namely: a macrolactonisation of the C1 *seco* acid **303** to OH15, a macro-cross-coupling of **304** to forge the C3-C4 bond, and a similar macro-cross-coupling of **305** to forge the C9-C10 bond (**Scheme 65**). Of the three options, macrolactonisation appeared to be the most promising strategy for closing the macrocycle in light of the multitude of examples surrounding its use in macrolide synthesis.[160] Additionally, the proposed biosynthesis for phormidolide A invokes a macrolactonisation as its final step before its liberation from the acyl carrier protein, further giving credence to this strategy.[82] This meant that the goal was now focused towards generating a suitable *seco* acid to verify the crucial macrolactonisation step.

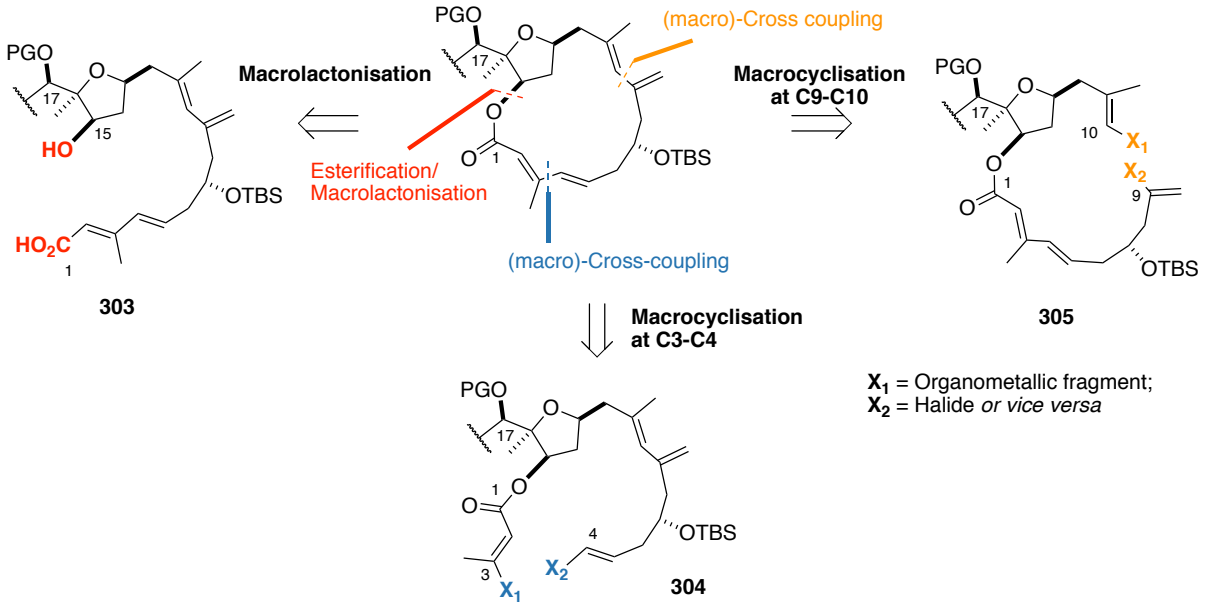

Scheme 65. *Sites identified in the phormidolide A macrocycle that are amenable to macrocyclisation processes and their respective seco precursors*

6.6.1. *The macrolactonisation approach*

With a reliable route developed by Muir and Rao Challa towards the THF core, Muir looked to develop a convergent method towards the C1-C17 *seco* acid **306** through a cross-coupling between vinyl iodide **241** and a suitable C1-C9 fragment. Muir planned to form the C9-C10 bond *via* a Suzuki reaction between the C10-C17 vinyl iodide **241** with a suitable C1-C9 boronate **307** (**Scheme 66a**). In practice, Muir commenced the synthesis of the C1-C9 boronate from (+)-epichlorohydrin **308** through an epoxide opening with the lithiated derivative of TMS-ethyne mediated by $BF_3{\cdot}OEt_2$ (**Scheme 66b**). A cyanide displacement of compound **309** generated nitrile **310**, where the TMS group was cleaved during the reaction. A Pd-catalysed formal hydroboration[161] was able to install the BPin functionality in the internal position in **311**. Following this, protection as the TBS ether **312** and a DIBAL reduction of the nitrile to aldehyde **313** was conducted. Here, Muir trialled several methods to elaborate **307** to the full C1-C9 fragment, though attempts at executing an HWE olefination, a Wittig reaction, or a Takai olefination were met with failure. While no conclusive reasons were given for its apparent lack of reactivity, Muir surmised that the potentially Lewis acidic BPin group was interfering with the nucleophilic component in these olefination reactions, hampering the reactivity of **313**.

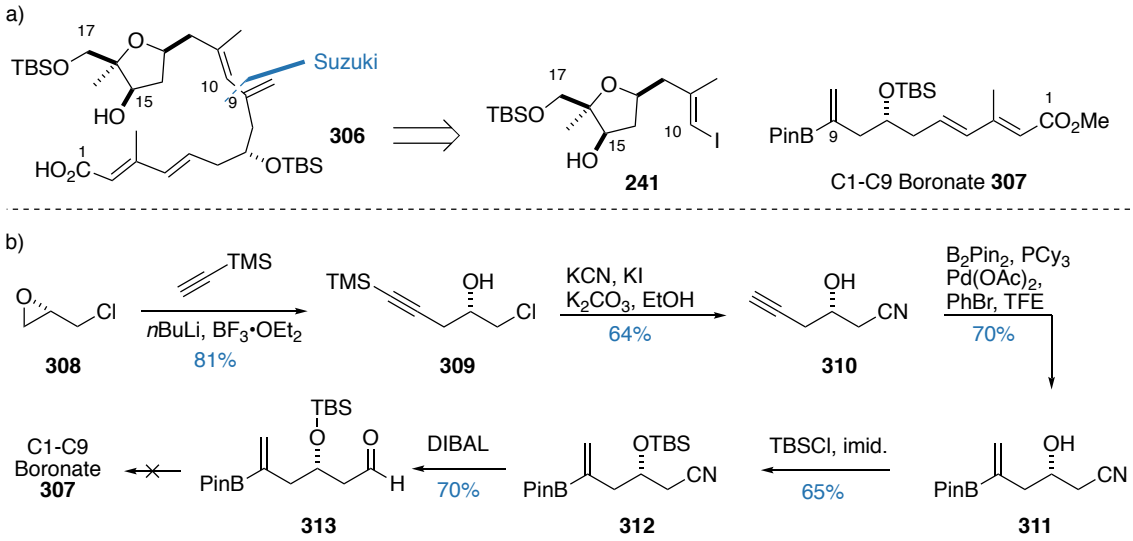

Scheme 66*. a) Retrosynthesis of seco acid **306** as planned by Muir. b) Synthesis of aldehyde **313** as conducted by Muir. Attempts at elaborating aldehyde **313** to the C1-C9 fragment **307** were unsuccessful. TFE = trifluoroethanol*

This forced Muir to conceive a step-wise approach towards the synthesis of the C1-C17 *seco* acid **306**. Muir initially obtained poor results with the Suzuki reaction of vinyl iodide **241** with aldehyde **313** to generate **314**, suspected to be due to competing self-condensation of aldehyde **313** under the basic cross-coupling conditions. To circumvent this, Muir reduced aldehyde **313** to the corresponding alcohol **315** (**Scheme 67**). Initially, employing conditions developed by Gopalarathnam and Nelson ($Pd(PPh_3)_4$, $Ba(OH)_2$)[162] with protected vinyl iodide **243** and boronate **315** delivered the product **316** in moderate yield, though dramatic improvements were observed in the author's hands using TlOEt as the stoichiometric base.[163] The exact

reason as to why TlOEt proved to be superior to other strong Brønsted bases is uncertain, though part of the reason may be attributed to its improved solubility under the reaction conditions which more efficiently generates the transmetallation-active 'ate' complex required for the cross-coupling to proceed. As the alcohol **316** was found to be inseparable from the excess boronate **315**, the mixture was used in subsequent transformations without further purification.

An initial attempt at oxidising alcohol **316** under Dess-Martin oxidation conditions yielded what appeared to be widespread isomerisation of the C9 double bond. This was solved by subjecting **316** under Swern conditions, which not only delivered aldehyde **317** in good yields (over two steps), but also successfully removed the excess boronate **315** from the previous reaction. Aldehyde **317** was then subjected to Takai olefination conditions to generate vinyl iodide **318** with moderate geometric control (3:1 *E*/*Z*). While it was reported that there is a degree of solvent dependence on the geometric selectivity for the olefination,[103] a solvent screen conducted by Muir failed to improve the selectivity of this reaction.

Moving forward with vinyl iodide **318** and vinyl stannane **319**, a Stille cross-coupling under Fürstner's conditions[73] reliably formed the C3-C4 bond to generate the C1-C17 skeleton **320**. At this point, the selective C17 deprotection of intermediate **320** to alcohol **321** would commit the material towards the planned total synthesis of phormidolide A. Muir's investigation into this process proved unfruitful, with a variety of acidic, acidic fluorous and basic fluorous conditions resulting in the unselective deprotection of the C7 and C17 TBS ethers, generating a statistical mixture of *mono* and *bis* deprotected products. In parallel, an attempt was undertaken to probe the efficacy of the planned macrolactonisation. Taking the C1-C17 diester **320**, a hydrolysis of both the methyl and dimethylacrylate esters afforded the *seco* acid **306**. Frustratingly however, a range of macrolactonisation conditions failed to deliver the C1-C17 macrocycle **322** (results summarised in **Table 15**), although trace amount of the minor 4*Z* isomer was observed to cyclise. This disappointing result was attributed to the steric demands of the proximal C16 group in relation to the all *syn* configuration in the THF, screening the C15 OH group required for the macrolactonisation.

This intelligence gathering exercise generated two key lessons that needed to be considered in the continual strategy evolution of phormidolide A: firstly, the negative results obtained from exploratory studies in macrolactonisation, attributed to steric factors, implied that the required macrocyclisation was likely to best proceed at a position distal to any steric bulk in the molecule. As the macrolactonisation process was deemed unviable, this meant that one of the two planned cross-coupling reactions would be needed to generate the macrocycle. Secondly, the poor results obtained from the selective TBS deprotection highlighted the sterically similar nature of an encumbered primary versus an unhindered secondary TBS group. Of course, this problem could be solved by modifying the protecting group strategy; for example, by the incorporation of a bulkier protecting group at C7 or an orthogonal protecting group at C17. However, at this stage, this was deemed to be a less pragmatic modification as compared to progressing with the

available supply of advanced intermediate. If no protecting group alterations were implemented, this would mean that any manipulations at C17, including side chain installation, would have to take place prior to the introduction of the C7 TBS group.

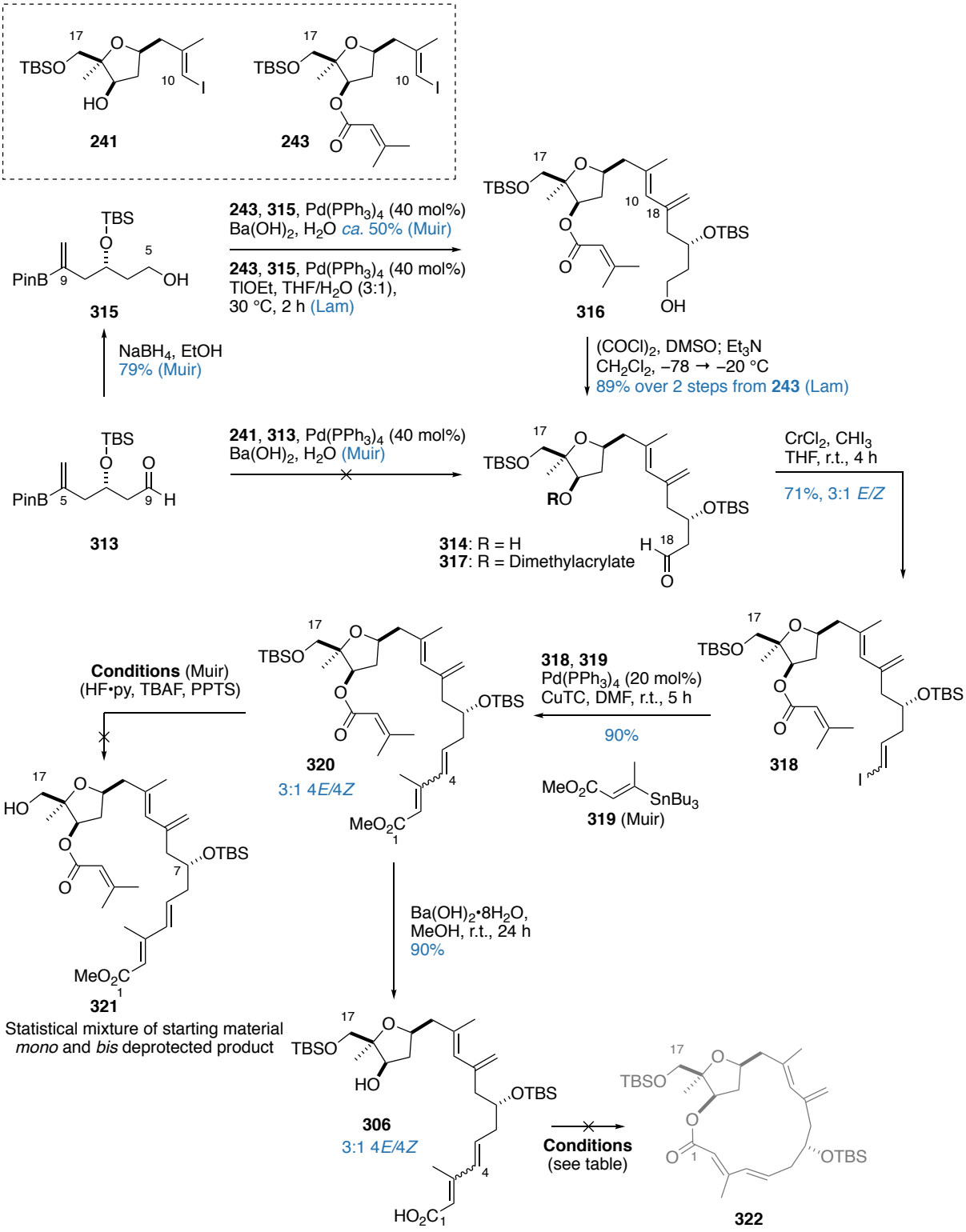

Scheme 67. *Synthesis of seco acid* ***306*** *and its attempted macrolactonisation, presented alongside deprotection studies of* ***320****. This work was conducted in close collaboration between Lam and Muir*

Table 15. *Conditions trialled for the macrolactonisation of seco acid* ***306*** *to macrocycle* ***322***

Conditions	Result
306, TCBC (10 eq.), Et_3N (20 eq.), PhMe, 1.5 h; Slow addition into DMAP (20 eq.), 50 °C, 20 h	No reaction; degradation observed Trace of 4*Z* macrocycle seen
306, MNBA (3.5 eq), PhMe; Slow addition into DMAP (7 eq.), PhMe, r.t., 24 h	No reaction; degradation observed

Taking these points into consideration, it was clear that a macro-cross coupling at either C3-C4 or C9-C10 was worth exploring to generate the macrocycle. Noting that the intermolecular Stille reaction to generate **320** proceeded more efficiently than the Suzuki reaction to give **316**, it was surmised that the required macrocyclisation was likely to best proceed through the macro-Stille reaction *via* the formation of the C3-C4 bond from **323** (**Scheme 68a**). While much less widely used compared to macrolactonisations, the macro-Stille reaction has been strategically used in several instances in natural product syntheses,[164] most recently in the synthesis of chivosazole F within the Paterson group.[165] Additionally, to circumvent the poorly selective C17 TBS deprotection in the presence of the C7 TBS ether, the side chain installation was proposed to take place prior to Suzuki cross-coupling with boronate **315** to reveal **324**. Fortunately, this sequence of steps was previously validated in model studies as described in section **6.3.2**. In this instance, vinyl iodide **325** bearing the C23 TES ether (itself generated from alcohol ***ent*-232 - Scheme 68b**) would be used instead of ***ent*-233** bearing the C23 TMS ether. This difference was not anticipated to impact the Grignard addition reaction, but the protecting group change was considered to be important owing to the number of basic conditions employed in the synthesis towards the macrocycle, where the TMS group was not considered likely to survive.

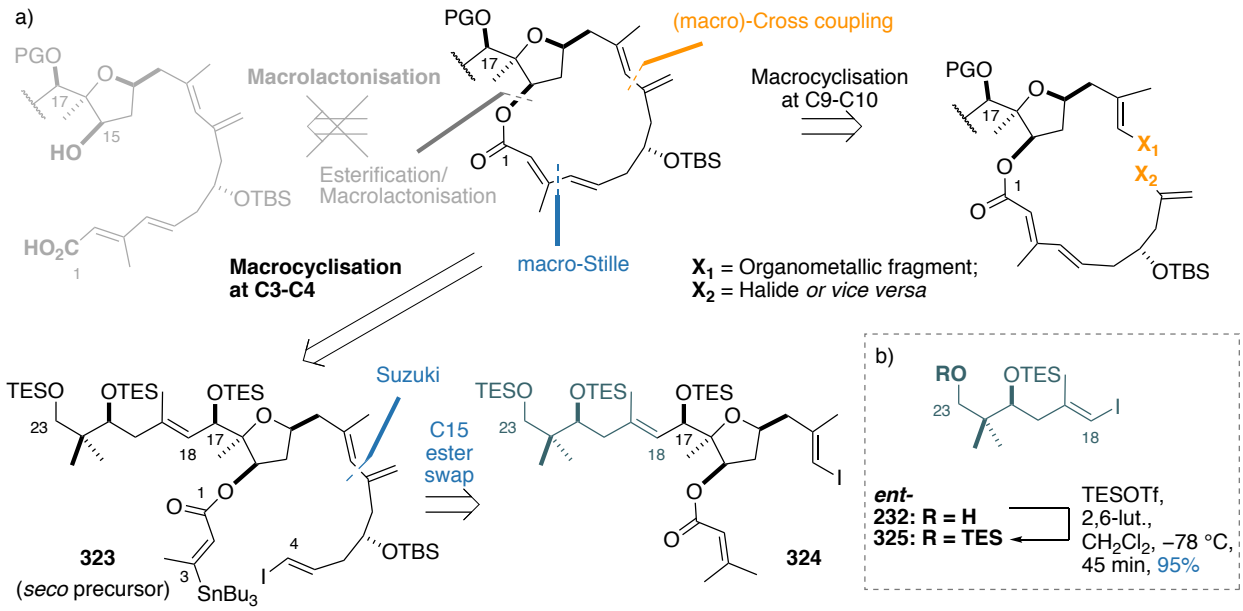

Scheme 68. *a) Strategy evolution towards the synthesis of the phormidolide A macrocycle involving seco precursor* ***323***

b) The synthesis of TES ether ***325*** *from alcohol* ***ent-232***

6.6.2. The C3-C4 macro-Stille approach

Pursuing the construction of an advanced *seco* precursor for the macro-Stille reaction **323** commenced with the chelation-controlled Grignard addition of vinyl iodide **325** into the previously synthesised aldehyde **245**. In accordance to previous studies, this generated the adduct **326** in good yields in a 5:1 *dr* (**Scheme 69**). Alcohol **326** was then protected as its TES ether in **324**, where Muir then elaborated **324** through an analogous Suzuki/Swern/Takai sequence as described above, to afford the C4-C23 vinyl iodide **327**. At this stage, the dimethylacrylate ester at C15 needed to be exchanged for a stannylacrylate ester to generate the required *seco* precursor. Interestingly, applying the same mildly basic conditions to **327** that were previously successful in cleaving the dimethylacrylate ester ($Ba(OH)_2 \cdot 8H_2O$ or K_2CO_3 in MeOH) gave no reaction; in the end, the dimethylacrylate ester was reductively cleaved by subjecting **327** to DIBAL at low temperatures to give alcohol **328**.

The unexpectedly poor reactivity in hydrolytically cleaving the dimethylacrylate ester was an apparent harbinger of the difficulties to be encountered surrounding the re-esterification of C15 to generate *seco* precursor **323**. As summarised in **Table 16**, no esterification was observed across a wide range of conditions, including transforming stannylacrylic acid **329** to the corresponding acyl chloride **330**. Hypothesising that the issue was due to the steric bulk of acid **329**, an attempt was conducted at re-esterifying with the smaller dimethylacrylic acid (**242**), which once again, gave no reactivity. In contrast with the ready esterification of alcohol **241**, as well as the facile ester hydrolysis of triols derived from silyl deprotection of Grignard adducts **249**, **253** and **256** (see section **6.3.2**), it appeared that the act of introducing a silyl protecting group at C17 deleteriously affected the reactivity of C15. Additionally, in combination with the lack of reactivity seen in *seco* acid **306**, the negative results observed in the intermolecular C15 esterification categorically eliminated the possibility of employing any form of macrolactonisation process as a key step towards the synthesis of phormidolide A. In both cases, it was clear that the required cross-coupling handle must be preinstalled, as the C15 alcohol was too hindered to be a productive nucleophile in any re-esterification processes.

In light of these frustrating results, a revision to the strategy for construction of the macrocycle was necessary. One solution to this impasse lay in the early installation of the stannylacrylate ester, though this was quickly deemed as an implausible solution given the instability of the C-Sn bond to the Brønsted and Lewis acidic conditions the motif would be required to survive prior to the Stille reaction. Another plausible route involved the site-selective Stille reaction of a *bis*-halide precursor **331** with a suitable stannane **332** (**Scheme 70**). Noting that the propensity for Pd^0 complexes to undergo oxidative addition is determined by a combination of the steric environment and the C-X bond strength,[165] one could reasonably expect that site-selective Stille reaction with a suitable stannane would preferentially occur at the terminal C10 vinyl iodide over the internal C3 vinyl bromide. It was conjectured that this property could be exploited in the synthesis of a suitable *seco* precursor **331**, itself generated from dihalide **333**, for the macro-Stille reaction.

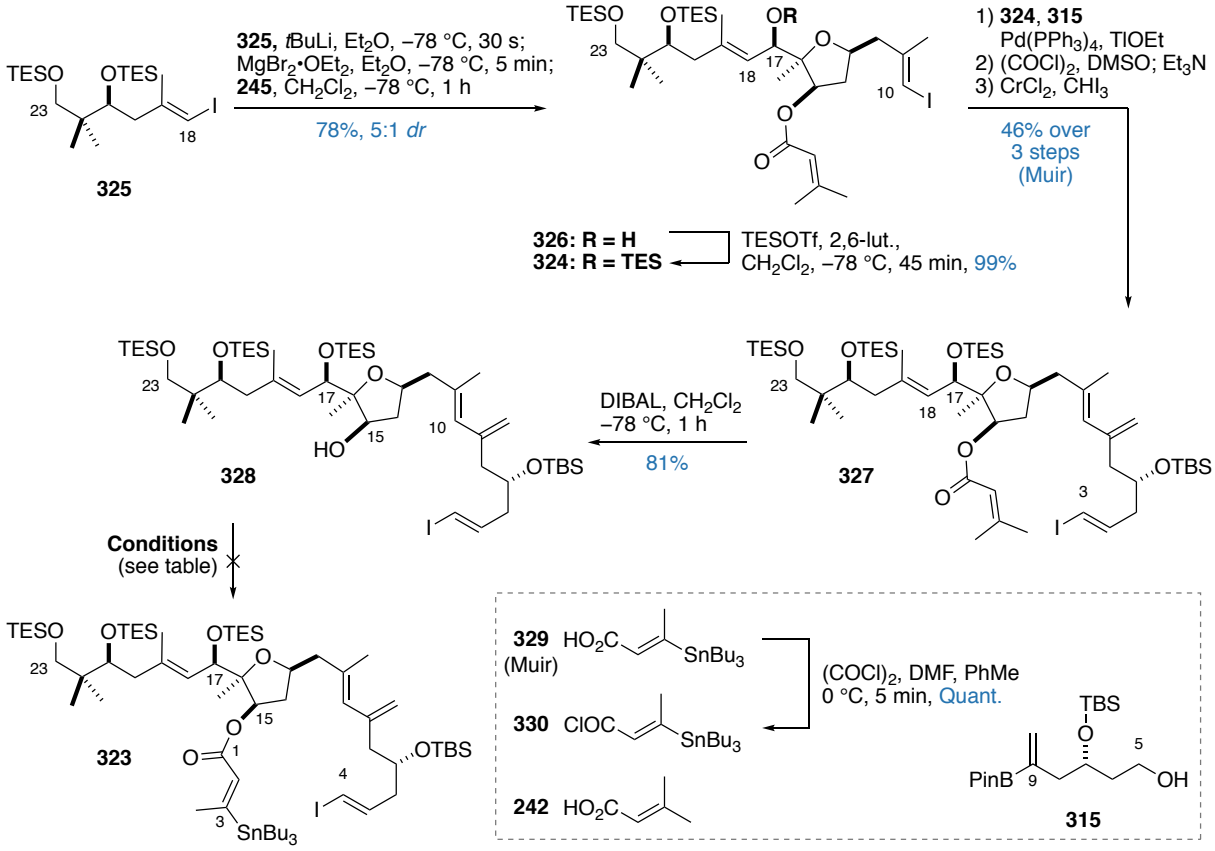

Scheme 69. *Attempted synthesis of seco precursor* ***323*** *via alcohol* ***328***

Table 16. *Conditions trialled for the attempted re-esterification of* ***328*** *to form seco precursor* ***323***

Acyl reagent	Conditions	Result
329	**329**, TCBC, Et_3N; **328**, DMAP, PhH, r.t., 3 – 24 h	No reaction (3 h and 24 h)
329	**329**, **328**, TCBC, Et_3N, DMAP, PhH, r.t., 3 – 24 h	No reaction (3 h and 24 h)
329	**329**, **328**, TCBC, Et_3N, DMAP, PhMe, 80 °C, r.t., 3 – 24 h	No reaction (3 h) Degradation with no **323** (24 h)
329	**329**, **328**, DCC, DMAP, DMAP·HCl, CH_2Cl_2, r.t., 24 h	Degradation with no **323**
330	Et_3N, DMAP (cat.), CH_2Cl_2, r.t., 3 – 24 h	No reaction
330	**328**, NaH, 15-crown-5, THF, 1 h; **330**, Et_3N, DMAP (cat.), r.t., 3 – 24 h	No reaction (3 h) Degradation with no **323** (24 h)
242	**242, 328,** TCBC, Et_3N, DMAP, PhMe, 80 °C, r.t., 24 h	No reaction

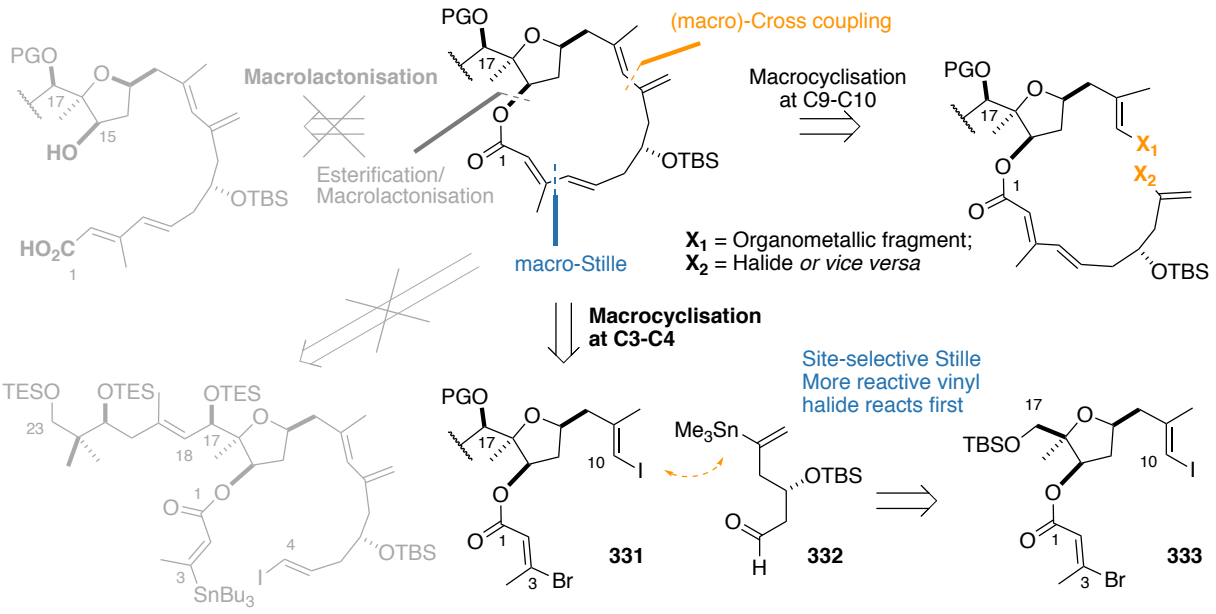

Scheme 70. *Alternative retrosythesis of the phormidolide A macrocycle using a site-selective Stille coupling of dihalide* ***331***

While plausible in theory, in practice this route was marred with the intractability of both the synthesis and manipulation of the bromoacrylate motif in *E*-**333**. Specifically, attempts at the direct esterification of acid **334** or acyl chloride **335** with alcohol **241** resulted in the degradation of the bromide motif (**Scheme 71**). In one instance, the attempted Yamaguchi esterification of acid **334** with alcohol **241** unexpectedly gave the allenyl ester **336**, postulated to have arisen from the elimination of the DMAP-activated intermediate **337**. Noting that the corresponding stannylacrylate ester **338** could be synthesised from alcohol **241** and acid **329**, it was hoped that treatment with an electrophilic Br^+ source could effect a Sn/Br exchange to install the required functionality. Treatment of the configurationally pure stannane **338** with NBS appeared to give a mixture of double bond isomers in the crude product in favour of *Z*-**333**, which can be attributed to a radical destannylative pathway. The intermediate vinyl radical is configurationally unstable, where it equilibrates to preferentially form the thermodynamically more stable radical; that is the radical where the methyl group is projected away from the ester. This radical could then capture a Br atom to primarily afford the undesired *Z*-bromacrylate ester.

In contrast, the use of Br_2 as the electrophilic Br^+ source cleanly gave the *E* isomer *E*-**333** based on NMR analysis of the crude product, ostensibly *via* a polar pathway. Frustratingly, this material was not amenable to any aqueous work up procedures and was unstable to silica chromatography; upon which the material quickly degraded. This degradation was not specific to the bromoacrylate ester; the analogous reaction conducted with I_2 gave the same mixture of degradation product upon aqueous work up or silica chromatography, highlighting that the two independent haloacrylate esters degraded to a common product.

The apparent extreme sensitivity of the bromoacrylate motif eliminated this as a possible route towards the total synthesis of phormidolide A. With both permutations of coupling handles for the C3-C4 macro-Stille approach trialled with no success, it was clear that this disconnection is unviable, and further revision to the overall strategy was required.

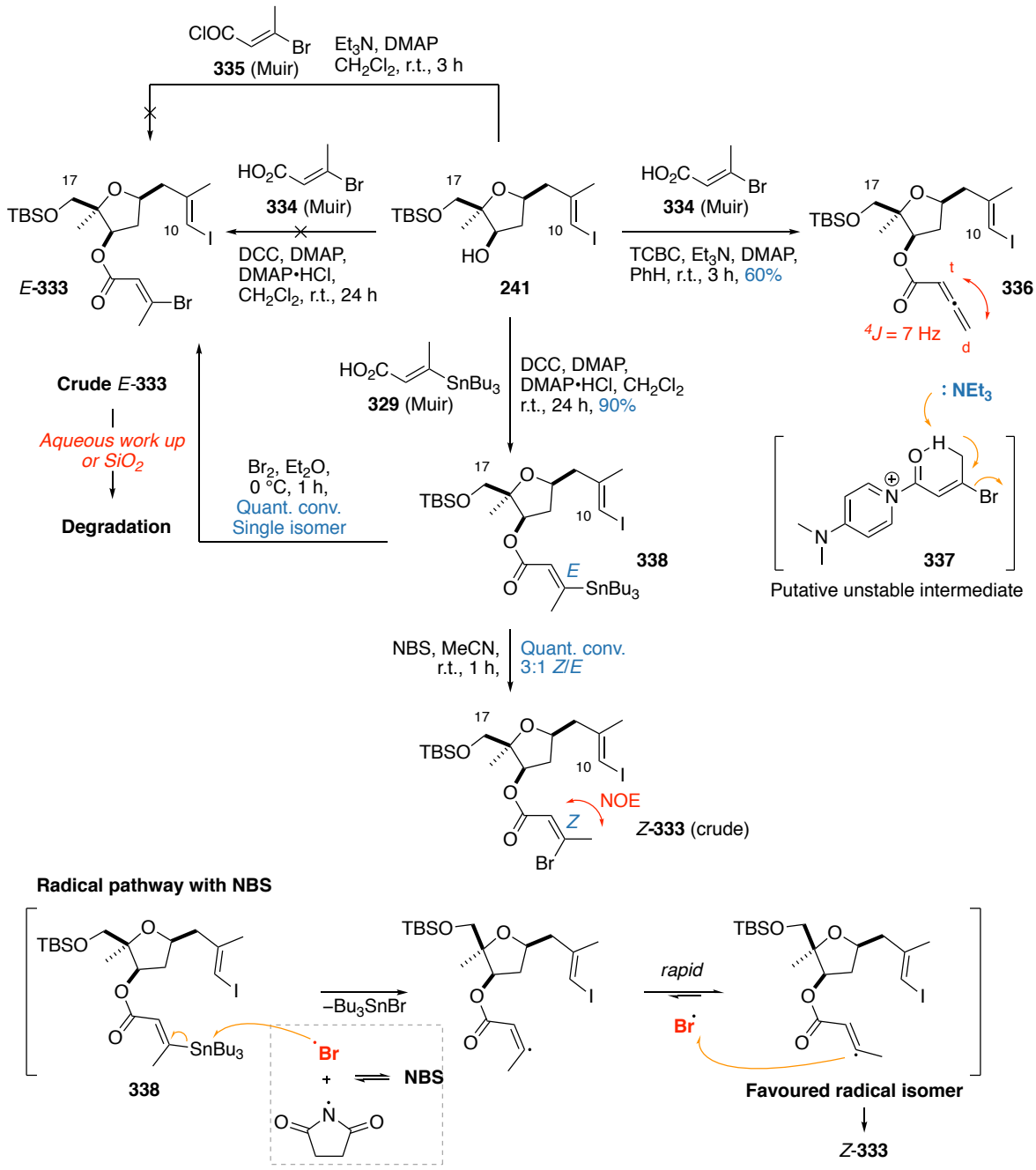

Scheme 71. *Attempted synthesis of E-**333** from **241***

6.6.3. *The C9-C10 macro-Stille approach*

With both the macrolactonisation and C3-C4 macrocyclisation approaches apparently exhausted, attention was then turned towards executing a macrocyclisation *via* the formation of the C9-C10 bond in **305**. In Muir's original synthesis, this bond was formed *via* a Suzuki cross-coupling that required comparatively forceful conditions in order to get any reaction. Noting that the Stille reaction has been successfully employed in demanding cross-couplings, and that high reactivity under dilute conditions is a requirement for effective macrocyclisations, the Suzuki coupling was deemed unacceptable for this purpose, and a C9-C10 macro-Stille cyclisation was adopted in the third strategy revision towards constructing the C1-C17 macrocycle of phormidolide A (**Scheme 72**).

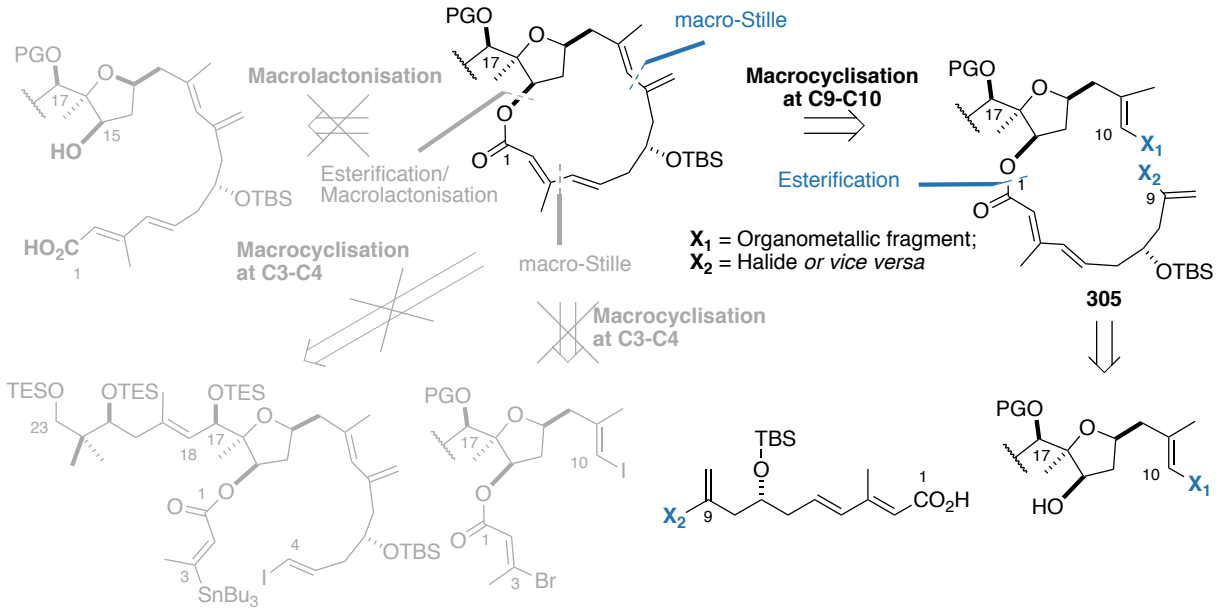

Scheme 72. *Strategy evolution towards the synthesis of the phormidolide A macrocycle: the C9-C10 macro-Stille approach*

This retrosynthetic revision to a macro-Stille reaction meant that a synthesis of the C1-C9 fragment could be revisited, with the aim of appending permutations of either the C9 stannane or the C10 stannane. Taking alkyne **339** synthesised by Muir, an iodoboration followed by acidic workup generated the internal vinyl iodide **340** regioselectively (**Scheme 73a**). An analogous DIBAL reduction revealed aldehyde **341**, which could be subjected to an HWE olefination with phosphonate **342**. Previous model studies conducted by Muir identified the crucial role of HMPA as an additive for this reaction; the omission of which resulted in the extensive isomerisation of the C2 double bond, presumably *via* an intermediary enolate type mechanism as described in **Scheme 73b**. While the exact role of HMPA is unknown, the addition of which as a co-solvent in the HWE olefination largely suppressed this isomerisation to give the C4 olefin in dienoate **343** as a single geometric isomer, and the C2 olefin as a 5:1 *E/Z* ratio of isomers. A hypothesised explanation rationalising this differential result could be attributed to the role of HMPA in solvating Li^+, where its sequestration prohibits the Li-mediated isomerisation to the alternative resonance form. This particular

resonance form contains a freely rotatable C2 bond, where the relative energies of the 2*E* and 2*Z* isomers are presumably similar in energy owing to comparable sized groups on one side of the double bond. Finally, it is worth noting that despite some degree of isomerisation observed, this HWE reaction has best generated the C1-C5 dienoate system in terms of both yield and geometric purity by far.

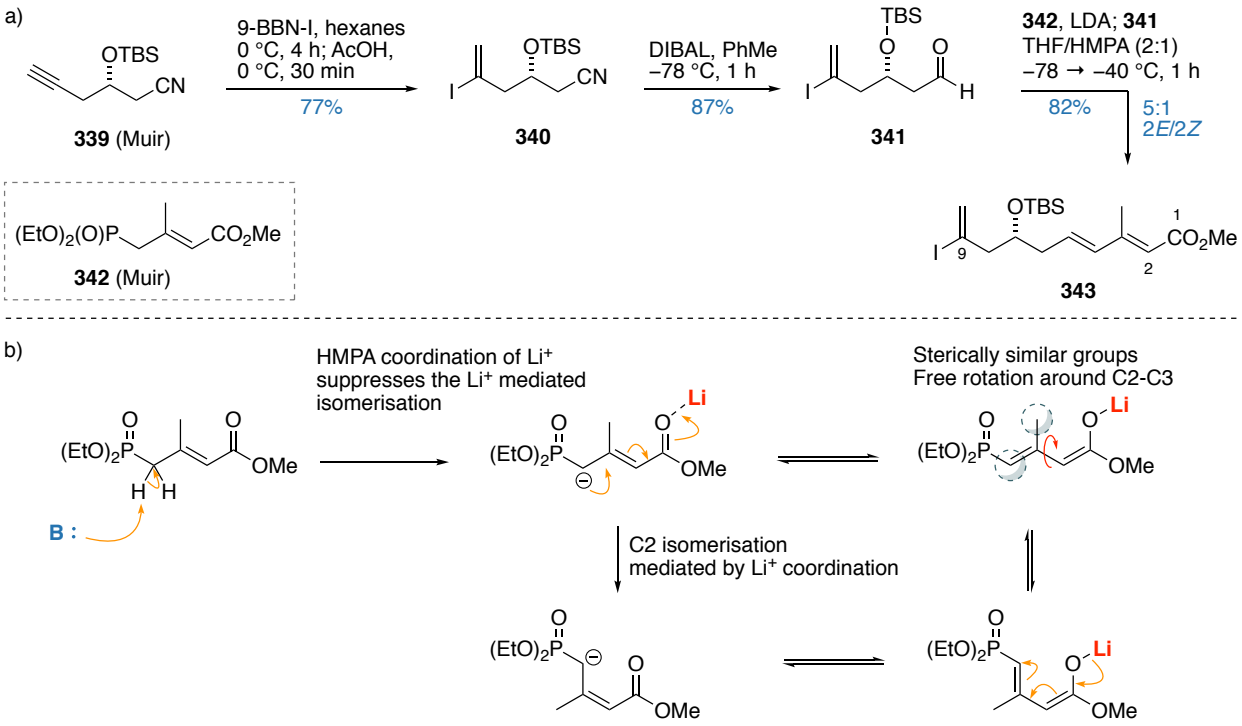

Scheme 73. *a) Synthesis of the C1-C9 dienoate* ***343****. b) Hypothesised mechanism to rationalise the observed C2 isomerisation*

Following this, a basic hydrolysis of the methyl ester **343** afforded acid **344**, which could be esterified onto a suitable alcohol in anticipation for the planned macro-Stille reaction. Despite the negative results observed for the re-esterification of alcohol **328**, it was thought that the use of a smaller silyl protecting group may perhaps open the window of reactivity for the C15 hydroxyl group. To verify this hypothesis, alcohol **326** was protected as the TMS ether **345** and the dimethylacrylate ester reductively cleaved to generate alcohol **346** (**Scheme 74**). Perhaps not surprisingly, attempts at esterifying alcohol **346** with the C1-C9 acid **344** to give **347** resulted in no reaction under Yamaguchi conditions, conclusively confirming the adverse impact C17 protection has on the reactivity of the C15 hydroxyl group. At this point, it was also worth noting the importance of employing the Yamaguchi protocol as the preferred esterification technique. During the course of this study, the prolonged exposure of acid **344** under DMAP-containing conditions resulted in an increased degree of isomerisation of the C2 olefin, which was presumed to occur from the reversible conjugate addition of DMAP into the activated dienoate system. This result highlighted the need to keep the time of DMAP exposure to a minimum, of which the Yamaguchi esterification is able to by virtue of its reliably fast reaction times as compared with the Keck protocol.

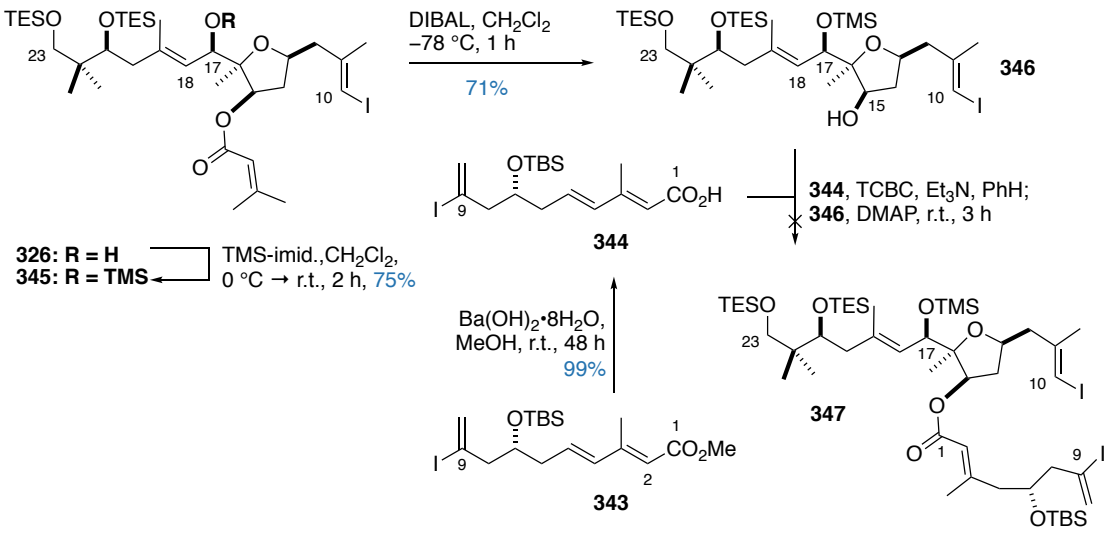

Scheme 74. *Synthesis of acid* ***344****, alcohol* ***346*** *and the attempted synthesis of* ***347***

Noting that the nature of the substitution at C17 appeared to directly impact the reactivity of C15, a more ambitious strategy was conjectured where one could take the C15,C17 diol **348** and conduct an unselective esterification with acid **344**. The regioisomeric esters **349** and **350** could then be macrocyclised to generate a mixture of macrolactone isomers (**Scheme 75**). Optimistically, one may be able to equilibrate the macrolactone to the presumedly thermodynamically more stable C15 regioisomer **351** *via* a Lewis acid. This tactic was used in the Paterson synthesis of aplyronine macrocycle[166] and towards the synthesis of elaiolide.[167] To explore this computationally, DFT optimisation of model C15 and C17 macrocycles were conducted and single point energies were evaluated for both structures. These results showed however, that the undesired C17 macrocycle was thermodynamically more stable by *ca.* 7.6 kcal/mol, highlighting the infeasibility of this idea.

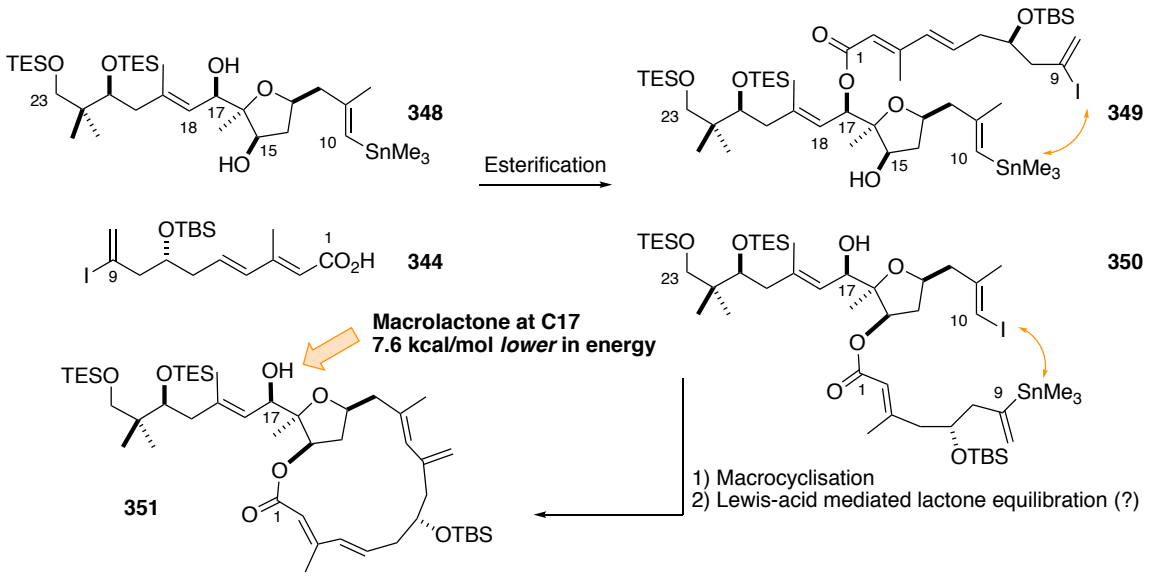

Scheme 75. *A hypothesised Lewis acid-mediated isomerisation strategy towards forming the phormidolide A macrocycle*

As any attempts to install the C1-C9 acid **344** with the C18-C23 side chain in place proved to be intractable, there was no choice but to esterify the C1-C9 fragment prior to side chain introduction. This switch in choreography would directly impact on the protecting group strategy, as the *mono*-desilylation of C17 could not be conducted selectively in the presence of the C7 TBS ether. To circumvent this, either a bulkier protecting group was required for C7, or a more labile/orthogonally labile protecting group was required at C17. Owing to availability of material, attention was first focused towards generating the C7 TIPS ether analogue for acid **344**, which commenced by the TIPS protection of alcohol **310** (**Scheme 76**a). An analogous sequence of steps involving iodoboration of **352** to afford vinyl iodide **353**, reduction, an HWE olefination of **354** to generate **355** and an ester hydrolysis gave acid **356** now bearing the C7 TIPS group.

In order to expeditiously verify the planned macro-Stille step, the C1-C17 macrocycle was once again targeted. At this stage, the stannane handle needed to be appended onto either the C9 or the C10 vinyl iodide. In previous studies, this stannylation could be conducted under Wulff-Stille conditions,[69] where the aldehyde bearing vinyl iodide **341** was successfully transformed to the corresponding stannane **332** (**Scheme 76b**). However, attempts to transform ester **355** to the corresponding stannane **357** proved unsuccessful, and so transforming the THF vinyl iodide **241** into stannane **358** was examined. Gratifyingly, this proceeded well under Wulff-Stille conditions, and the corresponding C10-C17 stannane **358** was esterified under Yamaguchi conditions to give the *seco* precursor **359**.

Taking inspiration from the Paterson synthesis of chivosazole F,[165] initial macrocyclisation attempts focused on using the Fürstner Stille conditions under high dilution. However, it became apparent that the C9 internal vinyl iodide was reticent towards oxidative addition processes at r.t. and required heating to initiate, as evidenced by the quantitative recovery of the protodestannylated product still bearing the vinyl iodide functionality (**Table 17**, entry 1). While the signals attributed to the vinyl iodide disappeared on heating, no product or oligomeric structures were seen and widespread disruption to the dienoate region was observed. Employing Nicolaou's conditions in the macro-Stille reaction towards sanglifehrin A[168] gave a similar outcome (**Table 17**, entry 3), which was rationalised to be from the susceptibility of the dienoate to conjugate addition processes by the phosphine and arsine ligands present in the reaction mixture.

These results suggested an avoidance of nucleophilic ligands was necessary to preserve the structural integrity of the reactant. Noting that the Stille reaction could proceed under Cu-mediated Pd-free conditions,[169] the Liebeskind protocol was trialled at increasing temperatures. Though the reaction was conducted at 1 mg scale, the CuTC promoted macro-Stille appeared to proceed at 110 °C, affording diagnostic m/z values and ^{1}H NMR signals that corresponded to macrocycle **360** (**Figure 55**). This represents a promising lead in which further optimisations can be conducted for the ongoing pursuit towards an effective macrocyclisation strategy. However, due to time constraints, the author's current progress towards the total synthesis of phormidolide A was halted here.

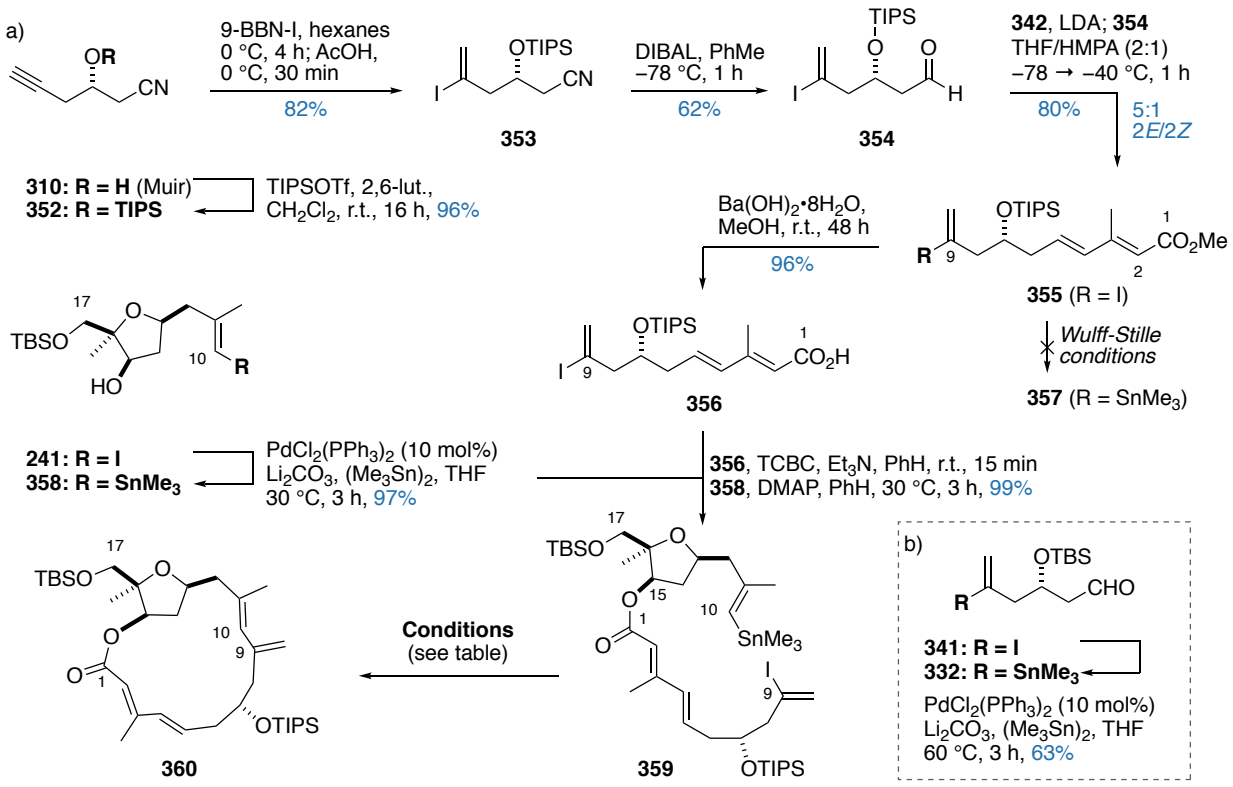

Scheme 76**. a) Synthesis of seco precursor **359** via acid **356**. b) The successful Wulff-Stille reaction of **341** to give **332

Table 17.** Conditions trialled for the macro-Stille reaction of seco precursor **359

Entry and Conditions	Result
1. $Pd(PPh_3)_4$ (20 mol%), CuTC, DMF, r.t., 2.5 h, c = 1 mM	C10 protodestannylated starting material
2. $Pd(PPh_3)_4$ (20 mol%), CuTC, DMF, 60 °C, 3 h, c = 1 mM	Degradation: no dienoate signals C9/C10 protodeiodination/stannylation
3. Pd_2dba_3 (20 mol%), $AsPh_3$, DIPEA, DMF, 80 °C, 3 h, c = 1 mM	Degradation: no dienoate signals C9/C10 protodeiodination/stannylation
4. CuTC, NMP, r.t., 16 h, c = 10 mM	C10 protodestannylated starting material
5. CuTC, NMP, 100 °C, 16 h, c = 10 mM	*ca.* 20% product, *ca.* 20% C10 protodestannylated starting material

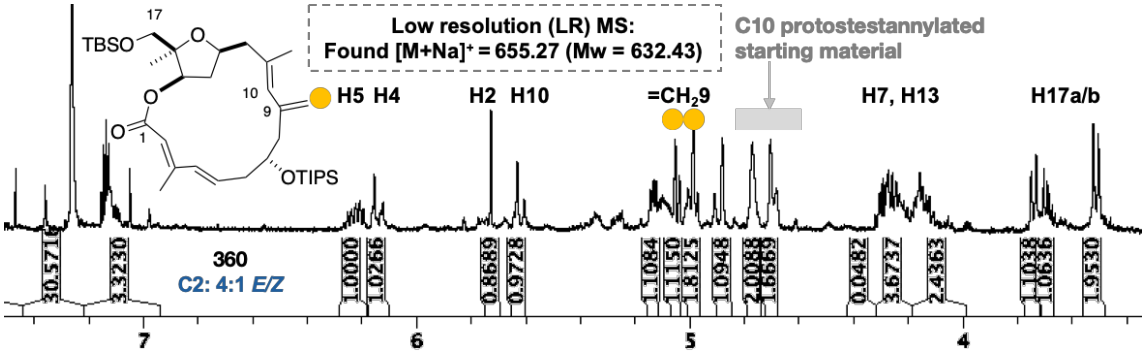

Figure 55.** Excerpt of the ^{1}H NMR spectrum for **360**, highlighting the diagnostic signals indicative of a successful macrocyclisation. The m/z value obtained via low resolution MS is also presented, giving further evidence for the successful synthesis of **360

7. Conclusions and Future Work

7.1. Conclusions

This chapter outlines the progress to date towards the total synthesis of phormidolide A, a complex polyketide of marine origins that bears a gamut of fascinating structural features. From the outset, configurational ambiguities presented in the original isolation paper meant that a parallel objective in this project was to achieve a synthesis-enabled stereochemical corroboration of the natural product.

This chapter first described the successful enantioselective synthesis of the C18-C23 vinyl iodide **233** in six steps, where it was used to investigate the pivotal chelation-controlled Grignard addition with aldehyde **245** to install the reported 17*S* configuration (**Scheme 77**). Unexpectedly, this planned addition delivered the 17*R* alcohol as the major adduct, contradicting the models rationalising its stereoselectivity. Moreover, corroborating the outcome of this addition with the reported triacetonide derivative of phormidolide A revealed yet more inconsistencies. This was addressed through the synthesis of three diastereomeric acetonides (**252**, **254** and **257**), which enabled the configurational reassignment of the side chain and seven of the 11 stereocentres present in phormidolide A. Crucially, this result was enabled through the ability to readily and flexibly generate single enantiomers of **218** and ***ent*-218** through a straightforward use of the appropriate enantiomeric form of the oxazaborolidinone promoter for the Mukaiyama reaction.

The resulting reassignment of the configuration of phormidolide A from **2** to **2a** then allowed for a focused synthetic campaign using the correct enantiomeric series of the side chain. A concise synthesis of the C24-C33 fragment **302** bearing the signature bromomethoxydiene motif was achieved in 14 steps, with a Sn-mediated Sakurai allylation between **286** and **294** employed as the key transformation. This result was enabled through the expeditious synthesis of allylstannane **286** *via* ester **289**, itself derived from known intermediate **276** through an NHC-catalysed oxidative esterification reaction. Finally, studies are presented towards the ongoing synthesis of the C1-C17 macrocycle, which revealed a myriad of unexpected challenges that has largely impeded the successful macrocyclisation of various *seco* precursors. A continual strategy evolution for this elusive target has led to the synthesis of acid **356** and alcohol **358**, to which the first successful macrocylisation result was achieved through the use of a CuTC-mediated macro-Stille reaction to forge the C9-C10 bond in **360**.

Overall, the results detailed in this chapter serve to highlight the lessons learnt in the ongoing synthetic campaign towards phormidolide A. Moreover, it is anticipated that these key findings are readily cross-applicable towards related congeners to phormidolide A. These cumulative results will hopefully allow for the eventual elucidation of the phormidolides elusive biological role in the living environment.

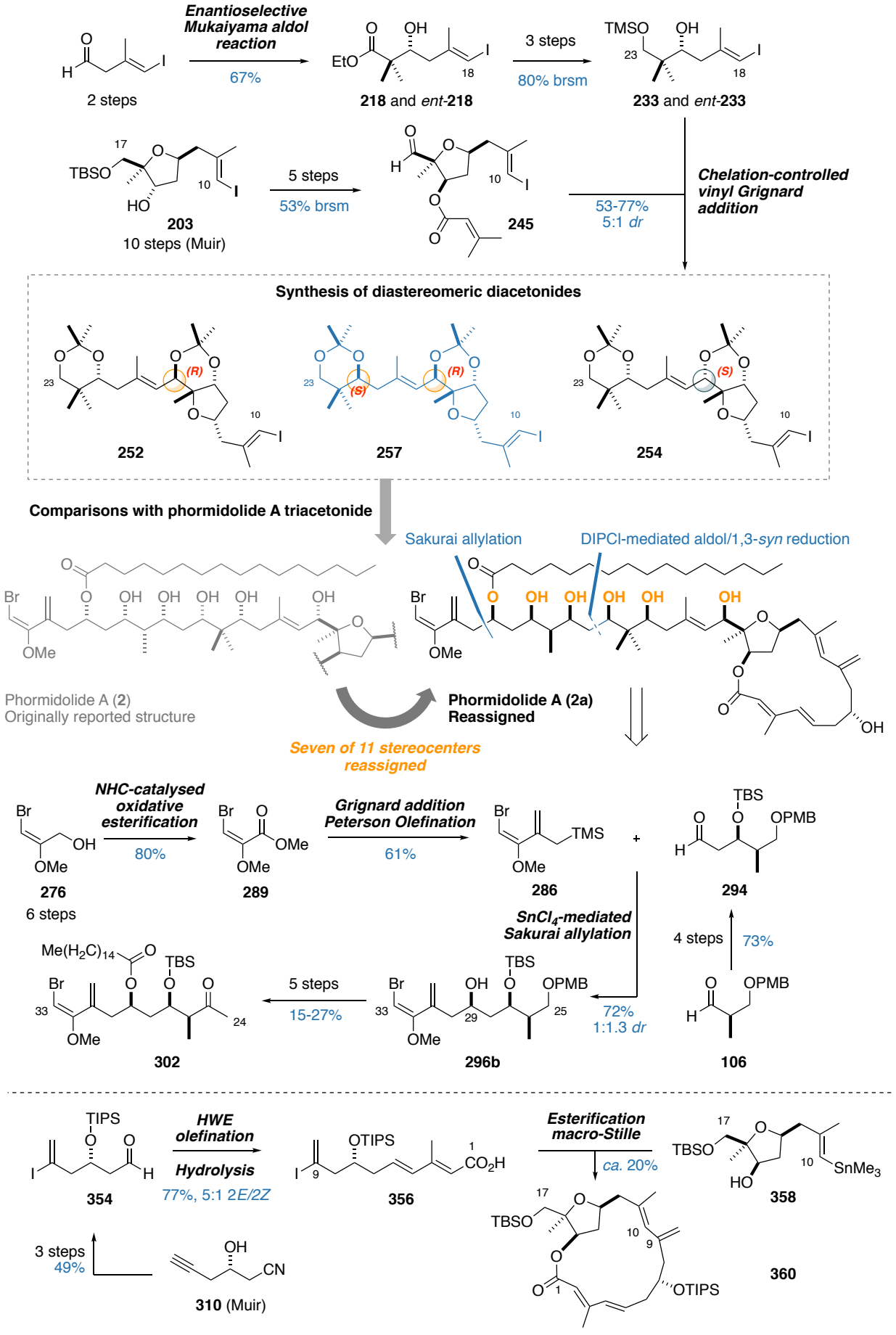

Scheme 77. Summary of the work towards the total synthesis of phormidolide A

7.2. Future work

To date, all the targeted fragments of phormidolide A have been synthesised. The challenge, as highlighted in previous sections, now lies in orchestrating the right sequence of events for fragment coupling and macrocyclisation. Preliminary studies have confirmed the use of a DIPCl-mediated aldol reaction to forge the C23-C24 bond and configure the C23 and C25 stereocentres. Additionally, the chelation-controlled Grignard addition has been validated as a robust strategy for configuring C17, as well as forming the C17-C18 bond. In the pursuit of this challenging target, the remaining fragment coupling step that needs further optimisation is the C9-C10 macro-Stille step, which will form much of the immediate future work for phormidolide A.

7.2.1. Synthesis of the C1-C17 macrocycle and endgame for phormidolide A

Based on the promising result obtained from the CuTC-mediated macro-Stille reaction, the initial focus will lie in its further optimisation with regards to other reaction parameters such as solvent and temperature to generate a reliable and robust method of forming the phormidolide A macrocycle.

As discussed in section **6.4**, the presence of the macrocycle was likely to impede the efficacy of the chelation-controlled vinyl Grignard addition – though this has to date not been experimentally proven. With this in mind, the proposed endgame for phormidolide A would involve the following sequence of reactions: starting with alcohol **241**, an esterification of the C1-C9 acid **356** would give ester **361** (**Scheme 78**). A selective C17 deprotection was then envisaged to occur due to the increased lability of the C17 TBS group as compared to the C7 TIPS group. After oxidation to aldehyde **362**, the planned chelation-controlled Grignard addition with vinyl iodide **325** is expected to deliver the desired 17*R* configuration in alcohol **363**.

At this point, the macrocycle can then be closed by first transforming the C10 vinyl iodide in **363**to the corresponding stannane. This adventurous site-selective Wulff-Stille strategy was conceived in light of the observation that the C10 vinyl iodide **241** readily underwent oxidative addition with Pd^0 at 30 °C, whereas in a previous model study, attempts at executing the analogous transformation for vinyl iodide **341** into the corresponding stannane **332** and indeed in attempting the macro-Stille reaction for substrate **359** required prolonged heating at >60 °C. This margin of reactivity could be exploited to selectively append the stannane handle at C10 while preserving the C9 vinyl iodide. At this stage, the *seco* precursor **364** could then be subjected to the optimised CuTC-mediated macrocyclisation conditions to deliver the advanced C1-C23 intermediate for phormidolide A (**365**).

From **365**, only four more steps would be required for the completion of the total synthesis. A selective C23 primary TES cleavage was anticipated to readily occur in the presence of the secondary C21 TES group. After which, the C23 alcohol could be selectively oxidised *via* a TEMPO-BAIB oxidation, which is known

to selectively target primary alcohols over hindered secondary alcohols.[170] The planned DIPCl-mediated aldol reaction/*in situ* 1,3-*syn* reduction with the C24-C33 ketone **302** could then occur to give the full carbon skeleton of phormidolide A **366**. From **366**, a global desilylation would then afford phormidolide A (**2a**) in 22 steps, with the longest linear sequence being the synthesis of the C10-C17 THF fragment **241** accounting for 12 of those steps. At this point, a careful side-by-side comparison of the spectroscopic data with an authentic sample would be performed to unambiguously assign the structure of phormidolide A.

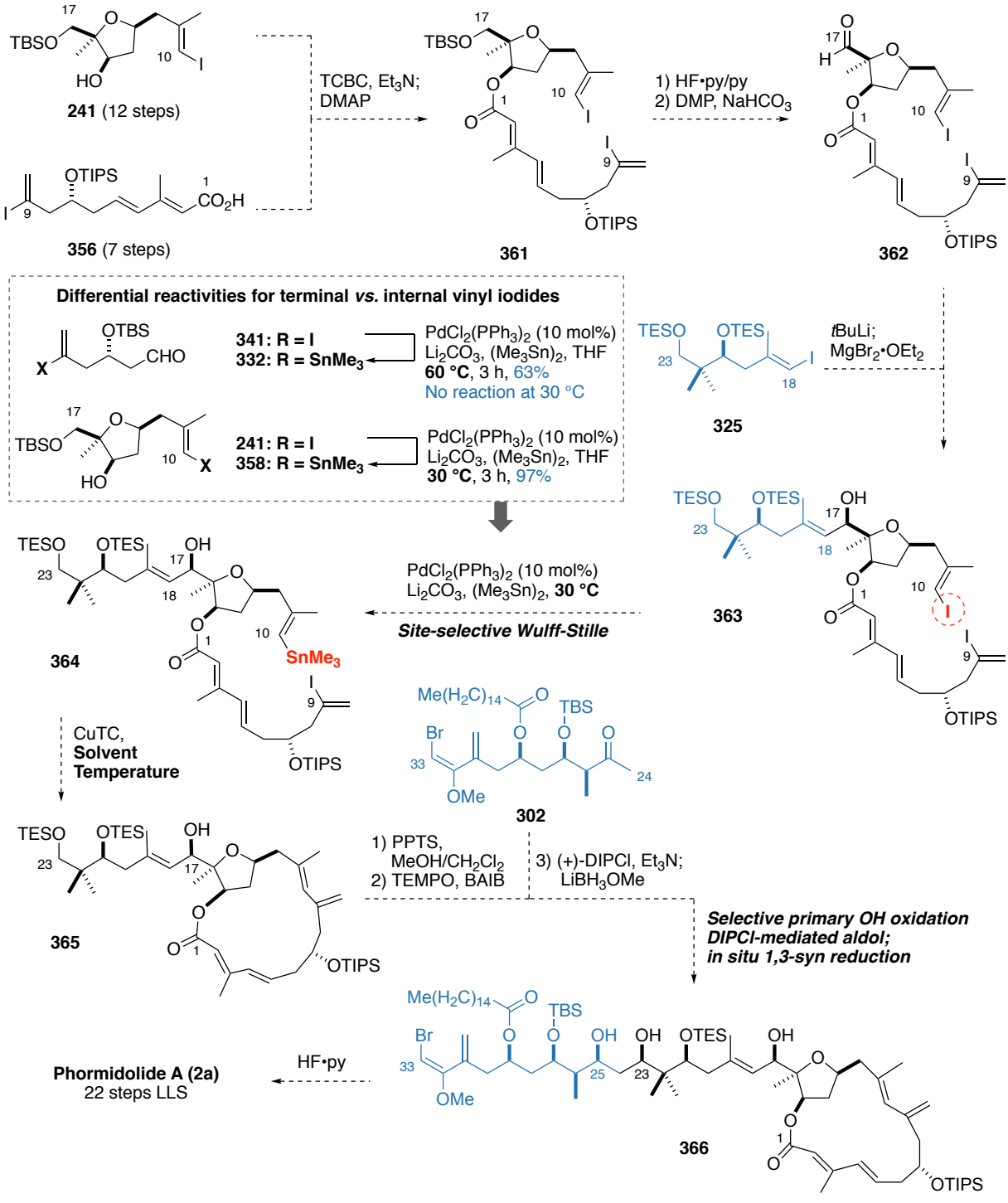

Scheme 78. *Proposed endgame for the total synthesis of revised phormidolide A (**2a**). BAIB = bisacetoxyiodobenzene*

7.2.2. Scope for further economy: a second-generation synthesis

The longest linear sequence towards the planned synthesis of phormidolide A lies in the synthesis of the THF fragment. In this route, the L-proline-catalysed desymmetrising aldol reaction, while a powerful transformation, created two extra stereocentres that required several manipulations to either correct or remove. The first of which is the extra oxygenation at C14 – that required a selective diol protection, triflation followed by reduction to remove, and the second is the undesired 15*S* stereocentre, that required a further two steps to invert to the desired 15*R* configuration. As detailed in section **6.3.3,** the exploratory studies investigating the stereochemical veracity of both C15 and C17 benefited from the ready accessibility of both 15*S* and 15*R* intermediates. This allowed for rapid spectroscopic comparisons to conclusively rule out C15 as a suspect stereocentre, and therefore facilitated the conclusive reassignment of C17 in phormidolide A.

With more confidence now attributed to the configuration of phormidolide A, a more focused synthetic approach can be adopted in order to streamline the synthesis even more. In particular, the opportunities identified in avoiding extra manipulations to edit unwanted stereocentres can be avoided. Noting that the biosynthesis of phormidolide A was hypothesised to proceed *via* an intramolecular conjugate addition to form the THF motif, a similar disconnection could be envisaged into a suitable Michael acceptor. This reveals a 1,2-*syn* diol motif **368**, which could arise from a Sharpless asymmetric dihydroxylation of **369**. The linear precursor **369** itself can be broken into its constituent fragments *via* an HWE olefination and a cross metathesis (**Scheme 79a**).

An example of how this strategy could be realised is presented in **Scheme 79b**. After protecting group installation, a three-step sequence involving cross-metathesis to give diol **370**, oxidative cleavage followed by HWE olefination with phosphonates **125** or **371,** and Sharpless asymmetric dihydroxylation of **369** would generate the linear precursor **368**, where it was expected that a cyclisation would spontaneously occur under Brønsted or Lewis acidic conditions to generate the THF moiety **372** or **373** diastereoselectively. At this point, transformation of the methyl ketone **372** to the *E*-vinyl iodide could optimistically be conducted under Takai conditions (with R = Me). Though there are literature examples of stereoselective Takai olefination of methyl ketones,[171] owing to the often poor reactivity and selectivity of ketones in the Takai olefination,[172,173] alternative strategies may be necessary. These include a validated three-step procedure involving HWE olefination with phosphonate **374**, ester hydrolysis and decarboxylative iodination.[174] Alternatively, taking the analogous thioester **373**, one could reduce to the aldehyde, conduct a Seyferth-Gilbert homologation with **375** followed by a Negishi carboalumination to afford the desired C10-C17 fragment **367**. This potential second-generation synthesis might be achieved in as little as seven steps, and has the opportunity to reduce the overall number of steps for phormidolide A from 22 down to 17 steps in the longest linear sequence.

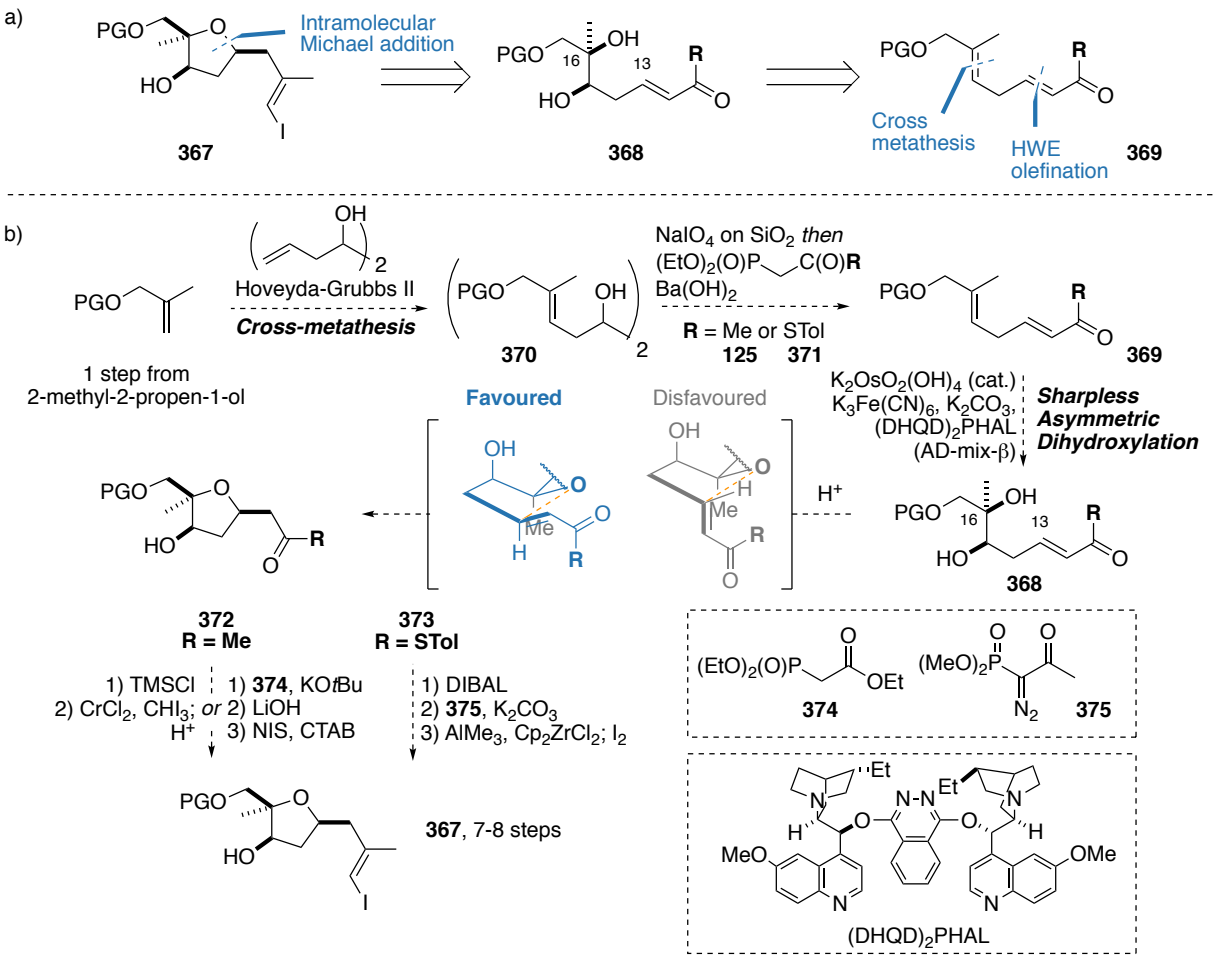

***Scheme 79**. a) Alternative retrosynthesis of the C10-C17 fragment **367**. b) Potential shorter second generation synthesis of the C10-C17 fragment **367**. PG denotes unspecified protecting group. STol = S-tolyl, CTAB = cetrimonium bromide*

7.2.3. The configurational identity of C7 – a case for a further misassignment?

During the writing of this thesis, an anomaly was spotted in the configurational assignment of the C7 stereocentre of phormidolide A as performed by Bertin *et al.*. In this report, Bertin *et al.* sought to confirm the stereochemical nature of a carbinol stereocentre set by a Type-B ketoreductase by forming the diastereomeric Mosher esters of phormidolide A triacetonide. While the ketoreductase responsible for setting C7 contains the D1758 residue – predictive of generating D-OHs, Bertin *et al.* claimed the result from Mosher analysis appeared to confirm the 7*R*, or L-OH configuration, and therefore the originally assigned configuration for the natural product.

A reinspection of the reported data presented for the *S*- and *R*-MTPA derivatives of triacetonide **151** however, directly contradicts this finding (**Table 18**). Applying Hoye's model to the reported NMR values revealed that C7 possesses the *S* configuration. This result also contradicts the modified Mosher method Williamson *et al.* conducted in the original isolation paper, which gave the 7*R* configuration (**Figure 56**).

***Table 18**. Diagnostic ^{1}H NMR signals for the configurational assignment of C7 as reported by Bertin et al.*

Proton	**δH (*S*)-MTPA** (ppm)	**δH (*R*)-MTPA** (ppm)	$\Delta\delta_{S-R}$ (ppm)
H2	5.71	5.72	-0.01
H4	6.17	6.19	-0.02
H5	6.17	6.18	-0.01
H6	2.38	2.43	-0.05
H6	2.34	2.36	-0.02
H7	5.64	5.31	+0.33
H8a	2.28	2.24	+0.04
H8b	2.25	2.21	+0.04
H10	5.73	5.71	+0.02
H12a	2.55	2.42	+0.13
H12b	2.43	2.40	+0.03
H13	3.97	3.96	+0.01

It is currently unknown whether or not this arose from a labelling error or from a misanalysis of the reported data, but these conflicting results give further stereochemical ambiguity for the natural product, especially since all the stereochemical information from the isolation paper was relayed to the C7 stereocentre. If C7 was indeed wrongly configured, there are two outcomes that can arise from this conundrum: the first outcome assumes the original *J*-based analysis was correctly formulated, which means that the remaining ten stereocentres in the molecule (or only three from the originally assigned structure) needs a further reassignment to their corresponding epimer. The second, and much more likely outcome, assumes that the *J*-based analysis was not definitive, where an alternative unconsidered configuration of the macrocycle could also explain the observed *J* values and NOEs observed for phormidolide A (**Figure 56**).

In the author's opinion, the second outcome is the more likely scenario, especially considering the published domain analysis for the ketoreductases responsible for configuring phormidolide A. In this chapter, the reassignment of phormidolide leaves C7 as the sole anomalous stereocentre that was not justified by the published domain analysis. The implications from the first scenario would mean that all carbinol stereocentres set by ketoreductases *except* for C7 are anomalous, On the other hand, the second scenario where the absolute configuration at C7 was revised without altering the configuration of the remaining stereocentres would align all carbinol stereocentres set by the ketoreductase enzyme. This would mean that *all* ketoreductases in the biosynthesis of phormidolide A that contain the D1758 residue will predictably generate the expected L-OH; a much more plausible scenario than the former.

However, it is important to note that this outcome, while providing a convenient stereochemical rationalisation, remains as an unsubstantiated claim. To further this investigation, ongoing DP4f

computational NMR studies are being conducted by the author towards identifying the diastereomer of the macrocycle that best fits the spectroscopic data from the natural product. Additionally, Muir is currently embarking on the synthesis of the enantiomeric C1-C9 fragment ***ent*-356** starting from (–)-epichlorohydrin, with the end goal of achieving a synthesis-enabled stereochemical corroboration of the deprotected C1-C17 macrocycle with phormidolide A, taken alongside the anticipated results from computational studies. Optimistically, the revision at C7 could help assuage the troubles faced with the stubborn macrocyclisation step previously faced, especially noting that distal stereocentres can have a noticeable impact on the overall conformation of the macrocycle.

Regardless of the various hypotheses put forth however, further stereochemical verification for C7 has now become a necessary objective towards the ongoing campaign towards phormidolide A.

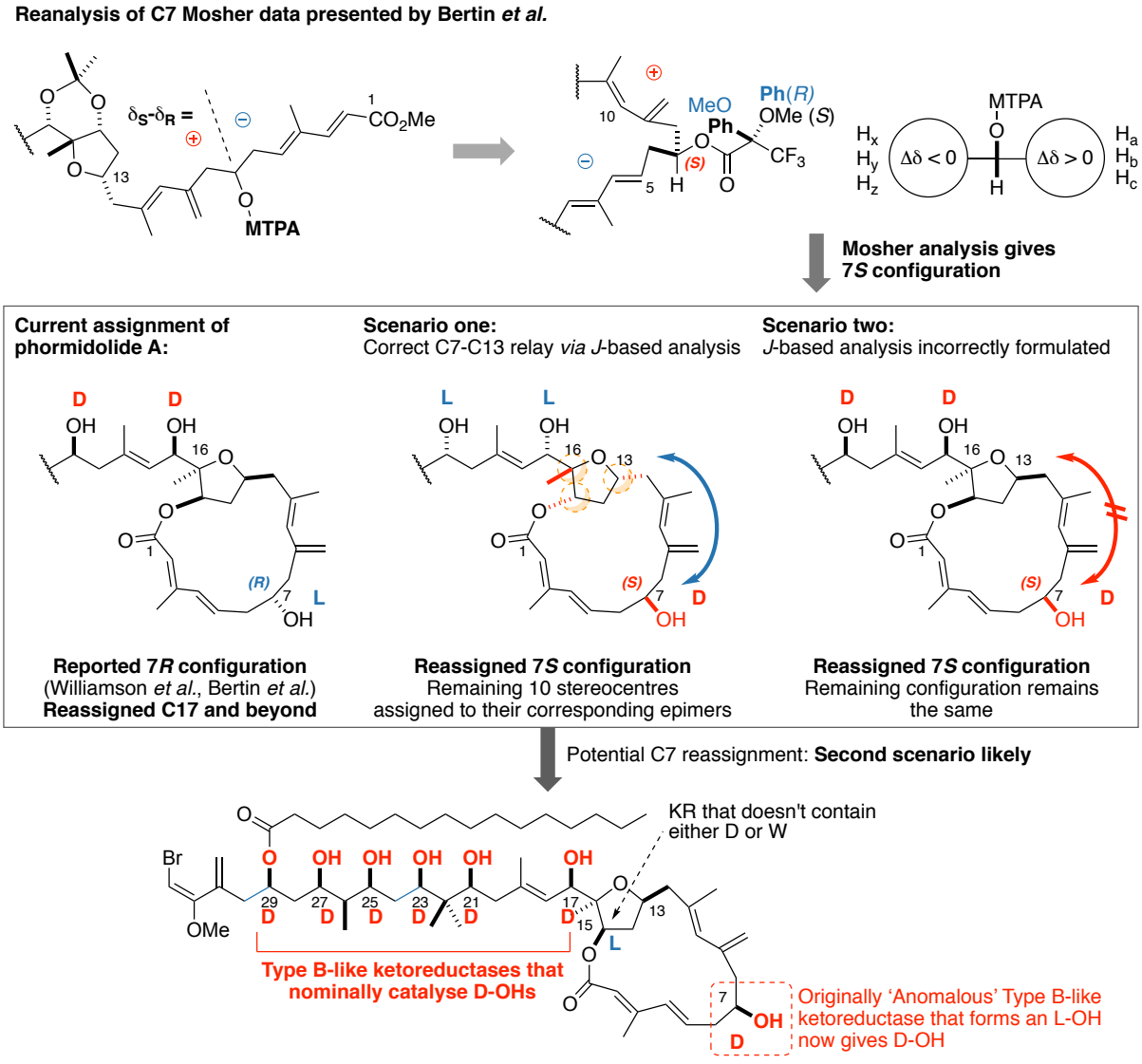

***Figure 56**. Reanalysis of the diastereomeric Mosher ester data by Bertin et al. suggest that C7 is misconfigured, which gives two broad scenarios for the overall configuration of phormidolide A*

Overall conclusions

This thesis examines the crucial role synthesis plays in the stereochemical elucidation of complex natural products. The first chapter outlines how synthetic chemistry, in particular, has allowed for the unambiguous elucidation of their complex architecture when other state-of-the-art techniques may not be applicable. This premise underpins the remaining chapters of this thesis, where developing the stereocontrolled syntheses of two architecturally complex polyketide natural products has enabled their ongoing stereochemical elucidation.

In chapter two, the hemicalide project presented a paramount example of the role a modular synthesis plays in the stereochemical elucidation of a natural product. The hemicalide project is unique, and perhaps unprecedented in the realm of natural product elucidation, that only 1D ^{1}H and ^{13}C listed NMR data was provided as the sole basis for determining all 21 unknown stereocentres. It is through years of fruitful collaboration between computational and synthetic chemists, employing state-of-the-art algorithms, that has allowed the eventual narrowing of over two million stereochemical permutations, down to 256 prior to this current work. With current limitations imposed by computational resources, the increasingly complex structures of truncates of hemicalide post a practical constraint for further *ab initio* prediction methods, and this thesis demonstrates the power stereocontrolled synthesis brings in the stereochemical elucidation of distal stereoclusters. Here, the synthesis of both candidate diastereomers unambiguously showed that hemicalide possesses the 13,18-*syn* configuration, further reducing the number of permutations down to 128 for the natural product.

Additionally, the independent synthetic development of hemicalide between the Paterson and Ardisson/Cossy groups has provided a great deal of understanding to the innate chemistry of the natural product. Embedded within this is the concept that academic research is not a zero-sum game (despite what the funding models may imply), and each team's successes and failures serve to guide the continual development of further stereochemical confirmation towards this alluring natural product.

Pursuing a total synthesis also has the advantage in being able to flexibly divert intermediates for biological testing. As Romo *et al.* demonstrated in their recent work,[175] a pharmacophore-guided retrosynthetic analysis can allow for the development of a comprehensive SAR study during a total synthesis campaign. Aspects of this can be incorporated to hemicalide, where a parallel objective is to investigate how the molecule imparts its stellar bioactivity, and whether or not simplification can be tolerated.

One could not anticipate from the outset of this project the challenges and opportunities phormidolide A, a continually moving target, has brought. As described in chapter three, the phormidolide A project further reinforces the role of synthesis in the unambiguous stereochemical confirmation of natural products. Again enabled through modular disconnections and enantioflexible syntheses, the Paterson/Britton approach towards phormidolide A rapidly generated candidate diastereomers to probe the likely configuration at C17 as well as C21 of the natural product. Underscoring this however, the project also highlights the role of serendipity in research; the reassignment of seven of 11 stereocentres of phormidolide A would have been a harder task such if the chelation-controlled vinylmetal addition proceeded exactly as planned.

The stereochemical reassignment of phormidolide A was additionally notable for the fact that it occurred despite a comprehensive analysis of spectroscopic data as well as the elucidation of its biosynthetic machinery, further reinforcing the role synthesis has as the final arbiter of a compound's 3D structure. Pleasingly, the correction of this error generated productive and ongoing collaborations in the attempt towards refining techniques used in structure elucidation and biosynthesis/informatics, so that these errors may not arise again. This additionally highlights the inherent symbiotic relationship between synthetic chemistry with natural products, where discoveries in either fields will mutually benefit each other.

The ongoing synthetic campaign towards phormidolide A also highlights the many deficiencies synthetic chemistry still has on the efficient construction of complex natural products. In light of several high profile debates,[176–178] of which many have proclaimed the passing of the golden-age of organic synthesis, the continual frustrations the present author encountered at executing notionally straightforward chemical reactions is a testament against the pessimists. The narrative that organic chemistry is a mature field, and research should be pursued in other high growth areas is detrimental to the pressing need for the development and, more importantly, improvement of chemical transformations. Especially noting that organic synthesis often lags behind other sciences as the rate-limiting step in discovery,[179,180] the focus now more than ever should firmly be on discovering methods to prospect and improve reactivity in order to facilitate the efficient construction of molecules large and small.

The study of natural products serves as an enabler for the co-discovery of medicine, biology and, as illustrated in this thesis, chemistry. The challenges and discoveries found in the productive journey towards these two marine polyketide natural products above all, illustrate how nature informs science, and in turn how science reveals nature. With continual advancements in technology, one can hope that the study of natural products across disciplines will continue to inspire the advancement of science for the betterment of mankind.

Experimental Procedures and Data

8.1. General Procedures

Unless the reaction contained aqueous reagents or otherwise stated, all reactions were carried out under an atmosphere of argon, using oven dried glassware and standard techniques for handling air sensitive chemicals.

Reagents were purified using standard laboratory procedures; benzene and dichloromethane were distilled from CaH_2 and stored under argon. THF and Et_2O were distilled from potassium or sodium wire/benzophenone ketyl radical and stored under argon. DMSO, 2,6-lutidine, *i*Pr_2NH, DIPEA and Et_3N were distilled from CaH_2 and stored over CaH_2 under argon. DBU was distilled from CaH_2 and stored over 4 Å MS. DMF was distilled from $MgSO_4$ and stored over 4 Å MS. EtOAc was distilled from $MgSO_4$, DDQ was recrystallised from $CHCl_3$. $(COCl)_2$ and $TiCl_4$ were distilled. Solvents used for extraction and chromatography were distilled. All other chemicals were used as received from the supplier unless otherwise stated.

Aqueous solutions of ammonium chloride (NH_4Cl), sodium bicarbonate ($NaHCO_3$), sodium thiosulfate ($Na_2S_2O_3$), brine (NaCl) and sodium/potassium (Na/K) tartrate were saturated. Buffer solutions were prepared as directed from stock tablets.

Flash column chromatography was carried out using Kieselgel 60 (230-400 mesh) and a positive solvent pressure. Chromatographic purification over alumina was carried out using Merck Millipore Aluminium oxide 90 and a positive solvent pressure.

8.2. Analytical Procedures

TLC was carried out using Merck Kieselgel 60 F_{254} or Aluminium oxide 60 F_{254} plates, which were visualised under UV light (254 nm) and stained with potassium permanganate or phosphomolybdic acid/$Ce_2(SO_4)_3$ dips.

NMR spectra were recorded using the following machines: Bruker Avance 500 BB (500 MHz), Avance TCI cryoprobe (500 MHz) and Avance 400 DRX (400 MHz). ^1H spectra were recorded at 298 K with an internal deuterium lock for the residual undeuterated solvent: $CDCl_3$ (δ_H = 7.26 ppm) and DMSO-d_6 (δ_H = 2.50 ppm), MeOD-d_4 (δ_H = 3.31 ppm). ^1H data are presented as: chemical shift (δ/ppm), relative to tetramethylsilane (δ_{TMS} = 0 ppm), integration, multiplicity (s = singlet, d = doublet, t = triplet, q = quartet,

qn = quintet, sext = sextet, sept = septet, m = multiplet, br = broad, obs = obscured) and coupling constants (*J* in Hz). Signals are assigned according to the numbering scheme for hemicalide (**1**) (**Figure 1**) or phormidolide (**2**) (**Figure 2)** unless otherwise indicated. Assignments have been made based on 1D data presented along with 2D spectra and comparison with fully assigned spectra for similar compounds.

^{13}C NMR spectra were recorded at 298 K with broadband proton decoupling and an internal deuterium lock for ^{13}C: $CDCl_3$ (δ_C = 77.0 ppm), DMSO-d_6 (δ_H = 39.5 ppm) or MeOD-d_4 (δ_H = 49.1 ppm). Data are listed by chemical shift (δ/ppm) relative to tetramethylsilane ($\delta_{TMS} = 0$ ppm).

Fourier transform IR spectroscopy (FT-IR) was carried out using a Perkin-Elmer Spectrum-One spectrometer and spectra were recorded as a thin film. Wavelengths of maximum absorption (ν_{max}) are reported in wavenumbers (cm^{-1}).

Optical rotations were measured using a Perkin-Elmer 241 polarimeter at the sodium D-line (589 nm) and are reported as $[\alpha]_D^{20}$, concentration (*c* in g/100 mL) and solvent used.

High resolution mass spectrometry (HRMS) was carried out by the EPSRC National Mass Spectrometry Facility (Swansea, UK) using electrospray ionisation (ESI). The parent ion $[M+H]^+$ or $[M+Na]^+$ is quoted.

Chiral HPLC was carried out on a Shimadzu XR-LC system, using a Chiralpak® IA column and a solvent system of mixed hexanes and isopropanol.

8.3. Preparation of Reagents

2-Iodoxybenzoic acid[181]

To a solution of Oxone® (53.0 g, 0.348 mol) in water (720 mL) was added iodobenzoic acid (60.0 g, 0.242 mol). The suspension was stirred vigorously at 70 °C for 3 h before cooling to r.t.. The resulting precipitate was filtered and washed with water (6 × 120 mL) and acetone (2 × 120 mL) and dried *in vacuo* to afford 2-iodoxybenzoic acid as a white solid (63.7 g, 0.227 mol, 94%).

Dess-Martin Periodinane[181]

A suspension of 2-iodoxybenzoic acid (63.7 g, 0.227 mol) and $TsOH{\cdot}H_2O$ (432 mg, 2.27 mmol) in acetic anhydride (318 mL) was stirred at 95 °C for 2.5 h to afford a pale-yellow solution. The mixture was cooled to r.t., then to 0 °C to facilitate the formation of a white precipitate. The precipitate was collected by filtration and washed with Et_2O (5 × 100 mL) then dried overnight *in vacuo* to afford Dess-Martin Periodinane as a white solid (63.2 g, 0.148 mol, 65%), which was stored at –20 °C without appreciable deterioration.

***i*PrMgCl**

Mg turnings (2.69 g, 120 mmol) and I_2 (2 crystals) were added to a solution of THF (10 mL) and *i*PrCl (0.91 mL, 10 mmol). The reaction was heated gently until the brown colour dissipated, at which point a solution of *i*PrCl (8.23 mL, 90.0 mmol) in THF (40 mL) was added dropwise over 30 min while maintaining a steady reflux. The reaction was heated to reflux for 1 h to afford a black solution of the Grignard reagent. This was titrated against menthol/1,10-phenanthroline to determine a final concentration of 1.42 M.

$[CuH(PPh_3)]_6$ (Stryker's Reagent)[182]

Tetramethyldisiloxane (1.40 mL, 7.56 mmol) was added to a stirred suspension of $Cu(OAc)_2{\cdot}H_2O$ (100 mg, 501 μmol) and PPh_3 (260 mg, 991 μmol) in toluene (18.6 mL) at r.t.. The mixture was stirred at r.t. for 24 h, during which the blue colouration faded to afford a solution of the Stryker's reagent as a red solution. The reagent was stored at 4 °C under Ar and was used as a 0.025 M solution with respect to $Cu(OAc)_2{\cdot}H_2O$.

***N*-Tosyl-L-valine – 215 and *ent*-215**

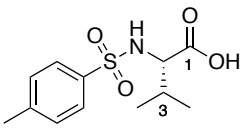

To a stirred solution of L-valine (1.76 g, 15.0 mmol) in aqueous NaOH (7.5 mL, 2 M) at 0 °C was added tosyl chloride (3.00 g, 15.8 mmol), DIPEA (2.87 mL, 16.5 mmol) and acetone (15 mL). The solution was

warmed to r.t. and stirred for 16 h to afford a pale-yellow solution. The reaction was neutralised with aqueous HCl (*ca.* 5 mL, 3 M) and the aqueous solution was extracted with EtOAc (5 × 15 mL). The combined organic phases were washed with brine (20 mL), dried (Na_2SO_4) and the solvent removed under reduced pressure to afford *N*-tosyl-L-valine as a white powder (3.89 g, 14.3 mmol, 95%). The enantiomeric compound was analogously prepared from D-valine (1.76 g, 15.0 mmol) to afford *N*-tosyl-D-valine (***ent*-215**) as a white powder (3.84 g, 14.1 mmol, 94%)

^{1}H NMR (400 MHz, $CDCl_3$) δ_H 7.72 (2H, d, *J* = 8.3 Hz, ArH), 7.28 (2H, d, *J* = 8.3 Hz, ArH), 5.12 (1H, d, *J* = 9.9 Hz, NH), 3.80 (1H, dd, *J* = 9.9, 4.6 Hz, H2), 2.41 (3H, s, Ar<u>Me</u>), 2.10 (1H, septd, *J* = 6.8, 4.6 Hz, H3), 0.96 (3H, d, *J* = 6.8 Hz, H4a), 0.87 (3H, d, *J* = 6.8 Hz, H4b); **^{13}C NMR** (125 MHz, $CDCl_3$) δ_c 176.5, 143.9, 136.6, 129.6, 127.2, 60.7, 31.4, 21.5, 19.0, 17.2.

Data in agreement with that presented by Berry[183]

***p*-Methoxybenzyl-2,2,2-trichloroacetimidate (PMBTCA)**

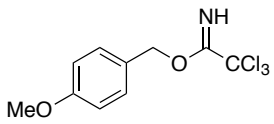

Trichloroacetonitrile (11.6 mL, 115 mmol) was added dropwise over 45 min to a stirred biphasic mixture of *p*-methoxybenzyl alcohol (13.8 g, 100 mmol), KOH (75.0 g, 1.34 mol) and $[Bu_4N][HSO_4]$ (435 mg, 10.0 mmol) in CH_2Cl_2 (150 mL) and water (150 mL) at –10 ˚C. The reaction was stirred for 16 h, with gradual warming to r.t.. The layers were separated and the aqueous phase was extracted with Et_2O (3 × 300 mL). The combined organic phases were washed with brine (500 mL), dried ($MgSO_4$) and the solvent removed under reduced pressure. Purification by flash column chromatography (EtOAc/PE 40-60: 5%) (alumina) afforded the title compound as a pale-yellow liquid (19.7 g, 69.7 mmol, 70%)

^{1}H NMR (500 MHz, $CDCl_3$) δ_H 8.36 (1H, br s, NH), 7.37 (2H, d, *J* = 8.8 Hz, ArH), 6.91 (2H, d, *J* = 8.8 Hz, ArH), 5.27 (2H, s, ArC<u>H</u>$_2$O), 3.80 (3H, s, <u>Me</u>OAr); **^{13}C NMR** (125 MHz, $CDCl_3$) δ_C 162.6, 159.7, 129.7, 127.5, 113.9, 91.5, 70.7, 55.3.

Data in agreement with that presented by Joly[184]

Trimethyl((3-methylbut-2-en-2-yl)oxy)silane – 207

TMSCl (7.61 mL, 60.0 mmol) was added dropwise to a stirred solution of methyl isopropyl ketone (4.44 mL, 50.0 mmol, dried over Na_2SO_4) and Et_3N (16.7 mL, 120 mmol) in DMF (15 mL). The reaction mixture was heated at 120 °C for 90 h to obtain a dark brown solution. The reaction mixture was allowed to cool to r.t. and diluted with Et_2O (160 mL). The mixture was washed with $NaHCO_3$ (200 mL), the aqueous phase was extracted with Et_2O (3 × 200 mL), and the combined organic fractions were rapidly washed with HCl (200 mL, 0.5 M), $NaHCO_3$ (2 × 200 mL) and brine (200 mL). The organic phase was dried (Na_2SO_4) and the solvent removed under reduced pressure. Purification by distillation under reduced pressure (90 °C, 3 mmHg) afforded the product as a colourless liquid (3.96 g, 25.0 mmol, 50%) as a 9:1 mixture of trimethyl((3-methylbut-2-en-2-yl)oxy)silane **(207**) and trimethyl((3-methylbut-1-en-2-yl)oxy)silane.

^{1}H NMR (500 MHz, $CDCl_3$) δ_H 1.79 (3H, s, Me), 1.61 (3H, s, $\underline{Me}_aMe_bC$), 1.60 (3H, s, $Me_a\underline{Me}_bC$), 0.19 ppm (9H, s, $Si\underline{Me}_3$); **^{13}C NMR** (125 MHz, $CDCl_3$) δ_C 140.1, 109.5, 18.8, 18.3, 17.6, 0.59.

Data in agreement with that presented by Fleming[112]

((1-ethoxy-2-methylprop-1-en-1-yl)oxy)trimethylsilane – 217

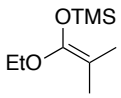

*n*BuLi (37.5 mL, 60.0 mmol, 1.6 M in hexanes) was added dropwise to a solution of *i*Pr_2NH (8.47 mL, 60.0 mmol) in THF (30 mL) at 0 °C. The solution was stirred at 0 °C for 2 h before cooling to –78 °C. Ethyl isobutyrate (6.72 mL, 50.0 mmol) was added dropwise to the mixture over 10 min, and the reaction was stirred for an additional 1 h before the addition of TMSCl (7.62 mL, 60.0 mmol). The reaction was warmed to r.t. and stirred for 16 h before quenching with a mixture of ice (20 g) and Et_2O (20 mL). The layers were separated and the aqueous phase was extracted with Et_2O (3 × 25 mL). The combined organic phases were washed with brine (50 mL), dried ($MgSO_4$) and the solvent removed under reduced pressure to afford a pale-yellow liquid. Purification by distillation under reduced pressure (68 °C, 25 mmHg) afforded the silyl ketene acetal **217** as a colourless liquid (8.28 g, 44.0 mmol, 88%).

^{1}H NMR (500 MHz, $CDCl_3$) δ_H 3.76 (2H, q, J = 7.1 Hz, C$\underline{H_2}$O), 1.57 (3H, s, $\underline{Me}_aMe_bC$), 1.52 (3H, s, $Me_a\underline{Me}_bC$), 1.20 (3H, t, J = 7.1 Hz, $\underline{Me}CH_2O$), 0.19 ppm (9H, s, $Si\underline{Me}_3$); **^{13}C NMR** (125 MHz, $CDCl_3$) δ_C 147.0, 91.8, 64.3, 16.9, 16.3, 14.8, 0.0.

Data in agreement with that presented by Inamoto[120]

(+)-Diisopinocampheyl (DIP) boron chloride[185]

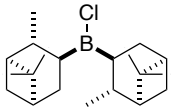

$ClBH_2{\cdot}SMe_2$ (0.50 mL, 4.80 mmol) was added dropwise to a stirred solution of freshly distilled (–)-α-pinene (1.60 g, 8.36 mmol) in Et_2O (2.2 mL) at –10 °C. The reaction was slowly warmed to 10 °C and stirred for 16 h to afford a colourless ethereal solution of (+)-DIPCl (*ca.* 1.0 M).

(–)-DIPCl was analogously prepared using the opposite enantiomer of α-pinene.

1,4-Dimethyl-1,2,4-triazolium iodide - 290

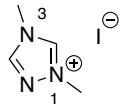

MeI (2.70 mL, 43.5 mmol) was added to a stirred suspension of 1,2,4-triazole (1.00 g, 14.5 mmol), K_2CO_3 (3.00 g, 21.7 mmol) in acetonitrile (8 mL) and methanol (2 mL). The mixture was stirred at 40 °C for 72 h before being filtered, washing the white solid with CH_2Cl_2 (3 × 5 mL). The solvent was removed under reduced pressure to afford the product as a white solid (3.21 g, 14.3 mmol, 99%).

^{1}H NMR (500 MHz, DMSO-d_6) δ_H 10.0 (1H, s, H2), 9.11 (1H, s, H4), 4.05 (3H, s, Me1), 3.89 (3H, s, Me3); **^{13}C NMR** (125 MHz, DMSO-d_6) δ_C 145.2, 143.3, 38.7, 34.1.

Data in agreement with that presented by Pan[186]

Anhydrous cerium trichloride[187]

$CeCl_3{\cdot}7H_2O$ was stirred *in vacuo* (0.05 Torr), gradually heating to 70 °C over 3 h. The mixture was stirred at 80 °C for 16 h, after which the mixture was gradually heated to 140 °C over 8 h. The mixture was then stirred at 140 °C for 16 h to afford anhydrous cerium trichloride as a fine white powder.

$TMSCH_2MgCl$[147]

Mg turnings (1.17 g, 48.0 mmol) and 1,2-dibromoethane (0.17 mL, 2.00 mmol) were added to a solution of $TMSCH_2Cl$ (1.12 mL, 8.00 mmol) in THF (7 mL) at r.t.. The solution was heated to initiate a gentle reflux, to which a solution of $TMSCH_2Cl$ (4.46 mL, 32.0 mmol) in THF (28 mL) was added dropwise over 30 min to maintain a steady reflux. After the addition was completed, the solution was stirred at 45 °C for 1 h to afford a black solution of the Grignard reagent. This was titrated against menthol/1,10-phenanthroline to determine a final concentration of 1.40 M.

(−)-Methoxydiisopinocampheylborane (Ipc_2BOMe)[188]

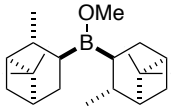

$BH_3{\cdot}SMe_2$ (5.25 mL, 52.5 mmol) was added to a stirred solution of (+)-α-pinene (20.0 mL, 126 mmol) in THF (16 mL) at r.t.. The stirring was stopped, and the solution was allowed to stand at r.t. for 16 h, during which a crystalline precipitate formed. The mixture was cooled to 0 °C for 1 h and the supernatant was removed *via* cannulation. The white solid was washed with anhydrous pentane (3 × 20 mL, dried over CaH_2) and dried *in vacuo* to afford Ipc_2BH as a white crystalline solid. Et_2O (50 mL) was added to the borane and the suspension was cooled to 0 °C. MeOH (2.55 mL, 63.0 mmol) was added dropwise to the stirred solution over 30 min *via* a syringe pump, during which a clear homogenous solution formed. The solvent and excess MeOH was distilled off at 40 °C and dried *in vacuo* to afford the product as a viscous clear oil that solidified into a crystalline solid upon standing (14.5 g, 45.8 mmol, 87% over two steps). The enantiomeric reagent was prepared analogously using (−)-α-pinene (20.0 mL, 126 mmol) to afford (+)-Ipc_2BOMe as a viscous oil (10.8 g, 34.2 mmol, 65% over two steps).

DMAP Hydrochloride (DMAP·HCl)

HCl (4.1 mL, 8.20 mmol, 2 M in Et_2O) was added dropwise to a stirred solution of DMAP (1.00 g, 8.20 mmol) in THF (15 mL) at 0 °C. The resulting white suspension was stirred for 10 min before filtering. The filtered precipitate was washed with Et_2O (30 mL) and dried *in vacuo* to afford DMAP hydrochloride salt as a white solid (1.03 g, 6.45 mmol, 79%).

8.4. Experimental Procedures for Part II – Hemicalide

8.4.1. Synthesis of the C16-C28 fragment

PMB ether 104

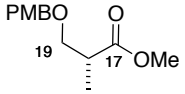

To a stirred solution of PMBTCA (17.9 g, 63.4 mmol) in CH_2Cl_2 (80 mL) was added (*R*)-methyl 3-hydroxy-2-methylpropionate (5.00 g, 42.3 mmol) and PPTS (1.06 g, 4.23 mmol). The solution was stirred for 16 h at r.t., during which the solution turned cloudy white. The reaction mixture was quenched with $NaHCO_3$ (70 mL), the layers separated and the aqueous phase extracted with CH_2Cl_2 (3 × 20 mL). The combined organic phases were washed with brine (100 mL), dried ($MgSO_4$) and the solvent removed under reduced pressure to afford a crude oil, which was triturated with PE 40-60 to facilitate the formation of a white precipitate. The precipitate was removed by filtration, the filtrate collected and the solvent removed *in vacuo*. Purification by flash column chromatography (EtOAc/PE 40-60: 8% → 20%) afforded the product **104** as a pale yellow liquid (10.0 g, 42.3 mmol, 99%).

R_f (EtOAc/PE 40-60: 20%) = 0.52; **^{1}H NMR** (500 MHz, $CDCl_3$) δ_H 7.23 (2H, d, *J* = 8.6 Hz, ArH), 6.87 (2H, d, *J* = 8.7 Hz, ArH), 4.45 (2H, s, Ar$\underline{CH_2}$O), 3.80 (3H, s, ArO$\underline{Me}$), 3.69 (3H, s, $CO_2\underline{Me}$), 3.62 (1H, dd, *J* = 9.1, 7.3 Hz, H19a), 3.45 (1H, dd, *J* = 9.2, 5.9, H19b), 2.77 (1H, sext, *J* = 7.1 Hz, H18), 1.16 (3H, d, *J* = 7.1 Hz, Me18).

Data in agreement with that presented by Paterson[189]

Alcohol 105

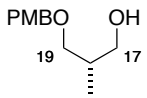

$LiAlH_4$ (2.00 g, 52.5 mmol) was added portion-wise to a stirred solution of PMB ether **104** (10.7 g, 47.7 mmol) in THF (120 mL) at 0 °C. The reaction was stirred at 0 °C for 3 h before quenching with water (25 mL) and aqueous NaOH (6 mL, 1 M in H_2O). The layers were separated and the aqueous phase was extracted with Et_2O (3 × 15 mL). The combined organic phases were washed with brine (120 mL), dried ($MgSO_4$) and the solvent removed under reduced pressure. Purification by flash column chromatography (EtOAc/PE 40-60: 15% → 25%) afforded the alcohol **105** as an orange liquid (9.75 g, 44.4 mmol, 93%).

R_f (EtOAc/PE 40-60: 30%) = 0.21; **^{1}H NMR** (400 MHz, $CDCl_3$) δ_H 7.24 (2H, d, *J* = 9.0 Hz, ArH), 6.88 (2H, d, *J* = 8.9 Hz, ArH), 4.45 (2H, s, Ar$\underline{CH_2}$), 3.81 (3H, s, ArO$\underline{Me}$), 3.64-3.55 (2H, m, H17a, OH), 3.53 (1H, dd, *J* = 9.0, 4.3 Hz, H19a), 3.39 (1H, dd, *J* = 9.0, 8.0 Hz, H19b), 2.56 (1H, dd, *J* = 7.1, 4.8 Hz, H17b), 2.11-2.02 (1H, m, H18), 0.87 (3H, d, *J* = 7.0 Hz, Me18).

Data in agreement with the enantiomeric compound presented by Janssen[190]

Vinyl dibromide *ent*-55

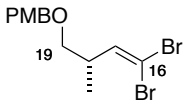

DMSO (10.1 mL, 142 mmol) was added dropwise to a stirred solution of $(COCl)_2$ (6.12 mL, 71.3 mmol) in CH_2Cl_2 (80 mL) at –78 °C. The solution was stirred for 15 min before the addition of a solution of alcohol **105** (5.00 g, 23.8 mmol) in CH_2Cl_2 (15 mL + 5 mL wash) *via* cannula. The reaction was stirred at –78 °C for 45 min, after which Et_3N (40.0 mL, 285 mmol) was added dropwise and the resulting pale-yellow solution was allowed to warm to r.t. over 30 min. The reaction was quenched by the addition of NH_4Cl solution (60 mL), the layers separated and the aqueous phase extracted with CH_2Cl_2 (3 × 20 mL). The combined organic phases were washed with brine (2 × 20 mL), dried ($MgSO_4$) and concentrated to *ca*. 20 mL under reduced pressure to yield a solution of the crude aldehyde **106** that was directly used in the subsequent step without further purification.

PPh_3 (24.9 g, 95.1 mmol) was added portion-wise to a stirred solution of CBr_4 (15.8 g, 47.5 mmol) in CH_2Cl_2 (100 mL). The resulting orange brown solution was stirred for 5 min before cooling to –78 °C. A solution of the crude aldehyde **106** (2.97 g, 14.3 mmol) in CH_2Cl_2 (20 mL + 5 mL wash) was added *via* cannula. The mixture was stirred for 1 h, during which it was allowed to warm to 0 °C before being quenched with a solution of NH_4Cl (100 mL). The layers were separated and the aqueous phase extracted with CH_2Cl_2 (3 × 30 mL). The combined organic phases were washed with brine (100 mL), dried ($MgSO_4$) and the solvent removed under reduced pressure. Purification by flash column chromatography (EtOAc/PE 40-60: 5% → 25%) afforded the product ***ent*-55** as an orange liquid (6.93 g, 19.0 mmol, 80% over 2 steps)

R_f (EtOAc/PE 40-60: 50%) = 0.73; **^{1}H NMR** (400 MHz, $CDCl_3$) δ_H 7.25 (2H, d, *J* = 8.8 Hz, ArH), 6.89 (2H, d, *J* = 8.8 Hz, ArH), 6.30 (1H, d, *J* = 9.2 Hz, H17), 4.46 (1H, d, *J* = 11.8 Hz, Ar$\underline{CH_a}H_bO$), 4.43 (1H, d, *J* = 11.8 Hz, $ArCH_a\underline{H_b}O$), 3.81 (3H, s, ArO$\underline{Me}$), 3.36 (1H, dd, *J* = 9.3, 6.3 Hz, H19a), 3.33 (1H, dd, *J* = 9.3, 6.0 Hz, H19b), 2.82-2.72 (1H, m, H18), 1.05 (3H, d, *J* = 6.5 Hz, Me18; $[\alpha]_D^{20}$ +16.7° (*c* 1.0, $CHCl_3$).

Data in agreement with the enantiomeric compound presented by Paterson[189]

Alkyne 107

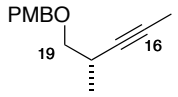

*n*BuLi (23 mL, 19.23 mmol, 1.6 M in hexanes) was added dropwise to a stirred solution of vinyl dibromide **55** (3.50 g, 9.61 mmol) in THF (50 mL) at –78 °C. The solution was stirred at –78 °C for 1 h before the dropwise addition of MeI (2.70 mL, 28.8 mmol). The reaction was stirred at –78 °C for a further 10 min before warming to 0 °C. The reaction was stirred for a further stirred for 1 h before quenching with a solution of NH_4Cl. The layers were separated and the aqueous phase was extracted with Et_2O (3 × 40 mL). The combined organic phases were washed with brine (100 mL), dried ($MgSO_4$) and the solvent removed under reduced pressure. Purification by flash column chromatography (EtOAc/PE 40-60: 10%) afforded the product **107** as a pale-yellow liquid (2.05 g, 9.39 mmol, 98%).

R_f (EtOAc/PE 40-60: 20%) = 0.66; **^{1}H NMR** (400 MHz, $CDCl_3$) δ_H 7.27 (2H, d, *J* = 8.2 Hz, ArH), 6.88 (2H, d, *J* = 8.7 Hz, ArH), 4.51 (1H, d, *J* = 11.7 Hz, Ar$\underline{CH_a}H_bO$), 4.47 (1H, d, *J* = 11.8 Hz, Ar$CH_a\underline{H_b}O$), 3.81 (3H, s, ArO$\underline{Me}$), 3.45 (1H, dd, *J* = 9.0, 6.1 Hz, H19a), 3.29 (1H, dd, *J* = 9.0, 7.5 Hz, H19b), 2.71-2.62 (1H, m, H18), 1.79 (3H, d, *J* = 2.4 Hz, Me16), 1.16 (3H, d, *J* = 6.9 Hz, Me18).

Data in agreement with the enantiomeric compound presented by Smith[191]

Vinyl iodide 108

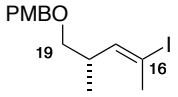

The following reaction was carried out in darkness due to the light sensitivity of $Cp_2Zr(H)Cl$.

DIBAL (9.16 mL, 9.16 mmol, 1 M in hexanes) was added dropwise to a stirred suspension of Cp_2ZrCl_2 (2.68 g, 9.16 mmol) in THF (13 mL) at 0 °C. The mixture was stirred at 0 °C for 30 min. A solution of alkyne **107** (1.00 g, 4.58 mmol) in THF (10 mL + 2 mL wash) was then added *via* cannula to the reaction mixture, after which the stirred mixture was allowed to warm to r.t. over 16 h. The reaction was cooled to –78 °C and a solution of I_2 (3.49 g, 13.7 mmol) in THF (10 mL + 5 mL wash) was added *via* cannula. The reaction was stirred for 10 min at –78 °C before being quenched with a solution of aqueous HCl (20 mL, 1 M in H_2O) and diluted with Et_2O (30 mL). The layers were separated and the aqueous phase was extracted with Et_2O (3 × 20 mL). The combined organic phases were successively washed with $Na_2S_2O_3$ (70 mL) and brine (100 mL), dried ($MgSO_4$) and the solvent removed under reduced pressure. Purification by flash column

chromatography (EtOAc/PE 40-60: 5%) afforded the product **108** as a colourless liquid (865 mg, 2.50 mmol, 54%).

R_f (EtOAc/PE 40-60: 20%) = 0.66; **^{1}H NMR** (400 MHz, $CDCl_3$) δ_H 7.24 (2H, d, *J* = 8.7 Hz, ArH), 6.88 (2H, d, *J* = 8.7 Hz, ArH), 5.99 (1H, dq, *J* = 9.5, 1.5 Hz, H17), 4.43 (2H, s, Ar$\underline{CH_2}$O), 3.81 (3H, s, ArO$\underline{Me}$), 3.28 (1H, dd, *J* = 9.1, 6.7 Hz, H19a), 3.25 (1H, dd, *J* = 9.2, 6.7 Hz, H19b), 2.77-2.66 (1H, m, H18), 2.39 (3H, d, *J* = 1.5 Hz, Me16), 0.98 (3H, d, *J* = 6.8 Hz, Me18).

Data in agreement with the enantiomeric compound presented by Paterson[43]

Alcohol 110

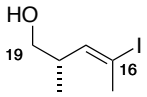

DDQ (393 mg, 1.73 mmol) was added to a stirred solution of the PMB-protected vinyl iodide **108** (400 mg, 1.16 mmol) in CH_2Cl_2 (40 mL). The reaction mixture was allowed to stir at r.t. for 1 h before quenching with a solution of $NaHCO_3$ (30 mL). The layers were separated and the aqueous phase extracted with CH_2Cl_2 (3 × 20 mL). The combined organic phases were washed with brine (40 mL), dried ($MgSO_4$) and the solvent removed under reduced pressure. Purification by flash column chromatography (Et_2O/PE 30-40: 0% → 25%) afforded the product **110** as a colourless liquid (244 mg, 1.08 mmol, 93%).

R_f (EtOAc/PE 40-60: 20%) = 0.66; **^{1}H NMR** (400 MHz, $CDCl_3$): δ_H 5.98 (1H, dq, *J* = 9.8, 1.5 Hz, H17), 3.51-3.39 (2H, m, H19), 2.72-2.60 (1H, m, H18), 2.43 (3H, d, *J* = 1.5 Hz, Me16), 1.41 (1H, dd, *J* = 7.7, 5.1 Hz, OH), 0.97 (3H, d, *J* = 6.8 Hz, Me18).

Data in agreement with the enantiomeric compound presented by MacGregor[43]

Methyl ketone *ent*-48

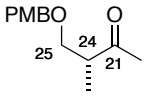

MeMgBr (7.06 mL, 21.2 mmol, 3 M in Et_2O) was added dropwise to a stirred solution of Weinreb amide **111** (2.83 g, 10.6 mmol) in Et_2O (20 mL) at 0 °C. The reaction mixture was stirred at 0 °C for 2 h before quenching with NH_4Cl solution (15 mL). The layers were separated and the aqueous phase extracted with Et_2O (3 × 20 mL). The combined organic phases were washed with brine (20 mL), dried ($MgSO_4$) and the solvent removed under reduced pressure. Purification by flash column chromatography (EtOAc/PE 40-60: 30%) afforded the product ***ent*-48** as a pale-yellow liquid (1.87 g, 9.01 mmol, 85%).

R_f (EtOAc/PE 40-60: 20%) = 0.64; **^{1}H NMR** (400 MHz, $CDCl_3$) δ_H 7.23 (2H, d, *J* = 8.7 Hz, ArH), 6.87 (2H, d, *J* = 8.7 Hz, ArH), 4.45 (1H, d, *J* = 11.6Hz, ArCH$_a$H$_b$O), 4.41 (1H, d, *J* = 11.7 Hz, ArCH$_a$H$_b$O), 3.80 (3H, s, ArOMe), 3.59 (1H, dd, *J* = 9.2, 7.5 Hz, H25a), 3.45 (1H, dd, *J* = 9.2, 5.5 Hz, H25b), 2.83 (1H, sext, *J* = 7.2, H24), 2.17 (3H, s, H20), 1.08 (3H, d, *J* = 7.1 Hz, Me24).

Data in agreement with that presented by Paterson[189]

Aldol adduct *ent*-50

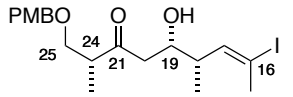

Dess-Martin Periodinane (1.01 g, 2.37 mmol) was added to a stirred suspension of alcohol **110** (134 mg, 0.593 mmol) and $NaHCO_3$ (597 mg, 7.11 mmol) in wet CH_2Cl_2 (10.0 mL). The reaction mixture was stirred at r.t. until TLC monitoring indicated full consumption of the starting material (*ca.* 1 h). The reaction mixture was quenched by the addition of $NaHCO_3$ (5 mL) and $Na_2S_2O_3$ (5 mL) and the mixture stirred at r.t. for 30 min. The layers were separated and the aqueous phase was extracted with CH_2Cl_2 (3 × 5 mL). The combined organic phases were dried (Na_2SO_4) and the solution concentrated under reduced pressure to *ca.* 8 mL. The solution of the crude aldehyde ***ent*-49** was filtered over a plug of SiO_2, dried over 4 Å MS and directly used in the subsequent step without further purification.

A solution of ketone ***ent*-48** (148 mg, 0.711 mmol, dried over CaH_2) in Et_2O (3 mL + 2 mL wash) was added *via* cannula to a stirred solution of Et_3N (133 μL, 0.948 mmol), (+)-DIPCl (652 μL, 0.652 mmol, *ca.* 1 M in Et_2O) in Et_2O (4 mL) at –10 °C to immediately form a white suspension. The mixture was stirred at –10 °C for 1 h before cooling to –78 °C. A solution of the crude aldehyde ***ent*-49** in CH_2Cl_2 (8 mL + 4 mL wash) was added *via* cannula to the reaction mixture, during which the mixture turned pale yellow. The reaction mixture was stirred at –78 °C for 5 h before warming slowly to –20 °C for 16 h. The reaction mixture was quenched at –20 °C by the addition of MeOH (3 mL), pH 7 buffer solution (3 mL) and H_2O_2 (5 mL) and warmed to r.t.. The layers were separated, and the aqueous phase extracted with Et_2O (3 × 10 mL). The combined organic extracts were washed with brine (15 mL), dried ($MgSO_4$) and the solvent removed under reduced pressure. Purification by flash chromatography (EtOAc/PE 40-60: 5% → 25%) afforded the product ***ent*-50** as a pale yellow oil (143 mg, 0.255 mmol, 53% over two steps).

R_f (EtOAc/PE 40-60: 30%) = 0.39; **^{1}H NMR** (500 MHz, $CDCl_3$) δ_H 7.21 (2H, d, *J* = 8.5 Hz, ArH), 6.88 (2H, d, *J* = 8.6 Hz, ArH), 5.96 (1H, dq, *J* = 10.2, 1.3 Hz, H17), 4.42 (2H, s, ArCH$_2$O), 3.81 (3H, s, ArOMe), 3.80 (1H, br s, H19), 3.56 (1H, t, *J* = 8.8 Hz, H25a), 3.45 (1H, dd, *J* = 9.1, 5.0 Hz, H25b), 3.16 (1H, br s, OH), 2.91-2.85 (1H, m, H24), 2.72 (1H, dd, *J* = 17.3, 2.3 Hz, H20a), 2.49 (1H, dd, *J* = 17.5, 9.4 Hz, H20b), 2.48-

2.42 (1H, m, H18), 2.38 (3H, d, *J* = 1.4 Hz, Me16), 1.05 (3H, d, *J* = 7.0 Hz, Me24), 1.01 (3H, d, *J* = 6.8 Hz, Me18); $[\alpha]_D^{20}$ −38.9° (*c* 0.5, $CHCl_3$).

Data in agreement with the enantiomeric compound presented by MacGregor [43]

(*S*)-Mosher ester 113

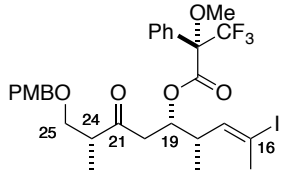

DCC (3.5 μL, 33.6 μmol, 1 M in CH_2Cl_2) was added to a stirred solution of ***ent*-50** (5.9 mg, 13.2 μmol), (*S*)-α-methoxy-α-trifluoromethylphenylacetic acid (MTPA) (7.9 mg, 33.6 μmol) and DMAP (one crystal) in CH_2Cl_2 (300 μL). The mixture was stirred for 2 days at r.t., during which a white precipitate formed. The mixture was filtered through cotton wool and the filtrate reduced to dryness. Purification by flash chromatography (EtOAc/PE 40-60: 15%) afforded the product **113** as a pale-yellow oil (4.0 mg, 6.03 μmol, 45%).

R_f (EtOAc/PE 40-60: 30%) = 0.52; **^{1}H NMR** (400 MHz, $CDCl_3$): δ_H 7.49 (2H, d, *J* = 6.6 Hz, MTPA-Ar<u>H</u>), 7.43-7.37 (3H, m, MTPA-Ar<u>H</u>), 7.18 (2H, d, *J* = 8.7 Hz, PMB-Ar<u>H</u>), 6.86 (2H, d, *J* = 8.7 Hz, PMB-Ar<u>H</u>), 5.97 (1H, dq, *J* = 8.1, 1.5 Hz, H17), 5.42 (1H, dt, *J* = 6.8, 5.3 Hz, H19), 4.41 (1H, d, *J* = 5.0 Hz, ArC<u>H</u>$_a$CH$_b$O), 4.37 (1H, d, *J* = 5.0 Hz, ArCH$_a$C<u>H</u>$_b$O), 3.79 (3H, s, ArO<u>Me</u>), 3.49 (1H, dd, *J* = 9.0, 8.3 Hz, H25a), 3.47 (3H, s, MTPA-O<u>Me</u>), 3.41 (1H, dd, *J* = 9.0, 4.1 Hz, H25b), 2.91–2.85 (1H, m, H18), 2.84 (1H, dd, *J* = 18.1, 7.0 Hz, H20a), 2.74 (1H, dd, *J* = 18.1, 5.5 Hz, H20b), 2.79-2.72 (1H, m, H24), 2.39 (3H, d, *J* = 1.5 Hz, Me16), 0.93 (3H, d, *J* = 7.0 Hz, Me18), 0.91 (3H, d, *J* = 7.0 Hz, Me24).

(*R*)-Mosher ester 114

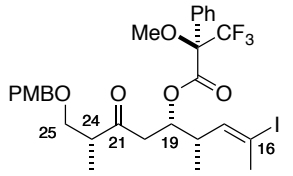

DCC (3.5 μL, 33.6 μmol, 1 M in CH_2Cl_2) was added to a stirred solution of ***ent*-50** (6.0 mg, 13.4 μmol), (*R*)-α-methoxy-α-trifluoromethylphenylacetic acid (MTPA) (7.9 mg, 33.6 μmol) and DMAP (one crystal) in CH_2Cl_2 (300 μL). The mixture was stirred for 2 days at r.t., during which a white precipitate formed. The mixture was filtered through cotton wool and the filtrate reduced to dryness. Purification by flash

chromatography (EtOAc/PE 40-60: 15%) afforded the product **114** as a pale yellow oil (9.0 mg, 13.4 μmol, 99%).

R_f (EtOAc/PE 40-60: 30%) = 0.52; **^{1}H NMR** (500 MHz, $CDCl_3$): δ_H 7.51-7.48 (2H, m, MTPA-ArH), 7.41-7.38 (3H, m, MTPA-ArH), 7.20 (2H, d, *J* = 8.7 Hz, PMB-ArH), 6.86 (2H, d, *J* = 8.7 Hz, PMB-ArH), 5.86 (1H, dq, *J* = 10.0, 1.5 Hz, H17), 5.42 (1H, dt, *J* = 5.7, 0.6 Hz, H19), 4.41 (1H, d, *J* = 11.5 Hz, ArCH$_a$CH$_b$O), 4.37 (1H, d, *J* = 11.5 Hz, ArCH$_a$CH$_b$O), 3.80 (3H, s, ArOMe), 3.52 (1H, d, *J* = 9.0, 8.4 Hz, H25a), 3.49 (3H, s, MTPA-OMe), 3.44 (1H, dd, *J* = 9.0, 5.1 Hz, H25b), 2.84-2.79 (4H, m, H18, 20, 24), 2.32 (3H, d, *J* = 1.6 Hz, Me16), 0.99 (3H, d, *J* = 7.0 Hz, Me18), 0.87 (3H, d, *J* = 6.9 Hz, Me24).

TBS ether 115

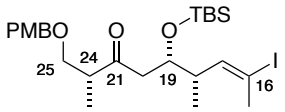

2,6-Lutidine (1.97 mL, 17.0 mmol) was added to a stirred solution of alcohol ***ent*-50** (3.80 g, 8.51 mmol) in CH_2Cl_2 (50 mL). The reaction mixture was cooled to –78 °C and stirred for 5 min, before the dropwise addition of TBSOTf (2.93 mL, 12.8 mmol). The mixture was stirred at –78 °C for 45 min. The reaction mixture was quenched with MeOH (1 mL), followed by $NaHCO_3$ (30 mL). Upon warming to r.t., the layers were separated and the aqueous phase extracted with CH_2Cl_2 (3 × 20 mL). The combined organic phases were washed with brine, dried ($MgSO_4$) and the solvent removed under reduced pressure to afford the product **115** as a colourless oil (4.76 g, 8.51 mmol, 99%), which is used in the next step without further purification. A small sample was purified by flash column chromatography (EtOAc/PE 40-60: 10%) for analytical purposes.

R_f (EtOAc/PE 40-60: 30%) = 0.74; **^{1}H NMR** (500 MHz, $CDCl_3$): δ_H 7.21 (2H, d, *J* = 8.6 Hz, ArH), 6.86 (2H, d, *J* = 8.5 Hz, ArH), 5.96 (1H, dq, *J* = 9.8, 1.4 Hz, H17), 4.43 (1H, d, *J* = 11.6 Hz, ArCH$_a$H$_b$), 4.39 (1H, d, *J* = 11.6 Hz, ArCH$_a$H$_b$), 4.13 (1H, dt, *J* = 5.8, 4.3 Hz, H19), 3.80 (3H, s, ArOMe), 3.57 (1H, dd, *J* = 9.3, 7.9 Hz, H25a), 3.44 (1H, dd, *J* = 9.1, 5.3 Hz, H25b), 2.79 (1H, dqn, *J* = 7.6, 5.4 Hz, H24), 2.67 (1H, dd, *J* = 17.7, 6.2 Hz, H20a), 2.60 (1H, dd, *J* = 17.7, 5.7 Hz, H20b), 2.53-2.46 (1H, m, H18), 2.39 (3H, d, *J* = 1.4 Hz, Me16), 1.05 (3H, d, *J* = 6.9 Hz, Me24), 0.89 (3H, d, *J* = 6.9 Hz, Me18), 0.86 (9H, s, Si*t*BuMe$_2$), 0.07 (3H, s, Si*t*BuMe$_a$Me$_b$), -0.02 (3H, s, Si*t*BuMe$_a$Me$_b$).

Data in agreement with the enantiomeric compound presented by MacGregor[43]

Ester 116

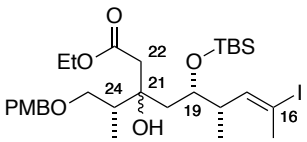

*n*BuLi (42.8 mL, 68.5 mmol, 1.6 M in hexanes) was added dropwise to a stirred solution of *i*Pr_2NH (12.0 mL, 85.6 mmol) in THF (18 mL) at 0 °C. The pale-yellow solution was stirred for 30 min at 0 °C before cooling to –78 °C. EtOAc (6.96 mL, 71.3 mmol) was added dropwise to the solution, and the mixture was stirred at –78 °C for 1 h to give a *ca.* 1.0 M solution of the lithium enolate.

The lithium enolate solution (36.0 mL, 36.0 mmol, 1.0 M in THF) was added dropwise to a stirred solution of TBS ether **115** (4.00 g, 7.12 mmol) in THF (36 mL) at –78 °C. The resulting solution was stirred at –78 °C for 3 h before being quenched with a solution of $NaHCO_3$ (50 mL) and warmed to r.t.. The mixture was diluted with Et_2O (50 mL), and the phases separated. The aqueous phase was extracted with Et_2O (3 × 25 mL). The combined organic phases were washed with brine, dried ($MgSO_4$) and the solvent removed under reduced pressure to afford the product **116** as a colourless oil (4.55 g, 7.01 mmol, 98%) as an inconsequential mixture of diastereomers (3.5:1 *dr*). A small sample was purified by flash column chromatography (EtOAc/PE 40-60: 4%) for analytical purposes.

Major isomer: $\mathbf{R_f}$ (EtOAc/PE 40-60: 5%) = 0.29; **^{1}H NMR** (500 MHz, $CDCl_3$) δ_H 7.24 (2H, d, *J* = 8.7 Hz, ArH), 6.88 (2H, d, *J* = 8.7 Hz, ArH), 6.18 (1H, dq, *J* = 9.5, 1.4 Hz, H17), 4.45 (1H, d, *J* = 11.5 Hz, ArC$H_a$$H_b$O), 4.39 (1H, d, *J* = 11.5 Hz, ArC$H_a$$H_b$O), 4.16-4.09 (2H, m, CH_3CH_2O), 3.99-3.95 (2H, m, H19, OH), 3.81 (3H, s, OMe), 3.60 (1H, dd, *J* = 9.2, 4.9 Hz, H25a), 3.39 (1H, dd, *J* = 9.2, 6.3 Hz, H25b), 2.70 (1H, dqd, *J* = 9.6, 6.8, 3.2 Hz, H18), 2.58 (1H, d, *J* = 14.5 Hz, H22a), 2.53 (1H, d, *J* = 15.3 Hz, H22b), 2.38 (3H, d, *J* = 1.3 Hz, Me16), 2.09-2.04 (1H, m, H24), 1.79 (1H, dd, *J* = 14.7, 5.8 Hz, H20a), 1.68 (1H, dd, *J* = 14.7, 5.8 Hz, H20b), 1.24 (3H, t, *J* = 7.2 Hz, CH_3CH_2O), 1.00 (3H, d, *J* = 6.9 Hz, Me24), 0.93 (3H, d, *J* = 6.8 Hz, Me18), 0.88 (9H, s, Si*t*BuMe$_2$), 0.08 (3H, s, Si*t*BuMe$_a$Me$_b$), 0.07 (3H, s, Si*t*BuMe$_a$Me$_b$).

Data in agreement with the enantiomeric compound presented by MacGregor[43]

Lactone 117

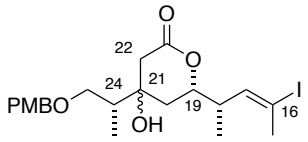

$TsOH{\cdot}H_2O$ (668 mg, 3.52 mmol) was added to a stirred solution of TBS ether **116** (5.70 g, 8.79 mmol) in MeOH (100 mL) at r.t.. The reaction mixture was stirred at r.t. for 16 h before being quenched with $NaHCO_3$ (100 mL). The mixture was extracted with EtOAc (4 × 30 mL), and the combined organic phases were washed with brine, dried ($MgSO_4$) and the solvent removed under reduced pressure. Purification by flash column chromatography (EtOAc/PE 40-60: 15% → 30%) afforded the product **117** as a colourless oil (3.56 g, 7.93 mmol, 90%) as an inconsequential mixture of diastereomers (3.5:1 *dr*).

Major isomer: $\mathbf{R_f}$ (EtOAc/PE 40-60: 40%) = 0.35; **^{1}H NMR** (500 MHz, $CDCl_3$) δ_H 7.22 (2H, d, *J* = 8.7 Hz, Ar<u>H</u>), 6.90 (2H, d, *J* = 8.7 Hz, Ar<u>H</u>), 5.98 (1H, dq, *J* = 10.2, 1.5 Hz, H17), 4.48 (1H, d, *J* = 11.5 Hz, ArC<u>H$_a$</u>H$_b$O), 4.41 (1H, d, *J* = 11.5 Hz, ArCH$_a$<u>H$_b$</u>O), 3.88 (1H, ddd, *J* = 11.4, 7.8, 4.4 Hz, H19), 3.81 (3H, s, O<u>Me</u>), 3.70 (1H, dd, *J* = 9.7, 3.5 Hz, H25a), 3.45 (1H, dd, *J* = 9.7, 5.0 Hz, H25b), 2.69 (1H, dqd, *J* = 9.7, 6.9, 3.6 Hz, H18), 2.58 (2H, s, H22), 2.40 (3H, d, *J* = 1.5 Hz, Me16), 2.00 (1H, dd, *J* = 14.5, 4.6 Hz, H20a), 1.85-1.77 (1H, m, H24), 1.65 (1H, dd, *J* = 14.5, 11.1 Hz, H20b), 1.09 (3H, d, *J* = 6.6 Hz, Me18), 1.04 (3H, d, *J* = 6.9 Hz, Me24).

Data in agreement with the enantiomeric compound presented by MacGregor[43]

Enoate *ent*-51

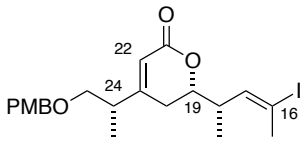

To a stirred solution of lactone **117** (3.56 g, 7.29 mmol) in Ac_2O (7.4 mL), pyridine (36 mL) and benzene (36 mL) was added DMAP (889 mg, 7.28 mmol) at r.t.. The reaction mixture was refluxed for 16 h before carefully quenching with $NaHCO_3$ (25 mL) and diluting with CH_2Cl_2 (25 mL). The layers were separated, and the aqueous phase was extracted with CH_2Cl_2 (3 × 25 mL). The combined organic phases were washed with citric acid (10% w/v in H_2O), brine, dried ($MgSO_4$) and the solvent removed under reduced pressure. Purification by flash column chromatography (EtOAc/PE 40-60: 20%) afforded the product ***ent*-51** as a pale-yellow oil (3.07 g, 6.53 mmol, 89%).

$\mathbf{R_f}$ (EtOAc/PE 40-60: 30%) = 0.79; **^{1}H NMR** (500 MHz, $CDCl_3$) δ_H 7.22 (2H, d, *J* = 8.7 Hz, Ar<u>H</u>), 6.89 (2H, d, *J* = 8.7 Hz, Ar<u>H</u>), 5.98 (1H, dq, *J* = 10.1, 1.7 Hz, H17), 5.58 (1H, s, H22), 4.44 (1H, d, *J* = 11.6 Hz,

ArC$\underline{H}_a$H$_b$O), 4.39 (1H, d, *J* = 11.6 Hz, ArCH$_a\underline{H}_b$O), 4.06 (1H, ddd, *J* = 11.2, 7.1, 4.3 Hz, H19), 3.81 (3H, s, O$\underline{Me}$), 3.45 (1H, dd, *J* = 9.2, 5.4 Hz, H25a), 3.41 (1H, dd, *J* = 9.2, 7.5 Hz, H25b), 2.71 (1H, dq, *J* = 10.1, 6.9 Hz, H18), 2.62 (1H, m, H24), 2.40 (3H, d, *J* = 1.7 Hz, Me16), 2.26 (1H, dd, *J* = 17.7, 4.5 Hz, H20a), 1.68 (1H, ddd, *J* = 17.6, 11.5, 1.4 Hz, H20b), 1.10 (3H, d, *J* = 7.0 Hz, Me24), 1.09 (3H, d, *J* = 7.0 Hz, Me18).

Data in agreement with the enantiomeric compound presented by MacGregor[43]

Dihydroxylactone *ent*-52

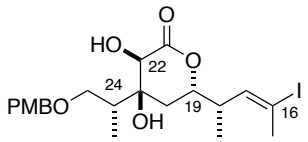

Citric acid (893 mg, 4.25 mmol), $K_2OsO_4{\cdot}2H_2O$ (16 mg, 42.5 μmol) and NMO (249 μL, 1.06 mmol, 50% w/w in H_2O) were successively added to a stirred mixture of enoate ***ent*-51** (1.00 g, 2.12 mmol) in THF (1.2 mL), *t*BuOH (1.2 mL) and H_2O (1.2 mL). The yellow-green solution was stirred for 5 h at r.t. before quenching with Na_2SO_3 (3 mL) and $NaHCO_3$ (3 mL). The mixture was extracted with EtOAc (3 × 5 mL) and the combined organic phases were washed with brine, dried (Na_2SO_4) and the solvent removed under reduced pressure. Purification by flash column chromatography (EtOAc/PE 40-60: 20%) afforded the product ***ent*-52** as a colourless oil (412 mg, 0.817 mmol, 79% brsm), as well as the recovered starting material (514 mg, 1.09 mmol).

R$_f$ (EtOAc/PE 40-60: 50%) = 0.50; **^{1}H NMR** (500 MHz, $CDCl_3$) δ_H 7.23 (2H, d, *J* = 8.6 Hz, Ar$\underline{H}$), 6.88 (2H, d, *J* = 8.7 Hz, Ar$\underline{H}$), 6.02 (1H, dq, *J* = 10.1, 1.5 Hz, H17), 4.50 (1H, ddd, *J* = 11.5, 6.4, 3.5 Hz, H19), 4.43 (2H, s, ArC$\underline{H}_2$O), 4.19 (1H, d, *J* = 1.7 Hz, H22), 3.92 (1H, d, *J* = 1.4 Hz, OH22), 3.81 (3H, s, O$\underline{Me}$), 3.67 (1H, dd, *J* = 10.0, 8.1 Hz, H25a), 2.72-2.58 (1H, m, H18), 2.38 (3H, d, *J* = 1.3 Hz, Me16), 2.09-2.04 (1H, m, H24), 1.79 (1H, dd, *J* = 14.7, 5.8 Hz, H20a), 1.68 (1H, dd, *J* = 14.7, 5.8 Hz, H20b), 1.06 (3H, d, *J* = 6.7 Hz, Me24), 0.98 (3H, d, *J* = 7.2 Hz, Me18). $[\alpha]_D^{20}$ +11.3 (*c* 0.2, $CHCl_3$).

Data in agreement with the enantiomeric compound presented by MacGregor[43]

***Bis*-TES ether 122**

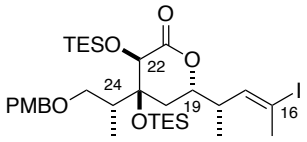

TESOTf (280 μL, 1.55 mmol) was added dropwise to a stirred solution of diol ***ent*-52** (130 mg, 258 μmol) and 2,6-lutidine (270 μL, 2.32 mmol) in CH_2Cl_2 (2.3 mL) at 0 °C. The reaction mixture was stirred at 0 °C for 24 h before quenching with MeOH (500 μL) followed by $NaHCO_3$ (1 mL). The layers were separated and the aqueous phase was extracted with CH_2Cl_2 (3 × 2 mL). The combined organic phases were washed with brine, dried ($MgSO_4$) and the solvent removed under reduced pressure. Purification by flash column chromatography (EtOAc/PE 40-60: 20%) afforded the product **122** as a colourless oil (178 mg, 243 μmol, 94%).

R_f (EtOAc/PE 40-60: 5%) = 0.48; **^{1}H NMR** (500 MHz, $CDCl_3$) δ_H 7.24 (2H, d, *J* = 8.6 Hz, Ar<u>H</u>), 6.92 (2H, d, *J* = 8.6 Hz, Ar<u>H</u>), 6.03 (1H, dq, *J* = 10.0, 1.4 Hz, H17), 4.43 (1H, d, *J* = 11.6 Hz, ArC<u>H$_a$</u>H$_b$O), 4.38-4.34 (2H, m, H19, ArCH$_a$<u>H$_b$</u>O), 4.24 (1H, s, H22), 3.83 (3H, s, O<u>Me</u>), 3.35 (1H, dd, *J* = 9.5, 5.0 Hz, H25a), 3.26 (1H, dd, *J* = 9.5, 5.5 Hz, H25b), 2.67 (1H, dqn, *J* = 9.9, 6.7 Hz, H18), 2.38 (3H, d, *J* = 1.4 Hz, Me16), 2.38-2.32 (1H, m, H24), 1.82 (1H, dd, *J* = 14.1, 3.4 Hz, H20a), 1.68 (1H, dd, *J* = 14.0, 11.6 Hz, H20b), 1.06 (3H, d, *J* = 7.0 Hz, Me24), 1.01 (3H, d, *J* = 6.9 Hz, Me18), 0.97 (9H, t, *J* = 7.9 Hz, OSiCH_2CH_3), 0.92 (9H, t, *J* = 8.0 Hz, OSiCH_2CH_3), 0.76-0.60 (12H, m, OSiCH_2CH_3).

Data in agreement with the enantiomeric compound presented by MacGregor[43]

Alcohol 123

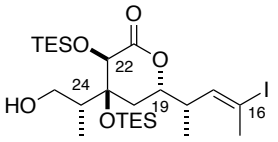

DDQ (28 mg, 123 μmol) was added to a stirred solution of PMB ether **122** (45 mg, 61.4 μmol) in CH_2Cl_2 (900 μL) and pH 7 buffer solution (100 μL). The dark green solution was stirred for 1.5 h at r.t., to which the mixture turned orange-red. The reaction mixture was quenched by addition of $NaHCO_3$ (1.5 mL), the layers separated and the aqueous phase extracted with CH_2Cl_2 (3 × 3 mL). The combined organic phases were washed with brine, dried ($MgSO_4$) and the solvent removed under reduced pressure. Purification by flash column chromatography (EtOAc/PE 40-60: 20%) afforded the product **123** as a colourless oil (35 mg, 57.1 μmol, 92%).

R_f (EtOAc/PE 40-60: 10%) = 0.19; **^{1}H NMR** (500 MHz, $CDCl_3$) δ_H 6.00 (1H, dq, *J* = 9.9, 1.5 Hz, H17), 4.36 (1H, ddd, *J* = 11.0, 6.6, 3.4 Hz, H19), 4.29 (1H, s, H22), 3.62-3.51 (2H, m, H25), 2.71-2.61 (1H, m, H18), 2.41 (3H, d, *J* = 1.5 Hz, Me16), 2.31-2.22 (1H, m, H24), 1.85 (1H, dd, *J* = 14.1, 3.5 Hz, H20a), 1.57 (1H, dd, *J* = 14.7, 11.7 Hz, H20b), 1.06 (3H, d, *J* = 6.8 Hz, Me18), 1.03-0.98 (12H, m, Me24, $OSiCH_2CH_3$), 0.92 (9H, t, *J* = 7.9 Hz, $OSiCH_2CH_3$), 0.83-0.73 (6H, m, $OSiCH_2CH_3$), 0.71-0.58 (6H, m, $OSiCH_2CH_3$).

Data in agreement with the enantiomeric compound presented by MacGregor[43]

Enoate 127

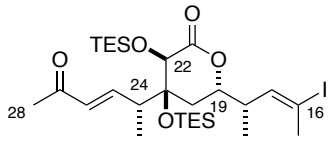

Dess-Martin Periodinane (208 mg, 490 μmol) was added to a stirred suspension of alcohol **123** (60 mg, 97.9 μmol) and $NaHCO_3$ (82 mg, 979 μmol) in wet CH_2Cl_2 (1.0 mL). The reaction mixture was stirred at r.t. until TLC monitoring indicated full consumption of the starting material (*ca*. 1 h). The reaction mixture was quenched by the addition of $NaHCO_3$ (1 mL) and $Na_2S_2O_3$ (1 mL) and the mixture stirred at r.t. for 30 min. The layers were separated and the aqueous phase was extracted with CH_2Cl_2 (3 × 2 mL). The combined organic phases were dried ($MgSO_4$) and the solvent removed under reduced pressure. The crude aldehyde **124** was directly used in the subsequent step without further purification.

Dimethyl (2-oxopropyl)phosphonate (81.3 mg, 490 μmol) was added to a stirred suspension of oven-dried $Ba(OH)_2$ (50.3 mg, 294 μmol) in THF (750 μL) at r.t.. After 30 min, the reaction mixture was cooled to 0 °C, and a solution of the crude aldehyde **124** (60 mg, 97.9 μmol) in THF (400 μL) and H_2O (10 μL) was added *via* cannula (400 μL wash). The reaction mixture was stirred at 0 °C for 30 min, warmed to r.t. over 16 h before being quenched with NH_4Cl (1 mL) and diluted with CH_2Cl_2 (5 mL). The layers were separated and the aqueous phase extracted with CH_2Cl_2 (3 × 2 mL). The combined organic phases were washed with brine, dried ($MgSO_4$) and the solvent removed under reduced pressure. Purification by flash column chromatography (EtOAc/PE 40-60: 5% → 10%) afforded the product **127** as a colourless oil (49 mg, 75 mmol, 77% over two steps).

R_f (EtOAc/PE 40-60: 20%) = 0.52; **^{1}H NMR** (500 MHz, $CDCl_3$) δ_H 6.65 (1H, dd, *J* = 15.8, 8.4 Hz, H25), 6.23 (1H, d, *J* = 15.8 Hz, H26), 5.98 (1H, dq, *J* = 9.9, 1.4 Hz, H17), 4.35 (1H, ddd, *J* = 10.9, 7.5, 4.0 Hz, H19), 3.98 (1H, s, H22), 3.02-2.91 (1H, m, H24), 2.70-2.60 (1H, m, H18), 2.41 (3H, d, *J* = 1.4 Hz, Me16), 2.26 (3H, s, H28), 1.89 (1H, dd, *J* = 13.7, 4.0 Hz, H20a), 1.40 (1H, dd, *J* = 13.7, 11.7 Hz, H20b), 1.10 (3H, d, *J* = 7.0 Hz, Me24), 1.07 (3H, d, *J* = 6.8 Hz, Me18), 1.00 (9H, t, *J* = 7.9 Hz, $OSiCH_2CH_3$), 0.93 (9H, t, *J* = 7.9 Hz, $OSiCH_2CH_3$), 0.83-0.704(6H, m, $OSiCH_2CH_3$), 0.72-0.61 (6H, m, $OSiCH_2CH_3$).

Data in agreement with the enantiomeric compound presented by MacGregor[43]

Ketone *ent*-53

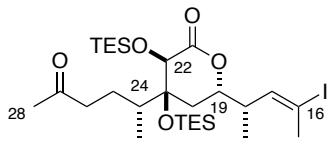

To a stirred solution of enone **127** (100 mg, 0.154 mmol) in toluene (220 μL) was added a solution of the Stryker's reagent (6.15 mL, 0.154 mmol, 0.025 M solution w.r.t Cu) and *t*BuOH (20 μL). The red solution was stirred at r.t. for 2.5 h before diluting with PE 40-60 (5 mL) and vigorously stirred in air for 2 h. The resulting amber solution was filtered over silica to afford a colourless filtrate. The solvent was removed under reduced pressure and the crude was purified by flash column chromatography (EtOAc/PE 40-60: 5% → 10%) to afford the product ***ent*-53** as a colourless oil (71.2 mg, 0.168 mmol, 70%).

R_f (EtOAc/PE 40-60: 5%) = 0.36; **^{1}H NMR** (500 MHz, $CDCl_3$) δ_H 5.98 (1H, dq, *J* = 10.0, 1.4 Hz, H17), 4.34 (1H, ddd, *J* = 10.6, 6.8, 3.5 Hz, H19), 4.22 (1H, s, H22), 2.65-2.55 (2H, m, H18, H26a), 2.41 (3H, d, *J* = 1.4 Hz, Me16), 2.35-2.29 (1H, m, H26b), 2.16 (3H, s, H28), 2.00-1.93 (1H, m, H24), 1.79 (1H, dd, *J* = 13.9, 3.5 Hz, H20a), 1.64-1.56 (1H, m, H25a), 1.43 (1H, dd, *J* = 13.8, 11.8 Hz, H20b), 1.27-1.16 (1H, m, H25b), 1.06 (3H, d, *J* = 6.7 Hz, Me18), 0.98 (9H, t, *J* = 7.9 Hz, $OSiCH_2CH_3$), 0.91 (9H, t, *J* = 7.9 Hz, $OSiCH_2CH_3$), 0.90 (3H, d, *J* = 7.0 Hz, Me24), 0.81-0.70 (6H, m, $OSiCH_2CH_3$), 0.69-0.56 (6H, m, $OSiCH_2CH_3$). $[\alpha]_D^{20}$ −2.7° (*c* 0.2, $CHCl_3$).

Data in agreement with the enantiomeric compound presented by MacGregor[43]

8.4.2. Fragment union and derivatisation of the C1-C28 truncate

13,18-*syn* C1-C28 ketone 101a

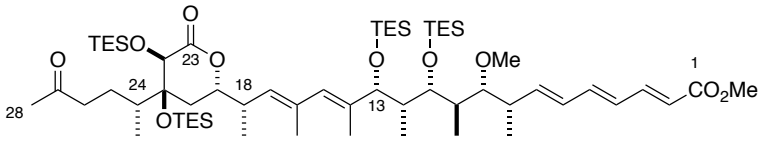

A solution of $Pd(PPh_3)_4$ (18.0 mg, 15.3 μmol) and CuTC (29.2 mg, 153 μmol) was prepared in degassed DMF (0.5 mL) and cooled to 0 °C. A degassed solution of vinyl iodide ***ent*-53** (50 mg, 76.6 μmol) and vinyl stannane **129**[***] (58.0 mg, 76.6 μmol) in DMF (1.0 mL) was added *via* cannula (2 x 0.1 mL wash) and the reaction mixture was stirred at 0 °C in the dark for 5 h. H_2O (10 mL) and Et_2O (10 mL) were added and the layers were separated. The aqueous phase was extracted with Et_2O (3 × 10 mL) and the combined organic extracts were washed with water (2 × 4 mL), dried (Na_2SO_4), concentrated *in vacuo* and purified by flash column chromatography (EtOAc/PE 40-60: 2% → 10%) to give the 13,18-*syn* C1-C28 ketone **101a** as a colourless oil (62.2 mg, 55.5 μmol, 72%).

R_f: (EtOAc/PE 40-60: 25%) = 0.45; **^{1}H NMR** (500 MHz, $CDCl_3$): δ_H 7.30 (1H, dd, *J* = 15.4, 11.4 Hz, H3), 6.52 (1H, dd, *J* = 14.8, 10.7 Hz, H5), 6.21 (1H, dd, *J* = 15.0, 11.2 Hz, H4), 6.13 (1H, dd, *J* = 15.0, 10.3 Hz, H6), 5.98 (1H, dd, *J* = 15.1, 7.3 Hz, H7), 5.85 (1H, d, *J* = 15.2 Hz, H2), 5.77 (1H, s, H15), 5.02 (1H, d, *J* = 9.8 Hz, H17), 4.32 (1H, ddd, *J* = 11.3, 8.3, 3.3 Hz, H19), 4.24 (1H, s, H22), 3.89 (1H, d, *J* = 7.6 Hz, H13), 3.74 (3H, s, CO_2Me), 3.76-3.73 (1H, obs m, H11), 3.28 (3H, s, OMe), 3.07 (1H, dd, *J* = 7.6, 3.9 Hz, H9), 2.65 (1H, m, H18), 2.56 (1H, ddd, *J* = 17.4, 11.7, 5.5 Hz, H26a), 2.49 (1H, m , H8), 2.30 (1H, ddd, *J* = 17.3, 11.3, 3.9 Hz, H26b), 2.15 (3H, s, H28), 2.00-1.93 (2H, m, H12, H24), 1.93-1.87 (2H, m, H10, H20a), 1.74 (3H, s, Me16), 1.66 (3H, s, Me14), 1.60-1.55 (1H, obs m, H25a), 1.45 (1H, dd, *J* = 13.7, 11.8 Hz, H20b), 1.17 (1H, dd, *J* = 12.3, 4.7 Hz, H25b), 1.09 (3H, d, *J* = 6.5 Hz, Me18), 1.04 (3H, d, *J* = 7.0 Hz, Me8), 1.00-0.87 (42H, m, Me10, Me12, $OSiCH_2CH_3$ ×4), 0.86 (3H, d, *J* = 6.9 Hz, Me24), 0.81-0.67 (6H, m, $OSiCH_2CH_3$), 0.67-0.52 (18H, m, $OSiCH_2CH_3$ ×3); **^{13}C NMR** (125 MHz, $CDCl_3$): δ_C 208.2, 172.8, 167.8, 145.1, 144.7, 141.4, 137.8, 133.5, 130.5, 130.2, 128.9, 128.3, 119.9, 86.8, 80.84, 80.79, 79.8, 74.1, 73.2, 60.1, 51.6, 42.5, 41.1, 39.7, 39.5, 38.3, 37.0, 33.1, 30.2, 25.8, 17.7, 17.4, 14.8, 14.1, 13.8, 12.8, 11.2, 7.35, 7.34, 7.2, 7.1, 6.8, 5.8, 5.3, 5.1; **IR** (thin film): ν_{max} 2954,

[***] Stannane **129** synthesised by Dr. Bing Yuan Han

2877, 1747, 1720, 1618, 1457, 1414, 1378, 1260, 1143, 1093, 1005, 802, 725; **HRMS** (ES^+) Calc. for $C_{61}H_{114}O_{10}Si_4H$ $[M+H]^+$ 1119.7562, found 1119.7571; $[\alpha]_D^{20}$ = +5.3 (*c* 0.15, $CHCl_3$).

Alcohol 131

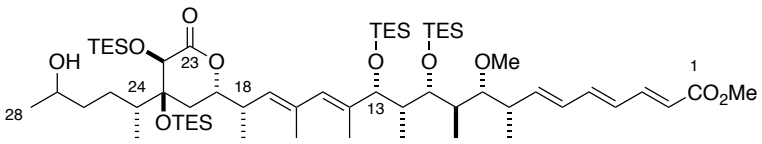

$NaBH_4$ (10.5 mg, 277 μmol) was added to a stirring solution of ketone **101a** (62.0 mg, 55.3 μmol) in MeOH (2.5 mL) at 0 °C. The reaction mixture was stirred at 0 °C for 30 min before quenching with a solution of NH_4Cl (2.5 mL) and diluting with Et_2O (5 mL). The layers were separated, and the aqueous phase was extracted with Et_2O (3 × 2.5 mL). The combined organic phases were dried ($MgSO_4$) and concentrated *in vacuo*. Purification by flash column chromatography (EtOAc/PE 40-60: 5%) afforded alcohol **131** as a colourless oil (59 mg, 52.6 μmol, 95%) as a 1:1.5 epimeric mixture at C27.

$\mathbf{R_f}$ (EtOAc/PE 40-60: 25%) = 0.34; **^{1}H NMR** (500 MHz, $CDCl_3$): δ_H 7.30 (1H, dd, *J* = 15.5, 11.6 Hz, H3), 6.52 (1H, dd, *J* = 14.8, 10.7 Hz, H5), 6.22 (1H, dd, *J* = 14.9, 11.4 Hz, H4), 6.13 (1H, dd, *J* = 15.2, 10.8 Hz, H6), 5.98 (1H, dd, *J* = 15.3, 7.4 Hz, H7), 5.85 (1H, d, *J* = 15.3 Hz, H2), 5.78 (1H, s, H15), 5.03 (1H, d, *J* = 9.0 Hz, H17), 4.35 (1H, ddd, J = 11.8, 7.2, 2.6 Hz, H19), 4.23 (1H, s, H22; minor epimer at 4.22, s), 3.89 (1H, d, *J* = 7.6 Hz, H13), 3.80-3.70 (5H, m, H11, H27, CO_2Me), 3.28 (3H, s, OMe9), 3.07 (1H, dd, *J* = 7.1, 4.0 Hz, H9), 2.68 (1H, m, H18), 2.50 (1H, m, H8), 2.04-1.94 (2H, m, H12, H24), 1.94-1.84 (2H, m, H10, H20a), 1.75 (3H, s, Me16), 1.67 (3H, s, Me14), 1.59 (1H, m, H26a), 1.51-1.40 (2H, m, H20b, H25a), 1.29 (1H, m, H26b), 1.21 (3H, d, *J* = 6.0 Hz, H28; minor epimer at 1.20 – d, *J* = 5.9 Hz), 1.08 (3H, d, *J* = 6.7 Hz, Me18), 1.04 (3H, d, J = 6.8 Hz, Me8), 1.02-0.81 (47H, m, Me10, Me12, Me24, H25b, $OSiCH_2CH_3$ ×4), 0.80-0.72 (6H, m, $OSiCH_2CH_3$), 0.68-0.53 (18H, m, $OSiCH_2CH_3$ ×3); **^{13}C NMR** (125 MHz, $CDCl_3$): δ_C 173.0, 167.8, 145.1, 144.6, 141.3, 137.9, 133.6, 130.6, 130.2, 128.9, 128.3, 119.9, 86.8, 80.9, 80.9, 79.9, 74.2, 73.2 (73.2 minor), 68.6 (68.9 minor), 60.1, 51.6, 41.1, 39.7, 39.5, 38.2, 38.0, 37.5, 32.7, 28.3 (minor 28.9), 23.9 (minor 24.2), 17.7, 17.3, 14.9, 14.2, 13.8, 13.0 (minor 12.9), 11.0, 7.2, 7.2, 6.9, 6.6, 5.7, 5.3, 5.2, 5.0; **IR** (thin film): ν_{max} 3502 (br), 2956, 2932, 2877, 1748, 1721, 1617, 1457, 1260, 1145, 1088, 1006, 789, 725 cm^{-1}; **HRMS** (ES^+) Calc. for $C_{61}H_{116}O_{10}Si_4NH_4$ $[M+NH_4]^+$ 1138.7984, found 1138.7993, $[\alpha]_D^{20}$ –17.5 (*c* 0.20, $CHCl_3$).

Methyl ether 132

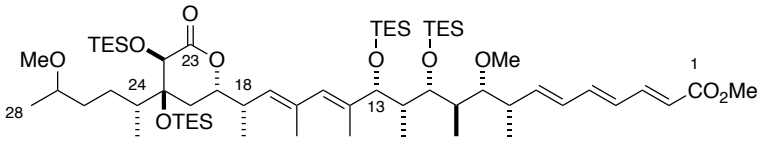

A solution of alcohol **131** (16 mg, 14.3 μmol) in CH_2Cl_2 (150 μL) was added to a suspension of $Me_3O{\cdot}BF_4$ (21 mg, 143 μmol), Proton Sponge® (46 g, 214 μmol) and crushed 4 Å molecular sieves (*ca*. 12 mg) in CH_2Cl_2 (200 μL). The resulting suspension was stirred for 3 h at r.t. before quenching with $NaHCO_3$ (1 mL). The layers were separated and the aqueous phase was extracted with CH_2Cl_2 (3 × 1 mL). The combined organic extracts were dried ($MgSO_4$) and concentrated *in vacuo*. Purification by flash column chromatography (EtOAc/PE 40-60: 5%) afforded methyl ether **132** as a colourless oil (13.9 mg, 12.2 μmol, 87%).

R_f (EtOAc/PE 40-60: 10%) = 0.24; **^{1}H NMR** (500 MHz, $CDCl_3$): δ_H 7.30 (1H, dd, *J* = 15.3, 11.4 Hz, H3), 6.52 (1H, dd, *J* = 14.9, 10.8 Hz, H5), 6.21 (1H, dd, *J* = 14.9, 11.4 Hz, H4), 6.13 (1H, dd, *J* = 15.5, 10.8 Hz, H6), 5.98 (1H, dd, *J* = 15.3, 7.5 Hz, H7; minor epimer 5.97, dd, *J* = 15.4, 7.5 Hz), 5.85 (1H, d, *J* = 15.4 Hz, H2), 5.78 (1H, s, H15), 5.03 (1H, d, *J* = 10.0 Hz, H17), 4.36 (1H, m, H19), 4.22 (1H, s, H22), 3.89 (1H, d, *J* = 7.6 Hz, H13; minor epimer 3.89), 3.77-3.65 (5H, m, H11, H27, CO_2Me), 3.29 (3H, s, OMe9), 3.28 (3H, s, OMe27; minor epimer 3.31, s), 3.07 (1H, dd, *J* = 7.4, 4.2 Hz, H9; minor epimer 3.07, dd, *J* = 7.4, 4.2 Hz), 2.69 (1H, m, H18), 2.49 (1H, m, H8), 2.01-1.93 (2H, m, H12, H24), 1.94-1.86 (2H, m, H10, H20a), 1.75 (3H, s, Me16), 1.67 (3H, s, Me14), 1.55 (1H, m, H26a), 1.45-1.36 (2H, m, H20b, H25a), 1.13 (3H, d, *J* = 6.1 Hz, H28; minor epimer 1.12, d, *J* = 6.1 Hz), 1.08 (3H, d, *J* = 6.9 Hz, Me18), 1.04 (3H, d, *J* = 6.7 Hz, Me8), 1.04-0.86 (38H, m, Me10, Me12, Me24, H25b, $OSiCH_2CH_3$ ×4), 0.82-0.71 (6H, m, $OSiCH_2CH_3$), 0.70-0.51 (16H, m, $OSiCH_2CH_3$ ×3); **^{13}C NMR** (125 MHz, $CDCl_3$): δ_C 172.9, 167.6, 144.0, 144.5 (minor 144.5), 141.2, 137.6, 133.5, 130.5 (minor 130.4), 130.0, 128.8, 128.2, 119.7, 86.7 (minor 86.6), 80.7, 80.6 (minor 80.6), 79.7, 74.1, 73.0, 59.9, 56.0, 51.5, 41.0, 39.6, 39.4, 38.0, 37.5, 35.3, 32.5 (minor 32.6), 28.3, 19.1, 17.6, 17.2, 14.7, 14.0 (minor 14.0), 13.6, 12.8 (minor 12.7), 11.0, 7.2, 7.2, 6.9, 6.6, 5.7, 5.3, 5.2 (minor 5.3), 5.0; **IR** (thin film): ν_{max} 2965, 2927, 1719, 1615, 1456, 1377, 1260, 1226, 1086, 1008, 803, 753 cm^{-1}; **HRMS** (ES^+) Calc. for $C_{62}H_{118}O_{10}Si_4H$ $[M + H]^+$ 1135.7875, found 1135.7880; $[\alpha]_D^{20}$ −15.0 (*c* 0.2, $CHCl_3$).

Tetraol 134

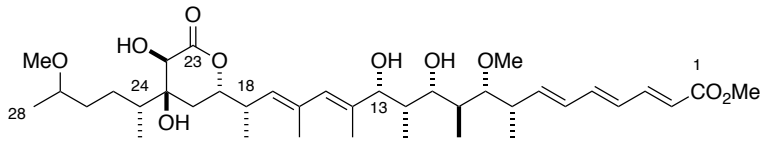

To a solution of TES ether **132** (14 mg, 12.3 μmol) in THF was added a solution of TASF (17 mg, 61.6 μmol) in DMF (300 μL) at 0 ˚C. The light pink solution was stirred at 0 ˚C for 30 min, before quenching with NH_4Cl (1 mL) and diluting with EtOAc (1 mL). The aqueous phase was extracted with EtOAc (5 × 0.5 mL), dried ($MgSO_4$), concentrated *in vacuo* and the crude immediately redissolved in THF (300 μL) and stirred at 0 ˚C. A solution of HF·py in py (1:3, 300 μL) was added and the solution was stirred at 0 ˚C for 3 h. The reaction mixture was quenched by slow addition of $NaHCO_3$ (1 mL), the layers separated and the aqueous phase extracted with EtOAc (5 × 1 mL). The combined organic phases were dried ($MgSO_4$) and concentrated *in vacuo*. Purification by flash column chromatography (EtOAc/PE 40-60: 80%) afforded the tetraol **134** as a colourless oil (8.0 mg, 11.7 μmol, 95% over two steps).

R_f (EtOAc/PE 40-60: 80%) = 0.34; **^{1}H NMR** (500 MHz, MeOD-d_4): δ_H 7.31 (1H, dd, *J* = 15.5, 11.3 Hz, H3), 6.58 (1H, dd, *J* = 14.8, 10.8 Hz, H5), 6.33 (1H, dd, *J* = 14.8, 10.8 Hz, H4), 6.21 (1H, dd, *J* = 15.3, 10.8 Hz, H6), 5.99 (1H, dd, *J* = 15.5, 8.6 Hz, H7), 5.95 (1H, s, H15), 5.90 (1H, d, *J* = 15.1 Hz, H2), 5.16 (1H, d, *J* = 9.6, H17), 4.42 (1H, ddd, *J* = 11.3, 7.4, 3.8 Hz, H19), 4.26 (1H, s, H22), 3.97 (1H, d, *J* = 7.9 Hz, H13), 3.73 (3H, s, CO_2Me) 3.52 (1H, d, *J* = 9.9 Hz, H11), 3.39 (3H, s, OMe9), 3.31 (3H, s, OMe27), 3.30-3.28 (2H, m, H9, H27), 2.80 (1H, m, H18), 2.54 (1H, m, H8), 2.00-1.92 (3H, m, H10, H20a, H24), 1.84-1.76 (4H, m, H12, Me16), 1.73-1.66 (4H, m, Me14, H20b), 1.62-1.43 (3H, m, H25a, H26a, H26b), 1.12 (3H, d, *J* = 6.1 Hz, H28), 1.10 (3H, d, *J* = 6.7 Hz, Me18), 1.08 (3H, d, *J* = 6.7 Hz, Me8), 0.97-0.91 (7H, m, Me12, Me24, H25b), 0.85 (3H, d, *J* = 6.9 Hz, Me10); **^{13}C NMR** (125 MHz, MeOD-d_4): δ_C 176.9, 169.3, 146.6, 145.0, 142.9, 137.4, 135.4, 131.8, 131.6, 130.5, 129.4, 120.6, 87.9, 82.7, 82.1, 78.5, 76.3, 75.3, 72.4, 59.4, 56.2, 52.0, 41.6, 40.0, 39.2, 39.2 (minor 39.1), 38.5, 35.9, 32.1, 28.7, 19.3 (minor 19.4), 17.8, 17.2, 17.1, 13.6, 13.0, 13.0, 7.7; **IR** (thin film): ν_{max} 3446 (br), 2965, 2927, 1719, 1615, 1456, 1377, 1260, 1226, 1086, 1008, 803, 753 cm^{-1}; **HRMS** (ES$^+$) Calc. for $C_{38}H_{62}O_{10}NH_4$ $[M + NH_4]^+$ 696.4681, found 696.4680; $[\alpha]_D^{20}$ +6.0 (*c* 0.01, $CHCl_3$),

^{1}H and ^{13}C NMR comparison between hemicalide, the 13,18-*syn* methyl ester truncate 134 and the 13,18-*anti* methyl ester truncate 136†

	δ_C					δ_H										
Atom	**Natural**	**13,18-*syn***	**Δ**	**13,18-*anti*†**	**Δ**	**Natural**	**mult**	***J* (Hz)**	**13,18-*syn***	**mult**	**J (Hz)**	**Δ**	**13,18-*anti*†**	**mult**	***J* (Hz)**	**Δ**
1	174.1	169.3	-4.8	169.3	-4.8	-			-			-	-			-
2	127.6	120.6	-7.0	120.5	-7.1	5.90	d	15.3	5.90	d	15.1	0.00	5.90	d	15.4	0.00
3	142.7	146.6	3.9	146.6	3.9	7.10	dd	15.1, 11.1	7.31	dd	15.5, 11.3	0.21	7.31	dd	15.4, 11.3	0.21
4	130.7	129.4	-1.3	129.4	-1.3	6.27	dd	15.0, 11.0	6.33	dd	14.8, 10.8	0.06	6.33	dd	14.6, 11.5	0.06
5	139.8	142.9	3.1	143.0	3.2	6.45	dd	15.0, 10.8	6.58	dd	14.8, 10.8	0.13	6.61	dd	14.8, 10.6	0.16
6	130.9	130.5	-0.4	130.5	-0.4	6.17	dd	15.3, 10.7	6.21	dd	15.3, 10.8	0.04	6.21	dd	15.3, 10.7	0.04
7	142.8	145.0	2.2	145.1	2.3	5.87	dd	15.1, 8.7	5.99	dd	15.5, 8.6	0.12	5.99	dd	15.3, 8.8	0.12
8	41.5	41.6	0.1	41.5	0.0	2.55	m		2.54	m		-0.01	2.58	m		0.03
Me8	17.2	17.2	0.0	17.0	-0.2	1.07	d	6.7	1.08	d	6.7	0.01	1.08	d	6.7	0.01
9	88.3	87.9	-0.4	88.1	-0.2	3.27	dd	6.7, 4.6	3.30	d	4.2**	0.03	3.28	dd	6.7, 4.4	0.01
OMe9	59.6	59.4	-0.2	59.5	-0.1	3.39	s		3.39	s		0.00	3.38	s		-0.01
10	40.1	40.0	-0.1	40.0	-0.1	1.22-2.02	m*		1.99	m		-	1.99	m		-
Me10	13.0	13.0	0.0	13.0	0.0	0.85	d	7.0	0.85	d	6.9	0.00	0.85	d	7.1	0.00
11	75.5	75.3	-0.2	75.7	0.2	3.57	dd	9.6, 2.0	3.52	d	9.9	-0.05	3.55	d	9.6	-0.02
12	38.5	38.5	0.0	38.4	-0.1	1.22-2.02	m*		1.80	m		-	1.80	m		-
Me12	7.6	7.7	0.1	7.5	-0.1	0.93	d	No *J* value	0.93	d	6.9	0.00	0.92	d	6.9	-0.01
13	82.1	82.1	0.0	82.0	-0.1	3.99	d	7.3	3.97	d	7.9	-0.02	3.99	d	7.4	0.00
14	137.4	137.4	0.0	137.4	0.0	-			-			-	-			-
Me14	14.0	13.6	-0.4	14.1	0.1	1.69	s		1.67	d	1.0	-0.02	1.67	d		-0.02
15	131.7	131.8	0.1	131.6	-0.1	5.95	s		5.95	s		0.00	5.95	s		0.00
16	135.4	135.4	0.0	135.3	-0.1	-			-			-	-			-
Me16	17.9	17.8	-0.1	17.9	0.0	1.82	s		1.81	d	0.9	-0.01	1.80	d	0.9	-0.02

17	131.6	131.6	0.0	131.3	-0.3	5.16	d	9.6	5.16	d	9.6	0.00	5.15	d	9.6	-0.01
18	39.3	39.2	-0.1	39.2	-0.1	2.81	m		2.80	m		-0.01	2.78	m		-0.03
Me18	17.2	17.1	-0.1	17.1	-0.1	1.10	d	6.8	1.10	d	6.7	0.00	1.12	d	6.8	0.02
19	82.8	82.7	-0.1	82.7	-0.1	4.42	ddd	11.4, 7.4, 3.9	4.42	ddd	11.3, 7.4, 3.8	0.00	4.42	ddd	11.4, 7.4, 3.9	0.00
20a	32.2	32.1	-0.1	32.1	-0.1	1.22-2.02	m*		1.97	m		-	1.94	m		-
20b	-	-	-	-	-	1.22-2.02	m*		1.69	m		-	1.64	m		-
21	76.4	76.3	-0.1	76.3	-0.1	-			-			-	-			-
22	72.5	72.4	-0.1	72.5	0.0	4.27	s		4.26	s		-0.01	4.24	s		-0.03
23	177.0	176.9	-0.1	176.9	-0.1	-			-			-	-			-
24	39.3	39.2	-0.1	39.2	-0.1	1.22-2.02	m*		1.94	m		-	1.92	m		-
Me24	13.1	13.0	-0.1	13.0	-0.1	0.96	d	6.7	0.95	d	6.9	-0.01	0.94	d	6.7	-0.02
25a	28.0	28.7	0.7	28.7	0.7	1.22-2.02	m*		1.56	m		-	1.57	m		-
25b	-	-	-	-	-	1.00	m		0.95	m		-0.05	0.95	m		-0.05
26a	40.8	35.9	-4.9	35.8	-5.0	1.22-2.02	m*		1.53	m		-	1.55	m		-
26b	-	-	-	-	-	1.22-2.02	m*		1.46	m		-	1.45	m		-
27	79.1	78.5	-0.6	78.5	-0.6	3.33	m		3.30	m		-0.03	3.33	m		0.00
OMe27	56.5	56.2	-0.3	56.2	-0.3	3.33	s		3.31	s		-0.02	3.31	s		-0.02
28	40.8	19.3	-21.5	19.3	-21.5	1.22-2.02	m*		1.12	d	6.1	-	1.13	d	6.1	-

† The analogous 13,18-*anti* methyl ester truncate **136** was synthesised by Dr. Bing Yuan Han

* m denotes the signal being enveloped in a 22H multiplet between δ_H 1.22-2.02 ppm

**Obscured by MeOH peak

All multiplets are assigned by their midpoint in COSY and HSQC spectra

Acid 103

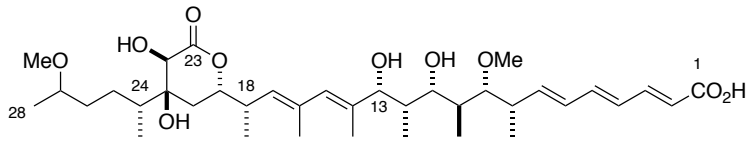

$Ba(OH)_2{\cdot}8H_2O$ (10.5 mg, 33.1 μmol) was added to a stirred solution of tetraol **134** (4.5 mg, 6.6 μmol) in MeOH (70 mL). The resulting pale-yellow suspension was stirred at rt for 24 h before quenching with 1 M HCl (1 mL) and partitioning with EtOAc (1 mL). The aqueous phase was extracted with EtOAc (5 × 0.5 mL), dried (Na_2SO_4), concentrated *in vacuo* and purified by flash column chromatography ($MeOH/CH_2Cl_2$: 10% + AcOH: 1%) to afford acid **103** as an amorphous white solid (2.0 mg, 3.0 μmol, 50%).

R_f ($MeOH/CH_2Cl_2$: 10%) = 0.30; **^{1}H NMR** (500 MHz, MeOD-d_4): δ_H 7.13 (1H, dd, *J* = 15.3, 11.1 Hz, H3), 6.47 (1H, dd, *J* = 14.6, 10.7 Hz, H5), 6.27 (1H, dd, *J* = 14.9, 11.2 Hz, H4), 6.18 (1H, dd, *J* = 15.0, 10.7 Hz, H6), 5.89 (1H, d, *J* = 15.4 Hz, H2), 5.95 (1H, s, H15), 5.89 (1H, dd, *J* = 15.0, 8.8 Hz, H7), 5.16 (1H, d, *J* = 9.6 Hz, H17), 4.42 (1H, ddd, *J* = 11.1, 7.3, 3.5 Hz, H19), 4.26 (1H, s, H22), 3.99 (1H, d, *J* = 7.2 Hz, H13), 3.57 (1H, dd, *J* = 9.8, 2.0 Hz, H11), 3.39 (3H, s, OMe9), 3.32 (3H, s, OMe27), 3.30-3.28 (2H, m, H9, H27), 2.81 (1H, m, H18), 2.54 (1H, m, H8), 2.01-1.92 (3H, m, H10, H20a, H24), 1.83-1.77 (4H, m, H12, Me16), 1.73-1.66 (4H, m, Me14, H20b), 1.62-1.43 (3H, m, H25a, H26a, H26b), 1.12 (3H, d, *J* = 6.0 Hz, H28), 1.10 (3H, d, *J* = 6.7 Hz, Me18), 1.07 (3H, d, *J* = 6.7 Hz, Me8), 0.97-0.90 (7H, m, Me12, Me24, H25b), 0.85 (3H, d, *J* = 7.1 Hz, Me10); **^{13}C NMR** (125 MHz, MeOD-d_4): δ_C 177.0, 143.2 (br), 143.1 (minor 143.1), 140.1, 137.3 (minor 137.4), 135.4, 131.8 (minor 131.7), 131.6 (minor 131.5), 130.8, 130.5, 128.2 (br), 88.3 (minor 88.4), 82.8, 82.1 (minor 82.0), 78.5 (minor 78.2), 76.4, 75.5 (minor 75.6), 72.5, 59.6 (minor 59.6), 56.3 (minor 56.3), 41.5 (minor 41.5), 40.1, 39.2, 39.2 (minor 39.1), 38.5, 35.9 (minor 36.0), 32.1, 28.7 (minor 28.6), 19.3 (minor 19.4), 17.8, 17.2 (minor 17.2), 17.2 (minor 17.0), 13.9 (minor 14.0), 13.1, 13.1 (minor 13.0), 7.5; **IR** (thin film): ν_{max} 3411, 2918, 2849, 1762, 1692, 1674, 1402, 1312, 1260, 1139, 1078, 969, 799 cm^{-1}; **HRMS** (ES^+) Calc. for $C_{37}H_{60}O_{10}Na$ $[M + Na]^+$ 687.4073, found 687.4079; $\mathbf{[\alpha]_D^{20}}$ +2.67 (*c* 0.15, $CHCl_3$),

Note: The C1 carboxylate signal is not seen in the ^{13}C NMR for **103**, but reappears in sodium salt **137**. This observation is noted alongside with the broadening of C2 and C3 – atoms most proximal to the C1 carboxylate. This is attributed to proton exchange arising from the partial deprotonation of the C1 carboxylate; an attribute also seen by Lecourt *et al.* in their C1-C27 truncate of hemicalide.[48]

Sodium salt 137

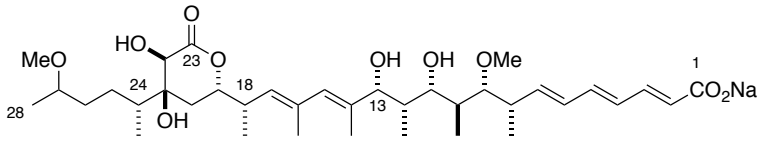

In a 5 mm NMR tube, Na_2CO_3 (*ca*. 5 mg) was added to a solution of the free acid **103** in MeOD-d_4 (500 µL). The mixture was vigorously shaken for *ca*. 30 seconds to afford the sodium salt **137** as a solution in MeOD-d_4.

^{1}H NMR (500 MHz, MeOD-d_4): δ_H 7.02 (1H, dd, *J* = 15.3, 11.3 Hz, H3), 6.41 (1H, dd, *J* = 15.0, 10.8 Hz, H5), 6.24 (1H, dd, *J* = 15.1, 11.2 Hz, H4), 6.16 (1H, dd, *J* = 15.2, 10.8 Hz, H6), 5.95 (1H, s, H15), 5.90 (1H, d, *J* = 15.4, H2), 5.83 (1H, d, *J* = 15.2, 8.8 Hz, H7; minor epimer 5.84, dd, *J* = 15.5, 9.0 Hz), 5.15 (1H, d, *J* = 9.9 Hz, H17), 4.42 (1H, ddd, *J* = 11.4, 7.6 3.9 Hz, H19), 4.26 (1H, s, H22), 4.00 (1H, d, *J* = 7.3 Hz, H13), 3.59 (1H, dd, *J* = 9.6, 2.2 Hz, H11), 3.39 (3H, s, OMe9), 3.32 (3H, s, OMe27), 3.30-3.28 (1H, m, H27), 3.27 (1H, dd, *J* = 6.3, 4.6 Hz, H9), 2.81 (1H, m, H18), 2.53 (1H, m, H8), 2.01-1.92 (3H, m, H10, H20a, H24), 1.85-1.77 (4H, m, H12, Me16), 1.73-1.65 (4H, m, Me14, H20b), 1.63-1.42 (3H, m, H25a, H26a, H26b), 1.12 (3H, d, *J* = 6.2 Hz, H28), 1.10 (3H, d, *J* = 6.7 Hz, Me18), 1.07 (3H, d, *J* = 6.7 Hz, Me8), 0.97-0.90 (7H, m, Me12, Me24, H25b), 0.85 (3H, d, *J* = 7.0 Hz, Me10); **^{13}C NMR** (125 MHz, MeOD-d_4): δ_C 177.0, 175.9, 161.5 (CO_3^{2-}), 142.0, 141.0, 138.6, 137.4 (minor 137.4), 135.5, 131.6 (minor 131.5), 131.5 (minor 131.4), 131.1, 131.0, 129.7 (minor 129.7), 88.5 (minor 88.6), 83.0, 82.0 (minor 82.0), 78.6 (minor 78.2), 76.4, 75.7 (minor 75.8), 72.5, 59.6 (minor 59.7), 56.3 (minor 56.3), 41.5 (minor 41.5), 40.1, 39.2, 39.2 (minor 39.1), 38.4, 35.9 (minor 36.0), 32.1, 28.7 (minor 28.6), 19.3 (minor 19.4), 17.9, 17.2, 17.1 (minor 17.0), 14.0 (minor 14.0), 13.1, 13.1, 7.5.

^{1}H and ^{13}C NMR comparison between hemicalide, the 13,18-*syn* free acid 103 and the 13,18-*anti* free acid 102[†]

	δ_C					δ_H										
Atom	**Natural**	**13,18-*syn***	**Δ**	**13,18-*anti*[†]**	**Δ**	**Natural**	**mult**	***J* (Hz)**	**13,18-*syn***	**mult**	***J* (Hz)**	**Δ**	**13,18-*anti*[†]**	**mult**	**J (Hz)**	**Δ**
1	174.1	[§]	-	174.9[§]	0.8	-			-				-	-		
2	127.6	(128.2) [§]	0.6	128.1[§]	0.5	5.90	d	15.3	5.89	d	15.4	-0.01	5.86	d	15.2	-0.04
3	142.7	143.2[§]	0.5	142.1[§]	-0.6	7.10	dd	15.1, 11.1	7.13	dd	15.3, 11.1	0.03	7.26	dd	14.9, 11.4	0.16
4	130.7	130.8	0.1	130.8	0.1	6.27	dd	15.0, 11.0	6.27	dd	14.9, 11.2	0.00	6.32	dd	14.7, 11.5	0.05
5	139.8	140.1	0.3	139.4	-0.4	6.45	dd	15.0, 10.8	6.47	dd	14.6, 10.7	0.02	6.57	dd	14.4, 10.4	0.12
6	130.9	130.5	-0.4	130.9	0.0	6.17	dd	15.3, 10.7	6.18	dd	15.0, 10.7	0.01	6.21	dd	15.1, 10.6	0.04
7	142.8	143	0.2	142.6	-0.2	5.87	dd	15.1, 8.7	5.89	dd	15.0, 8.8	0.02	5.96	dd	15.0, 8.7	0.09
8	41.5	41.5	0.0	41.4	-0.1	2.55	m		2.54	m		-0.01	2.56	m		0.01
Me8	17.2	17.2	0.0	16.8	-0.4	1.07	d	6.7	1.07	d	6.7	0.00	1.08	d	6.4	0.01
9	88.3	88.3	0.0	88.7	0.4	3.27	dd	6.7, 4.6	3.28	dd	6.4, 4.5	0.01	3.28	dd	6.4, 4.4	0.01
OMe9	59.6	59.6	0.0	59.8	0.2	3.39	s		3.39	s		0.00	3.39	s		0.00
10	40.1	40.1	0.0	40.0	-0.1	1.22-2.02	m*		1.98	m		-	1.98	m		-
Me10	13.0	13.1	0.1	13.0	0.0	0.85	d	7.0	0.85	d	7.1	0.00	0.85	d	7.1	0.00
11	75.5	75.5	0.0	76.1	0.6	3.57	dd	9.6, 2.0	3.57	dd	9.8, 2.0	0.00	3.61	dd	9.5, 1.5	0.04
12	38.5	38.5	0.0	38.3	-0.2	1.22-2.02	m*		1.80	m		-	1.81	m		-
Me12	7.6	7.5	-0.1	7.3	-0.3	0.93	d	No J value	0.93	d	6.7	0.00	0.92	d	7.0	-0.01
13	82.1	82.1	0.0	81.9	-0.2	3.99	d	7.3	3.99	d	7.2	0.00	4.00	d	7.0	0.01
14	137.4	137.3	-0.1	137.4	0.0	-			-			-	-			-
Me14	14.0	13.9	-0.1	14.3	0.3	1.69	s		1.68	s		-0.01	1.68	s		-0.01
15	131.7	131.7	0.0	131.3	-0.4	5.95	s		5.95	s		0.00	5.95	s		0.00
16	135.4	135.4	0.0	135.4	0.0	-			-			-	-			-

Me16	17.9	17.8	-0.1	17.9	0.0	1.82	s		1.82	s		0.00	1.80	s		-0.02
17	131.6	131.6	0.0	131.2	-0.4	5.16	d	9.6	5.16	d	9.6	0.00	5.15	d	10.0	-0.01
18	39.3	39.2	-0.1	39.2	-0.1	2.81	m		2.81	m		0.00	2.79	m		-0.02
Me18	17.2	17.2	0.0	17.1	-0.1	1.10	d	6.8	1.10	d	6.7	0.00	1.12	d	7.0	0.02
19	82.8	82.8	0.0	82.8	0.0	4.42	ddd	11.4, 7.4, 3.9	4.42	ddd	11.1, 7.3, 3.5	0.00	4.42	ddd	11.3, 7.3, 3.7	0.00
20a	32.2	32.1	-0.1	32.1	-0.1	1.22-2.02	m*		1.97	m		-	1.95	m		-
20b	-	-	-	-	-	1.22-2.02	m*		1.67	m		-	1.65	m		-
21	76.4	76.4	0.0	76.3	-0.1	-			-			-	-			-
22	72.5	72.5	0.0	72.5	0.0	4.27	s		4.26	s		-0.01	4.24	s		-0.03
23	177.0	177.0	0.0	177.0	0.0	-			-			-	-			-
24	39.3	39.2	-0.1	39.2	-0.1	1.22-2.02	m*		1.93	m		-	1.93	m		-
Me24	13.1	13.1	0.0	13.1	0.0	0.96	d	6.7	0.95	d	6.8	-0.01	0.94	d	7.0	-0.02
25a	28.0	28.7	0.7	28.7	0.7	1.22-2.02	m*		1.57	m		-	1.57	m		-
25b	-	-	-	-	-	1.00	m		0.96	m		-0.04	0.97	m		-0.03
26a	40.8	35.9	-4.9	35.8	-5.0	1.22-2.02	m*		1.50	m		-	1.54	m		-
26b	-	-	-	-	-	1.22-2.02	m*		1.44	m		-	1.47	m		-
27	79.1	78.5	-0.6	78.5	-0.6	3.33	m		3.31	m		-0.02	3.32	m		-0.01
OMe27	56.5	56.3	-0.2	56.2	-0.3	3.33	s		3.32	s		-0.01	3.31	s		-0.02
28	40.8	19.3	-21.5	19.3	-21.5	1.22-2.02	m*		1.12	d	6.0	-	1.13	d	6.1	-

† The analogous 13,18-*anti* acid truncate **102** was synthesised by Dr. Bing Yuan Han

* m denotes the signal being enveloped in a 22H multiplet between δ_H 1.22-2.02 ppm

**All multiplets are assigned by their midpoint in COSY and HSQC spectra

§ Broad signals due to proton exchange – C1 is not observed in **103** (and very broad in **102**), C2 and C3 are both very broad for **102** and **103**

^{1}H and ^{13}C NMR comparison between hemicalide, the 13,18-*syn* carboxylate salt 137 and the 13,18-*anti* carboxylate salt 138†

	δ_C					δ_H									
Atom	**Natural**	**13,18-*syn***	**Δ**	**13,18-*anti*†**	**Δ**	**Natural**	**mult**	***J* (Hz)**	**13,18-*syn***	**mult**	**J (Hz)**	**Δ**	**13,18-*anti*†**	**mult**	***J* (Hz)**	**Δ**
1	174.1	175.9	1.8	175.9	1.8	-			-				-	-		
2	127.6	129.7	2.1	129.7	2.1	5.90	d	15.3	5.90	d	15.4	0.00	5.91	d	15.3	0.01
3	142.7	142.0	-0.7	141.0	-1.7	7.10	dd	15.1, 11.1	7.02	dd	15.3, 11.3	-0.08	7.02	dd	15.3, 11.2	-0.08
4	130.7	131.0	0.3	131.0	0.3	6.27	dd	15.0, 11.0	6.24	dd	15.1, 11.2	-0.03	6.25	dd	14.9, 10.6	-0.02
5	139.8	138.6	-1.2	138.7	-1.1	6.45	dd	15.0, 10.8	6.41	dd	15.0, 10.8	-0.04	6.43	dd	14.8, 10.6	-0.02
6	130.9	131.1	0.2	131.0	0.1	6.17	dd	15.3, 10.7	6.16	dd	15.2, 10.8	-0.01	6.16	dd	15.2, 10.7	-0.01
7	142.8	141.0	-1.8	142.0	-0.8	5.87	dd	15.1, 8.7	5.83	dd	15.2, 8.8	-0.04	5.85	dd	15.2, 8.6	-0.02
8	41.5	41.5	0.0	41.4	-0.1	2.55	m		2.53	m		-0.02	2.53	m		-0.02
Me8	17.2	17.2	0.0	16.8	-0.4	1.07	d	6.7	1.07	d	6.7	0.00	1.07	d	6.7	0.00
9	88.3	88.5	0.2	88.7	0.4	3.27	dd	6.7, 4.6	3.27	dd	6.3, 4.6	0.00	3.26	dd	5.6, 4.8	-0.01
OMe9	59.6	59.6	0.0	59.8	0.2	3.39	s		3.39	s		0.00	3.39	s		0.00
10	40.1	40.1	0.0	40.1	0.0	1.22-2.02	m*		1.98	m		0.00	1.98	m		-
Me10	13.0	13.1	0.1	13.1	0.1	0.85	d	7.0	0.85	d	7.0	0.00	0.85	d	7.0	0.00
11	75.5	75.7	0.2	76.2	0.7	3.57	dd	9.6, 2.0	3.59	dd	9.6, 2.2	0.02	3.61	dd	9.5, 1.8	0.04
12	38.5	38.4	-0.1	38.3	-0.2	1.22-2.02	m*		1.80	m		0.00	1.82	m		-
Me12	7.6	7.5	-0.1	7.3	-0.3	0.93	d	No J value	0.92	d	6.8	-0.01	0.91	d	6.9	-0.02
13	82.1	82	-0.1	81.9	-0.2	3.99	d	7.3	4.00	d	7.3	0.01	4.02	d	6.6	0.03
14	137.4	137.4	0.0	137.4	0.0	-			-			-	-			
Me14	14.0	14.0	0.0	14.3	0.3	1.69	s		1.69	s		0.00	1.69	d	1.4	0.00
15	131.7	131.6	-0.1	131.2	-0.5	5.95	s		5.95	s		0.00	5.96	s		0.01
16	135.4	135.5	0.1	135.3	-0.1	-			-			-	-			-

Me16	17.9	17.9	0.0	17.9	0.0	1.82	s		1.82	s		0.00	1.80	d	0.9	-0.02
17	131.6	131.5	-0.1	131.2	-0.4	5.16	d	9.6	5.15	d	9.9	-0.01	5.15	d	9.8	-0.01
18	39.3	39.2	-0.1	39.2	-0.1	2.81	m		2.81	m		0.00	2.80	m		-0.01
Me18	17.2	17.1	-0.1	17.1	-0.1	1.10	d	6.8	1.10	d	6.7	0.00	1.11	d	6.6	0.01
19	82.8	83.0	0.2	82.8	0.0	4.42	ddd	11.4, 7.4, 3.9	4.42	ddd	11.4, 7.6, 3.9	0.00	4.42	ddd	11.4, 7.3, 4.0	0.00
20a	32.2	32.1	-0.1	32.1	-0.1	1.22-2.02	m*		1.97	m		-	1.95	m		-
20b	-	-	-	-	-	1.22-2.02	m*		1.68	m		-	1.67	m		-
21	76.4	76.4	0.0	76.4	0.0	-			-			-	-			-
22	72.5	72.5	0.0	72.5	0.0	4.27	s		4.26	s		-0.01	4.25	s		-0.02
23	177.0	177.0	0.0	177.0	0.0	-			-			-	-			-
24	39.3	39.2	-0.1	39.2	-0.1	1.22-2.02	m*		1.94	m		-	1.94	m		-
Me24	13.1	13.1	0.0	13.1	0.0	0.96	d	6.7	0.95	d	6.9	-0.01	0.94	d	6.9	-0.02
25a	28.0	28.7	0.7	28.7	0.7	1.22-2.02	m*		1.57	m		-	1.56	m		-
25b	-	-	-	-	-	1.00	m		0.96	m		-0.04	0.97	m		-0.03
26a	40.8	35.9	-4.9	35.9	-4.9	1.22-2.02	m*		1.51	m		-	1.53	m		-
26b	-	-	-	-	-	1.22-2.02	m*		1.43	m		-	1.46	m		-
27	79.1	78.6	-0.5	78.5	-0.6	3.33	m		3.32	m		-0.01	3.33	m		0.00
OMe27	56.5	56.3	-0.2	56.2	-0.3	3.33	s		3.31	s		-0.02	3.31	s		-0.02
28	40.8	19.3	-21.5	19.3	-21.5	1.22-2.02	m*		1.12	d	6.2	-	1.13	d	6.1	-

† The analogous 13,18-*anti* carboxylate salt truncate **138** was synthesised by Dr. Bing Yuan Han

* m denotes the signal being enveloped in a 22H multiplet between δ_H 1.22 – 2.02 ppm.

**All multiplets are assigned by their midpoint in COSY and HSQC spectra

8.5. Experimental Procedures for Part III – Phormidolide A

8.5.1. C18-C23/C24 fragment

Alcohol 210

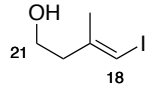

$AlMe_3$ (47.0 mL, 93.9 mmol) was added to a solution of Cp_2ZrCl_2 (1.95 g, 6.67 mmol) in CH_2Cl_2 (90 mL) at –20 °C. The solution was stirred for 10 min at –20 °C, before the addition of water (845 μL, 47.0 mmol). The pale-yellow suspension was stirred for 10 min at –20 °C. A solution of 3-butyn-1-ol (2.12 g, 30.3 mmol) in CH_2Cl_2 (20 mL) was treated with $AlMe_3$ (4.70 ml, 9.39 mmol) and transferred *via* cannula into the reaction mixture. The mixture was stirred overnight, with gradual warming to r.t., during which a yellow suspension formed. A solution of I_2 (9.16 g, 36.4 mmol) in Et_2O (200 mL) was transferred *via* cannula to the reaction mixture at –20 °C, resulting in a colour change to vivid yellow, then brown. The reaction mixture was allowed to warm to r.t. and stirred for 2 h. The reaction mixture was quenched by addition of Na/K tartrate (200 mL) and Et_2O (200 mL) and vigorously stirred at r.t. for 1.5 h. The layers were separated, and the aqueous phase was extracted with Et_2O (3 × 100 mL), dried ($MgSO_4$) and the solvent removed under reduced pressure to afford a yellow liquid. Purification by flash column chromatography (Et_2O/PE 30-40: 20% → 30%) afforded the product **210** as a pale-yellow oil (5.22 g, 26.4 mmol, 87%).

R_f (Et_2O/PE 30-40: 50%) = 0.54; **^{1}H NMR** (400 MHz, $CDCl_3$) δ_H 6.01 (1H, q, *J* = 1.0 Hz, H18), 3.72 (2H, t, *J* = 6.3 Hz, H21), 2.48 (2H, t, *J* = 6.3 Hz, H20), 1.87 (3H, s, Me19); **^{13}C NMR** (125 MHz, $CDCl_3$) δ_C 144.5, 76.8, 60.1, 42.4, 23.8.

Data in agreement with that presented by Penner[109]

Hydroxyketone (±)-197

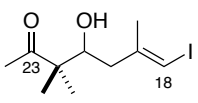

Dess-Martin Periodinane (616 mg, 1.45 mmol) was added to a stirred suspension of alcohol **210** (154 mg, 730 μmol) and $NaHCO_3$ (366 mg, 4.36 mmol) in wet CH_2Cl_2 (5.0 mL). The reaction mixture was stirred at r.t. until TLC monitoring indicated full consumption of the starting material (*ca.* 1.5 h). The reaction mixture was quenched by the addition of $Na_2S_2O_3$ solution (7 mL) and the mixture stirred at r.t. for 30 min. The layers were separated and the aqueous phase was extracted with CH_2Cl_2 (3 × 10 mL). The combined

organic phases were dried ($MgSO_4$) and concentrated under reduced pressure to ca. 4 mL. The solution of the crude aldehyde **196** was dried over 4 Å molecular sieves and directly used in the subsequent step without further purification.

Method A: Mukaiyama Aldol with $BF_3{\cdot}OEt_2$

A solution of the crude aldehyde **196** (152 mg, 0.73 mmol) in CH_2Cl_2 (4 mL + 4 mL wash) was added *via* cannula to a stirred solution of the silyl enol ether **207** (100 mg, 0.632 mmol, dried over CaH_2) in CH_2Cl_2 (2 mL) at –78 °C. The solution was allowed to stir at –78 °C for 10 min before the dropwise addition of $BF_3{\cdot}OEt_2$ (90 μL, 0.73 mmol). The reaction mixture was stirred at –78 °C for 1.5 h before quenching with $NaHCO_3$ solution (10 mL). Upon warming to r.t., the layers were separated, and the aqueous phase was extracted with CH_2Cl_2 (3 × 10 mL). The combined organic phases were washed with brine (15 mL), dried ($MgSO_4$) and the solvent removed under reduced pressure. Purification by flash column chromatography (EtOAc/PE 40-60: 20% → 40%) afforded the product **197** as an yellow oil (121 mg, 0.41 mmol, 64%).

Method B: Mukaiyama Aldol with $TiCl_4$

A solution of the crude aldehyde **196** (152 mg, 730 μmol) in CH_2Cl_2 (4 mL + 4 mL wash) was added *via* cannula to a stirred solution of the silyl enol ether **207** (100 mg, 632 μmol, dried over CaH_2) in CH_2Cl_2 (2 mL) at –78 °C. The solution was allowed to stir at –78 °C for 10 min before the dropwise addition of $TiCl_4$ (80 μL, 730 μmol). The reaction mixture was stirred at –78 °C for 1.5 h before quenching with $NaHCO_3$ solution (10 mL). Upon warming to r.t., the layers were separated and the aqueous phase was extracted with CH_2Cl_2 (3 × 10 mL). The combined organic phases were washed with brine (15 mL), dried ($MgSO_4$) and the solvent removed under reduced pressure. Purification by flash column chromatography (EtOAc/PE 40-60: 20% → 40%) afforded the product **197** as an yellow oil (128 mg, 430 μmol, 68%).

R_f (EtOAc/PE 40-60: 30%) = 0.55; **^{1}H NMR** (500 MHz, $CDCl_3$) δ_H 6.03 (1H, q, *J* = 0.7 Hz, H18), 3.85 (1H, dd, *J* = 10.1, 2.5 Hz, H21), 2.31-2.20 (3H, m, H20, OH), 2.18 (3H, s, H24), 1.90 (3H, d, *J* = 0.7 Hz, Me19), 1.17 (3H, s, MeC22a), 1.14 (3H, s, MeC22b); **^{13}C NMR** (125 MHz, $CDCl_3$) δ_C 214.5, 144.9, 77.2, 73.4, 51.5, 41.8, 26.4, 24.0, 21.6, 19.6; **IR** (thin film): ν_{max} 3469, 2975, 1694, 1467, 1354, 1273, 1143, 1120, 1068; **HRMS** (ESI^+) calculated for $C_{10}H_{18}O_2I$ $[M+H]^+$ 297.0346, found 297.0348.

Hydroxyester 218 and *ent*-218

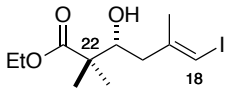

Dess-Martin Periodinane (2.50 g, 5.89 mmol) was added to a stirred suspension of alcohol **210** (500 mg, 2.35 mmol) and $NaHCO_3$ (1.50 g, 17.8 mmol) in wet CH_2Cl_2 (25 mL). The reaction mixture was stirred at r.t. until TLC monitoring indicated full consumption of the starting material (*ca*. 1.5 h). The reaction mixture was quenched by the addition of $NaHCO_3$ (20 mL) and $Na_2S_2O_3$ solution (20 mL) and stirred at r.t. for 30 min. The layers were separated and the aqueous phase was extracted with CH_2Cl_2 (3 × 10 mL). The combined organic phases were washed with brine (50 mL), dried ($MgSO_4$) and concentrated under reduced pressure to *ca*. 10 mL. The solution of the crude aldehyde **196** was dried over 4 Å molecular sieves and directly used in the subsequent step without further purification.

$BH_3{\cdot}SMe_2$ (279 μL, 2.95 mmol) was added dropwise to a stirred solution of *N*-tosyl-L-valine (**215**) (799 mg, 2.95 mmol) in CH_2Cl_2 (7 mL) and THF (1 mL) at 0 °C. The solution was stirred at 0 °C for 1 h before cooling to –78 °C. A combined solution of the crude aldehyde **196** and the silyl ketene acetal **217** (1.11 g, 5.89 mmol, dried over CaH_2) in CH_2Cl_2 (15 mL) was added *via* cannula to the reaction mixture. The mixture was stirred at –78 °C for 3 h before quenching with $NaHCO_3$ solution. Upon warming to r.t., the layers were separated and the aqueous phase extracted with CH_2Cl_2 (3 × 40 mL). The combined organic phases were washed with brine (100 mL), dried ($MgSO_4$), and the solvent removed under reduced pressure. Purification by flash column chromatography (EtOAc/PE 40-60: 5%) afforded the product **218** as an orange oil (516 mg, 3.95 mmol, 67% over 2 steps, 91% *ee*).

The enantiomeric compound was analogously prepared from alcohol **210** (1.00 g, 4.71 mmol), employing *N*-tosyl-D-valine (***ent*-215**) (1.92 g, 7.07 mmol) to give ***ent*-218** as an orange oil (818 mg, 2.51 mmol, 53%)

R_f (EtOAc/PE 40-60: 30%) = 0.57; **^{1}H NMR** (400 MHz, $CDCl_3$) δ_H 6.02 (1H, q, *J* = 0.9 Hz, H18), 4.16 (2H, q, *J* = 7.1 Hz, $CH_3\underline{CH_2}O$), 3.81 (1H, ddd, *J* = 10.0, 5.6, 2.5 Hz, H21), 2.39 (1H, d, *J* = 5.6 Hz, OH), 2.33 (1H, br d, *J* = 13.2 Hz, H20a), 2.26 (1H, dd, *J* = 13.9, 10.0 Hz, H20b), 1.90 (3H, d, *J* = 0.9 Hz, Me19), 1.27 (3H, t, *J* = 7.1 Hz, $\underline{CH_3}CH_2O$), 1.20 (3H, s, Me22a), 1.20 (3H, s, Me22b); **^{13}C NMR** (125 MHz, $CDCl_3$) δ_C 177.1, 145.1, 73.7, 60.8, 46.7, 42.0, 23.9, 21.6, 20.7, 14.2, 14.1; **IR** (thin film): ν_{max} 3526, 2984, 1716, 1469, 1386, 1269, 1134, 1070; $[\alpha]_D^{20}$ +13.9 (**218**, *c* 1.0, $CHCl_3$); $[\alpha]_D^{20}$ –12.6° (***ent*-218**, *c* 0.26, $CHCl_3$); **Chiral HPLC** (Chiralpak® IA, *i*PrOH:*n*-hexane: 5%) R_T (major) 10.02 min, R_T (minor) 10.74 min; **HRMS** (ESI^+) calculated for $C_{11}H_{20}O_3I$ $[M+H]^+$ 327.0452, found 327.0451.

TES ether 220 and *ent*-220

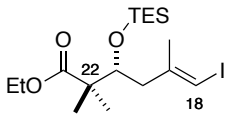

2,6-Lutidine (128 μL, 1.10 mmol) was added to a stirred solution of hydroxyester **218** (240 mg, 736 μmol) in CH_2Cl_2 (8 mL). The reaction mixture was cooled to –78 °C and stirred for 5 min, before the dropwise addition of TESOTf (208 μL, 920 μmol). The mixture was stirred at –78 °C for 45 min, before quenching with $NaHCO_3$ solution (10 mL). Upon warming to r.t., the layers were separated and the aqueous phase extracted with CH_2Cl_2 (3 × 10 mL). The combined organic phases were washed with brine (15 mL), dried ($MgSO_4$) and the solvent removed under reduced pressure. Purification by flash column chromatography (EtOAc/PE 40-60: 10%) afforded the product **220** as a colourless oil (319 mg, 721 μmol, 98%).

The enantiomeric compound was analogously prepared from hydroxyester ***ent*-218** (818 mg, 2.51 mmol) to give ***ent*-220** as a colourless oil (1.01 g, 2.29 mmol, 91%)

R_f (EtOAc/PE 40-60: 30%) = 0.80; **^{1}H NMR** (500 MHz, $CDCl_3$) δ_H 5.93 (1H, q, *J* = 1.0 Hz, H18), 4.15-4.08 (3H, m, Me$\underline{CH_2}$O, H21), 2.27 (1H, dd, *J* = 13.7, 7.9 Hz, H20a), 2.21 (1H, dd, *J* = 13.5, 3.4 Hz, H20b), 1.84 (3H, d, *J* = 1.0 Hz, Me19), 1.26 (3H, t, *J* = 7.1 Hz, Me$\underline{CH_2}$), 1.17 (3H, s, Me22a), 1.09 (3H, s, Me22b) 0.94 (9H, t, *J* = 8.0 Hz, Si($CH_2\underline{CH_3}$)$_3$), 0.57 (6H, q, *J* = 8.0 Hz, Si($\underline{CH_2}CH_3$)$_3$); **^{13}C NMR** (125 MHz, $CDCl_3$) δ_C 176.7, 144.5, 78.3, 74.3, 60.4, 48.0, 44.6, 23.8, 22.9, 17.8, 14.1, 7.0, 5.4; **IR** (thin film): ν_{max} 2955, 2913, 2877, 1723, 1466, 1384, 1261, 1132, 1095; **$[\alpha]_D^{20}$** +3.6 (**220**, *c* 1.0, $CHCl_3$); **$[\alpha]_D^{20}$** –3.7 (***ent*-220**, *c* 0.32, $CHCl_3$); **HRMS** (ESI^+) calculated for $C_{17}H_{34}O_3SiI$ $[M+H]^+$ 411.1316, found 411.1311.

Ketone 201

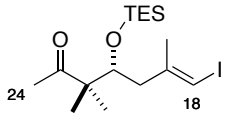

A solution of ester **220** (42.5 mg, 0.182 mmol) in PhMe (0.5 mL) was added *via* cannula to a stirred solution of MeMgBr (130 μL, 0.886 mmol, 3 M in Et_2O) and Et_3N (255 μL, 1.82 mmol) in PhMe (2.5 mL). The mixture was heated to 80 °C and stirred until TLC monitoring indicated complete consumption of the starting material (*ca.* 4 h). The mixture was allowed to cool to r.t. and quenched with NH_4Cl solution (2 mL). The layers were separated, and the aqueous phase extracted with Et_2O (3 × 3 mL). The combined organic phases were dried ($MgSO_4$) and the solvent removed under reduced pressure. Purification by flash column chromatography (EtOAc/PE 40-60: 4%) afforded the product **201** as a pale-yellow oil (36.5 mg, 0.168 mmol, 92%).

R_f (EtOAc/PE 40-60: 30%) = 0.78; **^{1}H NMR** (400 MHz, $CDCl_3$) δ_H 5.93 (1H, q, *J* = 1.0 Hz, H18), 4.08 (1H, t, *J* = 5.7 Hz, H21), 2.20 (2H, d, *J* = 5.7 Hz, H20), 2.15 (3H, s, H24), 1.84 (3H, d, *J* = 1.0 Hz, Me19), 1.12 (3H, s, Me22a), 1.10 (3H, s, Me22b) 0.94 (9H, t, *J* = 8.0 Hz, $Si(CH_2\underline{CH_3})_3$), 0.57 (6H, q, *J* = 8.0 Hz, $Si(\underline{CH_2}CH_3)_3$); **^{13}C NMR** (125 MHz, $CDCl_3$) δ_C 213.3, 144.5, 78.4, 74.6, 52.9, 44.4, 27.0, 23.9, 22.2, 19.8, 7.1, 5.4; **IR** (thin film): ν_{max} 2945, 2910, 2876, 1702, 1459, 1353, 1238, 1088, 1004; $[\alpha]_D^{20}$ +16.4 (*c* 0.5, $CHCl_3$); **HRMS** (ESI^+) calculated for $C_{16}H_{32}O_2SiI$ $[M+H]^+$ 411.1211, found 411.1206.

Mosher esters 221 and 222

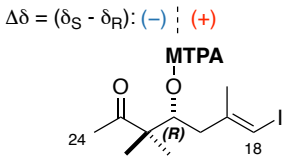

A solution of TBAF (54 µL, 53.6 µmol, 1 M in THF) was added to a stirred solution of TES ether **201** (20 mg, 48.7 µmol) in THF (0.5 mL). The pale-yellow solution was stirred for 1 h at r.t. before being quenched with a solution of NH_4Cl (0.5 mL). The layers were separated and the aqueous phase was extracted with Et_2O (3 × 1 mL). The combined organic phases were dried ($MgSO_4$) and the solvent removed under reduced pressure to afford the crude hydroxyketone (*R*)-**197** (11 mg, 38.5 µmol, 79%), which was used directly in subsequent steps without purification.

(S)-Mosher ester **221**

DCC (54 µL, 54.0 µmol, 1 M in CH_2Cl_2) was added in portion to a stirred solution of crude hydroxyketone (4.0 mg, 13.5 µmol), *(S)*-MTPA (12 mg, 54.0 µmol) and DMAP (one crystal) in CH_2Cl_2 (500 µL). The mixture was stirred for 24 h at r.t., during which the solution became a white suspension. The mixture was filtered through cotton wool and the filtrate reduced to dryness. Purification by flash chromatography (EtOAc/PE 40-60: 10%) afforded the product **221** as a colourless oil (4.6 mg, 8.97 µmol, 66%).

R_f (EtOAc/PE 40-60: 20%) = 0.48; **^{1}H NMR** (400 MHz, $CDCl_3$) δ_H 7.49-7.41 (5H, m, Ar<u>H</u>), 5.95 (1H, s, H18), 5.69 (1H, dd, *J* = 10.1, 2.3 Hz, H21), 3.49 (3H, s, OMe), 2.45 (1H, dd, *J* = 14.4, 10.1 Hz, H20a), 2.30 (1H, br d, *J* = 14.4 Hz, H20b), 2.11 (3H, s, H24), 1.94 (3H, s, Me19), 1.13 (3H, s, Me22a), 1.12 (3H, s, Me22b).

(R)-Mosher ester **222**

DCC (54 µL, 54.0 µmol, 1 M in CH_2Cl_2) was added in portion to a stirred solution of crude hydroxyketone (*R*)-**197** (4.0 mg, 13.5 µmol), *(R)*-MTPA (12 mg, 54.0 µmol) and DMAP (one crystal) in CH_2Cl_2 (500 µL). The mixture was stirred for 24 h at r.t., during which the solution became a white suspension. The mixture

was filtered through cotton wool and the filtrate reduced to dryness. Purification by flash chromatography (EtOAc/PE 40-60: 10%) afforded the product **222** as a colourless oil (4.0 mg, 7.80 μmol, 58%).

R_f (EtOAc/PE 40-60: 20%) = 0.48; **^{1}H NMR** (400 MHz, $CDCl_3$) δ_H 7.48-7.40 (5H, m, ArH), 5.94 (1H, s, H18), 5.66 (1H, dd, *J* = 9.8, 2.4 Hz, H21), 3.43 (3H, s, OMe), 2.43 (1H, dd, *J* = 14.3, 9.8 Hz, H20a), 2.31 (1H, d br, *J* = 14.3 Hz, H20b), 2.13 (3H, s, H24), 1.93 (3H, s, Me19), 1.17 (3H, s, Me22a), 1.15 (3H, s, Me22b).

Silyl enol ether 213

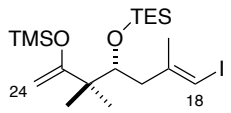

TMSOTf (17 μL, 95.1 μmol) was added dropwise to a stirred solution of ketone **201** (30.0 mg, 73.0 μmol) and Et_3N (31 μL, 219 μmol) in Et_2O (500 μL) at 0 °C. The resulting cloudy reaction mixture was stirred for 4 h at 0 °C before quenching with $NaHCO_3$ (500 μL). The layers were separated, and the aqueous phase extracted with Et_2O (3 × 500 μL). The combined organic phases were dried ($MgSO_4$) and the solvent removed under reduced pressure to afford the crude product **213** (35.0 mg, 72.5 μmol, 99%), which was used without further purification.

R_f (EtOAc/PE 40-60: 10%) = 0.74; **^{1}H NMR** (500 MHz, $CDCl_3$) δ_H 5.85 (1H, s, H18), 4.11 (1H, d, *J* = 2.0 Hz, H24a), 3.98 (1H, dd, *J* = 9.0, 1.5 Hz, H23), 3.96 (1H, d, *J* = 2.0 Hz, H24b), 2.31 (1H, dd, *J* = 13.7, 1.5 Hz, H20a), 2.18 (1H, dd, *J* = 13.7, 9.0 Hz), 1.81 (3H, s, Me19), 0.95 (9H, t, *J* = 7.9 Hz, $Si(CH_2CH_3)_3$), 0.54 (6H, q, *J* = 7.9 Hz, $Si(CH_2CH_3)_3$), 0.21 (9H, s, $SiMe_3$); **^{13}C NMR** (125 MHz, $CDCl_3$) δ_C 164.7, 145.7, 87.7, 74.6, 74.1, 45.4, 44.0, 25.0, 23.8, 18.9, 7.2, 5.6, 0.0; **IR** (thin film): ν_{max} 2955, 2877, 1619, 1378, 1274, 1252, 1091, 1010; $[\alpha]_D^{20}$ +2.9 (*c* 0.29, $CHCl_3$); **HRMS** (ESI^+) calculated for $C_{19}H_{39}O_2Si_2IH$ $[M+H]^+$ 483.1611, found 483.1593.

Aldehyde 227

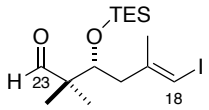

DIBAL (72 μL, 72 μmol, 1 M in hexanes) was added dropwise to a stirred solution of ester **220** (30.0 mg, 68.1 μmol) in PhMe (600 μL) at –78 °C. The reaction mixture was stirred at –78 °C for 1 h before quenching with MeOH (50 μL) and Na/K tartrate (500 μL) and allowed to warm to r.t.. The resulting emulsion was vigorously stirred at r.t. for 1 h until two distinct layers were observed. The layers were separated, and the aqueous phase extracted with EtOAc (3 × 1 mL). The combined organic phases were dried ($MgSO_4$) and

the solvent removed under reduced pressure. Purification by flash column chromatography (EtOAc/PE 40-60: 5%) afforded the product **227** as a colourless oil (25.2 mg, 63.6 μmol, 93%).

R_f (EtOAc/PE 40-60: 20%) = 0.83; **^{1}H NMR** (500 MHz, $CDCl_3$) δ_H 9.55 (1H, s, H23), 5.97 (1H, s, H18), 3.98 (1H, dd, *J* = 7.6, 4.0 Hz, H21), 2.35-2.27 (2H, m, H20), 1.84 (3H, s, Me18), 1.07 (3H, s, Me22a), 1.03 (3H, s, Me22b), 0.93 (9H, t, *J* = 8.0 Hz, $Si(CH_2C\underline{H}_3)_3$), 0.55 (6H, q, *J* = 8.0 Hz, $Si(C\underline{H}_2CH_3)_3$); **^{13}C NMR** (125 MHz, $CDCl_3$) δ_C 205.6, 143.9, 78.8, 74.0, 51.2, 43.7, 23.9, 18.5, 17.8, 6.9, 5.3; **IR** (thin film): ν_{max} 2953, 2875, 1725, 1464, 1378, 1274, 1097; **$[\alpha]_D^{20}$** +5.6 (*c* 1.0, $CHCl_3$); **HRMS** (ESI^+) calculated for $C_{15}H_{29}O_2SiINa$ $[M+Na]^+$ 419.0879, found 419.0903.

Alcohol 232 and *ent*-232

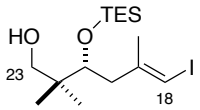

DIBAL (8.31 mL, 8.31 mmol, 1 M in hexanes) was added dropwise to a stirred solution of the ester **220** (1.80 g, 4.16 mmol) in CH_2Cl_2 (42 mL) at –78 °C. The reaction mixture was stirred at –78 °C for 30 min before the addition of an extra aliquot of DIBAL (4.16 mL, 4.16 mmol, 1 M in hexanes). The reaction mixture was warmed to –40 °C over 1 h before quenching with the successive addition of MeOH (2 mL) and Na/K tartrate (30 mL). The mixture was allowed to warm to r.t. and stirred for 2 h. The layers were separated, and the aqueous phase extracted with CH_2Cl_2 (3 × 20 mL). The combined organic phases were washed with brine (20 mL), dried ($MgSO_4$) and the solvent removed under reduced pressure. Purification by flash column chromatography (EtOAc/PE 40-60: 10% → 20%) afforded the product **232** as a colourless oil (1.31 g, 3.30 mmol, 79%, 90% brsm).

The enantiomeric product was analogously prepared from ester ***ent*-220** (1.00 g, 2.27 mmol) to give alcohol ***ent*-232** as a colourless oil (720 mg, 1.82 mmol, 73%).

R_f (EtOAc/PE 40-60: 30%) = 0.80; **^{1}H NMR** (500 MHz, $CDCl_3$) δ_H 5.98 (1H, s, H18), 3.72 (1H, dd, *J* = 8.6, 2.6 Hz, H21), 3.67 (1H, dd, *J* = 10.7, 3.2 Hz, H23a), 3.28 (1H, dd, *J* = 10.7, 7.4 Hz, H23b), 2.66 (1H, dd, *J* = 7.4, 3.4 Hz, OH), 2.48 (1H, dd, *J* = 14.1, 2.6 Hz, H20a), 2.36 (1H, dd, *J* = 14.1, 8.6 Hz, H20b), 1.85 (3H, d, *J* = 0.6 Hz, Me19), 1.04 (3H, s, Me22a), 0.96 (9H, t, *J* = 8.1 Hz, $Si(CH_2\underline{CH}_3)_3$), 0.80 (3H, s, Me22b), 0.59, 0.58 (6H, app dq, *J* = 8.0 Hz, $Si(\underline{CH}_2CH_3)_3$); **^{13}C NMR** (125 MHz, $CDCl_3$) δ_C 144.8, 78.2, 78.0, 70.0, 43.7, 39.5, 24.0, 23.3, 21.5, 7.1, 5.4; **IR** (thin film): ν_{max} 3477, 2955, 2927, 1459, 1318, 1274, 1090, 1006; **$[\alpha]_D^{20}$** +17.8 (**232**,

c 0.15, $CHCl_3$); $[\alpha]_D^{20}$ −14.7 (***ent*-232**, *c* 0.30, $CHCl_3$); **HRMS** (ESI^+) calculated for $C_{15}H_{31}O_2SiIH$ $[M+H]^+$ 399.1216, found 399.1217.

TMS ether 233 and *ent*-233

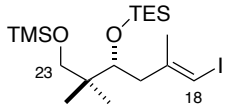

TMSCl (342 μL, 2.70 mmol) was added to a stirred solution of alcohol **232** (855 mg, 2.16 mmol), Et_3N (451 μL, 3.24 mmol) and DMAP (26.0 mg, 21.6 μmol) in CH_2Cl_2 (25 mL) at r.t.. The reaction mixture was stirred at r.t. for 1 h before quenching with MeOH (1 mL). The solvent was removed under reduced pressure and the residue resuspended in PE 40-60 before filtering over a pad of silica, eluting with PE 40-60. Removal of the solvent under reduced pressure afforded the TMS ether **233** as a colourless oil (924 mg, 1.96 mmol, 91%).

The enantiomeric product was analogously prepared from alcohol ***ent*-232** (100 mg, 252 μmol) to give TMS ether ***ent*-233** as a colourless oil (89 mg, 189 μmol, 75%).

$\mathbf{R_f}$ (EtOAc/PE 40-60: 20%) = 0.66; **^{1}H NMR** (500 MHz, $CDCl_3$) δ_H 5.88 (1H, s, H18), 3.77 (1H, dd, *J* = 8.8, 2.4 Hz, H21), 3.34 (1H, d, *J* = 9.6 Hz, H23a), 3.22 (1H, d, *J* = 9.6 Hz, H23b), 2.37 (1H, dd, *J* = 13.6, 2.4 Hz, H20a), 2.24 (1H, dd, *J* = 13.6, 8.8 Hz, H20b), 1.83 (3H, s, Me19), 0.94 (9H, t, *J* = 9.4 Hz, Si($\underline{CH_2}CH_3)_3$), 0.82 (3H, s, Me22a), 0.79 (3H, s, Me22b), 0.55 (6H, q, *J* = 9.4 Hz, Si($\underline{CH_2}CH_3)_3$), 0.08 (9H, s, $Si(CH_3)_3$); **^{13}C NMR** (125 MHz, $CDCl_3$) δ_C 145.8, 74.0, 69.2, 43.4, 40.3, 24.0, 21.1, 20.2, 7.2, 5.5, −0.6; **IR** (thin film): ν_{max} 2877, 2597, 1251, 1092, 1013, 874; $[\alpha]_D^{20}$ +9.6 (**233**, *c* 0.28, $CHCl_3$); $[\alpha]_D^{20}$ −9.0 (***ent*-233**, *c* 0.32, $CHCl_3$); **HRMS** (ESI^+) calculated for $C_{18}H_{39}O_2Si_2IH$ $[M+H]^+$ 471.1612, found 471.1615.

TES ether 325

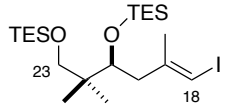

TESOTf (765 μL, 3.39 mmol) was added dropwise to a stirred solution of alcohol ***ent*-232** (1.22 g, 3.08 mmol) and 2,6-lutidine (535 μL, 4.62 mmol) in CH_2Cl_2 (35 mL) at −78 °C. The reaction mixture was stirred at −78 °C for 45 min before quenching with MeOH (1 mL) and $NaHCO_3$ (20 mL) and allowing to warm to r.t..

The layers were separated, and the aqueous phase extracted with CH_2Cl_2 (3 × 20 mL). The combined organic phases were washed with brine (20 mL), dried ($MgSO_4$) and the solvent removed under reduced pressure. Purification by flash column chromatography (EtOAc/PE 40-60: 10% → 20%) afforded the product **325** as a colourless oil (1.50 g, 2.93 mmol, 95%).

R_f (EtOAc/PE 40-60: 20%) = 0.68; **^{1}H NMR** (500 MHz, $CDCl_3$) δ_H 5.88 (1H, s, H18), 3.77 (1H, dd, *J* = 8.8, 2.4 Hz, H21), 3.34 (1H, d, *J* = 9.6 Hz, H23a), 3.22 (1H, d, *J* = 9.6 Hz, H23b), 2.37 (1H, dd, *J* = 13.6, 2.4 Hz, H20a), 2.24 (1H, dd, *J* = 13.6, 8.8 Hz, H20b), 1.83 (3H, s, Me19), 0.94 (9H, t, *J* = 9.4 Hz, Si($\underline{CH_2}CH_3)_3$), 0.82 (3H, s, Me22a), 0.79 (3H, s, Me22b), 0.55 (6H, q, *J* = 9.4 Hz, Si($\underline{CH_2}CH_3)_3$), 0.08 (9H, s, Si$(CH_3)_3$); **^{13}C NMR** (125 MHz, $CDCl_3$) δ_C 145.8, 74.0, 69.2, 43.4, 40.3, 24.0, 21.1, 20.2, 7.2, 5.5, –0.6; **IR** (thin film): ν_{max} 2877, 2597, 1251, 1092, 1013, 874; $[\alpha]_D^{20}$ +9.6 (*c* 0.28, $CHCl_3$); **HRMS** (ESI^+) calculated for $C_{18}H_{39}O_2Si_2IH$ $[M+H]^+$ 471.1612, found 471.1615.

8.5.2. Fragment union studies and the stereochemical reassignment of phormidolide A

Ketone 240

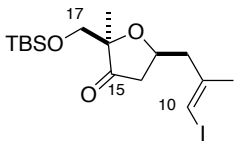

Dess-Martin Periodinane (311 mg, 733 μmol) was added to a stirred suspension of alcohol **203**[†††] (125 mg, 293 μmol) and $NaHCO_3$ (100 mg, 1.17 mmol) in wet CH_2Cl_2 (4 mL). The reaction mixture was stirred at r.t. until TLC monitoring indicated full consumption of the starting material (*ca.* 30 min). The reaction mixture was quenched by the addition of $NaHCO_3$ (2 mL) and $Na_2S_2O_3$ solution (2 mL) and stirred at r.t. for 30 min. The layers were separated, and the aqueous phase was extracted with CH_2Cl_2 (3 × 2 mL). The combined organic phases were dried ($MgSO_4$) and concentrated under reduced pressure. Purification by flash column chromatography (EtOAc/PE 40-60: 0% → 5%) afforded the product **240** as a colourless oil (123 mg, 290 μmol, 99%).

R_f (EtOAc/PE 40-60: 20%) = 0.71; **^{1}H NMR** (500 MHz, $CDCl_3$) δ_H 6.03 (1H, q, *J* = 0.9 Hz, H10), 4.33 (1H, app dq, *J* = 10.5, 6.1 Hz, H13), 3.64 (1H, d, *J* = 10.5 Hz, H17a), 3.53 (1H, d, *J* = 10.5 Hz, H17b), 2.71 (1H, dd, *J* = 14.3, 6.1 Hz, H14a), 2.55 (1H, dd, *J* = 14.3, 6.1 Hz, H14b), 2.48 (1H, dd, *J* = 17.4, 5.8 Hz, H12a), 2.19 (1H, dd, *J* = 17.4, 10.5 Hz, H12b), 1.92, (3H, d, *J* = 0.9 Hz, Me11), 1.09 (3H, s, Me16), 0.87 (9H, s, $SiMe_2$*t*Bu),

[†††] Alcohol **203** was synthesised by Garrett Muir

0.05, 0.02 (6H, s, $SiMe_2tBu$); **^{13}C NMR** (125 MHz, $CDCl_3$) δ_C 216.2, 144.1, 84.8, 77.5, 71.6, 67.3, 45.6, 43.3, 25.9, 24.6, 18.3, 17.7, –5.3, –5.6; **IR** (thin film): ν_{max} 2948, 2867, 1762, 1454, 1253, 1098, 898; $[\alpha]_D^{20}$ +16.3 (*c* 0.95, $CHCl_3$); **HRMS** (ESI^+) calculated for $C_{16}H_{29}O_3SiIH$ $[M+H]^+$ 425.1009, found 425.1006.

Alcohol 241

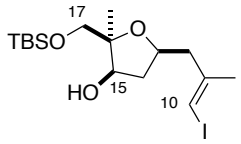

DIBAL (1.69 mL, 1.69 mmol, 1 M in hexanes) was added dropwise to a stirred solution of ketone **240** (239 mg, 563 μmol) in CH_2Cl_2 (6 mL) at –78 °C. The reaction mixture was stirred at –78 °C for 1 h before quenching with MeOH (500 μL), Na/K tartrate (5 mL) and the stirred mixture allowed to warm to r.t. over 3 h. The layers were separated, and the aqueous phase was extracted with CH_2Cl_2 (3 × 5 mL). The combined organic phases were dried ($MgSO_4$) and concentrated under reduced pressure. Purification by flash column chromatography (EtOAc/PE 40-60: 2%) afforded the product **241** as a colourless oil (238 mg, 559 μmol, 99%) as a single diastereomer.

R_f (EtOAc/PE 40-60: 20%) = 0.53; **^{1}H NMR** (500 MHz, $CDCl_3$) δ_H 5.99 (1H, s, H10), 4.14-4.11 (2H, m, H13, H15), 3.76 (1H, d, *J* = 10.3 Hz, H17a), 3.67 (1H, d, *J* = 10.3 Hz, H17b), 3.55 (1H, d, *J* = 6.2 Hz, OH15), 2.59 (1H, dd, *J* = 13.9, 6.8 Hz, H12a), 2.43 (1H, dd, *J* = 13.9, 6.3 Hz, H12b), 2.37-2.32 (1H, m, H14a), 1.88 (3H, s, Me11), 1.70-1.64 (1H, m, H14b), 1.15 (3H, s, Me16), 0.93 (9H, s, $SiMe_2tBu$), 0.13, 0.12 (6H, s, $SiMe_2tBu$); **^{13}C NMR** (125 MHz, $CDCl_3$) δ_C 144.9, 83.4, 79.3, 74.1, 67.9, 46.0, 41.0, 25.7, 24.3, 22.5, 18.0, –5.5, –5.8; **IR** (thin film): ν_{max} 3439, 2928, 2857, 1463, 1258, 1088 779; $[\alpha]_D^{20}$ –1.7 (*c* 0.24, $CHCl_3$); **HRMS** (ESI^+) calculated for $C_{16}H_{31}O_3SiIH$ $[M+H]^+$ 427.1165, found 427.1162.

Ester 243

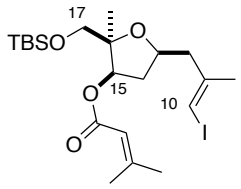

Method A: Yamaguchi esterification

Et_3N (325 μL, 2.34 mmol) was added to a stirred solution of dimethylacrylic acid (70.4 mg, 704 μmol) and TCBC (160 μL, 1.06 mmol) in PhH (7.5 mL). The solution was stirred for 30 min before the addition of a solution of alcohol **241** (100 mg, 235 μmol) and DMAP (86.0 mg, 704 μmol) in PhH (7.5 mL) *via* cannula, to which a white chunky precipitate immediately formed. The mixture was stirred for 3 h before filtering over SiO_2, eluting with Et_2O (15 mL) and the filtrate concentrated under reduced pressure. Purification by flash column chromatography (EtOAc/PE 40-60: 0% → 5%) afforded the product **243** as a colourless oil (103 mg, 202 μmol, 86%).

Method B: Keck esterification

DCC (2.27 mL, 2.27 mmol, 1 M in CH_2Cl_2) was added in one portion to a stirred solution of alcohol **241** (160 mg, 378 μmol), dimethylacrylic acid (227 mg, 2.27 mmol), DMAP (277 mg, 2.27 mmol) and DMAP·HCl (359 mg, 2.27 mmol) in CH_2Cl_2 (4 mL) at r.t.. The cloudy white suspension was stirred at r.t. for 24 h before quenching with NH_4Cl (5 mL). The layers were separated, and the aqueous phase was extracted with Et_2O (3 × 5 mL). The combined organic phases were dried ($MgSO_4$) and concentrated under reduced pressure. Purification by flash column chromatography (EtOAc/PE 40-60: 0% → 5%) afforded the product **243** as a colourless oil (178 mg, 350 μmol, 93%).

R_f (EtOAc/PE 40-60: 20%) = 0.72; **^{1}H NMR** (500 MHz, $CDCl_3$) δ_H 5.94 (1H, d, *J* = 1.0 Hz, H10), 5.66 (1H, sept, *J* = 1.2 Hz, =CH), 5.10 (1H, dd, *J* = 6.4, 3.9 Hz, H15), 4.22 (1H, ddt, *J* = 7.5, 6.8, 6.5 Hz, H13), 3.70 (1H, d, *J* = 9.7 Hz, H17a), 3.50 (1H, d, *J* = 9.7 Hz, H17b), 2.56 (1H, dd, *J* = 13.9, 6.8 Hz, H12a), 2.46 (1H, ddd, *J* = 13.8, 7.5, 6.6 Hz, H14a), 2.38 (1H, dd, *J* = 13.9, 6.6 Hz, H12b), 2.17 (3H, d, *J* = 1.7 Hz, $=CMe_aMe_b$), 1.91 (3H, d, *J* = 1.2 Hz, $=CMe_a\underline{Me}_b$), 1.85 (3H, d, *J* = 1.0 Hz, Me11), 1.70 (1H, ddd, *J* = 13.9, 6.4, 3.9 Hz, H14b), 1.20 (3H, s, Me16), 0.86 (9H, s, $SiMe_2tBu$), 0.03, 0.01 (6H, s, $SiMe_2tBu$); **^{13}C NMR** (125 MHz, $CDCl_3$) δ_C 165.7, 157.4, 144.9, 116.0, 84.5, 77.2, 74.5, 66.0, 46.3, 37.6, 27.4, 25.8, 24.5, 21.7, 20.3, 18.2, –5.5, –5.6; **IR** (thin film): ν_{max} 2927, 2853, 1723, 1561, 1444, 1144,1103; **$[\alpha]_D^{20}$** –13.0 (*c* 0.30, $CHCl_3$); **HRMS** (ESI^+) calculated for $C_{21}H_{37}O_4SiIH$ $[M+H]^+$ 509.1579, found 509.1572.

Alcohol 244

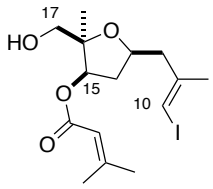

TsOH·H_2O (3.5 mg, 20.3 μmol) was added to a stirred solution of TBS ether **243** (103 mg, 203 μmol) in MeOH (1 mL) and CH_2Cl_2 (1 mL) at r.t.. The reaction mixture was stirred for 3 h at r.t., after which the reaction mixture was diluted with CH_2Cl_2 (5 mL) and quenched by the addition of $NaHCO_3$ (10 mL). The layers were separated, and the aqueous phase was extracted with CH_2Cl_2 (3 × 5 mL). The combined organic phases were dried ($MgSO_4$) and concentrated under reduced pressure. Purification by flash column chromatography (EtOAc/PE 40-60: 20%) afforded the product **244** as a colourless oil (54.6 mg, 138 μmol, 68%).

R_f (EtOAc/PE 40-60: 20%) = 0.23; **^{1}H NMR** (400 MHz, $CDCl_3$) δ_H 5.99 (1H, s, H10), 5.70 (1H, s, =CH), 5.08 (1H, dd, *J* = 6.8, 4.9 Hz, H15), 4.22 (1H, app qn, *J* = 6.8 Hz, H13), 3.57 (1H, dd, *J* = 11.8, 6.3 Hz, H17a), 3.51 (1H, dd, *J* = 11.8, 6.2 Hz, H17b), 2.57 (1H, dd, *J* = 13.9, 6.4 Hz, H12a), 2.52 (1H, ddd, *J* = 13.6, 6.8, 6.8 Hz, H14a), 2.42 (1H, dd, *J* = 13.9, 6.3 Hz, H12b), 2.18 (3H, s, =C$\underline{Me}_a$Me$_b$), 1.93 (3H, s, =CMe$_a$$\underline{Me}_b$), 1.87 (3H, s, Me11), 1.72 (1H, ddd, *J* = 13.5, 7.1, 4.9 Hz, H14b), 1.26 (3H, s, Me16); **^{13}C NMR** (100 MHz, $CDCl_3$) δ_C 166.4, 159.1 144.6, 115.3, 84.1, 78.1, 77.2, 74.1, 65.8, 46.0, 37.7, 27.6, 24.5, 21.7, 20.4; **IR** (thin film): ν_{max} 3511, 2919, 1717, 1649, 1377, 1228, 1145, 1008; **$[\alpha]_D^{20}$** +2.2 (*c* 0.19, $CHCl_3$); **HRMS** (ESI^+) calculated for $C_{15}H_{23}O_4INa$ $[M+Na]^+$ 417.0539, found 417.0535.

Aldehyde 245

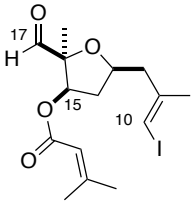

Dess-Martin Periodinane (250 mg, 583 μmol) was added to a stirred suspension of alcohol **244** (46.0 mg, 117 μmol) and $NaHCO_3$ (48 mg, 1.17 mmol) in wet CH_2Cl_2 (2 mL). The reaction mixture was stirred at r.t. for 30 min before quenching by the addition of $NaHCO_3$ (2 mL) and $Na_2S_2O_3$ solution (2 mL) and stirred at r.t. for 30 min. The layers were separated, and the aqueous phase was extracted with CH_2Cl_2 (3 × 2 mL). The combined organic phases were dried ($MgSO_4$) and concentrated under reduced pressure. Purification by flash column chromatography (EtOAc/PE 40-60: 0% → 5%) afforded the product **245** as a colourless oil

(30.3 mg, 77.2 μmol, 86% brsm), alongside with 20-30% of the C10 protodeiodinated product that is inseparable at this stage.

R_f (EtOAc/PE 40-60: 20%) = 0.35; **^{1}H NMR** (500 MHz, $CDCl_3$) δ_H 9.63 (1H, s, H17), 6.03 (1H, q, *J* = 1.1 Hz, H10), 5.59 (1H, s, =CH), 5.19 (1H, dd, *J* = 6.4, 4.1 Hz, H15), 4.41 (1H, dt, *J* = 13.7, 6.6 Hz, H13), 2.70 (1H, dd, *J* = 14.0, 6.7 Hz, H12a), 2.55 (1H, ddd, *J* = 13.7, 7.2, 6.4 Hz, H14a), 2.50 (1H, dd, *J* = 14.0, 6.4 Hz, H12b), 2.15 (3H, d, *J* = 1.3 Hz, =C$\underline{Me}_a$Me$_b$), 1.90 (6H, s, Me11, =CMe$_a$$\underline{Me}_b$), 1.79 (1H, ddd, *J* = 13.7, 6.2, 4.1 Hz, H14b), 1.31 (3H, s, Me16); **^{13}C NMR** (125 MHz, $CDCl_3$) δ_C 201.0, 165.1, 159.3, 144.4, 114.9, 87.6, 79.7, 77.6, 76.8, 45.9, 37.7, 27.5, 24.4, 20.4, 19.6; **IR** (thin film): ν_{max} 2918, 1738, 1723, 1649, 1443, 1377, 1224, 1138, 1076; $[\alpha]_D^{20}$ −3.4 (*c* 0.29, $CHCl_3$); **HRMS** (ESI^+) calculated for $C_{15}H_{21}IO_4Na$ $[M+Na]^+$ 415.0382, found 415.0373.

General protocol for the vinylmetal addition of the C18-C23 vinyl iodide to aldehyde 245

*t*BuLi (13 eq., molarity in pentane titrated before use) was added dropwise (down the side of the flask) to a stirred solution of vinyl iodide **233** or ***ent*-233** (6.5 eq., dried by azeotroping with PhH and over CaH_2) in Et_2O (0.1 M relative to vinyl iodide) at −78 °C, taking care that the reaction temperature does not exceed −78 °C. The solution was stirred for 30 seconds before the dropwise addition of a freshly prepared solution of $MgBr_2{\cdot}OEt_2$ (19 eq., 0.6 M in Et_2O) into the reaction mixture at −78 °C. The mixture was stirred for 5 min at −78 °C before the dropwise addition of aldehyde **245** (1 eq., dried by azeotroping with PhH × 3) in CH_2Cl_2 (0.1 M relative to aldehyde) *via* cannula (down the side of the flask). The pale-yellow reaction mixture was stirred at −78 °C for 1 h before quenching with NH_4Cl (3 mL) and warmed to r.t.. The layers were separated, and the aqueous phase was extracted with CH_2Cl_2. The combined organic phases were dried ($MgSO_4$) and concentrated under reduced pressure. Purification by flash column chromatography (Et_2O/PE 40-60: 0% → 5%) afforded the crude product as a colourless oil as an inseparable mixture of diastereomers, alongside with their C10 protodeiodinated counterparts. The crude product mixture was subjected to the acetonide formation sequence outlined below.

General protocol for the synthesis of diacetonides 252, 254 and 257

PPTS (one crystal) was added to a stirred solution of *bis*-silyl ethers **249**, **253** or **256** (1 eq.) in CH_2Cl_2 (100 μL) and methanol (100 μL) at r.t.. The reaction mixture was stirred for 16 h at r.t. before quenching with $NaHCO_3$ and diluting with EtOAc. The layers were separated, and the aqueous phase was extracted with EtOAc. The combined organic phases were dried ($MgSO_4$) and concentrated under reduced pressure. The crude triol was dissolved in MeOH (150 μL) and K_2CO_3 (6 mg, *ca.* 10 eq.) was added. The pale-yellow mixture was stirred overnight at r.t. before quenching with NH_4Cl and diluted with EtOAc. The layers were separated, and the aqueous phase was extracted with EtOAc. The combined organic phases were dried

($MgSO_4$) and concentrated under reduced pressure. The crude tetraol was redissolved in CH_2Cl_2 (100 μL) and 2,2-dimethoxypropane (100 μL) and PPTS (one crystal) was added. The solution was stirred for a further 16 h before quenching with $NaHCO_3$ and diluting with EtOAc. The layers were separated, and the aqueous phase was extracted with EtOAc. The combined organic phases were dried ($MgSO_4$) and concentrated under reduced pressure. Purification by preparative thin layer chromatography (EtOAc/PE 40-60: 20%) afforded the diacetonide as a colourless oil.

Alcohol **253** *and 15,17-anti acetonide* **252**

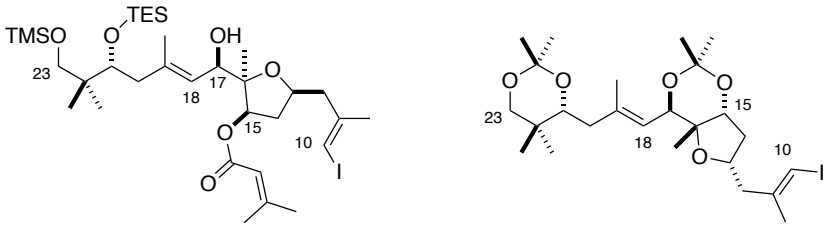

The addition reaction was performed according to the general protocol described above, using vinyl iodide **233** (42.0 mg, 88.9 μmol), *t*BuLi (120 μL, 185 μmol, 1.5 M in pentane), $MgBr_2{\cdot}OEt_2$ (381 μL, 229 μmol, 0.6 M in Et_2O), and aldehyde **245** (4.9 mg, 12.7 μmol) to afford the crude product **253** (7.2 mg, 9.78 μmol, 77%), a colourless oil as an inseparable 5:1 mixture of diastereomers at C17. alongside with the C10 protodeiodinated material.

The crude product was transformed to the corresponding acetonide **252** according to the general protocol described above to afford the pure diacetonide **252** as a colourless oil (1.3 mg, 2.37 mmol, 24% over three steps)

R_f (EtOAc/PE 40-60: 20%) = 0.85; **^{1}H NMR** (500 MHz, $CDCl_3$) δ_H 5.97 (1H, q, *J* = 0.9 Hz, H10), 5.19 (1H, dq, *J* = 8.6, 1.0 Hz, H18), 4.40 (1H, d, *J* = 8.6 Hz, H17), 4.21-4.14 (1H, m, H13), 3.94 (1H, dd, *J* = 7.0, 2.1 Hz, H15), 3.64 (1H, dd, *J* = 9.0, 2.7 Hz, H21), 3.61 (1H, d, *J* = 11.4 Hz, H23a), 3.28 (1H, d, *J* = 11.4 Hz, H23b), 2.63 (1H, dd, *J* = 13.9, 7.7 Hz, H12a), 2.48 (1H, dd, *J* = 13.9, 5.5 Hz, H12b), 2.32 (1H, app dt, *J* = 13.9, 7.0 Hz, H14a), 2.11-2.01 (2H, m, H20), 1.85 (3H, d, *J* = 0.9 Hz, Me11), 1.73-1.65 (4H, m, H14b, Me19), 1.39 (3H, s, $\underline{Me}_AMe_BCO(O))^A$, 1.38 (3H, s, $\underline{Me}_AMe_BCO(O))^B$, 1.36 (3H, s, $Me_A\underline{Me}_BCO(O))^B$, 1.34 (3H, s, $Me_A\underline{Me}_BCO(O))^A$, 1.06 (3H, s, Me16), 1.01 (3H, s, Me22a), 0.74 (3H, s, Me22b); **^{13}C NMR** (125 MHz, $CDCl_3$) δ_C 145.3, 137.6, 123.0, 100.3^A, 98.6^B, 87.0, 77.7, 76.6, 76.1, 75.5, 72.2, 72.1, 46.4, 39.9, 38.7, 36.7, 32.9, 29.7^B, 25.4^A, 24.2, 23.8^A, 21.8, 18.9^B, 18.5, 18.0, 17.8; **IR** (thin film): ν_{max} 2925, 1460, 1375, 1223, 1100; $\mathbf{[\alpha]_D^{20}}$ +19.5 (*c* 0.06, $CHCl_3$); **HRMS** (ESI^+) calculated for $C_{25}H_{41}O_5IH$ $[M+H]^+$ 549.2077, found 549.2082.

^{A}Signals attributed to the C15,C17 acetonide ^{B}Signals attributed to the C21,C23 acetonide

Alcohol **249** *and 15,17-syn acetonide* **254**

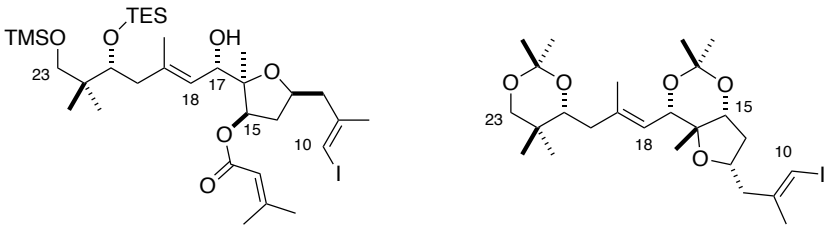

The addition reaction was performed according to the general protocol described above except omitting the addition of $MgBr_2OEt_2$, using vinyl iodide **233** (42.0 mg, 88.9 μmol), *t*BuLi (97 μL, 185 μmol, 1.9 M in pentane), and aldehyde **245** (4.9 mg, 12.7 μmol) to afford the crude product **249** (3.5 mg, 4.74 μmol, 37%), a colourless oil as an inseperable 4:1 mixture of diastereomers at C17, alongside with the C10 protodeiodinated material.

The crude product was transformed to the corresponding acetonide **254** according to the general protocol described above to afford the pure diacetonide as a colourless oil (1.8 mg, 3.28 mmol, 69% over three steps). Owing to competing lithium/iodine exchange at C10 from the formed vinyllithium species in the previous step, the product acetonide contains a 1:1 mixture of the C10 protodeiodinated species that was inseparable.

R_f (EtOAc/PE 40-60: 20%) = 0.87; **^{1}H NMR** (500 MHz, $CDCl_3$) δ_H 5.98 (1H, s, H10), 5.55 (1H, d, *J* = 8.6 Hz, H18), 4.50 (1H, d, *J* = 8.6 Hz, H17), 4.22-4.19 (1H, m, H13), 4.11 (1H, app d, *J* = 4.5 Hz, H15), 3.81 (1H, dd, *J* = 7.0, 2.2 Hz, H21), 3.66 (1H, d, *J* = 11.6 Hz, H23a), 3.27 (1H, d, *J* = 11.5 Hz, H23b), 2.73 (1H, dd, *J* = 13.5, 7.8 Hz, H12a), 2.44 (1H, dd, *J* = 13.5, 5.8 Hz, H12b), 2.38-2.30 (1H, m, H14a), 2.25 (1H, dd, *J* = 15.5 Hz, 7.0 Hz, H20a), 1.98-1.93 (1H, m, H20b), 1.88 (3H, d, *J* = 1.0 Hz, Me11), 1.76 (3H, s, Me19), 1.74-1.66 (1H, m, H14b), 1.49 (3H, s, $\underline{Me}_AMe_BCO(O))^A$, 1.42 (3H, s, $\underline{Me}_AMe_BCO(O))^A$, 1.42 (3H, s, $\underline{Me}_AMe_BCO(O))^B$, 1.37 (3H, s, $\underline{Me}_AMe_BCO(O))^B$, 1.03 (3H, s, Me22a), 0.93 (3H, s, Me16), 0.74 (3H, s, Me22b); **^{13}C NMR** (125 MHz, $CDCl_3$) δ_C 145.6, 140.2, 121.3, 98.5^B, 97.4^A, 78.8, 77.0, 76.9, 75.3, 74.5, 72.3, 69.7, 46.8, 38.5, 36.9, 32.9, 30.0^A, 29.9^B, 24.4, 21.8, 20.6, 19.2^A, 19.0, 18.8^B, 18.1; **IR** (thin film): ν_{max} 2928, 1464, 1377, 1261, 1129, 1098; $\mathbf{[\alpha]_D^{20}}$ +17.9 (*c* 0.08, $CHCl_3$); **HRMS** (ESI^+) calculated for $C_{25}H_{41}O_5IH$ $[M+H]^+$ 549.2077, found 549.2078.

Proof of 17S configuration in **249***: (R)- and (S)-MTPA-***255**

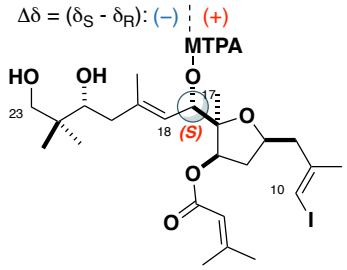

The assigned configuration at C17 was confirmed by forming the diastereomeric MTPA esters of alcohol **249** described below: DCC (15 µL, 14.9 µmol, 1 M in CH_2Cl_2) was added dropwise to a stirred solution of alcohol **254** (2.75 mg, 3.73 µmol), (*R*) or (*S*)-MTPA (3.5 mg, 14.9 µmol) and DMAP (one crystal) in CH_2Cl_2 (50 µL). The reaction mixture was stirred at r.t. for 16 h before filtering through a pad of silica‡‡‡ The crude product was dissolved in MeOH (25 µL) and CH_2Cl_2 (25 µL) and PPTS (one crystal) was added. The solution was stirred at r.t. for 24 h before quenching with $NaHCO_3$ (one drop), dried ($MgSO_4$), filtered and the solvent removed under reduced pressure to afford the (*S*)-MTPA ester diols [(*S*)-MTPA-**255**, 1.0 mg, 1.30 mmol, 46% over two steps] or (*R*)-MTPA ester diols [(*R*)-MTPA-**255**, 1.0 mg, 1.30 mmol, 46% over two steps. as a colourless oil.

(*S*)-MTPA-**255**

R_f (EtOAc/PE 40-60: 20%) = 0.25; **^{1}H NMR** (500 MHz, $CDCl_3$) δ_H 5.81 (1H, d, *J* = 10.0 Hz, H17), 5.79 (1H, s, H10), 5.66 (1H, s, =CH), 5.14 (1H, d, *J* = 10.0 Hz, H18), 5.04 (1H, dd, *J* = 7.0, 5.8 Hz, H15), 4.40 (1H, d, *J* = 10.8 Hz, H23a), 4.18 (1H, m, H13), 4.01 (1H, d, *J* = 10.8 Hz, H23b), 3.48 (1H, m, H21), 2.43 (1H, m, H14a), 2.41 (1H, m, H12a), 2.26 (1H, m, H12b), 2.19 (3H, s, =C$\underline{Me}_a$Me$_b$), 2.11 (1H, m, H20a), 1.94 (1H, m, H20b), 1.93 (3H, s, =CMe$_a$$\underline{Me}_b$), 1.82 (3H, s, Me11), 1.75 (3H, s, Me19), 1.65 (1H, m, H14b), 1.17 (3H, s, Me16), 0.92 (3H, s, Me22a), 0.88 (3H, s, Me22b)

(*R*)-MTPA-**255**

R_f (EtOAc/PE 40-60: 20%) = 0.22; **^{1}H NMR** (500 MHz, $CDCl_3$) δ_H 5.88 (1H, s, H10), 5.73 (2H, m, =CH, H17), 5.33 (1H, s, H18), 4.95 (1H, dd, *J* = 7.8, 7.0 Hz, H15), 4.29 (1H, d, *J* = 10.4 Hz, H23a), 4.09 (1H, d, *J* = 10.4 Hz, H23b), 4.09 (1H, m, H13), 2.52 (1H, m, H12a), 3.50 (1H, m, H21), 2.51 (1H, m, H20a), 2.32 (1H, m, H12b), 2.25 (1H, m, H20b), 2.21 (3H, s, =C$\underline{Me}_a$Me$_b$), 2.13 (1H, m, H14a), 1.98 (3H, s, =CMe$_a$$\underline{Me}_b$), 1.81

‡‡‡ Analysis of the MTPA esters at this stage gave inconclusive results

(3H, s, Me11), 1.76 (3H, s, Me19), 1.14 (3H, s, Me16), 1.10 (1H, m, H14b), 0.92 (3H, s, Me22a), 0.88 (3H, s, Me22b)

Alcohol **256** *and 21-epi-anti acetonide* **257**

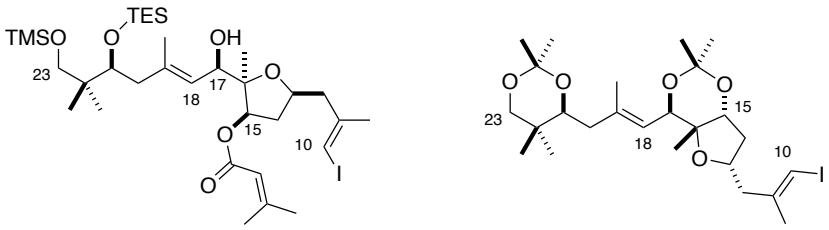

The addition reaction was performed according to the general protocol described above, using vinyl iodide ***ent*-233** (42.0 mg, 88.9 μmol), *t*BuLi (97 μL, 185 μmol, 1.9 M in pentane), $MgBr_2{\cdot}OEt_2$ (381 μL, 229 μmol, 0.6 M in Et_2O), and aldehyde **245** (4.9 mg, 12.7 μmol) to afford the crude product **256** (5.0 mg, 6.78 μmol, 53%), a colourless oil as an inseparable 5:1 mixture of diastereomers at C17, alongside with the C10 protodeiodinated material.

The crude product was transformed to the corresponding acetonide **257** according to the general protocol described above to afford the pure diacetonide **257** as a colourless oil (1.8 mg, 3.28 mmol, 48% over three steps)

R_f (EtOAc/PE 40-60: 20%) = 0.83; **^{1}H NMR** (500 MHz, $CDCl_3$) δ_H 5.98 (1H, q, *J* = 0.8 Hz, H10), 5.19 (1H, dq, *J* = 8.6, 1.2 Hz, H18), 4.42 (1H, d, *J* = 8.6 Hz, H17), 4.22-4.16 (1H, m, H13), 3.95 (1H, dd, *J* = 6.9, 1.9 Hz, H15), 3.77 (1H, dd, *J* = 9.2, 2.4 Hz, H21), 3.62 (1H, d, *J* = 11.4 Hz, H23a), 3.27 (1H, d, *J* = 11.4 Hz, H23b), 2.64 (1H, dd, *J* = 13.8, 7.8 Hz, H12a), 2.49 (1H, dd, *J* = 13.9, 6.2 Hz, H12b), 2.33 (1H, app dt, *J* = 14.0, 6.2 Hz, H14a), 2.21-2.18 (1H, m, H20a), 2.03-1.97 (1H, m, H20b), 1.86 (3H, d, *J* = 0.9 Hz, Me11), 1.76 (3H, d, *J* = 1.0 Hz, Me19), 1.75-1.68 (1H, m, H14b), 1.42 (3H, s, $\underline{Me}_AMe_BCO(O))^B$, 1.39 (3H, s, $\underline{Me}_AMe_BCO(O))^A$, 1.38 (3H, s, $Me_A\underline{Me}_BCO(O))^B$, 1.35 (3H, s, $Me_A\underline{Me}_BCO(O))^A$, 1.07 (3H, s, Me16), 1.02 (3H, s, Me22a), 0.73 (3H, s, Me22b); **^{13}C NMR** (125 MHz, $CDCl_3$) δ_C 145.3, 138.9, 120.7, 100.4^A, 98.5^B, 86.9, 78.2, 76.9, 76.7, 76.1, 71.9, 71.0, 46.5, 39.4, 36.6, 32.9, 30.9, 29.8^B, 25.3^A, 24.2, 23.6^A, 18.8^B, 18.7, 18.3, 18.1; **IR** (thin film): ν_{max} 2928, 2857, 1465, 1377, 1222, 1090, 1021; $[\alpha]_D^{20}$ –22.9 (*c* 0.05, $CHCl_3$); **HRMS** (ESI^+) calculated for $C_{25}H_{41}O_5INa$ $[M+Na]^+$ 571.1891, found 571.1885.

[A]Signals attributed to the C15,C17 acetonide [B]Signals attributed to the C21,C23 acetonide

Table of ^{1}H NMR data of phormidolide A triacetonide 151 and diacetonides 252, 254 and 257

	Phm A triacetonide ^{1}H (ppm)	**252** (15,17-*anti*)			**254** (15,17-*syn*)			**257** (21-*epi*-15,17-*anti*)		
		^{1}H	Δ	|Δ|	^{1}H	Δ	|Δ|	^{1}H	Δ	|Δ|
Ac1	1.34	1.34	0.00	0.00	1.49	0.15	0.15	1.35	0.01	0.01
Ac2	1.38	1.39	0.01	0.01	1.38	0.00	0.00	1.39	0.01	0.01
H13*	4.16	4.17	0.01	0.01	4.11	-0.05	0.05	4.19	0.03	0.03
H14A	2.32	2.32	0.00	0.00	2.34	0.02	0.02	2.33	0.01	0.01
H14B	1.75	1.70	-0.05	0.05	1.72	-0.03	0.03	1.71	-0.04	0.04
H15*	3.94	3.94	0.00	0.00	4.21	0.27	0.27	3.95	0.01	0.01
Me16	1.07	1.06	-0.01	0.01	0.93	-0.14	0.14	1.07	0.00	0.00
H17	4.42	4.40	-0.02	0.02	4.50	0.08	0.08	4.42	0.00	0.00
H18	5.18	5.19	0.01	0.01	5.55	0.37	0.37	5.19	0.01	0.01
Me19	1.74	1.72	-0.02	0.02	1.76	0.02	0.02	1.76	0.02	0.02
H20A	2.20	2.09	-0.11	0.11	2.25	0.05	0.05	2.18	-0.02	0.02
H20B	2.03	2.05	0.02	0.02	1.98	-0.05	0.05	2.03	0.00	0.00
H21	3.70	3.64	-0.06	0.06	3.81	0.11	0.11	3.78	0.08	0.08

*In the paper that describes the formation of the phormidolide triacetonide derivative, the ^{1}H values for H13 and H15 were erroneously swapped. A reexamination of their 2D ^{1}H-^{1}H COSY data as well as our NMR data supports this conclusion. Specifically, the signal attributed to δ_H 4.1x ppm couples to δ_H 2.50 and 2.34 ppm (signals that are attributed to H12). This means the signal attributed to 4.1x ppm arises from H13, rather than H15.

Table of ^{13}C NMR data of phormidolide A triacetonide 151 and diacetonides 252, 254 and 257

	Phm A triacetonide ^{13}C (ppm)	**252** (15,17-*anti*)			**254** (15,17-*syn*)			**257** (21-*epi*-15,17-*anti*)		
		^{13}C	Δ	|Δ|	^{13}C	Δ	|Δ|	^{13}C	Δ	|Δ|
Ac1	23.7	23.8	0.10	0.10	20.5	-3.2	3.2	23.6	0.1	0.1
Ac2	25.3	25.4	0.10	0.10	30.0	4.7	4.7	25.3	0.0	0.0
C13	76.8	76.6	-0.20	0.20	74.5	-2.3	2.3	76.7	-0.1	0.1
C14	36.7	36.7	0.00	0.00	36.9	0.2	0.2	36.6	-0.1	0.1
C15	78.2	77.7	-0.50	0.50	75.3	-2.9	2.9	78.2	0.0	0.0
C16	87.0	87.0	0.00	0.00	78.8	-8.2	8.2	86.9	-0.1	0.1
Me16	18.4	18.9	0.50	0.50	19.2	0.8	0.8	18.7	0.3	0.3
C17	71.8	73.0	1.20	1.20	70.0	-1.8	1.8	71.9	0.1	0.1
C18	120.3	123.0	2.70	2.70	121.5	1.2	1.2	120.7	0.4	0.4
Me19	18.2	17.8	-0.40	0.40	19.0	0.8	0.8	18.3	0.1	0.1
C20	39.0	40.0	1.00	1.00	38.5	-0.5	0.5	39.4	0.4	0.4
C21	77.6	76.1	-1.50	1.50	76.9	-0.7	0.7	76.1	-1.5	1.5

8.5.3. DFT optimised geometry for the Mg-chelated C10-C17 aldehyde

Structure optimisation was conducted as follows: A conformational search was carried out in MacroModel[192] using a hybrid of Monte Carlo multiple–minimum (MCMM)[193]/low–mode sampling[194] with the Merck Molecular Force Field (MMFF),[195] interfaced with Maestro 9.3.[196] The searches were carried out with a sufficient number of steps to find all conformers within 10 kJ $mol^{-1}$of the global minimum. All conformers within 10 kJ mol^{-1} of the global minimum were then further subjected to quantum mechanical calculations at the B3LYP[197]/6-31G** level of theory, implemented with Jaguar 7.9. The free energy in solution was derived from structures optimised in the gas phase by means of a single point calculation using B3LYP[197]/6-31G** level of theory with the polarisable continuum model (PCM) as implemented in the Jaguar program (version 9.3), using diethyl ether (probe radius = 2.74 Å) as the solvent. These values were used to correct the Gibbs free energy derived from the DFT calculations.

Mg-chelate structure 256

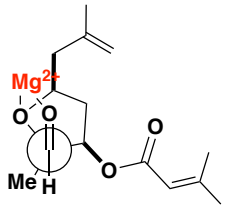

B3LYP/6-31G Free Energy:**	**B3LYP/6-31G** Free Energy in solution:**
–1085.2570 Hartrees	–1085.5556 Hartrees
Number of imaginary frequencies: 0	

Coordinates for the lowest energy conformer

Atom	x	y	z
C1	-0.2603	-0.3545	0.8179
C2	0.6585	0.7693	0.2948
C3	2.0712	0.3112	0.6238
O4	1.9797	-1.1941	0.5970
C5	0.5873	-1.6610	0.7018
O6	-1.4241	-0.5576	0.0355
C7	3.1665	0.6656	-0.4002
C8	-2.4935	0.3522	0.3466
O9	-2.2700	1.2147	1.1676
C10	-3.6643	0.0194	-0.4323
C11	-4.8595	0.6748	-0.3861
C12	-5.1696	1.8555	0.4833
C13	-5.9863	0.1980	-1.2565

C14	3.6692	2.1061	-0.3786
C15	4.5448	2.4821	0.7912
C16	3.3358	2.9404	-1.3723
C17	0.2760	-2.3904	-0.5910
C18	0.4320	-2.6235	1.8844
O19	1.1245	-2.5162	-1.4966
H20	-0.5293	-0.1781	1.8634
H21	0.4119	1.7257	0.7587
H22	0.5150	0.8767	-0.7878
H23	2.3918	0.5722	1.6342
H24	2.7706	0.4926	-1.4329
H25	4.0630	0.0220	-0.1970
H26	-3.5541	-0.8324	-1.0949
H27	-4.3123	2.2315	1.0363
H28	-5.5934	2.6601	-0.1292
H29	-5.9557	1.5765	1.1973
H30	-6.2982	0.9994	-1.9375
H31	-5.7251	-0.6823	-1.8473
H32	-6.8633	-0.0373	-0.6415
H33	4.0436	2.3356	1.7554
H34	5.4664	1.8864	0.8072
H35	4.8319	3.5332	0.7275
H36	3.6652	3.9746	-1.3632
H37	2.7319	2.6361	-2.2234
H38	-0.7051	-2.8595	-0.7134
H39	1.0348	-3.5285	1.7661
H40	0.7373	-2.1147	2.8022
H41	-0.6184	-2.9141	1.9840
Mg42	2.8637	-1.6683	-1.0962

8.5.4. Synthesis of the C24-C33 fragment

Alkyne 261

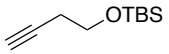

TBSCl (282 mg, 1.87 mmol) was added to a stirred solution of 4-butyn-1-ol (100 mg, 1.78 mmol) and imidazole (295 mg, 1.96 mmol) in CH_2Cl_2 (4 mL). The cloudy mixture was stirred at r.t. for 16 h before quenching with NH_4Cl (4 mL). The layers were separated and the aqueous phase extracted with CH_2Cl_2 (3 × 5 mL). The combined organic phases were dried ($MgSO_4$) and the solvent removed under reduced pressure. Purification by flash column chromatography (Et_2O/PE 30-40: 0 → 15%) afforded the product **261** as a colourless liquid (233 mg, 1.26 mmol, 71%).

R_f (EtOAc/PE 40-60: 20%) = 0.71; **^{1}H NMR** (500 MHz, $CDCl_3$) δ_H 3.74 (2H, t, *J* = 7.1 Hz, C<u>H</u>$_2$OTBS), 2.40 (2H, td, *J* = 7.1, 2.6 Hz, ≡CC<u>H</u>$_2$), 1.96 (1H, t, *J* = 2.6 Hz, ≡C<u>H</u>), 0.90 (9H, s, SiMe$_2$*t*<u>Bu</u>), 0.08 (6H, s, Si<u>Me</u>$_2$*t*Bu).

Data in agreement with that presented by Sneddon[198]

Alcohol 264

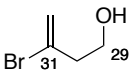

A mixture of 2,3-dibromoprop-1-ene (293 μL, 3.00 mmol), formalin (150 μL, 2.00 mmol, 37% wt solution in water), $SnCl_2{\cdot}2H_2O$ (677 mg, 3.00 mmol), KI (996 mg, 6.00 mmol) in water (5 mL) was vigorously stirred for 1 h, during which an opaque yellow suspension was formed. The mixture was diluted with Et_2O (10 mL), the layers separated and the aqueous phase extracted with Et_2O (3 × 5 mL). The combined organic phases were washed with brine (75 mL), dried (Na_2SO_4) and the solvent removed under reduced pressure. Purification by flash column chromatography (Et_2O/PE 30-40: 20%) afforded the alcohol **264** as a colourless liquid (343 mg, 2.27 mmol, 76%)

R_f (EtOAc/PE 40-60: 50%) = 0.71; **^{1}H NMR** (500 MHz, $CDCl_3$) δ_H 5.71 (1H, dt, *J* = 1.7, 1.2 Hz, C<u>H</u>$_a$H$_b$=C31), 5.54 (1H, d, *J* = 1.7 Hz, CH$_a$<u>H</u>$_b$=C31), 3.82 (2H, q, *J* = 5.9 Hz, H29), 2.68 (2H, td, *J* = 5.9, 0.9 Hz, H30), 1.51 (1H, t, *J* = 6.0 Hz, OH); **^{13}C NMR** (125 MHz, $CDCl_3$) δ_C 130.4, 119.4, 60.0, 44.4.

Data in agreement with that presented by Campbell[199]

TBS ether 265

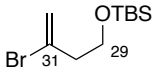

TBSCl (210 mg, 1.39 mmol) was added to a stirred solution of alcohol **264** (200 mg, 1.32 mmol) and imidazole (99.2 mg, 1.46 mmol) in CH_2Cl_2 (4 mL). The cloudy mixture was stirred at r.t. for 16 h before quenching with NH_4Cl (5 mL). The layers were separated and the aqueous phase extracted with CH_2Cl_2 (3 × 5 mL). The combined organic phases were dried ($MgSO_4$) and the solvent removed under reduced pressure. Purification by flash column chromatography (EtOAc/PE 40-60: 0 → 5%) afforded the product **265** as a colourless liquid (313 mg, 1.18 mmol, 89%).

R_f (EtOAc/PE 40-60: 20%) = 0.82; **^{1}H NMR** (400 MHz, $CDCl_3$) δ_H 5.63 (1H, d, *J* = 1.5 Hz, C$\underline{H}_a$H$_b$=C31), 5.46 (1H, d, *J* = 1.5 Hz, CH$_a$$\underline{H}_b$=C31), 3.79 (2H, t, *J* = 6.3 Hz, H29), 2.62 (2H, td, *J* = 6.3, 1.5 Hz, H30), 0.89 (9H, s, SiMe$_2$*t*$\underline{Bu}$), 0.07 (6H, s, Si$\underline{Me}_2$*t*Bu).

Data in agreement with that presented by Liu[200]

Bromoketone 269 *via* enol ether 267

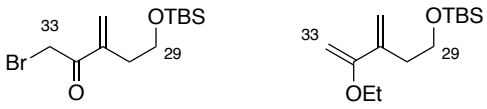

$Pd(PPh_3)_4$ (2.2 mg, 1.90 μmol) was added to a stirred suspension of vinyl bromide **265** (25.0 mg, 94.2 μmol), vinyl stannane **266**[§§§] (37.5 mg, 104 μmol), CuI (20.0 mg, 105 μmol), LiCl (7.5 mg, 177 μmol) in THF (500 μL). The resulting green-brown suspension was stirred for 16 h at r.t. before filtering over Celite® and a thin pad of SiO_2. The resulting filtrate was concentrated under reduced pressure to afford the crude enol ether **267** as a colourless liquid (21.0 mg, 82.0 μmol, 87%). An analytically pure sample of the enol ether was not obtained as the enol ether was unstable and degraded on further purification.

NBS (3.0 mg, 17.1 μmol) was added to a stirred solution of the crude enol ether **267** (4.0 mg, 15.6 μmol) in CH_2Cl_2 (200 μL) at 0 °C. The reaction mixture was stirred for 10 min before quenching with $Na_2S_2O_3$ (200 μL) and the layers separated. The aqueous phase was extracted with CH_2Cl_2 (3 × 200 μL). The combined organic phases were dried ($MgSO_4$) and the solvent removed under reduced pressure. Purification by flash

[§§§] Vinyl stannane **266** was synthesised by Dr. Simon Williams

column chromatography (EtOAc/PE 40-60: 5%) afforded the product **269** as a colourless liquid (4.1 mg, 13.4 μmol, 86%).

R_f (EtOAc/PE 40-60: 20%) = 0.43; **^{1}H NMR** (400 MHz, $CDCl_3$) δ_H 6.11 (1H, s, C$\underline{H}_a$H$_b$=C31), 5.96 (1H, t, *J* = 1.1 Hz, CH$_a\underline{H}_b$=C31), 4.24 (2H, s, H33), 3.69 (2H, t, *J* = 6.3 Hz, H29), 2.53 (2H, td, *J* = 6.3, 1.1 Hz, H30), 0.86 (9H, s, SiMe$_2$*t*$\underline{Bu}$), 0.02 (6H, s, Si$\underline{Me}_2$*t*Bu). **^{13}C NMR** (100 MHz, $CDCl_3$) δ_C 192.7, 143.3, 128.1, 61.6, 34.7, 30.7, 25.9, 18.3, −5.3, −5.4; **IR** (thin film): ν_{max} 2954, 2928, 2856, 1694, 1471, 1256, 1099; **HRMS** (ESI$^+$) calculated for $C_{12}H_{23}O_2{}^{79}BrSiNa$ $[M+Na]^+$ 306.0651, found 306.0639.

Acetal 178

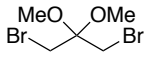

Bromine (8.50 mL, 167 mmol) was added to a stirred solution of methanol (100 mL) and acetone (6.30 mL, 167 mmol) at 0 °C. The red solution was allowed to warm to r.t. over 16 h, to which the colour faded to a pale-yellow solution. The stirring was stopped, and the solution was cooled to −40 °C for 3 h, to which a white precipitate formed. The solid was filtered, washed with cold MeOH (3 × 5 mL) and the solid dried *in vacuo* to afford the product **178** as white crystals (8.54 g, 32.2 mmol, 19%).

^{1}H NMR (500 MHz, $CDCl_3$) δ_H 3.58 (6H, s, MeO), 3.29 (4H, s, CH_2Br). **HRMS** (ESI$^+$) calculated for $C_4H_7Br_2O$ $[M-OMe]^+$ 230.8843, found 230.8848.

Data in agreement with that presented by Dieckmann[201]

Tribromide 277

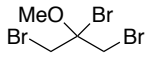

AcBr (11.0 mL, 153 mmol) was added to a stirred solution of acetal **178** (8.00 g, 30.5 mmol) in CH_2Cl_2 (75 mL) at 0 °C. The reaction mixture was stirred at 0 °C for 2 h before adding a further aliquot of AcBr (11.0 mL, 153 mmol) and allowing the mixture to warm to r.t. over 16 h. The solvent and excess reagents were removed under reduced pressure to afford the tribromide **277** as a yellow-orange liquid (9.08 g, 29.2 mmol, 96%).

^{1}H NMR (500 MHz, $CDCl_3$) δ_H 4.10 (2H, d, *J* = 11.8 Hz, C$\underline{H}_a$H$_b$Br), 4.07 (2H, d, *J* = 11.8 Hz, CH$_a\underline{H}_b$Br), 3.88 (3H, s, OMe). **HRMS** (ESI$^+$) calculated for $C_4H_7Br_2O$ $[M-Br]^+$ 230.8843, found 230.8841.

Data in agreement with that presented by Gil[100]

***Z*-Bromo enol ether *Z*-271**

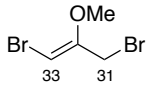

iPr_2NH (12.3 mL, 86.7 mmol) was added dropwise to a stirred solution of the tribromide **277** (9.00 g, 29.0 mmol) in CH_2Cl_2 (50 mL) at 0 °C. The reaction mixture was allowed to warm to r.t. over 4 h, after which the reaction mixture was quenched by the addition of NH_4Cl (40 mL). The layers were separated and the aqueous phase was extracted with CH_2Cl_2 (3 × 20 mL). The combined organic phases were washed with brine (75 mL), dried ($MgSO_4$) and the solvent removed under reduced pressure to afford the product ***Z*-271** as an amber liquid (6.61 g, 28.7 mmol, 99%) as a 1:10 mixture of *E*/*Z* isomers.

^{1}H NMR (500 MHz, $CDCl_3$) δ_H 5.67 (1H, s, H33), 4.02 (2H, s, H31), 3.88 (3H, s, OMe32). **^{13}C NMR** (125 MHz, $CDCl_3$) δ_C 153.1, 89.2, 57.0, 27.7.

Data in agreement with that presented by Gil[100]

***E*-Bromo enol ether *E*-271**

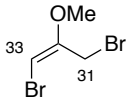

A solution of the *Z*-bromo enol ether *Z*-**271** (1.55 g, 6.74 mmol, *E*/*Z* = 1:10) in hexane (600 mL) was degassed by bubbling a stream of Ar for 30 min. The stirred solution was irradiated with UV light for 6 h to afford a brown mixture. The mixture was filtered over silica, eluting with PE 40-60 (100 mL). The solvent was removed under reduced pressure to afford the product *E*-**271** as an amber liquid (1.16 g, 5.04 mmol, 75%) as a 10:1 mixture of *E*/*Z* isomer.

^{1}H NMR (500 MHz, $CDCl_3$) δ_H 5.37 (1H, s, H33), 4.13 (2H, s, H31), 3.64 (3H, s, OMe32). **HRMS** (ESI^+) calculated for $C_4H_6Br_2OH$ $[M+H]^+$ 230.8843, found 230.8868.

Data in agreement with that presented by Gil[100]

Allylic alcohol 276

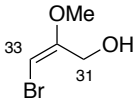

NaOAc (8.00 g, 97.9 mmol) and KI (216 mg, 1.30 mmol) was added to a stirred solution of *E*-bromo enol ether *E*-**271** (1.50 g, 6.52 mmol) in DMF (50 mL). The reaction mixture was stirred at 110 °C for 1 h before cooling to r.t. and diluting with Et_2O (50 mL) and H_2O (150 mL). The layers were separated, and the aqueous phase extracted with Et_2O (3 × 40 mL). The combined organic phases were washed with brine (3 × 20 mL), dried ($MgSO_4$) and the solvent removed under reduced pressure to afford the crude acetate ester, which was redissolved in MeOH (50 mL) and H_2O (50 mL). NaOH (5.20 g, 130 mmol) was added in one portion to a stirred solution of the crude ester, and the reaction mixture was stirred at 75 °C for 1 h. The mixture was allowed to cool to r.t., diluted with H_2O (50 mL) and partitioned with CH_2Cl_2 (25 mL). The layers were separated, and the aqueous phase extracted with CH_2Cl_2 (3 × 25 mL). The combined organic phases were washed with brine (3 × 20 mL), dried ($MgSO_4$) and the solvent removed under reduced pressure to afford the product **276** as a pale-yellow oil (993 mg, 5.95 mmol, 91% over two steps).

^{1}H NMR (500 MHz, $CDCl_3$) δ_H 5.25 (1H, s, H33), 4.36 (2H, s, H31), 3.63 (3H, s, OMe32). **HRMS** (ESI^+) calculated for $C_4H_7BrO_2H$ $[M+H]^+$ 166.9708, found 166.9708.

Data in agreement with that presented by Gil[100]

Aldehyde 278

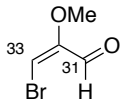

MnO_2 (4.00 g, 47.9 mmol) was added to a stirred solution of alcohol **276** (800 mg, 4.79 mmol) in CH_2Cl_2 (30 mL). The suspension was vigorously stirred for 24 h, before filtering over Celite® and washing the pad with CH_2Cl_2 (15 mL). The solvent was removed under reduced pressure to afford the product as a pale-yellow oil, which was used directly in the subsequent transformation without further purification. Note that owing to the volatility of the aldehyde, an accurate mass could not be obtained for the product. All yields using aldehyde **278** are quoted as a percentage yield over two steps from alcohol **276**.

^{1}H NMR (500 MHz, $CDCl_3$) δ_H 10.00 (1H, s, H31), 6.34 (1H, s, H33), 3.69 (3H, s, OMe32). **HRMS** (ESI^+) calculated for $C_4H_5BrO_2H$ $[M+H]^+$ 164.9552, found 164.9551.

Data in agreement with that presented by Gil[100]

Alcohol 279

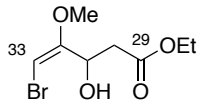

*n*BuLi (21.4 mL, 34.3 mmol, 1.6 M in hexane) was added dropwise to a stirred solution of *i*Pr_2NH (6.00 mL, 42.8 mmol) in THF (9 mL) at 0 °C. The pale-yellow solution was stirred for 30 min at 0 °C before cooling to –78 °C. EtOAc (3.48 mL, 35.7 mmol) was added dropwise to the solution, and the mixture was stirred at –78 °C for 1 h to give a *ca.* 1.0 M solution of the lithium enolate.

The lithium enolate solution (23.9 mL, 23.9 mmol, 1.0 M) was added dropwise to a stirred solution of aldehyde **278** (790 mg, 4.76 mmol, dried over CaH_2) in THF (20 mL) at –78 °C. The resulting solution was stirred at –78 °C for 2 h before being quenched with a solution of $NaHCO_3$ (40 mL) and warmed to r.t.. The mixture was diluted with Et_2O, separated and the aqueous phase extracted with Et_2O (3 × 20 mL). The combined organic phases were washed with brine, dried ($MgSO_4$) and the solvent removed under reduced pressure. Purification by flash column chromatography (Et_2O/PE 30-40: 30%) afforded the product **279** as a colourless oil (437 mg, 1.73 mmol, 30% over two steps from alcohol **276**).

R_f (EtOAc/PE 40-60: 30%) = 0.28; **^{1}H NMR** (500 MHz, $CDCl_3$) δ_H 5.25-5.21 (2H, m, H33, H31), 4.19 (2H, q, *J* = 7.1 Hz, $OC\underline{H}_2CH_3$), 3.63 (3H, s, OMe32), 2.94 (1H, d, *J* = 7.0 Hz, OH), 2.72 (1H, dd, *J* = 15.8, 8.8 Hz, H28a), 2.59 (1H, dd, *J* = 15.8, 4.2 Hz, H28b), 1.28 (3H, t, *J* = 7.1 Hz, $OCH_2C\underline{H}_3$); **^{13}C NMR** (125 MHz, $CDCl_3$) δ_C 171.4, 157.5, 78.8, 66.5, 60.9, 55.8, 38.9, 14.2; **IR** (thin film): ν_{max} 3471 (br), 2986, 1730, 1624, 1278, 1204, 1166, 1039; **HRMS** (ESI^+) calculated for $C_8H_{13}O_4{}^{79}BrNa$ $[M+Na]^+$ 274.9889, found 274.9884.

Alcohol 284

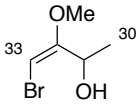

MeMgBr (2.42 mL, 7.26 mmol, 3 M in Et_2O) was added dropwise to a stirred solution of aldehyde **278** (*ca.* 400 mg, 2.42 mmol) in Et_2O (15 mL) at –78 °C. The reaction mixture was stirred at –78 °C for 30 min before quenching with NH_4Cl (10 mL) and the mixture warmed to r.t.. The layers were separated, and the aqueous phase extracted with Et_2O (3 × 5 mL). The combined organic phases were dried ($MgSO_4$) and the solvent

removed under reduced pressure. Purification by flash column chromatography (Et_2O/PE 30-40: 20%) afforded the product **284** as a colourless liquid (311 mg, 1.72 mmol, 71% from alcohol **276** over two steps).

R_f (EtOAc/PE 40-60: 20%) = 0.40; **^{1}H NMR** (500 MHz, $CDCl_3$) δ_H 5.15 (1H, s, H33), 4.93 (1H, dq, *J* = 8.4, 6.6 Hz, H31), 3.63 (3H, s, OMe32), 2.09 (1H, d, *J* = 8.4 Hz, OH), 1.33 (3H, d, *J* = 6.6 Hz, H30).

Data in agreement with that presented by Gil[100]

Ketone 179

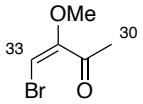

DMSO (401 μL, 5.65 mmol) was added dropwise to a solution of $(COCl)_2$ (242 μL, 2.82 mmol) in CH_2Cl_2 (5 mL) at –78 °C. The solution was stirred at –78 °C for 10 min before adding a solution of alcohol **284** (311 mg, 1.72 mmol, dried over 4 Å MS) in CH_2Cl_2 (5 mL) *via* cannula. The solution was stirred at –78 °C for 30 min before the dropwise addition to Et_3N (1.18 mL, 8.47 mmol) and allowing the reaction mixture to warm to –20 °C. The reaction mixture was quenched with NH_4Cl (10 mL), the layers were separated, and the aqueous phase extracted with CH_2Cl_2 (3 × 5 mL). The combined organic phases were dried ($MgSO_4$) and the solvent removed under reduced pressure. Purification by flash column chromatography (Et_2O/PE 30-40: 10%) afforded the product **179** as a colourless liquid (219 mg, 1.22 mmol, 71%).

R_f (EtOAc/PE 40-60: 20%) = 0.52; **^{1}H NMR** (500 MHz, $CDCl_3$) δ_H 5.64 (1H, s, H33), 3.65 (3H, s, OMe32), 2.35 (3H, s, H30).

Data in agreement with that presented by Gil[100]

Silyl enol ether 186

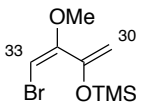

TMSOTf (133 μL, 736 μmol) was added dropwise to a stirred solution of ketone **179** (100 mg, 613 μmol) and Et_3N (128 μL, 920 μmol) in CH_2Cl_2 (3 mL) at 0 °C. The pale-yellow reaction mixture was allowed to warm to r.t. over 16 h, before quenching with $NaHCO_3$ (3 mL). The layers were separated, and the aqueous phase extracted with CH_2Cl_2 (3 × 2 mL). The combined organic phases were dried ($MgSO_4$) and the solvent removed under reduced pressure to afford the silyl enol ether **186** as an amber liquid (153 mg, 607 μmol, 99%)

R_f (EtOAc/PE 40-60: 20%) = 0.63; **^{1}H NMR** (500 MHz, $CDCl_3$) δ_H 5.39 (1H, s, H33), 4.76 (1H, s, H30a), 4.65 (1H, s, H30b), 3.60 (3H, s, OMe32).

Data in agreement with that presented by Gil[100]

Ester 289

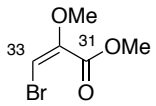

A solution of aldehyde **278** (790 mg, 4.79 mmol, dried over 4 Å MS) in CH_2Cl_2 (10 mL) was transferred *via* cannula into a stirred mixture of MnO_2 (4.20 g, 47.9 mmol), 1,4-dimethyl-1,2,4-triazolium iodide (215 mg, 958 μmol), crushed 4 Å MS (250 mg) in CH_2Cl_2 (40 mL) at r.t.. DBU (786 μL, 5.27 mmol) was added dropwise to the mixture and was vigorously stirred at r.t. for 16 h. The reaction mixture was filtered over Celite® and the solvent removed under reduced pressure. Purification by flash column chromatography (Et_2O/PE 30-40: 15%) afforded the product **289** as a colourless liquid (219 mg, 1.22 mmol, 80% from alcohol **276** over two steps).

R_f (EtOAc/PE 40-60: 20%) = 0.39; **^{1}H NMR** (500 MHz, $CDCl_3$) δ_H 5.84 (1H, s, H33), 3.86 (3H, s, CO_2Me), 3.68 (3H, s, OMe32); **^{13}C NMR** (125 MHz, $CDCl_3$) δ_C 162.4, 148.9, 87.5, 56.6, 52.5; **IR** (thin film): ν_{max} 1737, 1436, 1339, 1207, 1151; **HRMS** (ESI^+) calculated for $C_5H_7BrO_3H$ $[M+H]^+$ 194.9657, found 194.9653.

Alcohol 291

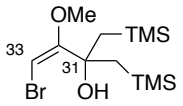

A freshly prepared solution of $TMSCH_2MgCl$ (7.20 mL, 10.0 mmol, 1.4 M in THF) was added to a stirred mixture of anhydrous $CeCl_3$ (2.46 g, 10.0 mmol) in THF (7 mL) at –78 °C. The mixture was stirred at –78 °C for 1 h before the dropwise addition of a solution of ester **289** (272 mg, 2.00 mmol) in THF (6 mL) *via* cannula at –78 °C. The reaction mixture was stirred at –78 °C for 2 h, before warming to r.t. over 16 h. The reaction mixture was quenched by addition of NH_4Cl (20 mL) at 0 °C and diluted with CH_2Cl_2 (20 mL). The layers were separated, and the aqueous phase extracted with CH_2Cl_2 (3 × 15 mL). The combined organic phases were washed with brine (20 mL), dried ($MgSO_4$) and the solvent carefully removed under reduced pressure (400 Torr). Purification by flash column chromatography (Et_2O/PE 30-40: 0% → 15%) afforded the product **291** as a colourless liquid (511 mg, 1.50 mmol, 75%).

R_f (EtOAc/PE 40-60: 20%) = 0.69; **^{1}H NMR** (500 MHz, $CDCl_3$) δ_H 5.03 (1H, s, H33), 3.53 (3H, s, OMe32), 2.97 (1H, s, OH), 1.29 (2H, dd, *J* = 14.5, 1.1 Hz, C$\underline{H}_a$H$_b$TMS), 1.61 (1H, d, *J* = 14.5 Hz, CH$_a\underline{H}_b$TMS), 0.01 (18H, s, TMS); **^{13}C NMR** (125 MHz, $CDCl_3$) δ_C 162.3, 74.7, 55.2, 34.1, 32.9, 22.3, 0.0; **IR** (thin film): ν_{max} 3512, 2954, 1246, 1202, 1157, 907; **HRMS** (ESI$^+$) calculated for $C_{12}H_{27}O_2{}^{79}BrSi_2H$ $[M+H]^+$ 339.0655, found 339.0655.

Allylsilane 286

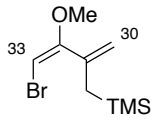

PPTS (67 mg, 0.27 mmol) was added to a stirred solution of alcohol **291** (450 mg, 1.33 mmol) in CH_2Cl_2 (14 mL) and methanol (1 mL) at r.t.. The solution was stirred at r.t. for 45 min before quenching with $NaHCO_3$ (10 mL). The layers were separated, and the aqueous phase extracted with CH_2Cl_2 (3 × 10 mL). The combined organic phases were dried ($MgSO_4$) and the solvent carefully removed under reduced pressure (400 Torr). Purification by flash column chromatography (Et_2O/PE 30-40: 0% → 2%) afforded the product **286** as a colourless liquid (267 mg, 1.07 mmol, 81%).

R_f (EtOAc/PE 40-60: 10%) = 0.69; **^{1}H NMR** (500 MHz, $CDCl_3$) δ_H 5.25 (1H, s, H33), 5.18 (1H, d, *J* = 1.7 Hz, H30a), 5.10 (1H, d, *J* = 1.7 Hz, H30b), 3.56 (3H, s, OMe32), 1.75 (2H, d, *J* = 1.0 Hz, CH_2TMS), 0.03 (9H, s, TMS); **^{13}C NMR** (125 MHz, $CDCl_3$) δ_C 160.1, 140.2, 117.0, 77.6, 55.4, 25.0, –1.5; **IR** (thin film): ν_{max} 2958, 1606, 1323, 1249, 1201, 1151; **HRMS** (ESI$^+$) calculated for $C_9H_{18}O^{79}BrSiH$ $[M+H]^+$ 249.0310, found 249.0307.

Alcohol 292

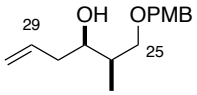

A solution of allylmagnesium chloride (3.92 mL, 6.66 mmol, 1.7 M in THF) was added to a stirred solution of (+)-Ipc$_2$BOMe (2.11 g, 6.66 mmol) in Et_2O (30 mL) at –78 °C. The solution was stirred at –78 °C for 30 min before allowing to warm to r.t. over 1 h, upon which a grey white suspension formed. The mixture was cooled to –78 °C, and a solution of aldehyde **106** (990 mg, 4.76 mmol, dried over 4 Å MS) in Et_2O (20 mL) was added dropwise to the reaction. The mixture was stirred at –78 °C for 2 h before quenching at –78 °C with the successive addition of MeOH (10 mL), pH 7 buffer (10 mL) and H_2O_2 (4 mL). The mixture was warmed to r.t. and the layers separated. The aqueous phase was extracted with Et_2O (3 × 20 mL), and the combined organic phases were successively washed with $Na_2S_2O_3$ (40 mL) and brine (40 mL). The organic

phases were then dried ($MgSO_4$) and the solvent removed under reduced pressure. Purification by flash column chromatography (EtOAc/PE 40-60: 10% → 15%) afforded the product **292** as a colourless oil (896 mg, 3.58 mmol, 75%) as a single diastereomer.

R_f (EtOAc/PE 40-60: 20%) = 0.38; **^{1}H NMR** (500 MHz, $CDCl_3$) δ_H 7.24 (2H, d, *J* = 8.6 Hz, ArH), 6.88 (2H, d, *J* = 8.6 Hz, ArH), 5.84 (1H, ddt, *J* = 17.1, 10.1, 7.0 Hz, H29), 5.11 (1H, d, *J* = 17.1 Hz, =C$\underline{H}_a$H$_b$), 5.08 (1H, d, *J* = 10.1 Hz, =CH$_a\underline{H}_b$), 4.44 (2H, s, CH_2Ar), 3.84-3.80 (1H, m, H27), 3.81 (3H, s, OMe), 3.49 (2H, d, *J* = 5.4 Hz, H25), 2.53 (1H, d, *J* = 3.8 Hz, OH), 2.27-2.16 (2H, m, H28), 1.92-1.85 (1H, m, H26), 0.95 (3H, d, *J* = 7.0 Hz, Me26).

Data in agreement with that presented by Liu[202]

The absolute stereochemical outcome at C27 was confirmed by Mosher ester analysis from the enantiomeric compound ***ent*-292**

Mosher esters (*R*)-MTPA-293 and (*S*)-MTPA-293

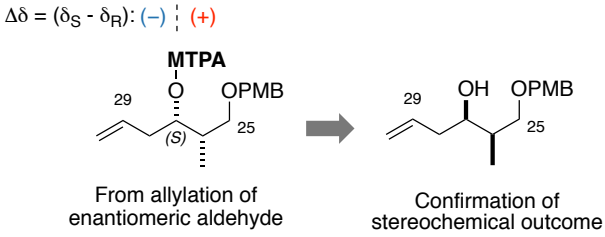

(R)-Mosher ester **(*R*)-MTPA-293**

DCC (64 µL, 64.0 µmol, 1 M in CH_2Cl_2) was added in portion to a stirred solution of alcohol ***ent*-292** (4.0 mg, 16.0 µmol), *(R)*-MTPA (15.0 mg, 63.9 5µmol) and DMAP (one crystal) in CH_2Cl_2 (500 µL). The mixture was stirred for 24 h at r.t., during which the solution became a white suspension. The mixture was filtered through cotton wool and the filtrate reduced to dryness. Purification by flash chromatography (EtOAc/PE 40-60: 10%) afforded the product **(*R*)-MTPA-293** as a colourless oil (4.0 mg, 8.6 µmol, 54%).

R_f (EtOAc/PE 40-60: 20%) = 0.52; **^{1}H NMR** (500 MHz, $CDCl_3$) δ_H 7.52-7.36 (5H, m, Ar$\underline{H}$), 7.24 (2H, d, *J* = 8.6 Hz, ArH), 6.87 (2H, d, *J* = 8.6 Hz, ArH), 5.67 (1H, m, H29), 5.34 (1H, m, H27), 5.05-4.99 (2H, m, =CH_2), 4.40 (1H, d, *J* = 11.5 Hz, C$\underline{H}_A$H$_B$Ar), 4.36 (1H, d, *J* = 11.5 Hz, CH$_A\underline{H}_B$Ar), 3.80 (3H, s, ArOMe), 3.47 (3H, s, OMe), 3.26 (2H, d, *J* = 7.1 Hz, H25), 2.43 (1H, m, H28a), 2.33 (1H, m, H28b), 2.07 (1H, m, H26), 0.92 (3H, d, *J* = 6.8 Hz, Me26).

(S)-Mosher ester **(*S*)-MTPA-293**

DCC (64 μL, 64.0 μmol, 1 M in CH_2Cl_2) was added in portion to a stirred solution of alcohol ***ent*-292** (4.0 mg, 16.0 μmol), *(S)*-MTPA (15.0 mg, 63.9 μmol) and DMAP (one crystal) in CH_2Cl_2 (500 μL). The mixture was stirred for 24 h at r.t., during which the solution became a white suspension. The mixture was filtered through cotton wool and the filtrate reduced to dryness. Purification by flash chromatography (EtOAc/PE 40-60: 10%) afforded the product **(*S*)-MTPA-293** as a colourless oil (5.3 mg, 11.4 μmol, 71%).

R_f (EtOAc/PE 40-60: 20%) = 0.52; **^{1}H NMR** (500 MHz, $CDCl_3$) δ_H 7.54-7.35 (5H, m, Ar<u>H</u>), 7.23 (2H, d, *J* = 8.6 Hz, ArH), 6.87 (2H, d, *J* = 8.6 Hz, ArH), 5.75 (1H, m, H29), 5.40 (1H, m, H27), 5.14-5.06 (2H, m, $=CH_2$), 4.36 (1H, d, *J* = 11.5 Hz, C<u>H</u>$_A$H$_B$Ar), 4.30 (1H, d, *J* = 11.5 Hz, CH$_A$<u>H</u>$_B$Ar), 3.80 (3H, s, ArOMe), 3.53 (3H, s, OMe), 3.16 (2H, m, H25), 2.50 (1H, m, H28a), 2.40 (1H, m, H28b), 2.05 (1H, m, H26), 0.87 (3H, d, *J* = 6.7 Hz, Me26).

General protocol for the synthesis of silyl ethers 288 and 295

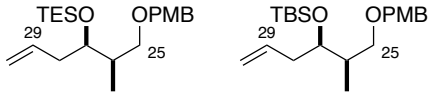

288 **295**

TBS or TES triflate (1.1 eq.) was added to a stirred solution of alcohol **292** (1 eq.) and 2,6-lutidine (1.2 eq.) in CH_2Cl_2 (c = 0.1 M relative to alcohol **292**) at −78 °C. The reaction mixture was stirred at −78 °C for 45 min before quenching with MeOH and $NaHCO_3$. The layers were separated, and the aqueous phase extracted with CH_2Cl_2. The combined organic phases were dried ($MgSO_4$) and the solvent removed under reduced pressure. Purification by flash column chromatography (EtOAc/PE 40-60: 0% → 2%) afforded the product as a colourless oil.

TES ether **288**

TES ether **288** was synthesised using the above general protocol from alcohol **292** (590 mg, 2.36 mmol), TESOTf (570 μL, 2.60 mmol) and 2,6-lutidine (329 μL, 2.84 mmol) as a colourless oil (628 mg, 1.72 mmol, 73%).

R_f (EtOAc/PE 40-60: 10%) = 0.54; **^{1}H NMR** (500 MHz, $CDCl_3$) δ_H 7.25 (2H, d, *J* = 8.4 Hz, ArH), 6.87 (2H, d, *J* = 8.4 Hz, ArH), 5.75 (1H, ddt, *J* = 17.2, 10.1, 7.2 Hz, H29), 5.03 (1H, d, *J* = 17.2 Hz, =C<u>H</u>$_a$H$_b$), 5.00 (1H, d, *J* = 10.1 Hz, =CH$_a$<u>H</u>$_b$), 4.44 (1H, d, *J* = 11.5 Hz, C<u>H</u>$_a$H$_b$Ar), 4.38 (1H, d, *J* = 11.5 Hz, CH$_a$<u>H</u>$_b$Ar), 3.85 (1H, td, *J* = 6.5, 2.9 Hz, H27), 3.80 (3H, s, OMe), 3.43 (1H, dd, *J* = 8.5, 7.0 Hz, H25a), 3.24 (1H, dd, *J* = 8.5, 7.0 Hz, H25a), 2.27-2.17 (2H, m, H28), 1.87 (1H, dq, *J* = 6.5, 2.9 Hz, H26), 0.94 (9H, t, *J* = 7.9 Hz, $SiCH_2CH_3$),

0.87 (3H, d, *J* = 6.8 Hz, Me26), 0.57 (6H, q, *J* = 7.9 Hz, $SiCH_2CH_3$); **^{13}C NMR** (125 MHz, $CDCl_3$) δ_C 159.1, 135.5, 130.8, 129.3, 116.6, 113.7, 72.8, 72.7, 72.0, 52.3, 39.7, 37.7, 10.8, 7.0, 5.2; **IR** (thin film): ν_{max} 2955, 2876, 1613, 1513, 1247, 1040; $[\alpha]_D^{20}$ +2.3 (*c* 0.31, $CHCl_3$); **HRMS** (ESI^+) calculated for $C_{21}H_{36}O_3SiH$ $[M+H]^+$ 365.2512, found 365.2514.

TBS ether **295**

TBS ether **295** was synthesised using the above general protocol from alcohol **292** (187 mg, 747 μmol), TBSOTf (190 μL, 822 μmol) and 2,6-lutidine (104 μL, 896 μmol) as a colourless oil (270 mg, 741 μmol, 99%).

R_f (EtOAc/PE 40-60: 10%) = 0.63; **^{1}H NMR** (500 MHz, $CDCl_3$) δ_H 7.25 (2H, d, *J* = 8.6 Hz, ArH), 6.88 (2H, d, *J* = 8.6 Hz, ArH), 5.74 (1H, ddt, *J* = 17.2, 10.1, 7.2 Hz, H29), 5.02 (1H, d, *J* = 17.2 Hz, $=C\underline{H_a}H_b$), 5.00 (1H, d, *J* = 10.1 Hz, $=CH_a\underline{H_b}$), 4.44 (1H, d, *J* = 11.5 Hz, $C\underline{H_a}H_bAr$), 4.37 (1H, d, *J* = 11.5 Hz, $CH_a\underline{H_b}Ar$), 3.84 (1H, td, *J* = 6.6, 2.9 Hz, H27), 3.80 (3H, s, OMe), 3.41 (1H, dd, *J* = 9.1, 6.8 Hz, H25a), 3.23 (1H, dd, *J* = 9.1, 6.8 Hz, H25a), 2.27-2.17 (2H, m, H28), 1.87 (1H, dq, *J* = 6.8, 3.0 Hz, H26), 0.88-0.86 (12H, m, Me26, $SiMe_2tBu$), 0.03 (3H, s, $SiMe_2tBu$), 0.02 (3H, s, $SiMe_2tBu$); **^{13}C NMR** (125 MHz, $CDCl_3$) δ_C 159.1, 135.5, 130.8, 129.2, 116.6, 113.7, 72.8, 72.6, 71.8, 52.3, 39.6, 37.5, 25.9, 18.1, 10.7, –4.3, –4.8; **IR** (thin film): ν_{max} 2935, 2858, 1613, 1514, 1250, 1040; $[\alpha]_D^{20}$ +0.73 (*c* 0.27, $CHCl_3$); **HRMS** (ESI^+) calculated for $C_{21}H_{36}O_3SiH$ $[M+H]^+$ 365.2512, found 365.2512.

General protocol for the synthesis of aldehydes 287 and 294

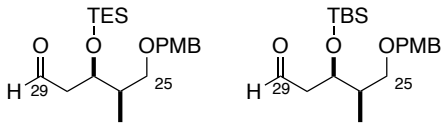

287 **294**

Method A: direct ozonolysis

A stream of O_3 was bubbled through a stirred red mixture of alkene, Sudan Red dye (one crystal), $NaHCO_3$ (10 eq.) in CH_2Cl_2 (8 mL) and MeOH (8 mL) at –78 °C. The stream of O_3 was immediately stopped once the reaction mixture turned pale yellow (*ca.* 5 min) and replaced with a stream of O_2, bubbling into the stirred mixture for 10 min at –78 °C. PPh_3 (1.05 eq.) was added in one portion, and the stirred solution was allowed to warm to r.t.. The solvent was then removed under reduced pressure, and the crude mixture was purified by flash column chromatography (EtOAc/PE 40-60: 10% → 20%) to afford the product as a colourless oil.

Method B: dihydroxylation followed by periodate cleavage

A solution of NMO (1.2 eq.) was added in one portion to a stirred mixture of the alkene, $K_2OsO_4{\cdot}2H_2O$ (0.02 eq.) in *t*BuOH, H_2O and THF (1:1:1, 0.3 M) at r.t.. The solution was stirred for 24 h at r.t., after which the reaction mixture was quenched by addition of Na_2SO_3, diluted with EtOAc and stirred for 30 min at r.t.. The layers were separated, and the aqueous phase extracted with EtOAc. The combined organic phases were washed with citric acid (10%), brine, dried ($MgSO_4$) and the solvent removed under reduced pressure to afford the crude diol. Silica-supported $NaIO_4$ (5 eq.) was added to a solution of the diol in CH_2Cl_2 (0.1 M) at r.t.. The mixture was stirred for 30 min at r.t. before filtering to remove all solids. The solvent was removed under reduced pressure to afford the aldehyde, which was pure enough for characterisation and to be used in the subsequent transformations.

Aldehyde **287**

Aldehyde **287** was prepared from alkene **288** (150 mg, 411 μmol) by Method A, employing PPh_3 (113 mg, 431 μmol) to afford the product **287** as a colourless oil (150 mg, 407 μmol, 80%).

$\mathbf{R_f}$ (EtOAc/PE 40-60: 20%) = 0.53; **^{1}H NMR** (500 MHz, $CDCl_3$) δ_H 9.77 (1H, t, *J* =2.4 Hz, H29), 7.24 (2H, d, *J* = 8.7 Hz, ArH), 6.87 (2H, d, *J* = 8.7 Hz, ArH), 4.42 (1H, d, *J* = 11.5 Hz, C$\underline{H}_a$H$_b$Ar), 4.39 (1H, d, *J* = 11.5 Hz, C$\underline{H}_a$H$_b$Ar), 4.37-4.33 (1H, m, H27), 3.80 (3H, s, OMe), 3.44 (1H, dd, *J* = 9.1, 6.0 Hz, H25a), 3.24 (1H, dd, *J* = 9.1, 5.9 Hz, H25a), 2.57 (1H, ddd, *J* = 16.1, 6.8, 2.6 Hz, H28a), 2.52 (1H, ddd, *J* = 16.1, 5.4, 2.1 Hz, H28b), 1.88 (1H, qd, *J* = 6.5, 4.0 Hz, H26), 0.94 (9H, t, *J* = 8.3 Hz, $SiCH_2CH_3$), 0.92 (3H, d, *J* = 6.6 Hz, Me26), 0.59 (6H, q, *J* = 8.3 Hz, $SiCH_2CH_3$); **^{13}C NMR** (125 MHz, $CDCl_3$) δ_C 202.0, 159.2, 130.5, 129.3, 113.7, 72.7, 71.7, 68.6, 55.2, 49.0, 39.7, 12.2, 6.9, 5.0; **IR** (thin film): ν_{max} 2956, 2875, 1727, 1612, 1513, 1463, 1247, 1099, 1015; $[\alpha]_D^{20}$ +1.5 (*c* 0.17, $CHCl_3$); **HRMS** (ESI^+) calculated for $C_{20}H_{34}O_4SiNa$ $[M+Na]^+$ 389.2124, found 389.2118.

Aldehyde **294**

Aldehyde **294** was prepared from alkene **295** (767 mg, 2.10 mmol) by Method B, employing $K_2OsO_4{\cdot}H_2O$ (16.0 mg, 42.0 μmol), NMO (523 μL, 2.52 mmol, 50% wt in H_2O) to afford the crude diol (801 mg, *ca.* 2.01 mmol, 95%). Treatment of crude diol (65.0 mg, 163 μmol) with $NaIO_4/SiO_2$ (1.00 g, 652 μmol, 14% w/w) afforded aldehyde **294** as a colourless oil (60.0 mg, 163 μmol, quant.).

Alternatively, aldehyde **294** can also be synthesised from alkene **295** (100 mg, 270 μmol) by Method A, employing PPh_3 (75.0 mg, 288 μmol) to afford the product as a colourless oil (81.3 mg, 222 μmol, 82%).

$\mathbf{R_f}$ (EtOAc/PE 40-60: 20%) = 0.53; **^{1}H NMR** (500 MHz, $CDCl_3$) δ_H 9.76 (1H, s, H29), 7.25 (2H, d, *J* = 8.5 Hz, ArH), 6.88 (2H, d, *J* = 8.5 Hz, ArH), 4.42 (1H, d, *J* = 11.6 Hz, C$\underline{H}_a$H$_b$Ar), 4.38 (1H, d, *J* = 11.6 Hz,

C<u>H</u>$_a$H$_b$Ar), 4.36-4.31 (1H, m, H27), 3.81 (3H, s, OMe), 3.43 (1H, dd, *J* = 9.1, 6.9 Hz, H25a), 3.28 (1H, dd, *J* = 9.1, 5.9 Hz, H25a), 2.59-2.50 (2H, m, H28), 1.89 (1H, qd, *J* = 6.9, 2.9 Hz, H26), 0.92 (3H, d, *J* = 6.9 Hz, Me26), 0.86 (9H, s, SiMe$_2$*t*Bu), 0.06 (3H, s, SiMe$_2$*t*Bu), 0.04 (3H, s, SiMe$_2$*t*Bu); **^{13}C NMR** (125 MHz, $CDCl_3$) δ_C 202.0, 159.0, 130.4, 129.1, 113.7, 72.6, 71.6, 68.3, 55.2, 48.9, 39.5, 25.7, 17.9, 11.9, –4.5, –4.8; **IR** (thin film): ν_{max} 2933, 2857, 1726, 1614, 1514, 1464, 1250, 1084, 1034; $[\alpha]_D^{20}$ +4.3 (*c* 1.34, $CHCl_3$); **HRMS** (ESI^+) calculated for $C_{20}H_{34}O_4SiNa$ $[M+Na]^+$ 389.2124, found 389.2124.

Alcohol 296b

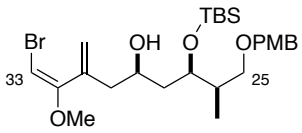

$SnCl_4$ (220 μL, 220 μmol, 1 M in CH_2Cl_2) was added dropwise to a stirred solution of allylsilane **286** (50.0 mg, 200 μmol, dried over CaH_2) in CH_2Cl_2 (1 mL) at –78 °C. The pale-yellow solution was stirred for 1 h at –78 °C before the addition of aldehyde **294** (110 mg, 302 μmol, dried by azeotroping with PhH × 3) in CH_2Cl_2 (1 mL) *via* cannula. The reaction mixture was stirred for a further 1 h before quenching with $NaHCO_3$ (2 mL). The layers were separated, and the aqueous phase extracted with CH_2Cl_2 (3 × 2 mL). The combined organic phases were dried ($MgSO_4$) and the solvent removed under reduced pressure. Purification by flash column chromatography (EtOAc/PE 40-60: 5% → 15%) afforded the 27,29-*syn* product **296b** (43.4 mg, 79.8 μmol) and the 27,29-*anti* product **296a** (34.3 mg, 63.0 μmol) as colourless oils (*syn*:*anti* 1.3:1, combined yield 72%).

The undesired C27 epimer in **296a** can be recycled to **296b** using the following method. To a stirred solution of 27,29-*anti* alcohol **296a** (20.0 mg, 36.8 μmol), PPh_3 (96.5 mg, 368 μmol) and 4-nitrobenzoic acid (55.0 mg, 331 μmol) in benzene (500 μL) was added DEAD (58 μL, 368 μmol) dropwise. The pale-yellow solution was stirred for 3 h at r.t. before quenching with $NaHCO_3$ (1 mL). The layers were separated, and the aqueous phase extracted with Et_2O (3 × 1 mL). The combined organic phases were dried ($MgSO_4$) and the excess Et_2O carefully removed under reduced pressure (400 Torr). The remaining solution was filtered over SiO_2, eluting with PE 40-60 (2 mL) and the solvent was removed under reduced pressure to afford the crude ester, which was immediately redissolved in MeOH (750 μL). K_2CO_3 (69.0 mg, 498 μmol) was added to this stirred solution and the reaction mixture was stirred at r.t. for 3 h before quenching with NH_4Cl (1 mL) and diluted with CH_2Cl_2 (2 mL). The layers were separated, and the aqueous phase extracted with CH_2Cl_2 (3 × 2 mL). The combined organic phases were dried ($MgSO_4$) and the solvent removed under reduced pressure. Purification by flash column chromatography (EtOAc/PE 40-60: 5% → 15%) afforded the 27,29-*syn* alcohol **296b** as a colourless oil (9.3 mg, 17.1 μmol, 52% over two steps).

27,29-*anti* alcohol **296a**

R_f (EtOAc/PE 40-60: 20%) = 0.43; **^{1}H NMR** (500 MHz, $CDCl_3$) δ_H 7.25 (2H, d, *J* = 8.7 Hz, ArH), 6.88 (2H, d, *J* = 8.7 Hz, ArH), 5.38 (2H, s, =Me31), 5.32 (1H, s, H33), 4.43 (1H, d, *J* = 11.5 Hz, C$\underline{H}_a$H$_b$Ar), 4.39 (1H, d, *J* = 11.5 Hz, C$\underline{H}_a$H$_b$Ar), 4.00 (1H, dt, *J* = 8.0, 3.8 Hz, H27), 3.88-3.77 (4H, m, H29, ArOMe), 3.56 (3H, s, OMe32), 3.52 (1H, dd, *J* = 9.0, 5.1 Hz, H25a), 3.23 (1H, dd, *J* = 9.0, 7.6 Hz, H25b), 2.43 (1H, dd, *J* = 13.6, 3.5 Hz, H30a), 2.26 (1H, dd, *J* = 13.6, 9.4 Hz, H30b), 1.97-1.90 (1H, m, H26), 1.52-1.47 (2H, m, H28), 0.93 (3H, d, *J* = 6.9 Hz, Me26), 0.87 (9H, s, SiMe$_2$*t*Bu), 0.06 (3H, s, SiMe$_2$*t*Bu), 0.05 (3H, s, SiMe$_2$*t*Bu); **^{13}C NMR** (125 MHz, $CDCl_3$) δ_C 159.0, 139.6, 130.9, 129.1, 122.3, 113.7, 93.4, 78.7, 72.6, 72.0, 70.8, 69.9, 55.6, 55.3, 43.5, 40.2, 39.4, 38.9, 25.8, 18.1, 13.0, –4.5, –4.8; **IR** (thin film): ν_{max} 3380, 2955, 2930, 2857 1611, 1513, 1462, 1219, 1201; $[\alpha]_D^{20}$ +7.3° (*c* 0.15, $CHCl_3$); **HRMS** (ESI$^+$) calculated for $C_{26}H_{43}{}^{79}BrO_5SiNa$ $[M+Na]^+$ 565.1966, found 565.1971.

27,29-*syn* alcohol **296b**

R_f (EtOAc/PE 40-60: 20%) = 0.37; **^{1}H NMR** (500 MHz, $CDCl_3$) δ_H 7.25 (2H, d, *J* = 8.6 Hz, ArH), 6.87 (2H, d, *J* = 8.6 Hz, ArH), 5.38 (2H, s, =Me31), 5.32 (1H, s, H33), 4.44 (1H, d, *J* = 11.3 Hz, C$\underline{H}_a$H$_b$Ar), 4.40 (1H, d, *J* = 11.3 Hz, C$\underline{H}_a$H$_b$Ar), 3.95 (1H, dt, *J* = 6.8, 3.2 Hz, H27), 3.80 (3H, s, ArOMe), 3.73-3.68 (1H, m, H29), 3.57 (3H, s, OMe32), 3.52 (1H, dd, *J* = 8.8, 5.4 Hz, H25a), 3.25 (1H, dd, *J* = 8.8, 8.4 Hz, H25b), 2.60 (1H, s, OH29), 2.40 (1H, dd, *J* = 13.8, 5.3 Hz, H30a), 2.34 (1H, dd, *J* = 13.8, 7.5 Hz, H30b), 1.98-1.92 (1H, m, H26), 1.68 (1H, ddd, *J* = 14.1, 6.8, 3.1 Hz, H28a), 1.51 (1H, ddd, *J* = 14.1, 8.7, 7.5 Hz, H28b), 0.90 (3H, d, *J* = 8.6 Hz, Me26), 0.87 (9H, s, SiMe$_2$*t*Bu), 0.06 (3H, s, SiMe$_2$*t*Bu), 0.05 (3H, s, SiMe$_2$*t*Bu); **^{13}C NMR** (125 MHz, $CDCl_3$) δ_C 159.1, 139.4, 130.8, 129.2, 122.5, 113.7, 93.8, 78.7, 72.8, 72.3, 72.0, 67.9, 55.6, 55.3, 42.0, 39.8, 38.4, 25.9, 18.0, 12.2, –4.4, –4.5 ; **IR** (thin film): ν_{max} 3381, 2954, 2920, 2857, 1611, 1513, 1462, 1249; $[\alpha]_D^{20}$ +4.2 (*c* 0.21, $CHCl_3$); **HRMS** (ESI$^+$) calculated for $C_{26}H_{43}{}^{79}BrO_5SiNa$ $[M+Na]^+$ 565.1966, found 565.1969.

Confirmation of stereochemistry at C29: general protocol for the synthesis of acetonides 297 and 298

The stereochemical outcome at C29 was confirmed by synthesising the acetonide derivatives of each diastereomeric alcohols using the protocol outlined below. To a purified sample of alcohol **296a** or **296b** was added TBAF (1.1 eq., 1 M in THF) at r.t.. The reaction mixture was stirred for 1 h before diluting with EtOAc and quenching with NH_4Cl. The layers were separated and the aqueous phase extracted with EtOAc (3 × 500 μL). The combined organic phases were dried ($MgSO_4$) and the solvent removed under reduced pressure. The crude diol was immediately redissolved in CH_2Cl_2 (100 μL) and 2,2-dimethoxypropane (100 μL). PPTS (one crystal) was added and the reaction mixture was stirred at r.t. for 16 h, after which the mixture was filtered over silica and the solvent removed under reduced pressure. Purification by flash column chromatography (EtOAc/PE 40-60: 10%) afforded the *syn*- or *anti*-acetonide for spectroscopic

analysis. The conformation of the acetonide reveals the diastereomeric relationship (27,29-*syn* or 27,29-*anti*). As the absolute configuration at C27 is known, the identity at C29 can be inferred.

27,29-anti acetonide **297**

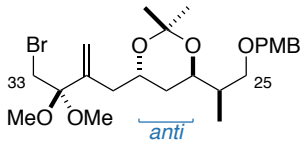

Anti acetonide **297** was synthesised from alcohol **296a** (6.8 mg, 12.5 µmol), employing TBAF (13.8 µL, 13.8 µmol) to remove the C27 silyl ether. Following the general protocol described above, acetonide **297** was obtained as a colourless oil (2.2 mg, 4.69 µmol, 37% over two steps) as a mixture of the C32 acetal and the C32 enol ether (2:1).

Major product – C32 acetal: $\mathbf{R_f}$ (EtOAc/PE 40-60: 20%) = 0.48; **^{1}H NMR** (500 MHz, $CDCl_3$) δ_H 7.25 (2H, d, *J* = 8.7 Hz, ArH), 6.88 (2H, d, *J* = 8.7 Hz, ArH), 5.52 (1H, d, *J* = 0.8 Hz, =Me31), 5.34 (1H, d, *J* = 1.9 Hz, =Me31), 4.43 (1H, d, *J* = 11.7 Hz, C$\underline{H_a}H_b$Ar), 4.39 (1H, d, *J* = 11.7 Hz, C$\underline{H_a}H_b$Ar), 4.04-3.98 (1H, m, H29), 3.85-3.80 (4H, m, H27, ArOMe), 3.50 (1H, d, *J* = 11.4 Hz, H33a), 3.43-3.38 (2H, m, H33b, H25a), 3.30 (1H, dd, *J* = 9.3, 5.9 Hz, H25b), 3.19 (3H, s, OMe32a), 3.18 (3H, s, OMe32b), 2.23 (1H, dd, *J* = 15.7, 7.8 Hz, H30a), 2.10 (1H, dd, *J* = 15.7, 4.7 Hz, H30b), 1.82 (1H, ddd, *J* = 12.7, 9.9, 6.0 Hz, H28a), 1.80-1.73 (1H, m, H26), 1.49 (1H, ddd, *J* = 12.7, 9.9, 6.0 Hz, H28b), 1.33 (3H, s, $\underline{Me}_A Me_B CO(O)$), 1.30 (3H, s, $Me_A \underline{Me}_B CO(O)$), 0.97 (3H, d, *J* = 6.8 Hz, Me26); **^{13}C NMR** (125 MHz, $CDCl_3$) δ_C 159.1, 141.2, 130.7, 129.2, 117.8, 113.7, 101.4, 100.3*, 72.9, 71.9, 67.2, 65.9, 55.3, 49.1, 49.1, 38.1, 36.8, 36.6, 31.8, 24.6*, 24.5*, 12.6

*Indicates ^{13}C signals that are diagnostic for the 27,29-*anti* configuration for the acetonide

27,29-syn acetonide **298**

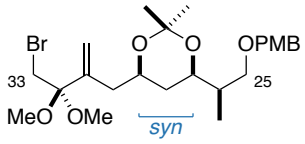

Syn acetonide **298** was synthesised from alcohol **296b** (3.1 mg, 5.70 µmol), employing TBAF (6.3 µL, 6.30 µmol) to remove the C27 silyl ether. Following the general protocol described above, acetonide **298** was obtained as a colourless oil (1.0 mg, 2.13 µmol, 37% over two steps).

$\mathbf{R_f}$ (EtOAc/PE 40-60: 20%) = 0.45; **^{1}H NMR** (500 MHz, $CDCl_3$) δ_H 7.25 (2H, d, *J* = 8.7 Hz, ArH), 6.88 (2H, d, *J* = 8.7 Hz, ArH), 5.53 (1H, d, *J* = 1.5 Hz, =Me31), 5.32 (1H, dd, *J* = 2.8, 1.5 Hz, =Me31), 4.43 (1H, d, *J* =

11.5 Hz, C<u>H</u>$_a$H$_b$Ar), 4.40 (1H, d, *J* = 11.5 Hz, C<u>H</u>$_a$H$_b$Ar), 4.07 (1H, dddd, *J* = 11.3, 7.4, 4.8, 2.2 Hz, H29), 3.91 (1H, ddd, *J* = 11.8, 4.9, 2.3 Hz, H27), 3.80 (3H, s, ArOMe), 3.53 (1H, d, *J* = 11.4 Hz, H33a), 3.43 (1H, dd, *J* = 9.0, 6.4 Hz, H25a), 3.42 (1H, d, *J* = 11.4 Hz, H33b), 3.31 (1H, dd, *J* = 9.0, 5.6 Hz, H25b), 3.19 (3H, s, OMe32), 3.18 (3H, s, OMe32), 2.22 (1H, ddd, *J* = 15.5, 7.5, 0.8 Hz, H30a), 2.07 (1H, dd, *J* = 15.5, 4.7 Hz, H30b), 1.80-1.72 (1H, m, H26), 1.42 (3H, s, <u>Me</u>$_A$Me$_B$CO(O)), 1.35 (3H, s, Me$_A$<u>Me</u>$_B$CO(O)), 1.51-1.43 (1H, m, H28a), 1.29-1.20 (1H, m, H28b), 0.94 (3H, d, *J* = 6.9 Hz, Me26); **^{13}C NMR** (125 MHz, $CDCl_3$) δ_C 159.1, 140.9, 130.7, 129.2, 118.2, 113.7, 101.4, 98.5*, 72.8, 71.8, 69.6, 68.4, 55.3, 49.1, 49.1, 38.5, 37.6, 34.4, 31.8, 30.1*, 19.7*, 12.2.

*Indicates ^{13}C signals that are diagnostic for the 27,29-*syn* configuration for the acetonide

Ester 299

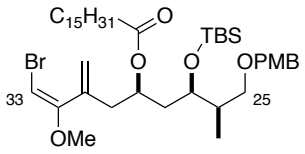

DCC (258 μL, 258 mmol, 1 M in CH_2Cl_2) was added to a stirred solution of alcohol **296b** (28.0 mg, 51.5 μmol), palmitic acid (66.0 mg, 258 μmol) and DMAP (one crystal) in CH_2Cl_2 (1 mL) at r.t.. The reaction mixture was stirred for 16 h before filtering over SiO_2 and eluting with Et_2O/PE 40-60 (2%). The solvent was removed under reduced pressure. Purification by flash column chromatography (Et_2O/PE 40-60: 2%) afforded ester **299** as a colourless oil (33.7 mg, 43.1 mmol, 84%).

R$_f$ (EtOAc/PE 40-60: 20%) = 0.70; **^{1}H NMR** (500 MHz, $CDCl_3$) δ_H 7.23 (2H, d, *J* = 8.7 Hz, ArH), 6.86 (2H, d, *J* = 8.7 Hz, ArH), 5.42 (1H, *J* = 1.2 Hz, =Me31a), 5.35 (1H, d, *J* = 1.2 Hz, =Me31b), 5.31 (1H, s, H33), 4.94 (1H, dtd, *J* = 9.0, 6.1, 4.0 Hz, H29), 4.40 (1H, d, *J* = 11.3 Hz, C<u>H</u>$_a$H$_b$Ar), 4.36 (1H, d, *J* = 11.3 Hz, C<u>H</u>$_a$H$_b$Ar), 3.88 (1H, ddd, *J* = 8.8, 4.9, 2.2 Hz, H27), 3.80 (3H, m, ArOMe), 3.57 (3H, s, OMe32), 3.39 (1H, dd, *J* = 9.2, 7.4 Hz, H25a), 3.22 (1H, dd, *J* = 9.2, 6.7 Hz, H25b), 2.54 (1H, dd, *J* = 13.9, 6.1 Hz, H30a), 2.50 (1H, dd, *J* = 13.9, 6.1 Hz, H30b), 2.20 (1H, t, *J* = 7.2 Hz, C(O)C<u>H</u>$_a$H$_b$R), 2.19 (1H, t, *J* = 7.2 Hz, C(O)CH$_a$<u>H</u>$_b$R), 1.92 (1H, m, H26), 1.83 (1H, ddd, *J* = 14.2, 8.8, 4.1 Hz, H28a), 1.68 (1H, ddd, *J* = 14.2, 9.0, 4.9 Hz, H28b), 1.32-1.21 (29H, m, C(O)CH$_2$<u>R</u>), 0.87 (9H, s, SiMe$_2$*t*Bu), 0.82 (3H, d, *J* = 6.9 Hz, Me26), 0.06 (3H, s, SiMe$_2$*t*Bu), 0.01 (3H, s, SiMe$_2$*t*Bu); **^{13}C NMR** (125 MHz, $CDCl_3$) δ_C 173.0, 158.9, 158.5, 138.2, 131.0, 129.0, 122.1, 113.6, 78.7, 72.7, 72.3, 69.5, 68.5, 55.6, 55.2, 39.2, 38.7, 36.6, 34.6, 31.9, 29.7, 29.7, 29.5, 29.4, 29.3, 29.2, 25.9, 24.9, 22.7, 18.1, 14.1, 10.1, –4.2, –4.8; **IR** (thin film): ν_{max} 2925, 2856, 1734, 1514, 1463, 1248, 1212, 1146, 1041; **$[\alpha]_D^{20}$** –1.2 (*c* 0.25, $CHCl_3$); **HRMS** (ESI$^+$) calculated for $C_{42}H_{73}{}^{79}BrO_6SiNa$ $[M+Na]^+$ 803.4253, found 803.4258.

Alcohol 300

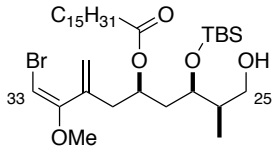

DDQ (60.0 mg, 263 μmol) was added to a stirred solution of PMB ether **299** (103 mg, 132 μmol) in CH_2Cl_2 (1.8 mL) and pH 7 buffer (0.2 mL). The reaction mixture was stirred at r.t. for 1 h before quenching with $NaHCO_3$. The layers were separated and the aqueous phase extracted with CH_2Cl_2 (3 × 2 mL). The combined organic phases were dried ($MgSO_4$) and the solvent removed under reduced pressure. Purification by flash column chromatography (EtOAc/PE 40-60: 25%) afforded the product **300** as a colourless oil (51.0 mg, 77.1 μmol, 58%).

R_f (EtOAc/PE 40-60: 20%) = 0.37; **^{1}H NMR** (500 MHz, $CDCl_3$) δ_H 5.43 (1H, d, *J* = 1.2 Hz, =Me31a), 5.36 (1H, d, *J* = 1.2 Hz, =Me31b), 5.33 (1H, s, H33), 4.96 (1H, dtd, *J* = 10.2, 6.5, 3.9 Hz, H29), 3.86 (1H, ddd, *J* = 9.0, 4.6, 2.4 Hz, H27), 3.58 (3H, s, OMe32), 3.55-3.49 (2H, m, H25), 2.52 (2H, d, *J* = 6.5 Hz, H30), 2.27 (1H, t, *J* = 7.7 Hz, C(O)C$\underline{H}_a$H$_b$R), 2.27 (1H, t, *J* = 7.7 Hz, C(O)C$\underline{H}_a$H$_b$R), 1.92-1.84 (3H, m, H28a, H26, OH), 1.71 (1H, ddd, *J* = 14.2, 9.5, 4.7 Hz, H28b), 1.63-1.58 (2H, m, C(O)C$H_2\underline{R}$), 1.32-1.24 (27H, m, C(O)C$H_2\underline{R}$), 0.89 (9H, s, SiMe$_2$*t*Bu), 0.82 (3H, d, *J* = 7.7 Hz, Me26), 0.08 (3H, s, SiMe$_2$*t*Bu), 0.07 (3H, s, SiMe$_2$*t*Bu); **^{13}C NMR** (125 MHz, $CDCl_3$) δ_C 173.4, 158.3, 138.2, 122.1, 78.8, 69.6, 69.5, 65.8, 55.6, 39.5, 38.8, 38.8, 34.6, 31.9, 29.7, 29.7, 29.5, 29.4, 29.3, 29.2, 25.8, 24.9, 22.7, 18.0, 14.1, 10.1, –4.3, –4.8 ; **IR** (thin film): ν_{max} 3550, 2956, 2926, 2856, 1724, 1463, 1216, 1147; $[\alpha]_D^{20}$ –5.8 (*c* 0.16, $CHCl_3$); **HRMS** (ESI^+) calculated for $C_{34}H_{65}{}^{79}BrO_5SiNa$ $[M+Na]^+$ 683.3682, found 683.3668.

C24-C33 Ketone 302

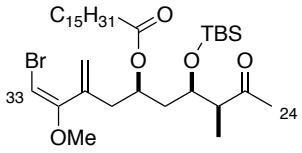

DMSO (17 μL, 242 μmol) was added dropwise to a stirred solution of $(COCl)_2$ (10 μL, 121 μmol) in CH_2Cl_2 (500 μL) at –78 °C. The solution was stirred at –78 °C for 5 min before the addition of a solution of alcohol **300** (20.0 mg, 30.2 μmol) in CH_2Cl_2 (500 μL) *via* cannula. The reaction mixture was stirred at–78 °C for 30 min before the dropwise addition of Et_3N (42 μL, 302 μmol). The mixture was allowed to warm to –20 °C over 30 min before quenching with NH_4Cl (1 mL). The layers were separated, and the aqueous phase extracted with Et_2O (3 × 1 mL). The combined organic phases were dried ($MgSO_4$) and the solvent removed under reduced pressure to afford a crude mixture, which was then resuspended in Et_2O (2 mL) and filtered

over Celite®. The resulting filtrate was concentrated under reduced pressure to afford the crude aldehyde. As the aldehyde was prone to epimerisation at C26, the crude product was used immediately in the next step without further purification.

MeMgBr (10 μL, 36.2 μmol, 3 M in Et_2O) was added dropwise to a solution of crude aldehyde (*ca*. 19.9 mg, 30.2 μmol, dried azeotropically with PhH × 3) in Et_2O (1 mL) at –78 °C. The reaction mixture was stirred at –78 °C for 1 h before quenching with NH_4Cl (1 mL) and allowing the mixture to warm to r.t.. The layers were separated, and the aqueous phase extracted with Et_2O (3 × 1 mL). The combined organic phases were dried ($MgSO_4$) filtered over SiO_2 (eluting with Et_2O) and the solvent removed under reduced pressure to afford the crude alcohol as an inconsequential mixture of C25 epimers.

Separately, DMSO (17 μL, 242 μmol) was added dropwise to a stirred solution of $(COCl)_2$ (10 μL, 121 μmol) in CH_2Cl_2 (500 μL) at –78 °C. The solution was stirred at –78 °C for 5 min before the addition of a solution of the crude alcohol (*ca*. 18.6 mg, 27.5 μmol) in CH_2Cl_2 (500 μL) *via* cannula. The reaction mixture was stirred at–78 °C for 30 min before the dropwise addition of Et_3N (42 μL, 302 μmol). The mixture was allowed to warm to –20 °C over 30 min before quenching with NH_4Cl (1 mL). The layers were separated, and the aqueous phase extracted with Et_2O (3 × 1 mL). The combined organic phases were dried ($MgSO_4$) and the solvent removed under reduced pressure. Purification by flash column chromatography (EtOAc/PE 40-60: 0% → 5%) afforded the product **302** as a colourless oil (11.2 mg, 16.6 μmol, 55% over three steps).

R_f (EtOAc/PE 40-60: 20%) = 0.73; **^{1}H NMR** (500 MHz, $CDCl_3$) δ_H 5.44 (1H, s, =Me31a), 5.36 (1H, s, =Me31b), 5.33 (1H, s, H33), 4.98-4.92 (1H, m, H29), 3.86 (1H, dt, *J* = 8.2, 4.0 Hz, H27), 3.58 (3H, s, OMe32), 2.67 (1H, qd, *J* = 11.5, 3.2 Hz, H26), 2.55-2.49 (2H, m, H30), 2.27 (2H, t, *J* = 7.2 Hz, C(O)CH_2R), 2.14 (3H, s, H24), 1.81 (1H, ddd, *J* = 14.6, 8.7, 4.1 Hz, H28a), 1.71 (1H, ddd, *J* = 14.6, 9.3, 4.5 Hz, H28b), 1.62-1.56 (2H, m, C(O)CH_2R), 1.32-1.24 (27H, m, C(O)CH_2R), 1.04 (3H, d, *J* = 6.8 Hz, Me26), 0.86 (9H, s, $SiMe_2$*t*Bu), 0.07 (3H, s, $SiMe_2$*t*Bu), 0.03 (3H, s, $SiMe_2$*t*Bu); **^{13}C NMR** (125 MHz, $CDCl_3$) δ_C 210.3, 173.1, 158.2, 137.9, 122.1, 78.7, 69.3, 69.1, 55.5, 50.5, 39.4, 39.3, 34.5, 31.8, 29.6, 29.5, 29.5, 29.2, 29.2, 29.1, 28.9, 25.6, 24.9, 22.6, 17.9, 14.0, 9.3, –4.3, –4.4; **IR** (thin film): ν_{max} 2926, 2855, 1734, 1716, 1463, 1251, 1149, 1101; $[\alpha]_D^{20}$ –18.3 (*c* 0.06, $CHCl_3$); **HRMS** (ESI^+) calculated for $C_{35}H_{65}{}^{79}BrO_5SiNa$ $[M+Na]^+$ 695.3682, found 695.3653.

8.5.5. Initial studies towards macrocyclisation: the macrolactonisation/C3-C4 Stille approach

Aldehyde 317 *via* alcohol 316

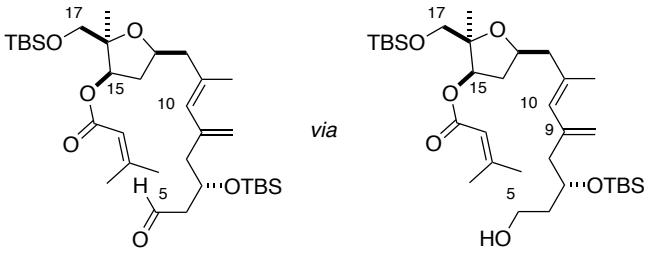

A stirred solution of vinyl iodide **243** (60.0 mg, 121 μmol), boronate **315**[****] (108 mg, 303 μmol) and $Pd(PPh_3)_4$ (56.0 mg, 48.4 μmol) in THF (7.5 mL) and H_2O (2.5 mL) was stirred at 30 °C, to which TlOEt (39 μL, 546 μmol) was added. The yellow-orange mixture was stirred at 30 °C for 2 h before quenching with NH_4Cl (10 mL) and diluting with Et_2O (10 mL). The layers were separated, and the aqueous phase extracted with Et_2O (3 × 10 mL). The combined organic phases were washed with brine (10 mL), dried ($MgSO_4$) and the solvent removed under reduced pressure. Purification by flash column chromatography (EtOAc/PE 40-60: 5%→ 10%) afforded the crude product. As the product was inseparable from the excess boronate, the crude mixture was directly subjected to the next step and an analytically pure sample of alcohol **316** was not obtained.

DMSO (76 μL, 1.05 mmol) was added dropwise to a solution of $(COCl)_2$ (46 μL, 536 μmol) in CH_2Cl_2 (2.5 mL) at –78 °C. The solution was stirred at –78 °C for 5 min before the addition of crude alcohol **316** (89.3 mg, *ca.* 134 μmol) in CH_2Cl_2 (2 mL) *via* cannula. The reaction mixture was stirred at –78 °C for a further 30 min before the dropwise addition of Et_3N (224 μL, 1.60 mmol), and the mixture was warmed to –20 °C over 30 min before quenching with NH_4Cl (10 mL). The layers were separated, and the aqueous phase extracted with Et_2O (3 × 5 mL). The combined organic phases were dried ($MgSO_4$) and the solvent removed under reduced pressure. Purification by flash column chromatography (EtOAc/PE 40-60: 2%) afforded the product **317** as a colourless oil (64.2 mg, 108 μmol, 89% over two steps).

[****] Boronate **315** was synthesised by Garrett Muir

R_f (EtOAc/PE 40-60: 20%) = 0.65; **^{1}H NMR** (500 MHz, $CDCl_3$) δ_H 9.78 (1H, s, H5), 5.67 (1H, s, =CH), 5.58 (1H, s, H10), 5.12 (1H, dd, *J* = 6.4, 4.5 Hz, H15), 5.04 (1H, s, =C$\underline{H}_a$H$_b$9), 4.87 (1H, s, =CH$_a\underline{H}_b$9), 4.27-4.20 (2H, m, H7, H13), 3.72 (1H, d, *J* = 9.6 Hz, H17a), 3.50 (1H, d, *J* = 9.6 Hz, H17b), 2.53-2.39 (5H, m, H6, H8a, H12a, H14a), 2.24 (1H, dd, *J* = 13.6, 8.6 Hz, H8b), 2.21 (1H, dd, *J* = 13.8, 7.2 Hz, H12b), 2.16 (3H, s, =C$\underline{Me}_a$Me$_b$), 1.90 (3H, s, =CMe$_a\underline{Me}_b$), 1.79 (3H, s, Me11), 1.76-1.74 (1H, m, H14b), 1.22 (3H, s, Me16), 0.86 (18H, s, SiMe$_2$*t*Bu), 0.07 (3H, s, SiMe$_2$*t*Bu), 0.05 (3H, s, SiMe$_2$*t*Bu), 0.04 (3H, s, SiMe$_2$*t*Bu), 0.01 (3H, s, SiMe$_2$*t*Bu); **^{13}C NMR** (125 MHz, $CDCl_3$) δ_C 202.2, 165.6, 156.9, 141.4, 136.2, 127.4, 116.0, 84.0, 77.1, 74.9, 67.4, 65.9, 50.0, 47.2, 46.5, 37.7, 25.7, 25.6, 21.7, 20.1, 18.6, 18.1, 17.8, 17.8, –4.5, –4.9, –5.7, –5.7; **IR** (thin film): ν_{max} 2928, 2857, 1723, 1472, 1361, 1253, 1226, 1144, 1094; **$[\alpha]_D^{20}$** –8.0 (*c* 0.05, $CHCl_3$); **HRMS** (ESI^+) calculated for $C_{33}H_{60}O_6Si_2Na$ $[M+Na]^+$ 631.3826, found 631.3805.

Ester 320

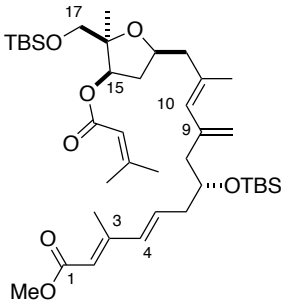

A solution of aldehyde **317** (20.0 mg, 33.6 μmol) and CHI_3 (40.0 mg, 101 μmol) in THF (250 μL) was added to a stirred mixture of $CrCl_2$ (41.0 mg, 336 μmol) in THF (250 μL) at r.t.. The resulting dark red suspension was stirred for 4 h before quenching with $Na_2S_2O_3$ (1 mL) and diluting with Et_2O (1 mL). The layers were separated, and the aqueous phase extracted with Et_2O (3 × 1 mL). The combined organic phases were washed with $Na_2S_2O_3$ (1 mL), dried ($MgSO_4$) and the solvent removed under reduced pressure. The residue was filtered over a plug of silica, eluting with PE 40-60 to afford the crude vinyl iodide **318** (*ca.* 17.5 mg, 23.9 μmol, 71%), which was used in the subsequent step without further purification as an inseparable mixture of *E*/*Z* isomers (3:1) at C4.

A solution of crude vinyl iodide **318** (7.0 mg, 10.0 μmol), stannane **319**[††††] (5.6 mg, 14.0 μmol), $Pd(PPh_3)_4$ (2.2 mg, 1.9 μmol) and CuTC (2.7 mg, 14.0 μmol) in DMF (1 mL) was stirred for 5 h at r.t.. The reaction mixture was subsequently quenched with H_2O and diluted with Et_2O. The layers were separated and the aqueous phase extracted with Et_2O (3 × 1 mL). The combined organic phases were dried ($MgSO_4$) and the

[††††] Stannane **319** was synthesised by Garrett Muir

solvent removed under reduced pressure. Purification by flash column chromatography (EtOAc/PE 40-60: 1%) afforded the product **320** as a colourless oil (6.0 mg, 8.5 μmol, 90%).

Major 4*E* isomer: $\mathbf{R_f}$ (EtOAc/PE 40-60: 20%) = 0.63; **^{1}H NMR** (500 MHz, $CDCl_3$) δ_H 6.21-6.09 (2H, m, H4, H5), 5.69 (1H, s, H2), 5.67 (1H, s, 1H, s, =CH), 5.56 (1H, s, H10), 5.12 (1H, dd, *J* = 6.6, 4.2 Hz, H15), 5.00 (1H, s, =C$\underline{H}_a$H$_b$9), 4.85 (1H, s, =CH$_a\underline{H}_b$9), 4.23 (1H, qn, *J* = 6.5 Hz, H13), 3.82 (1H, m, H7), 3.71-3.69 (4H, m, H17a, OMe), 3.53 (1H, d, *J* = 9.7 Hz, H17b), 2.48 (1H, dd, *J* = 13.2, 5.6 Hz, H12a), 2.42 (1H, ddd, *J* = 13.2, 7.9, 4.6 Hz, H14a), 2.38-2.30 (3H, m, H6a, H8), 2.27 (3H, d, *J* = 0.9 Hz, =C$\underline{Me}_a$Me$_b$) 2.22-2.17 (2H, m, H6b, H12b), 2.17 (3H, d, *J* = 0.8 Hz, Me3), 1.90 (3H, s, =CMe$_a\underline{Me}_b$), 1.79 (3H, d, *J* = 0.9 Hz, Me11), 1.73 (1H, ddd, *J* = 13.2, 6.8, 4.7 Hz, H14b), 1.21 (3H, s, Me16), 0.86 (18H, s, SiMe$_2$*t*Bu), 0.03 (3H, s, SiMe$_2$*t*Bu), 0.02 (3H, s, SiMe$_2$*t*Bu), 0.01 (6H, s SiMe$_2$*t*Bu); **^{13}C NMR** (125 MHz, $CDCl_3$) δ_C 167.7, 165.7, 157.0, 152.8, 142.2, 135.6, 128.0, 127.9, 117.4, 117.3, 116.0, 84.0, 75.0, 71.1, 66.1, 60.3, 51.0, 47.3, 46.3, 41.3, 38.4, 25.8, 25.8, 22.6, 20.2, 18.2, 18.1, 13.8, –4.4, –4.6, –5.4, –5.6 ; **IR** (thin film): ν_{max} 2931, 2861, 1732, 1720, 1440, 1361, 1361, 1256, 1226, 1147, 1101; $\mathbf{[\alpha]_D^{20}}$ –5.2 (*c* 0.16, $CHCl_3$); **HRMS** (ESI^+) calculated for $C_{39}H_{68}O_7Si_2Na$ $[M+Na]^+$ 727.4401 found 727.4395.

Alcohol 326

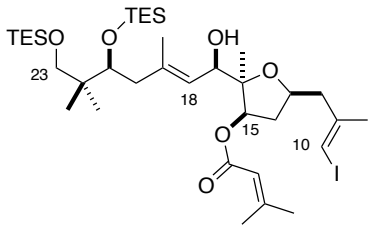

The addition reaction was performed according to the general protocol described in **8.5.2**, using vinyl iodide **325** (127.5 mg, 249 μmol), *t*BuLi (260 μL, 497 μmol, 1.9 M in pentane), $MgBr_2{\cdot}OEt_2$ (1.20 mL, 727 μmol, 0.6 M in Et_2O), and aldehyde **245** (15.0 mg, 38.3 μmol) to afford the product **326** (23.4 mg, 30.0 μmol, 78%), a colourless oil as an inseparable 5:1 mixture of diastereomers at C17, alongside with the C10 protodeiodinated material.

$\mathbf{R_f}$ (EtOAc/PE 40-60: 20%) = 0.58; **^{1}H NMR** (500 MHz, $CDCl_3$) δ_H 5.94 (1H, s, H10), 5.73 (1H, s, =CH), 5.31 (1H, d, *J* = 9.0 Hz, H10), 5.12 (1H, dd, *J* = 6.1, 2.4 Hz, H15), 4.49 (1H, dd, *J* = 9.0, 4.2 Hz, H17), 4.25-4.19 (1H, m, H13), 3.82 (1H, dd, *J* = 7.3, 3.8 Hz, H21), 3.37 (1H, d, *J* = 9.1 Hz, H23a), 3.32 (1H, d, *J* = 9.1 Hz, H23b), 2.59-2.50 (3H, m, H12a, H14a), 2.39 (1H, dd, *J* = 13.7, 6.2, H12b), 2.34 (1H, dd, *J* = 14.1, 3.8 Hz, H20a), 2.20 (3H, d, *J* = 1.3 Hz, =C$\underline{Me}_a$Me$_b$), 2.11 (1H, d, *J* = 4.2 Hz, OH), 2.04 (1H, dd, *J* = 14.1, 7.3 Hz, H20b), 1.94 (3H, d, *J* = 1.1 Hz, =CMe$_a\underline{Me}_b$), 1.84 (3H, d, *J* = 1.0 Hz, Me11), 1.72 (3H, d, *J* = 1.0 Hz, Me19), 1.69 (1H, ddd, *J* = 14.2, 5.0, 2.5 Hz, H14b), 1.17 (3H, s, Me16), 0.98-0.92 (18H, m, Si(CH$_2$C$\underline{H}_3$)$_3$), 0.85 (3H, s, Me22a), 0.80 (3H, s, Me22b), 0.61-0.55 (12H, m, Si($\underline{CH}_2$CH$_3$)$_3$); **^{13}C NMR** (125 MHz, $CDCl_3$) δ_C 166.2,

158.7, 144.8, 138.9, 125.2, 115.6, 87.1, 78.0, 77.1, 74.4, 73.8, 69.8, 69.6, 46.3, 44.4, 40.9, 37.5, 27.5, 24.4, 21.0, 20.4, 20.1, 19.1, 17.1, 7.2, 6.9, 5.5, 5.4, 4.5; **IR** (thin film): ν_{max} 3454, 2952, 2877, 1720, 1379, 1229, 1143, 1087, 1007; $[\alpha]_D^{20}$ –11.3 (*c* 0.08, $CHCl_3$); **HRMS** (ESI^+) calculated for $C_{36}H_{67}IO_6Si_2Na$ $[M+Na]^+$ 801.3419, found 801.3421.

TES ether 324

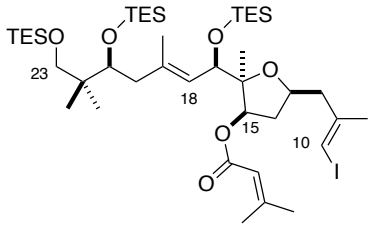

TESOTf (10 μL, 39.2 μmol) was added dropwise to a stirred solution of alcohol **326** (23.5 mg, 30.2 μmol) and 2,6-lutidine (10 μL, 91 μmol) in CH_2Cl_2 (500 μL) at –78 °C. The reaction mixture was stirred at –78 °C for 1 h before quenching with MeOH (50 μL) followed by $NaHCO_3$ (500 μL). The layers were separated, and the aqueous phase extracted with Et_2O (3 × 10 mL). The combined organic phases were dried ($MgSO_4$) and the solvent removed under reduced pressure. Purification by flash column chromatography (Et_2O/PE 40-60: 0% → 1%) afforded the product **324** as a colourless oil (26.0 mg, 29.1 mmol, μmol, 96%).

R_f (EtOAc/PE 40-60: 20%) = 0.82; **^{1}H NMR** (500 MHz, $CDCl_3$) δ_H 5.86 (1H, q, *J* = 1.0 Hz, H10), 5.73 (1H, sept, *J* = 1.3 Hz, =CH), 5.20 (1H, d, *J* = 8.7 Hz, H10), 4.98 (1H, dd, *J* = 5.7, 0.8 Hz, H15), 4.73 (1H, d, *J* = 8.7 Hz, H17), 4.19-4.13 (1H, m, H13), 3.85 (1H, dd, *J* = 7.6, 4.2 Hz, H21), 3.40 (1H, d, *J* = 9.2 Hz, H23a), 3.32 (1H, d, *J* = 9.2 Hz, H23b), 2.55-2.43 (3H, m, H12a, H14a, H20a), 2.32 (1H, dd, *J* = 13.5, 5.9 Hz, H12b), 2.20 (3H, d, *J* = 1.3 Hz, =C$\underline{Me}_a$Me$_b$), 2.06-2.01 (1H, m, H20b), 1.93 (3H, d, *J* = 1.2 Hz, =CMe$_a$$\underline{Me}_b$), 1.81 (3H, d, *J* = 1.0 Hz, Me11), 1.74 (3H, d, *J* = 0.8 Hz, Me19), 1.61 (1H, dd, *J* = 15.0, 4.3 Hz, H14b), 1.10 (3H, s, Me16), 0.96 (18H, t, *J* = 8.0 Hz, Si($CH_2C\underline{H}_3)_3$ ×2), 0.87 (9H, t, *J* = 8.0 Hz, Si($CH_2C\underline{H}_3)_3$), 0.63 (6H, q, *J* = 8.0 Hz, , Si($\underline{CH}_2CH_3)_3$, 0.59 (6H, q, *J* = 7.9 Hz, Si($CH_2\underline{CH}_3)_3$, 0.47 (6H, q, *J* = 7.9 Hz, Si($CH_2\underline{CH}_3)_3$, 1.17 (3H, s, Me16), 0.98-0.92 (18H, m, Si($CH_2C\underline{H}_3)_3$), 0.87 (3H, s, Me22a), 0.86 (3H, s, Me22b), 0.61-0.55 (12H, m, Si($\underline{CH}_2CH_3)_3$); **^{13}C NMR** (125 MHz, $CDCl_3$) δ_C 165.7, 156.8, 145.1, 137.0, 126.1, 116.5, 87.9, 77.5, 74.2, 74.1, 69.6, 69.5, 46.9, 45.2, 37.3, 27.3, 25.8, 24.2, 22.7, 20.3, 18.0, 17.6, 7.1, 6.9, 6.8, 5.3, 5.2, 4.5; **IR** (thin film): ν_{max} 2952, 2875, 1721, 1652, 1459, 1378, 1229, 1144, 1077; $[\alpha]_D^{20}$ –3.0 (*c* 0.14, $CHCl_3$); **HRMS** (ESI^+) calculated for $C_{42}H_{81}O_6Si_3INa$ $[M+Na]^+$ 915.4283, found 915.4271.

Alcohol 328

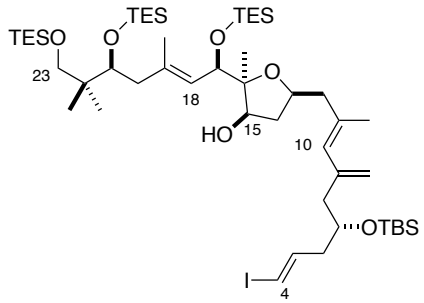

DIBAL (18 μL, 18 μmol, 1 M in hexanes) was added dropwise to a stirred solution of ester **327**‡‡‡‡ (10.0 mg, 8.90 μmol) in CH_2Cl_2 (250 μL) at –78 °C. The reaction mixture was stirred at –78 °C for 1 h before quenching with MeOH (10 μL) and Na/K tartrate (250 μL). The mixture was allowed to warm to r.t. and stirred for 30 min at r.t. before separating the layers. The aqueous phase extracted with EtOAc (3 × 250 μL). The combined organic phases were dried ($MgSO_4$) and the solvent removed under reduced pressure. Purification by flash column chromatography (EtOAc/PE 40-60: 5%) afforded the product **328** as a colourless oil (7.5 mg, 7.24 mmol, μmol, 81%).

Major 4*E* isomer: $\mathbf{R_f}$ (EtOAc/PE 40-60: 20%) = 0.69; **^{1}H NMR** (500 MHz, $CDCl_3$) δ_H 6.52 (1H, dt, *J* = 15.2, 7.3 Hz, H5), 5.98 (1H, d, *J* = 15.2 Hz, H5), 5.61 (1H, s, H10), 5.48 (1H, d, *J* = 11.0 Hz, H18), 5.01 (1H, s, =C$\underline{H}_a$H$_b$9), 4.84 (1H, s, =CH$_a\underline{H}_b$9), 4.60 (1H, d, *J* = 11.0 Hz, H17), 4.13-4.07 (2H, m, H13, H15), 3.89 (1H, dd, *J* = 7.3, 3.8 Hz, H21), 3.77-3.72 (1H, m, H7), 3.40 (1H, d, *J* = 9.3 Hz, H23a), 3.28 (1H, d, *J* = 9.3 Hz, H23b), 2.57-2.49 (2H, m, H12a, H20a), 2.33-2.13 (5H, m, H6a, H8, H12b, H14a), 2.11-2.03 (2H, m, H6b, H20b), 1.80 (3H, s, Me11), 1.76 (3H, s, Me19), 1.71-1.66 (1H, m, H14b), 0.98-0.93 (27H, m, SiCH$_2$C$\underline{H}_3$), 0.89 (9H, s, SiMe$_2$*t*Bu), 0.88 (3H, s, Me16), 0.83 (3H, s, Me22a), 0.81 (3H, s, Me22b), 0.64-0.56 (18H, m, SiC$\underline{H}_2$CH$_3$), 0.04 (6H, s, SiMe$_2$*t*Bu); **^{13}C NMR** (125 MHz, $CDCl_3$) δ_C 143.5, 142.2, 137.9, 136.0, 127.6, 125.6, 115.9, 86.1, 78.9, 76.4, 74.7, 74.4, 73.2, 70.2, 69.5, 47.5, 46.0, 45.2, 42.9, 41.4, 29.7, 21.5, 21.3, 19.1, 18.6, 18.0, 17.5, 7.1, 6.9, 6.8, 5.4, 5.4, 5.0, 4.5, 1.0, –4.5, –4.6; **IR** (thin film): ν_{max} 3379, 2953, 2928, 1462, 1377, 1258, 1078, 1011, 798; $[\alpha]_D^{20}$ –2.0 (*c* 0.10, $CHCl_3$); **HRMS** (ESI^+) calculated for $C_{50}H_{99}O_6Si_4INa$ $[M+Na]^+$ 1057.5461, found 1057.5473.

‡‡‡‡ Ester **327** was synthesised by Garrett Muir

Ester 338

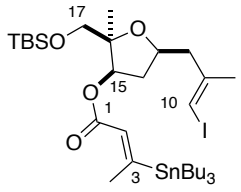

DCC (469 μL, 469 μmol, 1 M in CH_2Cl_2) was added to a stirred solution of alcohol **241** (40.0 mg, 93.8 μmol), acid **329**[§§§§] (176 mg, 469 μmol), DMAP (57.3 mg, 469 μmol) and DMAP·HCl (73.5 mg, 469 μmol) in CH_2Cl_2 (1 mL). The cloudy suspension was stirred for 16 h, to which it turned deep red. The reaction mixture was then filtered over SiO_2 and the filtrate concentrated under reduced pressure. Purification by flash column chromatography (Et_2O/PE 40-60: 5%) afforded the product **338** as a colourless oil (66.2 mg, 84.5 μmol, 90%).

R_f (EtOAc/PE 40-60: 20%) = 0.78; **^{1}H NMR** (500 MHz, $CDCl_3$) δ_H 6.40 (1H, s, H2), 5.93 (1H, s, H10), 5.05 (1H, dd, *J* = 6.0, 4.0 Hz, H15), 4.22 (1H, qn, *J* = 6.5 Hz, H13), 3.73 (1H, d, *J* = 9.7 Hz, H17a), 3.53 (1H, *J* = 9.7 Hz, H17b), 2.69 (3H, s, Me3), 2.55 (1H, dd, *J* = 13.9, 6.6 Hz, H12a), 2.47 (1H, dt, *J* = 13.8, 6.5 Hz, H14a), 2.37 (1H, dd, *J* = 13.9, 6.5 Hz, H12b), 1.85 (3H, s, Me11), 1.69 (1H, ddd, *J* = 13.8, 5.9, 4.0 Hz, H14b), 1.58-1.23 (36H, m, $SnBu_3$), 1.20 (3H, s, Me16), 1.11-0.83 (54H, m, $SiMe_2$*t*Bu, $SnBu_3$), 0.04 (3H, s, $SiMe_2$*t*Bu), 0.01 (3H, s, $SiMe_2$*t*Bu). **^{13}C NMR** (125 MHz, $CDCl_3$) δ_C 173.3, 167.1, 144.9, 128.9, 84.4, 77.8, 74.6, 74.5, 65.9, 46.3, 37.5, 29.2, 27.4, 25.9, 24.5, 21.7, 18.2, 13.8, 13.7, 11.3, 10.9, –5.5; **IR** (thin film): ν_{max} 2955, 2924, 2855, 1702, 1601, 1463, 1375, 1317, 1193, 1103; $[\alpha]_D^{20}$ –19.3 (*c* 1.37, $CHCl_3$); **HRMS** (ESI^+) calculated for $C_{32}H_{61}IO_4SiSnNa$ $[M+Na]^+$ 803.2299, found 803.2295.

[§§§§] Acid **329** was synthesised by Garrett Muir

8.5.6. Macrocyclisation *via* C9-C10 Stille coupling

TIPS ether 352

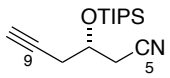

TIPSOTf (954 μL, 3.60 mmol) was added to a stirred solution of alcohol **310**[*****] (310 mg, 2.84 mmol) and 2,6-lutidine (491 μL, 4.26 mmol) in CH_2Cl_2 (30 mL) at r.t.. The solution was stirred at r.t. for 16 h before quenching with MeOH (1 mL) and stirring for 30 min. A solution of $NaHCO_3$ (20 mL) was then added and the layers were separated. The aqueous phase extracted with CH_2Cl_2 (3 × 10 mL). The combined organic phases were washed with brine (10 mL), dried ($MgSO_4$) and the solvent removed under reduced pressure. Purification by flash column chromatography (EtOAc/PE 30-40: 2%) afforded the product **352**, as a colourless liquid (725 mg, 2.73 mmol, 96%).

R_f (EtOAc/PE 40-60: 20%) = 0.60; **^{1}H NMR** (500 MHz, $CDCl_3$) δ_H 4.23 (1H, dq *J* = 8.0, 4.8 Hz, H7), 3.54 (1H, s, OH), 2.75 (1H, dd, *J* = 16.6, 5.0 Hz, H6a), 2.72 (1H, dd, *J* = 16.6, 4.9 Hz, H6b), 2.58 (1H, ddd, *J* = 15.9, 4.6, 2.7 Hz, H8a), 2.53 (1H, ddd, *J* = 16.9, 7.9, 2.7 Hz, H8b), 2.08 (1H, t, *J* = 2.7 Hz, ≡CH) ; **^{13}C NMR** (125 MHz, $CDCl_3$) δ_C 117.1, 79.1, 71.8, 67.2, 27.1, 25.4, 18.0, 12.3; **IR** (thin film): ν_{max} 3310, 2945, 2867, 2261, 1463, 1366, 1118, 1069; $[\alpha]_D^{20}$ +5.7 (*c* 0.35, $CHCl_3$); **HRMS** (ESI^+) calculated for $C_{15}H_{27}INOSiNa$ $[M+Na]^+$ 288.1754, found 288.1741.

Vinyl iodide 340 and 353

Iodo-9-BBN (4.0 mL 4.00 mmol, 1 M in hexanes) was added dropwise to a stirred solution of alkyne **339**[†††††] (400 mg, 1.79 mmol) in hexane (10 mL) at 0 °C. The reaction mixture was stirred for 4 h at 0 °C before adding glacial AcOH (1.0 mL, 17.5 mmol) in one portion. The mixture was stirred for 30 min at 0 °C before the addition of NaOH (1.5 mL, 1 M in H_2O), H_2O_2 (2.4 mL) and $NaHCO_3$ (10 mL) and stirred at r.t. for 1 h. The layers were separated, and the aqueous phase extracted with Et_2O (3 × 10 mL). The combined organic phases were washed with $Na_2S_2O_3$ (15 mL), brine (15 mL), dried ($MgSO_4$) and the solvent removed under

[*****] Alcohol **310** was synthesised by Garrett Muir

[†††††] Alkyne **339** was synthesised by Garrett Muir

reduced pressure. Purification by flash column chromatography (Et_2O/PE 40-60: 10%) afforded the product **340** as a colourless oil (486 mg, 1.38 mmol, μmol, 77%).

R_f (EtOAc/PE 40-60: 20%) = 0.61; **^{1}H NMR** (500 MHz, $CDCl_3$) δ_H 6.20 (1H, d, *J* = 1.2 Hz, =C$\underline{H}_a$H$_b$9), 5.83 (1H, d, *J* = 1.5 Hz, =CH$_a\underline{H}_b$9), 4.21 (1H, dddd, *J* = 6.6, 6.1, 5.0, 4.5 Hz, H7), 2.72 (1H, ddd, *J* = 14.2, 6.1, 1.0 Hz, H8a), 2.62 (1H, ddd, *J* = 14.1, 6.8, 1.1 Hz, H8b), 2.56 (1H, dd, *J* = 16.6, 6.6, 4.6 Hz, H6a), 2.45 (1H, dd, *J* = 16.6, 5.0 Hz, H6b), 0.91 (9H, s, SiMe$_2$*t*Bu), 0.16 (3H, s, SiMe$_2$*t*Bu), 0.13 (3H, s, SiMe$_2$*t*Bu); **^{13}C NMR** (125 MHz, $CDCl_3$) δ_C 129.7, 117.1, 104.7, 67.0, 52.3, 25.7, 25.3, 18.0, –4.4, –4.7; **IR** (thin film): ν_{max} 2929, 2857, 1618, 1471, 1363, 1257, 1105, 839; $[\alpha]_D^{20}$ –2.9 (*c* 0.21, $CHCl_3$); **HRMS** (ESI$^+$) calculated for $C_{12}H_{22}INOSiH$ $[M+H]^+$ 352.0594, found 352.0592.

The vinyl iodide **353** derived from alkyne **352** bearing the C7 TIPS ether (725 mg, 2.73 mmol) was analogously synthesised using iodo-9-BBN (8.19 mL, 8.19 mmol, 1 M in hexanes), followed by AcOH (2.0 mL, 35.0 mmol) to afford vinyl iodide **353** (884 mg, 2.25 mmol, 82%) as a colourless oil.

R_f (EtOAc/PE 40-60: 20%) = 0.67; **^{1}H NMR** (500 MHz, $CDCl_3$) δ_H 6.27 (1H, s, =C$\underline{H}_a$H$_b$9), 5.85 (1H, s, =CH$_a\underline{H}_b$9), 4.35 (1H, dt, *J* = 13.1, 4.4 Hz, H7), 2.81 (1H, dd, *J* = 14.2, 4.4 Hz, H8a), 2.71 (1H, dd, *J* = 14.2, 8.8 Hz, H8b), 2.61 (1H, dd, *J* = 16.7, 4.4 Hz, H6a), 2.50 (1H, dd, *J* = 16.7, 4.4 Hz, H6b), 1.10 (21H, m, OTIPS); **^{13}C NMR** (125 MHz, $CDCl_3$) δ_C 129.6, 116.7, 104.2, 67.1, 51.6, 24.9, 17.6, 12.1; **IR** (thin film): ν_{max} 2942, 2865, 1618, 1463, 1247, 1111; $[\alpha]_D^{20}$ –1.0 (*c* 0.49, $CHCl_3$); **HRMS** (ESI$^+$) calculated for $C_{15}H_{28}INOSiNa$ $[M+Na]^+$ 416.0939, found 416.0911.

Aldehyde 341 and 354

DIBAL (490 μL, 490 μmol, 1 M in hexanes) was added dropwise to a stirred solution of nitrile **340** (150 mg, 427 μmol, dried by azeotroping with PhH × 3) in PhMe (4.0 mL) at –78 °C. The reaction mixture was stirred at –78 °C for 1 h before quenching with MeOH (0.5 mL) followed by citric acid (2 mL, 10%). The mixture was allowed to warm to r.t. and stirred until two distinct layers were observed. The layers were separated, and the aqueous phase extracted with CH_2Cl_2 (3 × 2 mL). The combined organic phases were dried ($MgSO_4$) and the solvent removed under reduced pressure. Purification by flash column chromatography (Et_2O/PE 40-60: 10%) afforded the product **341** as a colourless oil (133 mg, 375 μmol, 87%).

R_f (EtOAc/PE 40-60: 20%) = 0.71; **^{1}H NMR** (500 MHz, $CDCl_3$) δ_H 9.85 (1H, dd, *J* = 2.9, 1.8 Hz, H5), 6.14 (1H, d, *J* = 1.2 Hz, =C$\underline{H}_a$H$_b$9), 5.82 (1H, d, *J* = 1.2 Hz, =CH$_a\underline{H}_b$9), 4.48 (1H, ddd, *J* = 12.8, 6.6, 4.7 Hz, H7),

2.71 (1H, ddd, *J* = 14.1, 6.0, 1.2 Hz, H8a), 2.64 (1H, ddd, *J* = 15.8, 4.7, 1.8 Hz, H6a), 2.58 (1H, ddd, *J* = 14.1, 6.6, 1.2 Hz, H8b), 2.53 (1H, ddd, *J* = 15.8, 6.5, 2.9 Hz, H6b), 0.90 (9H, s, $SiMe_2tBu$), 0.16 (3H, s, $SiMe_2tBu$), 0.14 (3H, s, $SiMe_2tBu$); **^{13}C NMR** (125 MHz, $CDCl_3$) δ_C 201.5, 129.0, 106.0, 67.1, 53.0, 49.8, 25.7, 18.0, –4.2, –4.6; **IR** (thin film): ν_{max} 2931, 2928, 1720, 1617, 1472, 1255, 1147, 1101; **$[\alpha]_D^{20}$** –2.3 (*c* 0.13, $CHCl_3$); **HRMS** (ESI^+) calculated for $C_{12}H_{23}IO_2SiNa$ $[M+Na]^+$ 377.0410, found 377.0412.

The aldehyde **354** derived from nitrile **353** bearing the C7 TIPS ether (301 mg, 764 μmol) was analogously synthesised using DIBAL (1.15 mL, 1.15 mmol, 1 M in hexanes) to afford aldehyde **354** (188 mg, 474 μmol, 62%) as a pale-yellow oil.

R_f (EtOAc/PE 40-60: 20%) = 0.69; **^{1}H NMR** (500 MHz, $CDCl_3$) δ_H 9.88 (1H, s, H5), 6.14 (1H, s, $=C\underline{H}_aH_b9$), 5.80 (1H, s, $=CH_a\underline{H}_b9$), 4.21 (1H, dt, *J* = 13.7, 4.8 Hz, H7), 2.81-2.71 (1H, m, H6a), 2.67-2.58 (2H, m, H8), 2.53-2.48 (1H, m, H6b), 1.09-1.05 (21H, m, OTIPS); **^{13}C NMR** (125 MHz, $CDCl_3$) δ_C 201.5, 129.0, 105.3, 67.8, 52.5, 49.1, 18.0, 12.3; **IR** (thin film): ν_{max} 2946, 1726, 1464, 1250, 1110, 1066; **$[\alpha]_D^{20}$** –3.3 (*c* 0.15, $CHCl_3$); **HRMS** (ESI^+) calculated for $C_{15}H_{29}IO_2SiNa$ $[M+Na]^+$ 419.0879, found 419.0885.

Dienoate 343 and 355

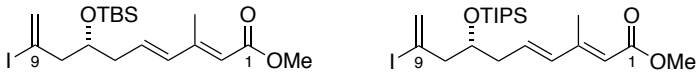

*n*BuLi (1.29 mL, 1.80 mmol, 1.4 M in hexane) was added dropwise to a stirred solution of *i*Pr_2NH (282 μL, 2.00 mmol) in THF (2.43 mL) at 0 °C. The pale-yellow solution was stirred for 30 min at 0 °C to give a 0.5 M solution of LDA.

An aliquot of freshly prepared LDA (1.52 mL, 762 μmol, 0.5 M in THF) was added to a stirred solution of phosphonate **342**[‡‡‡‡‡] (175 mg, 762 μmol, dried by azeotroping with PhH × 3) in THF (1 mL) and HMPA (1 mL) at –78 °C. The resulting yellow suspension was stirred for 30 min at –78 °C before the dropwise addition of a solution of aldehyde **341** (90.0 mg, 254 μmol) in THF (500 μL) *via* cannula. The stirred reaction mixture was then allowed to warm to –40 °C over 1 h before quenching with NH_4Cl (5 mL) and diluting with Et_2O (5 mL). The layers were separated, and the aqueous phase extracted with Et_2O (3 × 10 mL). The combined organic phases were washed with brine (10 mL), dried ($MgSO_4$) and the solvent removed under reduced pressure. Purification by flash column chromatography (EtOAc/PE 30-40: 2%)

[‡‡‡‡‡] Phosphonate **342** was synthesised by Garrett Muir

afforded product **343**, a pale-yellow oil (93.5 mg, 208 μmol, 82%), as an inseparable mixture of *E/Z* isomers (5:1) at C2.

R_f (EtOAc/PE 40-60: 20%) = 0.84; **^{1}H NMR** (500 MHz, $CDCl_3$) δ_H 6.16-6.13 (2H, m, H4, H5), 6.07 (1H, s, =C$\underline{H}_a$H$_b$9), 5.75 (1H, s, =CH$_a\underline{H}_b$9), 5.71 (1H, s, H2), 4.01 (1H, dt, *J* = 11.5, 6.0 Hz, H7), 3.71 (3H, s, OMe), 2.53 (1H, dd, *J* = 14.1, 6.0 Hz, H8a), 2.46 (1H, dd, *J* = 14.1, 6.0 Hz, H8b), 2.43-2.39 (1H, m, H6a), 2.30-2.25 (4H, m, Me3, H6b), 0.88 (9H, s, SiMe$_2$*t*Bu), 0.10 (3H, s, SiMe$_2$*t*Bu), 0.07 (3H, s, SiMe$_2$*t*Bu); **^{13}C NMR** (125 MHz, $CDCl_3$) δ_C 167.6, 152.5, 136.2, 133.1, 128.3, 117.8, 107.6, 70.4, 52.9, 51.0, 25.8, 18.0, 13.8, –4.2, –4.4; **IR** (thin film): ν_{max} 2951, 2929, 2857, 1717, 1614, 1471, 1434, 1240, 1157, 1091; $[\alpha]_D^{20}$ –1.3 (*c* 0.32, $CHCl_3$); **HRMS** (ESI^+) calculated for $C_{18}H_{31}IO_3SiNa$ $[M+Na]^+$ 473.0984, found 473.0970.

The dienoate **355** derived from aldehyde **354** bearing the C7 TIPS ether (188 mg, 475 μmol) was analogously synthesised using phosphonate **342** (166 mg, 721 μmol) and LDA (1.44 mL, 721 μL, 0.5 M in THF) to afford dienoate **355** (171 mg, 380 μmol, 80%) as an amber oil.

R_f (EtOAc/PE 40-60: 20%) = 0.70; **^{1}H NMR** (500 MHz, $CDCl_3$) δ_H 6.26-6.20 (1H, m, H5), 6.13 (1H, d, *J* = 15.6 Hz, H4), 6.08 (1H, s, =C$\underline{H}_a$H$_b$9), 5.76 (1H, s, =CH$_a\underline{H}_b$9), 5.70 (1H, s, H2), 4.24-4.20 (1H, m, H7), 3.70 (3H, s, OMe), 2.61 (1H, dd, *J* = 15.1, 4.9 Hz, H8a), 2.52-2.45 (2H, m, H8b, H6a), 2.35-2.24 (4H, m, Me3, H6b), 1.10-1.05 (21H, m, OTIPS); **^{13}C NMR** (125 MHz, $CDCl_3$) δ_C 167.5, 152.4, 136.2, 132.7, 128.1, 117.5, 107.0, 70.6, 52.1, 50.9, 39.2, 18.1, 13.7, 12.4; **IR** (thin film): ν_{max} 2945, 2866, 1716, 1614, 1462, 1356, 1239, 1157, 1109; $[\alpha]_D^{20}$ +4.8 (*c* 0.13, $CHCl_3$); **HRMS** (ESI^+) calculated for $C_{21}H_{37}IO_3SiNa$ $[M+Na]^+$ 515.1454, found 515.1458.

Acid 344 and 356

$Ba(OH)_2{\cdot}8H_2O$ (377 mg, 1.19 mmol) was added to a stirred solution of dienoate **343** (53.8 mg, 119 μmol) in MeOH (1.5 mL). The pale-yellow suspension was stirred at r.t. for 48 h before quenching with HCl (2 mL, 1 M in H_2O) and diluting with EtOAc (3 mL). The layers were separated, and the aqueous phase extracted with Et_2O (3 × 10 mL). The combined organic phases were washed with brine (10 mL), dried ($MgSO_4$) and the solvent removed under reduced pressure to afford acid **344** as an amorphous yellow solid (52.0 mg, 119 μmol, 99%).

R_f (EtOAc/PE 40-60: 20%) = 0.10; **^{1}H NMR** (500 MHz, $CDCl_3$) δ_H 10.60 (1H, br s, OH), 6.25-6.16 (2H, m, H4, H5), 6.07 (1H, s, =C$\underline{H}_a$H$_b$9), 5.76 (1H, s, =CH$_a\underline{H}_b$9), 5.74 (1H, s, H2), 4.02 (1H, qn, *J* = 5.6 Hz, H7), 2.54 (1H, dd, *J* = 14.0, 5.6 Hz, H8a), 2.48-2.41 (2H, m, H6a, H8b), 2.32-2.26 (4H, m, Me3, H6b), 0.88 (9H, s,

$SiMe_2tBu$), 0.10 (3H, s, $SiMe_2tBu$), 0.08 (3H, s, $SiMe_2tBu$); **^{13}C NMR** (125 MHz, $CDCl_3$) δ_C 171.5, 154.8, 136.1, 134.1, 128.3, 117.2, 107.6, 70.4, 52.8, 40.0, 25.8, 18.0, 14.0, –4.2, –4.4; **IR** (thin film): ν_{max} 2951 (br), 2928, 2855, 1682, 1607, 1413, 1253, 1186, 1088; $[\alpha]_D^{20}$ +0.6 (*c* 0.33, $CHCl_3$); **HRMS** (ESI^+) calculated for $C_{17}H_{29}IO_3SiNa$ $[M+Na]^+$ 459.0828, found 459.0822.

The acid **356** derived from dienoate **355** bearing the C7 TIPS ether (171 mg, 380 μmol) was analogously synthesised using $Ba(OH)_2{\cdot}8H_2O$ (1.09 g, 3.47 mmol) to afford acid **356** (159 mg, 332 μmol, 96%) as a brown oil.

R_f (EtOAc/PE 40-60: 20%) = 0.05; **^{1}H NMR** (500 MHz, $CDCl_3$) δ_H 9.40 (1H, br s, OH), 6.33-6.28 (1H, m, H5), 6.19 (1H, d, *J* = 15.8 Hz, H4), 6.11 (1H, s, =C$\underline{H}_a$H$_b$9), 5.80 (1H, s, =CH$_a\underline{H}_b$9), 5.75 (1H, s, H2), 4.27-4.23 (1H, m, H7), 2.64 (1H, dd, *J* = 14.0, 4.5 Hz, H8a), 2.54-2.50 (2H, m, H6a, H8b), 2.36 (1H, ddd, *J* = 14.2, 8.2, 5.5 Hz, H6b), 2.31 (3H, s, Me3), 1.11-1.10 (21H, m, OTIPS); **^{13}C NMR** (125 MHz, $CDCl_3$) δ_C 169.9, 154.9, 136.2, 133.8, 128.2, 116.6, 107.1, 70.6, 52.2, 39.3, 18.2, 13.9, 12.5; **IR** (thin film): ν_{max} 2944, (br) 2866, 1687, 1609, 1461, 1258, 1188, 1109; $[\alpha]_D^{20}$ +3.3 (*c* 0.09, $CHCl_3$); **HRMS** (ESI^+) calculated for $C_{20}H_{35}IO_3SiNa$ $[M+Na]^+$ 501.1275, found 501.1298.

TMS ether 345

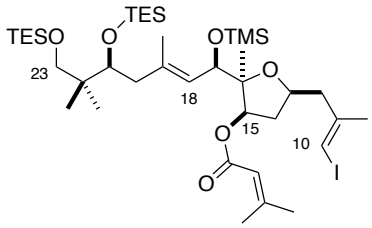

TMS-imidazole (13.9 μL, 95.0 μmol) was added to a stirred solution of alcohol **326** (18.5 mg, 23.7 μmol) in CH_2Cl_2 (240 μL) at 0 °C. The mixture was allowed to warm to r.t. over 2 h before quenching with MeOH (50 μL) and stirring for 10 min. The solvent was evaporated under reduced pressure, and the residue was purified by flash column chromatography (EtOAc/PE 40-60: 2%) to afford product **345** as a colourless oil (15.2 mg, 17.9 μmol, 75%).

R_f (EtOAc/PE 40-60: 20%) = 0.83; **^{1}H NMR** (500 MHz, $CDCl_3$) δ_H 5.87 (1H, s, H10), 5.72 (1H, s, =CH), 5.19 (1H, d, *J* = 9.0 Hz, H18), 5.02 (1H, d, *J* = 5.0 Hz, H15), 4.69 (1H, d, *J* = 9.0 Hz, H19), 4.20-4.15 (1H, m, H13), 3.86 (1H, dd, *J* = 7.1, 4.4 Hz, H21), 3.40 (1H, d, *J* = 9.3 Hz, H23a), 3.32 (1H, d, *J* = 9.3 Hz, H23b), 2.52-2.45 (3H, m, H12a, H14a, H20a), 2.33 (1H, dd, *J* = 13.9, 5.7 Hz, H12b), 2.20 (3H, s, =C$\underline{Me}_a$Me$_b$), 2.04 (1H, dd, *J* = 14.9, 4.4 Hz, H20b), 1.93 (3H, s, =CMe$_a\underline{Me}_b$), 1.81 (3H, s, Me11), 1.74 (3H, s, Me19), 1.60 (1H, dd, *J* =

14.7, 4.6 Hz, H14b), 1.09 (3H, s, Me16), 0.96 (18H, t, J = 7.9 Hz, $SiCH_2C\underline{H}_3$), 0.83 (3H, s, Me22a), 0.83 (3H, s, Me22b), 0.62 (6H, q, J = 7.9 Hz, $SiC\underline{H}_2CH_3$), 0.58 (6H, q, J = 7.9 Hz, $SiC\underline{H}_2CH_3$), –0.03 (9H, s, $SiMe_3$); **^{13}C NMR** (125 MHz, $CDCl_3$) δ_C 165.7, 157.0, 145.1, 137.0, 126.2, 116.5, 87.9, 77.4, 76.9, 74.3, 74.2, 69.8, 69.7, 46.9, 45.0, 41.3, 37.3, 29.7, 27.4, 24.2, 21.6, 20.3, 19.0, 18.1, 7.2, 6.9, 5.4, 4.5, 0.4; **IR** (thin film): ν_{max} 2952, 2927, 2873, 1724, 1462, 1377, 1248, 1230, 1145; $[\alpha]_D^{20}$ +1.3 (*c* 0.16, $CHCl_3$); **HRMS** (ESI^+) calculated for $C_{39}H_{75}IO_6Si_3Na$ $[M+Na]^+$ 873.3814, found 873.3819.

Alcohol 346

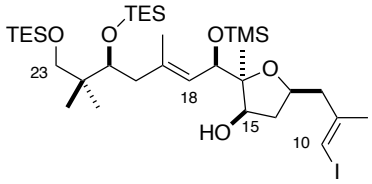

DIBAL (80 μL, 80.0 μmol, 1 M in hexanes) was added dropwise to a stirred solution of ester **345** (15.2 mg, 17.9 μmol) in CH_2Cl_2 (300 μL) at –78 °C. The reaction mixture was stirred at –78 °C for 30 min before quenching with MeOH (50 μL) and Na/K tartrate (500 μL). The mixture was warmed to r.t. and vigorously stirred for 1 h, until two clear layers were observed. The layers were separated, and the aqueous phase extracted with Et_2O (3 × 1 mL). The combined organic phases were dried ($MgSO_4$) and the solvent removed under reduced pressure to afford alcohol **346** as a colourless oil (9.7 mg, 12.6 μmol, 71%).

R_f (EtOAc/PE 40-60: 20%) = 0.73; **^{1}H NMR** (500 MHz, $CDCl_3$) δ_H 5.99 (1H, s, H10), 5.46 (1H, d, J = 9.7 Hz, H18), 4.68 (1H, J = 5.6 Hz, OH), 4.57 (1H, d, J = 9.7 Hz, H17), 4.17-4.07 (2H, m, H13, H15), 3.86 (1H, dd, J = 6.1, 4.9 Hz, H21), 3.39 (1H, d, J = 9.4 Hz, H23a), 3.29 (1H, d, J = 9.4 Hz, H23b), 2.62 (1H, dd, J = 13.6, 6.9 Hz, H12a), 2.48 (1H, dd, J = 14.4, 6.4 Hz, H20a), 2.44 (1H, dd, J = 13.6, 6.4 Hz, H12b), 2.32 (1H, ddd, J = 13.6, 7.7, 6.0 Hz, H14a), 2.07 (1H, dd, J = 14.4, 4.2 Hz, H20b), 1.85 (3H, s, Me11), 1.73 (3H, s, Me19), 1.65 (1H, ddd, J = 13.6, 5.4, 2.7 Hz, H14b), 1.25 (3H, s, Me16), 0.96 (9H, t, J = 8.0 Hz, $SiCH_2C\underline{H}_3$), 0.95 (9H, t, J = 8.0 Hz, $SiCH_2C\underline{H}_3$), 0.83 (3H, s, Me22a), 0.80 (3H, s, Me22b), 0.60 (6H, q, J = 8.0 Hz, $SiC\underline{H}_2CH_3$), 0.58 (6H, q, J = 8.0 Hz, $SiC\underline{H}_2CH_3$), 0.12 (9H, s, $SiMe_3$); **^{13}C NMR** (125 MHz, $CDCl_3$) δ_C 145.2, 138.1, 125.5, 86.4, 78.4, 77.2, 74.3, 74.2, 73.4, 69.5, 46.7, 45.0, 41.3, 40.9, 24.3, 21.4, 21.3, 19.3, 17.4, 7.1, 6.9, 5.4, 4.5, 0.4; **IR** (thin film): ν_{max} 3424, 2953, 2877, 1457, 1250, 1086, 1009; $[\alpha]_D^{20}$ –15.9 (*c* 0.44, $CHCl_3$); **HRMS** (ESI^+) calculated for $C_{34}H_{69}O_5Si_3INa$ $[M+Na]^+$ 791.3395, found 791.3375.

Stannane 358

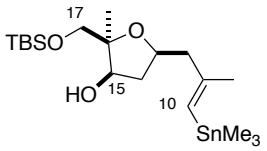

A suspension of vinyl iodide **241** (10.0 mg, 23.5 μmol), $(Me_3Sn)_2$ (35.6 μL, 117 μmol), $PdCl_2(PPh_3)_2$ (1.6 mg, 2.3 μmol) and Li_2CO_2 (8.7 mg, 117 μmol) in THF (1 mL) was stirred at 30 °C for 3 h, during which the mixture turned dark brown. After this time, the suspension was filtered over a plug of Al_2O_3, eluting with Et_2O. The resulting filtrate was concentrated under reduced pressure and the residue was purified by flash column chromatography (EtOAc/PE 40-60: 0% → 5%) (alumina) to afford the product **358** as a colourless oil (10.5 mg, 22.7 μmol, 97%).

R_f (EtOAc/PE 40-60: 20%) = 0.75; **^{1}H NMR** (500 MHz, $CDCl_3$) δ_H 5.53 (1H, s, H10), 4.13-4.07 (2H, m, H13, H15), 3.75 (1H, d, *J* = 10.3 Hz, H17a), 3.65 (1H, *J* = 10.3 Hz, H17b), 3.53 (1H, d, *J* = 6.5 Hz, OH), 2.55 (1H, dd, *J* = 13.6, 5.9 Hz, H12a), 2.34 (1H, dt *J* = 12.6, 6.3 Hz, H14a), 2.31 (1H, dd, *J* = 13.6, 7.5 Hz, H12b), 1.79 (3H, s, Me11), 1.67 (1H, ddd, *J* = 12.6, 8.5, 6.5 Hz, H14b), 1.15 (3H, s, Me16), 0.91 (9H, s, $SiMe_2t\underline{Bu}$), 0.13 (9H, s, $SnMe_3$), 0.11 (3H, s, $SiMe_2t$Bu), 0.10 (3H, s, $SiMe_2t$Bu); **^{13}C NMR** (125 MHz, $CDCl_3$) δ_C 151.7, 125.6, 82.9, 79.7, 74.8, 68.0, 48.6, 41.4, 25.8, 24.7, 22.6, 18.1, –5.4, –5.6, –8.8; **IR** (thin film): ν_{max} 2930, 2853, 1606, 1463, 1255, 1087; $[\alpha]_D^{20}$ –2.6 (*c* 0.09, $CHCl_3$); **HRMS** (ESI^+) calculated for $C_{19}H_{40}O_3SiSnNa$ $[M+Na]^+$ 487.1666, found 487.1651.

Ester 359

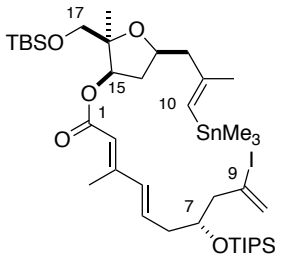

Et_3N (30 μL, 215 μmol) was added to a stirred solution of acid **356** (41.0 mg, 86.3 μmol), TCBC (20 μL, 130 μmol) in PhH (150 μL), to which the solution became cloudy. The reaction mixture was stirred at r.t. for 15 min before the addition of a solution of alcohol **358** (10.0 mg, 21.6 μmol) and DMAP (10.5 mg, 21.6 μmol) in PhH (150 μL) *via* cannula, to which a clumpy precipitate immediately formed. The suspension was stirred at r.t. for 3 h at 30 °C, before filtering the mixture over Al_2O_3, eluting with Et_2O. The resulting filtrate was concentrated under reduced pressure and the residue was purified by flash column chromatography (PE 40-60: 100%) (alumina) to afford the product **359** as a colourless oil (19.0 mg, 21.4 μmol, 99%).

R_f (PE 40-60: 100%) = 0.18; **^{1}H NMR** (500 MHz, $CDCl_3$) δ_H 6.28-6.21 (1H, m, H5), 6.14 (1H, d, *J* = 15.7 Hz, H4), 6.09 (1H, s, =C$\underline{H}_a$$\underline{H}_b$9), 5.77 (1H, s, =C$H_a\underline{H}_b$9), 5.69 (1H, s, H2), 5.48 (1H, s, H10), 5.14-5.09 (1H, m, H15), 4.29-4.20 (2H, m, H7, H13), 3.73 (1H, d, *J* = 9.7 Hz, H17a), 3.51 (1H, d, *J* = 9.7 Hz, H17b), 2.65-2.43 (6H, m, H6a, H8, H12, H14a), 2.30-2.25 (4H, m, Me3, H6b), 1.79-1.75 (4H, m, Me11, H14b), 1.23 (3H, s, Me16), 1.11-1.05 (21H, m, OTIPS), 0.13 (9H, s, $SnMe_3$), 0.07 (3H, s, $SiMe_2$*t*Bu), 0.03 (3H, s, $SiMe_2$*t*Bu); **^{13}C NMR** (125 MHz, $CDCl_3$) δ_C 166.4, 151.7, 136.3, 132.9, 128.2, 125.8, 118.1, 107.1, 84.0, 75.2, 70.7, 66.0, 52.1, 48.8, 39.3, 37.7, 29.7, 25.9, 24.7, 18.1, 13.8, 12.6, 1.0, –5.5, –8.8; **IR** (thin film): ν_{max} 2929, 2857, 1742, 1437, 1363, 1254, 1151, 1119;; $[\alpha]_D^{20}$ +11.1 (*c* 0.22, $CHCl_3$); **HRMS** (ESI^+) calculated for $C_{39}H_{73}IO_5Si_2SnNa$ $[M+Na]^+$ 947.2961, found 947.2979.

8.5.7. Computational studies on the C1-C17 macrocycle

Structure optimisation was conducted as follows: A conformational search was carried out in MacroModel[192] using a hybrid of Monte Carlo multiple–minimum (MCMM)[193]/low–mode sampling[194] with the Merck Molecular Force Field (MMFF),[195] interfaced with Maestro 9.3.[196] The searches were carried out with a sufficient number of steps to find all conformers within 10 kJ $mol^{-1}$of the global minimum. Calculations were carried out in gas phase. All conformers within 10 kJ mol^{-1} of the global minimum were then further subjected to quantum mechanical calculations at the B3LYP[197]/6–31G** level of theory. Finally, single point energies of each conformer were evaluated at the B3LYP/6–31G** level of theory, implemented with Jaguar 7.9.

C15 Macrocycle

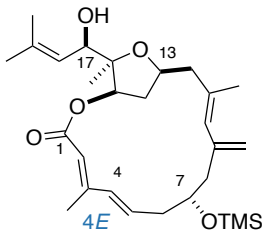

B3LYP/6-31G Free Energy:**	**Number of Imaginary Frequencies:** 0
–1758.5472 Hartrees	

Coordinates for the lowest energy conformer

Atom	x	y	z
C1	-0.9065	0.6341	10.6247
C2	-1.0938	1.7639	11.6600
O3	-0.1224	2.7690	11.2978
C4	0.5170	2.4364	10.0517
C5	-0.3624	1.3696	9.3925
C6	0.8627	3.7323	9.3014
C7	-2.4821	2.4486	11.6967
O8	-1.4922	1.9392	8.7128
C9	-0.3129	4.6189	8.9837
C10	-0.5248	5.3141	7.8560
C11	-1.7293	6.2160	7.7274
C12	0.3671	5.2900	6.6397
O13	1.8352	4.4395	10.0908
C14	-1.8577	1.4324	7.4932
O15	-1.1023	0.8069	6.7733
C16	-3.2848	1.7301	7.3120

C17	-3.6789	1.5372	11.8796
C18	-3.6357	0.6054	13.0654
C19	-4.7261	1.6504	11.0339
C20	-5.9852	0.8745	10.9909
C21	-6.0139	-0.4646	11.1118
C22	-7.2820	1.6485	10.7944
C23	-7.5184	2.4127	9.4655
C24	-4.1160	1.3460	6.3142
C25	-5.5607	1.5488	6.5527
C26	-3.6808	0.7404	5.0076
C27	-6.1211	1.2260	7.7308
C28	-7.5156	1.5301	8.1884
O29	-8.8062	3.0200	9.5699
Si30	-9.0988	4.6580	9.8120
C31	10.9671	4.7984	9.9403
C32	-8.2758	5.2586	11.4027
C33	-8.4474	5.6608	8.3505
H34	-1.8278	0.0931	10.3987
H35	-0.1612	-0.0839	10.9827
H36	-0.8394	1.4047	12.6646
C37	1.8674	1.7650	10.3638
H38	0.1930	0.7406	8.6945
H39	1.3925	3.4449	8.3891
H40	-2.5918	3.0197	10.7723
H41	-2.4427	3.1739	12.5229
H42	-1.0231	4.7347	9.8004
H43	-2.3589	5.9159	6.8791
H44	-2.3468	6.2044	8.6299
H45	-1.4254	7.2538	7.5357
H46	1.2457	4.6539	6.7555
H47	-0.1882	4.9438	5.7583
H48	0.7195	6.3032	6.4067
H49	1.4060	4.6155	10.9412
H50	-3.7197	2.2456	8.1578
H51	-2.9452	-0.2324	12.9021
H52	-3.2700	1.1395	13.9516
H53	-4.6170	0.1840	13.2903
H54	-4.6563	2.4427	10.2883
H55	-6.9502	-1.0146	11.0817
H56	-5.1078	-1.0503	11.2244
H57	-7.3694	2.3953	11.5935
H58	-8.1308	0.9657	10.9108
H59	-6.7440	3.1843	9.3404
H60	-6.1644	1.9587	5.7415
H61	-4.1322	-0.2502	4.8752

H62	-4.0417	1.3601	4.1762
H63	-2.5971	0.6494	4.9476
H64	-5.4892	0.7266	8.4596
H65	-8.0735	0.6084	8.4047
H66	-8.0690	2.0706	7.4139
H67	-11.2747	5.8377	10.1020
H68	-11.4529	4.4435	9.0260
H69	-11.3496	4.2019	10.7747
H70	-8.4671	6.3268	11.5576
H71	-8.6621	4.7232	12.2766
H72	-7.1886	5.1234	11.3834
H73	-8.6392	6.7302	8.4958
H74	-7.3667	5.5399	8.2167
H75	-8.9336	5.3598	7.4162
H76	2.3684	1.5048	9.4314
H77	2.4931	2.4532	10.9321
H78	1.6977	0.8612	10.9490

C17 Macrolactone Regioisomer

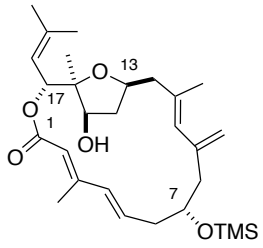

B3LYP/6-31G Free Energy:**

–1758.5593 Hartrees

Number of Imaginary Frequencies: 0

Coordinates for the lowest energy conformer

Atom	x	y	z
C1	0.1413	-5.2375	0.4900
C2	-0.7253	-6.4524	0.0867
O3	0.2019	-7.4725	-0.3438
C4	1.5570	-6.9837	-0.3204
C5	1.5250	-5.8577	0.7427
O6	1.6434	-6.3259	2.0829
C7	2.4903	-8.1857	-0.0011
C8	-1.6034	-6.9383	1.2555
C9	1.9450	-6.4389	-1.7048
O10	1.8718	-8.9133	1.0970

C11	3.8878	-7.7783	0.3739
C12	5.0336	-8.1758	-0.2027
C13	5.1341	-9.1286	-1.3678
C14	6.3569	-7.6607	0.3106
C15	-2.3613	-8.2396	1.0681
C16	-3.0604	-8.4124	-0.2554
C17	-2.4430	-9.0978	2.1078
C18	1.9798	-10.2779	1.0793
O19	2.7378	-10.8639	0.3263
C20	1.0045	-10.8455	2.0159
C21	0.8997	-12.1360	2.4154
C22	1.8474	-13.2364	2.0147
C23	-0.2463	-12.5313	3.2517
C24	-0.9112	-11.7169	4.0845
C25	-2.1756	-12.0471	4.8187
C26	-3.1633	-10.3863	2.1899
C27	-3.1588	-11.2939	1.1981
C28	-3.9589	-10.6702	3.4592
C29	-3.2218	-10.9046	4.8005
O30	-2.6024	-9.6994	5.2569
Si31	-2.9507	-8.9516	6.7256
C32	-2.6469	-10.1483	8.1560
C33	-1.7757	-7.4905	6.8150
C34	-4.7495	-8.3786	6.7530
H35	-0.2208	-4.7343	1.3893
H36	0.1876	-4.4976	-0.3150
H37	-1.3672	-6.2095	-0.7700
H38	2.3310	-5.1330	0.5847
H39	1.4743	-7.2809	2.0910
H40	2.4871	-8.8530	-0.8636
H41	-2.3342	-6.1298	1.4245
H42	-0.9871	-6.9911	2.1585
H43	3.0073	-6.1802	-1.7428
H44	1.7427	-7.1996	-2.4643
H45	1.3648	-5.5485	-1.9598
H46	3.9386	-7.1064	1.2282
H47	4.2202	-9.7000	-1.5286
H48	5.3873	-8.5913	-2.2914
H49	5.9436	-9.8470	-1.1937
H50	6.9236	-7.1667	-0.4897
H51	6.2311	-6.9482	1.1302
H52	6.9831	-8.4887	0.6678
H53	-3.5440	-7.4737	-0.5568
H54	-2.3443	-8.6647	-1.0472
H55	-3.8178	-9.1975	-0.2193

H56	-1.9691	-8.7911	3.0390
H57	0.2437	-10.1393	2.3260
H58	2.6392	-12.8772	1.3608
H59	2.2858	-13.6968	2.9089
H60	1.2957	-14.0301	1.4955
H61	-0.5871	-13.5604	3.1281
H62	-0.5308	-10.7140	4.2603
H63	-1.9439	-12.2320	5.8780
H64	-2.6287	-12.9663	4.4284
H65	-3.7121	-12.2256	1.2815
H66	-2.5768	-11.1538	0.2945
H67	-4.5768	-11.5594	3.2837
H68	-4.6530	-9.8388	3.6407
H69	-4.0132	-11.2030	5.5066
H70	-2.8716	-9.6702	9.1164
H71	-3.2743	-11.0441	8.0862
H72	-1.6017	-10.4744	8.1844
H73	-1.9199	-6.9242	7.7417
H74	-0.7323	-7.8207	6.7839
H75	-1.9328	-6.8050	5.9761
H76	-4.9865	-7.8836	7.7018
H77	-4.9483	-7.6653	5.9460
H78	-5.4489	-9.2143	6.6388

References

(1) Carletti, I.; Debitus, C.; Massiot, G. Molécules Polykétides Comme Agents Anticancéreux. WO2011051380 (A1). 2011.

(2) Williamson, R. T.; Boulanger, A.; Vulpanovici, A.; Roberts, M. A.; Gerwick, W. H. *J. Org. Chem.* **2002**, *67*, 7927–7936.

(3) Masamune, S.; Ali, S. A.; Snitman, D. L.; Garvey, D. S. *Angew. Chem. Int. Ed.* **1980**, *19*, 557–558.

(4) Simmons, T. L.; Andrianasolo, E.; McPhail, K.; Flatt, P.; Gerwick, W. H. *Mol. Cancer Ther.* **2005**, *4*, 333–342.

(5) Haefner, B. *Drug Discov. Today* **2003**, *8*, 536–544.

(6) Cragg, G. M.; Grothaus, P. G.; Newman, D. J. *Chem. Rev.* **2009**, *109*, 3012–3043.

(7) Newman, D. J.; Cragg, G. M. *J. Nat. Prod.* **2004**, *67*, 1216–1238.

(8) Molinski, T. F.; Dalisay, D. S.; Lievens, S. L.; Saludes, J. P. *Nat. Rev. Drug Discov.* **2009**, *8*, 69–85.

(9) Newman, D. J.; Cragg, G. M. *J. Nat. Prod.* **2016**, *79*, 629–661.

(10) Norcross, R. D.; Paterson, I. *Chem. Rev.* **1995**, *95*, 2041–2114.

(11) Nicolaou, K. C.; Snyder, S. A. *Angew. Chem. Int. Ed.* **2005**, *44*, 1012–1044.

(12) Williamson, R. T.; Brian, L. M.; Gerwick, W. H.; Katalin, E. K. *Magn. Reson. Chem.* **2000**, *38*, 265–273.

(13) Matsumori, N.; Kaneno, D.; Murata, M.; Nakamura, H.; Tachibana, K. *J. Org. Chem.* **1999**, *64*, 866–876.

(14) Smith, S. G.; Goodman, J. M. *J. Am. Chem. Soc.* **2010**, *132*, 12946–12959.

(15) Jones, C. G.; Martynowycz, M. W.; Hattne, J.; Fulton, T. J.; Stoltz, B. M.; Rodriguez, J. A.; Nelson, H. M.; Gonen, T. *ACS Cent. Sci.* **2018**, *4*, 1587–1592.

(16) Winter, J. M.; Behnken, S.; Hertweck, C. *Curr. Opin. Chem. Biol.* **2011**, *15*, 22–31.

(17) McAlpine, J. B.; Bachmann, B. O.; Piraee, M.; Tremblay, S.; Alarco, A. M.; Zazopoulos, E.; Farnet,

C. M. *J. Nat. Prod.* **2005**, *68*, 493–496.

(18) Phillips, A. W.; Anketell, M. J.; Balan, T.; Lam, N. Y. S.; Williams, S.; Paterson, I. *Org. Biomol. Chem.* **2018**, *16*, 6908–6913.

(19) Paterson, I.; Williams, S. *Isr. J. Chem.* **2017**, *57*, 192–201.

(20) Suyama, T. L.; Gerwick, W. H.; McPhail, K. L. *Bioorg. Med. Chem.* **2011**, *19*, 6675–6701.

(21) Gould, S. J.; Tamayo, N.; Melville, C. R.; Cone, M. C. *J. Am. Chem. Soc.* **1994**, *116*, 2207–2208.

(22) Liu, Y.; Saurí, J.; Mevers, E.; Peczuh, M. W.; Hiemstra, H.; Clardy, J.; Martin, G. E.; Williamson, R. T. *Science* **2017**, *356*.

(23) Trost, B. M.; Gunzner, J. L.; Dirat, O.; Rhee, Y. H. *J. Am. Chem. Soc.* **2002**, *124*, 10396–10415.

(24) Nicolaou, K. C.; Koftis, T. V.; Vyskocil, S.; Petrovic, G.; Tang, W.; Frederick, M. O.; Chen, D. Y. K.; Li, Y.; Ling, T.; Yamada, Y. M. A. *J. Am. Chem. Soc.* **2006**, *128*, 2859–2872.

(25) Lei, H.; Yan, J.; Yu, J.; Liu, Y.; Wang, Z.; Xu, Z.; Ye, T. *Angew. Chem. Int. Ed.* **2014**, *53*, 6533–6537.

(26) Veerasamy, N.; Ghosh, A.; Li, J.; Watanabe, K.; Serrill, J. D.; Ishmael, J. E.; McPhail, K. L.; Carter, R. G. *J. Am. Chem. Soc.* **2016**, *138*, 770–773.

(27) Nguyen, M. H.; Imanishi, M.; Kurogi, T.; Smith, A. B. *J. Am. Chem. Soc.* **2016**, *138*, 3675–3678.

(28) Willwacher, J.; Heggen, B.; Wirtz, C.; Thiel, W.; Fürstner, A. *Chem. Eur. J.* **2015**, *21*, 10416–10430.

(29) Willwacher, J.; Fürstner, A. *Angew. Chem. Int. Ed.* **2014**, *53*, 4217–4221.

(30) Paterson, I.; Haslett, G. W. *Org. Lett.* **2013**, *15*, 1338–1341.

(31) Ben-David, U.; Siranosian, B.; Ha, G.; Tang, H.; Oren, Y.; Hinohara, K.; Strathdee, C. A.; Dempster, J.; Lyons, N. J.; Burns, R.; et al. *Nature* **2018**, *560*, 325–330.

(32) Kumagai, K.; Tsuda, M.; Masuda, A.; Fukushi, E.; Kawabata, J. *Heterocycles* **2015**, *91*, 265–274.

(33) Sakamoto, K.; Hakamata, A.; Tsuda, M.; Fuwa, H. *Angew. Chem. Int. Ed.* **2018**, *57*, 3801–3805.

(34) Sakamoto, K.; Hakamata, A.; Iwasaki, A.; Suenaga, K.; Tsuda, M.; Fuwa, H. *Chem. Eur. J.* **2019**, *25*, 8528–8542.

(35) Tripathi, A.; Schofield, M. M.; Chlipala, G. E.; Schultz, P. J.; Yim, I.; Newmister, S. A.; Nusca, T. D.; Scaglione, J. B.; Hanna, P. C.; Tamayo-Castillo, G.; et al. *J. Am. Chem. Soc.* **2014**, *136*, 1579–1586.

(36) Guchhait, S.; Chatterjee, S.; Ampapathi, R. S.; Goswami, R. K. *J. Org. Chem.* **2017**, *82*, 2414–2435.

(37) Wu, J.; Lorenzo, P.; Zhong, S.; Ali, M.; Butts, C. P.; Myers, E. L.; Aggarwal, V. K. *Nature* **2017**, *547*, 436–440.

(38) Bhalla, K. N. *Oncogene* **2003**, *22*, 9075–9086.

(39) Holohan, C.; Van Schaeybroeck, S.; Longley, D. B.; Johnston, P. G. *Nat. Rev. Cancer* **2013**, *13*, 714–726.

(40) Chari, R. V. J.; Miller, M. L.; Widdison, W. C. *Angew. Chem. Int. Ed.* **2014**, *53*, 3796–3827.

(41) Fleury, E.; Lannou, M.-I.; Bistri, O.; Sautel, F.; Massiot, G.; Pancrazi, A.; Ardisson, J. *J. Org. Chem.* **2009**, *74*, 7034–7045.

(42) Fleury, E.; Sorin, G.; Prost, E.; Pancrazi, A.; Sautel, F.; Massiot, G.; Lannou, M.-I.; Ardisson, J. *J. Org. Chem.* **2013**, *78*, 855–864.

(43) MacGregor, C. I.; Han, B. Y.; Goodman, J. M.; Paterson, I. *Chem. Commun.* **2016**, *52*, 4632–4635.

(44) Specklin, S.; Boissonnat, G.; Lecourt, C.; Sorin, G.; Lannou, M.-I.; Ardisson, J.; Sautel, F.; Massiot, G.; Meyer, C.; Cossy, J. *Org. Lett.* **2015**, *17*, 2446–2449.

(45) Sorin, G.; Fleury, E.; Tran, C.; Prost, E.; Molinier, N.; Sautel, F.; Massiot, G.; Specklin, S.; Meyer, C.; Cossy, J.; et al. *Org. Lett.* **2013**, *15*, 4734–4737.

(46) MacGregor, C. I. PhD Thesis, Studies Towards the Structural Elucidation and Total Synthesis of Hemicalide, University of Cambridge, 2015.

(47) Lecourt, C.; Dhambri, S.; Yamani, K.; Boissonnat, G.; Specklin, S.; Fleury, E.; Hammad, K.; Auclair, E.; Sablé, S.; Grondin, A.; et al. *Chem. Eur. J.* **2019**, *25*, 2745–2749.

(48) Lecourt, C.; Boinapally, S.; Dhambri, S.; Boissonnat, G.; Meyer, C.; Cossy, J.; Sautel, F.; Massiot, G.; Ardisson, J.; Sorin, G.; et al. *J. Org. Chem.* **2016**, *81*, 12275–12290.

(49) Paterson, I.; Wallace, D. J. *Tetrahedron Lett.* **1994**, *35*, 9087–9090.

(50) Evans, D. A.; Bartroli, J.; Shih, T. L. *J. Am. Chem. Soc.* **1981**, *103*, 2127–2129.

(51) Han, B. Y.; Lam, N. Y. S.; MacGregor, C. I.; Goodman, J. M.; Paterson, I. *Chem. Commun.* **2018**, *54*, 3247–3250.

(52) Thompson, J. MSci Dissertation, Studies Towards the Total Synthesis of Hemicalide, University of Cambridge, 2016.

(53) Dias, L. C.; Steil, L. J. *Tetrahedron Lett.* **2004**, *45*, 8835–8841.

(54) Paterson, I.; Collett, L. A. *Tetrahedron Lett.* **2001**, *42*, 1187–1191.

(55) Evans, D. A.; Cee, V. J.; Siska, S. J. *J. Am. Chem. Soc.* **2006**, *128*, 9433–9441.

(56) Paterson, I.; Lam, N. Y. S. *J. Antibiot. (Tokyo).* **2018**, *71*.

(57) Corey, E. J.; Fuchs, P. L. *Tetrahedron Lett.* **1972**, No. 36, 3769–3772.

(58) Hart, D. W.; Blackburn, T. F.; Schwartz, J. *J. Am. Chem. Soc.* **1975**, *97*, 679–680.

(59) Schwartz, J.; Labinger, J. A. *Angew. Chem. Int. Ed.* **1976**, *15*, 333–340.

(60) Paton, R. S.; Goodman, J. M. *J. Org. Chem.* **2008**, *73*, 1253–1263.

(61) Paterson, I.; Anne Lister, M. *Tetrahedron Lett.* **1988**, *29*, 585–588.

(62) Neises, B.; Steglich, W. *Angew. Chem. Int. Ed.* **1978**, *17*, 522–524.

(63) Sullivan, G.; Dale, J.; Mosher, H. *J. Org. Chem.* **1973**, *38*, 2143–2147.

(64) Dale, J. A.; Mosher, H. S. *J. Am. Chem. Soc.* **1973**, *95*, 512–519.

(65) Hoye, T. R.; Jeffrey, C. S.; Shao, F. *Nat. Protoc.* **2007**, *2*, 2451–2458.

(66) Dupau, P.; Epple, R.; Thomas, A. A.; Fokin, V. V.; Sharpless, K. B. *Adv. Synth. Catal.* **2002**, *344*, 421–433.

(67) Paddon-Row, M. N.; Rondan, N. G.; Houk, K. N. *J. Am. Chem. Soc.* **1982**, *104*, 7162–7166.

(68) Vedejs, E.; McClure, C. K. *J. Am. Chem. Soc.* **1986**, *108*, 1094–1096.

(69) Wulff, W. D.; Peterson, G. A.; Bauta, W. E.; Chan, K.-S.; Faron, K. L.; Gilbertson, S. R.; Kaesler, R. W.; Yang, D. C.; Murray, C. K. *J. Org. Chem.* **1986**, *51*, 277–279.

(70) Paterson, I.; Ng, K. K.-H.; Williams, S.; Millican, D. C.; Dalby, S. M. *Angew. Chem. Int. Ed.* **2014**, *53*, 2692–2695.

(71) Fürstner, A.; Nevado, C.; Tremblay, M.; Chevrier, C.; Teplý, F.; Aïssa, C.; Waser, M. *Angew. Chem. Int. Ed.* **2006**, *45*, 5837–5842.

(72) Li, J.; Yang, P.; Yao, M.; Deng, J.; Li, A. *J. Am. Chem. Soc.* **2014**, *136*, 16477–16480.

(73) Fürstner, A.; Funel, J.-A.; Tremblay, M.; Bouchez, L. C.; Nevado, C.; Waser, M.; Ackerstaff, J.; Stimson, C. C. *Chem. Commun.* **2008**, No. 25, 2873–2875.

(74) Mee, S. P. H.; Lee, V.; Baldwin, J. E. *Angew. Chem. Int. Ed.* **2004**, *43*, 1132–1136.

(75) Han, B. Y. PhD Thesis, Studies Towards the Total Synthesis of Hemicalide, University of Cambridge, 2018.

(76) Nicolaou, K. C.; Dalby, S. M.; Majumder, U. *J. Am. Chem. Soc.* **2008**, *130*, 14942–14943.

(77) Meng, Z.; Yu, H.; Li, L.; Tao, W.; Chen, H.; Wan, M.; Yang, P.; Edmonds, D. J.; Zhong, J.; Li, A. *Nat. Commun.* **2015**, *6*, 6096.

(78) Lassen, K. M.; Joullié, M. M. *Org. Lett.* **2010**, *12*, 5306–5309.

(79) Dalby, S. M.; Goodwin-Tindall, J.; Paterson, I. *Angew. Chem. Int. Ed.* **2013**, *52*, 6517–6521.

(80) Chatterjee, A. K.; Choi, T.-L.; Sanders, D. P.; Grubbs, R. H. *J. Am. Chem. Soc.* **2003**, *125*, 11360–11370.

(81) Rodríguez, A.; Nomen, M.; Spur, B. W.; Godfroid, J. J. *Tetrahedron Lett.* **1999**, *40*, 5161–5164.

(82) Bertin, M. J.; Vulpanovici, A.; Monroe, E. A.; Korobeynikov, A.; Sherman, D. H.; Gerwick, L.; Gerwick, W. H. *ChemBioChem* **2016**, *17*, 164–173.

(83) Pumiglia, K.; Chow, Y. H.; Fabian, J.; Morrison, D.; Decker, S.; Jove, R. *Mol. Cell. Biol.* **1995**, *15*, 398–406.

(84) Lorente, A.; Gil, A.; Fernández, R.; Cuevas, C.; Albericio, F.; Álvarez, M. *Chem. Eur. J.* **2015**, *21*, 150–156.

(85) Staunton, J.; Weissman, K. J. *Nat. Prod. Rep.* **2001**, *18*, 380–416.

(86) Murakami, M.; Matsuda, H.; Makabe, K.; Yamaguchi, K. *Tetrahedron Lett.* **1991**, *32*, 2391–2394.

(87) Rychnovsky, S. D.; Rogers, B.; Yang, G. *J. Org. Chem.* **1993**, *58*, 3511–3515.

(88) Murata, M.; Matsuoka, S.; Matsumori, N.; Paul, G. K.; Tachibana, K. *J. Am. Chem. Soc.* **1999**, *121*, 870–871.

(89) Barfield, M.; Smith, W. B. *J. Am. Chem. Soc.* **1992**, *114*, 1574–1581.

(90) Imai, K.; Ōsawa, E. *Magn. Reson. Chem.* **1990**, *28*, 668–674.

(91) Latypov, S. K.; Seco, J. M.; Quiñoá, E.; Riguera, R. *J. Am. Chem. Soc.* **1998**, *120*, 877–882.

(92) El-Sayed, A. K.; Hothersall, J.; Cooper, S. M.; Stephens, E.; Simpson, T. J.; Thomas, C. M. *Chem. Biol.* **2003**, *10*, 419–430.

(93) Bolaños, J. P.; Almeida, A.; Moncada, S. *Trends Biochem. Sci.* **2010**, *35*, 145–149.

(94) Doughty, C. C.; Hayashi, J. A.; Guenther, H. L. *J. Biol. Chem.* **1966**, *241*, 568–572.

(95) Bonnett, S. A.; Whicher, J. R.; Papireddy, K.; Florova, G.; Smith, J. L.; Reynolds, K. A. *Chem. Biol.* **2013**, *20*, 772–783.

(96) Reid, R.; Piagentini, M.; Rodriguez, E.; Ashley, G.; Viswanathan, N.; Carney, J.; Santi, D. V.; Richard Hutchinson, C.; McDaniel, R. *Biochemistry* **2003**, *42*, 72–79.

(97) Gil, A.; Lorente, A.; Albericio, F.; Álvarez, M. *Org. Lett.* **2015**, *17*, 6246–6249.

(98) Gil, A.; Giarrusso, M.; Lamariano-Merketegi, J.; Lorente, A.; Albericio, F.; Álvarez, M. *ACS Omega* **2018**, *3*, 2351–2362.

(99) Edvardsen, K. R.; Benneche, T.; Tius, M. A. *J. Org. Chem.* **2000**, *65*, 3085–3089.

(100) Gil, A.; Lamariano-Merketegi, J.; Lorente, A.; Albericio, F.; Álvarez, M.; Alvarez, M. *Chem. Eur. J.* **2016**, *22*, 7033–7035.

(101) Gil, A.; Lamariano-Merketegi, J.; Lorente, A.; Albericio, F.; Álvarez, M. *Org. Lett.* **2016**, *18*, 4485–4487.

(102) Lamariano-Merketegi, J.; Lorente, A.; Gil, A.; Albericio, F.; Álvarez, M. *Eur. J. Org. Chem.* **2015**, *2015*, 235–241.

(103) Evans, D. A.; Fitch, D. M.; Smith, T. E.; Cee, V. J. *J. Am. Chem. Soc.* **2000**, *122*, 10033–10046.

(104) Evans, D. A.; Dart, M. J.; Duffy, J. L.; Yang, M. G. *J. Am. Chem. Soc.* **1996**, *118*, 4322–4343.

(105) Bergeron-Brlek, M.; Meanwell, M.; Britton, R. *Nat. Commun.* **2015**, *6*, 6903.

(106) Bergeron-Brlek, M.; Teoh, T.; Britton, R. *Org. Lett.* **2013**, *15*, 3554–3557.

(107) Wipf, P.; Lim, S. *Angew. Chem. Int. Ed.* **1993**, *32*, 1068–1071.

(108) Negishi, E.; Van Horn, D. E.; Yoshida, T. *J. Am. Chem. Soc.* **1985**, *107*, 6639–6647.

(109) Penner, M.; Rauniyar, V.; Kaspar, L. T.; Hall, D. G. *J. Am. Chem. Soc.* **2009**, *131*, 14216–14217.

(110) Allais, C.; Tsai, A. S.; Nuhant, P.; Roush, W. R. *Angew. Chem. Int. Ed.* **2013**, *52*, 12888–12891.

(111) Nuhant, P.; Allais, C.; Roush, W. R. *Angew. Chem. Int. Ed.* **2013**, *52*, 8703–8707.

(112) Fleming, I.; Paterson, I. *Synthesis* **1979**, *1979*, 736–738.

(113) Kiyooka, S.; Hena, M. A. *J. Org. Chem.* **1999**, *64*, 5511–5523.

(114) Kiyooka, S.; Shahid, K. A.; Goto, F.; Okazaki, M.; Shuto, Y. *J. Org. Chem.* **2003**, *68*, 7967–7978.

(115) Kumar, R. N.; Meshram, H. M. *Tetrahedron Lett.* **2011**, *52*, 1003–1007.

(116) Keck, G. E.; Krishnamurthy, D. *J. Am. Chem. Soc.* **1995**, *117*, 2363–2364.

(117) Corey, E. J.; Barnes-Seeman, D.; Lee, T. W. *Tetrahedron Lett.* **1997**, *38*, 4351–4354.

(118) Kan, S. B. J.; Ng, K. K.-H.; Paterson, I. *Angew. Chem. Int. Ed.* **2013**, *52*, 9097–9108.

(119) Mayr, H.; Kempf, B.; Ofial, A. R. *Acc. Chem. Res.* **2003**, *36*, 66–77.

(120) Inamoto, Y.; Kaga, Y.; Nishimoto, Y.; Yasuda, M.; Baba, A. *Chem. Eur. J.* **2014**, *20*, 11664–11668.

(121) Ralston, K. J.; Ramstadius, H. C.; Brewster, R. C.; Niblock, H. S.; Hulme, A. N. *Angew. Chem. Int. Ed.* **2015**, *127*, 7192–7196.

(122) Kikkawa, I.; Yorifuji, T. *Synthesis* **1980**, *1980*, 877–880.

(123) Fürstner, A.; Mathes, C.; Grela, K. *Chem. Commun.* **2001**, No. 12, 1057–1059.

(124) Dieckmann, M.; Rudolph, S.; Lang, C.; Ahlbrecht, W.; Menche, D. *Synthesis* **2013**, *45*, 2305–2315.

(125) Bahmanyar, S.; Houk, K. N.; Martin, H. J.; List, B. *J. Am. Chem. Soc.* **2003**, *125*, 2475–2479.

(126) Boden, E. P.; Keck, G. E. *J. Org. Chem.* **1985**, *50*, 2394–2395.

(127) Inanaga, J.; Hirata, K.; Saeki, H.; Katsuki, T.; Yamaguchi, M. *Bull. Chem. Soc. Jpn.* **1979**, *52*, 1989–1993.

(128) Ohba, Y.; Takatsuji, M.; Nakahara, K.; Fujioka, H.; Kita, Y. *Chem. Eur. J.* **2009**, *15*, 3526–3537.

(129) Omura, K.; Swern, D. *Tetrahedron* **1978**, *34*, 1651–1660.

(130) Parikh, J. R.; Doering, W. von E. *J. Am. Chem. Soc.* **1967**, *89*, 5505–5507.

(131) Chamberlin, A. R.; Dezube, M.; Reich, S. H.; Sall, D. J. *J. Am. Chem. Soc.* **1989**, *111*, 6247–6256.

(132) Seiple, I. B.; Zhang, Z.; Jakubec, P.; Langlois-Mercier, A.; Wright, P. M.; Hog, D. T.; Yabu, K.; Allu, S. R.; Fukuzaki, T.; Carlsen, P. N.; et al. *Nature* **2016**, *533*, 338–345.

(133) Wolfrom, M. L.; Hanessian, S. *J. Org. Chem.* **1962**, *27*, 1800–1804.

(134) Seyferth, D. *Organometallics* **2009**, *28*, 1598–1605.

(135) Mowat, J.; Kang, B.; Fonovic, B.; Dudding, T.; Britton, R. *Org. Lett.* **2009**, *11*, 2057–2060.

(136) Nguyen, K. H.; Tomasi, S.; Le Roch, M.; Toupet, L.; Renault, J.; Uriac, P.; Gouault, N. *J. Org. Chem.* **2013**, *78*, 7809–7815.

(137) Corma, A.; Ruiz, V. R.; Leyva-Pérez, A.; Sabater, M. J. *Adv. Synth. Catal.* **2010**, *352*, 1701–1710.

(138) Sethofer, S. G.; Mayer, T.; Toste, F. D. *J. Am. Chem. Soc.* **2010**, *132*, 8276–8277.

(139) Barluenga, J.; Aznar, F.; Bayod, M. *Synthesis* **1988**, *1988*, 144–146.

(140) Hoye, T. R.; Kurth, M. J. *J. Org. Chem.* **1979**, *44*, 3461–3467.

(141) Marion, N.; Lemière, G.; Correa, A.; Costabile, C.; Ramón, R. S.; Moreau, X.; de Frémont, P.; Dahmane, R.; Hours, A.; Lesage, D.; et al. *Chem. Eur. J.* **2009**, *15*, 3243–3260.

(142) Lin, M. H.; Lin, L. Z.; Chuang, T. H. *Synlett* **2011**, *2011*, 1871–1874.

(143) Houk, K. N.; Paddon-Row, M. N. *J. Am. Chem. Soc.* **1986**, *108*, 2659–2662.

(144) Kobayashi, S.; Hachiya, I. *J. Org. Chem.* **1994**, *59*, 3590–3596.

(145) Maki, B. E.; Chan, A.; Phillips, E. M.; Scheidt, K. A. *Org. Lett.* **2007**, *9*, 371–374.

(146) Narayanan, B. A.; Bunnelle, W. H. *Tetrahedron Lett.* **1987**, *28*, 6261–6264.

(147) Xuan, M.; Paterson, I.; Dalby, S. M. *Org. Lett.* **2012**, *14*, 5492–5495.

(148) Jadhav, P. K.; Bhat, K. S.; Perumal, P. T.; Brown, H. C. *J. Org. Chem.* **1986**, *51*, 432–439.

(149) Li, Y.; Houk, K. N. *J. Am. Chem. Soc.* **1989**, *111*, 1236–1240.

(150) Vulpetti, A.; Gardner, M.; Gennari, C.; Bernardi, A.; Goodman, J. M.; Paterson, I. *J. Org. Chem.* **1993**, *58*, 1711–1718.

(151) Veysoglu, T.; Mitscher, L. A.; Swayze, J. K. *Synthesis* **2003**, *1980*, 807–810.

(152) Hosomi, A.; Iguchi, H.; Endo, M.; Sakurai, H. *Chem. Lett.* **2006**, *8*, 977–980.

(153) Denmark, S. E.; Almstead, N. G. *Tetrahedron* **1992**, *48*, 5565–5578.

(154) Hosomi, A. *Acc. Chem. Res.* **1988**, *21*, 200–206.

(155) Yamasaki, S.; Fujii, K.; Wada, R.; Kanai, M.; Shibasaki, M. *J. Am. Chem. Soc.* **2002**, *124*, 6536–6537.

(156) Dias, L. C.; Meira, P. R. R.; Ferreira, E. *Org. Lett.* **2002**, *1*, 1335–1338.

(157) Evans, D. A.; Dart, M. J.; Duffy, J. L.; Yang, M. G.; Livingston, A. B. *J. Am. Chem. Soc.* **1995**, *117*, 6619–6620.

(158) Mahrwald, R. *Chem. Rev.* **1999**, *99*, 1095–1120.

(159) Hughes, D. L.; Reamer, R. A. *J. Org. Chem.* **1996**, *61*, 2967–2971.

(160) Parenty, A.; Moreau, X.; Campagne, J. M. *Chem. Rev.* **2006**, *106*, 911–939.

(161) Ojha, D. P.; Prabhu, K. R. *Org. Lett.* **2016**, *18*, 432–435.

(162) Gopalarathnam, A.; Nelson, S. G. *Org. Lett.* **2006**, *8*, 7–10.

(163) Frank, S. A.; Chen, H.; Kunz, R. K.; Schnaderbeck, M. J.; Roush, W. R. *Org. Lett.* **2000**, *2*, 2691–2694.

(164) Duncton, M. A. J.; Pattenden, G. *J. Chem. Soc. Perkin Trans. 1* **1999**, *0*, 1235–1246.

(165) Williams, S.; Jin, J.; Kan, S. B. J.; Li, M.; Gibson, L. J.; Paterson, I. *Angew. Chem. Int. Ed.* **2017**, *56*, 645–649.

(166) Paterson, I.; Woodrow, M. D.; Cowden, C. J. *Tetrahedron Lett.* **1998**, *39*, 6041–6044.

(167) Paterson, I.; Lombart, H.-G.; Allerton, C. *Org. Lett.* **2002**, *1*, 19–22.

(168) Nicolaou, K. C.; Murphy, F.; Barluenga, S.; Ohshima, T.; Wei, H.; Xu, J.; Gray, D. L. F.; Baudoin, O. *J. Am. Chem. Soc.* **2000**, *122*, 3830–3838.

(169) Allred, G. D.; Liebeskind, L. S. *J. Am. Chem. Soc.* **1996**, *118*, 2748–2749.

(170) De Mico, A.; Margarita, R.; Parlanti, L.; Vescovi, A.; Piancatelli, G. *J. Org. Chem.* **1997**, *62*, 6974–6977.

(171) Ghosh, A. K.; Ma, N.; Effenberger, K. A.; Jurica, M. S. *Org. Lett.* **2014**, *16*, 3154–3157.

(172) Takai, K. In *Organic Reactions*; John Wiley & Sons, Inc.: Hoboken, NJ, USA, 2004; pp 253–612.

(173) Takai, K.; Nitta, K.; Utimoto, K. *J. Am. Chem. Soc.* **1986**, *108*, 7408–7410.

(174) Novaes, L. F. T.; Pastre, J. C. *Org. Lett.* **2017**, *19*, 3163–3166.

(175) Abbasov, M. E.; Alvariño, R.; Chaheine, C. M.; Alonso, E.; Sánchez, J. A.; Conner, M. L.; Alfonso, A.; Jaspars, M.; Botana, L. M.; Romo, D. *Nat. Chem.* **2019**, *11*, 342–350.

(176) Baran, P. S. *J. Am. Chem. Soc.* **2018**, *140*, 4751–4755.

(177) Whitesides, G. M. *Isr. J. Chem.* **2018**, *58*, 142–150.

(178) Keasling, J. D.; Mendoza, A.; Baran, P. S. *Nature* **2012**, *492*, 188–189.

(179) Blakemore, D. C.; Castro, L.; Churcher, I.; Rees, D. C.; Thomas, A. W.; Wilson, D. M.; Wood, A. *Nat. Chem.* **2018**, *10*, 383–394.

(180) Campos, K. R.; Coleman, P. J.; Alvarez, J. C.; Dreher, S. D.; Garbaccio, R. M.; Terrett, N. K.; Tillyer,

R. D.; Truppo, M. D.; Parmee, E. R. *Science* **2019**, *363*.

(181) Ireland, R. E.; Liu, L. *J. Org. Chem.* **1993**, *58*, 2899–2899.

(182) Anžiček, N.; Williams, S.; Housden, M. P.; Paterson, I. *Org. Biomol. Chem.* **2018**, *16*, 1343–1350.

(183) Berry, M. B.; Craig, D. *Synlett* **1992**, *1992*, 41–44.

(184) Joly, G. D.; Jacobsen, E. N. *Org. Lett.* **2002**, *4*, 1795–1798.

(185) Moeder, C. W.; Sowa, J. R. *J. Phys. Org. Chem.* **2004**, *17*, 317–324.

(186) Pan, X.; Lacôte, E.; Lalevée, J.; Curran, D. P. *J. Am. Chem. Soc.* **2012**, *134*, 5669–5674.

(187) Paquette, L. A. In *Encyclopedia of Reagents for Organic Synthesis*; John Wiley & Sons, Ltd: Chichester, 2001.

(188) Lautens, M.; Maddess, M. L.; Sauer, E. L. O.; Ouellet, S. G. *Org. Lett.* **2002**, *4*, 83–86.

(189) Paterson, I.; Florence, G. J.; Gerlach, K.; Scott, J. P.; Sereinig, N. *J. Am. Chem. Soc.* **2001**, *123*, 9535–9544.

(190) Janssen, D.; Albert, D.; Jansen, R.; Müller, R.; Kalesse, M. *Angew. Chem. Int. Ed.* **2007**, *46*, 4898–4901.

(191) Smith, A. B.; Lee, D. *J. Am. Chem. Soc.* **2007**, *129*, 10957–10962.

(192) MacroModel, Version 9.9, Schrodinger LLC; New York, 2012.

(193) Chang, G.; Guida, W. C.; Still, W. C. *J. Am. Chem. Soc.* **1989**, *111*, 4379–4386.

(194) Kolossváry, I.; Guida, W. C. *J. Am. Chem. Soc.* **1996**, *118*, 5011–5019.

(195) Halgren, T. A. *J. Comput. Chem.* **1996**, *17*, 490–519.

(196) Maestro, Version 9.3, Schrodinger LLC,; New York, 2012.

(197) Becke, A. D. *J. Chem. Phys.* **1993**, *98*, 5648–5652.

(198) Sneddon, H. F.; Gaunt, M. J.; Ley, S. V. *Org. Lett.* **2003**, *5*, 1147–1150.

(199) Campbell, C. D.; Greenaway, R. L.; Holton, O. T.; Walker, P. R.; Chapman, H. A.; Russell, C. A.;

Carr, G.; Thomson, A. L.; Anderson, E. A. *Chem. Eur. J.* **2015**, *21*, 12627–12639.

(200) Liu, Y.; Yeung, Y. Y. *Org. Lett.* **2017**, *19*, 1422–1425.

(201) Dieckmann, A.; Beniken, S.; Lorenz, C. D.; Doltsinis, N. L.; Von Kiedrowski, G. *Chem. Eur. J.* **2011**.

(202) Liu, J.; De Brabander, J. K. *J. Am. Chem. Soc.* **2009**, *131*, 12562–12563.

Appendix

Selected ^{1}H and ^{13}C NMR spectra for hemicalide and phormidolide A are included below

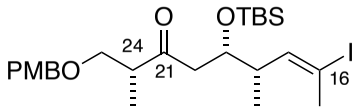

115

^{1}H NMR ($CDCl_3$, 500 MHz)

^{13}C NMR ($CDCl_3$, 125 MHz)

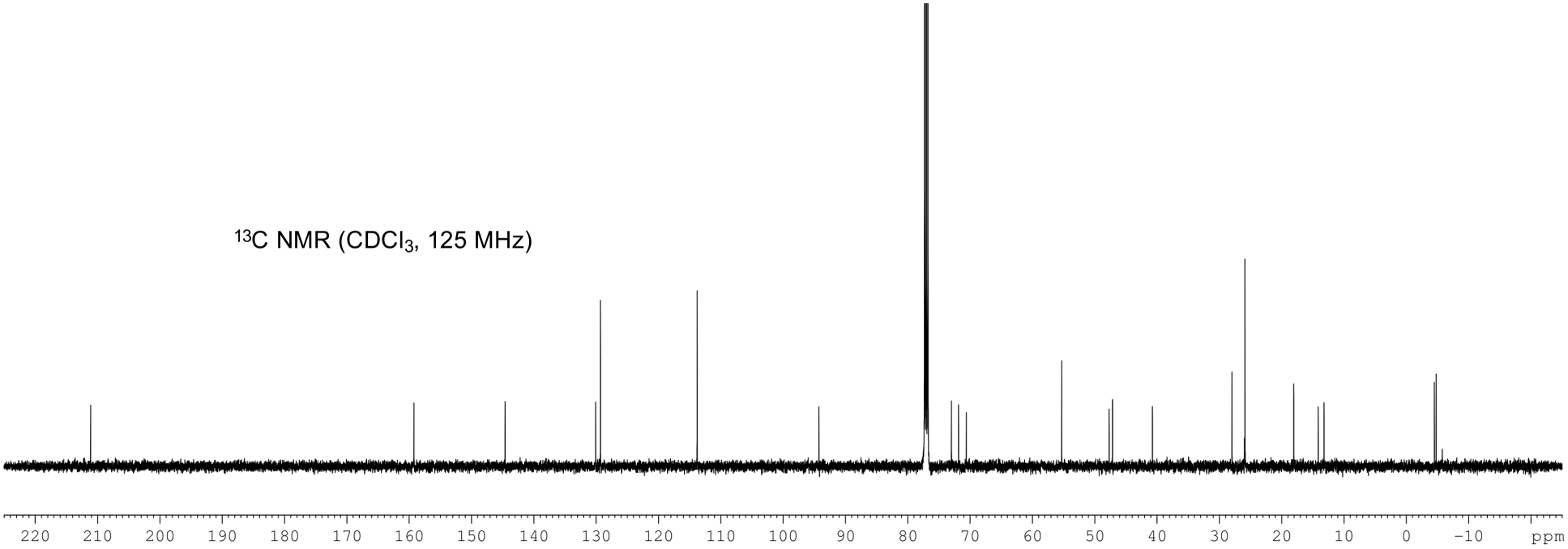

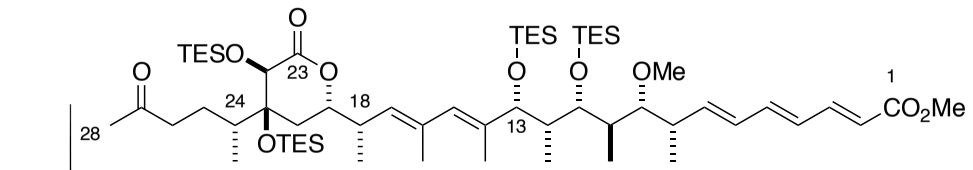

101a

^{1}H NMR ($CDCl_3$, 500 MHz)

^{13}C NMR ($CDCl_3$, 125 MHz)

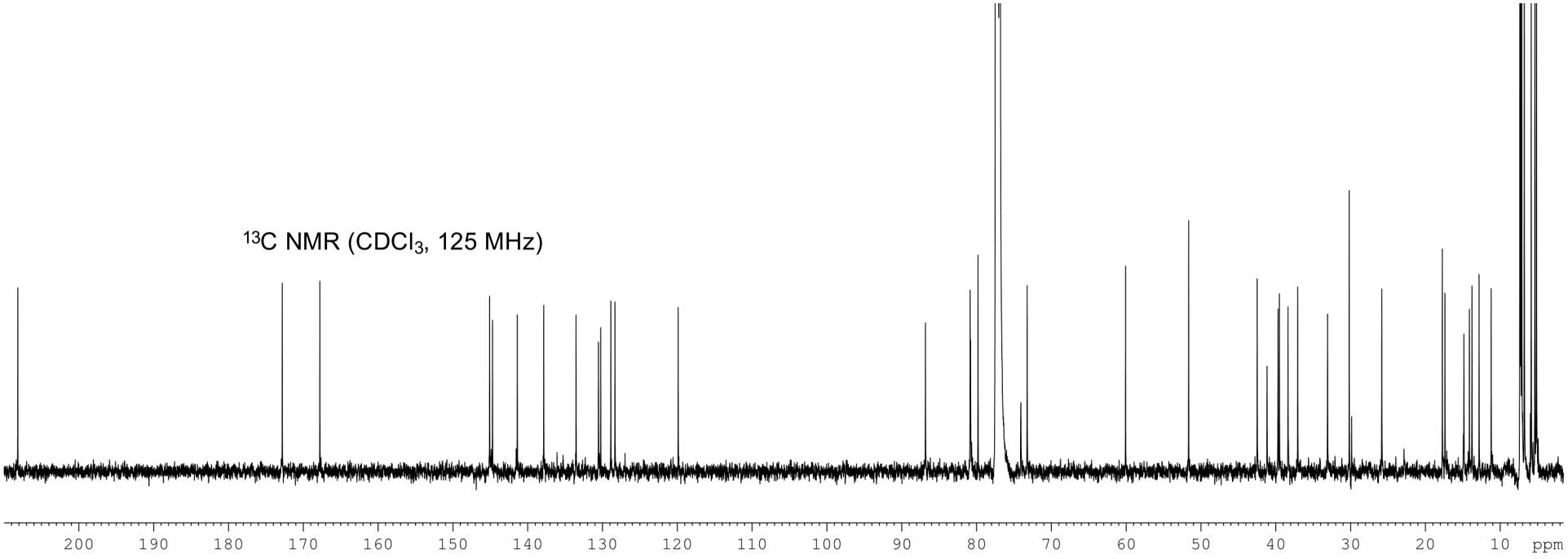

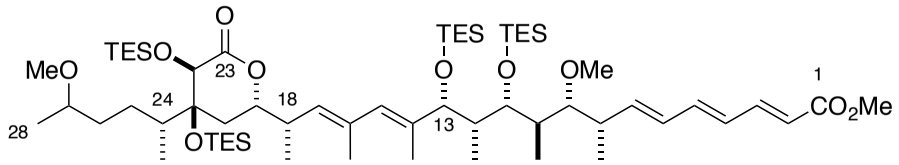

132

^{1}H NMR ($CDCl_3$, 500 MHz)

^{13}C NMR ($CDCl_3$, 125 MHz)

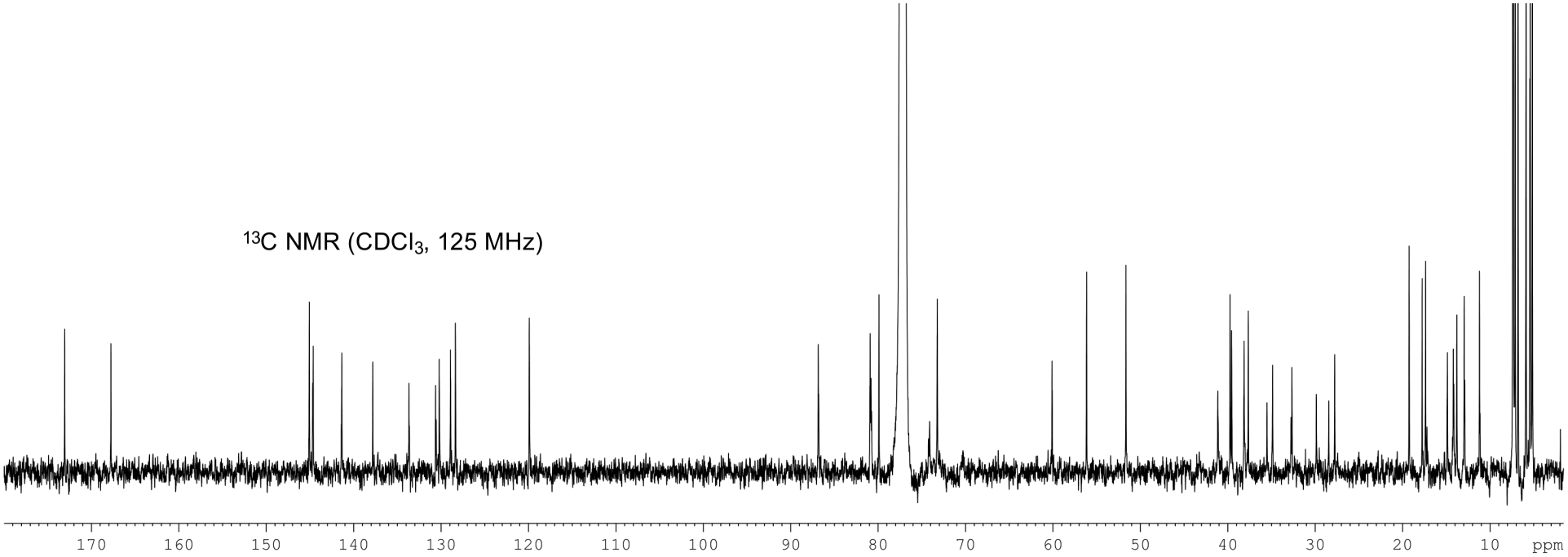

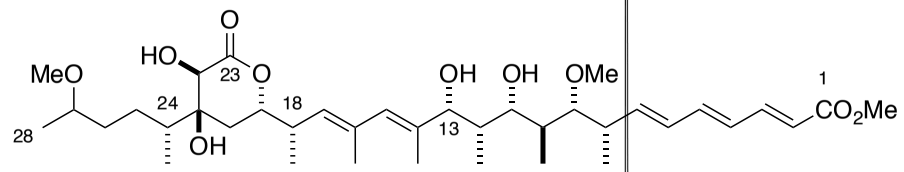

134

^{1}H NMR ($CDCl_3$, 500 MHz)

^{13}C NMR ($CDCl_3$, 125 MHz)

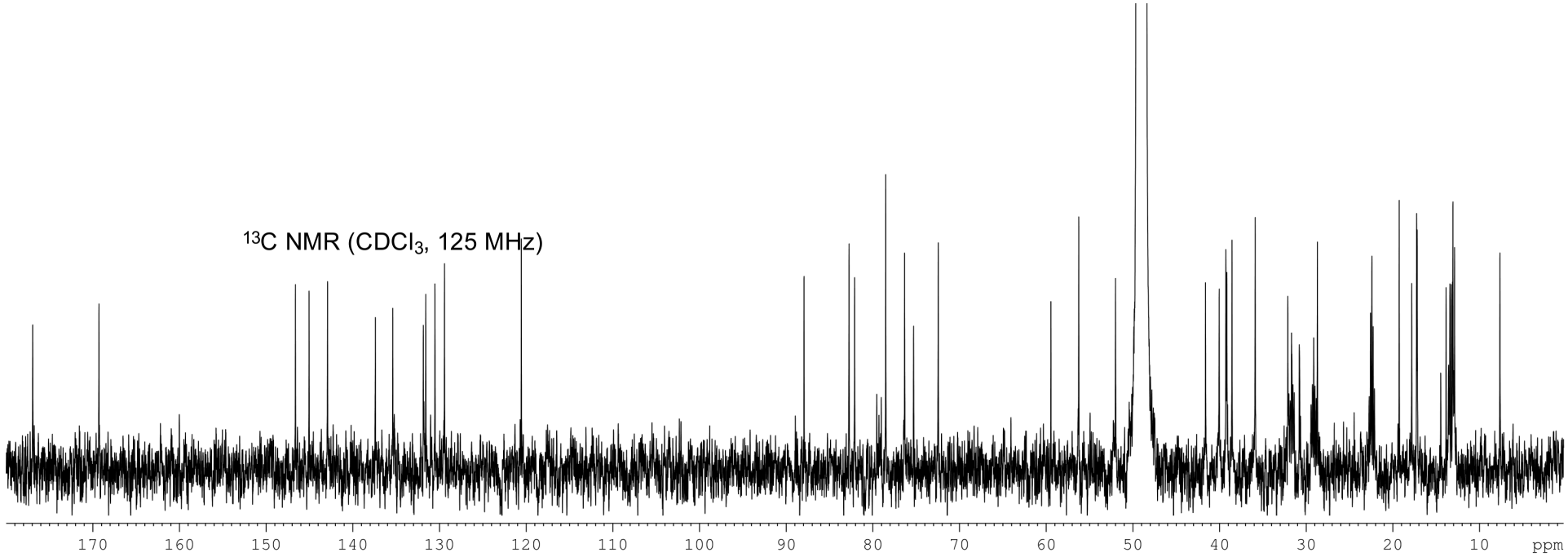

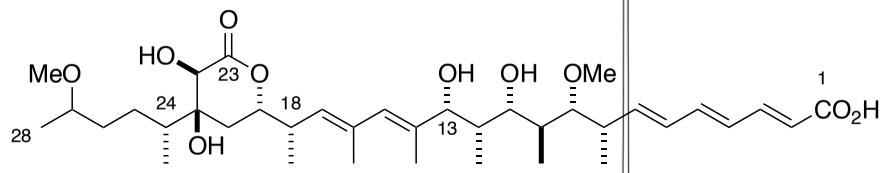

103

^{1}H NMR ($CDCl_3$, 500 MHz)

^{13}C NMR ($CDCl_3$, 125 MHz)

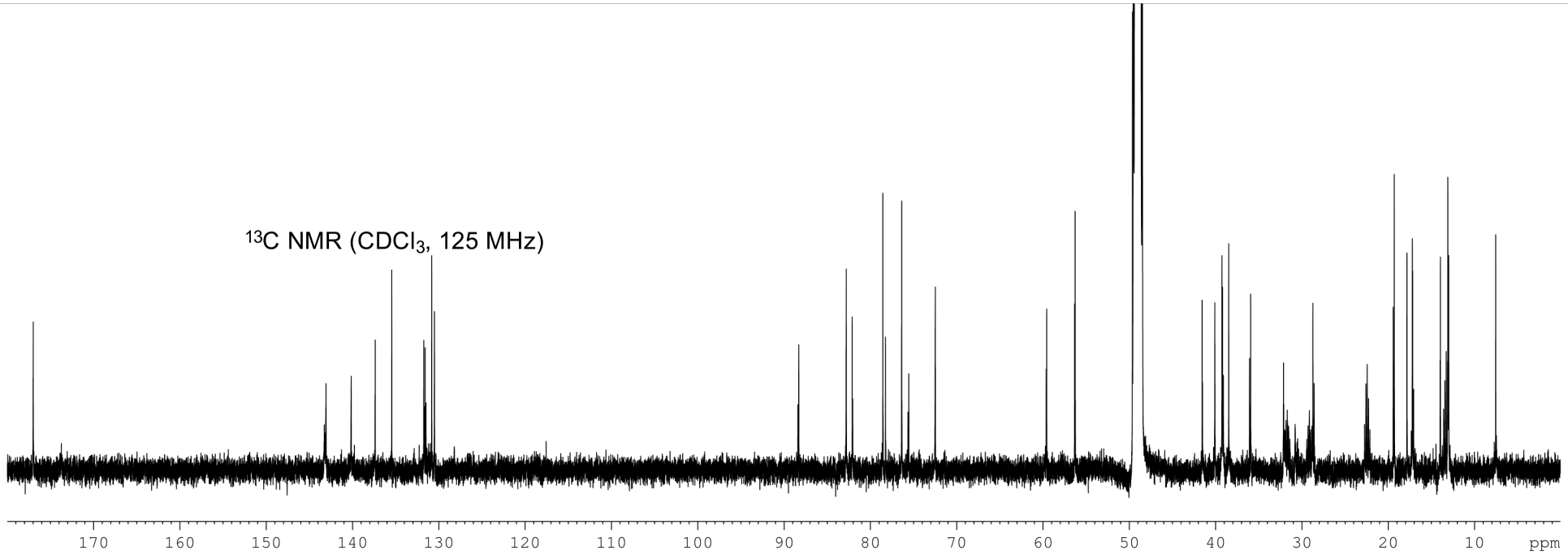

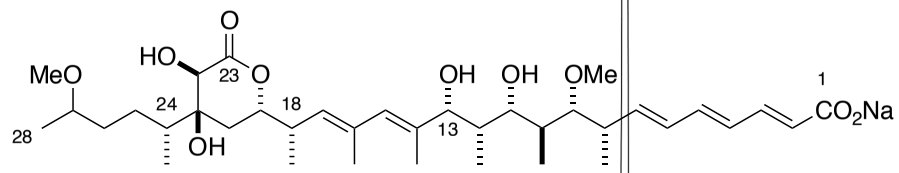

137

^{1}H NMR ($CDCl_3$, 500 MHz)

^{13}C NMR ($CDCl_3$, 125 MHz)

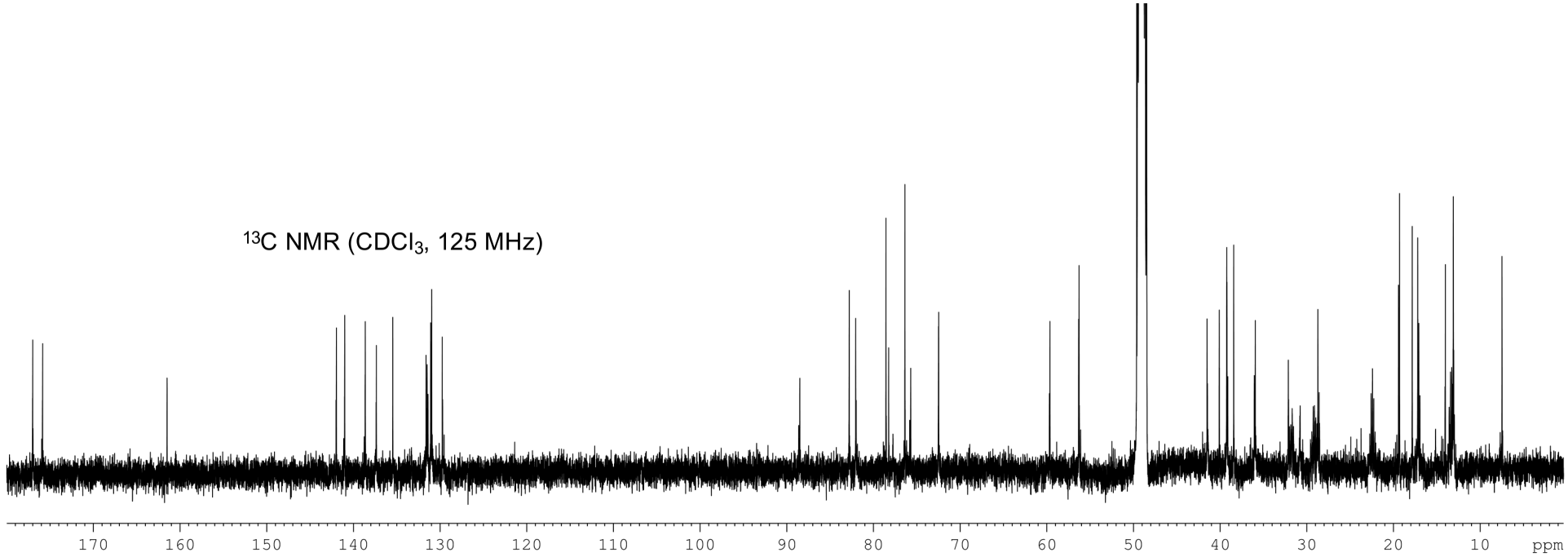

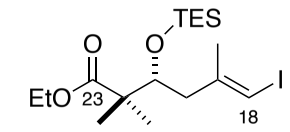

220

^{1}H NMR ($CDCl_3$, 500 MHz)

^{13}C NMR ($CDCl_3$, 125 MHz)

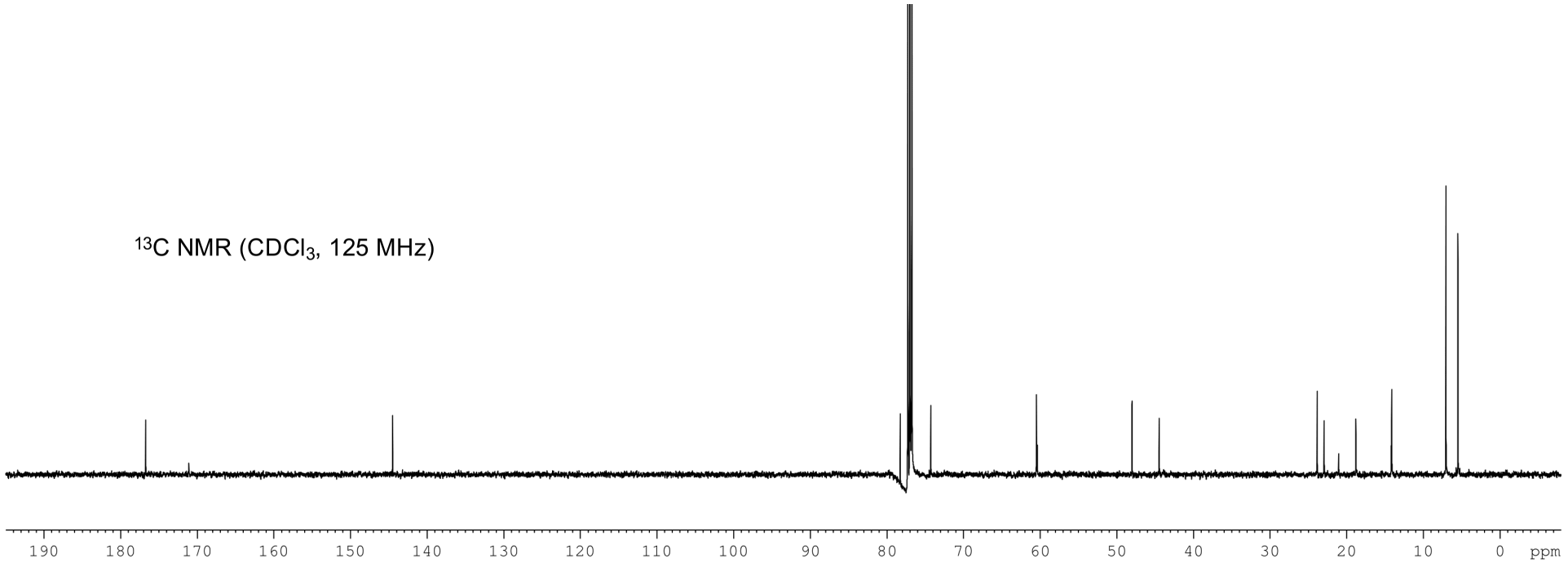

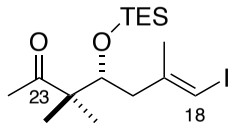

201

^{1}H NMR ($CDCl_3$, 500 MHz)

^{13}C NMR ($CDCl_3$, 125 MHz)

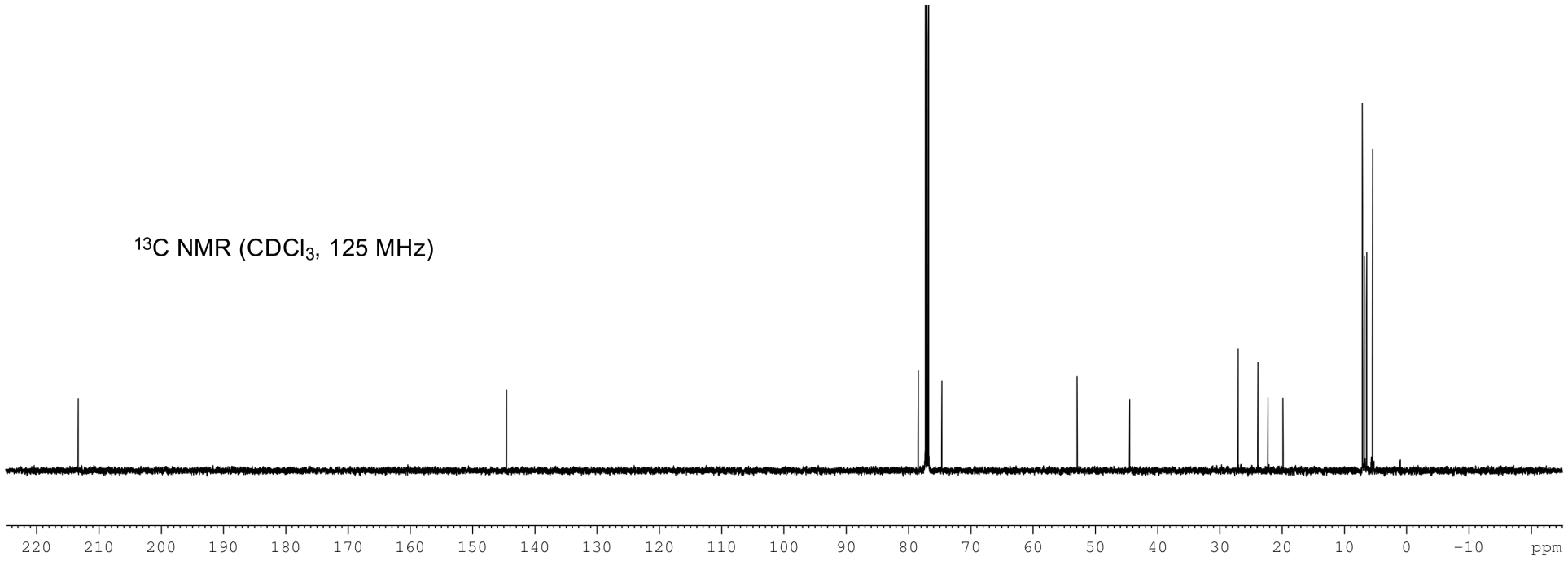

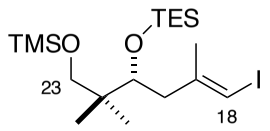

233

^{1}H NMR ($CDCl_3$, 500 MHz)

^{13}C NMR ($CDCl_3$, 125 MHz)

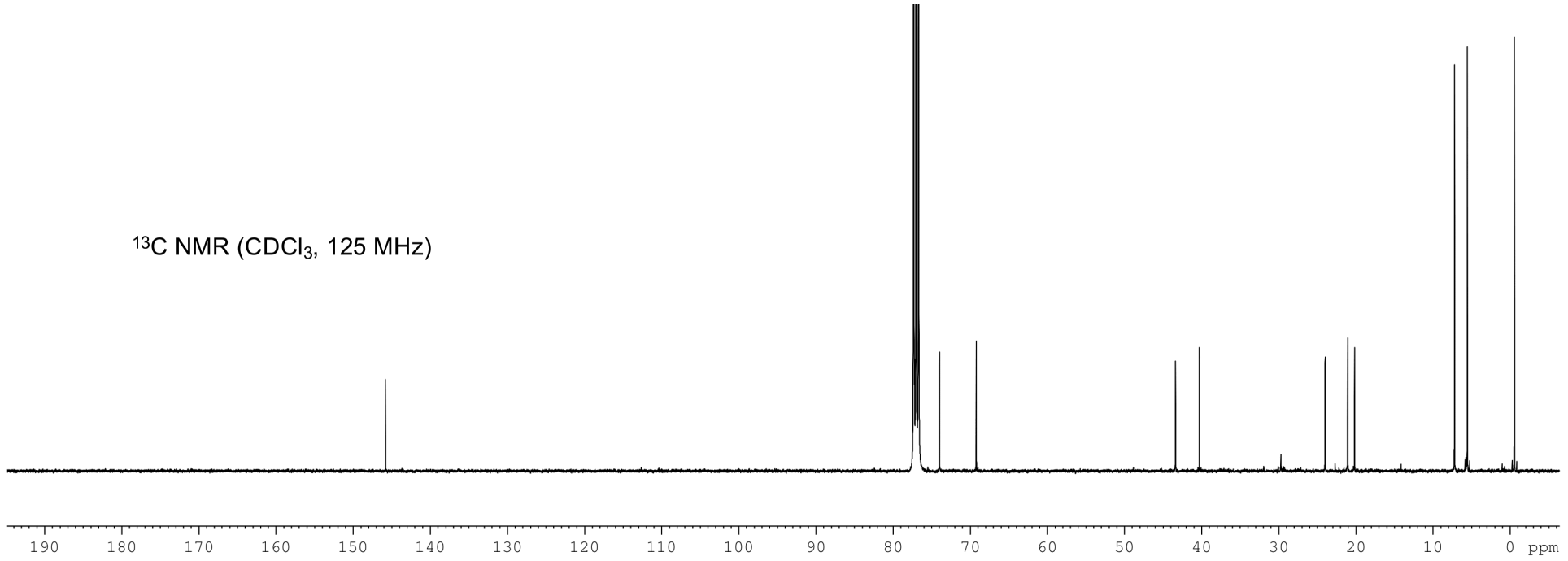

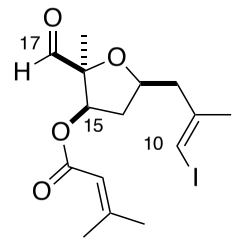

245

^{1}H NMR ($CDCl_3$, 500 MHz)

^{13}C NMR ($CDCl_3$, 125 MHz)

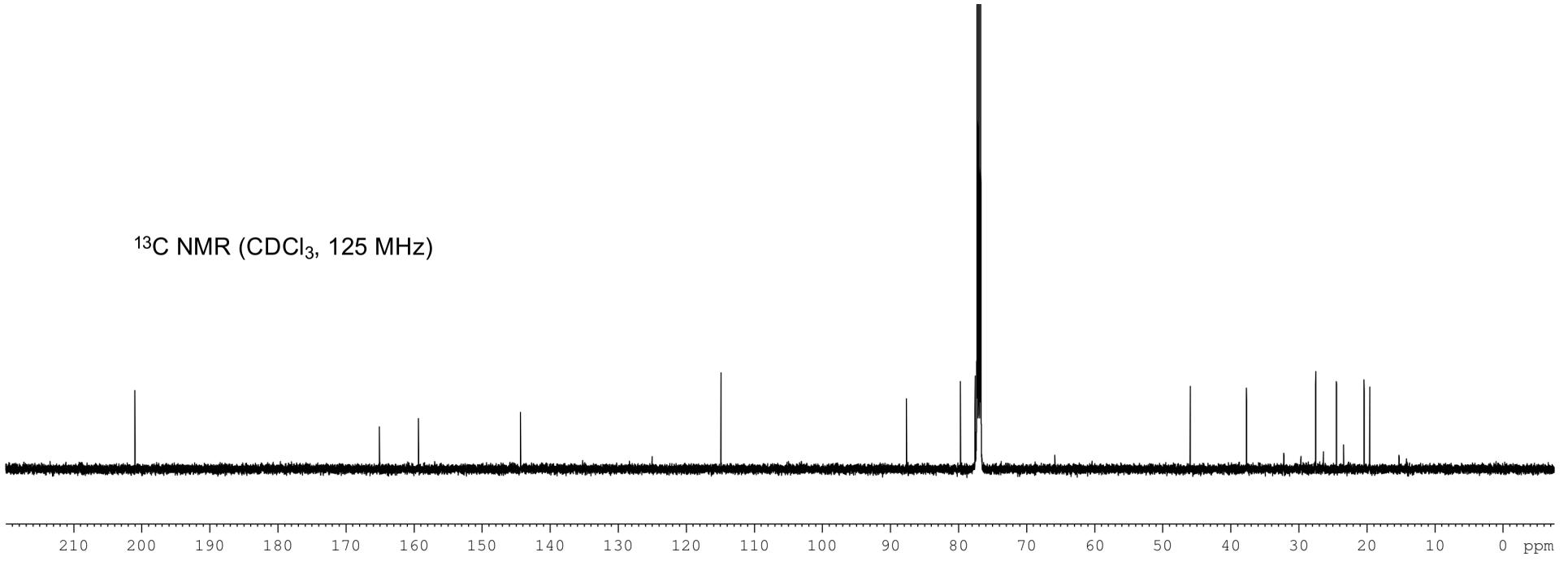

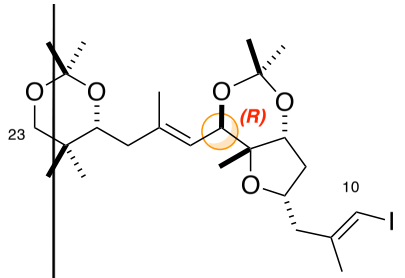

252 (15,17-*anti*)

^{1}H NMR ($CDCl_3$, 500 MHz)

^{13}C NMR ($CDCl_3$, 125 MHz)

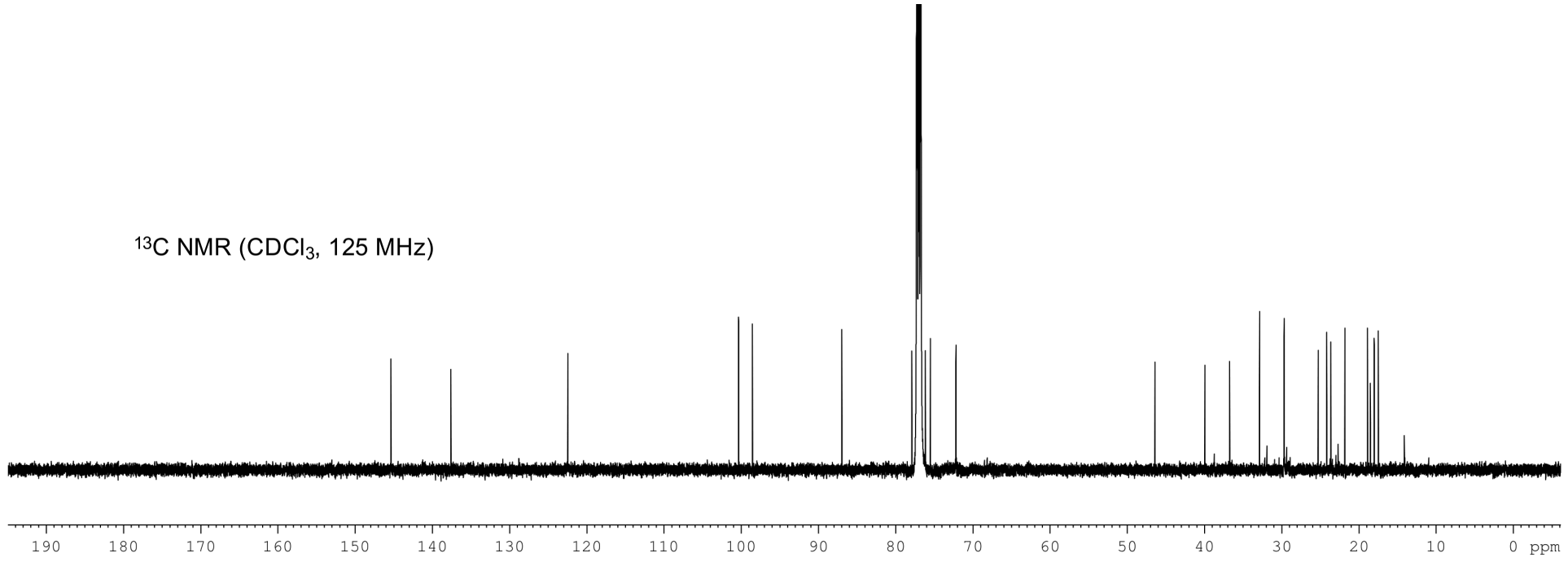

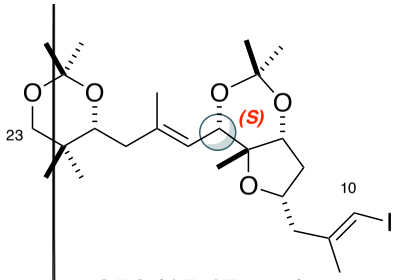

254 (15,17-*syn*)

^{1}H NMR ($CDCl_3$, 500 MHz)

^{13}C NMR ($CDCl_3$, 125 MHz)

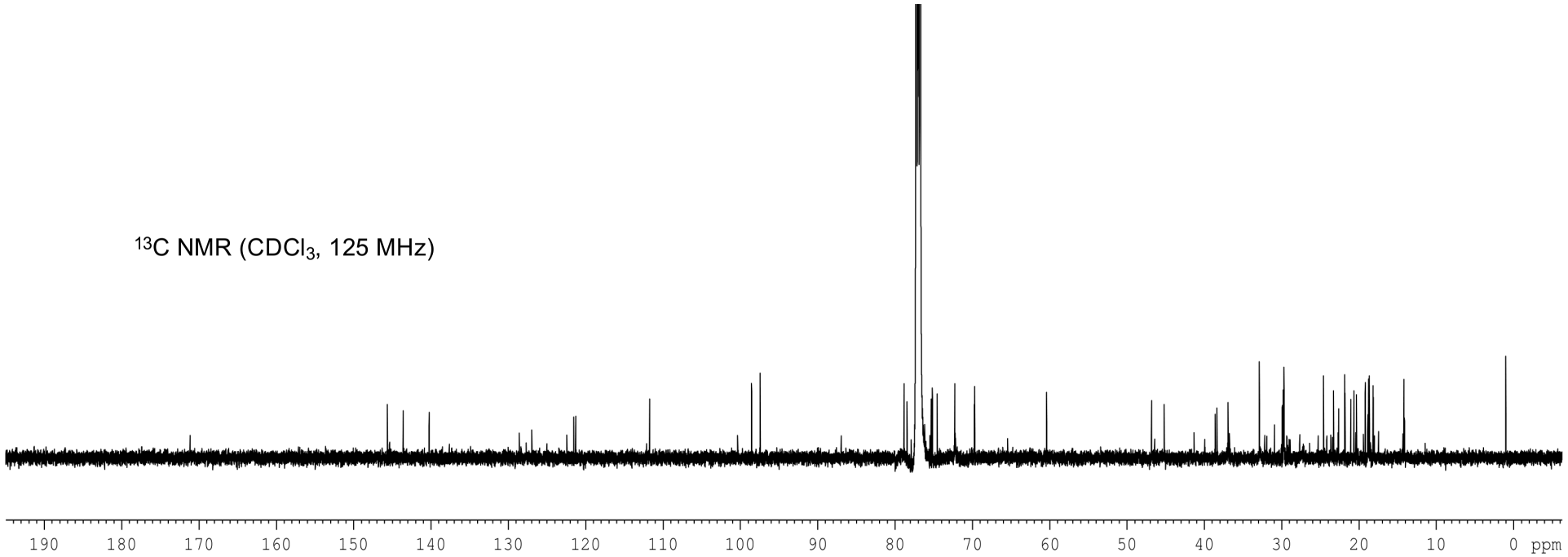

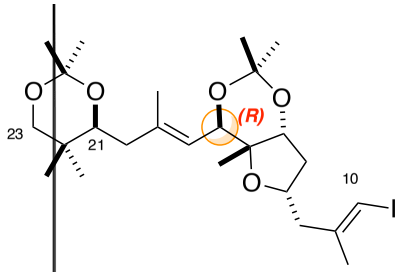

257 (21-*epi*-15,17-*anti*)

^{1}H NMR ($CDCl_3$, 500 MHz)

^{13}C NMR ($CDCl_3$, 125 MHz)

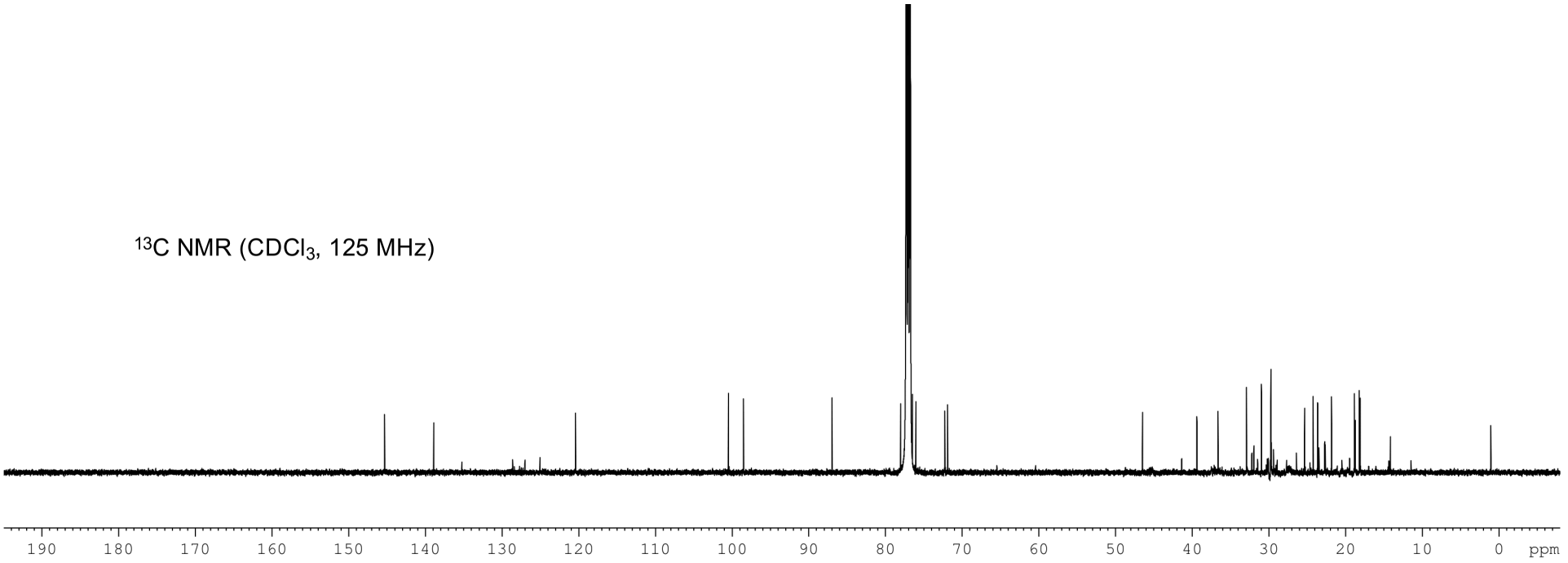

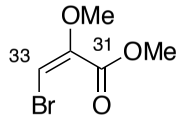

289

^{1}H NMR ($CDCl_3$, 500 MHz)

^{13}C NMR ($CDCl_3$, 125 MHz)

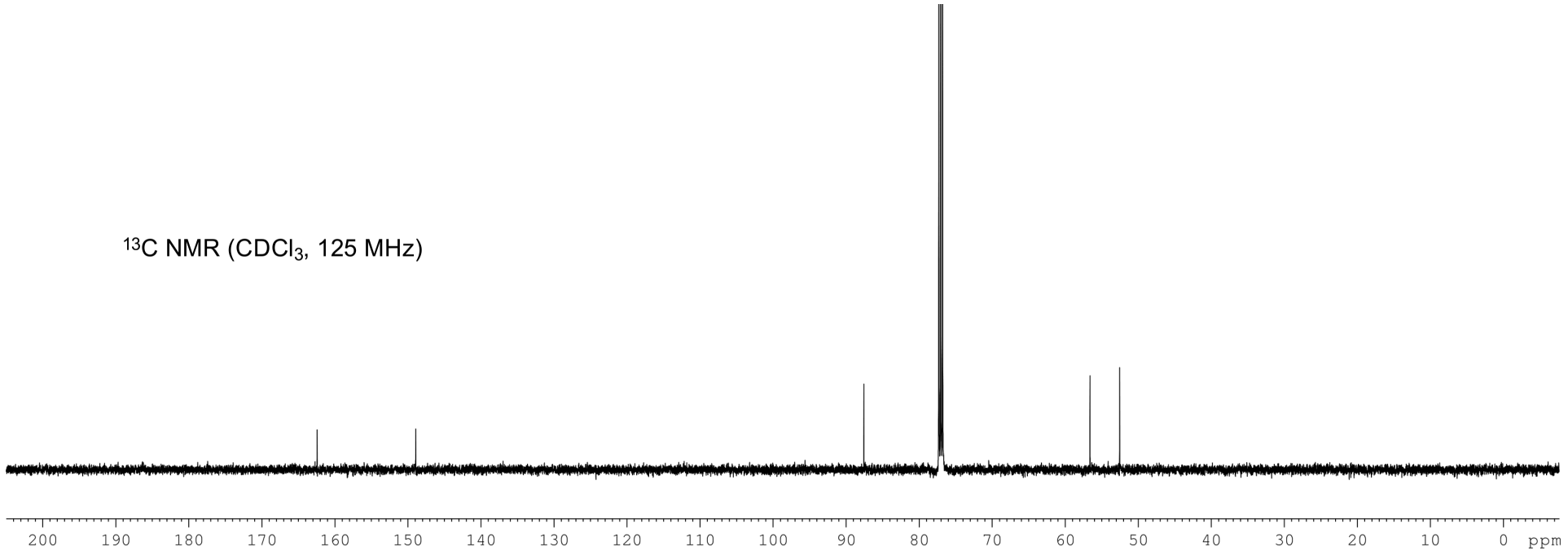

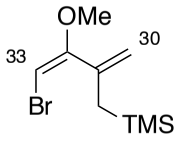

286

^{1}H NMR ($CDCl_3$, 500 MHz)

^{13}C NMR ($CDCl_3$, 125 MHz)

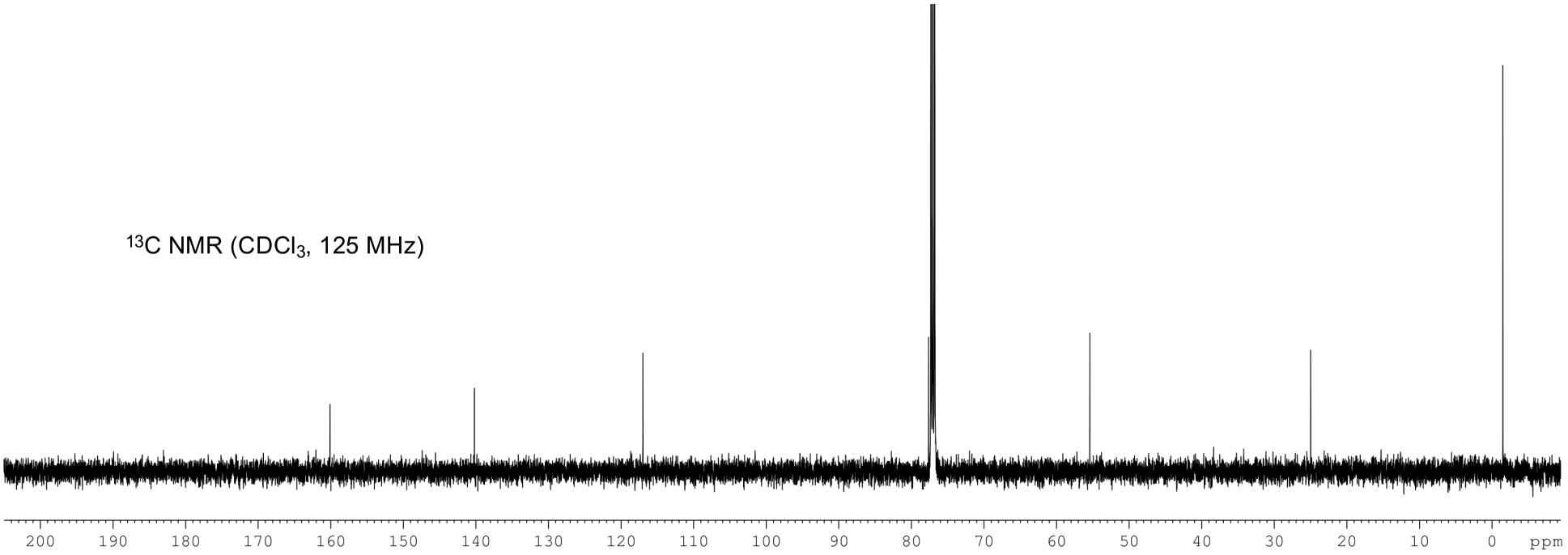

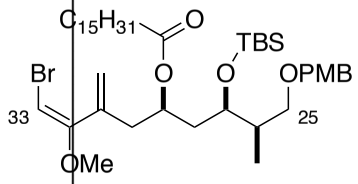

299

^{1}H NMR ($CDCl_3$, 500 MHz)

^{13}C NMR ($CDCl_3$, 125 MHz)

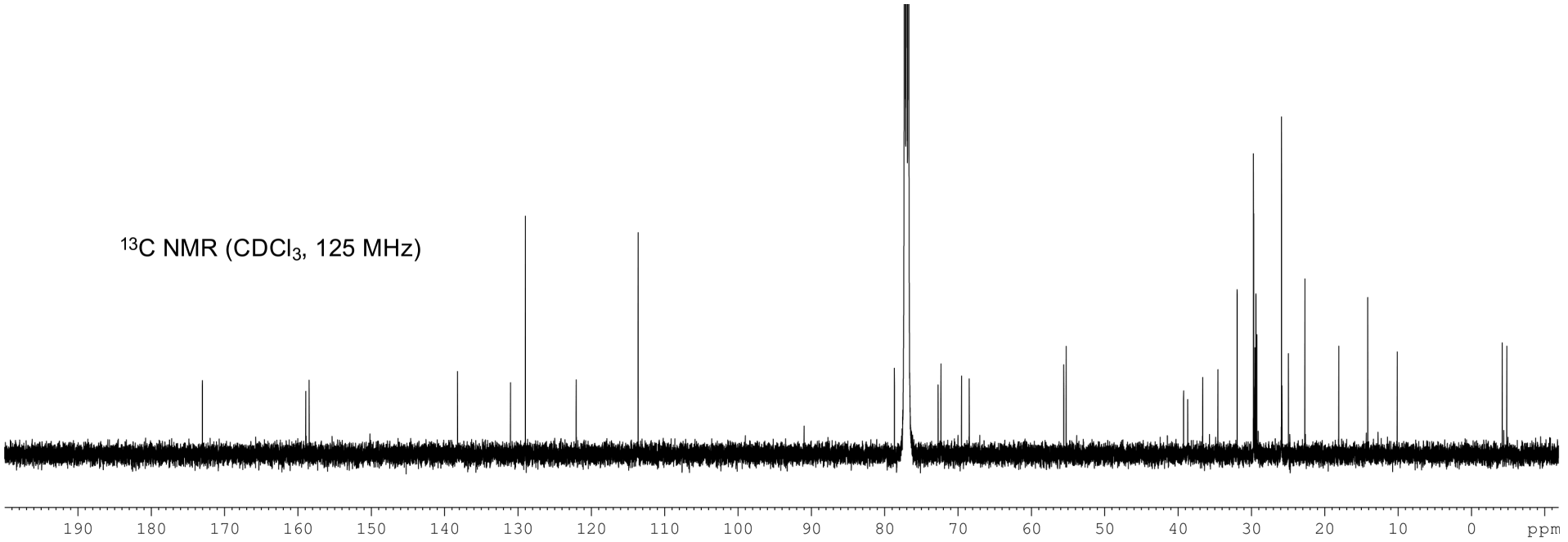

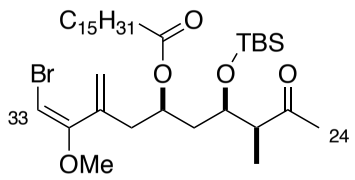

302

^{1}H NMR ($CDCl_3$, 500 MHz)

^{13}C NMR ($CDCl_3$, 125 MHz)

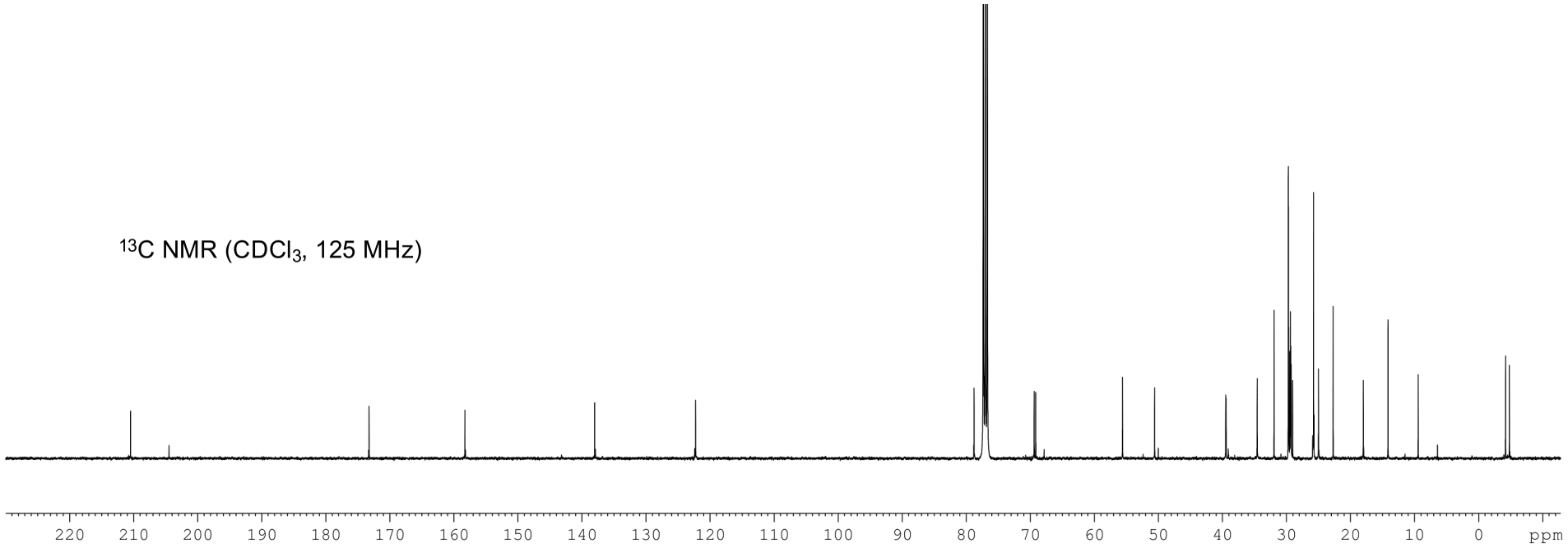

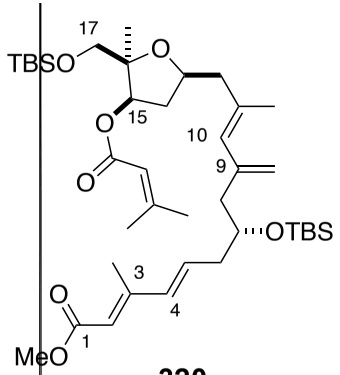

320

^{1}H NMR ($CDCl_3$, 500 MHz)

^{13}C NMR ($CDCl_3$, 125 MHz)

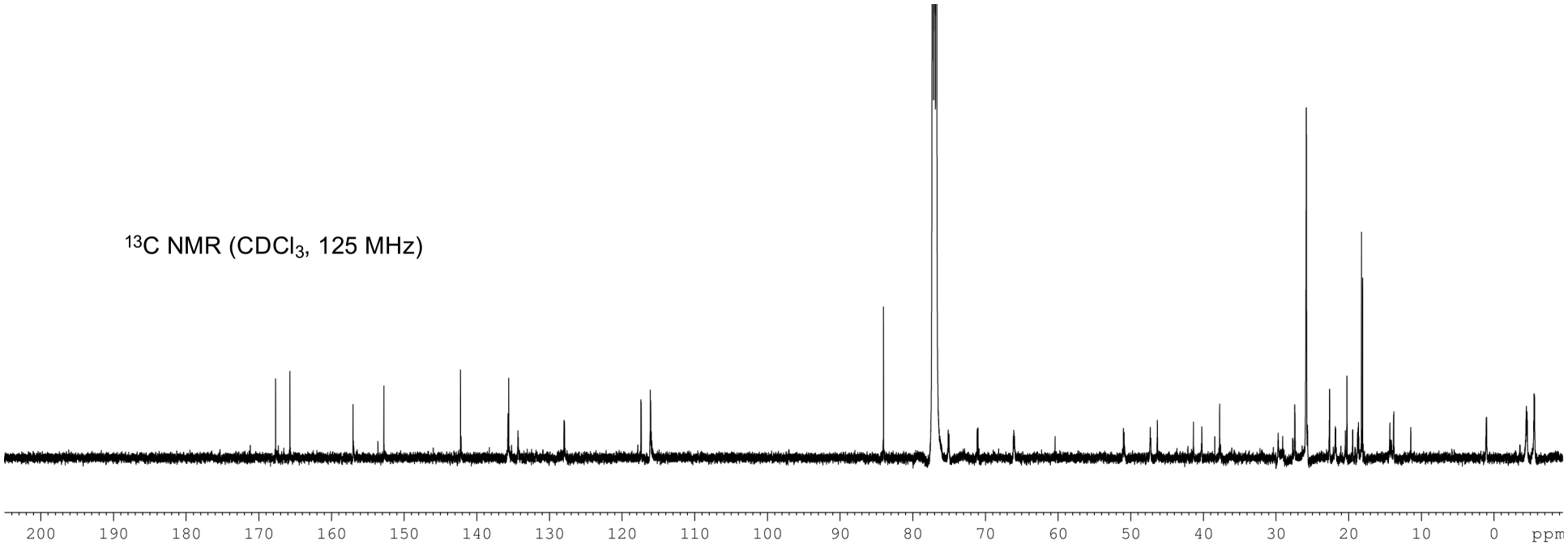

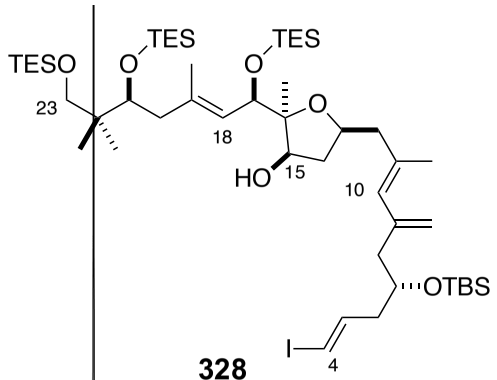

328

^{1}H NMR ($CDCl_3$, 500 MHz)

^{13}C NMR ($CDCl_3$, 125 MHz)

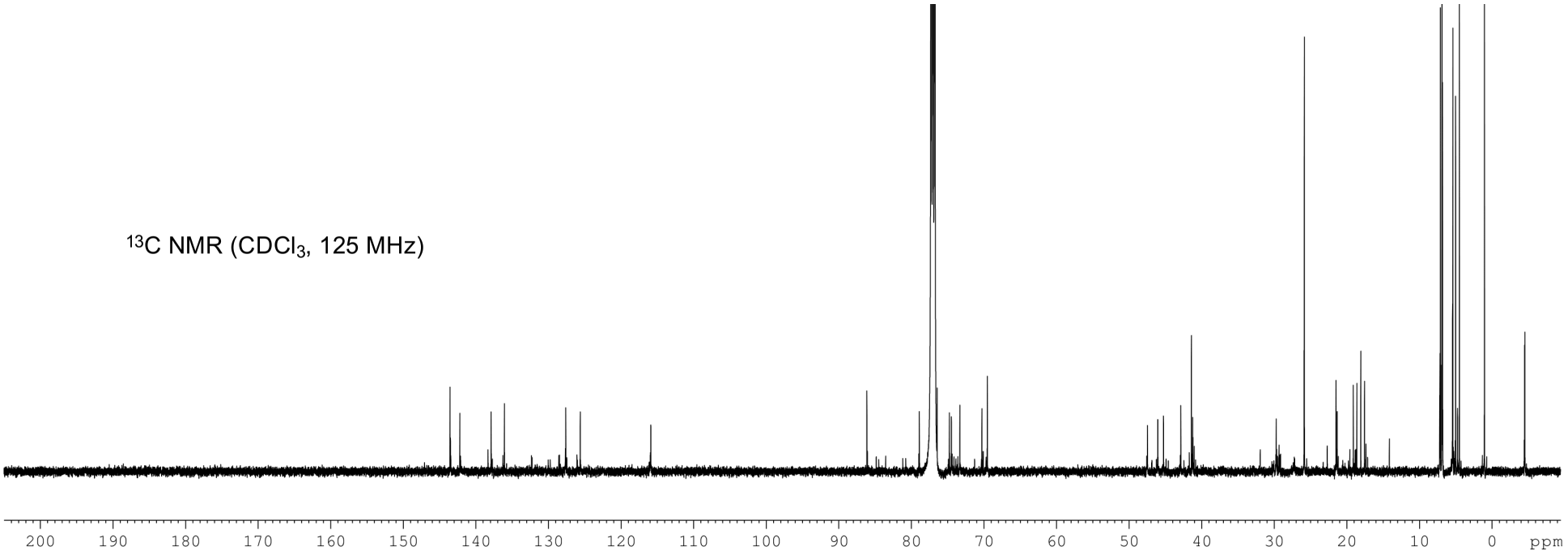

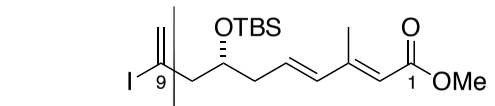

343

^{1}H NMR ($CDCl_3$, 500 MHz)

^{13}C NMR ($CDCl_3$, 125 MHz)

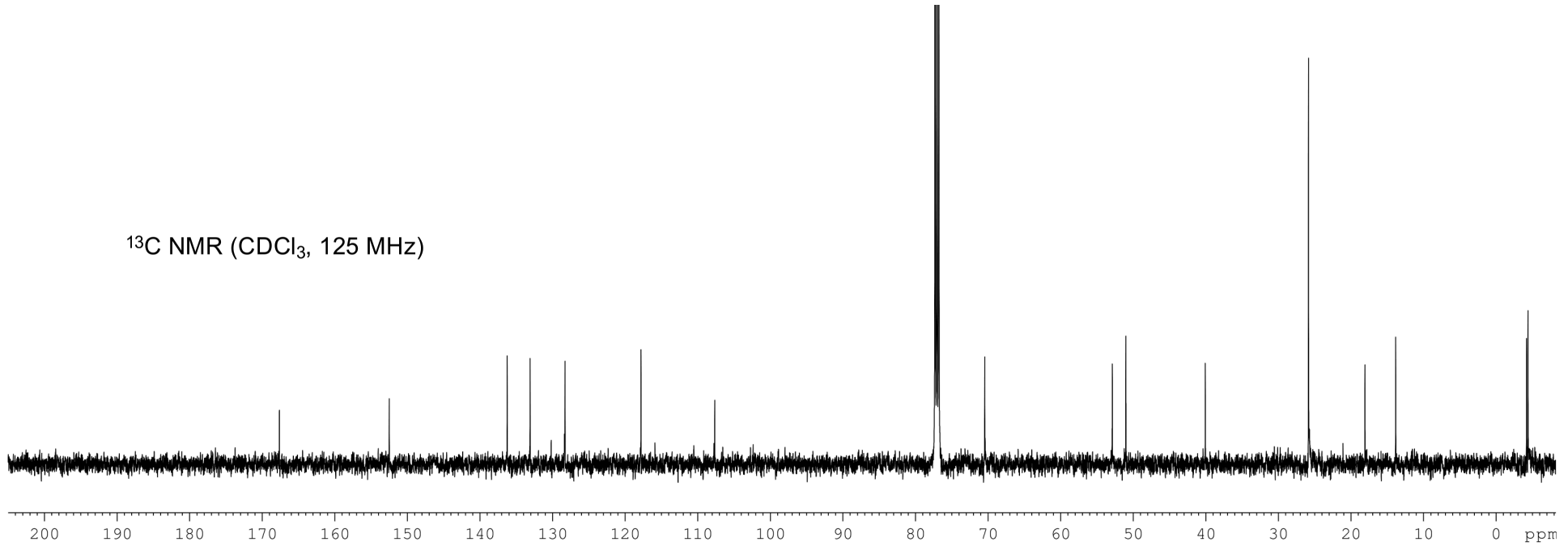

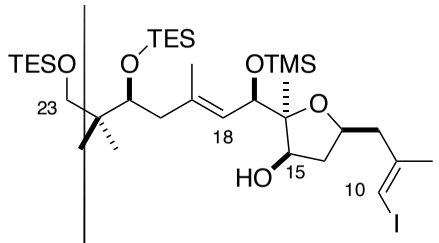

346

^{1}H NMR ($CDCl_3$, 500 MHz)

^{13}C NMR ($CDCl_3$, 125 MHz)